



**Phytochemical, Anticancer and  
Antidiabetic Studies on Libyan Plants:**

*Arum cyrenaicum, Pituranthos tortuosus, Teucrium zanonii, Hypochaeris radicata  
and Solanum sodomaeum*

Thesis submitted by

**Ebtisam Salem Saleh Saad**

For the degree of Doctor of Philosophy

Strathclyde Institute of Pharmacy and Biomedical Sciences,  
University of Strathclyde  
161 Cathedral Street  
Glasgow G4 0NR  
UK

‘This thesis is the result of the author’s original research. It has been composed by the author and has not been previously submitted for examination which has lead to the award of a degree.’

‘The copyright of this thesis belongs to the author under the terms of the United Kingdom Copyright Acts as qualified by University of Strathclyde Regulation 3.50. Due acknowledgement must always be made of the use of any material contained in, or derived from, this thesis.’

Signed:

Date:

**By the name of Allah**

*Dedicated to my husband and my father and my mother*

## **Acknowledgements**

I would like to express my sincere gratitude and appreciation to my Supervisors: Dr. Valerie Ferro and Prof. Alexander Gray for their inspiration, moral support and encouragement, during the entire period of this research and also for their guidance, and patience during this project, perseverance which paved a successful way for my work.

My sincere thanks also goes to Prof. John Igoli for his valuable time, knowledge and support. I would also like to thank my colleagues for their support and friendship which helped me to finish my work smoothly and made my life easy and comfortable in Glasgow.

My acknowledgements also go to the Ministry of Higher Education in Libya for awarding me the scholarship and providing me with the opportunity to study abroad to undertake my PhD degree in the United Kingdom.

Finally, my deepest gratitude goes to my parents, Salem Saleh Saad and Raja Kalled; my husband, Jamal Benkato; brothers, sisters, friends and my son Mohamed whose unconditional love and support make everything possible.

## Abstract

This thesis examined the *in vitro* anticancer and/ or antidiabetic activities of five Libyan medicinal plants which are traditionally used. They included: *Arum cyrenaicum*, *Pituranthos tortuosus*, *Teucrium zanonii*, *Hypochaeris radicata* and *Solanum sodomaeum*. Plants were investigated phytochemically and a range of compounds, including daucosterol ester of *trans p*-coumaric acid, were elucidated; one of which appears to be novel. In addition, phenolic compounds, phenolic acids, flavonoids, flavonoids glycosides, pheophytins, phenylethanoid glycoside, steroidal glycoalkaloid and fatty acid were isolated from these plants.

The work focused on the evaluation of the plant extracts and some of the isolated compounds for cytotoxicity based on metabolic activity to evaluate the potential anticancer activity against human melanoma A375, HeLa cervical, prostate LNCaP and PC-3M, pancreas PANC-1 and liver HepG2 and non cancerous cells PNT2 and HEKa cells as the normal controls. Crude extracts and isolated compounds that showed weak or no inhibitory activity on the cell lines were then further investigated for hypoglycaemic activity by evaluating inhibition of carbohydrate-hydrolysing enzymes protein tyrosine phosphatase 1B (PTP1B), alpha-glycosidase and alpha-amylase.

Among the *A. cyrenaicum* extracts, the root hexane extract showed weak activity at 250 µg/ml on cancer cells and HeLa, HepG2, HEKa and PNT2 cells with an IC<sub>50</sub> of 181.3, 128.3, 136.6, and 140.7 µg/ml, respectively, while *A. cyrenaicum* fruit showed toxicity on normal cells. The hexane extract of *P. tortuosus* showed no selective toxicity toward cancers cells, as it killed normal and cancer cells (A375, PANC-1 and PNT2) at the lowest concentration with IC<sub>50</sub> values of 76.97, 86.57 and 80.30 µg/ml, respectively and this extract was toxic to LNCaP, PC-3M and HepG2 at 250 µg/ml. However, PTH-6-7 from hexane extract, showed selective activity on A375, PC-3M

and PANC-1 cells with an  $IC_{50}$  of 70.11, 72.20 and 75.88  $\mu\text{g/ml}$ , respectively. The ethyl acetate extract of *P. tortuosus* showed weak activity at 250  $\mu\text{g/ml}$  against A375, PANC-1 and PNT2 cells, but the methanol extract of *P. tortuosus* showed no toxicity on cancer cells.

The ethyl acetate extract of *T. zanonii* showed selective activity against A375 and LNCaP cancer cells, while the methanol extract showed selective activity against PANC-1 cells with an  $IC_{50}$  of 62.02  $\mu\text{g/ml}$  and this effect was linked in part to the extracts' contents of phenylethanoid glycoside types. However, the hexane extract of *T. zanonii* showed weak activity on PANC-1 cells with an  $IC_{50}$  of 132.9  $\mu\text{g/ml}$ ; this could be due to the presence of salvigenin.

The hexane extract of *H. radicata* showed no selective activity against cancer cells, but the ethyl acetate extract of *H. radicata* showed selective activity against hepatoma cells with an  $IC_{50}$  of 63.43  $\mu\text{g/ml}$  and this effect was linked in part to the extracts' flavonoids. The methanol extract of *H. radicata* did not exhibit activity on cancer cells.

*S.sodomaenum* methanol crude extract (SSM) and chlorogenic acid (SSM-56) were the most active against cancer cells. SSM showed toxicity against LNCaP, PC-3M, A375, HeLa, PANC-1 and HepG2 cells at different concentrations with different  $IC_{50}$  values 18.95  $\mu\text{g/ml}$ , 18.37  $\mu\text{g/ml}$ , 93.58  $\mu\text{g/ml}$ , 29.20  $\mu\text{g/ml}$ , 8.72  $\mu\text{g/ml}$  and 18.98  $\mu\text{g/ml}$ , respectively. Compound SSM-56 was toxic to LNCaP, PC-3M and HepG2 with  $IC_{50}$  values of 371.90  $\mu\text{M}$ , 266.97  $\mu\text{M}$  and 337.83  $\mu\text{M}$ , respectively. However, both SSM and SSM-56 were most toxic to PANC-1 cells with  $IC_{50}$  values of 15.6  $\mu\text{g/ml}$  and 20.19  $\mu\text{g/ml}$ , respectively. On PNT2, the SSM extract showed toxic effects at concentrations above 125  $\mu\text{g/ml}$  while SSM-56 did not show toxicity on normal cells. Therefore SSM extract and SSM-56 showed selective activity on PANC-1 cells. On further analysis,

both SSM and SSM-56 had an inhibitory effect on adhesion, migration and invasion of PANC-1 cells. The effect of SSM and SSM-56 inhibited adhesion of PANC-1 cells to fibronectin and collagen IV. Therefore, SSM and SSM-56 have the potential to treat pancreatic cancer by inhibition of cell migration and invasion as a result of reduced or inhibited attachment to ECM proteins (collagen IV and fibronectin).

In terms of antidiabetic assessment, protein tyrosine phosphatase inhibition was observed for the hexane extract of *T. zanonii* (Ki  $1.18 \pm 0.006$   $\mu\text{g/ml}$ ), hexane and ethyl acetate extracts of *H. radicata* (Ki  $1.207 \pm 0.008$  and  $1.301 \pm 0.006$   $\mu\text{g/ml}$ ) and the hexane root and aerial part extracts of *A. cyrenaicum* (Ki  $1.902 \pm 1.51$   $\mu\text{g/ml}$  and  $1.65 \pm 1.37$   $\mu\text{g/ml}$ ). The extract of *H. radicata* displayed alpha-glucosidase inhibition (Ki value of  $2.160 \pm 1.007$   $\mu\text{g/ml}$ ) and no activity for alpha-amylase. Results obtained indicated that all four plant extracts tested had the potential to lower blood glucose levels to some extent and therefore in part corroborates the ethnomedicinal use of these four species in the treatment of diabetes.

In conclusion, traditional Libyan plants can provide an excellent source of natural raw material to isolate anticancer or antidiabetic's agents, in addition, to phytochemicals, preliminary data showed the possibility from these plants having an anti-cancer or anti-diabetic role to play.

## Table of Contents

Acknowledgements .....	I
Abstract .....	II
Table of Contents .....	V
List of Abbreviations .....	XII
List of Figures .....	XIV
List of Tables .....	XXI
List of Schemes .....	XXIV
<b>Chapter 1</b> .....	<b>0</b>
1.1 Herbal medicine .....	1
1.2 Review of cancer and diabetes .....	6
1.2.1 Cancer .....	7
1.2.2 Cancer and herbal medicine .....	9
1.3 Diabetes mellitus .....	12
1.3.1 Diabetes and Herbal Medicine .....	13
1.4 Herbal medicinal plant use in Libya .....	19
1.4.1 <i>Arum cyrenaicum</i> .....	21
1.4.2 <i>Pituranthos tortuosus</i> .....	27
1.4.3 <i>Teucrium zanonii</i> .....	33
1.4.4 <i>Hypochaeris radicata</i> .....	41
1.4.5 <i>Solanum sodomaeum</i> .....	48
1.5 Aims and Objectives .....	56
<b>Chapter 2</b> .....	<b>57</b>
2. Materials and methods .....	58
2.1. Solvents .....	58
2.2 Reagents and chemicals .....	58
2.3 Equipment .....	59

2.4 Plant material .....	62
2.5 Extraction and Partitioning .....	62
2.5.1 Hot extraction.....	62
2.5.2 Maceration.....	62
2.6 Fractionation work and isolation of compounds.....	63
2.6.1 Analytical Thin layer (TLC).....	63
2.6.2 Vacuum liquid chromatography (VLC) .....	64
2.6.3 Size-Exclusion Chromatography (SEC) .....	64
2.6.4 Column Chromatography (CC).....	64
2.6.5 Preparative TLC .....	65
2.6.6 Solvent extraction.....	65
2.7 Spectroscopic examination.....	66
2.7.1 Nuclear Magnetic Resonance (NMR).....	66
2.7.2 Mass spectrometry .....	67
2.7.3 Infrared spectroscopy (IR) .....	67
2.8 Bioactivity examination .....	68
2.8.1 Tissue culture .....	68
28.1.1 Maintenance of the cells .....	68
28.1.2 Preparation of complete culture medium .....	68
28.1.3 Cytotoxicity assay .....	70
2.8.2 SYTOX®Green assay .....	72
2.8.3 Effect of staurosporine and cisplatin.....	72
2.8.4 ApoTox-Glo™ Triplex Assay .....	72
2.8.5 ADP/ATP Ratio Assay Kit.....	74
2.8.6 Apoptosis, necrosis and healthy cell quantitation kit plus .....	75
2.8.7 Adhesion of PANC-1 cells to fibronectin using an InnoCyte™ ECM Cell Adhesion Assay (Fibronectin) .....	76

2.8.8 Adhesion of PANC-1 cells to collagen IV using a CytoSelect™ 48-Well Cell Adhesion Assay (Collagen IV).....	76
2.8.9 Migration assay using a Cytoselect™ 24-well Cell Migration Assay .....	77
2.8.10 Invasion assay using a Cytoselect™ 24-well Cell Invasion Assay .	77
29 Effect of the extracts and compounds on the activities of PTP1B, $\alpha$ -glucosidase and $\alpha$ -amylase enzymes .....	78
2.9.1 Z-factor.....	78
2.9.2 Plant sample preparation.....	78
2.9.3 PTP1B assay .....	79
2.9.4 $\alpha$ -glucosidase assay.....	80
2.9.5 $\alpha$ -amylase assay.....	81
<b>Chapter 3.....</b>	<b>83</b>
Part1: Phytochemistry .....	84
3.1 Solvent extraction and yield.....	84
3.2 Fractionation of <i>A. cyrenaicum</i> crude extracts.....	84
3.2.1 Characterisation of ARE-6-6 as a <i>para</i> -hydroxybenzoic acid .....	85
3.2.2 Characterisation of ARE-6-18 as <i>p</i> -coumaric acid (a) and 3, 4-dimethoxycinnamic acid (b).....	88
3.3 Fractionation of <i>P. tortuosus</i> crude extracts.....	92
3.3.1 Characterisation of PTM-1 as luteolin-7-o-rutinoside-4'-methylether (diosmin) .....	92
3.3.2 Characterisation of PTH6-7 as 2-hydroxy-3-(4-hydroxy-3-methoxyphenyl)-propionic acid (vanillic acid) .....	99
3.4 Fractionation of <i>T. zanonii</i> Crude Extracts .....	103
3.4.1 Characterisation of TZH-103-107-9 as 5-hydroxy-6, 7, 4'-trimethoxyflavone or salvigenin .....	103

3.4.2	Characterisation of TZH-150-170-7 as 5-hydroxy-3', 4', 6, 7-tetramethoxyflavone OR as 5-hydroxy-3, 4, 7, 8 tetramethoxyflavone...	108
3.4.3	Characterisation of TzM-24 as poliumoside .....	113
3.4.4	Characterisation of TZH-68 as pheophytin A .....	121
3.2.5	Characterisation of TZH-41-49 as ferulic acid ester of (a) fatty alcohol(s).....	128
3.5	Fractionation of <i>H. radicata</i> crude extracts .....	133
3.5.1	Characterisation of HRE-21 as 3', 4', 5, 7-tetrahydroxyflavone or luteolin .....	133
3.5.2	Characterisation of HRM- 50-59 as Cinaroside (luteolin-7-O-glucoside).....	138
3.5.3	Characterisation of HRE-94 of a novel daucosterol ester of <i>trans p</i> -coumaric acid .....	143
3.5.4	Characterisation of HRE-121 as 1-monoacetylglycerol .....	150
3.5.5	Characterisation of HRH-42 as linoleic acid .....	152
3.6	Fractionation of <i>S. sodomaeum</i> crude extracts.....	153
3.6.1	Characterisation of SSM-30-2 as solamargine.....	153
3.6.2	Characterisation of SSM-56 as 3- <i>O</i> -caffeoyl quinic acid or cholorgenic acid .....	163
3.4.3	Characterisation SSH and SSE as trilinolein .....	168
	<b>Part 2: Biology Results</b> .....	170
3.7	Cytotoxicity screening of crude extracts and isolated compounds using AlamarBlue®assay .....	170
3.7.1	Cytotoxicity of <i>A. cyrenaicum</i> crude extracts and isolated compounds .....	174
3.7.2	Cytotoxicity of <i>P. tortuosus</i> crude extracts and isolated compounds .....	176

3.7.3 Cytotoxicity of <i>T. zanonii</i> crude extracts and isolated compounds	180
3.7.4 Cytotoxicity of <i>H. radicata</i> crude extracts and isolated compounds	185
3.7.5 Cytotoxicity of <i>S. Sodomaeum</i> crude extracts and isolated compounds	192
3.7.5.1 Effects of <i>S. sodomaeum</i> methanol extract (SSM) and chlorogenic acid (SSM-56) on PANC-1 cells	197
3.7.5.1.1 Effect of SSM and SSM 56 on PANC-1 and PNT2 cells viability after 48 h	197
3.7.5.1.2 Effect of SSM and SSM-56 on the morphology of PANC-1 cells after 48 h	200
3.7.5.1.3 Effect of SSM and SSM 56 on membrane integrity of PANC-1 cells after 24 h	201
3.7.5.1.4 Effects of SSM and SSM-56 on adhesion, migration and invasion of PANC-1 cells	204
3.7.5.1.4.1 Effect of SSM and SSM-56 on adhesion of PANC-1 cells to ECM (fibronectin and collagen IV)	204
3.7.5.1.4.2 Effect of SSM and SSM56 on migration of PANC-1 cells using a Cytoselect™ 24-well Cell Migration Assay	208
3.7.5.1.4.3 Effect of SSM and SSM-56 on invasion of PANC-1 cells across the basement membrane using a Cytoselect™ 24-well Cell Invasion Assay	210
3.7.5.1.4 Effect of SSM and SSM-56 on viability, cytotoxicity and apoptosis of PANC-1 cells using the ApoTox-Glo™ Triplex Assay	212
3.7.5.1.6 Effect of SSM and SSM-56 on PANC-1 cells by measuring an apoptosis, necrosis and Healthy Cell Quantitation Kit Plus	215
3.8 <i>In vitro</i> antidiabetic activity assessment	216

3.8.1 Screening of antidiabetic assays, of PTP1B, $\alpha$ -glucosidase and $\alpha$ -amylase enzymes.....	216
3.8.2 PTP1B enzyme.....	216
3.8.2.1 Z-factor of PTP1B and TFMS Reference Standard Curve .....	216
3.8.2.2 PTP1B inhibition by crude extracts and isolated compounds.....	218
3.8.2.3 Concentration dependent inhibition of crude extracts .....	220
3.8.3 $\alpha$ -Glucosidase enzyme .....	223
3.8.3.1 Z-Factor of $\alpha$ -Glucosidase assay and Acarbose Reference Standard Curve.....	223
3.8.3.2 Effect of crude extracts and isolated compounds.....	225
3.8.3.3 Concentration dependent inhibition of crude extracts .....	226
3.8.4 $\alpha$ -Amylase enzyme.....	226
3.8.4.1 Z-factor of $\alpha$ -Amylase assay and A carbose Reference Standard Curve.....	226
3.8.4.2 $\alpha$ -amylase inhibition by crude extracts .....	228
<b>Chapter 4.....</b>	<b>229</b>
4.1 Discussion .....	230
4.2 <i>In vitro</i> cytotoxicity activity assessment .....	230
4.2.1 Effects of crude extracts from the <i>A. cyrenaicum</i> and its components on cell viability.....	230
4.2.2 Effects of crude extracts from the <i>P. tortuosus</i> and its components on cell viability.....	232
4.2.3 Effects of crude extracts from the <i>T. zanonii</i> and their components on cell viability.....	233
4.2.4 Effects of crude extracts from the <i>H. radicata</i> and its components on cell viability.....	241
4.2.5 Effects of crude extracts from the <i>S. sodomaeum</i> and its components	

on cell viability.....	245
4.2.5.1 SSM extract and SSM-56 had an inhibitory effect on morphology, adhesion, migration and invasion of PANC-1 cells .....	251
4.3 <i>In vitro</i> anti- diabetic activity assessment .....	254
4.2.4 Overall evaluation of the cytotoxicity and anti-diabetic activities of the crude extracts .....	259
5.1 Recommendations for future.....	263
<b>5.2 Conclusion.....</b>	<b>265</b>
<i>Appendix I</i> .....	268
<i>Appendix II</i> .....	278
<i>Appendix III</i> .....	287
<i>Appendix IV (A) Arum cyrenaicum</i> .....	300
<i>Appendix V H. radicata</i> .....	303
References .....	309

## List of Abbreviations

Acetone- <i>d</i> <sub>6</sub>	Deuterated acetone
<i>brs</i>	Broad singlet
BSA	Bovine Serum Albumin
CC	Column Chromatography
CDCl <sub>3</sub>	Deuterated Chloroform
COSY	<sup>1</sup> H- <sup>1</sup> H COrrrelation SpectroscopY
<i>d</i>	Doublet
DEPT	Distortionless Enhancement by Polarisation Transfer
<i>dd</i>	Doublet of a doublet
DMEM	Dulbecco's Modified Eagle Medium
DMSO	Dimethyl sulphoxide
DMSO- <i>d</i> <sub>6</sub>	Deuterated dimethyl sulphoxide
EtOAc	Ethyl acetate
FCS	Foetal Calf Serum
HRESI-MS	High-resolution Electrospray Ionisation Mass Spectroscopy
HMBC	Heteronuclear Multiple Bond Coherence
HMQC	Heteronuclear Multiple Quantum Coherence
LC-MS	Liquid Chromatography- Mass Spectroscopy
Hz	Hertz
<i>m</i>	Multiple
MeOH	Methanol
MIC	Minimum Inhibitory Concentration
MS	Mass Spectroscopy
MTT	3-[4,5-Dimethylthiazol-2-yl]-2,5 diphenyl tetrazolium bromide
NMR	Nuclear Magnetic Resonance
NOESY	Nuclear Overhauser Enhancement SpectroscopY
PBS	Phosphate-Buffered Saline
PTP1B	Tyrosine-protein phosphatase non-receptor type 1
RPMI	Roswell Park Memorial Institute
PTLC	Preparative Thin Layer Chromatography
<i>S</i>	Singlet
SEC	Size-Exclusion Chromatography

TLC	Thin Layer Chromatography
UV	Ultraviolet
VLC	Vacuum Liquid Chromatography

## List of Figures

Figure 1.1: Examples of some therapeutic agents from plants. ....	3
Figure 1.2: Examples of some anticancer agents from plants.....	11
Figure 1.3: (A) map showed the location of Libya and the major phytogeographical regions of the country: Tripolitania, Cyrenaica, Fezzan and (B) location Al- <i>Jabal Al-Akhdar</i> (The Green Mountain) region in Libya .....	20
Figure 1.4: (A) The fruit, (B) aerial part, (C) root of <i>Arum cyrenaicum</i> collected from Wadi Buoreequ, Libya. ....	21
Figure 1.5: Aerial part of <i>Pituranthos tortuosus</i> , .....	27
Figure 1.6: The aerial parts of <i>Teucrium zanonii</i> collected from Libya.....	33
Figure 1.7: <i>Hypochaeris radicata</i> plant; .....	41
Figure 1.8: Fruit of <i>Solanum sodomaeum</i> collected from Libya. ....	48
Figure 2.1: Template of a cytotoxicity plate layout. ....	71
Figure 3.1: Structure of <i>para</i> -hydroxybenzoic acid. ....	86
Figure 3.2 A: $^1\text{H}$ and 3.2B: HMBC spectra (500 MHz) of ARE-6-6 in $\text{DMSO-}d_6^*$ ... ..	87
Figure 3.3: Structure of ARE-6-18 as a <i>p</i> -coumaric acid (ARE-6-18 a) and 3, 4-dimethoxycinnamic acid (ARE-6-18 b). ....	90
Figure 3.4A: $^1\text{H}$ NMR and 3.4B: HMBC spectra (500 MHz) of ARE-6-18 in $\text{DMSO-}d_6^*$ . ....	91
Figure 3.5: Structure of luteolin-7- <i>O</i> -rutinoside-4'-methylether (diosmin). Key HMBC (  ) and NOESY (  ) correlations observed in PTM-1. ....	94
Figure 3.6A: $^1\text{H}$ NMR and 3.6B: $^{13}\text{C}$ NMR spectra (500 MHz) of PTM-1 in $\text{DMSO-}d_6^*$ . ....	96
Figure 3.7A: HMBC and 3.7B: HSQC spectra (500 MHz) of PTM-1 in $\text{DMSO-}d_6^*$ . ....	97
Figure 3.8: NOESY spectrum (500 MHz) of PTM1 in $\text{DMSO-}d_6^*$ .....	98

Figure 3.9: Structure of 2-hydroxy-3-(4-hydroxy-3-methoxyphenyl)-propionic acid (vanillic acid).....	100
Figure 3.10A: $^1\text{H}$ (400MHz) and 3.10B: $^{13}\text{C}$ NMR spectra (100MHz) of PTH 6-7 in $\text{CDCl}_3^*$ .....	101
Figure 3.11A: COSY (500 MHz) and 3.11B: HMBC (400MHz) spectra of of PTH 6-7 in $\text{CDCl}_3^*$ .....	102
Figure 3.12: Structure of 5-hydroxy-6, 7, 4'-trimethoxyflavone or salvigenin. ....	104
Figure 3.13A: $^1\text{H}$ NMR (400 MHz) and 3.13B: $^{13}\text{C}$ NMR spectra (100 MHz) of TZH 103-107-9 in $\text{CDCl}_3^*$ . ....	106
Figure 3.14A: HMBC and 3.14B: HSQC spectra (400 MHz) of TZH-103-107-9 in $\text{CDCl}_3^*$ .....	107
Figure 3.15: Structure of 5-hydroxy-6, 7, 3', 4'-tetramethoxy flavone. ....	109
Figure 3.16A: $^1\text{H}$ (400 MHz) and 3.16B: $^{13}\text{C}$ (100 MHz) NMR spectra of TZH-150-170-7 in $\text{CDCl}_3^*$ .....	111
Figure 3.17A: HMBC and 3.17B: HSQC spectra (400 MHz) of TZH-150-170-7 in $\text{CDCl}_3^*$ .....	112
Figure 3.18: Structure of poliumoside. Key HMBC (  ) and NOESY (  ) correlations observed in TZM-24.....	115
Figure 3.19A: $^1\text{H}$ and 3.19B: COSY (500 MHz) spectra of TZM-24 in $\text{DMSO-}d_6^*$ . ....	118
Figure 3.20A: HMBC and 3.20B: HSQC spectra (500 MHz) of TZM-24 in $\text{DMSO-}d_6^*$ .....	119
Figure 3.21 A: NOESY and 3.21B: TOCSY spectra (500 MHz) of TZM-24 in $\text{DMSO-}d_6^*$ . ....	120
Figure 3.22: Structure of pheophytin A. ....	122
Figure 3.23: $^1\text{H}$ NMR spectrum (500 MHz) of TZH-68 in $\text{CDCl}_3^*$ .....	125
Figure 3.24 A: and 3.24B: Selected expansion $^{13}\text{C}$ NMR spectra (100 MHz) of TZH-	

68 in CDCl <sub>3</sub> *.....	126
Figure 3.25A: HMBC and 3.25B: HSQC spectra (500 MHz) of TZH-68 in CDCl <sub>3</sub> *. .....	127
Figure 3.26: Structure of ferulic acid ester fatty alcohol. ....	129
Figure 3.27A: <sup>1</sup> H NMR and 3.27B: <sup>13</sup> C NMR spectra (500MHz) of TZH-41-49 inCDCl <sub>3</sub> *.....	131
Figure 3.28A: HMBC and 3.28B: HSQC (500 MHz) spectra of TZH-41-49 in CDCl <sub>3</sub> *. .....	132
Figure 3.29: Structure of luteolin.....	135
Figure 3.30A: <sup>1</sup> H NMR and 3.30B: <sup>13</sup> C NMR spectra (500 MHz) of HRE-21 in Acetone- <i>d</i> <sub>6</sub> *.....	136
Figure 3.31A: HMBC and 3.31B: HSQC (500 MHz) spectra of HRE-21 in Acetone- <i>d</i> <sub>6</sub> *.....	137
Figure 3.32: Structure of luteolin-7-O-glucoside.....	138
Figure 3.33A: <sup>1</sup> H NMR and 3.33B: <sup>13</sup> C NMR spectra (500 MHz) of HRM-50-59 in DMSO- <i>d</i> <sub>6</sub> *.....	141
Figure 3.34A: HMBC and 3.34B: HSQC (500 MHz) spectra of HRM-50-59 DMSO- <i>d</i> <sub>6</sub> *.....	142
Figure 3.35: Structure of daucosterol ester of <i>trans</i> <i>p</i> -coumaric acid.....	145
Figure 3.36A: <sup>1</sup> H NMR and 3.36B: COSY spectra (400 MHz) of HRE-94 in CDCl <sub>3</sub> *. .....	148
Figure 3.37A: HMBC and 3.37B: HSQC (400 MHz) spectra of HRE-94 in CDCl <sub>3</sub> *. .....	149
Figure 3.38: Structure of 1-monoacetylglycerol.....	151
Figure 3.39: <sup>1</sup> H NMR spectrum (400 MHz) of HRE-121 in Acetone- <i>d</i> <sub>6</sub> *.....	151
Figure 3.40: Structure of linoleic acid.....	152
Figure 3.41: <sup>1</sup> H NMR spectrum (400 MHz) of HRH-42 in CDCl <sub>3</sub> *.....	152

Figure 3.42: Structure of solamargine.....	156
Figure 3.43A: <sup>1</sup> H NMR and 3.43B& C: <sup>13</sup> C NMR spectra (500 MHz) of SSM-30-2 in DMSO- <i>d</i> <sub>6</sub> *. ....	159
Figure 3.44A: COSY and 3.44B: HMBC spectra (500 MHz) of SSM-30-2 in DMSO- <i>d</i> <sub>6</sub> *. ....	160
Figure 3.45A: HSQC and 3.45B: expansion HSQC spectra (500 MHz) of SSM-30-2 in DMSO- <i>d</i> <sub>6</sub> *. ....	161
Figure 3.46: NIOSY spectrum (500 MHz) of SSM-30-2 in DMSO- <i>d</i> <sub>6</sub> *.....	162
Figure 3.47: Structure of cholorgenic acid.....	164
Figure 3.48A: <sup>1</sup> H NMR and 3.48B: <sup>13</sup> C NMR spectra (400 MHz) of SSM-56 in DMSO- <i>d</i> <sub>6</sub> *. ....	166
Figure 3.49A: HMBC and 3.49B: HSQC spectra (400 MHz) of SSM-56 in DMSO- <i>d</i> <sub>6</sub> *. ....	167
Figure 3.50: Structure of SSH as triglyceride. ....	168
Figure 3.51: <sup>1</sup> H NMR spectrum (400 MHz) of SSH CDCl <sub>3</sub> .....	169
Figure 3.52: Effect 50% of DMSO on cell viability of (A) cancers cells and (B) normal cells after 48h. ....	171
Figure 3.53: Effect of 5μM of staurosporine on cell viability of LNCap, A375, PC-3M and PNT2 cells. ....	172
Figure 3.54: Morphology and substrate coverage of the cells for the cytotoxicity assay.....	173
Figure 3.55: Effect of <i>P. tortuosus</i> hexane on cell viability of (A) A375 cells, (B) PANC-1 cells, (C) LNCaP cells, (D) PC-3M cells, (E) HepG2 cells, and (F) PNT2 cells after 48h. ....	178
Figure 3.56: Effect of PTH-6-7 on cell viability of (A) A375 cells, (B) PC-3M cells, (C) PANC-1 cells, (D) HepG2 cells and (E) PNT2 cells after 48 h.....	179
Figure 3.57: Effect of <i>T.zanonii</i> EtOAc extract on cell viability of (A) A375 cells, (B)	

LNCaP cells, (C) PANC-1 cells, (D) HEKa cells and (E) PNT2 cells after 48h. .....	182
Figure 3.58: Effect of <i>T zanonii</i> MeOH extract on cell viability of (A) PANC-1 cells, (B) LNCaP cells, (C) HEKa cells and (D) PNT2 cells after 48h. ....	183
Figure 3.59: Effect of TZH-103-107-9 on cell viability of (A) PANC-1 cells and (B) PNT2 cells after 48 h.....	184
Figure 3.60: Effect of TZH-41-49 on HeLa cells after 48h. ....	184
Figure 3.61: Effect of <i>H. radicate</i> hexane on cell viability of (A) PC-3M cells, (B) LNCap cells, (C) PANC-1 cells, (D) HepG2 cells, (E) A375 cells and (F) HeLa cells after 48h. ....	187
Figure 3.62: Effect of <i>H. radicate</i> hexane extract on cell viability of (A) PNT2 cells and (B) HEKa cells after 48 h. ....	188
Figure 3.63: Effect of <i>H. radicate</i> MeOH extract on cell viability of PNT2 cells after 48 h.....	188
Figure 3.64: Effect of <i>H. radicate</i> EtOAc extract on cell viability of (A) HepG2, (B) PC-3M, (C) PANC-1, (D) HeLa, (E) PNT2 and (F) HEKa cells after 48 h..	189
Figure 3.65: Effect HRE-21 on cell viability of (A) HepG2 cells, (B) PC-3M cells and (C) PNT2 cells after 48h. ....	190
Figure 3.66: Effect of HRE-94 on cell viability of (A) LNCaP cells, (B) HepG2 cells, (C) A375 cells and (D) PNT2 cells after 48h.....	191
Figure 3.67: Effect of SSM extract on cell viability of (A) LNCaP cells, (B) PC-3M cells, (C) A375 cells, (D) HeLa cells, (E) PANC-1 cells and (F) HepG2 cells after 48 h.....	194
Figure 3.68: Effect of SSM extract on cell viability of normal cells (A) PNT2 cells and (B) HEKa cells after 48 h.....	195
Figure 3.69: Effect of SSM-56 on cell viability of (A) PANC-1 cells, (B) HepG2 cells, (C) PC-3M cells and (D) LNCaP cells after 48 h. ....	196

Figure 3.70: Effect of SSM on viability of (A) PANC-1 cells and (B) PNT2 cells after 48 h.....	198
Figure 3.71: Effect of SSM 56 on viability of (A) PANC-1 cells and (B) PNT2 cells after 48 h. ....	198
Figure 3.72: Effect of (A) 250µg/ml cisplatin and (B) staurosporine on cell viability of PANC-1 cells after 48 h. ....	199
Figure 3.73: Morphology of PANC-1 cells before and after treatment with SSM, SSM56 and staurosporine after 48 h. ....	200
Figure 3.74: Effect of (A) SSM extract and (B) SSM-56 on PANC-1 cell membrane integrity after 24 h. ....	202
Figure 3.75: Effect of (A) SSM extract, (B) SSM-56 and (C) 5µM staurosporine on PNT2 cell membrane integrity after 24 h.....	203
Figure 3.76: Effect of (A) SSM extract and (B) SSM-56 on adhesion of PANC-1 cells coated plates of fibronectin, with BSA as a negative.....	206
Figure 3.77: Effect of (A) SSM extract (B) SSM-56 on adhesion of PANC-1 cells to a collagen IV coated plate, with BSA as a negative control. ....	207
Figure 3.78: Effect of (A) SSM extract and (B) SSM-56 on migration of PANC-1 cells. ....	209
Figure 3.79: Effect of (A) SSM and (B) SSM-56 on invasion of PANC-1 cells. ....	211
Figure 3.80: Effect of (A) SSM and (B) SSM-56 on PANC-1 cells by measuring viability, cytotoxicity and apoptosis.....	212
Figure 3.81: Effect of SSM extract and SSM-56 on PANC-1 cells with (A) ATP and (B) ADP level. ....	214
Figure 3.82: Shows the PANC-1 cells exhibiting green florescence with (A) SSM and red florescence with (B) SSM-56... ..	215
Figure 3.83: Z factor for PTP1B inhibition assay. ....	217
Figure 3.84: Effect of TFMS inhibitor on PTP1B enzyme in the presence of DiFMUP	

substrate.....	217
Figure 3.85: Effect (A) <i>T. zanonii</i> (hexane, ethyl acetate crude methanol crude extracts) on PTP1B enzyme.....	219
Figure 3.86: The effect of (A) root and (B) aerial part of hexane crude extract of <i>A. cyrenaicum</i> on PTP1B enzyme. ....	221
Figure 3.87: The effect of (A) hexane and (B) EtOAc of crude extract of <i>H. radicata</i> on the PTP1B enzyme. ....	221
Figure 3.88: The effect of hexane crude extract of <i>T. zanonii</i> on the PTP1B enzyme. ....	222
Figure 3.89: Z factor for $\alpha$ -glucosidase assay. ....	223
Figure 3.90: Effect of acarbose on the $\alpha$ -glucosidase assay in the presence of 4-nitrophenyl-glucopyranoside (substrate).....	224
Figure 3.91: Effect of <i>H. radicate</i> from hexane, ethyl acetate and methanol crude extract on the $\alpha$ -glucosidase enzyme. ....	225
Figure 3.92: The effect of the hexane extract of <i>H. radicate</i> on $\alpha$ -glucosidase enzyme. ....	226
Figure 3.93: High-throughput screening fitness for $\alpha$ -amylase assay using 4-nitrophenyl- $\alpha$ -D-maltohexaside as substrate and $\alpha$ -amylase enzyme.....	227
Figure 3.94: Effect of acarbose on $\alpha$ -amylase enzyme in the presence of 4- nitrophenyl- $\alpha$ -D-maltohexaside substrate.....	227

## List of Tables

Table 1.1: Some natural products: currently used, originally derived from plants and their clinical use .....	2
Table 1.2: Some anticancer compounds: currently used, originally derived from plants. ....	10
Table 1.3: Some anti-diabetic compounds isolated from various plant species .....	15
Table 1.4: Selection of phytochemicals previously isolated from <i>Arum</i> . AM: refers to the name of the plant <i>Arum cyrenaicum</i> .....	24
Table 1.5: Selection of phytochemicals previously isolated from <i>P.tortuosus</i> PT: refers to the name of the plant <i>tortuosus</i> .....	30
Table 1.6: Selection of phytochemicals previously isolated from <i>T. zanonii</i> . T: refers to the name of the plant <i>Teucrium</i> .....	36
Table 1.7: Selection of phytochemicals previously isolated from Asteraceae. HR: refers to the name of the <i>H. radicata</i> . ....	45
Table 1.8: Selection of phytochemicals previously isolated from <i>S.sodomaicum</i> . SS: refers to the name of the plant <i>Solanum</i> .....	54
Table 2.1: Collection details of plants and amount used in the study .....	62
Table 2.2: Cell culture media of the cell lines used in this study .....	69
Table 3.1: Yields of solvent extractions .....	84
Table 3.2: <sup>1</sup> H (400MHz), <sup>13</sup> C (100MHz), and HMBC data of ARE-6-6 in DMSO- <i>d</i> <sub>6</sub> . ....	86
Table 3.3: <sup>1</sup> H (500MHz), <sup>13</sup> C (100MHz), and HMBC data of ARE-6-18 in DMSO- <i>d</i> <sub>6</sub> . ....	90
Table 3.4: <sup>1</sup> H (400MHz), <sup>13</sup> C (100MHz), and HMBC data of PTM-1 in DMSO- <i>d</i> <sub>6</sub> . ....	95
Table 3.5: <sup>1</sup> H (400MHz), <sup>13</sup> C (100MHz), and HMBC data of PTH 6-7 in CDCl <sub>3</sub> ... ..	100
Table 3.6: <sup>1</sup> H (400MHz), <sup>13</sup> C (100MHz), and HMBC data of TZH-103-117-9 in CDCl <sub>3</sub> . ....	104

Table 3.7: $^1\text{H}$ (400MHz), $^{13}\text{C}$ (100MHz), and HMBC data of TZH-150-170-7 in $\text{CDCl}_3$ . .....	110
Table 3.8: $^1\text{H}$ (500MHz), $^{13}\text{C}$ (100MHz), HMBC data of TZM-24 in $\text{DMSO-}d_6$ ....	116
Table 3.9: $^1\text{H}$ (500MHz), $^{13}\text{C}$ (100MHz), and HMBC data of TZH-68 in $\text{CDCl}_3$ ...	123
Table 3.10: $^1\text{H}$ (500MHz), $^{13}\text{C}$ (100MHz), and HMBC data of TZH-41-49 in $\text{CDCl}_3$ . .....	130
Table 3.11: $^1\text{H}$ (400MHz), $^{13}\text{C}$ (100MHz), and HMBC data of HRE-21 in $\text{Acetone-}d_6$ . .....	135
Table 3.12: $^1\text{H}$ (400MHz), $^{13}\text{C}$ (100MHz), and HMBC data of HRM-50-59 in $\text{DMSO-}d_6$ . .....	140
Table 3.13: $^1\text{H}$ (400MHz), $^{13}\text{C}$ (100MHz), and HMBC data of of HRE-94 in $\text{CDCl}_3$ . .....	146
Table 3.14: $^1\text{H}$ (400MHz), $^{13}\text{C}$ (100MHz), and HMBC data of HRE-121 in $\text{Acetone-}d_6^*$ . .....	151
Table 3.15: $^1\text{H}$ (500MHz), $^{13}\text{C}$ (100MHz), and HMBC data of SSM-30-2 in $\text{DMSO-}d_6$ . .....	156
Table 3.16: $^1\text{H}$ (400MHz), $^{13}\text{C}$ (100MHz), and HMBC data of SSM-56 in $\text{DMSO-}d_6$ . .....	165
Table 3.17: $\text{IC}_{50}$ of 50% DSMO on normal and cancer cell lines. ....	171
Table 3.18: Summary of $\text{IC}_{50}$ of <i>A. cyrenaicum</i> extracts and compounds on each cell line.....	175
Table 3.19: Summary of $\text{IC}_{50}$ of <i>P. tortuosus</i> extracts and compounds on each cell line. .....	177
Table 3.20: Summary of $\text{IC}_{50}$ of <i>T. zanonii</i> extracts and compounds on each cell line.. .....	181
Table 3.21: Summary $\text{IC}_{50}$ of cytotoxicity of <i>H. radicata</i> extracts and compounds on each cell line.....	186

Table 3.22: Summary IC <sub>50</sub> of cytotoxicity of <i>S. sodomaeum</i> extracts and compounds on each cell line.....	193
Table 4.1: Cytotoxicity activity of <i>T. zanonii</i> extracts and other species of <i>Teucrium</i> on different cancer cell lines. ....	239
Table 4.2: Selected of mechanism of action of SSM-56 on tumour cell lines. ....	248
Table 4.3: Cytotoxic activity of SSM-30-2 on human tumour cell lines.....	250
Table 4.4: Summary of the cytotoxicity effects of crude extracts and their constituents from the plants in this study.....	260

## List of Schemes

Scheme 1	Isolation of compounds from the extracts of <i>Arum Cyrenaicum</i>	304
Scheme 2	Isolation of compounds from the extracts of <i>Pituranthos tortuosus</i>	305
Scheme 3	Isolation of compounds from the extracts of <i>Teucrium zanonii</i>	306
Scheme 4	Isolation of compounds from the extracts of <i>Hypochaeris radicata</i>	307
Scheme 5	Isolation of compounds from the extracts of <i>Solanum sodomaeum</i>	308

# **Chapter 1**

## ***Introduction***

## 1.1 Herbal medicine

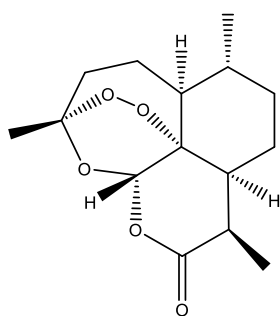
Plants have been used as medicine for centuries and still remain the main source of new drugs. According to the World Health Organization (WHO), about 65% of the world's population and 80% of developing countries depend primarily on 85% of plant-derived traditional medicine (Cragg and Newman, 2013, Ekor, 2014). The WHO reported that the use of herbal remedies throughout the world exceeds that of conventional drugs by two to three times (Pal and Shukla, 2003). The demand for herbal medicines has increased, with over 800 plants being used in indigenous medicine (Sheng-Ji, 2001). The use of herbal medicine is common because they are inexpensive and there is a belief that they have fewer side effects (Wachtel-Galor and Benzie, 2011).

Natural products and their derivatives represent over 50% of all drugs clinically used worldwide (Kingston, 2011) where natural products from medicinal plants contribute 25% of the total drugs (Balandrin *et al.*, 1993; Gurib-Fakim, 2006). Natural products and related drugs are reported for use as antibacterials, anticancer, antiparasitic and antidiabetic agents (Newman and Cragg, 2016a). For example, 49% of anticancer drugs introduced into the market were derived from natural products (Xiong *et al.*, 2013; Newman and Cragg, 2016b). More than 100 new products particularly anticancer agents and anti-infectives are derived from natural products (Harvey, 2008; Newman and Cragg, 2016a).

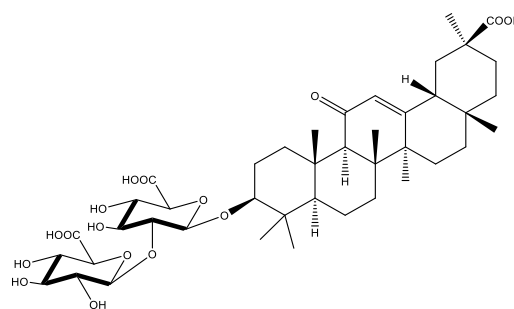
Natural products can also serve as pharmacological tools, such as digoxin from foxglove has been shown to have a role in the sodium-potassium-ATPase pump in humans, while muscarine, nicotine and tubocurarine have helped to identify different types of acetylcholine receptors (Harvey, 2008). Some examples of drugs, derived from plants, are shown in Table 1.1 and their structures in Figure 1.

**Table 1.1:** Some natural products: currently used, originally derived from plants and their clinical use (Lohar *et al.*, 1979; De Abreu *et al.*, 2005; Pi *et al.*, 2005; Dias *et al.*, 2012; Sharma and Purkait, 2012; Fachini-Queiroz *et al.*, 2012; Alizadeh *et al.*, 2014; Lobay, 2015; Oliveira *et al.*, 2015; Chamikara *et al.*, 2016; Iqbal *et al.*, 2017; Black, 2017).

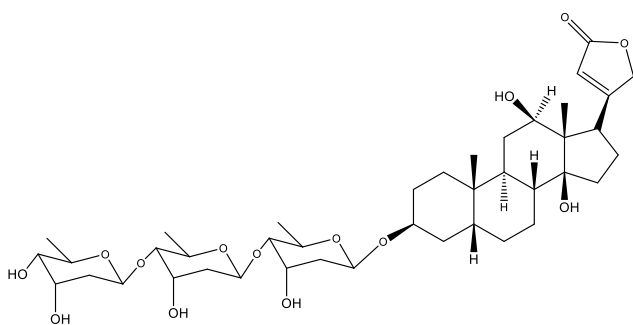
<b>Drug</b>	<b>Plant</b>	<b>Activity</b>
Artemisinin (1)	<i>Artemisia annua</i> plant (qinghao, sweet worm wood)	Antimalarial
Glycyrrhizin (2)	<i>Glycyrrhiza glabra</i> roots	Used as a sweetener; Addison's disease
Digoxin (3)	<i>Digitalis purpurea</i> leaves	Treatment atrial fibrillation and congestive heart failure (CHF)
Colchicine (4)	<i>Colchicum autumnale</i> plant	Arthritis, cirrhosis and gout
Capsaicin (5)	Red pepper (genus <i>Capsicum</i> ) fruits	Anticancer and antimutagenic
Morphine (6)	Opium poppy ( <i>Papaver somniferum</i> )	Analgesic and pain relievers
Hyoscyamine (7)	<i>Hyoscyamus niger</i> leaves	Anticholinergic
Quinine (8)	<i>Cinchona succirubra</i> bark	Antimalarial
Pilocarpine (9)	<i>Pilocarpus microphyllus</i> leaves	Treatment of chronic open- angle glaucoma and acute angle-closure glaucoma
Salicylic acid (10)	<i>Salix alba</i> plant	Analgesic and a prophylactic antithrombic agent
Reserpine (11)	<i>Rauwolfia serpentine</i> roots	Antihypertensive and tranquilizer
Papavarine (12)	<i>Papaver somniferum</i> seeds	Smooth muscle relaxant
Thymol (13)	<i>Thymus vulgaris</i> (thyme) herb	Topical antifungal
Sennosides A (14)	<i>Cassia acutifolia</i> leaves	Laxative
Theophylline (15)	<i>Theobroma cacao</i> seeds	Diuretic and bronchodilator



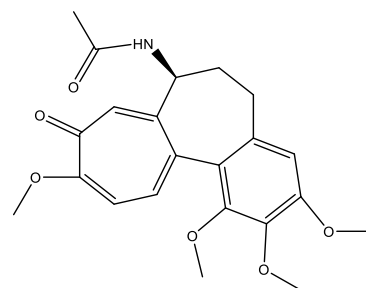
**Artemisinin (1)**



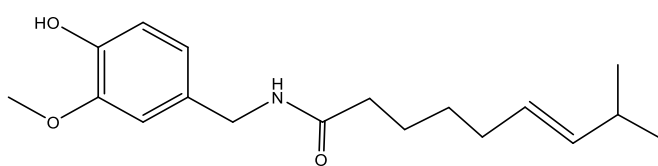
**Glycyrrhizin (2)**



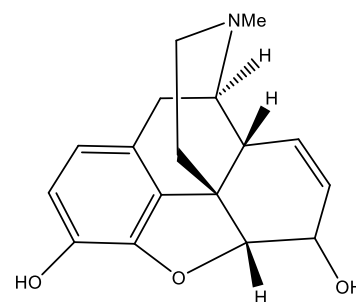
**Digoxin (3)**



**Colchicine (4)**

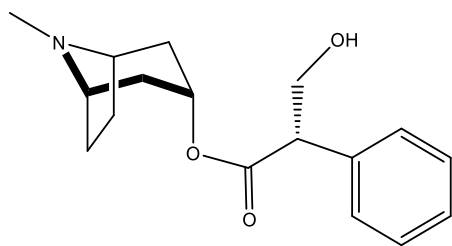


**Capsaicin (5)**

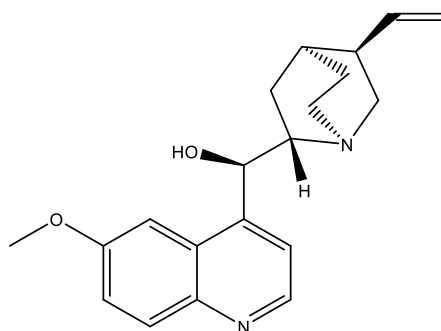


**Morphine (6)**

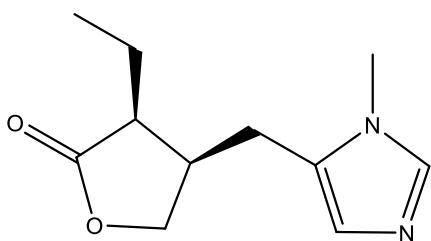
**Figure 1.1:** Examples of some therapeutic agents from plants.



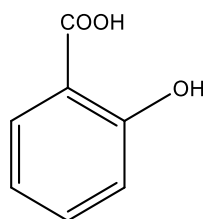
**Hyoscyamine (7)**



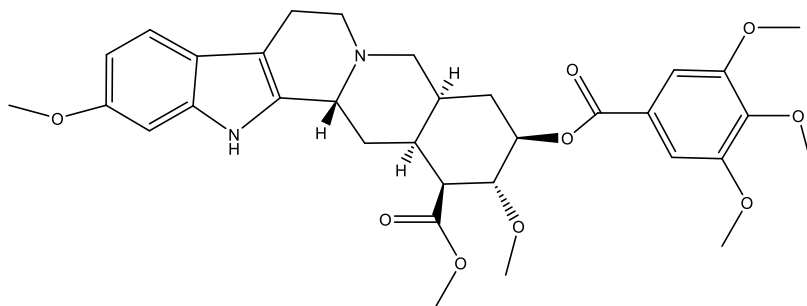
**Quinine (8)**



**Pilocarpine (9)**

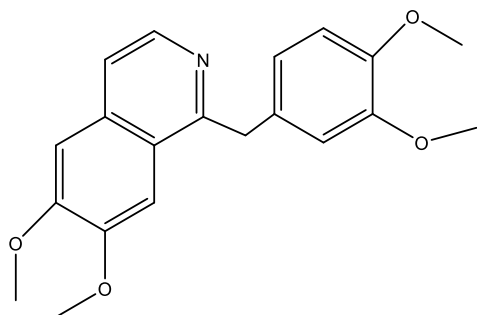


**Salicylic acid (10)**

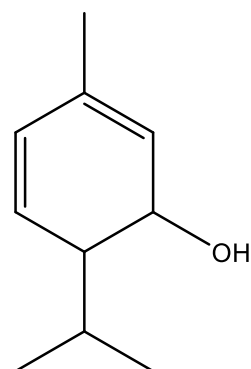


**Reserpine (11)**

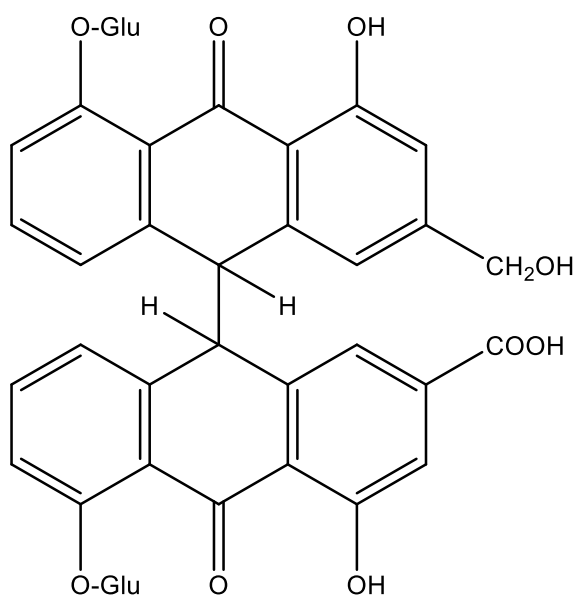
**Figure 1.1(continued):** Examples of some therapeutic agents from plants.



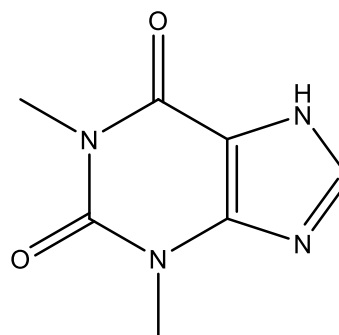
**Papaverine (12)**



**Thymol (13)**



**Sennoside A (14)**



**Theophylline (15)**

**Figure 1.1(continued):** Examples of some therapeutic agents from plants.

The present research focussed on the use of some medicinal plants in cancer and diabetes. Worldwide, many plants have a long history of traditional use for the treatment of cancer and diabetes

## 1.2 Review of cancer and diabetes

Cancer and diabetes are common diseases with significant impact on health worldwide (Giovannucci *et al.*, 2010). Globally, cancer is the second and diabetes is the twelfth leading cause of death. In the U.S., cancer is the second and diabetes is the seventh leading cause of death (Giovannucci *et al.*, 2010; Zaorsky *et al.*, 2017). Currently, about 8%–18% of all cancer patients also have pre-existing diabetes (Barone *et al.*, 2010). More recently, the results of several studies have shown that some cancers develop more commonly in patients with diabetes (predominantly type 2); the relative risks imparted by diabetes are greatest (about twofold or higher) for cancers of the liver, pancreas, and endometrium, while cancer mortality is moderately increased in diabetic patients (Vigneri *et al.*, 2009).

A study reported that the antidiabetic drug metformin inhibited cell proliferation, reduced colony formation, and caused partial cell cycle arrest in MCF-7, BT-474, and SKBR-3 human breast cancer cells (Zakikhani *et al.*, 2006; Liu *et al.*, 2009; Alimova *et al.*, 2009; Nguyen *et al.*, 2012). It has also been shown that the anticancer molecular activity of metformin is mainly associated with the inhibition of the mammalian target of rapamycin complex 1 (mTORC1). The mTOR pathway plays an essential role in metabolism, growth and proliferation of cancer cell. Metformin is supposed to inhibit mTORC1 pathway. The inhibition of mTOR pathway by metformin proceeds dependent and independent on AMP-activated protein kinase (AMPK) activation (Kasznicki *et al.*, 2014). AMPK is activated by the phosphorylation of liver kinase B1 (LKB1), a tumour suppressor, at threonine-172 within the catalytic subunit (alpha) of AMPK (Thr172), and anabolic and catabolic pathways are subsequently inhibited and activated, respectively (Yu *et al.*, 2017; Pernicova and Korbonits, 2014). In particular, AMPK activation inhibits the mTOR pathway via the phosphorylation of tuberous sclerosis 1 and 2 (TSC1/2), tumour suppressors that negatively regulate mTOR

(Pernicova and Korbonits, 2014). Metformin-mediated activation of AMPK also leads to activation of p53, a tumor suppressor that promotes apoptosis, autophagy and inhibition of the protein kinase B (Akt) and mTOR pathways (Pernicova and Korbonits, 2014). Furthermore, AMPK activation can inhibit receptor tyrosine kinase pathways, including epidermal growth factor receptor (EGFR) and ErbB2 signaling, which further target the downstream effectors Akt, mTOR, and extracellular signal-regulated kinase (Erk) (Zhang and Guo, 2016). It also inhibits the mTOR pathway in an AMPK-independent manner by inactivating Rag GTPases (it is a GTPase-activating protein for Rag subunits A/B) (Kalender *et al.*, 2010) or by upregulating the expression of regulated in development and DNA damage responses 1 (REDD1), a negative regulator of mTOR (Ben Sahra *et al.*, 2011; Yu *et al.*, 2017). mTOR inhibition further suppresses downstream targets, including 4EBPs, pS6Ks, and initiation factor eukaryotic translation initiation factor 4 G (eIF4G) (Dowling *et al.*, 2012). mTOR is also a critical mediator of the PI3K signaling pathway, which is involved in cellular growth and survival (Yu *et al.*, 2017). Thus, metformin restricts cancer cell proliferation by inhibiting protein translation via (phosphatidylinositol-4,5-bisphosphate 3-kinase) (PI3K)/Akt/mTOR pathways (Evans *et al.*, 2005).

### **1.2.1 Cancer**

In the last 20 years, numerous factors, such as overweight, obesity, type 2 diabetes (T2D), oestrogen and testosterone imbalance and chronic inflammation have been identified as enabling cancers to develop (Shikata *et al.*, 2013). Normal cells develop into cancerous cells through a complex process, including initiation (DNA damage from a carcinogen or reactive molecule), promotion (stimulation of initiated cells' growth), and progression (more aggressive growth with angiogenesis and metastasis) (Collins, 2014).

Cancer is defined as the uncontrolled growth of abnormal cells, which results from alterations in deoxyribonucleic acid (DNA). These alterations change genetic information and prevent the proper function of normal cells, leading them to divide without stopping and spreading to surrounding tissues (Almeida and Barry, 2011). Serious implications may result if the tumour begins to spread (metastasise) throughout the body. Globally, the WHO reported that in 2016, there were 14 million new cases and 6.2 million deaths worldwide and it is expected that these figures will rise to 22 million new cases within the two next decades (Jacques *et al.*, 2015; McGuire, 2016). Two factors cause cancer: internal factors such as genes that control basic cell function such as hormones, immune conditions, mutation for metabolism and they grow and divide are altered or mutated. These genetic changes can be inherited or modified by external environmental factors such smoking, poor diet, physical inactivity, radiation, infectious organism and ultraviolet rays from the sun (Vineis and Wild, 2014; Freddie *et al.*, 2015).

In addition, cancer is fundamentally a disease of tissue growth regulation. In order for a normal cell to transform into a cancer cell, the genes that regulate cell growth and differentiation must be altered. The affected three main groups of genes, including proto-oncogenes, tumour suppressor genes, and DNA repair genes, which are also called the drivers of cancer. Proto-oncogenes play an important role in regulating cell growth and division in normal cells, but in cancer cells they are altered or activated to become cancer causing genes (oncogenes). Tumour suppressor genes control cell growth and division in normal cells, whereas in cancer cells these genes are mutated, leading to dysregulated and uncontrolled cell division. DNA repair genes are involved in the repair of damaged DNA in normal cells, but these genes are altered in cancer, leading to the development of other mutations, ending up causing the cells to become cancerous. These genes are important in the fidelity of DNA replication, assuring

normal cell growth and division. Furthermore, including uncontrolled growth of cells, loss of cell differentiation, ability to ignore signals involved in normal cell growth and death, and the capability to influence normal cells, molecules, and blood vessels to supply the tumour with oxygen and nutrients (microenvironment) can include the presence of disruptive substances called carcinogens, changes in multiple genes are required to transform a normal cell into a cancer cell (Hejmadi, 2009).

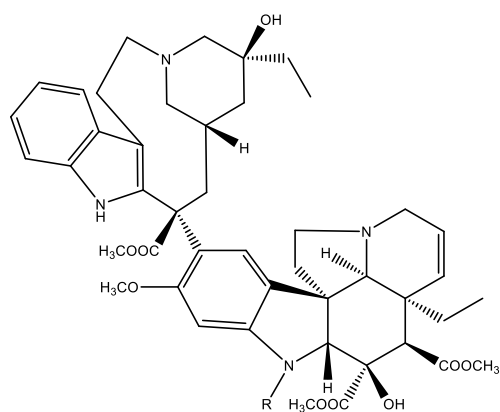
### **1.2.2 Cancer and herbal medicine**

Over the centuries, many medicinal herbs have been used for the prevention and treatment of cancer (Mans *et al.*, 2000). Around 47% of antitumour and antiinfectious drugs on the market are from natural origin under clinical trials and the numbers of new anticancer drugs are increasing (Newman and Cragg, 2007; Newman and Cragg, 2012). It is presumed that natural compounds are safer than synthetic compounds because of their presence in diet, wide availability, low cost and tolerability (Gullett *et al.*, 2010). Many studies have demonstrated the anti-tumour properties of products isolated from plant sources such as *Camellia sinensis* (green tea), which is the most common drink used in the world. It has a distinctive group of polyphenols called catechins (epigallocatechin-3-gallate (EGCG), epigallocatechin (EGC), epicatechin-3-gallate (ECG), and epicatechin (EC). Green tea has been shown to suppress cell growth and kill cancer after distinguishing tumour cells from normal cells (Kaur and Verma, 2015). Studies found that topical application or oral administration of green tea in mice prevents skin tumour development, and this prevention is mediated, through rapid repair of DNA through the induction of interleukin (IL)-12 in particular anti-non-melanoma skin cancer (Wang *et al.*, 1992; Katiyar, 2011; Cao *et al.*, 2016), invasion and metastasis in B16-F3m melanomas (Liu *et al.*, 2001). Many studies suggest that people who drink more green tea have a lower risk of prostate (Heilbrun *et al.*, 1986) and breast cancers (Inoue *et al.*, 2001). Many current anticancer agents are

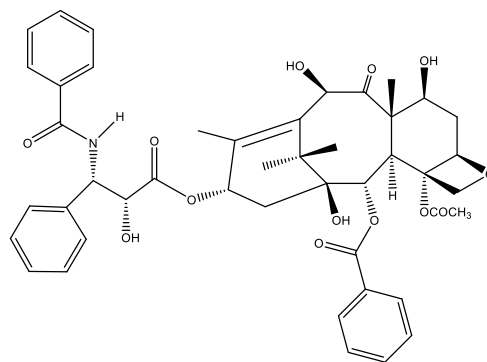
phytochemicals or derivatives such as paclitaxel (Taxol) and artemisinin. Synthetic compounds include etoposide, teniposide derived from podophyllotoxin, navelbine from vinblastine and vincristine, and topotecan and irinotecan from camptothecin (da Rocha *et al.*, 2001; Cragg and Newman, 2005; Dholwani *et al.*, 2008). Examples of drugs, with anticancer activity derived from plant sources that are currently in use, are shown in Table 1.2 and their structures in Figure 2.

**Table 1.2:** Some anticancer compounds: currently used, originally derived from plants.(Endo *et al.*, 1987; Van Uden *et al.*, 1995; Gupta *et al.*, 2005; Zou and Zhan, 2005; Leonelli *et al.*, 2008; Fulda, 2008; Zu *et al.*, 2011; Stiborova *et al.*, 2011; Prakash *et al.*, 2013; Larsson and Ronsted, 2014; Liang *et al.*, 2016).

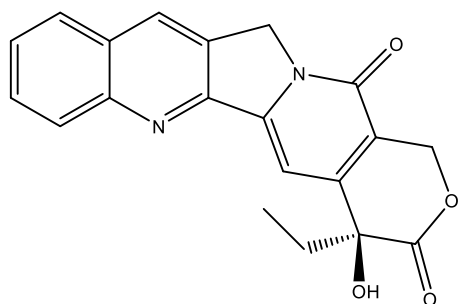
<b>Drug</b>	<b>Plant</b>	<b>Activity</b>
Vincristine and vinblastine (1)	The periwinkle plant ( <i>Catharanthus roseus</i> )	Cytotoxic agents used in cancer chemotherapy, particularly in leukaemia
Paclitaxel (2)	Bark of the Pacific Yew tree ( <i>Taxus brevifolia</i> )	Treatment of breast, ovarian and lung cancer
Camptothecin (3)	Bark and stems of <i>Camptotheca acuminata</i>	Gastric, rectal, colon, bladder ovarian and cervical cancer
Ellipticine (4)		antitumour (antineoplastic agent) and anti-HIV activities
Podophyllotoxin (5)	Rhizomes of <i>Podophyllum hexandrum</i>	Treatment of testicular teratoma, Hodgkin`s , non-Hodgkin`s lymphoma and small-cell cancer
Ricin (from castor beans)	Whole plant <i>Ricinus communis</i>	Treatment of metastatic melanoma and colon cancer
Betulinic acid (6)	Whole plant <i>Ziziphus mauritiana</i>	Treatment of melanoma
Combretastatin (7)	Bark of <i>Combretum caffrum</i>	Treatment of bladder and thyroid cancer



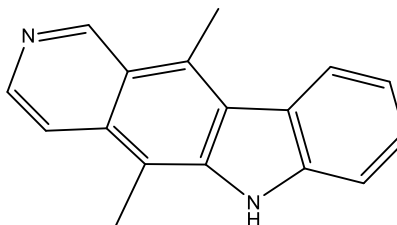
**Vincristine R = CHO (1)**  
**Vinblastine R = Me**



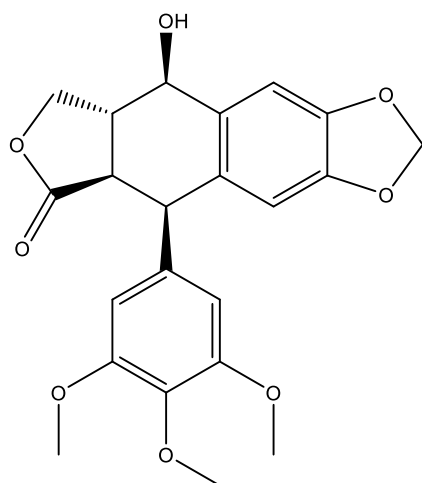
**Paclitaxel (2)**



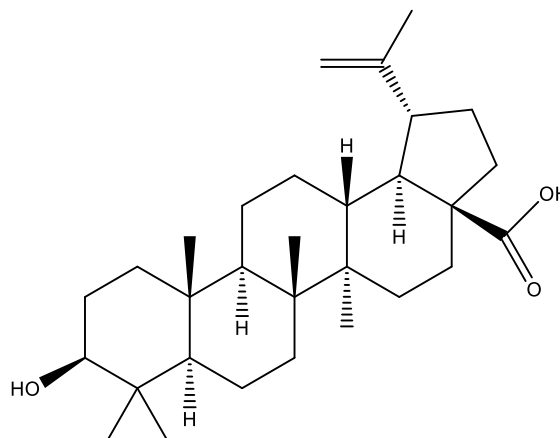
**Camptothecin (3)**



**Ellipticine (4)**

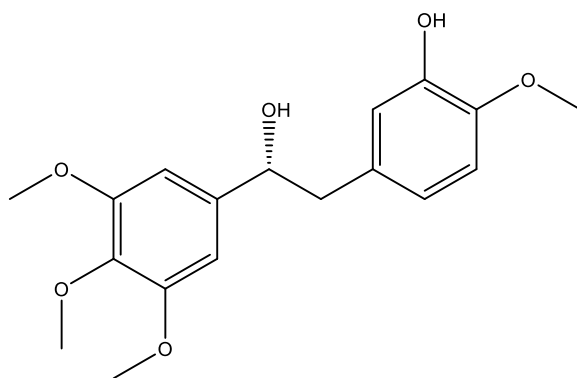


**Podophyllotoxin (5)**



**Betulinic acid (6)**

**Figure 1.2:** Examples of some anticancer agents from plants.



**Combretastatin (7)**

**Figure 1.2 (continued):** Examples of some anticancer agents from plants.

### 1.3 Diabetes mellitus

Diabetes mellitus is a metabolic disorder characterised by a loss of glucose homeostasis with disturbances of carbohydrate, fat and protein metabolism resulting from defects in insulin secretion, insulin action, or both. There are two main forms of diabetes mellitus; type 1 and type 2 (Shouip, 2014). Type 1 diabetes (T1D), also known as insulin dependent diabetes (IDDM), is due to an inadequate insulin secretion resulting from a large decrease in the number of beta-cells in the islets of Langerhans and Type 2 diabetes (T2D), or non-insulin dependent diabetes mellitus (NIDDM), is due to a lack of insulin action in target tissues and/or insulin resistance that leads to impaired tissue glucose uptake and impaired suppression of hepatic glucose production (Olokoba *et al.*, 2012; Gregory *et al.*, 2013).

IDDM is usually treated by injection of insulin and NIDDM may be controlled by dietary means such as weight loss and restricted diet; however, around 50% of NIDDM patients cannot achieve satisfactory control through diet alone and require treatment

with a class of drugs collectively referred to as oral hypoglycaemic agents (Moore *et al.*, 2004; Olokoba *et al.*, 2012).

Diabetes is the third leading cause of morbidity and mortality, after heart attacks and cancer (Bharti *et al.*, 2018) and it is estimated that 25% of the world's population is affected by this disease (Arumugam *et al.*, 2013). In addition to hyperglycemia, diabetes also causes many complications, such as hyperlipidemia, hyperinsulinemia, hypertension and atherosclerosis (Babu *et al.*, 2007).

### **1.3.1 Diabetes and Herbal Medicine**

Plants have been used in treatment of diabetes mellitus all over the world for many years (Kooti *et al.*, 2016). Several plant species have been used as hypoglycaemic agents such as *Aloe vera*, *Allium cepa* (Onion) and *Allium sativum* (Garlic) *Cinnamomum cassie*, *Citrullus colocynthis*, *Ficus bengalensis*, *Gymnema sylvestre*, *Momordica charantia* (Bitter Melon), *Opuntia streptacantha*, *Polygala senega*, *Trigonella foenum graecum* (Fenugreek), (Patel *et al.*, 2012).

In Mediterranean regions, *Artemisia herba-alba*, *Teucrium polium*, *Coriandrum sativum* and *Rosmarinus officinalis* are plants widely used in traditional medicine for the treatment of diabetes (Eddouks *et al.*, 2002; Mandal and Mandal, 2015).

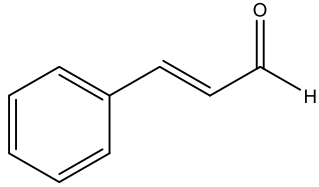
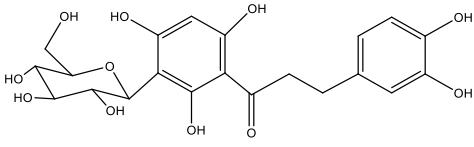
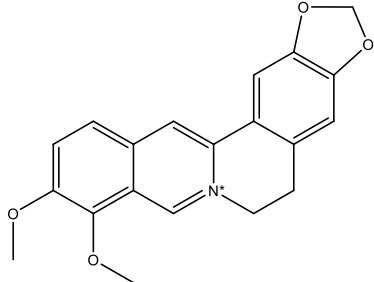
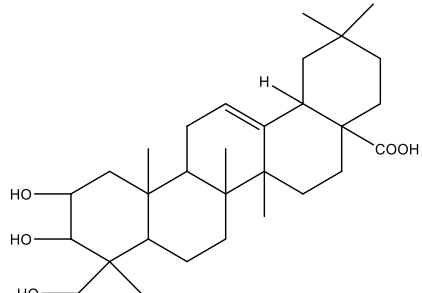
Compounds isolated for treatment of diabetes include alkaloids, glycosides, galactomannan, gum, peptidoglycan, glycopeptide, amino acids and inorganic ions (Shukia *et al.*, 2000). Around 1200 species of plants have been investigated in the therapy of diabetes mellitus (Marles and Farnsworth, 1995). Metformin is the only drug approved for treatment of NIDDM derived from a medicinal plant, galegine and

guanidine isolated from *Galega officinalis*, which is used as a substrate for the synthesis of biguanides and metformin (Mooney *et al.*, 2008).

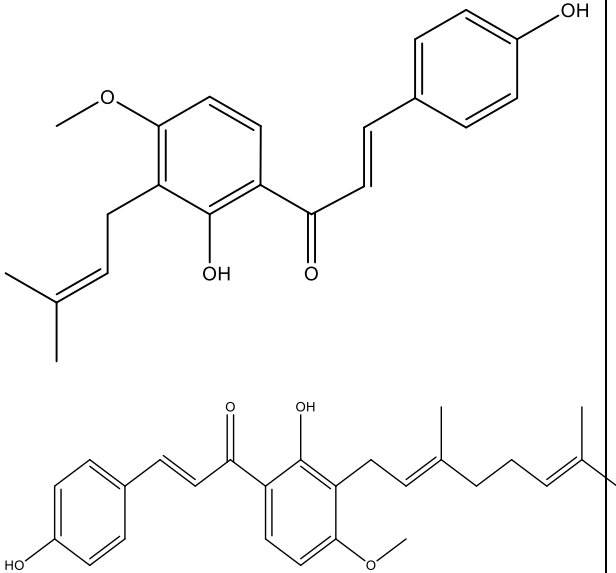
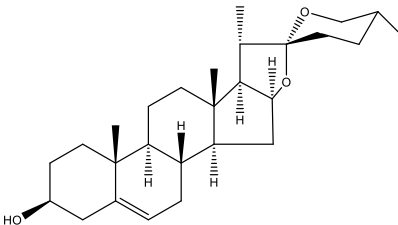
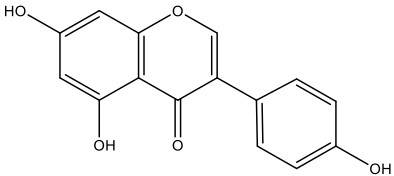
A number of medicinal plants and herbs have been studied for their hypoglycaemic potential using experimental animal models of diabetes (Ali *et al.*, 2000; Basch *et al.*, 2003; Ribnicky *et al.*, 2006; Wani and Kumar, 2018;). It has been found that fagasterol from *Phyllanthus emblica* leaves reduced blood glucose in alloxan-induced hyperglycemic mice; ginsenoside from *Panax ginseng* leaves had a hypoglycemic effect in rats in streptozotocin (STZ)-induced diabetes. Another example comes from polyhydroxylated triterpenoids from *Eriobotrya japonica* leaves, which produced marked inhibition of glycosuria and reduced blood glucose levels in normoglycemic rats (Perez *et al.*, 1998). In Mediterranean countries, *Teucrium polium* has been used by people to treat T2D, due to its terpenoids and flavonoids content (Sabet *et al.*, 2013).

*Brassica juncea* aqueous seed extract with doses 250, 350, 450 mg/kg had a potent hypoglycemic activity in STZ-induced diabetic male albino rats. In addition, consumption of the methanolic extract bark of *Albizia odoratissima* showed significantly reduced levels of serum cholesterol, triglycerides, serum glutamic-oxaloacetic transaminase (SGOT), serum glutamic pyruvic transaminase, (SGPT), alkaline phosphatase and of total proteins in alloxan-induced albino mice (Arumugam *et al.*, 2013). Examples of drugs, with antidiabetic use derived from plants, are shown in Table 1.3.

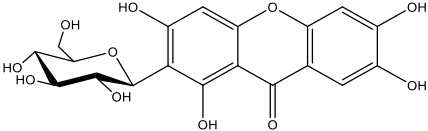
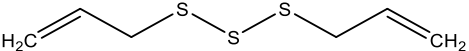
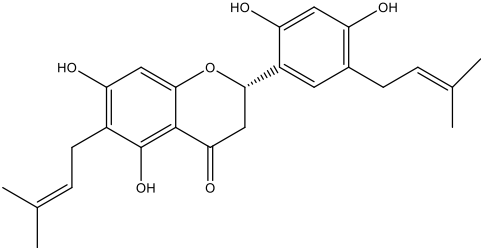
**Table 1.3:** Some anti-diabetic compounds isolated from various plant species

Compound (Plant name)	Biological activity	Reference
<p><b>Cinnamaldehyde</b> (<i>Cinnamomum zeylanicum</i> bark) (cinnamon)</p> 	<p>Decreases glycosylated haemoglobin (HbA1C) and improved lipid profile in an STZ-induced diabetic rat model</p>	<p>(Subash Babu <i>et al.</i>, 2007; Al-Bayati and Mohammed, 2009)</p>
<p><b>Aspalathin</b> (<i>Aspalathus linearis</i> plant) herbal tea</p> 	<p>Increases glucose uptake in a dose-dependent manner, and increases insulin secretion from cultured RIN-5F cells in <i>db/db</i> mice</p>	<p>(Kamakura <i>et al.</i>, 2015)</p>
<p><b>Berberine</b> (<i>Coptis chinensis</i> herb)</p> 	<p>Regulates glucose and lipid metabolism <i>in vitro</i> and <i>in vivo</i>, and decreases haemoglobin A1c</p>	<p>(Yin <i>et al.</i>, 2008; Osadebe <i>et al.</i>, 2014;)</p>
<p><b>Arjunolic acid</b> (<i>Terminalia arjuna</i> wood)</p> 	<p>Inhibits <math>\alpha</math>-amylase and <math>\alpha</math>-glucosidase activity</p>	<p>( Ramesh <i>et al.</i>, 2012; Elekofehinti, 2015)</p>

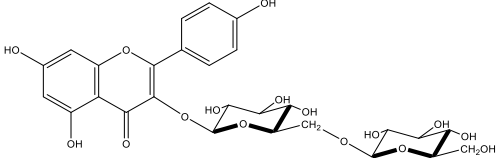
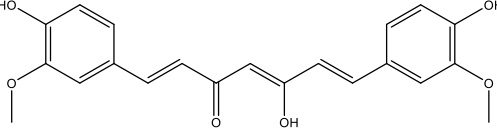
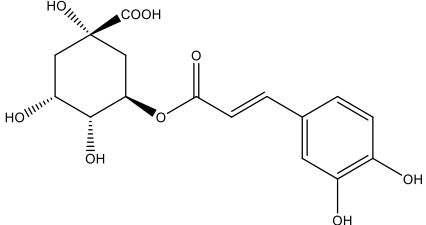
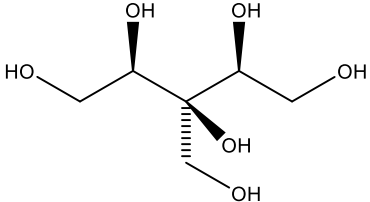
**Table 1.3 (continued):** anti-diabetic compounds isolated from various plant species

Compound (Plant name)	Biological activity	Reference
<p><b>4-Hydroxyderricin and xanthoangelol</b> (<i>Angelica keiskei</i> stems)</p> 	<p>Insulin like activities via a pathway independent of the peroxisome proliferator-activated receptor-<math>\gamma</math> (PPAR-<math>\gamma</math>) activation</p>	<p>( Tabata <i>et al.</i>, 2005; Enoki <i>et al.</i>, 2007)</p>
<p><b>Diosgenin</b> (<i>Trigonella foenum-graecum</i> seeds)</p> 	<p>Inhibits carbohydrate digestion/absorption</p>	<p>(Elekofehint i, 2015)</p>
<p><b>Genistein</b> (<i>Genista tinctoria</i> flowers)</p> 	<p><math>\alpha</math>-Amylase and <math>\alpha</math>-glucosidase inhibitors</p>	<p>(Gilbert and Liu, 2013)</p>

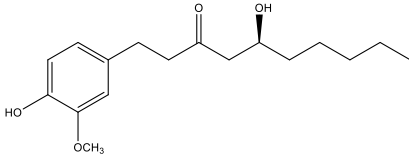
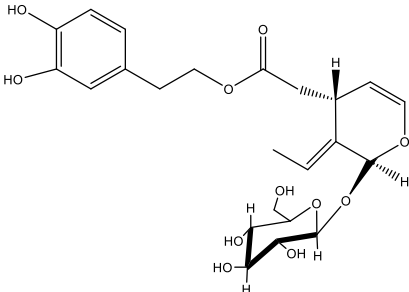
**Table 1.3 (continued):** anti-diabetic compounds isolated from various plant species

Compound (Plant name)	Biological activity	Reference
<p><b>Mangiferin</b> (<i>Mangifera indica</i> leaves mango)</p> 	<p>Inhibits glomerular extracellular matrix expansion and transforming growth factor-beta 1 overexpression in glomeruli of a diabetic nephropathy rat model</p>	<p>(Muruganandan <i>et al.</i>, 2005; Li <i>et al.</i>, 2010b; Matkowski <i>et al.</i>, 2013; )</p>
<p><b>Allitridin</b> (Diallyl trisulfide (DATS) produced by the hydrolysis of alliin, <i>Allium sativum</i> leaves and bulbs (Garlic))</p> 	<p>Stimulates <i>in vitro</i> insulin secretion, inhibits glucose production by the liver</p>	<p>(Liu <i>et al.</i>, 2005)</p>
<p><b>Cudraflavanone D</b> (<i>Cudrania tricuspidata</i> roots)</p> 	<p>Inhibits PTP1B</p>	<p>(Quang <i>et al.</i>, 2015)</p>

**Table 1.3 (continued):** anti-diabetic compounds isolated from various plant species

Compound (Plant name)	Biological activity	Reference
<p><b>Kaempferol 3-O- gentiobioside</b> (<i>Cassia alata</i> leaves)</p> 	<p><math>\alpha</math>-glucosidase inhibition</p>	<p>(Varghese <i>et al.</i>, 2013)</p>
<p><b>Curcumin</b> (<i>Curcuma longa</i> rhizomes, Turmeric)</p> 	<p>Reduces glycemia and hyperlipidemia in rodent models</p>	<p>(Zhang <i>et al.</i>, 2013; Seyed Fazel <i>et al.</i>, 2015)</p>
<p><b>Chlorogenic acid</b> (<i>Marrubium vulgare</i> herb)</p> 	<p>Improves glucose and lipid metabolism, via the activation of AMPK</p>	<p>(Ong <i>et al.</i>, 2013b; Ong <i>et al.</i>, 2013a)</p>
<p><b>3-Hydroxymethyl xylitol</b> (<i>Casearia esculenta</i> roots)</p> 	<p>Increases the level of hexose, hexosamine, and fucose in the liver and kidney of diabetic rats</p>	<p>(Govindasamy <i>et al.</i>, 2011; Wang <i>et al.</i>, 2013;)</p>

**Table 1.3 (continued):** anti-diabetic compounds isolated from various plant species

Compound (Plant name)	Biological activity	Reference
<b>Gingerol</b> ( <i>Zingiber officinale</i> roots, Ginger) 	Increases glucose uptake through promotion of GLUT4 translocation via AMPK activation in L6 myocytes	(Mahady <i>et al.</i> , 2003; Son <i>et al.</i> , 2015)
<b>Oleuropein</b> ( <i>Olea europaea</i> leaves, Olive) 	Antidiabetic due to their antioxidant activities preventing oxidative stress which is associated with diabetes	(Jemai <i>et al.</i> , 2009a; Jemai <i>et al.</i> , 2009b)

The purpose of this study was to investigate anticancer or antidiabetic activities in plants that are grown in Libya, which may contain compounds with significant cytotoxic effects on cancer or any hypoglycaemic effect.

#### 1.4 Herbal medicinal plant use in Libya

Libya has a remarkable wealth of medicinal plants, distributed all over an enormous area especially in the Al-jabal Al-akhdar region (Figure 1.3). Al-jabal Al-akhdar has a high diversity of plant species that show both economic and medicinal importance

(Aljaiyash *et al.*, 2014). Indigenous people in the region of the eastern Mediterranean coast of Libya tend to be dependent on medicinal plants and possess medicinal plant knowledge (El-Mokasabi, 2014).



(A)

(B)

**Figure 1.3:** (A) map showed the location of Libya and the major phytogeographical regions of the country: Tripolitania, Cyrenaica, Fezzan and (B) location Al-Jabal Al-Akhdar (The Green Mountain) region in Libya (Hegazy *et al.*, 2011).

### 1.4.1 *Arum cyrenaicum*

*A. cyrenaicum* (Figure 1.4) is locally known as renish belonging to the family Araceae, or the Arum family. The family is a large and monocotyledon, including the smallest known angiosperms and some of the largest vegetative and reproductive structures. Araceae comprises about 3800 species in 118 genera, mainly located in the tropics, but may range into temperate regions. The stems can be rhizomatous, cormose, tuberous or reduced to a thallus-like structure and leaves can be simple, highly divided or fenestrate. It is distinguished from other families by having a great diversity of calcium oxalate crystals such as raphides, possessing a spadix of small, bisexual or unisexual flowers, subtended by a spathe, and they lack ethereal oil cells ( Nauheimer *et al.*, 2012; Henriquez *et al.*, 2014). The collection of the plant materials was carried out by the Mr Adella-Salem (Botany Department, Benghazi University). A voucher specimen has been kept in Benghazi University herbarium.

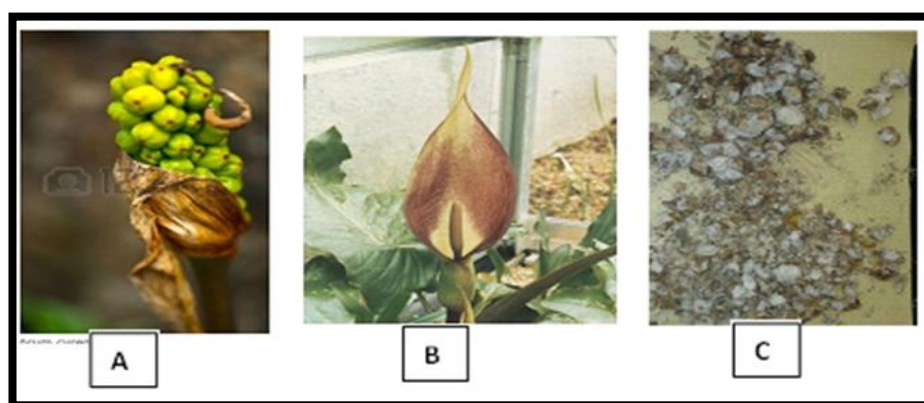


**Figure1.4:** (A) The fruit, (B) aerial part, (C) root of *Arum cyrenaicum* collected from Wadi Buoreequ, Libya.

#### 1.4.1.1 Traditional uses

It is used externally to cure dermal diseases, viral and bacterial infections, insect and animal bites, burns and sometimes for the treatment of hair problems. El-Mokasabi

(2014) has reported the use of *A. cyrenaicum* in folk medicine in treatment of dermatitis, psoriasis, corns, and bone spurs.

#### **1.4.1.2 Active ingredients and biological activities**

There are no scientific studies reporting any phytochemicals and medicinal activities for *A. cyrenaicum*.

The Araceae family is reported to produce valuable phytochemicals as summarised in Table 1.4. The family possess different activities such as antibacterial against *Escherichia coli*, *Bacillus subtilis*, *Staphylococcus aureus*, *Klebsiella pneumoniae* and *Pseudomonas aeruginosa*, antifungal activity against *Pichia guilliermondii*, anthelmintic, pesticidal, treatment of diarrhoea and other gastrointestinal disorders, antioxidant and anticancer activity (Perrett and Whitfield, 1995; Chan *et al.*, 2005; Mandal *et al.*, 2010; Roy *et al.*, 2013; Salako *et al.*, 2015; Pornprasertpol *et al.*, 2015).

##### **1.4.1.2.1 Antitumour activity**

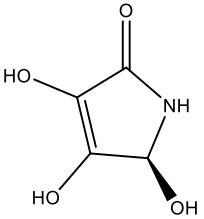
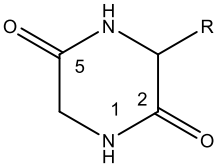
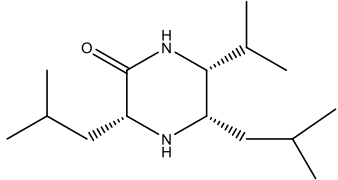
An aqueous methanol extract of *A. palaestinum* had strong antiproliferative activity against breast (MCF7), liver (HepG2), larynx (Hep2) and cervix (HeLa) cancer cell lines while the butanol fraction also revealed significant activity against MCF7 and HepG2 cancer cell lines and chrysoeriol-7-*O*-neohesperidoside showed moderate activity against Hep2 cells with an IC<sub>50</sub> value of 37.8 µM (Farid *et al.*, 2017). A study found that the ethyl acetate fraction of *A. palaestinum* had a dose-dependent suppression against the proliferation of breast (MCF-7) and leukemia (1301) cell lines with IC<sub>50</sub> of 59.01 and 53.1 µg/ml, respectively (El-Desouky *et al.*, 2007a). In addition, the ethyl acetate, methanol and chloroform extracts of *A. palaestinum* showed a dose-dependent reduction in cell proliferation against T cell lymphoblastic leukemia and Jurkat cells after 48 h, with IC<sub>50</sub> values of 17.5±2.1µg/ml, 19.7±2.8 µg/ml and 23.3±2.8 µg/ml, respectively (Diab-Assaf *et al.*, 2012). An aqueous boiled extract of

*A. Palaestinum* (leaves) showed variable activity on mouse myoblasts (C2C12), embryo tissue (3T3-L1) and cervix (HeLa) cell lines. Piperazirum (AM-4) is an alkaloid from *A. palaestinum*, reported to show significant inhibition on non-small cell lung (A549), ovary (SK-OV-3), melanoma (SK-MEL-2) and colon (HCT-15) cancer cell lines (El-Desouky *et al.*, 2007b).

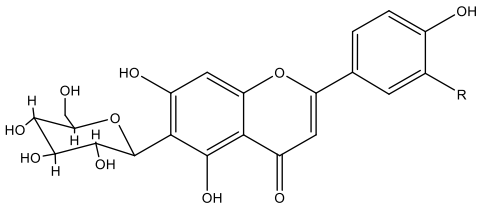
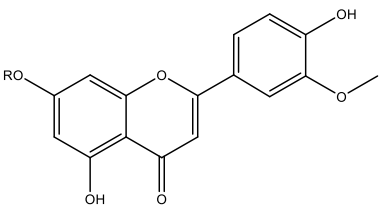
#### **1.4.1.2.2 Other activity**

El-Desouky *et al.* (2007) observed that the ethyl acetate fraction of *A. palaestinum* leaves had antioxidant activity; acting with a strong scavenging capacity for 1,1 - diphenyl-2-picrylhydrazyl (DPPH) radicals. A study reported that an essential oil obtained from *A. maculatum* (palmitic acid, phytol, methyl 9, 12, 15-octadecatrienoate and methyl linolenate) had antimicrobial activity against various pathogenic bacteria such as *Staph. aureus*, *Staph. epidermidis* and *E. coli*. They also showed antioxidant activity using DPPH free radical scavenging with an IC<sub>50</sub> value of 24.86 ± 21.4 mg/ml (Kianinia and Farjam, 2016). It was also reported that ethanol and methanol extracts of the leaves of *A. dioscoridis* had *in vitro* antioxidant activities due to the highest phenolic and flavonoid contents (Karahan *et al.*, 2015). Majumder *et al.* (2005) reported insecticidal activity of *A. maculatum* tuber on *Lipaphis erysimi* and *Aphis craccivora* with LC<sub>50</sub> values of 21 µg/ml and 16 µg/ml, respectively (Majumder *et al.*, 2005).

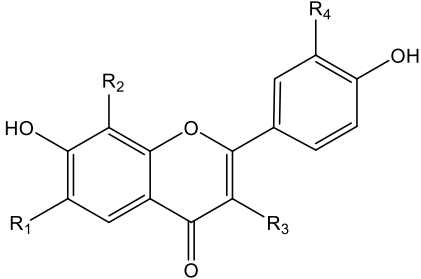
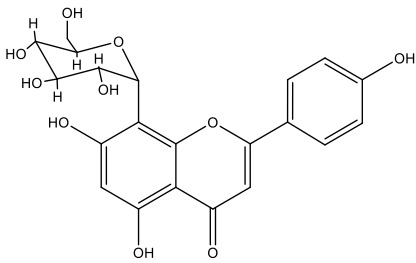
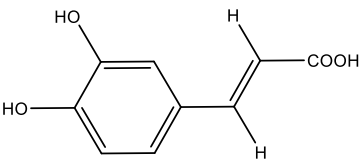
**Table 1.4:** Selection of phytochemicals previously isolated from Araceae family. AM: refers to the name of the plant *Arum cyrenaicum*.

Classification	Compound	Parts of the plant	Reference
Alkaloids	 <p>(S)-3, 4, 5-trihydroxy-1H-pyrrole-2(5H)-one (<b>AM-1</b>)</p>  <p>3-Hydroxypiperazine-2,5-dione (<b>AM-2</b>); <b>R=OH</b> piperazine-2,5-dione (<b>AM-3</b>); <b>R=H</b></p>  <p>Piperazirum (<b>AM-4</b>)</p>	Leaves of <i>A. palaestinum</i>	(El-Desouky <i>et al.</i> , 2007a; El-Desouky <i>et al.</i> , 2007b; El-Desouky <i>et al.</i> , 2014)

**Table 1.4 (continued):** Selection of phytochemicals previously isolated from Araceae family. AM: refers to the name of the plant *Arum cyrenaicum*.

Classification	Compound	Parts of the plant	Reference
Phenolic derivatives	 <p>Isovitexin (AM-5); R=H Isoorientin (AM-6); R=OH</p>	Aerial parts of <i>A. palaestinum</i>	(El-Desouky <i>et al.</i> , 2007a; Farid <i>et al.</i> , 2015)
	 <p style="text-align: center;"><b>R</b></p> <p>Chrysoeriol-7-<i>O</i>-neohesperidoside (AM-7)    neohesperidoside Chrysoeriol-7-<i>O</i>-(<math>\beta</math>-apiosyl)-<math>\beta</math>-glucopyranoside (AM-8)    apiosyl-glucoside</p>		

**Table 1.4 (continued):** Selection of phytochemicals previously isolated from Araceae family. AM: refers to the name of the plant *Arum cyrenaicum*.

Classification	Compound	Parts of the plant	Reference																											
Phenolic derivatives		Leaves of <i>A. palaestinum</i>	(El-Desouky <i>et al.</i> , 2007a)																											
	<table border="0"> <tr> <td></td> <td><b>R<sub>1</sub></b></td> <td><b>R<sub>2</sub></b></td> <td><b>R<sub>3</sub></b></td> <td><b>R<sub>4</sub></b></td> </tr> <tr> <td>Isoorientin (<b>AM-9</b>)</td> <td>C-Glu</td> <td>H</td> <td>H</td> <td>OH</td> </tr> <tr> <td>Luteolin (<b>AM-10</b>)</td> <td>H</td> <td>H</td> <td>H</td> <td>OH</td> </tr> <tr> <td>Vicenin (<b>AM-11</b>)</td> <td>C-Glu</td> <td>C-Glu</td> <td>H</td> <td>H</td> </tr> <tr> <td>3, 6, 8-trimethoxy, (<b>AM-12</b>)</td> <td>OCH<sub>3</sub></td> <td>OCH<sub>3</sub></td> <td>OCH<sub>3</sub></td> <td>OH</td> </tr> <tr> <td>5, 7, 3', 4'-tetrahydroxy flavone</td> <td></td> <td></td> <td></td> <td></td> </tr> </table>				<b>R<sub>1</sub></b>	<b>R<sub>2</sub></b>	<b>R<sub>3</sub></b>	<b>R<sub>4</sub></b>	Isoorientin ( <b>AM-9</b> )	C-Glu	H	H	OH	Luteolin ( <b>AM-10</b> )	H	H	H	OH	Vicenin ( <b>AM-11</b> )	C-Glu	C-Glu	H	H	3, 6, 8-trimethoxy, ( <b>AM-12</b> )	OCH <sub>3</sub>	OCH <sub>3</sub>	OCH <sub>3</sub>	OH	5, 7, 3', 4'-tetrahydroxy flavone	
	<b>R<sub>1</sub></b>	<b>R<sub>2</sub></b>	<b>R<sub>3</sub></b>	<b>R<sub>4</sub></b>																										
Isoorientin ( <b>AM-9</b> )	C-Glu	H	H	OH																										
Luteolin ( <b>AM-10</b> )	H	H	H	OH																										
Vicenin ( <b>AM-11</b> )	C-Glu	C-Glu	H	H																										
3, 6, 8-trimethoxy, ( <b>AM-12</b> )	OCH <sub>3</sub>	OCH <sub>3</sub>	OCH <sub>3</sub>	OH																										
5, 7, 3', 4'-tetrahydroxy flavone																														
																														
																														

### 1.4.2 *Pituranthos tortuosus*

The genus *Pituranthos* includes more than 20 species; one of these is *P. tortuosus* (Figure 1.5) known in Arabic as Guezzah. It belongs to the Family Umbellifereae (Apiaceae, parsley family or carrot family) and it comprises three subfamilies, 275 genera and 2850 species. Plants of this are generally known to be rich in essential oils showing antimicrobial activity against bacteria and fungi (Abdelwahed *et al.*, 2006). It is a small shrub without leaves and grows naturally in North Africa, and is widespread in central and southern Tunisia. The collection of the plant materials was carried out by the Mr Adella-Salem (Botany Department, Benghazi University). A voucher specimen has been kept in Benghazi University herbarium.



**Figure1.5:** Aerial part of *Pituranthos tortuosus*, and an image of the plant taken from <http://www.panoramio.com/photo/56689622>.

#### 1.4.2.1 Traditional uses

In Tunisia, *P. tortuosus* is used traditionally as an anti-asthmatic and against scorpion stings, while it is used traditionally by the Egyptian people for the preparation of a carminative drink and to relieve stomach pain, when blood is excreted in urine or when

coughing blood. It is also used for relief of stomach pains, against intestinal parasites, and for the regulation of menstruation (Mighri *et al.*, 2015).

#### **1.4.2.2 Active ingredients and biological activities**

Previous studies examining the chemical constituents of *P. tortuosus* have demonstrated the existence of essential oils (EO), furocoumarins and flavonoids (Table 1.5). Studies have identified a range of potential biological properties and applications for extracts from *P. tortuosus*.

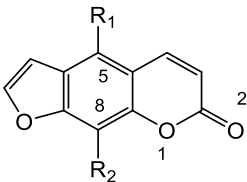
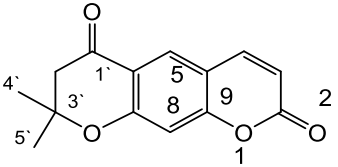
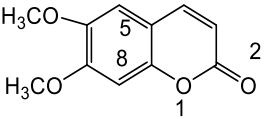
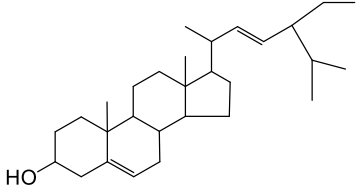
*P. tortuosus* extracts display antimicrobial activity against several bacteria and yeasts. EO obtained in November harvests are more effective than in April against the Gram-positive bacteria *Enterococcus faecalis* and *Staph. aureus* that could be due to the concentration of terpenes and particularly a relative high concentration of  $\alpha$ -pinene (Abdelwahed *et al.*, 2006). The oil isolated from fresh aerial parts resulted in potent antibacterial activity against *Streptococcus pyogenes*, and *Enterobacter aerogenesa* (Mighri *et al.*, 2015).

Anticancer activity has been documented for an acetonitrile/water extract which showed high cytotoxicity against a murine macrophage (RAW 264.7) cell line with an IC<sub>80</sub> value of 1.55  $\mu$ g/ml (Fatma *et al.*, 2017). The EO (terpinen-4-ol, sabinene,  $\gamma$ -terpinene, and  $\beta$ -myrcene) displayed potent activity against liver (HepG2), colon (HCT116), and breast (MCF7) cancer cell lines, with IC<sub>50</sub> values of 1.67, 1.34, and 3.38 mg/ml, respectively (Abdallah and Ezzat, 2011). The EO also displayed *in vitro* and *in vivo* antimelanoma activities against B16F10 cancer cells and was shown to induce apoptosis and to inhibit migration and invasion processes (Mounira *et al.*, 2016). Abdel-Wahed *et al.* (2008) studied the antimutagenic activities against direct acting mutagens, nifuroxazide (NF) and sodium azide (SA), and indirect acting

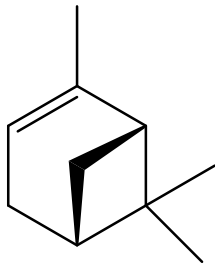
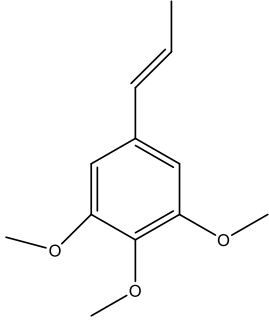
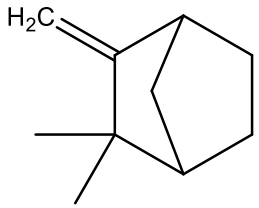
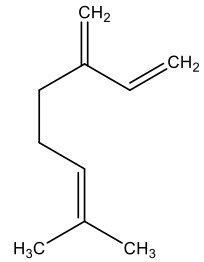
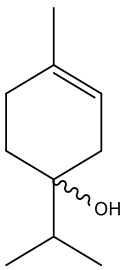
mutagen of latoxin B1 (AFB<sub>1</sub>) using extracts prepared from aerial parts of *P. tortuosus*. It was found that all extracts decreased the mutagenicity induced by AFB<sub>1</sub>, SA, and NF. In addition, ethyl acetate, acetone, and methanol extracts showed significant cytotoxic effects against two leukemia cell lines, L1210 and K562; the effect was greater against the latter, but did not induce apoptosis (Abdelwahed *et al.*, 2008b).

Ahmeda *et al.* (2011) tested 10 EOs extracted from 10 plants issued from the Sned region (Tunisia). They showed that the EOs obtained from *P. tortuosus* has moderate leishmanicidal effects against *Leishmania major* and *L. infantum* with IC<sub>50</sub> 0.64 and 0.66 µg/mL respectively, and showed cytotoxicity against the murine macrophage cell line RAW 264.7 with an IC<sub>80</sub> of 0.5 µg/ml (Ahmed *et al.*, 2011).

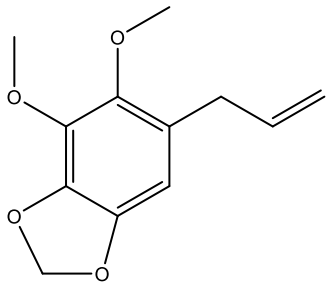
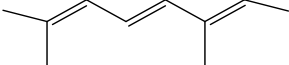
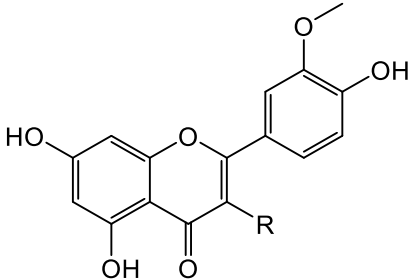
**Table 1.5:** Selection of phytochemicals previously isolated from *P.tortuosus* PT: refers to the name of the plant *tortuosus*.

Classification	Compound	Parts of the plant	Reference												
Furanocoumarins		Roots of <i>P. tortuosus</i>	(Abdel-Kader, 2003)												
	<table border="0"> <tr> <td></td> <td><b>R<sub>1</sub></b></td> <td><b>R<sub>2</sub></b></td> </tr> <tr> <td>Bergapten</td> <td>(PT-1)</td> <td>OCH<sub>3</sub>    H</td> </tr> <tr> <td>Xanthotoxin</td> <td>(PT-2)</td> <td>H        OCH<sub>3</sub></td> </tr> <tr> <td>Isopimpinellin</td> <td>(PT-3)</td> <td>OCH<sub>3</sub>    OCH<sub>3</sub></td> </tr> </table>				<b>R<sub>1</sub></b>	<b>R<sub>2</sub></b>	Bergapten	(PT-1)	OCH <sub>3</sub> H	Xanthotoxin	(PT-2)	H        OCH <sub>3</sub>	Isopimpinellin	(PT-3)	OCH <sub>3</sub> OCH <sub>3</sub>
				<b>R<sub>1</sub></b>	<b>R<sub>2</sub></b>										
	Bergapten			(PT-1)	OCH <sub>3</sub> H										
	Xanthotoxin			(PT-2)	H        OCH <sub>3</sub>										
Isopimpinellin	(PT-3)	OCH <sub>3</sub> OCH <sub>3</sub>													
	Graveolone (PT-4)														
	Aesculetin dimethyl ether (PT-5)														
Sterols		Stigmasterol (PT-6)													

**Table 1.5 (continued):** Selection of phytochemicals previously isolated from *P.tortuosus* PT: refers to the name of the plant *tortuosus*.

Classification	Compound	Parts of the plant	Reference
Essential oil	 <p>(+)-<math>\alpha</math>-Pinene (PT-7)</p>	Aerial parts of <i>P. tortuosus</i>	(Abdallah and Ezzat, 2011)
	 <p>Isoelemicin (PT-8)</p>		
	 <p>Camphene (PT-9)</p>		
	 <p><math>\beta</math>-myrcene (10)</p>		
	 <p>Terpinen-4-ol (-11)</p>		
	 <p>Sabinene (PT-12)</p>		
	 <p><math>\gamma</math>-Terpinene (PT-13)</p>		

**Table 1.5 (continued):** Selection of phytochemicals previously isolated from *P. tortuosus* PT: refers to the name of the plant *tortuosus*.

Classification	Compound	Parts of the plant	Reference
	 Dill apiol (PT-14)	Aerial parts of <i>P. tortuosus</i>	(Abdallah and Ezzat, 2011)
	 Allo-ocimene (PT-15)		
Flavonoids	 Isorhamnetin (PT-16) Chrysoeriol (PT-17) Isorhamnetin-3-O-glucoside (PT-8) Isorhamnetin-3-O-rutinoside (PT-19)	Aerial parts of <i>P. tortuosus</i>	(Singab <i>et al.</i> , 1998; Al-Gaby and Allam, 2000; Abdel-Kader, 2003; Mighri <i>et al.</i> , 2015)
			<b>R</b> OH H O-Glu O-rutinoside

### 1.4.3 *Teucrium zanonii*

*T. zanonii* (Figure 1.6) is known as Jaida in Arabic and belongs to the family Lamiaceae (Labiatae) also known as the mint or aromatic family and it has a high content of EO. The family includes about 252 genera and 6700 species. In the flora of Libya, it is represented by 13 species, five of which are endemic. They are *T. appollinis*, *T. barbeyanum*, *T. davaeanum*, *T. linivaccarii*, and *T. zanonii* wherein *T. zanonii* is the most common (Abdelshafeek *et al.*, 2009; Naghibi *et al.*, 2010). A voucher specimen has been kept in Benghazi University herbarium.

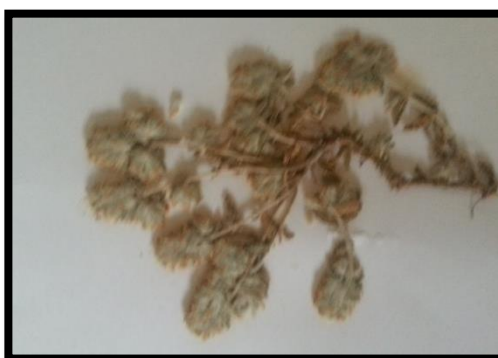


**Figure 1.6:** The aerial parts of *Teucrium zanonii* collected from Libya.

#### 1.4.3.1 Traditional uses

Many *Teucrium* species are known to have important biological activities such as diuretic, diaphoretic, antiseptic, antipyretic, antispasmodic, hypoglycemic and antifeedant. In folk medicine, the preparation of *Teucrium* extracts depend on the illness (such as stomach and intestinal troubles, cold and as a stimulant vermifuge, tonic, for rheumatism, hemorrhoids and renal inflammatory). In the Abofakhra region (25 Km from Benghazi City), this endemic plant is used in folk medicine for gastrointestinal troubles, as a tonic, for renal inflammation and as an antidiabetic agent (Abdelshafeek *et al.*, 2009; Naghibi *et al.*, 2010).

### 1.4.3.2 Active ingredients and biological activities

The family Lamiaceae (Labiatae) is reported to produce valuable phytochemicals, such as flavonoids (T-17-T-21), terpenoids (diterpenoids (T-22-T-54), sesquiterpenes (T-55-T-62), triterpenes (T-63-T-64), iridoid (T-65-T-69), phenylethanol glycosides (T-70-71), saponins (T-73-T-74) and steroids (T75-76) (Table 1.6, Appendix I). Examples of compounds, with biological activity derived from Lamiaceae family are shown in Table 1.6 and their structures. (Labbe *et al.*, 1989; Bedir *et al.*, 1999; Bruno *et al.*, 2004; Abdelshafeek *et al.*, 2006; D'Abrosca *et al.*, 2013; Hao *et al.*, 2013; Lv *et al.*, 2014b; Elmasri *et al.*, 2014a; Lv *et al.*, 2015; Elmasri *et al.*, 2015a; Elmasri *et al.*, 2015b; Elmasri *et al.*, 2016; Venditti *et al.*, 2017 ).

### 1.4.3.3 Previous phytochemical and biological reports of *T. zanonii*

Abdelshafeek *et al.* (2006) isolated flavonoids from an ethyl acetate extract of *T. zanonii* cirsiol (T-1), luteolin (T-2), chrysoeriol (T-3) and xanthomicrol (T-4) and from a butanol extract apigenin 6, 8-di-*O*-glucoside (T-5) and luteolin-7-*O*-rutinoside (T-6) (Table 1.6). In 2009, Abdelshafeek *et al.* showed that an aqueous extract of *T. zanonii* had the highest insecticidal activity against the adult the olive bark beetle, *Phloeotribus oleae* and Abdelshafeek *et al.* (2010) reported that a *T. zanonii* volatile oil contained 74 compounds where germacrene-D was the main compound and the ethyl acetate and butanol extracts of *T. zanonii* showed antioxidant activity.

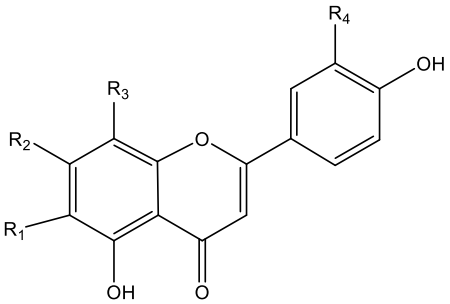
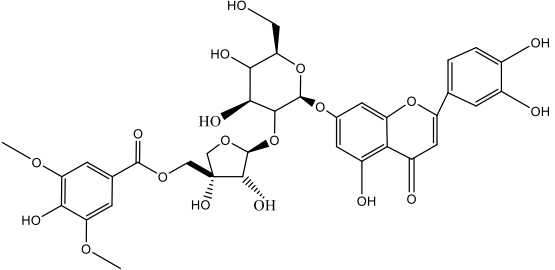
### 1.4.3.4 Antidiabetic activities of *Teucrium* species

A study found that an ethyl acetate extract of *T. stocksianum* produced a decrease in blood glucose levels and an increase in insulin levels in alloxan-induced diabetic rabbits after an oral glucose load leading to reduced HbA1c levels (Alamgeer *et al.*, 2013). Studies have shown significant histological changes in the pancreas of induced diabetic rats treated with a *T. polium* aerial parts extract that reduced the level of serum glucose (Yazdanparas *et al.*, 2005; Tatar *et al.*, 2012). Esmaili and Yazdanparast (2004) also reported that an aqueous extract of *T. polium* reduced high blood glucose levels through enhancing insulin secretion by the pancreas.

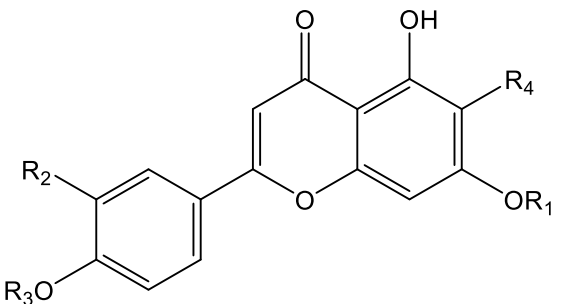
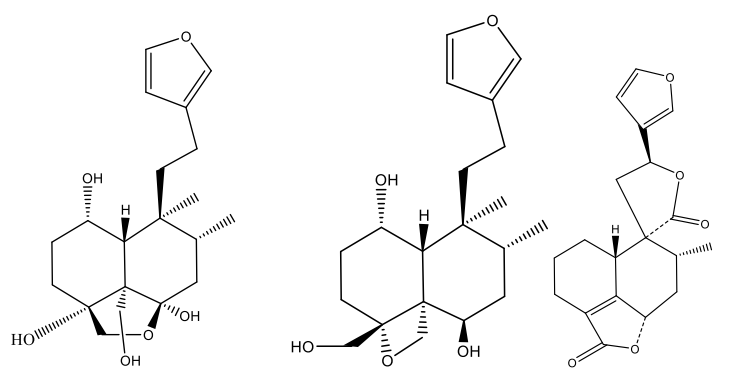
#### **1.4.3.5 Antibacterial activities of *Teucrium* species**

A methanol extract of *T. stocksianum* roots had significant bactericidal activity against *E. coli*, *Staph. aureus*, *S. typhi*, *Shigella flexneri* and *B. subtilis* and showed fungicidal action against *Aspergillus niger*, *A. flavus*, *A. fumigatus* and *Fusariumsolani* at different minimum inhibitory concentrations. An ethyl acetate fraction exhibited inhibition of *L. atropica* growth (Shah *et al.*, 2015), while an ethanolic extract of *T. chamaedrys* had high antimicrobial activity, and antioxidant activity (Vlase *et al.*, 2014). Sesquiterpenes in the extract showed antibacterial activity against *Staph. aureus* biofilm activity in the low range (Elmasri *et al.*, 2014b). In addition, the crude saponins of *T. stocksianum* had cytotoxic and anthelmintic activity (Ali *et al.*, 2011).

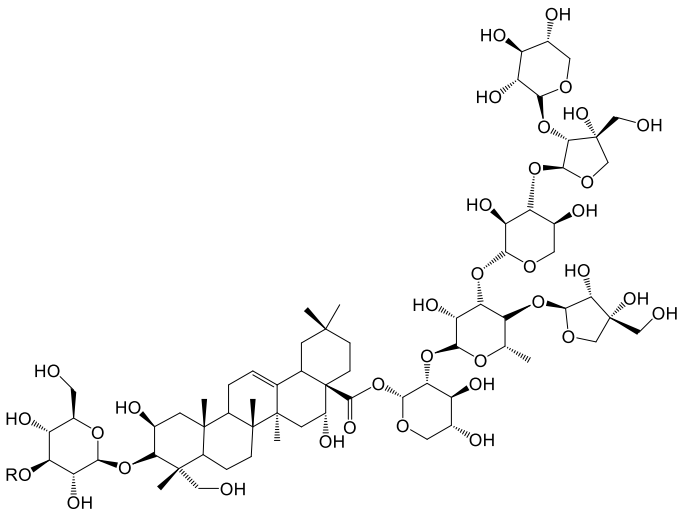
**Table 1.6:** Selection of phytochemicals previously isolated from *T. zanonii*. T: refers to the name of the plant *Teucrium*.

Classification	Compound	Parts of the plant	Reference																																
Flavonoids		Aerial parts of <i>T. zanonii</i>	(Abdelshafeek <i>et al.</i> , 2009)																																
	<table border="0"> <thead> <tr> <th></th> <th>R<sub>1</sub></th> <th>R<sub>2</sub></th> <th>R<sub>3</sub></th> <th>R<sub>4</sub></th> </tr> </thead> <tbody> <tr> <td>Cirsiliol (T-1)</td> <td>OCH<sub>3</sub></td> <td>OCH<sub>3</sub></td> <td>H</td> <td>OH</td> </tr> <tr> <td>Luteolin (T-2)</td> <td>H</td> <td>OH</td> <td>H</td> <td>OH</td> </tr> <tr> <td>Chrysoeriol (T-3)</td> <td>H</td> <td>OH</td> <td>H</td> <td>OCH<sub>3</sub></td> </tr> <tr> <td>Xanthomicrol (T-4)</td> <td>OCH<sub>3</sub></td> <td>OCH<sub>3</sub></td> <td>OCH<sub>3</sub></td> <td>H</td> </tr> <tr> <td>Apigenin 6, 8-di-O-glucoside (T-5)</td> <td>c-glu</td> <td>OH</td> <td>c-glu</td> <td>H</td> </tr> <tr> <td>Luteolin-7-O-rutinoside (T-6)</td> <td>H</td> <td>o-rutinoside</td> <td>H</td> <td>OH</td> </tr> </tbody> </table>				R <sub>1</sub>	R <sub>2</sub>	R <sub>3</sub>	R <sub>4</sub>	Cirsiliol (T-1)	OCH <sub>3</sub>	OCH <sub>3</sub>	H	OH	Luteolin (T-2)	H	OH	H	OH	Chrysoeriol (T-3)	H	OH	H	OCH <sub>3</sub>	Xanthomicrol (T-4)	OCH <sub>3</sub>	OCH <sub>3</sub>	OCH <sub>3</sub>	H	Apigenin 6, 8-di-O-glucoside (T-5)	c-glu	OH	c-glu	H	Luteolin-7-O-rutinoside (T-6)	H
	R <sub>1</sub>	R <sub>2</sub>	R <sub>3</sub>	R <sub>4</sub>																															
Cirsiliol (T-1)	OCH <sub>3</sub>	OCH <sub>3</sub>	H	OH																															
Luteolin (T-2)	H	OH	H	OH																															
Chrysoeriol (T-3)	H	OH	H	OCH <sub>3</sub>																															
Xanthomicrol (T-4)	OCH <sub>3</sub>	OCH <sub>3</sub>	OCH <sub>3</sub>	H																															
Apigenin 6, 8-di-O-glucoside (T-5)	c-glu	OH	c-glu	H																															
Luteolin-7-O-rutinoside (T-6)	H	o-rutinoside	H	OH																															
		Leaves of <i>T. polium</i>	(D'Abrosca <i>et al.</i> , 2013)																																

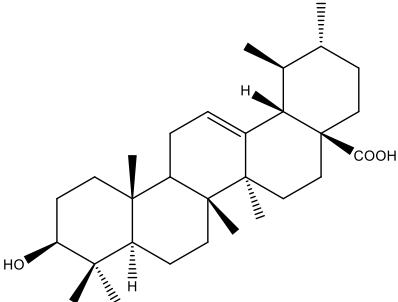
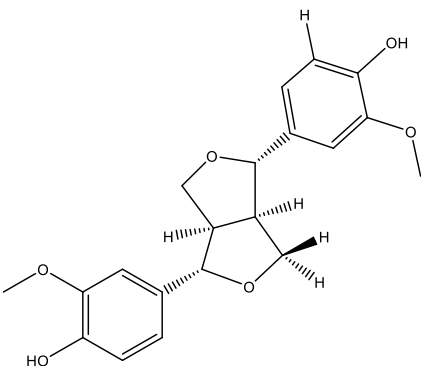
**Table 1.6 (continued):** Selection of phytochemicals with pharmacological activities previously isolated from *Teucrium* species.

Classification	Compound	Parts of the plant	Biological activity	Reference
	 <p>3',4',5-trihydroxy-6,7-dimethoxy-flavone; <math>R_1=OCH_3</math>, <math>R_2=OH</math>, <math>R_3=OH</math>, <math>R_4=OCH_3</math> (<b>T-8</b>)</p>	Aerial parts of <i>T. polium</i>	Inhibit the biofilm-forming strain <i>Staphylococcus aureus</i>	(Elmasri <i>et al.</i> , 2015b)
	<p>5,6,7,3',4'-pentahydroxyflavone (<b>T-9</b>) <math>R_1, R_2, R_3, R_4=OH</math></p> <p><b><i>nor</i>-neoclerodane diterpenoids</b></p>	Aerial parts of <i>T. fruticans</i>	No cytotoxicity activity against osteosarcoma (U-2OS), lung (NCI-H460), and breast (MCF-7) cancer cell lines	(Lv <i>et al.</i> , 2015)
	 <p>Teufruintin B (<b>T-10</b>)      Teufruintin C (<b>T-11</b>)      Teucvin (<b>T-12</b>)</p>	Whole plant of <i>T. polium</i>	Reduced feeding by larvae of <i>Leptinotarsa decemlineata</i> on Colorado potato beetle	(Ortego <i>et al.</i> , 1995)
			Did not have activity against P 388 Lymphocytic Leukemia in mice	(Nagao <i>et al.</i> , 1982)

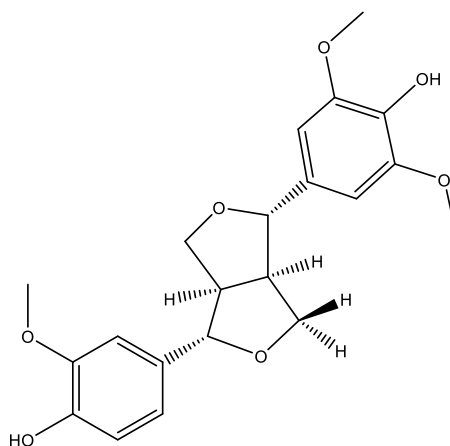
**Table 1.6 (continued):** Selection of phytochemicals with pharmacological activities previously isolated from *Teucrium* species.

Classification	Compound	Parts of the plant	Biological activity	Reference
Saponins		Aerial parts of <i>T. polium</i>	Highly active against breast (MDA-MB468) and colon (HCC-2998) cancer cells and moderately active against colon (COLO 205), renal (A-498) and melanoma (SK-MEL-498) cancer cells	(Elmasri <i>et al.</i> , 2015a)
	Poliusaposide C (T-13)			

**Table 1.6 (continued):** Selection of phytochemicals with pharmacological activities previously isolated from *Teucrium* species.

Classification	Compound	Parts of the plant	Biological activity	Reference
<b>Triterpenoids</b>	 <p>Ursolic acid (T-14)</p>	Whole parts of <i>T. viscidum</i>	Antibacterial activity against <i>E. coli</i> , <i>Sarcina lutea</i> , <i>K. pneumoniae</i> and <i>Staph. aureus</i>  Antioxidant activity and anticancer activity on prostate and breast cancer	(do Nascimento <i>et al.</i> , 2014)  (Sultana <i>et al.</i> , 2010; Gai <i>et al.</i> , 2016; Yin <i>et al.</i> , 2018)
<b>Lignan</b>	 <p>Pinoresinol (T-15)</p>	Whole parts of <i>T. viscidum</i>	Cytotoxic, anti-proliferative and pro-oxidant activity in human breast tumour cells  Antibacterial activities against five food-related bacteria ( <i>E. coli</i> , <i>Pseudomonas aeruginosa</i> , <i>Staph. aureus</i> , <i>B. subtilis</i> and <i>Salmonella enterica</i> )	(Hao <i>et al.</i> , 2013; Lopez-Biedma <i>et al.</i> , 2016)  (Zhou <i>et al.</i> , 2017)

**Table 1.6 (continued):** Selection of phytochemicals with pharmacological activities previously isolated from *Teucrium* species.

Classification	Compound	Parts of the plant	Biological activity	Reference
		Whole parts of <i>T. viscidum</i>	Antifungal activity	(Hwang <i>et al.</i> , 2012)
	(+)-medioresinol ( <b>T-16</b> )		Antioxidant activity	(Amiri, 2010)
	essential oil containing linalool, caryophyllene oxide, 1, 8-cineol, $\beta$ -pinene, 3-octanol, $\beta$ -caryophyllene, and germacrene-D		Cytotoxic effects on the HepG2 cancer cells with antioxidant and antiviral properties	(Hammami <i>et al.</i> , 2015)

#### 1.4.4 *Hypochoeris radicata*

*H. radicata* L. (Figure 1.7), known as catsear or flatweed, belongs to the family Asteraceae. Asteraceae (Compositae) is the largest family of flowering plants and contains about 1,600 genera and some 25,000 species (Tähtiharju *et al.*, 2012). It grows 15-60 cm tall, is perennial, and rosulate. It has a taproot and stems which ascends to erect leaves and yellow flowers (Senguttuvan *et al.*, 2014b; Senguttuvan and Subramaniam, 2016). It is native in Europe and it is spread in Africa, and Asia, Australia, India, Japan, North and South America, and Pacific islands the high hills of Nilgiris and the Western Ghats India (Senguttuvan *et al.*, 2014b; Senguttuvan and Subramaniam, 2016). It is included in the flora of Libya in 1983 (Jamuna *et al.*, 2013) (Thompson, 2007). The the plant materials was provided by SIPBS colleague Dr Ibrahim Khadra (Strathclyde University).



**Figure 1.7:** *Hypochoeris radicata* plant; and an image of the plant taken from [https://middlepath.com.au/plant/Catsear\\_Hypochoeris-radicata.php](https://middlepath.com.au/plant/Catsear_Hypochoeris-radicata.php)

#### 1.4.4.1 Traditional uses

It is used for various medical ailments, mainly for the treatment of inflammation. It is prescribed by local healers for the treatment of jaundice, rheumatism, dyspepsia, constipation, hypoglycaemia, anticancer, anti-inflammatory, antidiuretic, hepatoprotective activity and to treat kidney problems (Pal and Shukla, 2003).

#### 1.4.4.2 Active ingredients and biological activities

The Asteraceae family is reported to contain a wide variety of phytochemicals, such as terpenoids (sesquiterpene lactones (HR-17-HR47) and triterpenoids (HR-48-HR-61), lignans (HR-62), alkaloids (HR-63-HR-67), sterols (HR-68-HR-69), and polyphenols (HR-70-HR-88), EO, tannins, acids and carbohydrates (Table 1.7, Appendix II). This family has also been reported to have biological activities including antioxidant, antimicrobial, antifungal, antiviral, anti-cancer, anti-inflammatory and insecticidal activities (Niño *et al.*, 2006; Jbilou *et al.*, 2008; Boussaada *et al.*, 2008; Dewan *et al.*, 2013; Visintini Jaime *et al.*, 2013; Süntar, 2014; Koc *et al.*, 2015; Iqbal *et al.*, 2017). Examples of compounds, with pharmacological activities derived from the family Asteraceae, are shown in Table 1.7.

The preliminary analysis of an alcoholic and aqueous extract of leaf and root parts of *H. radicata* by Senguttuvan *et al.* (2014) reported the presence of alkaloids, flavonoids, tannins, glycosides, terpenoids and saponins with excellent antioxidant activity (Senguttuvan *et al.*, 2014b; Senguttuvan and Subramaniam, 2016). Kim *et al.* (2014) identified luteolin (HR-16) by HPLC methods; a common flavonoid widely distributed in the plant. HR-16 is reported to have different biological activities including anticancer activity (Lopez-Lazaro, 2009) and antimicrobial activities against *Staph. aureus*, *B. cereus* and *E. coli* (Wang and Xie, 2010; Lee *et al.*, 2010; Rashed *et*

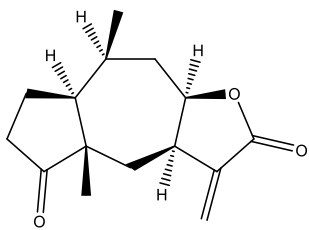
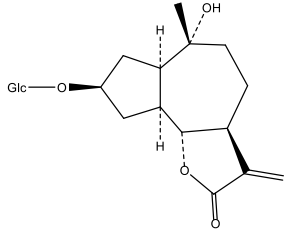
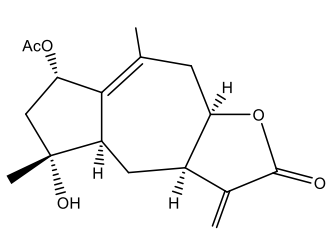
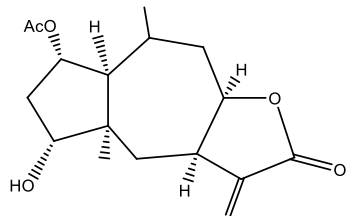
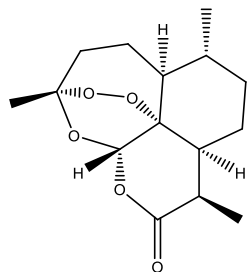
*al.*, 2013), antiinflammatory and antioxidant activity (Odontuya *et al.*, 2005; Popov *et al.*, 2016). Jamuna *et al.* (2015) isolated confertin (HR-1) and scopoletin (HR-14) from *H. radicata* and found they suppressed the production of proinflammatory cytokines such as TNF- $\alpha$ , IL-1 $\beta$  and IL-6 and enhanced more prominent antioxidant activity. There may be a use for inflammatory disorders since confertin (HR-1) and scopoletin (HR-14) compounds inhibited paw oedema. The sesquiterpene lactones from Asteraceae plants, inuchinenolide B (HR-3) and aucherinolide (HR-4) showed cytotoxicity activity against liver (HepG-2), breast (MCF-7) and lung (A-549) cancer cell lines with IC<sub>50</sub> values of 56.6, 19.0, 39.0, 11.8, 55.7 and 15.3  $\mu$ g/ml, respectively (Gohari *et al.*, 2015) while the sesquiterpene lactone ixerin D (HR-2) showed no toxicity against colon (HT29) and lung (A-549) cancer cell lines (Ahn *et al.*, 2006). However, the sesquiterpene lactone artemisinin (HR-5) is a naturally occurring antimalarial compound, with potent anticancer activity (Crespo-Ortiz and Wei, 2012). While another sesquiterpene  $\beta$ -eudesmol (HR-6) (10–100  $\mu$ M) inhibited proliferation of cervix (HeLa), gastric (SGC-7901), and liver (BEL-7402) cancer cell lines. It acts in a dose-dependent manner to inhibit angiogenesis by suppressing cAMP response element binding protein (CREB) activation in a growth factor signalling pathway (Ma *et al.*, 2008). HR-6 is reported to have antibacterial activity against *Pseudomonas aeruginosa* ATCC, *Enterococcus faecalis*, *Staph. subtilis* and *Entrobacter aerogenes* (Mohsenzadeh *et al.*, 2011; Salah-Fatnassi *et al.*, 2017). Parthenolide (HR-7) is also a sesquiterpene that showed leishmanicidal activities against *L. amazonensis* (Tiuman *et al.*, 2005).

Arctiin (HR-8), trachelogenin (HR-9), and arctigenin (HR-10) are lignans, isolated from Asteraceae plants such as *Tussilago farfara* L and *Arctium lappa* L. These have been reported to have antiviral activity against influenza A virus (A/NWS/33, H1N1) (IFV) (Hayashi *et al.*, 2010; Qian *et al.*, 2016). It has also been found that HR-8 induces

cell detachment and decreases cell numbers via the up-regulation of MUC-1 mRNA and protein in a prostate (PC-3) cancer cell line (Huang *et al.*, 2004), while HR-10 was reported to have antiviral, neuroprotective, antiinflammatory and antioxidant activities (Hayashi *et al.*, 2010). Oil such as 1,8-cineole,  $\alpha$ -terpineol, terpinen-4-ol,  $\alpha$ -pinene,  $\beta$ -pinene,  $\alpha$ -phellandrene, and *p*-cymene from the Asteraceae family are reported to have antifungal activity against *A. fumigatus* (Zapata *et al.*, 2010; Salah-Fatnassi *et al.*, 2017). Lupeol (HR- 11) is a triterpenoid, reported to have antileishmanial against *L. donovani* parasite (Das *et al.*, 2017). In addition, HR-11 is reported to have anti-inflammatory, antimicrobial, antiprotozoal, antiproliferative, anti-invasive, anti-angiogenic and cholesterol lowering properties (Siddique and Saleem, 2011). N-(*p*-coumaroyl) serotonin (HR- 12) is an alkaloid that improves vascular distensibility and inhibits aortic hyperplasia by blocking the increase of  $Ca^{2+}$  and blocking platelet-derived growth factor (PDGF) signalling (Takimoto *et al.*, 2011).

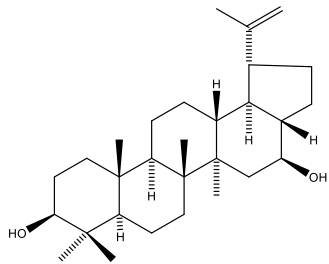
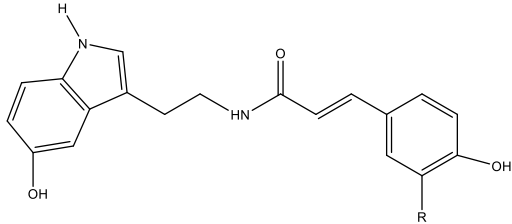
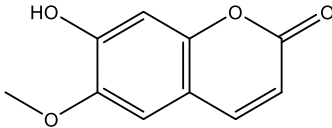
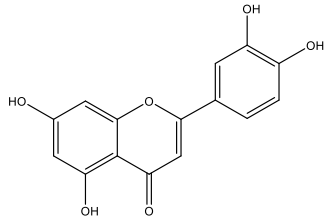
Kim *et al.* (2014) showed that an ethyl acetate extract of *H. radicata* inhibited the production of pro-inflammatory molecules nitric oxide (NO), iNOS, prostaglandin E<sub>2</sub> (PGE<sub>2</sub>) and cyclooxygenase (COX-2), and cytokines such as TNF- $\alpha$ , IL-1 $\beta$ , and IL-6 in lipopolysaccharide (LPS)-stimulated RAW 264.7 cells. Therefore, the phosphorylation of mitogen-activated protein kinase (MAPK) for example MAPK p38, extracellular regulated kinase (ERK), and c-Jun NH<sub>2</sub>-terminal kinase (JNK) were inhibited by an ethyl acetate extract in a concentration-dependent manner. 11 $\beta$ ,13-dihydrolactucin is reported to have sedative properties (Wesołowska *et al.*, 2006).

**Table 1.7:** Selection of phytochemicals previously isolated from Asteraceae. HR: refers to the name of the *H. radicata*.

Classification	Compound	Parts of the plant	Reference
Terpenoids			( Ohmura <i>et al.</i> , 1989; Jamuna <i>et al.</i> , 2015)
Sesquiterpenes	 <p>Confertin (HR-1)</p>	leaves and roots <i>H. radicata</i>	
	 <p>Ixerin D (HR-2)</p>		
	 <p>Inuchinenolide B (HR-3)</p>		
		Aerial parts of <i>Inula aucheriana</i>	(Gohari <i>et al.</i> , 2015; Ivanescu <i>et al.</i> , 2015)
	 <p>Aucherinolide (HR-4)</p>		
	 <p>Artemisinin (HR-5)</p>		



**Table 1.7 (continued):** Selection of phytochemicals previously isolated from Asteraceae. HR: refers to the name of the *H. radicata*.

Classification	Compound	Parts of the plant	Reference
Triterpenoids		Genus <i>Calendula</i>	(Arora <i>et al.</i> , 2013; Hodaj <i>et al.</i> , 2017)
Alkaloid		Seeds of <i>C. vlachorum</i>	
	Lupeol (HR-11)		
	N-(p-coumaroyl) serotonin (HR-12) R=H		
	Moschamine (HR-13) R= OCH <sub>3</sub>		(Ohmura <i>et al.</i> , 1989; Jamuna <i>et al.</i> , 2015)
Coumarin phenylbutanoid glucoside		Leaf and root parts of <i>H. radicata</i>	
	Scopoletin (HR-14)		
	4-(3-Glucopyranosyloxy-4-hydroxyphenyl)- (E)-3-buten-2-one (HR-15)		
Flavonoid			
	Luteolin (HR-16)		

#### 1.4.5 *Solanum sodomaeum*

*Solanum* is one of the largest genera in the plant kingdom. It includes about 1400 species distributed throughout the world. *S. sodomaeum* (Figure 1.8) is an annual herb, widely distributed in the Libyan desert and belongs to the Solanaceae family. *Solanum* have steroidal alkaloids and isoprenoids (El Sayed *et al.*, 1998).

*Solanum* species herbs have been utilised for treatment of cancer; although, their mechanisms and effectiveness *in vivo* remain unclear. Also, *Solanum* extracts have been shown to possess anticancer activities for centuries around the world, including China. Numerous active ingredients, such solamargine, solasodine and solasonine, decrease cancer growth *in vitro* and *in vivo*. *S. sodomaeum* studies have demonstrated that steroidal glycosides have strong antileukemic activity (Wu *et al.*, 2011). A voucher specimen has been kept in Benghazi University herbarium.



**Figure 1.8:** Fruit of *Solanum sodomaeum* collected from Libya.

#### **1.4.5.1 Traditional uses**

*S. sodomaeum* is traditionally used to treat eczema by decoction (one kilo of plant in 3 litres of water, boiled to reduce the volume down to one litre) used three times daily. For haemorrhoids, the fruit is crushed and applied locally as a poultice, In Arabic, it known as teffah elgoul, French pomme de Sodom and in English it is known as apple of Sodom.

#### **1.4.5.2 Active ingredients and biological activities**

The flowering plant family Solanaceae contains important plants for humans, in agriculture (potatoes, tomatoes, peppers), medicine (mandrake, tobacco, deadly nightshade, henbane), and as ornamentals (*Solanum* spp., tobaccos, petunias) (Spooner *et al.*, 1993; Bohs and Olmstead, 1997). *Solanum* is one of the largest genera in the Solanaceae family, it includes valuable plants like eggplant (Weese and Bohs, 2007; Species, 2008). This genus *Solanum* (Solanaceae) is a source of steroidal glycoalkoids, which is an important group of plant secondary metabolites and glycoalkaloids are remarkable metabolites because they can have both harmful and beneficial effects on human health (Gürbüz Öztürk *et al.*, 2015). These compounds are used as a starting material for the synthesis of steroidal drugs. In the majority of solanaceous plants, solasodine occurs as a glycone part of glycoalkoids, which is a nitrogen analogue of sapogenins (Patel and Patel, 2013). Various phytochemicals, mainly steroidal glycoalkoids, alkaloids have been isolated from different parts of *Solanum* (Table 1.8, Appendix III).

#### 1.4.5.3 Previous phytochemical and biological studies of *S. sodomaicum*

El Sayed *et al.* (1998) isolated two pyrrole alkaloids, solasodamine A and B (SS-7-SS-8) from the fresh berries of *S. Sodomaicum* L. SS-7 exhibits activity against *Mycobacterium intracellulare* (Cham *et al.*, 1987). Cham and Wilson (1987) isolated glycoalkaloids from *S. sodomaicum* L, which contain a sugar moiety, consisting of a mixture of glucose, rhamnose, and galactose. Cham and Meares (1987) reported that a glycoalkaloid isolated from *S. sodomaicum* is highly effective in the treatment of malignant human skin basal cell carcinomas (BCCs), squamous cell carcinomas (SCCs) and benign tumours (keratoses and keratoacanthomas) and found that the histological analyses of biopsies taken before, during and after treatment give compelling evidence of the efficacy of the glycoalkaloid formulation. Biochemical, haematological and urinal analytical studies demonstrated that there were no adverse effects on the liver, kidneys or haematopoietic system during treatment. Normal skin treated with the glycoalkaloid formulation likewise was free from adverse histological or clinical effects.

Solamargine (SS-3) is a glycoside of solasodine with a significant anticancer effect against cancer cells such as human bone (U2OS) cells hepatoma cells (Hep3B), colon (HT29, SW 620), liver (HepG2), adenocarcinoma (H441), lung (H520), large cell lung cancer (H661) and small cell lung cancer (H69), human K562 leukemia and squamous cell carcinoma KB cells, breast cancer cells (MCF-7 and SK-BR-3 cells), stomach (NUGC-3) (Nakamura *et al.*, 1996; Kuo *et al.*, 2000; Lee *et al.*, 2004; Liu *et al.*, 2004; Shiu *et al.*, 2007; Shiu *et al.*, 2009; Sun *et al.*, 2010; Sun *et al.*, 2011). SS-3 showed greater cytotoxicity than cisplatin, methotrexate, 5-fluorouracil, epirubicin and cyclophosphamide against human breast cancer cells (HBL-100, ZR-75-1 and SK-BR-

3) (Shiu *et al.*, 2007). It was reported that it triggers extrinsic and intrinsic apoptotic pathways of breast cancer cells through activation of caspase-3, -8 and -9 and up-regulated external death receptors (Shiu *et al.*, 2007). Studies reported that due to overexpression of Bcl-2 and Bcl-xL which may cause resistance to anticancer drugs such as cisplatin, combination therapy of solamargine and cisplatin might be effective in treatment of cisplatin-resistant in breast cancer (Chang *et al.*, 1998b; Pietras *et al.*, 1999; Shiu *et al.*, 2007;). Furthermore, solamargine induced apoptosis on human hepatoma cells (SMMC-7721 and HepG2) through activating caspase-3 and leading to G2/M arrest (Ding *et al.*, 2012). A study conducted by Hsu *et al.* (2014) reported that the anticancer activity of SS-3 involves triggering the gene expression of human tumor necrosis factor receptor 1 (TNFR I) which may lead to cell apoptosis (Hsu *et al.*, 1996). TNFR-I acts as important regulator in inducing apoptosis and TNFR-I acts in almost every cell type and can independently transmit most biological activities of TNF- $\alpha$  (Kuo *et al.*, 2000). It induces apoptosis in lung cancer cells (H441, H520, H661 and H69) by phospholipid phosphatidylserine externalisation in a dose-dependent manner and increases sub-G1 (Liu *et al.*, 2004). It also induces apoptosis in human hepatoma cells (SMMC-7721, Hep3B and HepG2) by causing cell cycle arrest at the G2/M phase and up-regulate the expression of caspase-3 through the activation of caspase-3 (Chang *et al.*, 1998a; Kuo *et al.*, 2000; Ding *et al.*, 2011; Ding *et al.*, 2012). Another study demonstrated that solamargine induces apoptosis in gastric cancer cells MGC-803 through a decrease of mutation p53, an increase of the ratio of Bax to Bcl-2 and the activation of caspase-3, which could be due to three sugar units and  $\alpha$ -L-rhamnopyranose at C-2 or a hydroxyl group on the steroidal backbone leading to potential candidates for the treatment of gastric cancer (Ding *et al.*, 2013b). It has also been found that solasonine and SS-3 from *S. sodomaeum* showed antineoplastic activity against Sarcoma 180 with single dosages of 8 mg/kg given on two consecutive days resulted in inhibition of tumour progression with greater than 40% survival

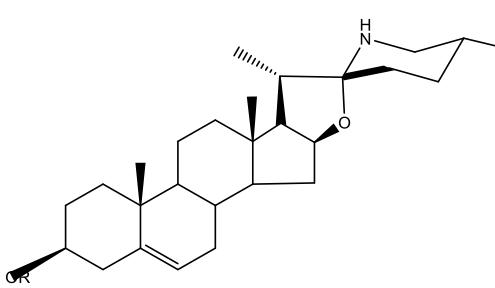
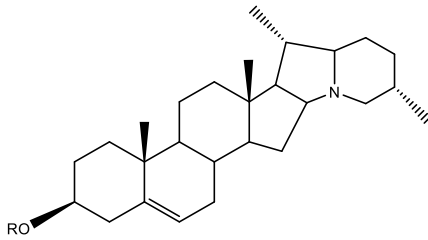
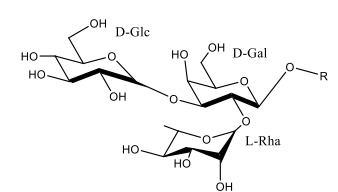
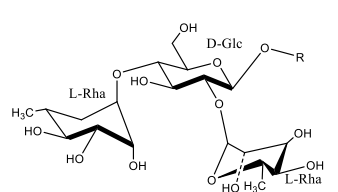
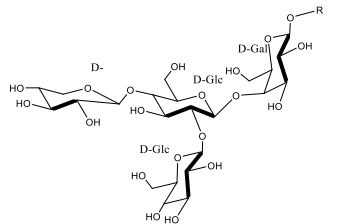
however, the use of the same dosages given on three or four consecutive days resulted in greater than 90% survival (Cham *et al.*, 1987). Thus solasodine glycosides are effective *in vivo* against murine sarcoma 180 (S180), whereas the aglycone solasodine at an equimolar concentration is ineffective (Cham *et al.*, 1987). SS-3, diosgenin 3-*O*- $\beta$ -solatrioside and protodioscin showed stronger antiproliferative activity against leukemia cells (HL-60) cells than cisplatin *in vitro* (Ono *et al.*, 2006). SS-3 also inhibited the growth of metastatic and primary melanoma cells (WM239 and WM115) and caused cellular necrosis to the melanoma cell lines WM115 and WM239, by rapid induction of lysosomal membrane permeabilisation as confirmed by cathepsin B upregulation which triggered the extrinsic mitochondrial death pathway represented by the release of cytochrome c and upregulation of TNFR1 (Al Sinani *et al.*, 2016). Solamargine showed a liver protective effect against CCL4 (carbon tetrachloride)-induced liver damage. It was also effective in the treatment of actinic keratosis (AKs), squamous cell carcinoma (SCC) and basal cell carcinoma (Wua *et al.*, 2011).

Solasonine (SS-5) is one of the steroidal glycoalkaloids and has been found in *Solanum* species. It has shown potent cytotoxicity activity against colon (HT29), breast (MCF-7, Bcap-37), cervical (HeLa), liver (HepG2), gastric (MGC-803), murine melanoma (B16F10), glioblastoma (MO59J, U343 and U251) PC-12 and HCT-116 cell, and Leukaemia K562, ileocecal (HCT-8) cells (Esteves-Souza *et al.*, 2002; Ikeda *et al.*, 2003; Lee *et al.*, 2004; Li *et al.*, 2007; Munari *et al.*, 2014a; Li *et al.*, 2016; Ding *et al.*, 2013a; Munari *et al.*, 2013). Solasonine shows potent anticonvulsant and CNS depressant activities (Chauhan *et al.*, 2011).

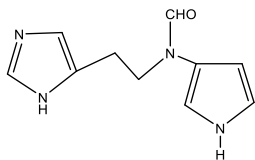
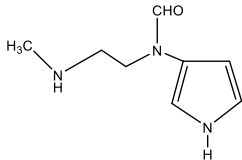
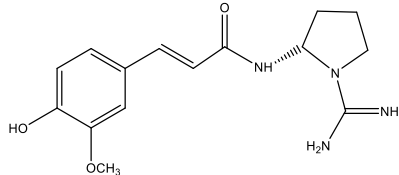
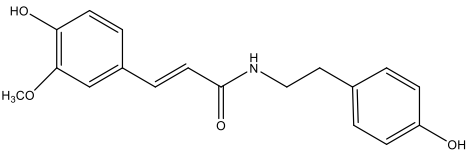
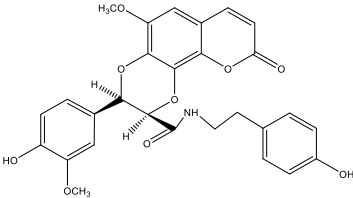
Antileishmanial activities have been evaluated for solamargine, solasonine and an equimolar mixture against promastigote forms of *L. amazonensis*. Results revealed that the equimolar mixture of solamargine/solasonine showed more activity with an

IC<sub>50</sub> value of 1.1 μM than solamargine with an IC<sub>50</sub> value of 14.4 μM compared with amphotericin B as positive control (Miranda *et al.*, 2013). Also, solamargine and solasonine alkaloids have been reported to kill intracellular and extracellular *L. mexicana* parasites more efficiently than the reference drug sodium stibogluconate (Lezama-Dávila *et al.*, 2016). α-Chaconine (SS-6) was reported as the most active glycoalkaloids against *Plasmodium yoelii* in terms of antimalarial activity. The activity was due to compounds containing the solatriose sugar chain moiety (Chen *et al.*, 2010). A study found that saponins from *S. anguivi* fruit can enhance the hypoglycemic, hypolipidemic properties in alloxan-induced diabetic rats (Elekofehinti *et al.*, 2013). The methanol extracts of *S. sodomaicum* fruit peel showed insecticidal activity against *Schistocera gregaria* fifth instar larvae (Zouiten *et al.*, 2006).

**Table 1.8 :** Selection of phytochemicals previously isolated from *S.sodomaeum*. SS: refers to the name of the plant *Solanum*.

Classification	Compound	Parts of the plant	Reference
Steroidal glycosides	 <p style="text-align: center;"><b>R</b></p>	<i>S. tuberosum</i> L (potato plants), <i>S. melongena</i> L (eggplants) and <i>Lycopersicon</i> <i>esculentum</i> (tomato plants)	(Chowanski <i>et al.</i> , 2016)
	 <p style="text-align: center;"><b>R</b></p>		
	Solasodine ( <b>SS-1</b> )    H Solasonine ( <b>SS-2</b> )    salatriose Solamargine ( <b>SS-3</b> )    chacotriose		
	Solanidine ( <b>SS-4</b> )    H α-Solanine ( <b>SS-5</b> )    solatriose α-Chaconine ( <b>SS-6</b> )    chacotriosa		
			
			
			
	Solatriose	Chacotriose	Lycotetrose

**Table 1.8 (continued):** Selection of phytochemicals previously isolated from *S. sodomaeum*. SS: refers to the name of the plant *Solanum*.

Classification	Compound	Parts of the plant	Reference	
alkaloids	 <p>Solsodamine A (SS-7)</p>	Berries <i>S. sodomaeum</i> , leaves of <i>S. cernuum</i> , roots of <i>S. erianthum</i> , seeds of <i>S. indicum</i> and aerial parts of <i>S. leuocarpum</i>	(El Sayed <i>et al.</i> , 1998)	
	 <p>Solsodamine B (SS-8)</p>			
	 <p>Cernidine (SS-9)</p>			(Ramos and de Oliveira, 2017)
	 <p><i>N-trans</i>-Feruloyltyramine (SS-10)</p>			(Yin <i>et al.</i> , 2013)
 <p>Indicumines A (coumarinolignoid alkaloids) (SS-11)</p>				

## 1.5 Aims and Objectives

The present work aimed to investigate plants from Libya in search of cytotoxic agents which could be active against cancer cells and not active against normal cells. Screening was also carried out for antidiabetic activity. These two diseases were chosen because they are very common diseases and the most common causes of death in the world.

The objectives of the work were to:

- Develop suitable methods to purify phytochemicals from selected plant extracts, using techniques such as thin layer chromatography, vacuum liquid chromatography, open column chromatography, solvent extraction and preparative thin layer chromatography
- Elucidate the structures of isolated compounds using  $^1\text{H}$  and  $^{13}\text{C}$  nuclear magnetic resonance, including extensive two-dimensional  $^1\text{H}$ - $^1\text{H}$  homonuclear (COSY, NOESY) and  $^1\text{H}$ - $^{13}\text{C}$  heteronuclear (HMBC, HSQC) experiments and mass spectrometry
- *In vitro* screening of the crude extracts, fractions and isolated pure compounds for some biological activities in the light of the traditional use of these plant. These tests included:

Cytotoxicity assessment against the cancer cell line A375 (melanoma), HeLa (cervical), LNCaP (prostate), PC-3M (prostate), PANC-1 (pancreas) and HePG2 (liver) and non-cancer PNT2 normal and HEKa (normal) cell lines using an AlamarBlue® assay which were then re examined for their effect on cell morphology, viability, adhesion, migration and invasion. In this way, it was anticipated that identification of the active components against the process of metastasis could be made

- *In vitro* screen extracts and isolated compounds for antidiabetic activity using three different enzyme inhibition assays (PTP1B,  $\alpha$ -glucosidase and  $\alpha$ -amylase)

## **Chapter 2**

### ***Materials and Methods***

## 2. Materials and methods

### 2.1 Solvents

Solvents listed below were used for the different processes of extraction, chromatographic separation and analytical TLC. All the solvents were stored at room temperature and transferred to 500 mL solvent bottles for routine use. Deuterated (99.9%) solvents ( $\text{CDCl}_3$ ,  $\text{DMSO-}d_6$ ,  $\text{CD}_3\text{OD}$  and  $\text{Acetone-}d_6$ ) were utilised for the NMR analysis.

- *n*-Butanol (Analytical grade, VWR, UK Ltd)
- *n*-Hexane (HPLC grade, VWR, UK Ltd)
- Acetone (Analytical grade, VWR, UK Ltd)
- DCM (HPLC grade, VWR, UK Ltd)
- Deuterated oxide ( $\text{D}_2\text{O}$ ) (Sigma-Aldrich, UK Ltd)
- Deuterated chloroform ( $\text{CDCl}_3$ ) (Sigma-Aldrich, UK Ltd)
- Deuterated dimethyl sulfoxide ( $\text{DMSO-}d_6$ ) (Sigma-Aldrich, UK Ltd)
- Deuterated methanol (methanol- $d_4$ ) (Sigma-Aldrich, UK Ltd)
- Deuterated pyridine ( $\text{C}_5\text{D}_5\text{N}$ ) (Sigma-Aldrich, UK Ltd)
- Ethanol (Analytical grade, VWR, UK Ltd)
- Ethyl acetate (HPLC grade, VWR, UK Ltd)
- Methanol (HPLC grade, VWR, UK Ltd)

### 2.2 Reagents and chemicals

- 0.22  $\mu\text{m}$  filter (Merck, Darmstadt, Germany)
- 4-nitrophenyl- $\alpha$ -D-glucopyranoside (Sigma N1377,UK)
- 4-nitrophenyl- $\alpha$ -D-maltohexaside (Sigma 73681 ,UK)
- Acarbose (Sigma A8980 ,UK)
- AlamarBlue® Cell Viability Assay (Invitrogen, Renfrew, UK)
- $\alpha$ -amylase (3.2.1.1) from porcine pancreas, ( Sigma A6255 ,UK)
- Anisaldehyde (FSA laboratory, UK)
- Antibumping granules (BDH, UK)
- ADP/ATP Ratio Assay Kit (Sigma-Aldrich, UK)

- Apoptosis, Necrosis and healthy cell quantitation kit plus (Biotium, USA)
- ApoTox-Glo™ Triplex Assay (Promega, USA)
- Cisplatin(Sigma-Aldrich, UK Ltd)
- Column grade silica gel (Silica gel 60, mesh size 20-200 µm (Merck, Germany)
- CytoSelect™ 48-well cell adhesion assay (collagen IV-coated, colorimetric format) (Cell Biolabs, Inc, USA)
- (DiFMUP) (Invitrogen,Thermo Fisher Scientific, UK)
- Dithiothreitol (Sigma,UK)
- DMEM (Dulbecco's Modified Eagle's medium) (Sigma Aldrich, UK)
- Ethylenediaminetetraacetic acid (Sigma E1644,UK)
- Foetal calf serum (FCS) (Invitrogen, Renfrew, UK)
- α-glucosidase (Sigma G0660,UK)
- HEPES (Sigma , UK)
- InnoCyte™ Cell Migration Assay, 96-well (Calbiochem®, Merck KGaA, Darmstadt, Germany)
- InnoCyte™ ECM Cell Adhesion Assay, Fibronectin(Calbiochem®, Merck KGaA, Darmstadt, Germany)
- Invasion assay kits (Cambridge Bioscience Ltd, Cambridge, UK)
- L-glutamine (Thermo Fisher Scientific Inc, Renfrew, UK )
- Lipophilic Sephadex LH-20 (Sigma Aldrich, UK)
- Mg<sup>2+</sup>-Ca<sup>2+</sup> -free Hank's balanced salt solution (HBSS) (Invitrogen, Renfrew, UK)
- Migration assay kits (Cambridge Bioscience Ltd, Cambridge, UK)
- Non-essential amino acids (Thermo Fisher Scientific Inc, Renfrew, UK)
- Protein tyrosine phosphatase 1B (Sigma ,UK)
- Resazurin sodium salt (Sigma Aldrich, Germany)
- RPMI 1640 (Sigma-Aldrich Ltd, Dorset, UK)
- Silica gel 60H for thin layer chromatography (Merck, Germany)
- Silica gel 60 0.063-0.200 mm for column chromatography (Merck, Germany)
- Sodium chloride (Sigma S9625,UK)
- Sodium phosphate dibasic heptahydrate Na<sub>2</sub>HPO<sub>4</sub>.7H<sub>2</sub>O (Sigma S9390-,UK)

- Sodium phosphate monobasic dehydrate  $\text{NaH}_2\text{PO}_4 \cdot 2\text{H}_2\text{O}$  (Sigma 04269-1k,UK)
- Sodium pyruvate (Thermo Fisher Scientific Inc, Renfrew, UK)
- Staurosporine (Merck KGaA, Darmstadt, Germany)
- Streptomycin/ Penicillin (Cambrex, UK)
- TFMS inhibitor (Bis(4-Trifluoromethylsulfonamidophenyl)-1,4-diisopropylbenzine), (Calbiochem 540211- 10 mg, Km 6  $\mu\text{M}$ )
- TLC grade silica gel (60H, Merck, Germany)
- TLC grade silica gel coated aluminium sheet (Precoated Silica gel PF254, Merck, Darmstadt, Germany)
- TrypLE Express (Invitrogen, Renfrew, UK)
- Virkon® (Antec International, Sudbury, UK)

### 2.3 Equipment

- 25cm<sup>2</sup> and 75cm<sup>2</sup> sterile flask (Thermo Fisher, Renfrew, UK)
- 12 and 96 well plates (Sigma-Aldrich, Poole, UK)
- 0.22 $\mu\text{m}$  filter (Millipore, UK)
- 96-well plates (TPP, Switzerland)
- 96-well round-bottom clear plate (U-shape plate, Greiner bio-one, Germany)
- A sintered glass Buchner filter funnel (Schott Duran, Germany)
- Avance DRX500 MHz NMR (Bruker, UK)
- Centrifuge 5415D (Eppendorf, Hamburg, Germany)
- Decon Sanicator (Decon laboratories, UK)
- Edwards freeze dryer ((Edwards, Crawley,UK)
- Epi florescence upright microscope (Nikon Eclipse) E600 under X60 1.40 NA objective lens was used under the following settings; Alexa555: TRITC, YFP: FITC, Nuclei: Dapi
- Haemocytometer (Hawksley, Lancing, UK)
- Infrared spectrometer ATI Mattson (Genesis series FTIR spectrometer, UK)
- Jeol Eclipse 400 NMR spectrometer (Jeol, Pleasanton, USA)
- LC-MS (Thermo fisher, Hemel Hempstead, UK)
- Microcentrifuge (Centaur, SANYO, Japan)

- Microscope (Olympus, Japan)
- Neubauer-Improved Haemocytometer (Marienfeld, Germany)
- Ninety six well plates (Greiner Bio-one, Stonehouse, UK)
- Nikon Eclipse TE300 Epifluorescent Inverted microscope (Nikon, Kingston upon Thames, UK)
- NMR tubes (5mm x178 mm, Sigma-Aldrich, UK)
- Orbitrap HRESI mass spectrometer (Thermo Fisher, Hemel Hempstead, UK)
- Rotary evaporator (Büchi, Switzerland)
- Safety Cabinet (Walker Safety Cabinets Ltd, UK)
- Soxhlet apparatus (Quickfit, UK)
- SpectraMax M5 Microplate Reader (Molecular Devices, Sunnyvale, USA)
- UV-detector 254nm and 364nm UVGL-58 (UVP, USA)
- Water Bath (Grant Instruments Ltd, UK)

## 2.4 Plant material

Plant materials were collected from Libya in March and April, 2014 (Table 2.1) by Mr Adella -Salem Botany Department, Faculty of Science, Benghazi University. The plants were air dried to prevent mould or any type of degradation. The dried plant material was ground to a fine powder. The *H. radicata* was provided by SIPBS colleague Dr Ibrahim Khadra (Strathclyde University).

**Table 2.1:** Collection details of plants and amount used in the study

Plant Species	Location and Time	Plant Amount
<i>Arum cyrenaicum</i>	Wadi Buoreequ Libya, March 2014	Root 640g, Aerial part 360g and Fruit 173 g
<i>Solanum sodomaeum</i>	Tokara, Libya, April 2014	332g
<i>Teucrium zanonii</i>	Tariha, Libya, 2014	1Kg
<i>Pituranthos tortuosus</i>	Benina, Libya March 2014	1Kg
<i>Hypochaeris radicata</i>		1Kg

## 2.5 Extraction and Partitioning

### 2.5.1 Soxhlet extraction

The plant materials were extracted in a Soxhlet apparatus using different solvents starting with lowest polarity to highly polar, hexane, ethyl acetate and finally methanol (3.5 L each). All extracts obtained were evaporated at 40 °C under vacuum using a rotary evaporator.

### 2.5.2 Maceration

The powdered plant material was soaked using five litres of solvent at one time starting with n-hexane, ethyl acetate and finally methanol. Each solvent with plant material was left for three days. Filtration was carried out after each extraction using Whatman™ filter paper, and the filtrates were evaporated at 40°C under vacuum using

a rotary evaporator until all the solvent was removed. Then the extracts were transferred into small vials using small amounts of the same solvent used for extraction and left under a fume hood at room temperature to obtain solvent-free extracts. The extraction was repeated three times for each solvent. TLC and NMR spectroscopies of the three different crude extracts were carried out.

## **2.6 Fractionation work and isolation of compounds**

Several chromatographic techniques were used for the isolation of compounds from the crude solvent extracts.

### **2.6.1 Analytical Thin Layer (TLC)**

Thin layer chromatography (TLC) was used to screen crude extracts and fractions. It was also used to analyse the collected fractions from different separation methods. In addition, it was used to choose the elution system for mobile phases of other separation methods such as column chromatography (CC), and vacuum liquid chromatography (VLC). The fractions were dissolved in an appropriate solvent and spotted approximately 1cm above the bottom edge of a TLC grade silica gel coated aluminium sheet. Solvent combinations of *n*-hexane, *n*-hexane/ethyl acetate or ethyl acetate/methanol were used as mobile phases depending on the expected polarity of the sample under analysis. Filter paper was placed inside the tank in order to saturate the jar with solvent. Spotted TLC plates were then placed in the TLC tank to develop in an ascending direction. The TLC plates were taken out of the tank, the solvent front was marked with a pencil line and the plates air-dried immediately. Plates were first examined under UV light using short ( $\lambda=254$  nm) and long ( $\lambda=366$  nm) wavelengths and subsequently sprayed with anisaldehyde- $\text{H}_2\text{SO}_4$  spray (5 ml sulphuric acid, 85 ml methanol, 10 ml glacial acetic acid and 0.5 ml anisaldehyde) and heated at  $110^\circ\text{C}$  for a minute to allow colour develop. The  $R_f$  values for each spot were calculated by dividing the distance the spot travelled, by the distance of the solvent front. TLC was used to pool similar fractions together, which were then dried and further analysed by Nuclear Magnetic Resonance (NMR) to attempt to elucidate the structure of the compounds (Gray *et al.*, 2012).

### **2.6.2 Vacuum liquid chromatography (VLC)**

Vacuum liquid chromatography (VLC) is one technique used for rapid fractionation of crude extracts using a sintered glass funnel attached to a water pump. Silica gel 60H (TLC grade) was loaded into the funnel and vacuum was applied to compress silica gel to a hard layer. The methanol or ethyl acetate extracts were dissolved in an appropriate solvent, absorbed on a small amount of silica gel 60 (mesh size 0.063-0.200 mm) and dried to achieve a free flowing powder. The powder was loaded and packed as a uniform thin layer on the top of the compressed silica gel column and the thin layer was covered with a filter paper. Hexane and ethyl acetate were used as mobile phases in different ratios of increasing polarity from hexane to methanol. Each fraction was collected, evaporated to dryness at 40°C under vacuum using a rotary evaporator. Then the fractions were checked by TLC and pooled according to similar chemical profiles (Targett *et al.*, 1979; Coll and Bowden, 1986).

### **2.6.3 Size-Exclusion Chromatography (SEC)**

This technique is also known as gel filtration chromatography or molecular sieve chromatography. The principle of SEC is the separation of molecules according to their molecular size. In this work, a slurry of Sephadex LH-20 (40g) was added to a glass column of approximately 22 cm height and 2 cm diameter. The methanol extract was dissolved in a small quantity of methanol to the top of the column. Elution was started with 100% methanol and vials of 5 ml were used to collect different fractions. Also the SEC was carried out for some fractions to purify them (Gray *et al.*, 2012).

### **2.6.4 Column Chromatography (CC)**

This technique was applied to fractionate polar and non-polar components, using an open glass column plugged with cotton wool. The glass column 55×3 cm was packed with 300 g silica gel 60 (mesh size 0.063-0.200 mm). Silica gel 60 was made into a wet slurry using the least polar solvent of the eluting system and then poured in a glass chromatography column of appropriate size. The hexane and ethyl acetate extracts were dissolved in a suitable solvent and adsorbed on a small amount of silica gel 60 (mesh size 0.063-0.200 mm), then loaded at the top of the column. A small amount of silica 60 was applied over the sample to prevent any distortion in separation. The elution was started with low polar to high polar solvents and air bubbles were

eliminated by taping. The collected fractions were analysed by TLC and pooled according to similar chemical profiles.

### **2.6.5 Preparative TLC**

This technique was mostly used for some fractions which required separating and purifying in low amounts. TLC plates 20× 20 cm were used for fractions which were dissolved in a small amount of methanol and spotted on TLC plates (20× 20 cm) as a narrow streak about 2.5 cm from the bottom. The plates were allowed to dry and then developed in an appropriate solvent system. After drying, the plates were observed under UV light (sometimes sprayed at one side with a suitable reagent if they were invisible), and the bands of interest were cut into strips along with the absorbent. The strips attributed to each separate component were cut into small pieces and soaked in a polar solvent overnight for maximum recovery. After filtration and evaporation, the recovered components were analysed by NMR spectroscopy.

### **2.6.6 Solvent extraction**

This technique is used to remove the sugars and tannins in extracts. The methanol extract was evaporated to minimise the amount of solvent then water was added to it and allowed to stand overnight. The 500 ml of solvent was filtered using filter paper then the filtrate was placed in a separating funnel. The extraction procedure was carried out starting with a low to high polar solvent (dichloromethane, ethyl acetate and n.butanol). Each solvent was added to the separating funnel, then shaken well and the solution left to form into two layers. This method was carried out for the three solvents. The extract from each step was evaporated by using a rotatory evaporator, weighed, then the crude solvent extract was fractionated using different methods. For example, the extract from dichloromethane (2g) was further purified by carrying out a small sephadex column separation, then the fractions analysed by NMR.

## 2.7 Spectroscopic examination

### 2.7.1 Nuclear Magnetic Resonance (NMR)

1D and 2D  $^1\text{H}$  and  $^{13}\text{C}$  NMR experiments were carried out on a Jeol Eclipse 400 spectrometer at 400 MHz for  $^1\text{H}$  and 100 MHz for  $^{13}\text{C}$  and Distortionless Enhancement of Polarization Transfer (DEPT) spectra and a Bruker Avance DRX-500 (500MHz) spectrometer 500 for heteronuclear multiple quantum coherence (HSQC) and heteronuclear multiple bond connectivity (HMBC). Each fraction was dissolved in about 500  $\mu\text{l}$  of a suitable deuterated solvent ( $\text{CDCl}_3$  or  $\text{DMSO}-d_6$ ) and taken in 5 mm internal diameter NMR tubes. The structures of the compounds were elucidated from the resulting spectra. The NMR spectroscopic data were processed using MestReNova software 8.1.2 (Mestrelab Research, A Coruña, and Spain) and ChemBioDraw Ultra, Version 14 (PerkinElmer, Yokohama, Japan) was used to draw compound structures. Spectra obtained for known compounds were identified following comparison with published spectral data.

#### 2.7.1.1 One-Dimensional NMR (1D)

This is the simplest technique used in structure elucidation.  $^1\text{H}$  NMR experiments were used for the determination of the types of protons in the compounds and  $^{13}\text{C}$  NMR for providing data on the number and kinds of carbon atoms in the compounds. Both  $^1\text{H}$  and  $^{13}\text{C}$  1D spectra can be less informative than two-dimensional (2D) NMR analysis especially in the case of some of the more complex organic molecules.

#### 2.7.1.2 Two-Dimensional NMR (2D)

2D NMR includes Correlation Spectroscopy (COSY), Nuclear Overhauser Enhancement Spectroscopy (NOESY), Heteronuclear Single Quantum Coherence (HSQC) and Heteronuclear Multiple Bond Coherence (HMBC).

COSY shows  $^1\text{H}$ - $^1\text{H}$  connectivities. The proton shifts are plotted on both axes with the contour plot along the diagonal of the square. NOESY records all the  $^1\text{H}$ - $^1\text{H}$  NOE correlations occurring in a molecule. HSQC was used to identify the correlation between protons and carbons atoms in samples through the  $^1J$  coupling between them.

HMBC provided the correlation between the chemical shift of the protons in the samples and the heteronucleus  $^{13}\text{C}$  through  $^2J$  and  $^3J$  coupling interaction between the nuclei (long-range H-X-C-C-C correlations).

### **2.7.2 Mass spectrometry**

This technique is used to elucidate the elemental composition of a sample. One mg of each sample was dissolved in 1ml methanol and 10  $\mu\text{L}$  of the solution was then injected along with an infusion of 0.1% (v/v) formic acid in water (solution A) and 0.1% (v/v) formic acid in acetonitrile (solution B) at a flow rate of 300  $\mu\text{L}/\text{min}$ . A gradient method was used for elution of the mobile phase starting with 10% (v/v) solution B in solution A to reach 100% of solution B then reduced again to 10% (v/v) solution B. Positive ion and negative ion mode electrospray (ESI) experiments were carried out on a Dionex ultimate 5000 LC-Exactive Orbitrap mass spectrometer.. MS data acquisition was carried out by Dr. Tong Zhang (SIPBS, University of Strathclyde).

### **2.7.3 Infrared spectroscopy (IR)**

The sample was prepared in disc form by pressing with potassium bromide and measured between 4000 and 667  $\text{cm}^{-1}$ . An infrared spectrum was obtained using an ATI Mattson spectrometer.

## **2.8 Bio activity examination**

### **2.8.1 Tissue culture**

#### **2.8.1.1 Maintenance of the cells**

All cell lines used were kindly provided by researchers at the University of Strathclyde and Mrs. Louise Young (University of Strathclyde, UK). All cell lines were grown in a humidified incubator at 37°C with 5% CO<sub>2</sub>. Every 3-4 days, a 75 cm<sup>2</sup> flask of cells (75% confluency), the growth medium was discarded (or used in bioassays). The medium was decanted into Virkon disinfectant, the cells were washed with 5 ml Mg<sup>2+</sup>-Ca<sup>2+</sup>-free Hank's Balanced Salt solution (HBSS) solution and trypsinised by adding 5 ml of TrypLE Express and then incubated at 37°C for 4 to 6 min according to the cell type. The cells were then observed under the microscope to ensure complete detachment of the cells. The action of TrypLE Express was stopped by adding 10 ml of complete culture medium (Table 2.2). The cells were then centrifuged at 1000×g for 5 min, the medium was removed, and the pellet resuspended in 10 ml of fresh complete medium. The cell numbers were counted using a haemocytometer and adjusted to the required number according to the cell type.

#### **2.8.1.2 Preparation of complete culture medium**

All procedures were carried out in a sterile environment and the medium for each cell line was prepared in a sterile flow hood and was then stored at 4°C until required (Table 2.2). Cells were grown in an incubator at 37°C, 100% humidity and 5% CO<sub>2</sub> and subcultured every 3 days. All the cell lines used in this study were adherent with an epithelial morphology.

**Table 2.2:** Cell culture media of the cell lines used in this study.

<b>Cell lines</b>	<b>Complete Culture Medium</b>
1. HeLa cells cervical cancer	500 ml Dulbecco's Modified Eagle's Medium (DMEM) supplemented with 50 ml foetal calf serum 10% (v/v), 5 ml penicillin/streptomycin and 5 ml L-glutamine
2. LNCaP cells prostate carcinoma	500 ml RPMI 1640 medium supplemented with 50 ml foetal calf serum 10% (v/v), 5 ml penicillin/streptomycin, 5 ml L-glutamine and 5 ml sodium pyruvate
3. PC-3M cells prostate carcinoma	500 ml DMEM supplemented with 50 ml foetal calf serum 10% (v/v), 5 ml penicillin/streptomycin and 5 ml L-glutamine
4. PANC-1 cells pancreatic carcinoma	500 ml DMEM supplemented with 50 ml foetal calf serum 10% (v/v), 5 ml penicillin/streptomycin and 5 ml L-glutamine
5. HepG2 cells liver hepatocellular carcinoma	500 ml DME) supplemented with 50 ml foetal calf serum 10% (v/v), 5 ml penicillin/streptomycin and 5 ml L-glutamine
6. A375 cells malignant melanoma	500 ml DMEM supplemented with 50 ml foetal calf serum 10% (v/v), 5 ml penicillin/streptomycin and 5 ml L-glutamine
7. PNT2 cells normal prostate	500 ml RPMI 1640 medium supplemented with 50 ml foetal calf serum 10% (v/v), 5 ml penicillin/streptomycin and 5 ml L-glutamine.
8. HEKa cells normal Human Epidermal Keratinocytes	500 ml DMEM supplemented with 50 ml foetal calf serum 10% (v/v), 5 ml penicillin/streptomycin and 5 ml L-glutamine

### 2.8.1.3 Cytotoxicity assay

An AlamarBlue® assay, based on resazurin, was used to detect the effect of sample on cell metabolic activity. Resazurin is a non-toxic, cell permeable compound that is blue in colour and virtually non-fluorescent. Upon entering metabolically active cells, resazurin is reduced to resorufin, a compound that is red in colour and highly fluorescent. The cytotoxicity of the crude extracts and compounds were determined using 0.01% (w/v) resazurin solution (5mg in 50 ml deionised H<sub>2</sub>O). This was then filtered sterilised using a 0.22 µm filter unit. The number of cells required for the cytotoxicity bioassay was 1x10<sup>5</sup> cells/ml per plate (ie 1x10<sup>4</sup> cells in 100 µg /well). For the crude extracts and compounds, one gram of each sample was dissolved in 1.0 ml DMSO and diluted 1:9 with complete medium to give 1mg/ml of plant extract or compound in 5% (v/v) DMSO. On day one, the cell plates were prepared with numbers of cells required then incubated for 24 h at 37°C, 5% CO<sub>2</sub>, before the samples were added. On day two, a 1:1 serial dilution of each sample was performed in a dilution plate to give a concentration range from 500µg/ml to 3.9µg/ml µg/ml. The diluted test sample (100 µl) was transferred to the corresponding assay well in the cell plate to give a final assay volume of 200 µl. The final serial dilution was from 250µg/ml to 1.9µg/ml. Controls (serial dilutions of 0.5% upto 50% DMSO as solvent controls) were added to the appropriate control wells and staurosporine was added for a cell death control. The plate was then incubated for 24 h at 37°C in a humidified atmosphere containing 5% CO<sub>2</sub>. On day 3, 10% (v/v) resazurin solution was added to each well and the assay plate was wrapped with tin foil and returned to the incubator under the previous conditions. Fluorescence intensity was measured after 24 h using a SpectraMax M5 micro-plate reader at the excitation and emission wavelengths of 560 nm and 590 nm, respectively. These results were transferred to Microsoft Excel for analysis. Readings after 24 h were deemed as optimal.

Each sample was tested in triplicate and the results are expressed as cell viability as a percentage of the cell only control. The equation used to determine the cell viability is shown below:

$$\% \text{ Cell Viability} = \frac{\text{Mean of Sample (OD560-590)}}{\text{Mean of Control (OD560-590)}} \times 100$$

Extracts were considered to be toxic if they caused a reduction in cell viability by at least 50% or more. Statistical analysis was carried out using analysis of variance (ANOVA) with a Dunnet's post-test using MiniTab 16 and graphs were plotted using GraphPad Prism5.0.

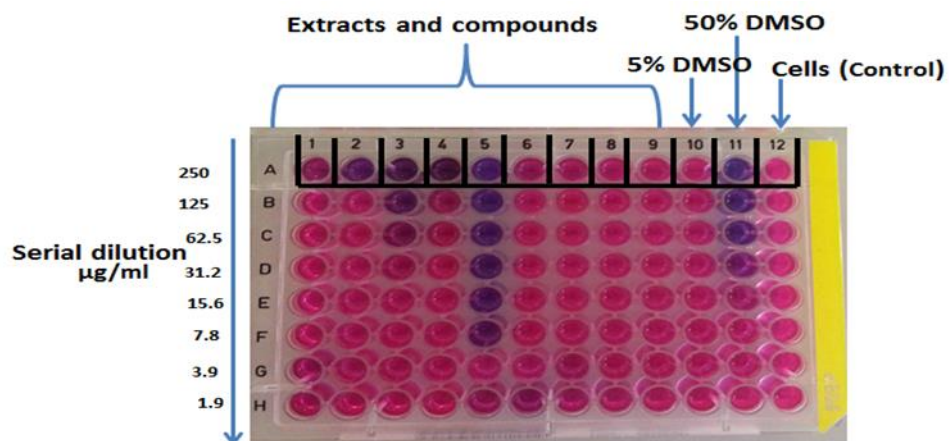


**Figure 2.1:** Template of a cytotoxicity plate layout.

### **2.8.2 SYTOX®Green assay**

SYTOX®Green is a high-affinity nucleic acid stain that easily penetrates cells with compromised plasma membranes, but will not penetrate intact cell membranes. Cells were seeded at  $1 \times 10^5$  cells per well in complete medium in a 96 well plate (100µl) and incubated for 24 h. Samples were prepared in complete medium and 100µl added to the wells and incubated for 24 h (sample prepared at concentrations of 1.9 to 250µg/ml). SYTOX®Green was used at a final concentration of 5µM in each well and incubated for 15min at 37°C in a humidified atmosphere with 5% CO<sub>2</sub>. A SpectraMax M5 micro plate reader was used to measure the fluorescence intensity at 485-535nm.

### **2.8.3 Effect of staurosporine and cisplatin**

Staurosporine was used as a positive control to induce apoptosis in the cells, used at 5 µl/ml. (The stock solution consisted of 250 µg/ml of staurosporine in 535 ml DMSO; 5 µg from stock was add to 995 µl of medium). The staurosporine was added to the cells and incubated for 24 h at 37°C in an atmosphere containing 5% CO<sub>2</sub> in air before lysing the cells. Cisplatin, cisplatinum, or cis-diamminedichloroplatinum (II) is an anticancer or cytotoxic agent (chemotherapy drug). It is as an alkylating agent and it has been used for treatment of various types of cancers, including carcinomas, germ cell tumors, lymphomas, and sarcomas. Here it was used at 100 µg/ml (stock solution 1mg/ml in one ml DMSO; 100 µl from stock was added into 900 µl of medium), added to the cells and incubated for 24 h at 37°C in an atmosphere containing 5% CO<sub>2</sub>.

### **2.8.4 ApoTox-Glo™ Triplex Assay**

The ApoTox-Glo™ Triplex Assay is a combination of three Promega assay chemistries to assess viability, cytotoxicity and caspase activation. The first part of the assay simultaneously measures two protease activities; one is a marker of cell viability, and the other for cytotoxicity. The live-cell protease activity intact with viable cells and is measured using a fluorogenic, cell-permeant, peptide substrate (glycyl-phenylalanyl-aminofluorocoumarin; GF-AFC).The GF-AFC substrate can enter live cells where it is cleaved by the live-cell protease to release AFC. The bis-AAF-R110 substrate (bis-alanylalanyl-phenylalanyl-rhodamine 110; bis-AAF-R110) cannot enter live cells, but instead can be cleaved by dead-cell proteases to release R110. The live-

and dead-cell proteases produce different products, AFC and R110, which have different excitation and emission spectra, allowing them to be detected simultaneously.

The assay for a 96-well plate, contained 10ml assay buffer, 10 $\mu$ l GF-AFC substrate (100mM in DMSO), 10 $\mu$ l bis-AAF-R110 substrate (100mM in DMSO), 10ml Caspase-Glo® 3/7 buffer, Caspase-Glo® 3/7 substrate (lyophilized), all components stored at -20°C protected from light.

For the preparation of reagents, warmed assay buffer, GF-AFC substrate and bis-AAF-R110 substrate at 37°C in a water bath, while caspase-Glo® 3/7 buffer and caspase-Glo® 3/7 substrate were used at room temperature. The contents of the GF-AFC and bis-AAF-R110 substrates were transferred into 2.5 ml of assay buffer, (for 96-well plates, transferred 10 $\mu$ l of each substrate into 2 ml of assay buffer). The assay buffer containing substrates were mixed by vortexing the contents until the substrates were thoroughly dissolved. This mixture will be referred to as the viability/cytotoxicity reagent. Once prepared, the viability/cytotoxicity reagent containing both substrates were used within 24 h if stored at room temperature. Unused viability/cytotoxicity reagent was stored at 4°C for up to 7 days with no appreciable loss of activity. The contents of the caspase-Glo® 3/7 buffer was transferred into an amber bottle containing caspase-Glo® 3/7 substrate. They were mixed by inverting the contents until the substrate was thoroughly dissolved to form the caspase-Glo® 3/7 reagent for 20 seconds.

Cells were seeded at 1x10<sup>6</sup> cells per well in complete medium in a 96 well plate (100  $\mu$ l) and incubated for 24 h. Compounds and controls were added to appropriate wells for a final volume of 100 $\mu$ l per well and incubated for 3 h. A 20  $\mu$ l aliquot of viability/cytotoxicity reagent containing both GF-AFC and bis-AAF-R110 substrates were added to all wells, and briefly mixed by orbital shaking (for 30 seconds) and incubated for 30 min at 37°C. A SpectraMax M5 micro plate reader was used to measure fluorescence at the two wavelengths 400Ex/505Em (for viability) and 485Ex/520Em (for cytotoxicity). After reading, 100  $\mu$ l of Caspase-Glo® 3/7 reagent was added to all wells, and briefly mixed by orbital shaking (for 30 seconds), incubated for 30 min at room temperature, and the luminescence measured.

### 2.8.5 ADP/ATP Ratio Assay Kit

The ADP (adenosine diphosphate) /ATP (adenosine triphosphate) ratio assay kit provides a simple and direct procedure for measuring ADP and ATP levels in cells for the screening of apoptosis, necrosis, and cell proliferation. The assay includes two steps. In the first step, the working reagent lyses cells to release ATP and ADP. In the presence of luciferase, ATP immediately reacts with the substrate D-luciferin to produce light. The light intensity is a direct measure of the intracellular ATP concentration. In the second step, the ADP is converted to ATP through an enzyme reaction. This newly formed ATP then reacts with the D-luciferin as in the first step. The second light intensity measured represents the total ADP and ATP concentration in the sample.

Components of the assay: assay buffer 10 ml, substrate 120  $\mu$ l, cosubstrate 120  $\mu$ l, ATP Enzyme 120  $\mu$ l and ADP Enzyme 120  $\mu$ l

**Assay Reaction:** before beginning the assay, the assay buffer was warmed, the substrate and cosubstrate were kept at room temperature and ADP enzyme reagents was defrosted on at  $-20^{\circ}\text{C}$ .

Cells were seeded at  $1 \times 10^6$  cells per well in complete medium in a 96 well plate (100 $\mu$ l) and incubated for 24 h and After which, samples were added to the wells at a final concentration between 250-125 $\mu$ g/ml. After 24 h, ATP reagent was prepared which contained assay buffer 95 $\mu$ l, substrate 1 $\mu$ l, cosubstrate 1 $\mu$ l and ATP enzyme 1  $\mu$ l. The medium was removed from the wells of the plate; 90  $\mu$ l of ATP reagent was added to each well and the plate tapped briefly to mix. The plate was incubated for 1 min at room temperature and read at luminescence for the ATP assay ( $\text{RLU}_A$ ). The plate was incubated for an additional 10 min, during the incubation; ADP reagent was prepared containing water 5  $\mu$ l and ADP Enzyme 1 $\mu$ l. After incubation, the luminescence for ATP ( $\text{RLU}_B$ ) was read. This measurement provided the background prior to measuring ADP (i.e., the residual ATP signal). Immediately following the reading of  $\text{RLU}_B$ , 5  $\mu$ l of ADP reagent was added to each well and mixed by tapping the plate or pipetting. After 1 min, the luminescence ( $\text{RLU}_C$ ) was read. The ADP/ATP ratio was calculated using the formula below.

$$\text{ADP/ATP ratio} = \frac{\text{RLUC} - \text{RLU}_B}{\text{RLUA}} \times 100$$

### **2.8.6 Apoptosis, necrosis and healthy cell quantitation kit plus**

Apoptosis and necrosis are two processes by which cells die. During apoptosis, phosphatidylserine (PS) is translocated from the inner to the outer surface of the cell, allowing the dying cell to be engulfed by phagocytic cells. Annexin V is a 35 kD  $\text{Ca}^{2+}$ -dependent phospholipid binding protein with a high affinity for PS. The assay contains Annexin V labeled with CF<sup>TM</sup>488A (excitation/emission: 490/515 nm) for staining PS on the surface of apoptotic cells with green fluorescence. Necrosis resulted due to both internal organelle and plasma membrane integrity loss, resulting in spilling of cell contents into the surrounding environment. Ethidium Homodimer III (EthD-III) is a highly positively charged nucleic acid probe, which is impermeant to live cells and early apoptotic cells, but stains necrotic cells and late apoptotic cells with red fluorescence.

Cells of  $1 \times 10^6$  were fixed onto the coverslip per well in a 12well plate (100 $\mu$ l) then incubated at 37°C in an atmosphere containing 5%  $\text{CO}_2$ . After 24 h, the cells were washed twice with PBS and 1X binding buffer was prepared by diluting 5X Annexin V binding buffer 1:5 with  $\text{H}_2\text{O}$ , and staining solution by adding the following 5  $\mu$ L of CF<sup>TM</sup>488-Annexin V, and 5 $\mu$ L of EthD-III in 100  $\mu$ L 1X binding buffer (enough staining solution to cover cells). The samples and stains were added to the cells, incubated for 15 min at room temperature covered with foil to protect from light. After incubation the cells were washed twice with 1X binding buffer, then the coverslips carefully removed and placed cells face down, washed 3 times in PBS, dried carefully and mounted onto a microscope slide using 8 $\mu$ l of MOWIOL and left for 30 min to fix. The covered cells were then examined and all images were captured on a Epi fluorescence upright microscope (Nikon Eclipse) E600. X60 1.40 NA objective lens was used under the following settings; Alexa555: TRITC, YFP: FITC, Nuclei: Dapi and ImageJ used to open the pictures.

### **2.8.7 Adhesion of PANC-1 cells to fibronectin using an InnoCyte™ ECM Cell Adhesion Assay (Fibronectin)**

Following the manufacturer's instructions, 100µl of  $5 \times 10^5$  cells/ml containing samples at final concentrations of 250 to 1.9µg/ml in serum-free medium, and incubated at 37°C in a humidified atmosphere with 5% CO<sub>2</sub>. After incubation for 4 h, The non-adherent cells were then washed away twice with 200 µl of PBS solution. After washing the cells, 100 µl of calcein-AM solution was added to each well. The plate was incubated for 1 h at 37°C in a cell culture incubator. A SpectraMax M5 micro plate reader was used to measure fluorescence at 485 and 520 nm. The results were calculated as % adhesion, where the untreated control was considered 100% adhesion.

### **2.8.8 Adhesion of PANC-1 cells to collagen IV using a CytoSelect™ 48-Well Cell Adhesion Assay (Collagen IV)**

Following the manufacturer's instructions and under sterile conditions, the collagen IV adhesion plate was warmed up at room temperature for 10 min. After which, 150 µl of a cell suspension containing  $0.5 \times 10^6$  cells/ml in serum-free medium and samples (at 250 to 1.9 µg/ml) were added directly to the cell suspension in the wells of the plate. One hundred fifty µl of the cell suspension was added to each well containing BSA (BSA-coated wells are provided as a negative control) and incubated at 37°C in a humidified atmosphere with 5% CO<sub>2</sub>. After 90 min, the media carefully discarded from each well. Each well was washed 4 times with 250 µl PBS, then the PBS aspirated from each well. A 200 µl of cell stain solution was added to each well and incubated at room temperature. After 10 min, the cell stain solution discarded from the wells and gently washed 4times with 500 µl deionized. The deionized water discarded and left the wells to air dry. Subsequently, 200 µl extraction solution was added to each well and then incubated for 10 min. 150 µl from each extracted sample was transferred to a 96-well microtiter plate. A SpectraMax M5 micro plate reader was used to measure the absorbance at 540nm.

### **2.8.9 Migration assay using a Cytoselect™ 24-well Cell Migration Assay**

Following the manufacturer's instructions, 300 µl of a cell suspension containing  $5 \times 10^5$  cells/ml in serum-free medium with the sample at final concentrations of 15.6 to 250 µg/ml were added to the inside of each upper chamber of the cell culture inserts (polycarbonate membrane, 8µm pore size to assay the migratory properties of cells) in a 48 well plate. Culture medium (500 µl) containing 30% (v/v) foetal calf serum (chemo attractant) was added to the lower chamber of the migration plate; 1µM of latrunculin B was added as a negative control and incubated at 37°C in a humidified atmosphere with 5% CO<sub>2</sub>. After 24 h, 300 µl of the labeling/detachment solution was added to the unused rows of the cell culture insert. The upper chamber was removed from using forceps and carefully discarded remaining cells then the upper chambers were replaced in the wells containing the cell labeling/detachment solution and incubated at 37°C in a humidified atmosphere with 5% CO<sub>2</sub>. After 20 min, each upper chamber was removed by forceps and gently tapped against the bottom of the well to ensure complete removal of cells. The cell culture insert containing the dislodged cells was incubated for an additional 40 min at 37°C in a CO<sub>2</sub> tissue culture incubator. Finally, 200 µl of the dislodged and labeled cells were transferred to an appropriate number of wells on a black Module strip and the fluorescence measured at 485 and 520 nm using a SpectraMax M5 micro plate reader. The results were calculated as % migration of the untreated control, which was considered 100% migration.

### **2.8.10 Invasion assay using a Cytoselect™ 24-well Cell Invasion Assay**

Following the manufacturer's instructions, the protocol was as above (2.6.9), except the basement membrane layer of the cell culture inserts was rehydrated by adding 300 µl of warm serum-free media to the inner compartment and incubated at room temperature for 1 h. The difference between the invasion and migration assay kit is the inserts are coated with a uniform layer of dried basement membrane matrix solution in the invasion assay, which serves as a barrier to discriminate invading from non-invading cells. The results were calculated as a % invasion of the untreated control, which was considered 100% invasion.

## **2.9 Effect of the extracts and compounds on the activities of PTP1B, $\alpha$ -glucosidase and $\alpha$ -amylase enzymes**

### **2.9.1 Z-factor**

The Z Factor (also known as Z prime, Z') is a measure of quality of an assay and has been proposed for use in high throughput assays to determine whether a result is large enough to be investigated further. It shows the separation between the positive and negative controls and indicates the likelihood of a false positive or negative. The Z Factor is defined by four parameters: the means and standard deviations of both the positive and negative controls in an assay. Given these values, the Z-factor is defined as:

$$Z \text{ Factor} = 1 - \frac{3 \times \text{StDev} (-) + 3 \times \text{StDev} (+)}{\text{Mean} (-) + \text{Mean} (+)}$$

SD-: the negative control standard deviation

SD+ : the positive control standard deviation

Ave+: the positive control average

Ave- : the negative control average

The Z Factor was determined for each enzyme assay below: PTP1B,  $\alpha$ -glucosidase and  $\alpha$ -amylase inhibition assays. The positive control was added to half of a 96 well plate while the negative control was added to the remaining half of the same 96-well plate. The assay was then carried out according to the specific protocols by adding the enzyme and substrate before the plate was analysed on a plate reader. Following this, the Z factor was determined. Values between 0.5 – 1 are excellent, 0 – 0.5 are acceptable and less than 0 indicate that the assay will not perform well in a high throughput context. The higher the Z factor value, the more reliable and reproducible the assay is thought to be.

### **2.9.2 Plant sample preparation**

Plant stock was prepared at 10 mg/ml in DMSO (stored at -20°C). In all the enzyme assays, samples (crude or pure compounds) were screened at 30 $\mu$ g/ml in a 96-well

round-bottom clear plate. Ten  $\mu\text{l}$  of the prepared sample was added to the enzyme and substrate in the enzyme assay plate.

### **2.9.3 PTP1B assay**

#### **2.9.3.1 Buffer preparation**

The buffer was composed of the following: 25 mM HEPES, 50 mM sodium chloride, 2 mM dithiothreitol, 2.5 mM ethylenediaminetetraacetic acid (EDTA) and 0.01 mg/ml BSA. All were dissolved in 500 ml of distilled water and the pH was adjusted to 7.2. An amended protocol was also used which consisted of the addition of catalase (0.25mg/ml) to the assay buffer. Due to the addition of dithioreitol, some natural extracts may produce hydrogen peroxide, which can interfere in the assay causing potential false positive results. Therefore, by adding catalase to the buffer, the false positives are minimised. All other procedures and reagents remained the same.

#### **2.9.3.2 Enzyme preparation**

One hundred  $\mu\text{l}$  of the enzyme PTP1B was added to 25 ml of the buffer and aliquoted into 1 ml (100  $\mu\text{l}$  was sufficient for each plate) then stored at  $-80^{\circ}\text{C}$ . A working solution of 2 nM was needed, therefore, 100  $\mu\text{l}$  of the stock was added to 2.5 ml of PTP1B buffer.

#### **2.9.3.3 Substrate preparation**

6, 8-difluoro-4-methylumbelliferyl phosphate (DiFMUP) was used as a substrate. The stock was prepared in DMSO and the final concentration on the assay plate was  $10\mu\text{M}$ .  $K_m = 6\mu\text{M}$ .

#### **2.9.3.4 Inhibitor preparation**

Bis(4-trifluoromethylsulfonamidophenyl)-1,4-diisopropylbenzine (PTP Inhibiter IV) (TFMS) was used as a positive control. A serial dilution of TFMS was prepared to produce a final concentration range of  $100\mu\text{M}$  to  $30\mu\text{M}$ .

#### **2.9.3.5 Assay method**

In a 96-half-well flat-bottom black plate (Costar®), 10  $\mu\text{l}$  of the standard (TFMS) or samples were added. Then 20  $\mu\text{l}$  of PTP1B enzyme was added to each well, and incubated for 30 min at  $37^{\circ}\text{C}$  in an atmosphere containing 5%  $\text{CO}_2$ . Ten  $\mu\text{l}$  of the

substrate was added to the wells then incubated for another 10 min. The plate was tested on a Wallac Victor2, (ex 355 nm/em 460 nm). Each sample was tested in triplicate and the results are expressed as % inhibition compared to the control and was calculated as follows:

$$\% \text{ Inhibition} = \frac{\text{Control Reading} - \text{Sample Reading}}{\text{Control Reading}} \times 100$$

The control consisted of assay buffer with enzyme and substrate to a final volume of 40 $\mu$ l. The  $K_i$  for the reference standard was also calculated. Statistical analysis was carried out using ANOVA with a Dunnet's post-test using MiniTab 16 and graphs were plotted using GraphPad Prism 5.0.

#### **2.9.4 $\alpha$ -Glucosidase assay**

##### **2.9.4.1 Buffer preparation**

Phosphate buffer at a concentration of 0.1 mM was freshly prepared by mixing 25.5 ml of solution A and 24.5 ml of solution B. The volume was topped up to 100 ml with distilled water. The pH was adjusted to 6.8.

**Solution A:** sodium phosphate monobasic dehydrate  $\text{NaH}_2\text{PO}_4 \cdot 2\text{H}_2\text{O}$  prepared at a concentration of 0.2 M in distilled water (13.9 g in 500 ml distilled  $\text{H}_2\text{O}$ ).

**Solution B:** sodium phosphate dibasic heptahydrate  $\text{Na}_2\text{HPO}_4 \cdot 7\text{H}_2\text{O}$  prepared at a concentration of 0.2 M in distilled water (26.8 g in 500 ml distilled  $\text{H}_2\text{O}$ ).

Stock solutions A and B were kept at room temperature.

##### **2.9.4.2 Enzyme preparation**

The enzyme used was yeast  $\alpha$ -glucosidase. A stock concentration was made up in water to 75units/ml and kept at  $-20^\circ\text{C}$  until required. A final concentration of 0.2units/ml was used.

#### **2.9.4.3 Substrate preparation**

P-nitrophenyl- $\alpha$ -D-glucopyranoside was used as the substrate. A stock solution was prepared in phosphate buffer and stored at  $-20^{\circ}\text{C}$  until required. A final concentration of 1mM was used.

#### **2.9.4.4 Inhibitor preparation**

Acarbose was used as a positive control and a standard curve was prepared to produce a final concentration range from 25mM to 10 $\mu$ M.  $K_m = 0.83\text{mM}$ .

#### **2.9.4.5 Assay method**

In a 96-half-well clear flat-bottom plate (Costar®), 10  $\mu$ l of standard (Acarbose) or samples were added to the wells. Twenty  $\mu$ l of  $\alpha$ -glucosidase enzyme was added to each well and incubated for 10 min at  $37^{\circ}\text{C}$  in an atmosphere containing 5%  $\text{CO}_2$ . Ten  $\mu$ l of the substrate was added to the wells and then incubated for another 10 min at  $37^{\circ}\text{C}$  in an atmosphere containing 5%  $\text{CO}_2$ . The optical density was tested on a Spectramax plate reader at 450 nm. Each sample was tested in triplicate and the results are expressed as % inhibition compared to the control. The % inhibition was calculated as follows:

$$\% \text{ Inhibition} = \frac{\text{Control Reading} - \text{Sample Reading}}{\text{Control Reading}} \times 100$$

The control consisted of assay buffer with enzyme and substrate to a final volume of 40 $\mu$ l. The  $K_i$  for the reference standard was also calculated. Statistical analysis was carried out using ANOVA with a Dunnet's post-test using MiniTab 16 and graphs were plotted using GraphPad Prism version 4.0.

### **2.9.5 $\alpha$ -amylase assay**

#### **2.9.5.1 Buffer preparation**

The assay buffer consisted of 50mM HEPES in water at pH 7.1.

#### **2.9.5.2 Enzyme preparation**

The enzyme used was porcine pancreas  $\alpha$ -amylase. A stock concentration was made

up in water to 250 units/ml and kept at -20°C until required. A final concentration of 125units/ml was used.

### **2.9.5.3 Substrate preparation**

4-nitrophenyl  $\alpha$ -D-maltohexaside was used as the substrate. A stock solution was prepared in assay buffer and stored at -20°C until required. A final concentration of 1.5mM was used.

### **2.9.5.4 Inhibitor preparation**

Acarbose was used as a positive control and a standard curve was prepared to produce a final concentration range from 300nM to 1mM.  $K_m = 01.8mM$ .

### **2.9.5.5 Assay method**

In a 96-half-well flat-bottom clear plate (Costar®), 10  $\mu$ l of standard (acarbose) or samples were added to the plate, and then 20  $\mu$ l of  $\alpha$ -amylase enzyme was added to each well. The plate was incubated for 30 min at 37°C in an atmosphere containing 5% CO<sub>2</sub>. 10  $\mu$ l of the substrate was added to the wells and then incubated for another 30 min at 37°C in an atmosphere containing 5% CO<sub>2</sub>. The optical density was tested using a Spectramax plate reader at 450 nm. Each sample was tested in triplicate and the results are expressed as percent inhibition compared to the control. The percent inhibition was calculated as follows:

$$\% \text{ Inhibition} = \frac{\text{Control Reading} - \text{Sample Reading}}{\text{Control Reading}} \times 100$$

## **Chapter 3**

### ***Results***

## Part1: Phytochemistry

### 3.1 Solvent extraction and yield

Solvent extraction using a Soxhlet apparatus was carried out to obtain crude extracts from the aerial parts of *T. zanonii*, *A. cyrenaicum* and *P. tortuosus* and from the fruit of *S. sodomaeum*, and *A. cyrenaicum* and from the root of *A. cyrenaicum*, while maceration was used to obtain crude extracts from *H. radicata* whole plant. The aim of maceration was to reduce the decomposition of active compounds. Table 3.1 shows the yields obtained from the extractions.

**Table 3.1:** Yields of solvent extractions

Plant Name and Part	Starting material (g)	Yield hexane (%)	Yield ethyl acetate (%)	Yield methanol (%)
<i>T. zanonii</i> aerial part	400	1.5	1.75	3.5
<i>H. radicata</i> whole plant	1000	2.4	2.1	2.1
<i>S.sodomaeum</i> fruit	331	5.1	2.3	7.8
<i>P. tortuosus</i> aerial part	510	2.9	1.5	3.7
<i>A. cyrenaicum</i> .fruit	173	1.4	1.2	7.51
<i>A. cyrenaicum</i> aerial part	364	7.857	2.2	ND
<i>A. cyrenaicum</i> root	640	0.628	1	4.3

ND = not determined.

### 3.2 Fractionation of *A. cyrenaicum* crude extracts

CC was used to fractionate the hexane extract of the aerial part (8g, 2.1% of yield), the hexane fruit (2g, 1.1% of yield) and the EtOAc extract of the fruit (2g, 1.2% of yield) and root (6g, 0.93% of yield) of *A. cyrenaicum*. The methanol extract of *A. cyrenaicum* fruit (13.0g, 7.5% of yield) was divided into two parts for further fractionation. A VLC column was used to fractionate the first part of the extract (6g, 3.4% of yield). The second part of the extract (1.5g, 0.86% of yield) was subjected to fractionation using a Sephadex column. The methanol extract of *A. cyrenaicum* root (28g, 4.3% of yield) was subjected to VLC. The ethyl acetate aerial part of *A. cyrenaicum* (6g, 1.6% of yield) was subjected to VLC. The silica gel and sephadex columns were used to purify fractions from *Arum cyrenaicum* extracts. TLC was used to compare compound

profiles. From the bands that showed on the plate, the  $R_f$  values were calculated. Fractions were assessed using NMR, which also enabled elucidation of the structure of ARE-6-6 and ARE-6-18, isolated from the EtOAc extract of the aerial part of *A. cyrenaicum*. ARH32 was isolated from the hexane extract of the aerial part of *A. cyrenaicum*. The fractions coded ARH 11-18, ARH 62-68 and ARH 38 were examined by  $^1\text{H-NMR}$ , and identified as cycloartane type, pheophytin A, a mixture of  $\beta$ -sitosterol and stigmasterol and mainly associated with some unsaturated fatty acids (data not shown, Appendix IV). The purification methods were applied to those fractions; however the  $^1\text{H NMR}$  spectra of the fractions obtained from purification showed no differences from the original spectrum, therefore, the separation process should be repeated in the future using different conditions.

### 3.2.1 Characterisation of ARE-6-6 as a *para*-hydroxybenzoic acid

The compound ARE-6-6 (Figure 3.1) was isolated from the ethyl acetate of *A. cyrenaicum* extract using a Sephadex column. After spraying with *p*-anisaldehyde-sulphuric acid reagent and heating, a brown spot appeared with  $R_f$  value of 0.70 using 10% (v/v) MeOH in EtOAc as the mobile phase on TLC.

The  $^1\text{H NMR}$  spectrum (Figure 3.2A, Table 3.2) indicated the presence of a 1,4-disubstituted aromatic ring with proton signals at  $\delta_{\text{H}}$  6.93 ppm (2H, *d*, 8.8Hz) and  $\delta_{\text{H}}$  7.93 ppm (2H, *d*, 8.8Hz). In the HMBC (Figure 3.2B, Table 3.2) the proton at  $\delta_{\text{H}}$  7.93 ppm (H-2) showed  $^3J$  correlation to  $\delta_{\text{C}}$  131.6 (C-6), 162.3 (C-4) and 171.9 (C-7) a carbonyl group. The proton at  $\delta_{\text{H}}$  6.93 ppm (H-3) showed also  $^3J$  correlation to  $\delta_{\text{C}}$  121.6 (C-1),  $\delta_{\text{C}}$  114.5 (C-5) and  $^2J$  correlation  $\delta_{\text{C}}$  162.3 ppm (C-4). The COSY showed the protons H-2 and H-6 at  $\delta_{\text{H}}$  7.93 (2H, *d* 8.8) correlate to protons H-3 and H-5 at  $\delta$  6.93 (2H, *d* 8.8 Hz).

The HRESI-MS data showed a molecular ion  $[\text{M}]^-$  at  $m/z$  137.0246, suggesting a molecular formula of  $\text{C}_7\text{H}_6\text{O}_3$ . The NMR results were consistent with the literature (Cho *et al.*, 1998) this is the first report of its isolation from *A. cyrenaicum*.

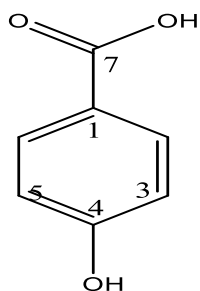
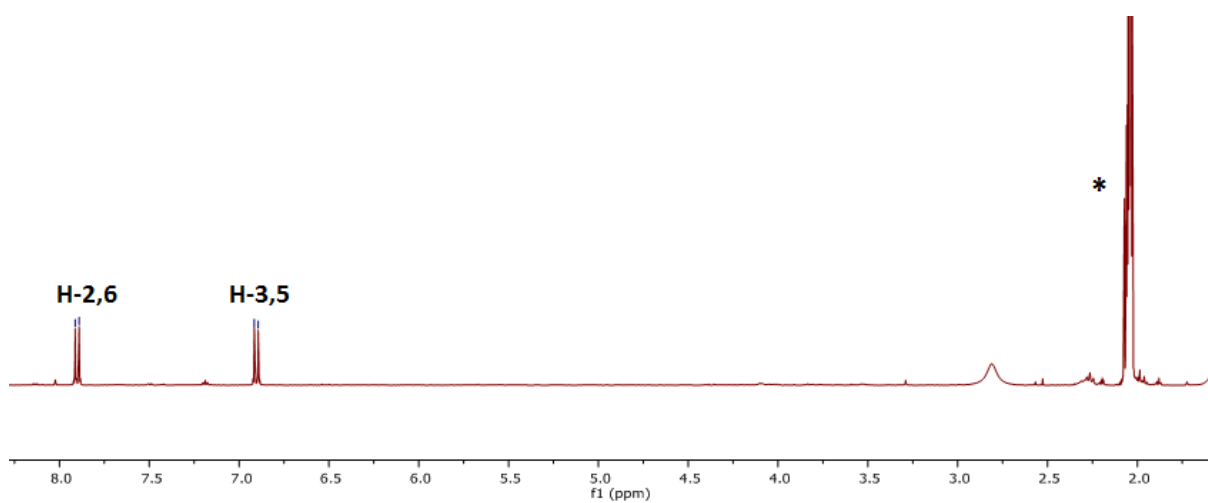


**Figure 3.1:** Structure of *para*-hydroxybenzoic acid.

**Table 3.2:**  $^1\text{H}$  (400MHz),  $^{13}\text{C}$  (100MHz), and HMBC data of ARE-6-6 in DMSO- $d_6$ .

Position	$^1\text{H}$ ( $\delta$ ppm)	$^{13}\text{C}$	HMBC correlations
1	-	121.6	-
2	7.93 (1H, <i>d</i> , 8.8Hz)	131.6	C-6( $^3J$ ), C-4( $^3J$ ), C-7( $^3J$ )
3	6.93 (1H, <i>d</i> , 8.8Hz)	114.5	C-5( $^3J$ ), C-1( $^3J$ ), C-4( $^2J$ )
4	-	162.3	-
5	6.93 (1H, <i>d</i> , 8.8Hz)	114.5	C-3( $^3J$ ), C-1( $^3J$ ), C-4( $^2J$ )
6	7.93 (1H, <i>d</i> , 8.8Hz).	131.6	C-2( $^3J$ ), C-4( $^3J$ ), C-7( $^3J$ )
7	-	171.9	-

**A**



**B**

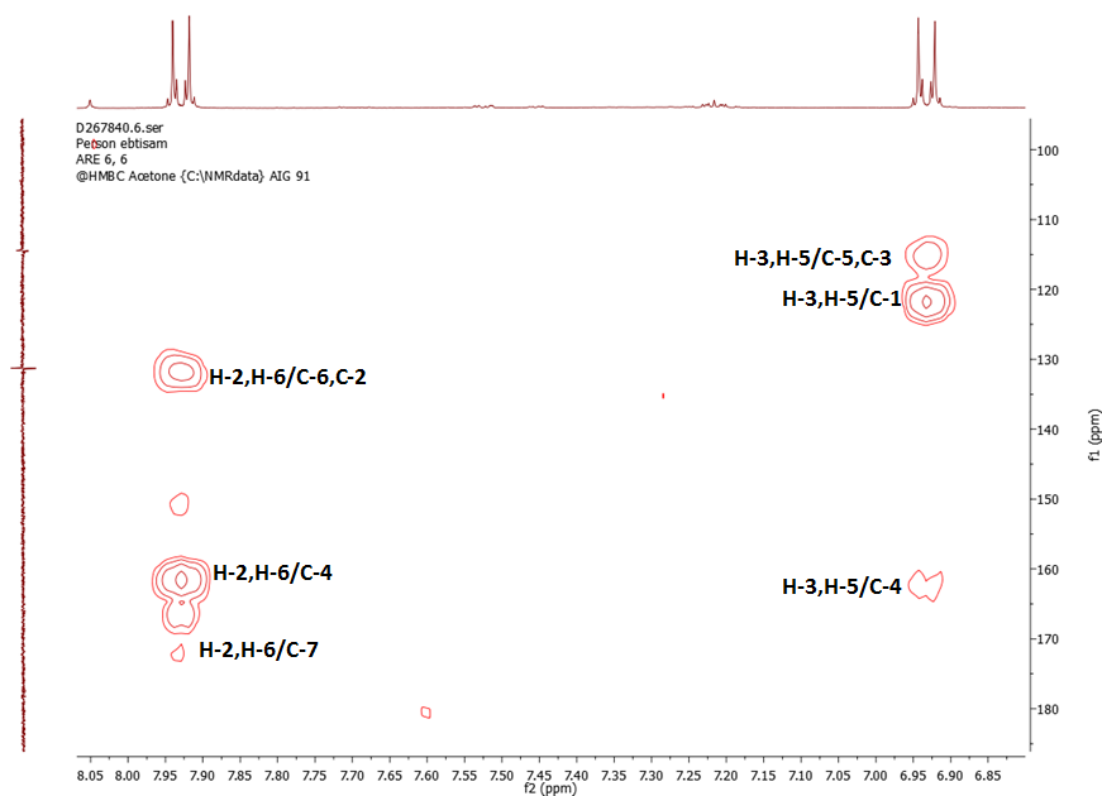


**Figure 3.2 A:**  $^1\text{H}$  and **3.2B:** HMBC spectra (500 MHz) of ARE-6-6 in  $\text{DMSO-}d_6^*$ .

### 3.2.2 Characterisation of ARE-6-18 as *p*-coumaric acid (a) and 3, 4-dimethoxycinnamic acid (b)

The mixture ARE-6-18 (Figure 3.3) was isolated from the ethyl acetate extract of *A. cyrenaicum* using a Sephadex column. On a TLC plate, a brown spot was observed after spraying with anisaldehyde-sulphuric acid reagent followed by heating with a  $R_f$  value of 0.60 using 10% (v/v) MeOH in EtOAc as the mobile phase.

The  $^1\text{H}$  NMR spectrum of the major compound ARE-6-18 a (Table 3.3, Figure 3.4A) showed two *trans* olefinic protons at  $\delta_{\text{H}}$  7.62 (1H, *d*,  $J=16.0$  Hz, H-7a) and  $\delta_{\text{H}}$  6.35 (1H, *d*,  $J=16.0$  Hz, H-8a) and a pair of *ortho*, *meta*-coupled signals at  $\delta_{\text{H}}$  7.56 (2H, *dd*,  $J=1.8, 6.9$  Hz) and  $\delta_{\text{H}}$  6.91 (2H, *dd*,  $J=2.2, 6.6$  Hz) indicating a 1, 4-*para* disubstituted aromatic ring. The  $^1\text{H}$  NMR spectrum for the minor compound ARE-6-18b (Table 3.3, Figure 3.4A) followed the same pattern as that of ARE-6-18a except for the presence of two methoxy groups instead of a hydroxyl group and proton at C-4 and C-3, respectively. The  $^1\text{H}$  NMR spectrum of ARE-6-18b (Table 3.3, Figure 3.4A) indicated the presence of three aromatic protons at signals at  $\delta_{\text{H}}$  6.89 (1H, *d*, H-5b), 7.16 (1H, *dd*, H-6b) 7.35(1H, *d*, H-2b). The presence of two protons at  $\delta_{\text{H}}$  7.61 (1H, *d*,  $J=16.0$  Hz, H-7b) and 6.39 (1H, *d*,  $J = 15.9$  Hz, H-8b) also suggested a *trans*-olefinic H-7b and H-8b in the compound. The spectrum also showed two singlets for 6H at  $\delta_{\text{H}}$  3.92 and 3.94 representing two methoxy groups.

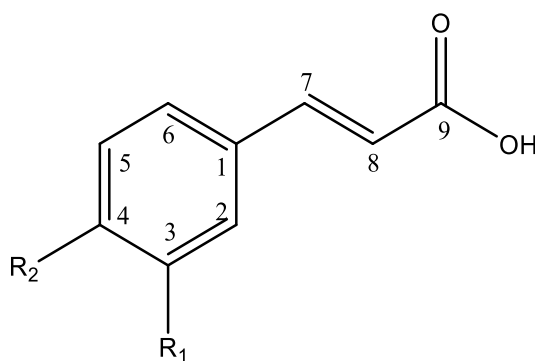
The  $^{13}\text{C}$  NMR spectrum (Table 3.3) displayed six methines at  $\delta_{\text{C}}$  114.9 (C-8a), 115.6 (C-3a/5a), 130.1(C-2a/6a), and 144.6(C-7a) and the three quaternary carbons at  $\delta_{\text{C}}$  126.4(C-1a), 159.5 (C-4a) and 166.8 (C-9a) for the major compound, were extracted from the HMBC spectrum. The  $^{13}\text{C}$  NMR spectrum for the minor compound was five methines at  $\delta_{\text{C}}$  114.8 (C-8b), 122.8 (C-6b), 110.5(C-2b), and 144.9(C-7b).

In the HMBC spectrum (Figure 3.4B), the olefinic proton at  $\delta_{\text{H}}$  7.62 (H-7a) showed a  $^3J$  correlation to the methine carbons at  $\delta_{\text{C}}$  130.1 (C-2a/6a) and the carbonyl at  $\delta_{\text{C}}$  166.8 (C-9a). The other olefinic proton at  $\delta_{\text{H}}$  6.35 (H-8a) showed a  $^3J$  coupling to the quaternary carbon at  $\delta_{\text{C}}$  126.4 (C-1a) and a  $^2J$  coupling to the carbonyl carbon at  $\delta_{\text{C}}$  166.8

(C-9a). The signal at  $\delta_{\text{H}}$  7.56 (H-2a/6a) showed  $^3J$  couplings to carbons at  $\delta_{\text{C}}$  130.1 (C-6a/2a),  $\delta_{\text{C}}$  144.6 (C-7a) and  $\delta_{\text{C}}$  159.5 (C-4a). The signal at  $\delta_{\text{H}}$  6.91 (H-3a/5a) showed  $^3J$  correlations to carbons at  $\delta_{\text{C}}$  126.4 (C-1a),  $\delta_{\text{C}}$  115.6 (C-5a/3a) and a  $^2J$  coupling to the carbon at  $\delta_{\text{C}}$  159.5 (C-4a). Additionally, in the minor compound, the methoxy groups showed  $^3J$  correlation to the carbons at  $\delta_{\text{C}}$  147.3 (C-3b) and 147.6 (C-4b) (Figure 3.4B, Table 3.3). Therefore, these carbons were assigned to C-3 and C-4 in the minor compound.

The HRESI-MS data showed a molecular ion  $[\text{M}]^-$  at  $m/z$  163.0473, suggesting a molecular formula of  $\text{C}_9\text{H}_8\text{O}_3$ . The above information identified ARE-6-18 a as 4-hydroxycinnamic acid (*p*-coumaric acid). The NMR results showed agreement with previous reports (Yi *et al.*, 2011). This is the first report of its isolation from *A. cyrenaicum*.

The HRESI-MS data showed a molecular ion  $[\text{M}]^-$  at  $m/z$  207.21, suggesting a molecular formula of  $\text{C}_{11}\text{H}_{12}\text{O}_4$ . The above information identified ARE-6-18b as 3,4-dimethoxycinnamic acid (b). The NMR results showed agreement with previous reports (Chang *et al.*, 2009). This is the first report of its isolation from *A. cyrenaicum*.



ARE 6-18 a : $R_1=H$ ,  $R_2=OH$

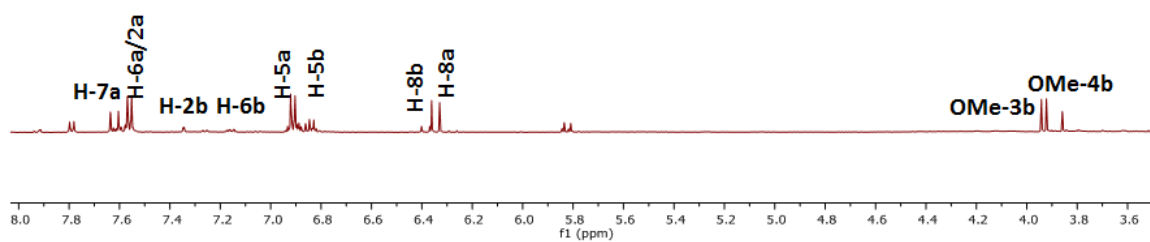
ARE 6-18 b : $R_1=R_2=OCH_3$

**Figure 3.3:** Structure of ARE-6-18 as a *p*-coumaric acid (ARE-6-18 a) and 3, 4-dimethoxycinnamic acid (ARE-6-18 b).

**Table 3.3:**  $^1H$  (500MHz),  $^{13}C$  (100MHz), and HMBC data of ARE-6-18 in DMSO- $d_6$ .

Position	ARE 6-18 a		ARE 6-18 b	
	$^1H$	$^{13}C$	$^1H$	$^{13}C$
1	-	126.4	-	132.0
2	7.56 (1H, <i>dd</i> , $J=1.8, 6.9$ Hz)	130.1	7.35 (1H, <i>d</i> , $J = 8.0$ )	110.5
3	6.91 (1H, <i>dd</i> , $J=2.0, 6.6$ Hz)	115.6	-	147.6
4	-	159.5	-	147.3
5	6.91 (1H, <i>dd</i> , $J=2.0, 6.6$ Hz)	115.6	6.89 (1H, <i>d</i> , $J = 2.0$ Hz)	-
6	7.56 (1H, <i>dd</i> , $J=1.8, 6.9$ Hz)	130.1	7.16(1H, <i>dd</i> , $J = 8.0, 2.0$ )	122.8
7	7.62 (1H, <i>d</i> , $J=16.0$ Hz)	144.6	7.61 (1H, <i>d</i> , $J=16.0$ Hz)	144.9
8	6.35 (1H, <i>d</i> , $J=16.0$ Hz)	114.9	6.39 (1H, <i>d</i> , $J = 15.9$ Hz)	114.8
9	-	166.8	-	166.9
3-OCH <sub>3</sub>	-	-	3.94(3H, <i>s</i> )	55.4
4-OCH <sub>3</sub>	-	-	3.92(3H, <i>s</i> )	55.2

A



B

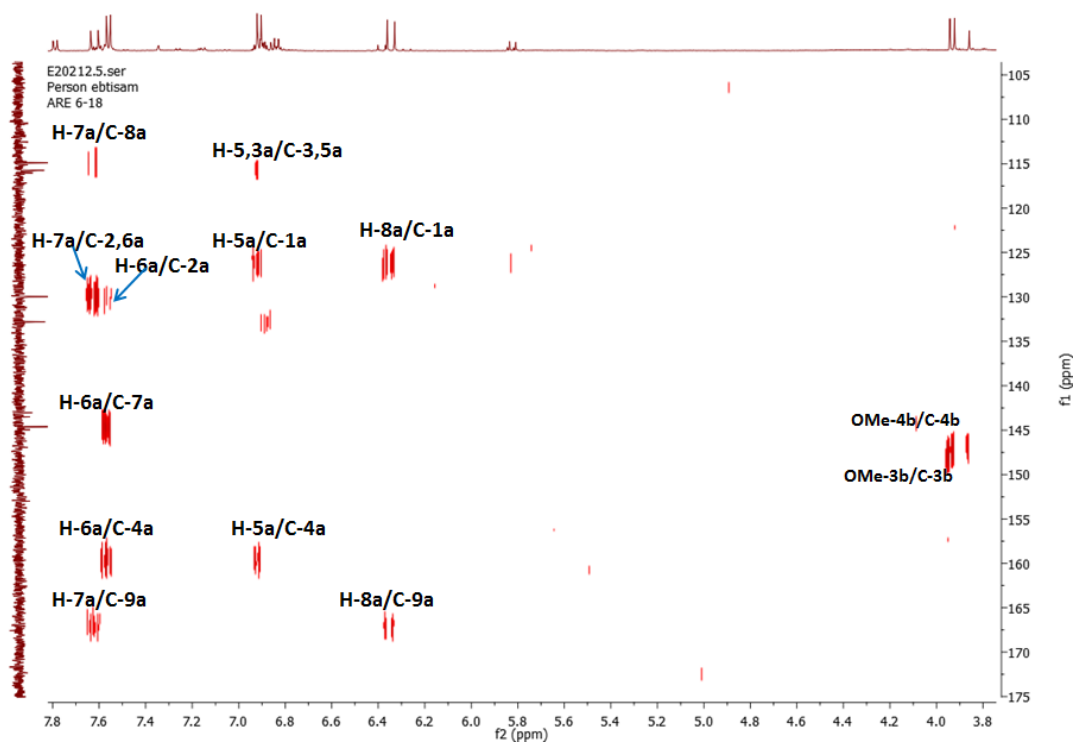


**Figure 3.4A:** <sup>1</sup>H NMR and **3.4B:** HMBC spectra (500 MHz) of ARE-6-18 in DMSO-*d*<sub>6</sub>\*.

### 3.3 Fractionation of *P. tortuosus* crude extracts

The dried hexane extract of *P. tortuosus* was dissolved in hexane and adsorbed on a small amount of silica 60 H and left to dry in the hood before being subjected to separation on a silica gel column chromatography and eluted with hexane increasing polarity to methanol. The fractions collected were assessed using NMR and enabled elucidation of the structure of one compound designated PTH-6-7. CC was used to fractionate the EtOAc extract of *P. tortuosus*; no compounds were separated. The methanol extract for *P. tortuosus* produced a white precipitate in the flask after extraction. The white powder was filtered and weighed to yield 15g (PTM-1). The remaining extract was filtered and concentrated under vacuum pressure and further purified on a silica C-18; no compounds were obtained.

#### 3.3.1 Characterisation of PTM-1 as luteolin-7-o-rutinoside-4'-methylether (diosmin)

The  $^1\text{H}$  NMR spectrum (Figure 3.6A, Table 3.4) indicated the presence H-bounded at  $\delta_{\text{H}}$  12.93 (1H, *s*) indicating an OH- at C-5 of a flavonoid moiety. The ring A of the flavonoid structure had the *meta* coupled protons at  $\delta_{\text{H}}$  6.47 (1H, *d*,  $J = 2.2$  Hz, H-6) and 6.77 (1H, *d*,  $J = 2.2$  Hz, H-8) and an ABX substitution pattern on the B ring with protons at  $\delta_{\text{H}}$  7.45 (1H,*d*,  $J = 2.3$  Hz, H-2'), 7.14(1H,*d*,  $J = 8.6$  Hz, H-5') and 7.57(1H,*dd*,  $J = 8.6, 2.3$  Hz,H-6') and a proton singlet at  $\delta_{\text{H}}$  6.82 (1H, *s*, H-3). The proton spectrum (Figure 3.6A, Figure 3.8) also indicated the presence of a methoxy group at  $\delta_{\text{H}}$  3.85 (3H, *s*), and two sugar residues with their anomeric protons at  $\delta_{\text{H}}$  5.05 (1H, *d*, 7.2 Hz) and 4.57 (1H, *d*,  $J = 1.6$ Hz) along with some oxymethines between  $\delta_{\text{H}}$  3.16 and 3.86 and a methyl doublet at 1.06 (3H, *d*,  $J = 6.2$  Hz). The  $^{13}\text{C}$  NMR spectrum (Figure 3.6B, Table 3.4) indicated the presence of 28 carbons including a carbonyl carbon at  $\delta_{\text{C}}$  182.3. Using  $^1\text{H}$  NMR and COSY spectra, the two sugar units were identified as  $\beta$ -D-glucose due to the large coupling constant (7.2 Hz) of its anomeric proton and  $\beta$ -L-rhamnose for the small coupling constant of the anomeric proton.

In the HMBC and HSQC spectra (Figure 3.7A, Figure 3.7B), the proton at  $\delta_{\text{H}}$  6.82 (H-3) showed  $^3J$  correlations to carbons at  $\delta_{\text{C}}$  105.8 (C-10), 123.1(C-1') and  $^2J$  correlations  $\delta_{\text{C}}$  182.3 (C-4) and 164.5 (C-2). The protons at  $\delta_{\text{H}}$  6.77 (H-8) and 6.47 (H-6) showed

$^3J$  correlations to the carbons 105.8 (C-10) and  $^2J$  correlations to  $\delta_C$  163.3 (C-7). The protons at  $\delta_H$  6.77 (H-8) showed  $^2J$  correlations to 157.3 (C-9) and  $^3J$  coupling to  $\delta_C$  99.4 (C-6). The protons at  $\delta_H$  6.47 (H-6) showed  $^3J$  correlation to the carbon at 95.3 (C-8) and  $^2J$  coupling to carbon at  $\delta_C$  161.5 (C-5). In ring B, the protons at  $\delta_H$  7.57 (H-6') and  $\delta_H$  7.45 (H-2') showed  $^3J$  correlation to carbon  $\delta_C$  164.5 (C-2) and to an oxygen bearing carbon at  $\delta_C$  151.6 (C-4'). The proton at  $\delta_H$  7.57 (H-6') showed  $^3J$  correlation to the carbon at  $\delta_C$  113.4 (C-2') and  $\delta_H$  7.45 (H-2') showed  $^3J$  correlations to carbon at  $\delta_C$  119.3 (C-6') and  $^2J$  coupling to carbon at  $\delta_C$  147.2 (C-3'). The protons at  $\delta_H$  7.14 (H-5') showed  $^3J$  correlations to carbons at  $\delta_C$  123.1 (C-1'), 147.2 (C-3') and  $^2J$  correlations to carbon at 151.6 (C-4'). Furthermore, the methoxy group at  $\delta_H$  3.85 (3H, s) showed  $^3J$  correlation to the carbon at  $\delta_C$  151.6 (C-4') proving its connectivity to ring B. The anomeric proton of  $\beta$ -L-rhamnose ( $\delta_H$  4.57) showed  $^3J$  correlation to carbon at  $\delta_C$  66.8 (C-6'') of glucose residue. While the anomeric proton of  $\beta$ -D-glucose at  $\delta_H$  5.07 showed  $^3J$  correlation to carbon at  $\delta_C$  163.3 (C-7) proving its connectivity to ring A.

The HRESI-MS data showed a molecular ion  $[M]^+$  at  $m/z$  609.1817 suggesting the molecular formula of  $C_{28}H_{32}O_{15}$ . Thus PTM-1 was identified as luteolin-7-*O*-rutinoside-4'-methylether. All the spectral data were in agreement with those published in the literature (Gopalakrishnan *et al.*, 2015) This is the first report of luteolin-7-*O*-rutinoside-4'-methylether from *P. tortuosus*.

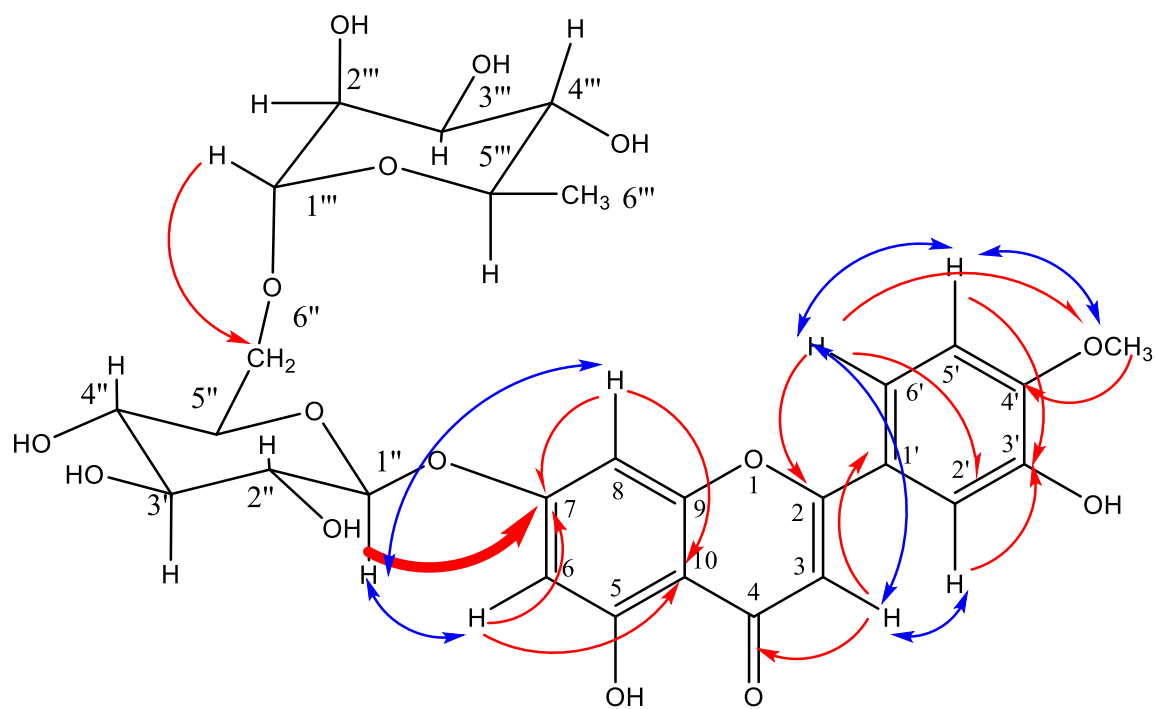
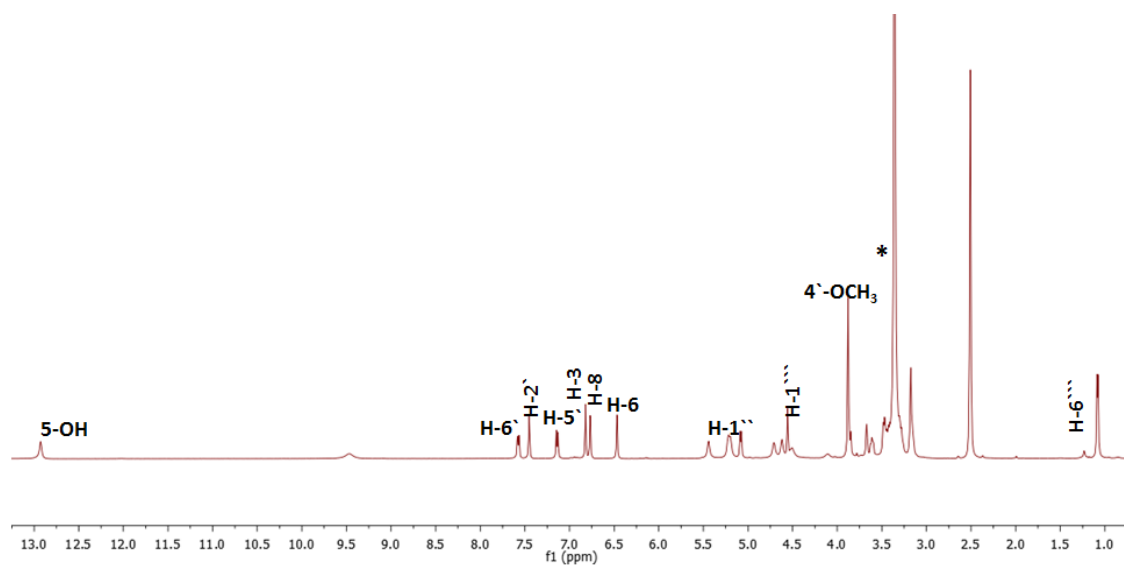


**Figure 3.5:** Structure of luteolin-7-*O*-rutinoside-4'-methylether (diosmin). Key HMBC (  ) and NOESY (  ) correlations observed in PTM-1.

**Table 3.4:**  $^1\text{H}$  (400MHz),  $^{13}\text{C}$  (100MHz), and HMBC data of PTM-1 in DMSO- $d_6$ .

Position	$^1\text{H}$ (ppm)	$^{13}\text{C}$ (ppm)	HMBC correlation
1	-	-	-
2	-	164.5	-
3	6.82(1H, <i>s</i> )	104.2	C-10( $^3J$ ), C-1( $^3J$ ), C-2( $^2J$ ), C-4( $^2J$ )
4	-	182.3	-
5	-	161.5	-
6	6.47(1H, <i>d</i> , 2.2 Hz)	99.9	C-8( $^3J$ ) / C-10( $^3J$ ), C-5( $^2J$ ), C-7( $^2J$ )
7	-	163.3	-
8	6.77(1H, <i>d</i> , 2.2Hz)	95.3	C-6( $^3J$ ), C-10( $^3J$ ), C-9( $^2J$ ), C-7( $^2J$ )
9	-	157.3	-
10	-	105.8	-
1 $\prime$	-	123.1	-
2 $\prime$	7.45(1H, <i>d</i> , 2.3 Hz)	113.5	C-6( $^3J$ ), C-3( $^2J$ ), C-4( $^3J$ ), C-2( $^3J$ )
3 $\prime$	-	147.2	-
4 $\prime$	-	151.6	-
5 $\prime$	7.14 (1H, <i>d</i> , 8.6 Hz)	112.5	C-1( $^3J$ ), C-3( $^3J$ ) / C-4( $^2J$ )
6 $\prime$	7.57(1H, <i>dd</i> 2.3, 8.6 Hz)	119.5	C-2( $^3J$ ), C-4( $^3J$ ), C-2( $^3J$ )
5-OH	12.93	-	-
1 $\prime\prime$	5.05(1H, <i>d</i> , $J = 7.2$ Hz)	100.4	C-7( $^3J$ )
2 $\prime\prime$	3.27(1H, <i>m</i> )	72.7	-
3 $\prime\prime$	3.33(1H, <i>m</i> )	76.0	-
4 $\prime\prime$	3.61(1H, <i>m</i> )	75.2	-
5 $\prime\prime$	3.18(1H, <i>m</i> )	69.8	-
6 $\prime\prime$	3.86/3.47(2H)	66.5	-
1 $\prime\prime\prime$	4.5( <i>d</i> , $J = 1.6$ Hz, 2H)	100.9	C-6( $^3J$ ), C-5( $^3J$ ), C-3( $^3J$ )
2 $\prime\prime\prime$	3.67(1H)	70.0	-
3 $\prime\prime\prime$	3.47(1H)	70.3	C-1( $^3J$ )
4 $\prime\prime\prime$	3.16(1H, <i>m</i> )	71.7	-
5 $\prime\prime\prime$	3.42(1H, <i>m</i> )	68.6	-
6 $\prime\prime\prime$	1.06 (3H, <i>d</i> , $J = 6.2$ Hz, 5H)	17.7	C-5( $^2J$ ), C-4( $^3J$ )
4'OCH <sub>3</sub>	3.85(3H, <i>s</i> )	56.2	-

**A**



**B**

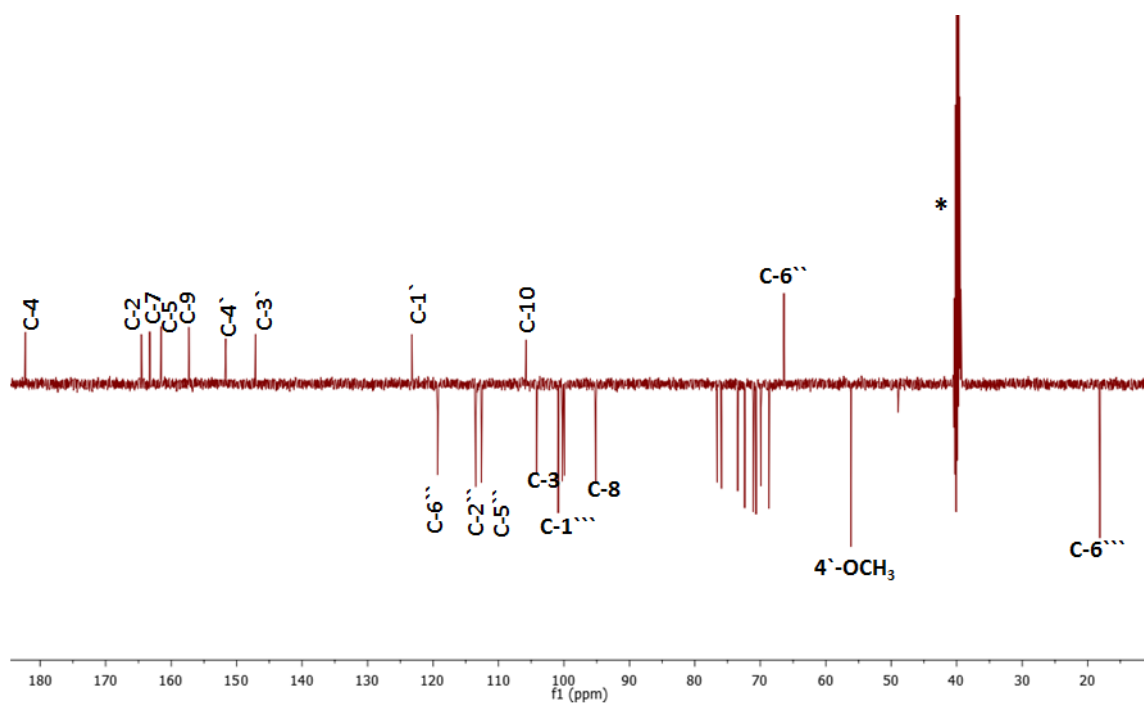
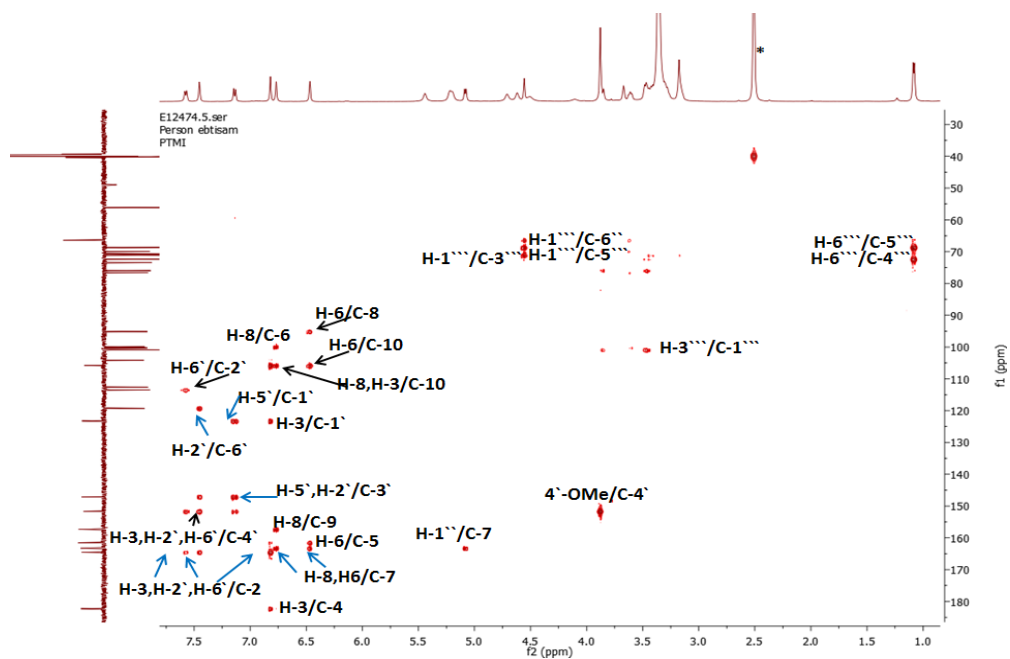


**Figure 3.6A:**  $^1\text{H}$  NMR and **3.6B:**  $^{13}\text{C}$  NMR spectra (500 MHz) of PTM-1 in  $\text{DMSO-}d_6^*$ .

A



B

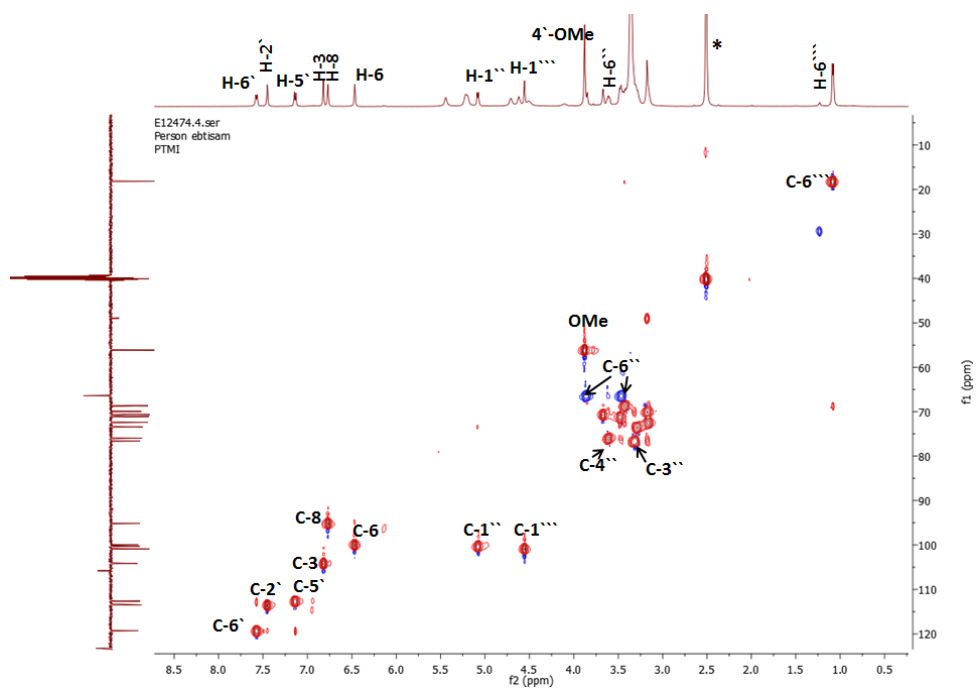
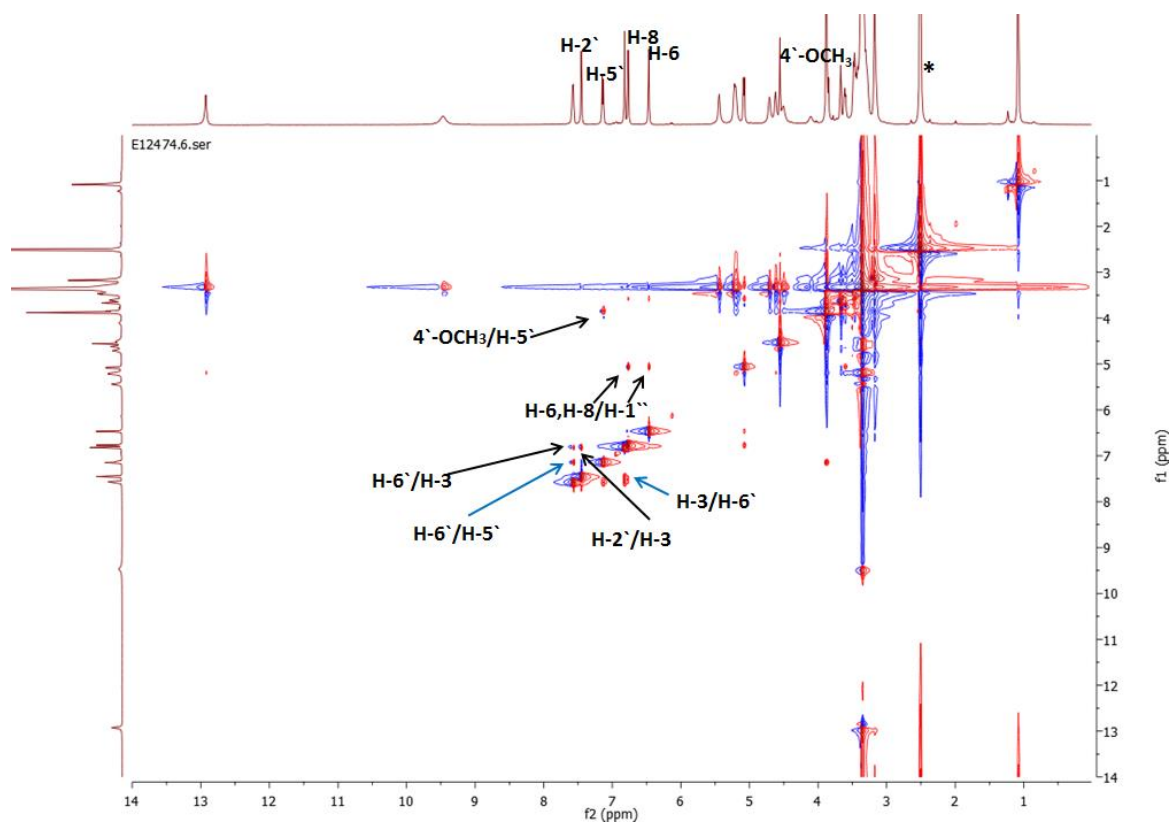


Figure 3.7A: HMBC and 3.7B: HSQC spectra (500 MHz) of PTM-1 in DMSO- $d_6^*$ .

A



**Figure 3.8:** NOESY spectrum (500 MHz) of PTM1 in DMSO- $d_6^*$ .

### 3.3.2 Characterisation of PTH6-7 as 2-hydroxy-3-(4-hydroxy-3-methoxyphenyl)-propionic acid (vanillic acid)

The compound PTH6-7 (Figure 3.9) was isolated from the hexane extract of the aerial part of *P. tortuosus* using CC. After spraying with *p*-anisaldehyde-sulphuric acid reagent and heating, a yellow spot appeared with  $R_f$  value of 0.75 using 20% EtOAc in hexane as the mobile phase on TLC.

The  $^1\text{H}$  NMR spectrum of PTH6-7 (Figure 3.10A, Table 3.5) revealed the presence of an aromatic ring with protons at  $\delta_{\text{H}}$  6.83 (1H, *d*,  $J = 1.8$  Hz, H-2'),  $\delta_{\text{H}}$  6.88 (1H, *d*,  $J = 8.0$  Hz, H-5') and  $\delta_{\text{H}}$  6.78 (1H, *dd*,  $J = 8.0$  1.8 Hz, H-6'). The coupling constants and multiplicity of these signals indicated an aromatic ABX spin system. The spectrum also showed the presence of methylene signals at  $\delta_{\text{H}}$  4.37 (2H, *d*,  $J = 5.6$  Hz, H-3) and from COSY  $^1\text{H}$ - $^1\text{H}$  (Figure 3.11A) the proton at  $\delta_{\text{H}}$  5.70 (1H, *m*, H-2) were assigned to attached to H-3. A signal for a 3H singlet at  $\delta_{\text{H}}$  3.90 represented a methoxy group.

The  $^{13}\text{C}$  NMR spectrum (Figure 3.10B, Table 3.5) indicated the presence of carbon atoms including one methylene carbon at 43.38 ppm, one methoxy carbon at 55.9 ppm, three quaternary carbons at 130.3, 145.0, 146.6 ppm and four CH carbons at 110.8, 120.8, 114.3, 80.4 ppm.

The HMBC spectrum (Figure 3.11B, Table 3.5) showed  $^3J$  correlation between protons at  $\delta_{\text{H}}$  6.78 (H-6'), 6.83 (H-2') and a carbon signal at  $\delta_{\text{C}}$  43.3 (C-3). The protons at  $\delta_{\text{H}}$  6.78 (H-6')  $^3J$  coupling to the carbons at  $\delta_{\text{C}}$  110.8 (C-2'). The protons at  $\delta_{\text{H}}$  6.83 (H-2') showed a  $^3J$  correlation to the carbons at  $\delta_{\text{C}}$  120.8 (C-6') and 145.0 (C-4'). The proton signal at  $\delta_{\text{H}}$  6.88 (H-5') showed a  $^3J$  correlation to the quaternary carbon 130.3 (C-1') and 146.6 (C-3'). The singlet of the methoxy group showed a  $^3J$  correlation with an aromatic carbon bearing it at  $\delta_{\text{C}}$  146.6. The  $^3J$  correlations between methylene signals at  $\delta_{\text{H}}$  4.37 and the signal carbons at  $\delta_{\text{C}}$  110.8 (C-2'), 120.8 (C-6') and a carbonyl at 173.1 (C-1) and  $^2J$  correlation to carbon at  $\delta_{\text{C}}$  at 130.3 (C-1'), which therefore confirmed the methylene proton and carbon C-3.

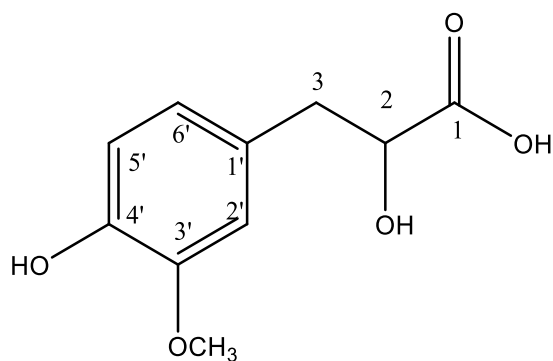


**Figure 3.9:** Structure of 2-hydroxy-3-(4-hydroxy-3-methoxyphenyl)-propionic acid (vanillic acid)

**Table 3.5:**  $^1\text{H}$  (400MHz),  $^{13}\text{C}$  (100MHz), and HMBC data of PTH 6-7 in  $\text{CDCl}_3$ .

Position	$^1\text{H}$ (ppm)	$^{13}\text{C}$ (ppm)	HMBC correlations
1	-	173.1	-
2	5.70 (1H,m)	80.4	-
3	4.37 (2H,d, $J = 5.6$ Hz)	43.3	$\text{C-2}^{\prime} (^3J)$ , $\text{C-6}^{\prime} (^3J)$ , $\text{C-1}^{\prime} (^2J)$ , $\text{C-1}^{\prime} (^3J)$
1 $\prime$	-	130.3	-
2 $\prime$	6.83 (1H, $d$ , $J = 1.8$ Hz)	110.8	$\text{C-6}^{\prime} (^3J)$ , $\text{C-3}^{\prime} (^3J)$
3 $\prime$	-	146.6	-
4 $\prime$	-	145.0	-
5 $\prime$	6.88 (1H, $d$ , $J = 8.0$ Hz)	114.3	$\text{C-1}^{\prime} (^3J)$ , $\text{C-3}^{\prime} (^3J)$
6 $\prime$	6.78 (1H, $dd$ , $J = 8.0, 1.8$ Hz)	120.8	$\text{C-2}^{\prime} (^3J)$ , $\text{C-4}^{\prime} (^3J)$ , $\text{C-3}^{\prime} (^3J)$
3 $\prime$ -OMe	3.90	55.9	$\text{C-3}^{\prime} (^3J)$

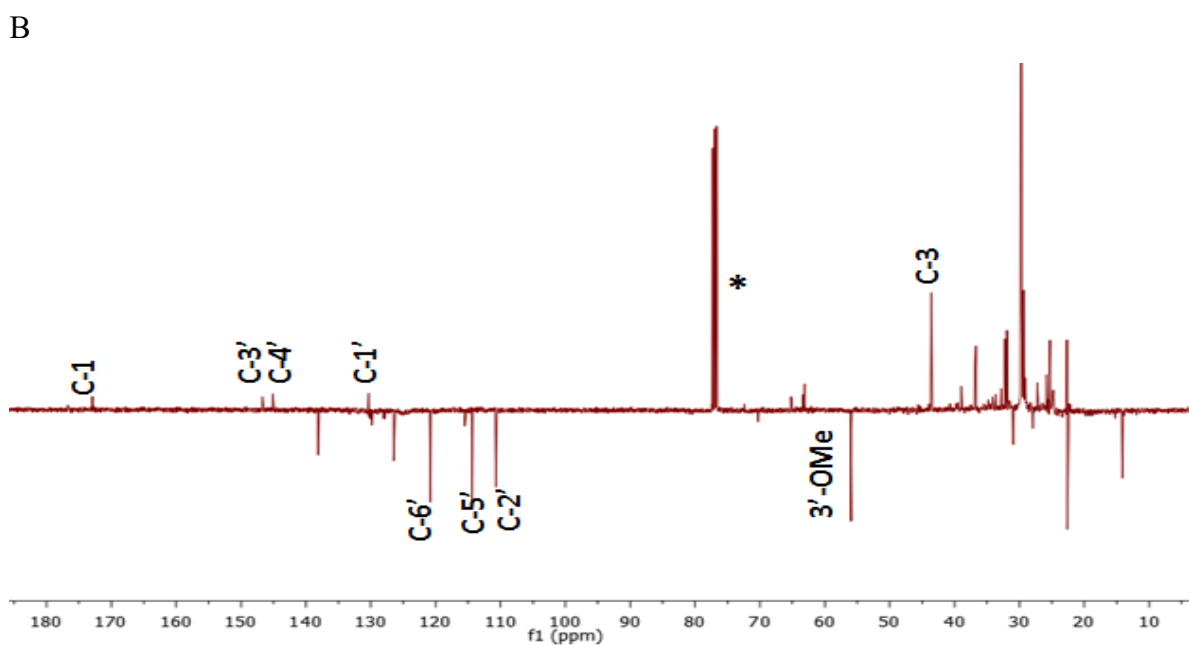
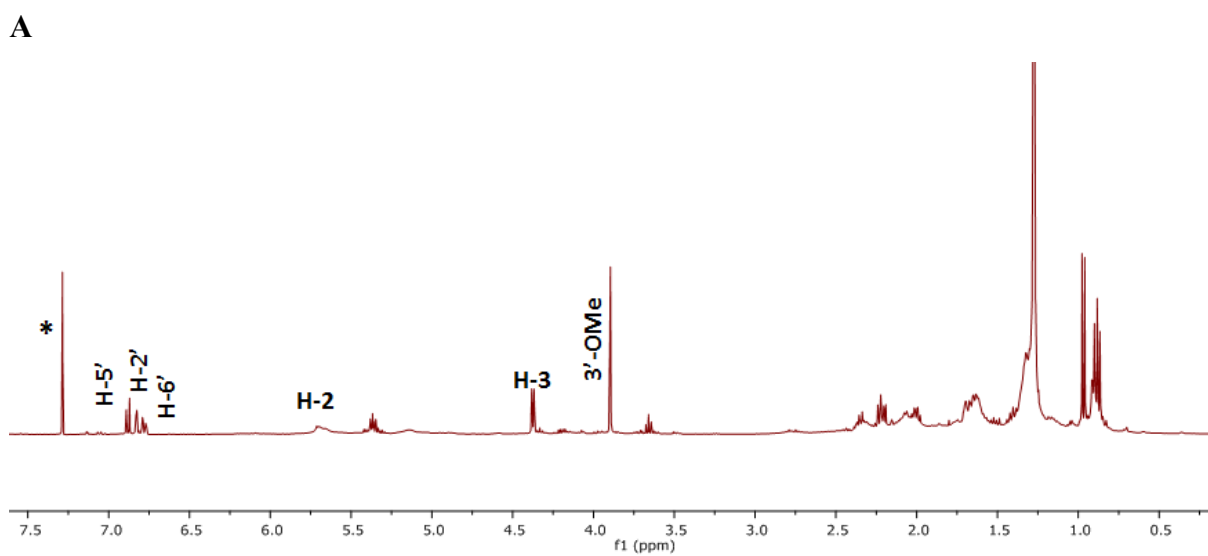
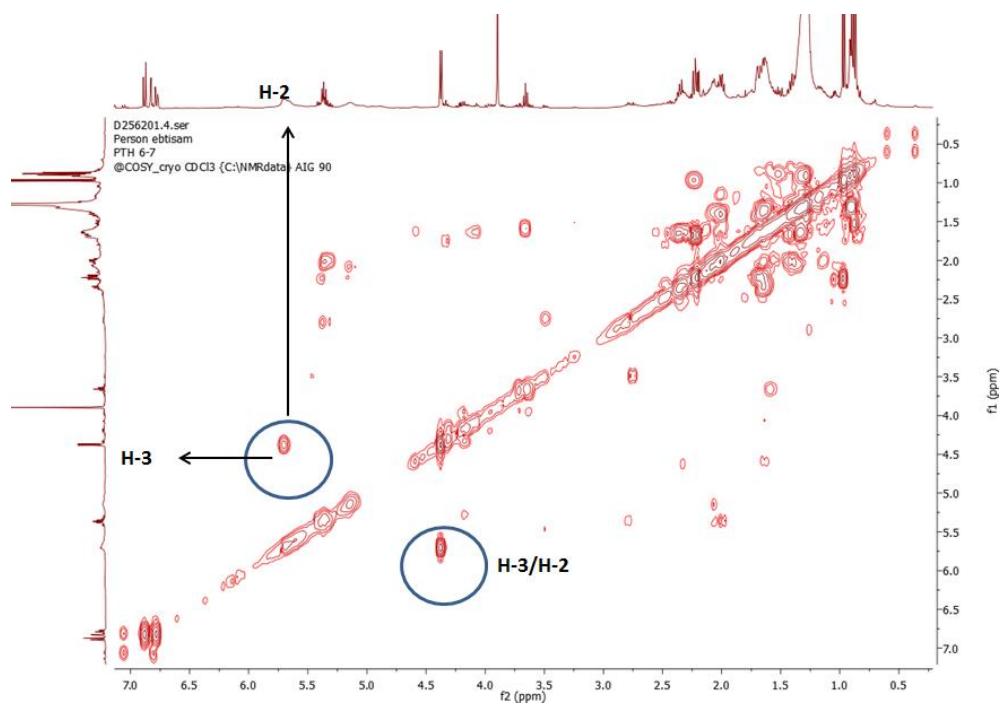


**Figure 3.10A:** <sup>1</sup>H (400MHz) and **3.10B:** <sup>13</sup>C NMR spectra (100MHz) of PTH 6-7 in CDCl<sub>3</sub>\*.

A



B

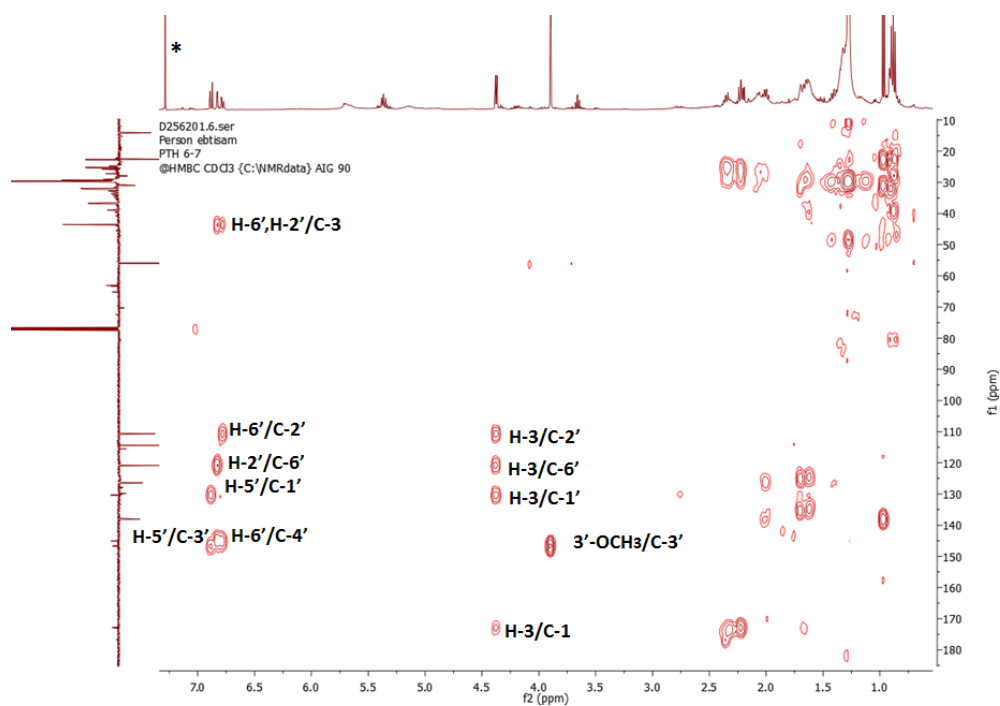


**Figure 3.11A:** COSY (500 MHz) and **3.11B:** HMBC (400MHz) spectra of of PTH 6-7 in CDCl<sub>3</sub>\*.

### 3.4 Fractionation of *T. zanonii* Crude Extracts

A silica gel column was used to fractionate the hexane extracts of *T. zanonii* and the EtOAc. The fractions collected from the hexane extract were assessed using NMR and enabled elucidation of the structure of two compounds designated TZH-68 and TZH-41-49. Other fractions from the same hexane extract from 103 to 107 and 150 to 170 were combined and further purified using Sephadex which afforded TZH-103-107-9 and TZH-150-170-9. The methanol extract was fractionated using Sephadex and fractions were collected and examined using NMR and enabled the isolation of TZM-24. No compounds were separated from the fractionation of the EtOAc extract of *T. zanonii* using silica gel.

#### 3.4.1 Characterisation of TZH-103-107-9 as 5-hydroxy-6, 7, 4'-trimethoxyflavone or salvigenin

TZH-103-107-9 (Figure 3.12) was obtained as a pale yellow solid from the hexane extract of *T. zanonii* using a silica gel column and purified by Sephadex column. A brown spot with an  $R_f$  value of 0.61 was observed when this compound was run on a TLC plate using 50% (v/v) MeOH in EtOAc as the mobile phase.

In the  $^1\text{H}$  NMR spectrum (Figure 3.13A, Table 3.6), the A ring of a flavone structure was identified with a proton at  $\delta_{\text{H}}$  6.58 (1H, *s*, H-8). A pair of signals showing *ortho* coupling at  $\delta_{\text{H}}$  7.03 (2H, *d*,  $J=9.0$ , Hz, H-3'/5') and  $\delta_{\text{H}}$  7.86 (2H, *d*,  $J=9.0$  Hz, H-2'/6') established the presence of a 1, 4-*para* di-substituted B ring and proton singlet at  $\delta_{\text{H}}$  6.62 (1H, *s*) for H-3 of ring C. The NMR spectrum also exhibited three methoxy groups at  $\delta_{\text{H}}$  3.92, 3.95 and 4.00. A single singlet proton at  $\delta_{\text{H}}$  12.78 confirmed the presence of OH at C-5.

In the HMBC spectrum (Figure 3.14A) a proton at  $\delta_{\text{H}}$  6.58 (H-8) showed  $^3J$  correlations to the carbons at  $\delta_{\text{C}}$  106.2 (C-10) and 132.6 (C-6) and  $^2J$  coupling to carbons at  $\delta_{\text{C}}$  154.45 (C-9), 159.2 (C-7). The proton at  $\delta_{\text{H}}$  7.03 (H-3',5') showed  $^3J$  correlation to a quaternary carbon at  $\delta_{\text{C}}$  123.7 (C-1') and  $^2J$  to a carbon at  $\delta_{\text{C}}$  162.6 (C-

4'). The proton at  $\delta_H$  6.62 (H-3) showed  $^2J$  coupling to the carbons at  $\delta_C$  164.1 (C-2) and 182.8 (C-4) and  $^3J$  coupling to the carbons at  $\delta_C$  123.7 (C-1') and 106.2 (C-10). The proton at  $\delta_H$  7.86 (H-2'/6') showed  $^3J$  coupling to the carbon at  $\delta_C$  162.6 (C-4'). The methoxy at  $\delta_H$  4.00 showed  $^3J$  correlation to the carbon at  $\delta_C$  159.2 (C-7), the methoxy at  $\delta_H$  3.95 showed  $^3J$  correlation to  $\delta_C$  132.6 (C-6) while the methoxy at  $\delta_H$  3.92 showed  $^3J$  correlations to  $\delta_C$  162.6 (C-4'). From the HSQC spectrum (Figure 3.14B) the methoxy carbons were identified as methoxy at 3.92 belong to  $\delta_C$  55.3, methoxy (C-6) 3.95 at  $\delta_C$  60.93 and methoxy (C-7) at 4.00 at  $\delta_C$  56.2.

The HRESI-MS data showed a molecular ion  $[M]^-$  at  $m/z$  327.087 suggesting the molecular formula  $C_{18}H_{16}O_6$ . A NMR spectrum in the literature (Facundo *et al.*, 2012; Hossain and Mizanur Rahman, 2015) supported the structure of TZH-103-107-9 being a 5-hydroxy-6, 7, 4'-trimethoxyflavone. This is the first report of 5-hydroxy-6, 7, 4'-trimethoxyflavone from *T. zanonii*.

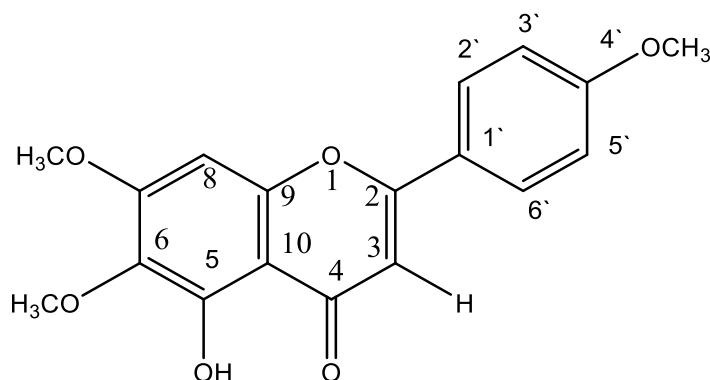
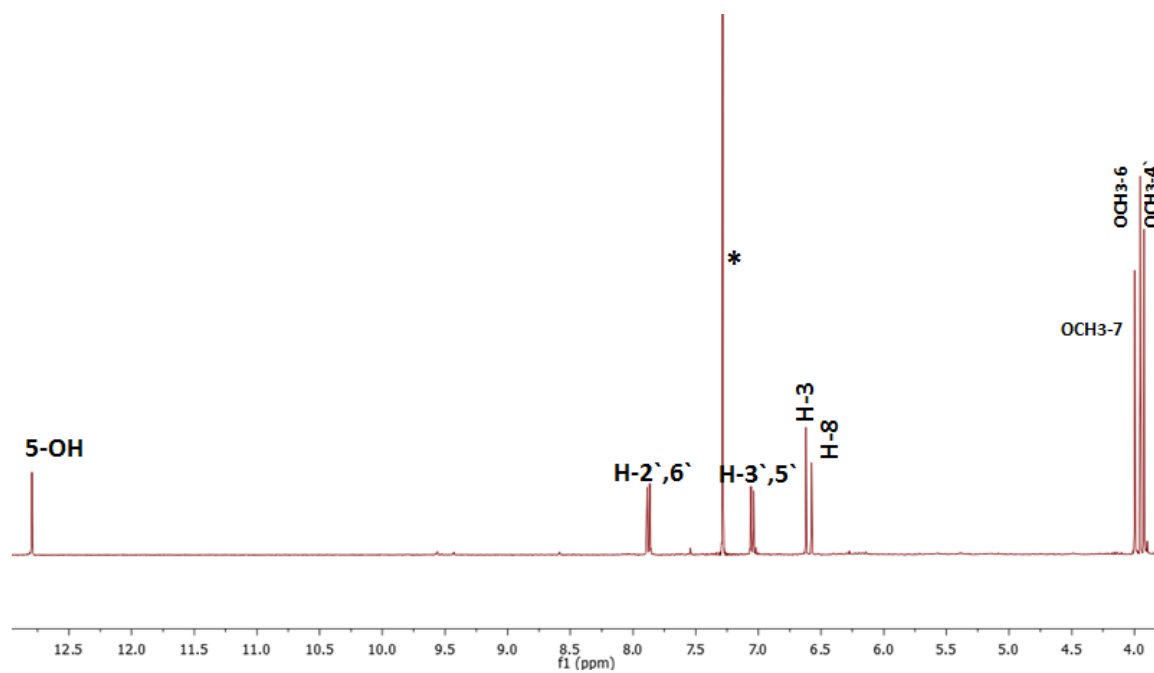


**Figure 3.12:** Structure of 5-hydroxy-6, 7, 4'-trimethoxyflavone or salvigenin.

**Table 3.6:**  $^1\text{H}$  (400MHz),  $^{13}\text{C}$  (100MHz), and HMBC data of TZh-103-107-9 in  $\text{CDCl}_3$ .

Position	$^1\text{H}$ (ppm)	$^{13}\text{C}$ (ppm)	HMBC correlations
1	-	-	-
2	-	164.1	-
3	6.62 (1H, s)	104.0	C-10 ( $^3J$ ), C-1' ( $^3J$ ), C-2 ( $^2J$ ), C-4 ( $^3J$ )
4	-	182.8	-
6	-	132.6	-
7	-	159.2	-
8	6.58(1H, s)	90.8	C-10 ( $^3J$ ), C-6 ( $^3J$ ), C-9 ( $^2J$ ), C-7 ( $^2J$ )
9	-	153.2	-
10	-	106.2	-
1'	-	123.7	-
2'	7.86(1H, d, $J=9.0$ Hz)	128.2	C-4' ( $^3J$ ), C-6' ( $^3J$ )
3'	7.03(1H, d, $J=9.0$ , Hz)	114.36	C-1' ( $^3J$ ), C-4' ( $^2J$ ), C-5' ( $^3J$ )
4'	-	162.6	-
5'	7.03(1H, d, $J=9.0$ , Hz)	114.36	C-1' ( $^3J$ ), C-4' ( $^2J$ ), C-3' ( $^3J$ )
6'	7.86(1H, d, $J=9.0$ Hz)	128.2	C-4' ( $^3J$ ), C-2' ( $^3J$ )
5-OH	12.78 (s)		C-10 ( $^2J$ ), C-6 ( $^2J$ ), C-9 ( $^3J$ )
6-OCH <sub>3</sub>	3.95 (3H, s)	60.93	C-6 ( $^3J$ )
7-OCH <sub>3</sub>	4.00 (3H, s)	56.24	C-7 ( $^3J$ )
4'-OCH <sub>3</sub>	3.92 (3H, s)	55.31	C-4' ( $^3J$ )

A



B

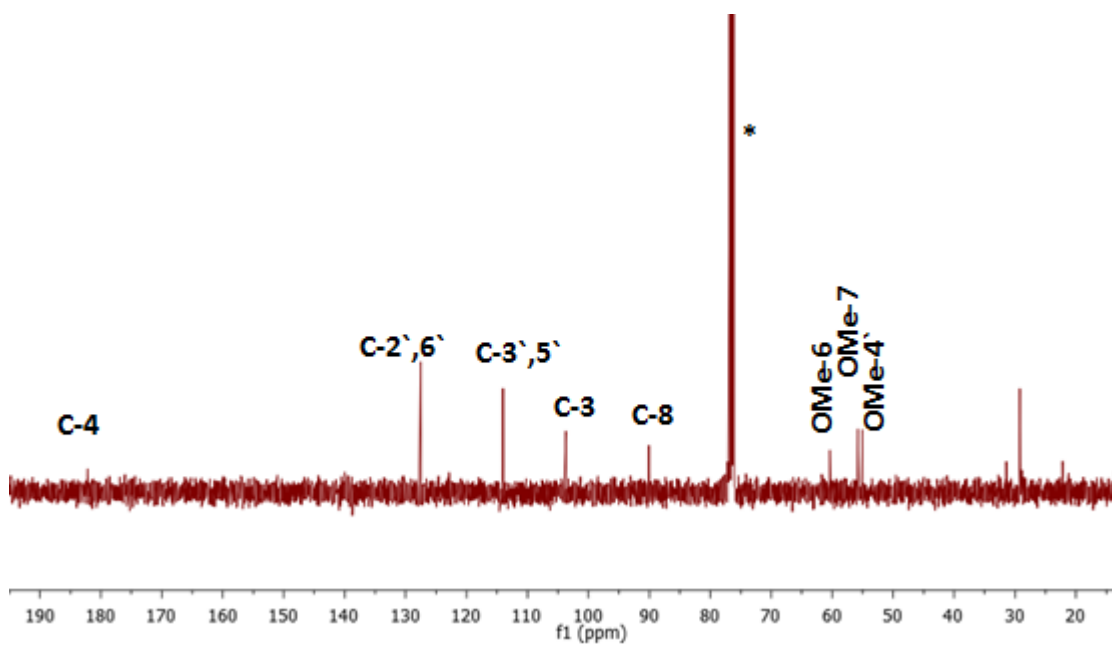
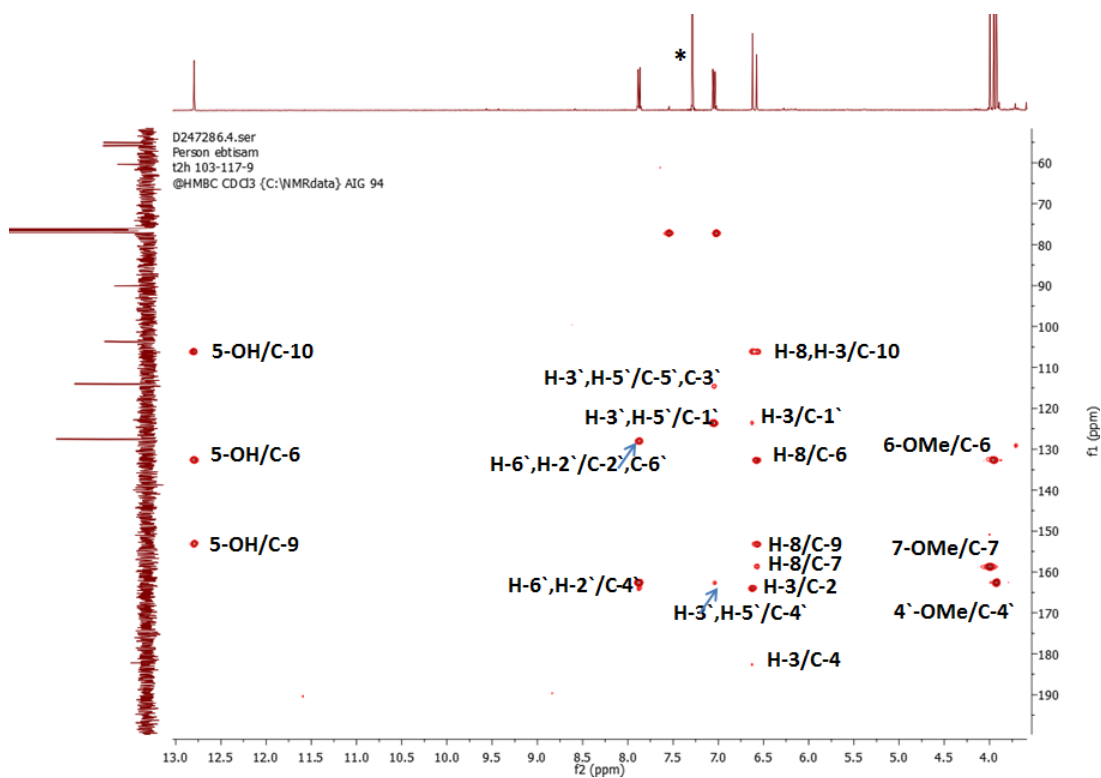


**Figure 3.13A:** <sup>1</sup>H NMR (400 MHz) and **3.13B:** <sup>13</sup>C NMR spectra (100 MHz) of TZH 103-107-9 in CDCl<sub>3</sub>\*.

A



B

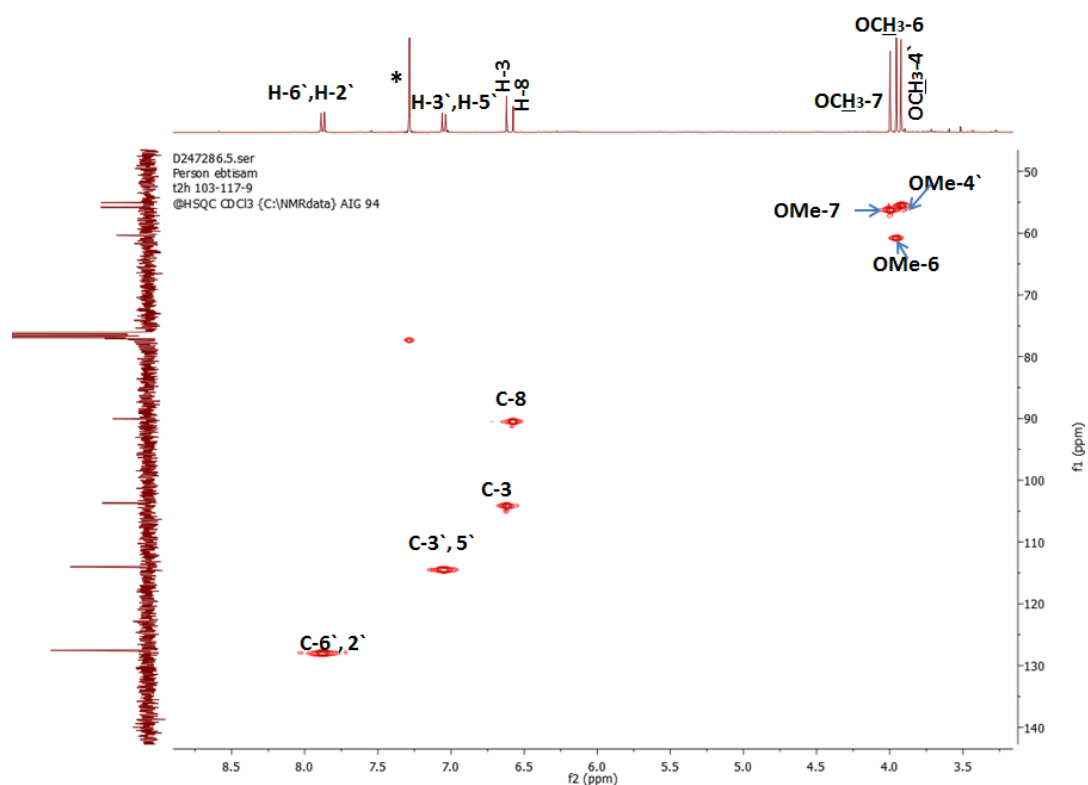


**Figure 3.14A:** HMBC and **3.14B:** HSQC spectra (400 MHz) of TZH-103-107-9 in CDCl<sub>3</sub>\*.

### 3.4.2 Characterisation of TZH-150-170-7 as 5-hydroxy-3', 4', 6, 7-tetramethoxyflavone OR as 5-hydroxy-3, 4, 7, 8 tetramethoxyflavone

TZH-150-170-7 (Figure 3.15) was obtained from silica gel separation of the hexane extract of *T. zanonii*, which was subjected to Sephadex column, eluted with 100% methanol. On TLC, the compound showed up as a dark spot under UV light. After treatment with *p*-anisaldehyde-sulphuric acid reagent and heating, the compound turned yellow with an  $R_f$  value of 0.33 using a mobile phase of 40% (v/v) EtOAc in hexane.

The  $^1\text{H}$  NMR spectrum (Figure 3.16A) revealed the presence of a hydroxyl signal at 12.76 ppm (OH-5), a three spin aromatic system at  $\delta_{\text{H}}$  7.39(1H, *d*,  $J= 2.1$  Hz, H-2') 7.01 (1H, *d*,  $J=8.4$  Hz, H-5') and 7.56 (1H, *dd*,  $J= 8.5, 2.1$  Hz, H-6'). Two other aromatic singlets were observed at  $\delta_{\text{H}}$  6.58 (H-8) and 6.63 (H-3) (Table 3.7).

In the HMBC spectrum (Figure 3.17A), one methoxy at  $\delta_{\text{H}}$  3.93 attached to C-6 also showed  $^3J$  correlation to the carbon at  $\delta_{\text{C}}$  132.5 (C-6) and thus was assigned as 6- OMe. The proton at  $\delta_{\text{H}}$  6.58(H-8) showed a strong  $^3J$  correlation to (C-6) at  $\delta_{\text{C}}$  132.02 and (C-10) at  $\delta_{\text{C}}$  (106.4) and  $^2J$  correlation to the carbon (C-9) at  $\delta_{\text{C}}$  153.2. The protons at  $\delta_{\text{H}}$  7.56 (H-6'), 7.39 (H-2') and the methoxy at 4'.00 showed  $^3J$  correlations to the carbon at  $\delta_{\text{C}}$   $\delta$  152.3 (C-4') and thus the methoxy is attached to C-4'. The protons  $\delta_{\text{H}}$  7.56 (H-6') and 7.39 (H-2') showed  $^3J$  correlation to the carbon (C-2) at  $\delta_{\text{C}}$  164.2. The proton at  $\delta_{\text{H}}$  7.01(H-5') showed  $^3J$  correlation to the carbon(C-3') at  $\delta_{\text{C}}$   $\delta$  149.4 and the carbon (C-1') at  $\delta_{\text{C}}$  123.5. Protons at  $\delta_{\text{H}}$  7.39 (H-2') and 7.56 (H-6') showed  $^3J$  correlation to the carbons signals (C-6'), (C-2') at  $\delta_{\text{C}}$  120.1, 108.9 respectively. The proton at  $\delta_{\text{H}}$  6.63 (H-3) showed a  $^2J$  coupling to the carbons at  $\delta_{\text{C}}$   $\delta$ 164.2 (C-2) and  $^3J$  coupling to  $\delta_{\text{C}}$  106.4 (C-10). The methoxy at  $\delta_{\text{H}}$  4.02 showed  $^3J$  correlation to the carbon at  $\delta_{\text{C}}$  159.06 (C-7) and the methoxy was thus assigned as 7-OMe and the methoxy at  $\delta_{\text{H}}$  4.01 showed  $^3J$  correlation to the carbon at  $\delta_{\text{C}}$  149.4 (C-3') and the methoxy was thus assigned as 3-OMe.

The HRESI-MS data showed a molecular ion  $[M]^+$  at 359.1123 suggesting a molecular formula of  $C_{19}H_{18}O_7$ . TZH-150-170-7 was identified as 5-hydroxy-3', 4', 6, 7-tetramethoxyflavone and confirmed by (Ayatollahi *et al.*, 2015), this is the first report of this compound from *T. zanonii*.

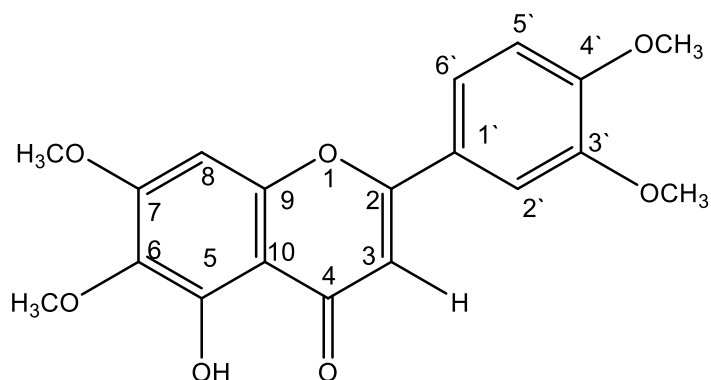


**Figure 3.15:** Structure of 5-hydroxy-6, 7, 3', 4'-tetramethoxy flavone.

**Table 3.7:**  $^1\text{H}$  (400MHz),  $^{13}\text{C}$  (100MHz), and HMBC data of TZH-150-170-7 in  $\text{CDCl}_3$ .

Position	$^1\text{H}$ (ppm)	$^{13}\text{C}$ (ppm)	HMBC correlations
2	-	164.2	-
3	6.63(1H, <i>s</i> )	104.4	C-10( $^3J$ ), C-2( $^2J$ )
4	-	185	-
5	12.76		-
6	-	132.5	-
7	-	159.06	-
8	6.58(1H, <i>s</i> )	90.54	C-10( $^3J$ ), C-6( $^3J$ ), C-9( $^2J$ )
9	-	153.63	-
10	-	106.4	-
1'	-	123.6	-
2'	7.39(1H, <i>d</i> , $J=2.1\text{Hz}$ )	108.9	C-6'( $^3J$ ), C-4'( $^3J$ ), C-2'( $^3J$ )
3'	-	149.4	-
4'	-	152.3	-
5'	7.01(1H, <i>d</i> , $J=8.4\text{Hz}$ )	111.2	C-1'( $^3J$ ), C-3'( $^3J$ )
6'	7.56(1H, <i>dd</i> , $J=8.5, 2.1\text{Hz}$ )	120.1	C-2'( $^3J$ ), C-4'( $^3J$ ), C-2'( $^3J$ ),
6-OMe	3.96 (3H, <i>s</i> )	60.93	C-6( $^3J$ )
7-OMe	4.02 (3H, <i>s</i> )	56.13	C-7( $^3J$ )
3'-OMe	4.01(3H, <i>s</i> )	56.16	C-3'( $^3J$ )
4'-OMe	4.00 (3H, <i>s</i> )	56.30	C-4'( $^3J$ )
5-OH	12.76 (1H, <i>s</i> )	-	-

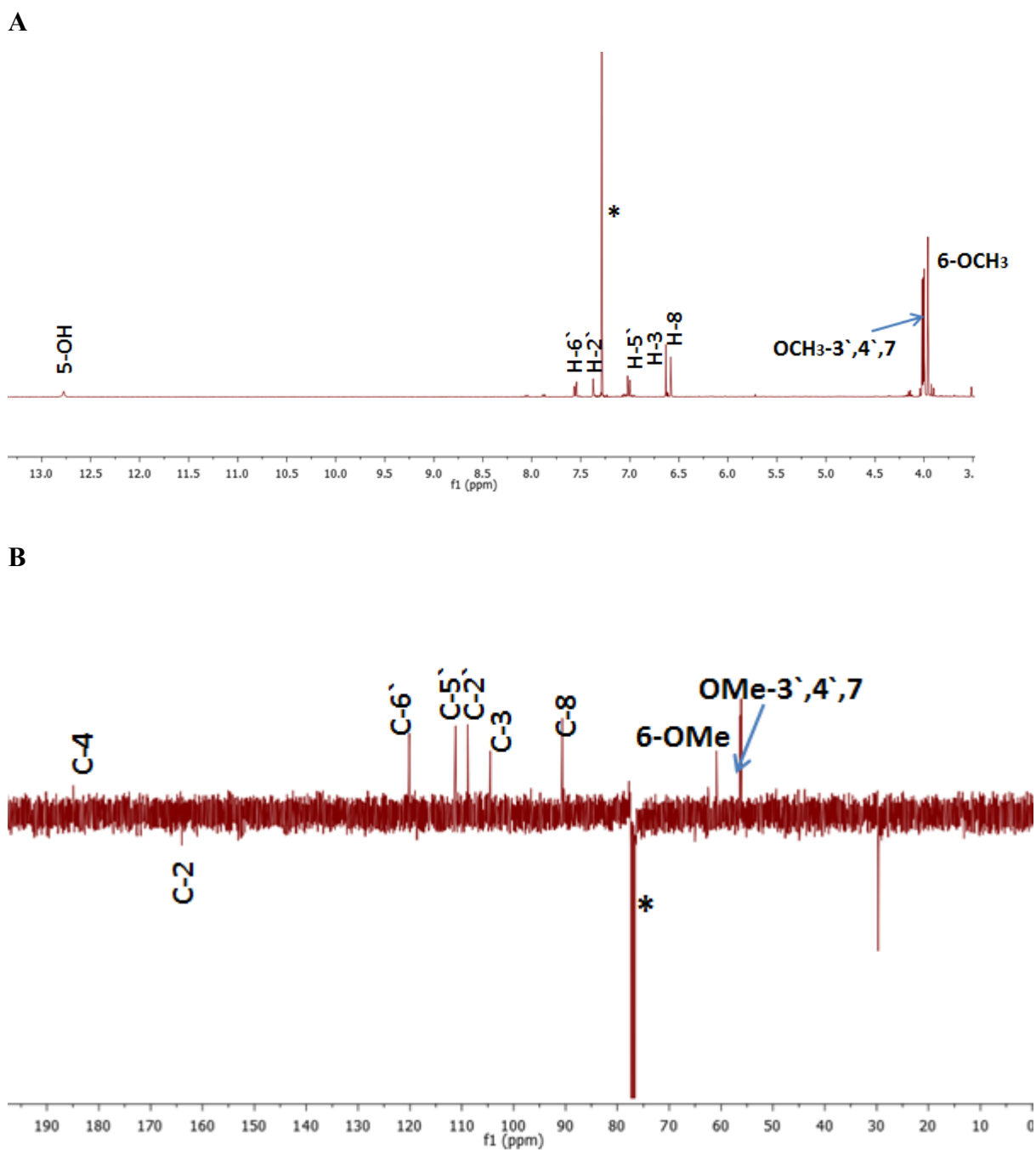
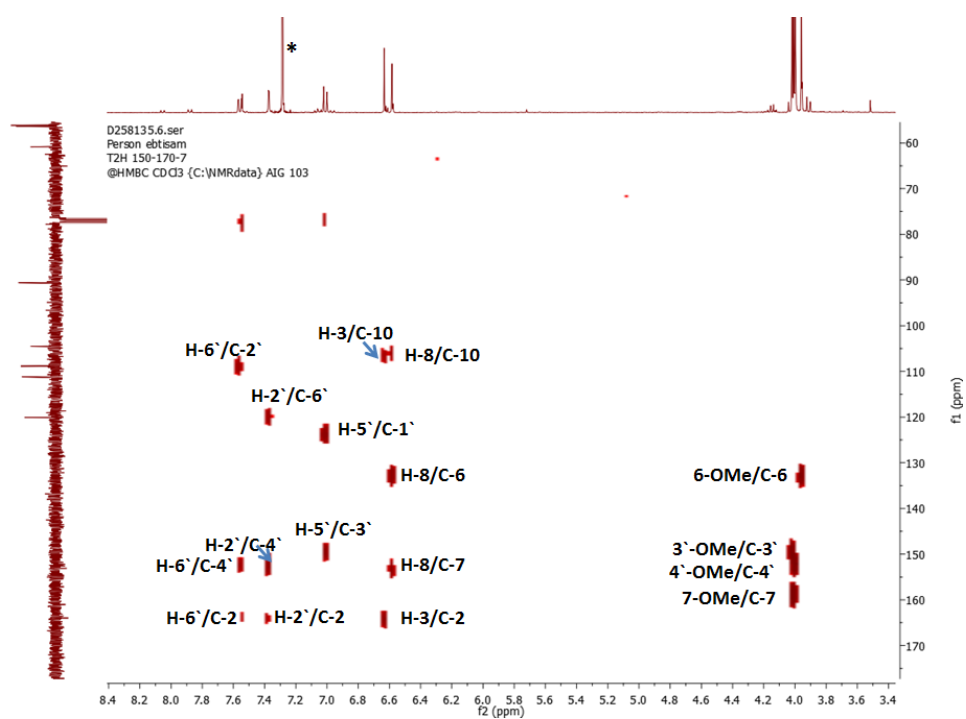


**Figure 3.16A:**  $^1\text{H}$  (400 MHz) and **3.16B:**  $^{13}\text{C}$  (100 MHz) NMR spectra of TZH-150-170-7 in  $\text{CDCl}_3^*$ .

A



B

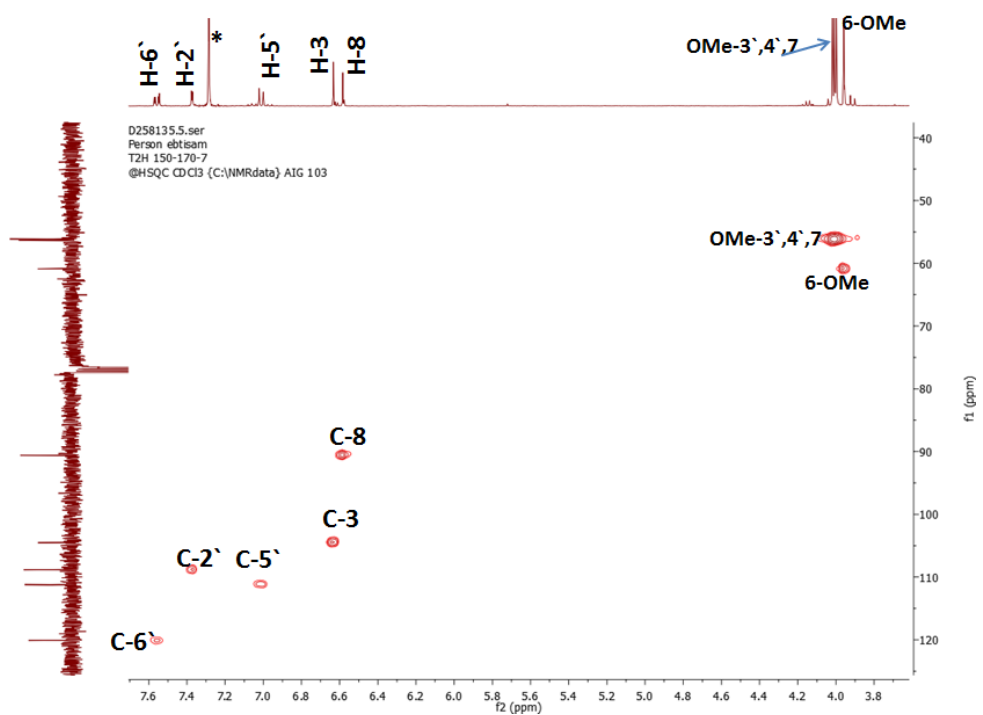


**Figure 3.17A:** HMBC and **3.17B:** HSQC spectra (400 MHz) of TZH-150-170-7 in CDCl<sub>3</sub>\*.

### 3.4.3 Characterisation of TZM-24 as poliumoside

TZM-24 was isolated from the methanol extract of *T. zanonii* as a greenish yellow amorphous solid using a Sephadex column. After spraying with *p*-anisaldehyde-sulphuric acid reagent and heating, a brown spot was observed with an  $R_f$  value of 0.62 using 30% (v/v) MeOH in EtOAc as a mobile phase on TLC.

The  $^1\text{H}$  NMR spectrum (Table 3.8, Figure 3.19A) showed signals typical for a caffeoyl group with an ABX system at  $\delta_{\text{H}}$  7.05 (1H, *d*,  $J=2.0$  Hz, H-2),  $\delta_{\text{H}}$  6.78 (1H, *d*,  $J=8.1$  Hz, H-5) and  $\delta_{\text{H}}$  6.97 (1H, *dd*,  $J=8.1, 2.0$  Hz, H-6) and two olefinic protons at  $\delta_{\text{H}}$  7.48 (1H, *d*,  $J=15.9$  Hz, H-7) and  $\delta_{\text{H}}$  6.21 (1H, *d*,  $J=15.9$  Hz, H-8).

The NMR spectrum also showed another ABX system with aromatic protons at  $\delta_{\text{H}}$  6.49 (1H, *d*,  $J=6.3$  Hz, H-6'),  $\delta_{\text{H}}$  6.64 (1H, *d*, H-5') and  $\delta_{\text{H}}$  6.65 (1H, *brs*, H-2'). The COSY and HSQC experiment spectra (Figure 3.19B, Figure 3.20B) further revealed one methylene at  $\delta_{\text{H}}$  2.70 (2H, *m*, H-7') and an oxymethylene group at  $\delta_{\text{H}}$  3.83 (1H, *m*, H-8a')/ $\delta_{\text{H}}$  3.63 (1H, *m*, H-8b'). These data suggested the presence of one hydroxytyrosol moiety. The two methyl groups at  $\delta_{\text{H}}$  1.12 (3H, *d*,  $J=6.1$  Hz, H-6'') and  $\delta_{\text{H}}$  0.96 (3H, *d*,  $J=6.1$  Hz, H-6''') and two anomeric proton at  $\delta_{\text{H}}$  4.51 (1H, *d*,  $J=1.6$  Hz, H-1'')  $\delta_{\text{H}}$  5.03 (1H, *d*,  $J=1.6$  Hz, H-1''') accounted for two 6-deoxy sugar units. Another anomeric proton at  $\delta_{\text{H}}$  4.38 (1H, *d*,  $J=7.7$  Hz, H-1''), one oxymethylene and four additional oxymethines were also observed, suggesting the presence of a third sugar unit. With the aid of COSY, TOCSY and NOESY experiments (Figure 3.19B, Figure 3.21B, Figure 3.21A), three sugar units were identified as two rhamnose and glucose. Protons H-1'', H-1''' and H-2'', H-2''' of the two rhamnose units were assigned as equatorial due to the small coupling constant detected for H-1'', H-1''' ( $J=1.6$  Hz). The coupling constant for H-4''' ( $\delta_{\text{H}}$  3.13, *t*,  $J=9.0$  Hz) indicated a *trans*-diaxial orientation of H-3'''/H-4'''/H-5'''. In contrast, the large coupling constant for H-1'' ( $\delta_{\text{H}}$  4.38,  $J=7.7$  Hz) indicated that H-1'' and H-2'' were *trans*-diaxial. Proton H-4'' ( $\delta_{\text{H}}$  4.74, *t*,  $J=9.6$  Hz) also appeared as a triplet with a large coupling constant, thus allowing the assignment of H-3'', H-4'' and H-5'' as *trans*-diaxial. On the basis of the above data, two sugar moieties were identified as  $\alpha$ -L-rhamnopyranose and  $\beta$ -D-glucopyranoside.

The  $^{13}\text{C}$  NMR spectrum (Table 3.8) showed 35 carbons including one carbonyl, two methyl, three methylenes, eighteen methines and six quaternary carbons. Distinctive signals for three anomeric carbons at  $\delta_{\text{C}}102.8$  (C-1''),  $\delta_{\text{C}}100.9$  (C-1''') and  $\delta_{\text{C}}101.7$  (C-1'''), one oxymethylene at  $\delta_{\text{C}}66.3$  (C-6'') and the two methyl groups at  $\delta_{\text{C}}18.24$  (C-6''') and at  $\delta_{\text{C}}18.64$  (C-6''') further confirmed the presence of one glucose and one rhamnose unit.

In the HMBC spectrum (Table 3.8, Figure 3.20A), the olefinic proton on the caffeoyl group at  $\delta_{\text{H}}7.48$  (H-7) correlated via  $^3J$  couplings to the carbonyl at  $\delta_{\text{C}}166.3$  (C-9) and two aromatic methines at  $\delta_{\text{C}}121.2$  (C-6) and  $\delta_{\text{C}}115.2$  (C-2). The other olefinic proton at  $\delta_{\text{H}}6.21$  (H-8) showed a  $^3J$  correlation to one quaternary carbon at  $\delta_{\text{C}}126.3$  (C-1) and to  $^2J$  coupling to carbon at  $\delta_{\text{C}}166.3$  (C-9). The protons at  $\delta_{\text{H}}7.05$  (H-2) and  $\delta_{\text{H}}6.97$  (H-6) showed  $^3J$  and  $^2J$  couplings to oxygen-bearing quaternary carbons at  $\delta_{\text{C}}148.7$  (C-4) and  $\delta_{\text{C}}146.4$  (C-3), respectively. On the hydroxytyrosol moiety, the methylene protons at  $\delta_{\text{H}}2.7$  (H-7') displayed  $^3J$  couplings to carbons at  $\delta_{\text{C}}116.9$  (C-2') and  $\delta_{\text{C}}119.9$  (C-6'), and  $^2J$  correlation to the oxymethylene carbons at  $\delta_{\text{C}}70.9$  (C-8') and at  $\delta_{\text{C}}129.6$  (C-1'). The oxymethylene signals at  $\delta_{\text{H}}3.83$  and  $\delta_{\text{H}}3.63$  (H-8'a/b) correlated via  $^3J$  coupling to one anomeric carbon at  $\delta_{\text{C}}102.8$  (C-1''), indicating the hydroxytyrosol was linked to the C-1'' of  $\beta$ -D-glucopyranoside. On the glucose unit, the  $^3J$  correlation between the anomeric proton at  $\delta_{\text{H}}4.38$  (H-1'') and the oxymethylene carbon at  $\delta_{\text{C}}70.9$  (C-8') further established the bridge link between  $\beta$ -D-glucopyranoside and hydroxytyrosol. The link between the caffeoyl group and  $\beta$ -D-glucopyranoside was also detected with the  $^3J$  coupling between the proton at  $\delta_{\text{H}}4.74$  (H-4'') the carbonyl at  $\delta_{\text{C}}166.3$  (C-9). In addition, the protons at  $\delta_{\text{H}}3.72$  (H-3'') and  $\delta_{\text{H}}5.03$  (H-1''') showed  $^3J$  correlations to the carbons at  $\delta_{\text{C}}101.7$  (C-1''') and  $\delta_{\text{C}}79.4$  (C-3''), respectively, suggesting that the glucose and rhamnose units were linked through C-3'' and C-1'''. Furthermore, the protons at  $\delta_{\text{H}}4.51$  (H-1''') showed  $^3J$  correlations to the carbons at  $\delta_{\text{C}}66.6$  (C-6'') and  $\delta_{\text{H}}3.51$  (H-6'') showed  $^3J$  correlation to the carbon at  $\delta_{\text{C}}100.9$  (C-1''') suggesting that the glucose and other rhamnose units were linked through C-6'' and C-1''''.

The HRESI-MS data showed molecular ion  $[\text{M-H}]^-$  at  $m/z$  769.73, suggesting a

molecular formula of  $C_{35}H_{46}O_{19}$ . The above data led to the identification of TZM-24 as poliumoside. The NMR results were in good agreement with a previous report (Boghrati *et al.*, 2016b). This is the first report of poliumoside from *T. zanonii*.

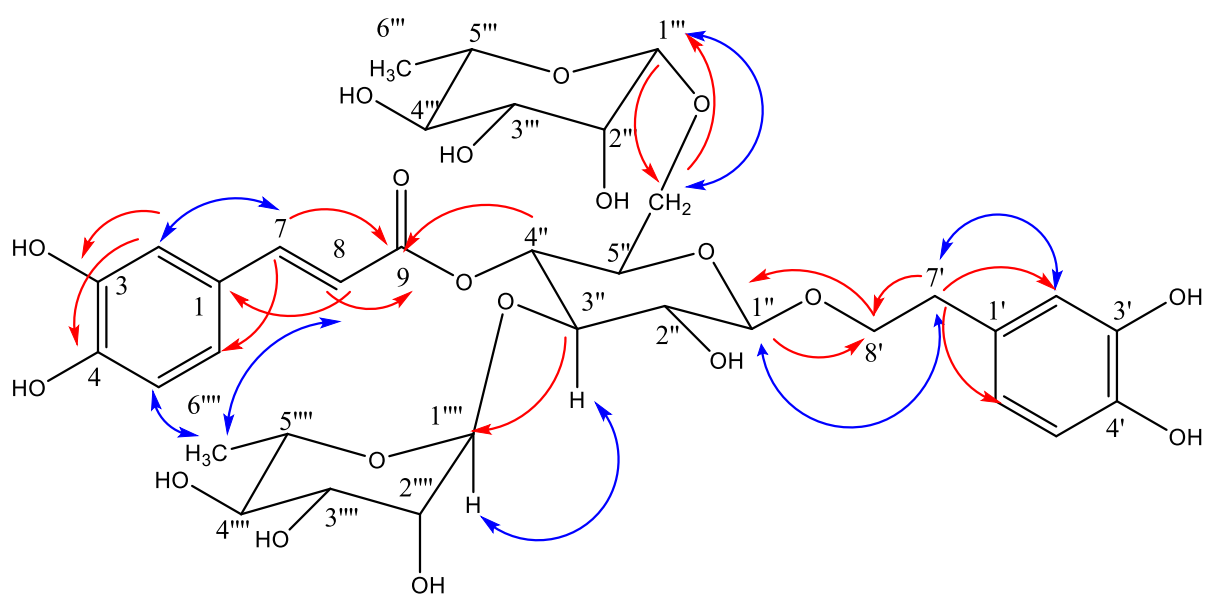


**Figure 3.18:** Structure of poliumoside. Key HMBC (  ) and NOESY (  ) correlations observed in TZM-24.

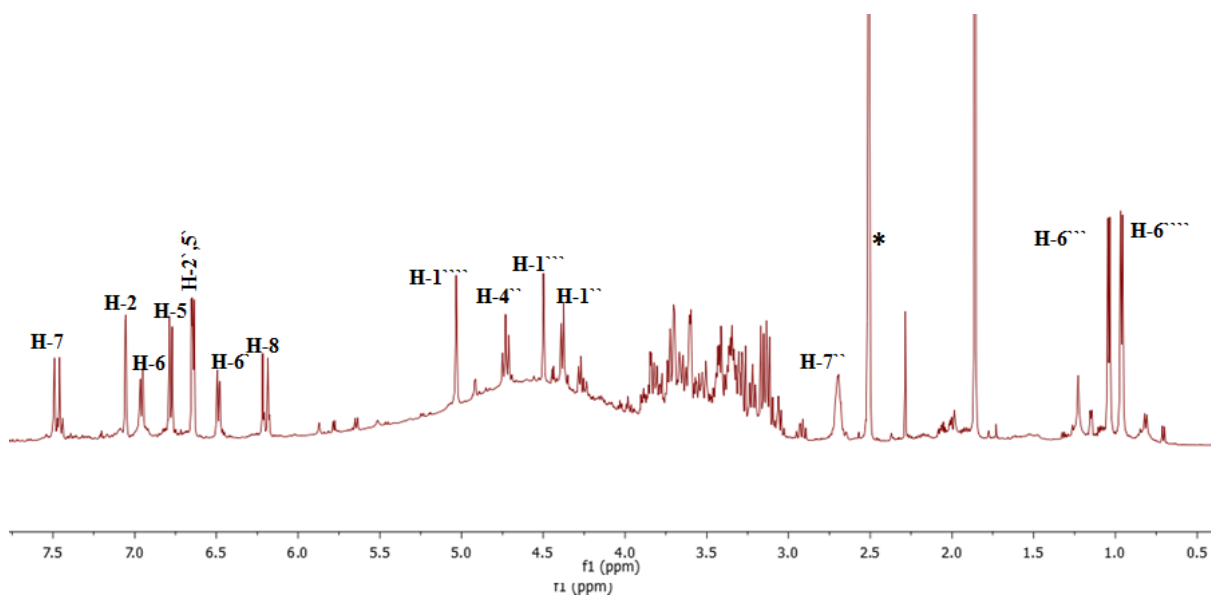
**Table 3.8:**  $^1\text{H}$  (500MHz),  $^{13}\text{C}$  (100MHz), HMBC data of TZM-24 in DMSO- $d_6$ .

Position	$^1\text{H}$ ( $\delta$ ppm)	$^{13}\text{C}$ ( $\delta$ ppm)	HMBC correlations
Caffeoyl moiety	-	-	-
1	-	126.3	-
2	7.05 (1H, <i>d</i> , $J=2.0$ Hz)	115.2	C-6( $^3J$ ), C-4( $^3J$ ), C-7( $^3J$ ), C-3( $^2J$ )
3	-	146.4	-
4	-	148.7	-
5	6.78 (1H, <i>d</i> , $J=8.1$ Hz)	116.2	C-1( $^3J$ ), C-3( $^2J$ ), C-4( $^3J$ ), C-6( $^3J$ )
6	6.97 (1H, <i>dd</i> , $J=8.1, 2.0$ Hz)	121.2	C-2( $^3J$ ), C-4( $^3J$ ), C-7( $^3J$ ), C-3( $^4J$ )
7	7.48 (1H, <i>d</i> , $J=15.9$ Hz)	146.1	C-9( $^3J$ ), C-8( $^2J$ ), C-1( $^2J$ ), C-6( $^3J$ ), C-2( $^3J$ )
8	6.21 (1H, <i>d</i> , $J=15.9$ Hz)	113.9	C-1( $^3J$ ), C-9( $^2J$ ), C-7( $^2J$ )
9	-	166.3	-
Hydroxytyrosol	-	-	-
1'	-	130.2	-
2'	6.65 (1H, <i>brs</i> )	116.9	C-6'( $^3J$ ), C-4'( $^3J$ ), C-7'( $^3J$ ), C-1'( $^2J$ )
3'	-	144.8	-
4'	-	143.2	-
5'	6.64 (1H, <i>d'</i> )	115.7	C-1'( $^3J$ ), C-3'( $^3J$ )
6'	6.49 (1H, <i>d</i> , $J=6.3$ Hz)	119.9	C-7'( $^3J$ ), C-2'( $^3J$ ), C-4'( $^3J$ )
7'	2.70 (2H, <i>m</i> )	35.5	C-8'( $^2J$ ), C-2'( $^3J$ ), C-6'( $^3J$ ), C-1'( $^2J$ )
8'	3.63 (1H, <i>m</i> ) / 3.83 (1H, <i>m</i> )	70.9	C-7'( $^2J$ ), C-1''( $^3J$ ), C-1'( $^3J$ )
Glucose	-	-	-
1''	4.38 (1H, <i>d</i> , $J=7.7$ Hz)	102.8	C-8'( $^3J$ )
2''	3.22 (1H, <i>t</i> , $J=8.5$ Hz)	74.9	C-1''( $^2J$ ), C-3''( $^2J$ )
3''	3.72 (1H, <i>t</i> , $J=9.2$ Hz)	79.4	C-4''( $^2J$ ), C-2''( $^2J$ ), C-1'''( $^3J$ )
4''	4.74 (1H, <i>t</i> , $J=9.6$ Hz)	69.4	C-9'( $^3J$ ), C-3''( $^2J$ ), C-5''( $^2J$ ), C-6''( $^3J$ )
5''	3.66 (1H, <i>m</i> )	74.5	C-1''( $^3J$ )
6''	3.32 (1H, <i>m</i> ) / 3.51 (1H, <i>m</i> )	66.3	C-1'''( $^3J$ )
Rhamnose 1	-	-	-
1'''	4.51 (1H, <i>d</i> , $J=1.6$ Hz, )	100.9	C-6''( $^3J$ ), C-5'''( $^2J$ ), C-2'''( $^3J$ )
2'''	3.60 (1H, <i>dt</i> , $J = 3.5, 1.7$ Hz,)	71.0	C-3'''( $^2J$ ), C-4'''( $^3J$ ), C-1'''( $^2J$ )
3'''	3.41 (1H, <i>dd</i> )	71.3	C-5'''( $^3J$ ), C-2'''( $^3J$ )
4'''	3.16 (1H, <i>t</i> , $J=9.1$ Hz)	72.7	C-6'''( $^3J$ ), C-5'''( $^2J$ ), C-3'''( $^2J$ )
5'''	3.37 (1H, <i>m</i> )	68.1	C-6'''( $^2J$ ), C-4'''( $^2J$ )

**Table 3.8:** (continued).

6 <sup>''''</sup>	1.12 (3H, <i>d</i> , $J=6.1$ Hz)	18.2	C-5 <sup>''''</sup> ( <sup>2</sup> $J$ ), C-4 <sup>''''</sup> ( <sup>3</sup> $J$ )
Rhamnose 2			
1 <sup>''''</sup>	5.03 (1H, <i>d</i> , $J=1.5$ Hz)	101.7	C-3 <sup>''''</sup> ( <sup>3</sup> $J$ ), C-3 <sup>''''</sup> ( <sup>3</sup> $J$ ), C-5 <sup>''''</sup> ( <sup>3</sup> $J$ )
2 <sup>''''</sup>	3.70 (1H, <i>brs</i> )	70.9	C-3 <sup>''''</sup> ( <sup>2</sup> $J$ )
3 <sup>''''</sup>	3.30 (1H, <i>m</i> )	70.9	C-4 <sup>''''</sup> ( <sup>2</sup> $J$ ), C-5 <sup>''''</sup> ( <sup>3</sup> $J$ )
4 <sup>''''</sup>	3.14 (1H, <i>t</i> , $J=9.1$ Hz)	72.2	C-2 <sup>''''</sup> ( <sup>3</sup> $J$ ), C-5 <sup>''''</sup> ( <sup>2</sup> $J$ )
5 <sup>''''</sup>	3.33 (1H, <i>m</i> )	69.1	C-1 <sup>''''</sup> ( <sup>3</sup> $J$ )
6 <sup>''''</sup>	0.96 (3H, <i>d</i> , $J=6.1$ Hz)	18.6	C-4 <sup>''''</sup> ( <sup>3</sup> $J$ ), C-5 <sup>''''</sup> ( <sup>2</sup> $J$ )

A



B

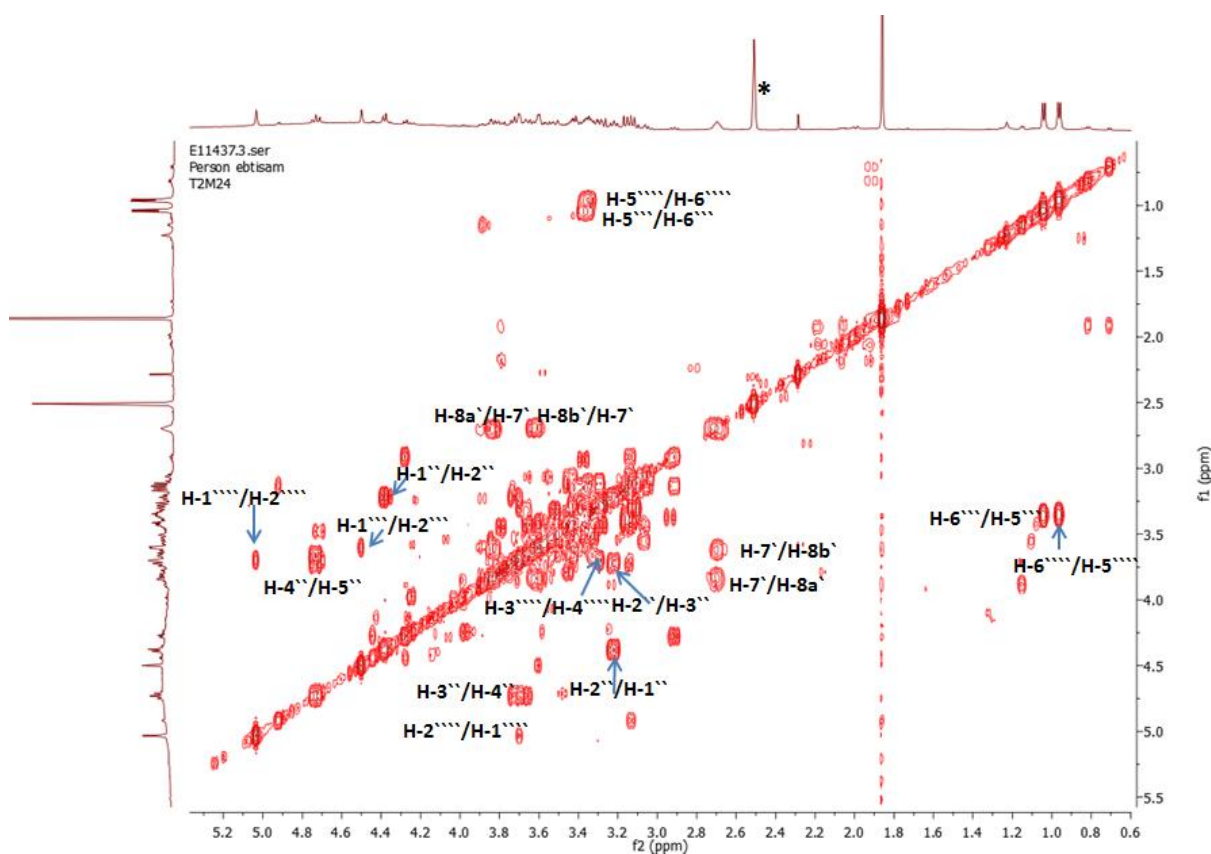
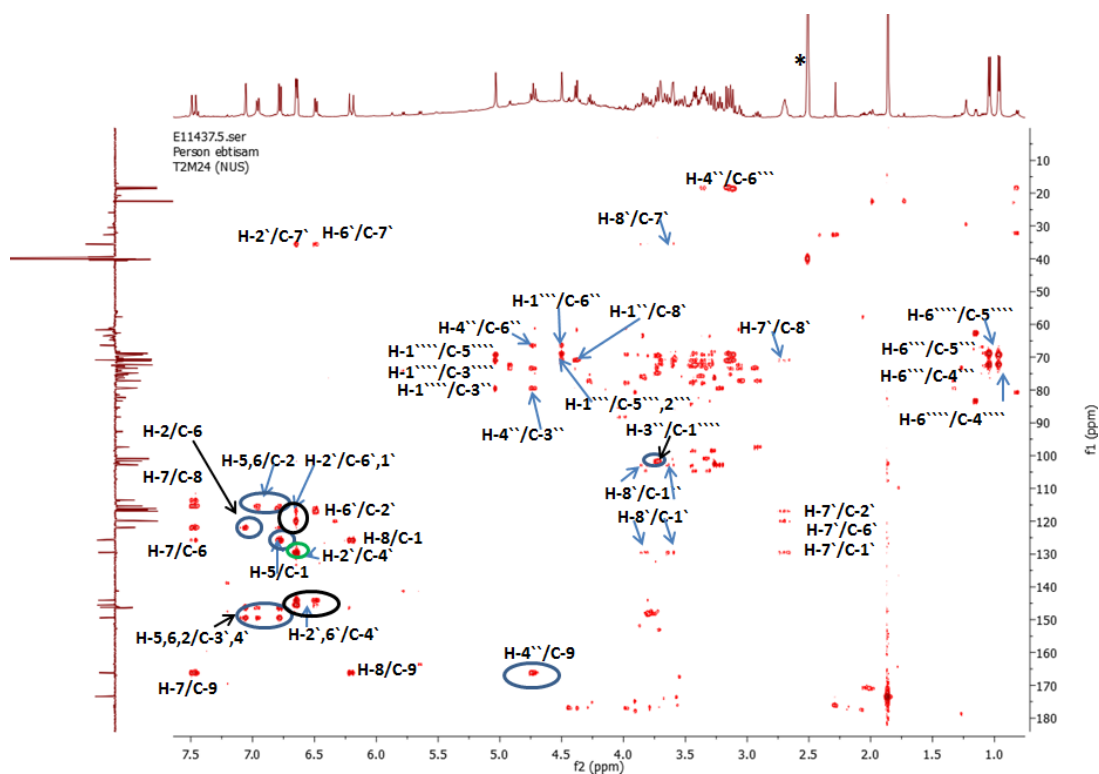


Figure 3.19A:  $^1\text{H}$  and 3.19B: COSY (500 MHz) spectra of TzM-24 in  $\text{DMSO-}d_6$  \*.

A



B

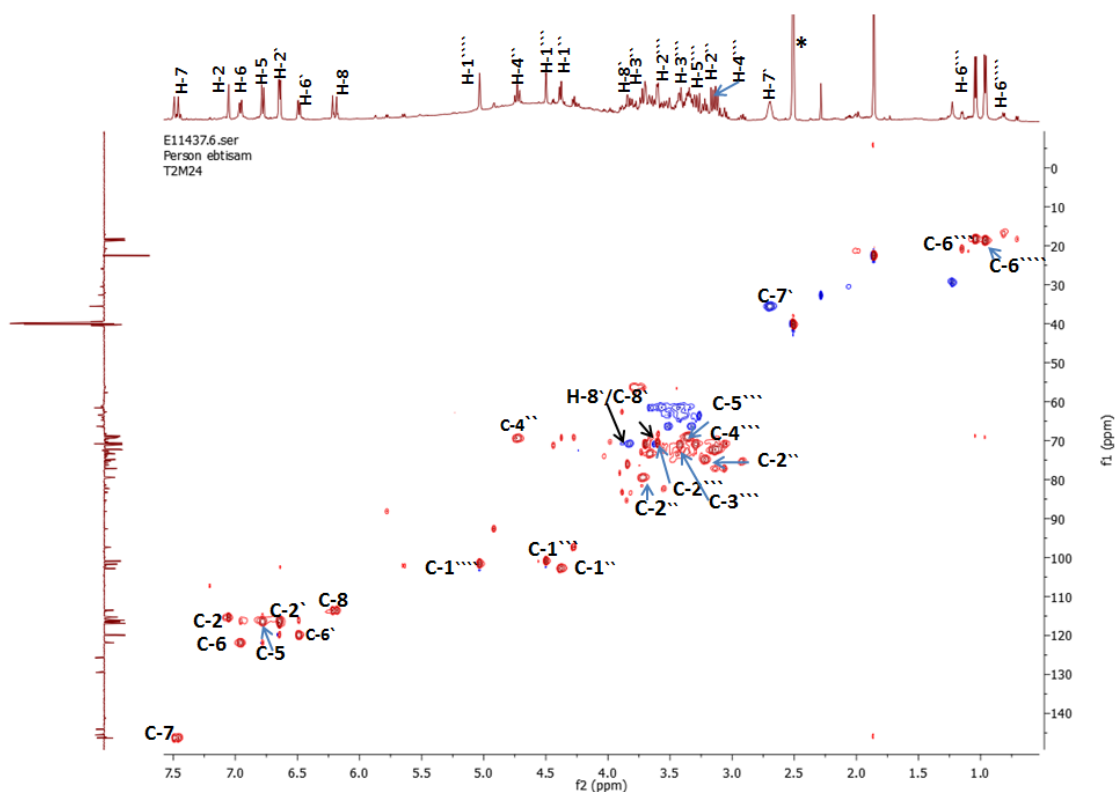
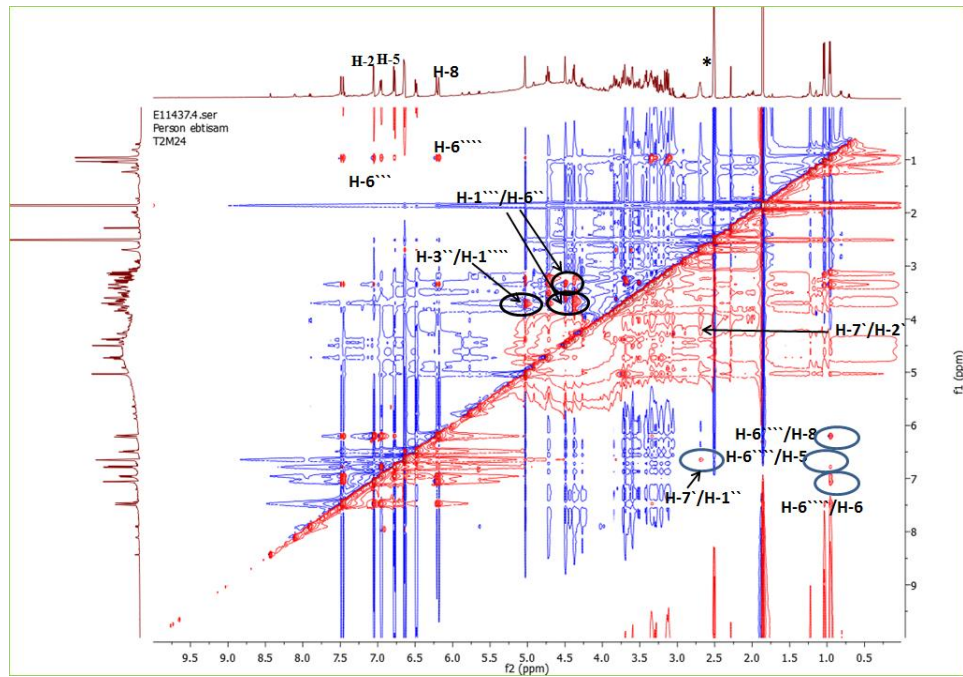
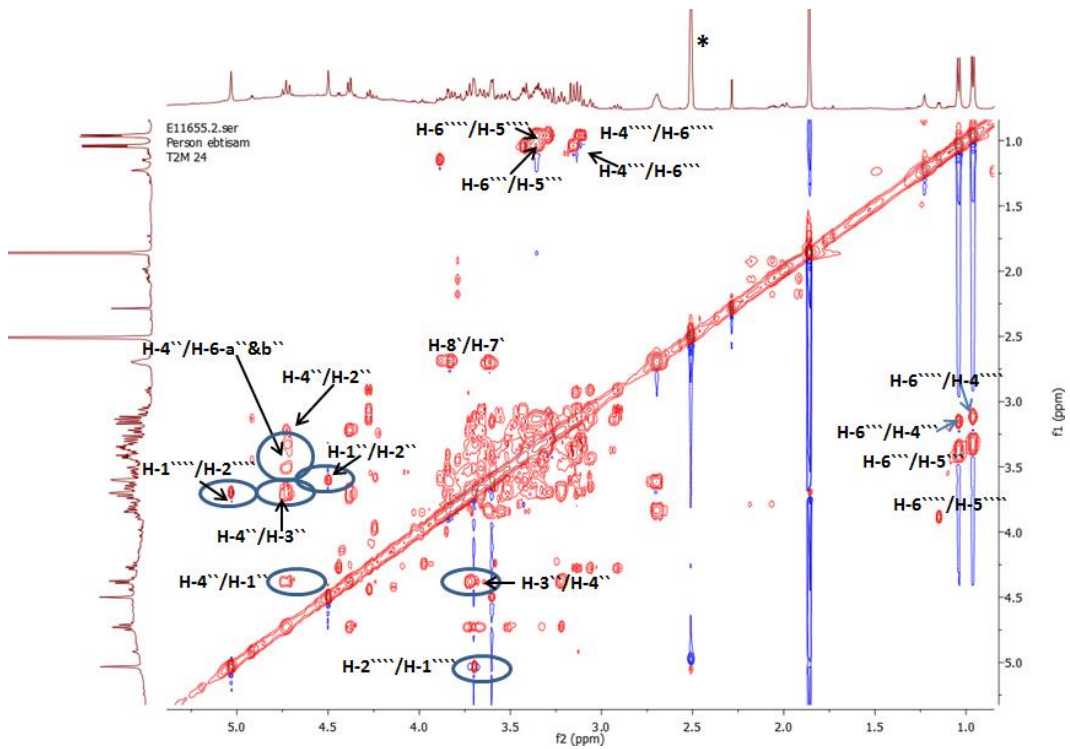


Figure 3.20A: HMBC and 3.20B: HSQC spectra (500 MHz) of TZM-24 in DMSO- $d_6$  \*.

A



B



**Figure 3.21 A: NOESY and 3.21B: TOCSY spectra (500 MHz) of T2M-24 in DMSO- $d_6$  \*.**

### 3.4.4 Characterisation of TZH-68 as pheophytin A

The compound TZH-68 (Figure 3.22) was isolated from the hexane extract of *T. zanonii* as dark-green amorphous solid using silica gel column. It gave a green color after spraying with anisaldehyde-sulphuric acid reagent followed by heating, with a  $R_f$  value of 0.65 using 70% (v/v) hexane in EtOAc as the mobile phase on TLC.

The  $^1\text{H}$  NMR spectrum (Table 3.9, Figure 3.23) revealed the presence of three proton singlets in the region of  $\delta_{\text{H}}$  8.5 to 10 ppm, a singlet around 6.2 ppm and a multiplet around 8 accounting for a  $-\text{CH}=\text{CH}_2$  group. Singlets were also observed between 3 and 4 ppm for the methoxy groups and singlets detected between 1.55 and 1.9 ppm for the methyl.

The  $^1\text{H}$  NMR spectrum (Figure 3.23) showed three deshielded protons at 9.55 ppm (1H, *s*, H-10), 9.42 ppm (1H, *s*, H-5) and 8.58 (1H, *s*, H-20). Another three signals between 6 to 8 ppm for H-3<sup>1</sup>, H-3<sup>2</sup> and H-13<sup>2</sup>. In addition, an oxymethylene multiplet at  $\delta_{\text{H}}$  4.50, a triplet at  $\delta_{\text{H}}$  5.17 assigned as an olefinic proton attached to a methylene and methyl signals at  $\delta_{\text{H}}$  0.80 (6H, *d*),  $\delta_{\text{H}}$  0.87 (6H, *d*) and  $\delta_{\text{H}}$  1.60 (3H, *s*) were observed, suggesting the presence of a phytol group.

The  $^{13}\text{C}$  NMR spectrum (Figure 3.24A and 3.24B, Table 3.9) showed a total of 55 carbons, including five methyls, one methoxy at  $\delta_{\text{C}}$  52.9, seven methines including four olefinic carbons at  $\delta_{\text{C}}$  129.1,  $\delta_{\text{C}}$  97.4,  $\delta_{\text{C}}$  103.8 and  $\delta_{\text{C}}$  93.2, three methylenes at  $\delta_{\text{C}}$  19.5, 29.7 and 31.5, one exomethylene at  $\delta_{\text{C}}$  122.9 and eighteen quaternary carbons including three carbonyls at  $\delta_{\text{C}}$  189.7, 173.7 and 169.5. The other 20 carbons could be attributed to the phytol moiety with one olefinic methine at  $\delta_{\text{C}}$  117.7, one oxymethylene at  $\delta_{\text{C}}$  61.5, five methyls at  $\delta_{\text{C}}$  16.0, 19.6, 19.7, 22.65 and 22.55, nine methylenes (three at  $\delta_{\text{C}}$  24.6, 24.8 and 25.6, four at 37.0 ~ 37.38 and two at  $\delta_{\text{C}}$  39.5 and 39.9), and three methines at  $\delta_{\text{C}}$  27.9, 32.6 and 32.7 as well as one quaternary carbon at  $\delta_{\text{C}}$  142.9. In addition, the HMBC and HSQC spectra (Figure 3.25A, and 3.25B) showed typical correlations between the protons and carbons (Table 3.9) confirming the structure of pheophytin A.

The HRESI-MS data showed molecular ion  $[M]^+$  at  $m/z$  871.5715, indicating a molecular formula of  $C_{55}H_{74}O_5N_4$ . Data from  $^1H$  NMR spectra of TZH-68 was similar to the data obtained for pheophytin A by (Oba *et al.*, 1997, Lv and Xu, 2008).

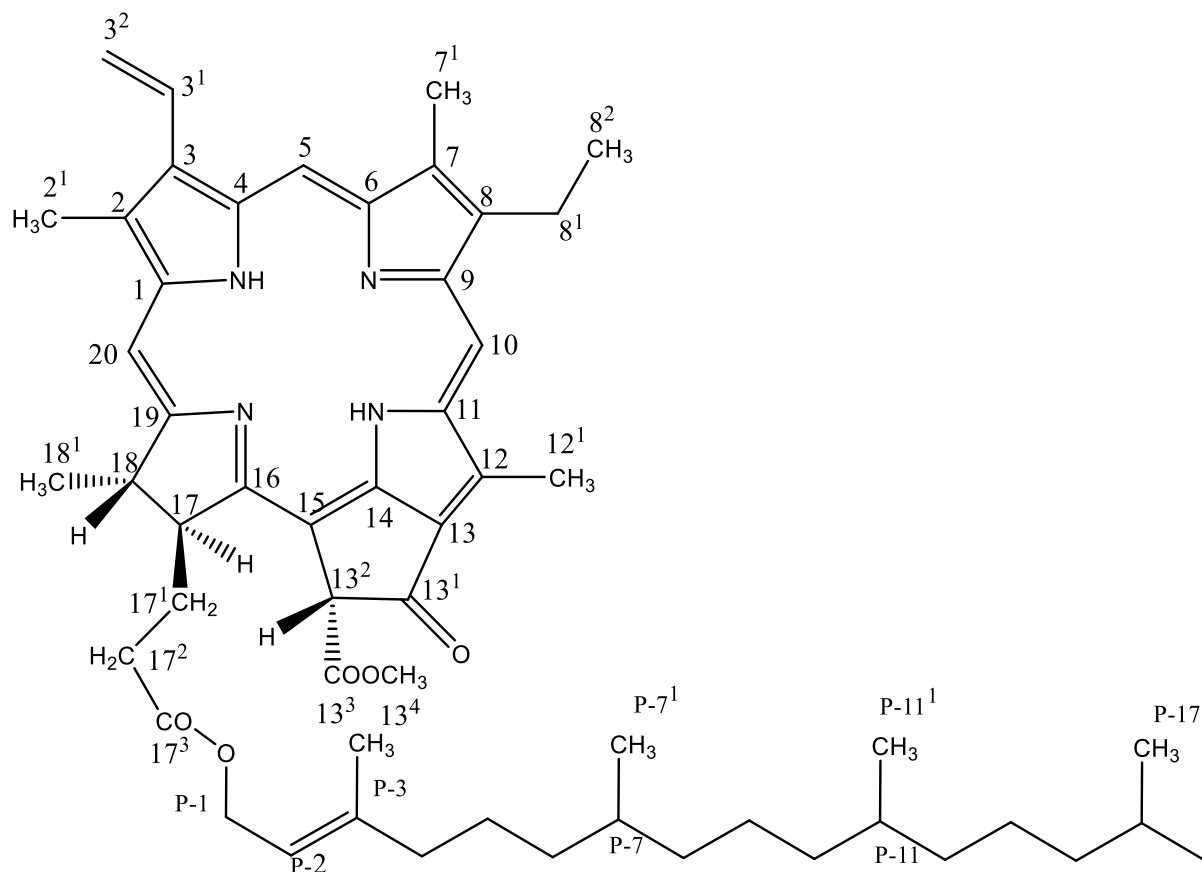


**Figure 3.22:** Structure of pheophytin A.

**Table 3.9:**  $^1\text{H}$  (500MHz),  $^{13}\text{C}$  (100MHz), and HMBC data of TZH-68 in  $\text{CDCl}_3$ .

Position	$^1\text{H}$ ( $\delta$ ppm)	$^{13}\text{C}$ ( $\delta$ ppm)	HMBC correlation
1	-	142.5	-
2	-	131.9	-
2 <sup>1</sup>	3.43 (3H, <i>s</i> )	12.0	H-2 <sup>1</sup> /C-2( <sup>2</sup> <i>J</i> ), C-1( <sup>3</sup> <i>J</i> ), C-3( <sup>3</sup> <i>J</i> )
3	-	136.3	-
3 <sup>1</sup>	8.03 (1H, <i>dd</i> , <i>J</i> =17.8, 11.5 Hz)	129.1	-
3 <sup>2</sup>	6.20 (1H, <i>d</i> , /6.32 (1H, <i>d</i> ))	122.9	H-3 <sup>2</sup> /C-3( <sup>3</sup> <i>J</i> )
4	-	136.5	-
5	9.42 (1H, <i>s</i> )	97.4	H-5/C-7( <sup>3</sup> <i>J</i> ), C-3( <sup>3</sup> <i>J</i> ), C-4( <sup>2</sup> <i>J</i> )
6	-	155.3	-
7	-	136.1	-
7 <sup>1</sup>	3.27 (3H, <i>s</i> )	11.4	H-7 <sup>1</sup> /C-6( <sup>3</sup> <i>J</i> ), C-8( <sup>3</sup> <i>J</i> ), C-7( <sup>2</sup> <i>J</i> )
8	-	145.5	-
8 <sup>1</sup>	3.73 (2H, <i>m</i> )	19.5	-
8 <sup>2</sup>	1.73 (3H, <i>t</i> , <i>J</i> =7.7 Hz)	17.5	H-8 <sup>2</sup> /C-8 <sup>1</sup> ( <sup>2</sup> <i>J</i> ), C-8( <sup>3</sup> <i>J</i> )
9	-	150.9	-
10	9.55 (1H, <i>s</i> )	103.8	H-10/C-12( <sup>3</sup> <i>J</i> ), C-11( <sup>2</sup> <i>J</i> ), C-8( <sup>3</sup> <i>J</i> )
11	-	137.9	-
12	-	129.7	-
12 <sup>1</sup>	3.71 (3H, <i>s</i> )	12.2	H-12 <sup>1</sup> /C-11( <sup>3</sup> <i>J</i> ), C-13( <sup>3</sup> <i>J</i> ), C-12( <sup>2</sup> <i>J</i> )
13	-	128.9	-
13 <sup>1</sup>	-	189.7	-
13 <sup>2</sup>	6.28(1H, <i>s</i> )	64.55	H-13 <sup>2</sup> /C-15( <sup>2</sup> <i>J</i> ), C-14( <sup>3</sup> <i>J</i> ), C-13 <sup>1</sup> , ( <sup>2</sup> <i>J</i> ) C-13 <sup>3</sup> ( <sup>2</sup> <i>J</i> )
13 <sup>3</sup>	-	169.5	-
13 <sup>4</sup>	3.91 (3H, <i>s</i> )	52.9	H-13 <sup>4</sup> /C-13 <sup>3</sup> ( <sup>3</sup> <i>J</i> )
14	-	149.5	-
15	-	105.7	-
16	-	161.4	-
17	4.23 (1H, <i>d</i> )	51.1	-
17 <sup>1</sup>	2.36 (1H, <i>m</i> ) /2.66 (1H, <i>m</i> )	29.7	-
17 <sup>2</sup>	2.22 (1H, <i>m</i> ) /2.51 (1H, <i>m</i> )	31.5	-
17 <sup>3</sup>	-	173.7	-
18	4.49 (1H)	50.8	-
18 <sup>1</sup>	1.82 (3H, <i>d</i> , <i>J</i> =7.3 Hz)	23.1	H-18 <sup>1</sup> /C-17( <sup>3</sup> <i>J</i> ), C-18( <sup>2</sup> <i>J</i> ), C-19( <sup>3</sup> <i>J</i> )
19	-	172.8	-

**Table 3.9:** (continued).

20	8.58 (1H, <i>s</i> )	93.2	H-20/C-2( <sup>3</sup> <i>J</i> )
P-1	4.50	61.5	-
P-2	5.17	117.7	-
P-3	-	142.9	-
P-3 <sup>1</sup>	1.60	16.0	H-P-3 <sup>1</sup> /C-P-4( <sup>3</sup> <i>J</i> ), C-P-2( <sup>3</sup> <i>J</i> ), C-P-3( <sup>2</sup> <i>J</i> )
P-4	1.91	39.9	-
P-5	1.30	24.9	-
P-6	123/1.02	37.3	-
P-7	1.32	32.6	-
P-7 <sup>1</sup>	0.82	19.7	H- P-7 <sup>1</sup> /C-P-7( <sup>2</sup> <i>J</i> ), C-P-8( <sup>3</sup> <i>J</i> )
P-8	123/1.02	37.3	-
P-9	1.30	24.8	-
P-10	123/1.02	37.2	-
P-11	1.32	32.7	-
P-11 <sup>1</sup>	0.80	19.6	H- P-11 <sup>1</sup> /C-P-12( <sup>3</sup> <i>J</i> ), C-P-11( <sup>2</sup> <i>J</i> )
P-12	123/1.02	37.5	-
P-13	1.30	25.6	-
P-14	1.13	39.5	-
P-15	1.56	27.9	-
P-16	0.87	22.5	H-P-16/C-P-17( <sup>3</sup> <i>J</i> ), C-P-15( <sup>2</sup> <i>J</i> ), C-P-14( <sup>3</sup> <i>J</i> )
P-17	0.88	22.6	H-P-17/C-P-16( <sup>3</sup> <i>J</i> ), C-P-15( <sup>2</sup> <i>J</i> ), C-P-14( <sup>3</sup> <i>J</i> )

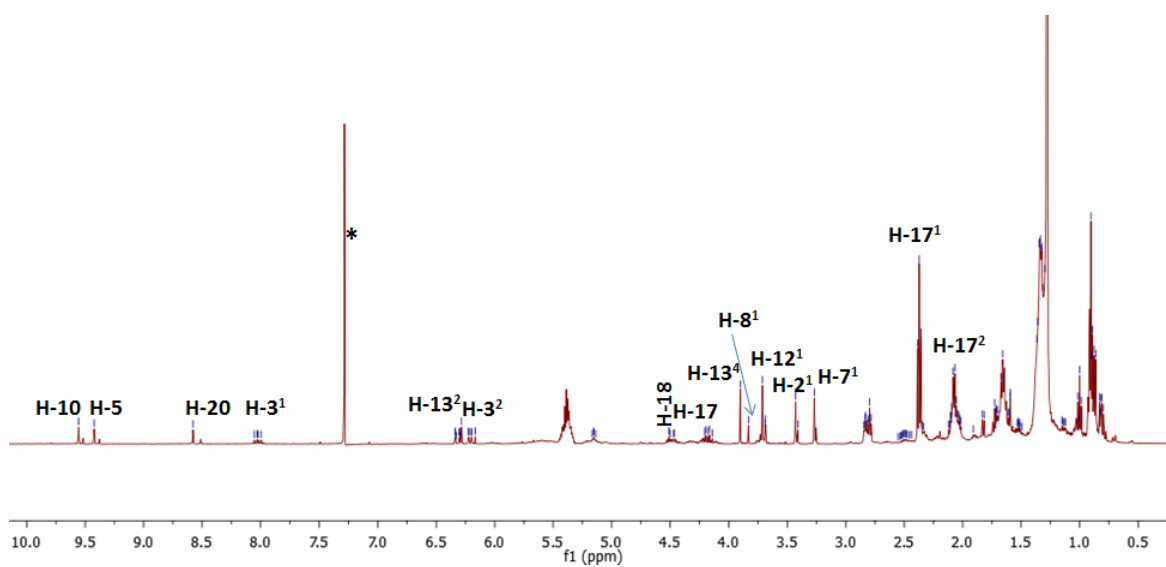
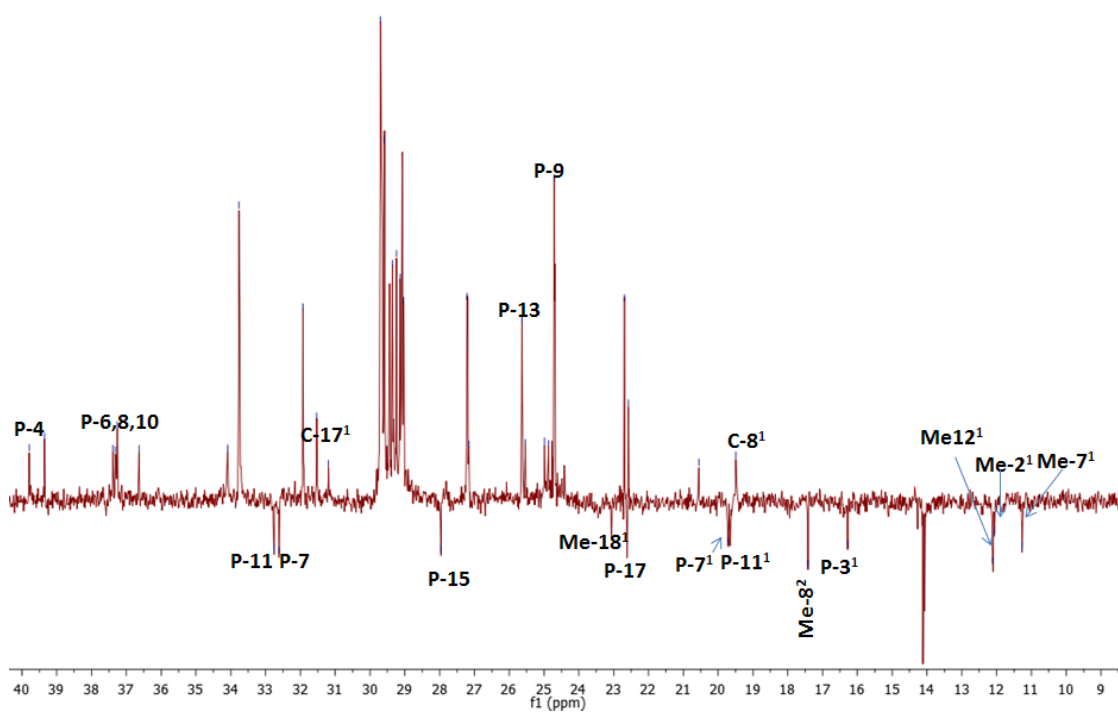


**Figure 3.23:** <sup>1</sup>H NMR spectrum (500 MHz) of TZH-68 in CDCl<sub>3</sub>\*.

A



B

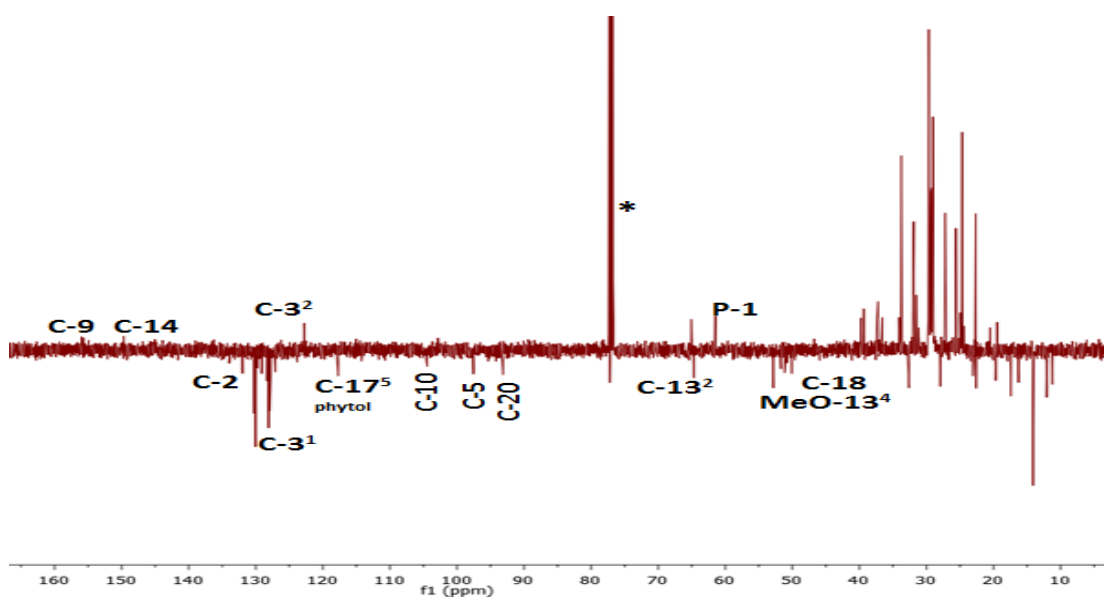
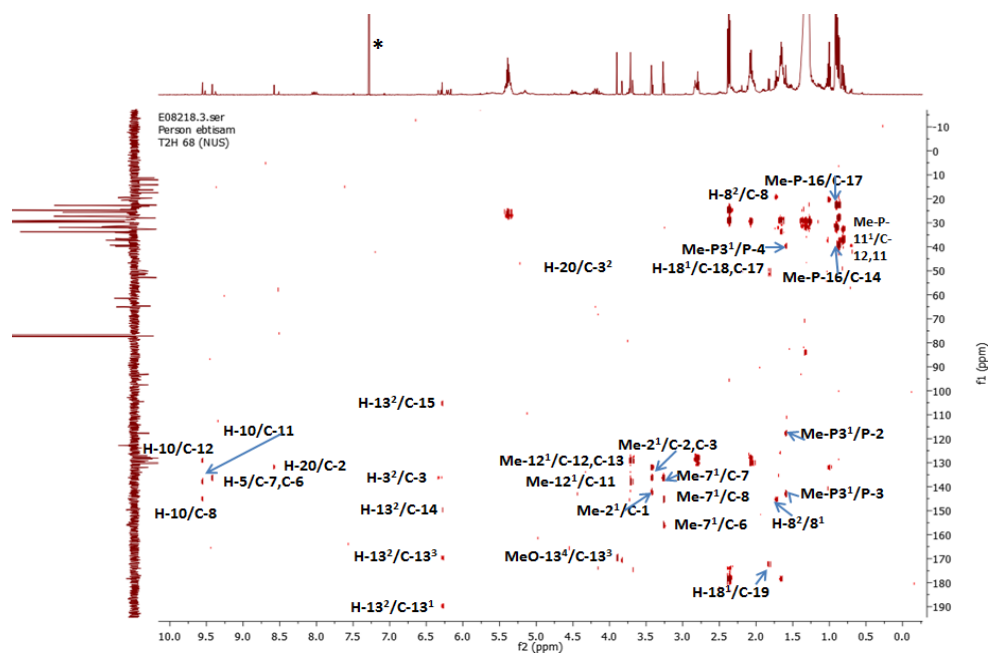


**Figure 3.24 A:** and **3.24B:** Selected expansion  $^{13}\text{C}$  NMR spectra (100 MHz) of TZH-68 in  $\text{CDCl}_3^*$ .

A



B

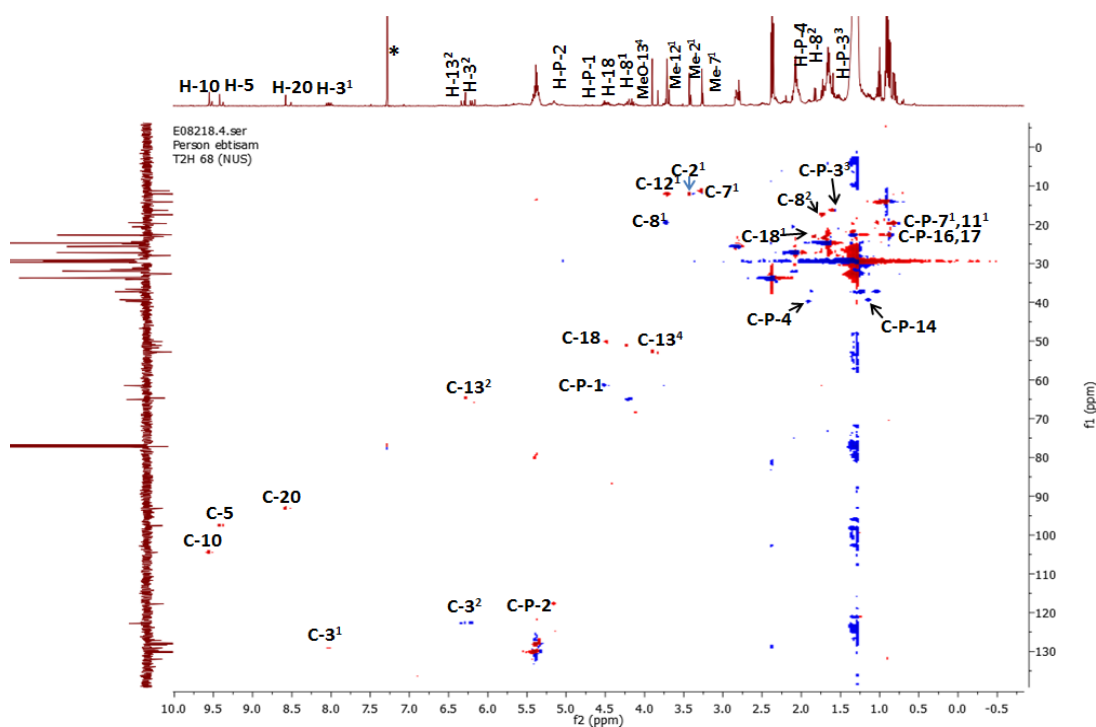


Figure 3.25A: HMBC and 3.25B: HSQC spectra (500 MHz) of TZH-68 in  $\text{CDCl}_3^*$ .

### 3.2.5 Characterisation of TZH-41-49 as ferulic acid ester of (a) fatty alcohol(s)

The compound TZH-41-49 (Figure 3.26) was isolated from the hexane extract of *T. zanonii* using column chromatography on silica gel. Using 70% (v/v) hexane in EtOAc as the mobile phase for TLC, it appeared as a brown spot with a  $R_f$  value of 0.74 after spraying with *p*-anisaldehyde sulphuric acid reagent and heating.

The  $^1\text{H}$  NMR spectrum (Figure 3.27A) of the compound TZH-41-49 (Figure 3.26) revealed the presence of an aromatic ring with three protons at  $\delta_{\text{H}}$  6.91 (1H, *d*,  $J = 8.1$  Hz, H-5),  $\delta_{\text{H}}$  7.03 (1H, *d*,  $J = 1.9$  Hz, H-2), and  $\delta_{\text{H}}$  7.07 (1H, *dd*,  $J = 8.1, 1.9$  Hz, H-6). The spectrum also showed the presence of *trans* olefinic protons at  $\delta_{\text{H}}$  7.60 (1H, *d*,  $J = 15.9$  Hz) and  $\delta_{\text{H}}$  6.28 (1H, *d*,  $J = 15.9$ ) were assigned to H-1' and H-2' respectively. A signal for a 3H singlet at  $\delta_{\text{H}}$  3.92 represented a methoxy group.

The  $^{13}\text{C}$  spectrum (Figure 3.27B, Table 3.10) showed carbon signals made up of a methoxy at  $\delta_{\text{C}}$  56.1 ppm and six aromatic carbons at  $\delta_{\text{C}}$  109.4, 114.6, 122.9, 126.5, 146.2, 148.0 (carbons at 146.2 and 148.0 ppm were observed to be oxygen bearing carbons), and two olefinic carbons at  $\delta_{\text{C}}$  115.6 and 144.6, and a carbonyl carbon at  $\delta_{\text{C}}$  167.3 ppm.

Using 2D NMR (HMBC and HSQC) (Figure 3.28A, Figure 3.28B), the structure of the compound was elucidated as follows: The HMBC (Figure 3.28A, Table 3.10) showed  $^3J$  correlations between  $\delta_{\text{H}}$  7.60 (H-1') and carbon signals at  $\delta_{\text{C}}$  122.9 (C-6),  $\delta_{\text{C}}$  109.1 (C-2) and to carbonyl at  $\delta_{\text{C}}$  167.8 (C-3') and  $^2J$  correlation to carbon at  $\delta_{\text{C}}$  115.6 (C-2'). The protons at  $\delta_{\text{H}}$  6.28 (H-2') showed a  $^2J$  correlation to carbonyl at  $\delta_{\text{C}}$  167.8 (C-3') and  $^3J$  correlations to carbon at  $\delta_{\text{C}}$  126.5 (C-1). The proton signal at  $\delta_{\text{H}}$  7.03 (H-2) showed  $^3J$  correlation to carbons at  $\delta_{\text{C}}$  122.9 (C-6), 144.6 (C-1') and 148.0 (C-4). The protons at  $\delta_{\text{H}}$  6.91 (H-6) showed a  $^3J$  coupling to carbons at  $\delta_{\text{C}}$  126.5 (C-1) and 146.2 (C-4). The methoxy at  $\delta_{\text{H}}$  3.92 showed  $^3J$  correlation to carbon  $\delta_{\text{C}}$  146.2 (C-3). The proton at  $\delta_{\text{H}}$  4.13 showed  $^3J$  correlation to a carbonyl at  $\delta_{\text{C}}$  167.8 (C-3') which confirmed the esterification of the ferulic acid by a long aliphatic chain. Thus the fraction seems to be a ferulic acid residue (Figure 3.26) associated with a saturated

fatty alcohol and the aliphatic region show correlation to the keto of the ferulic acid, which was shown in the HMBC spectrum (Figure 3.28A). The ferulic acid is esterified with an aliphatic saturated fatty chain.

The HRESI-MS data showed a molecular ion  $[M]^-$  at  $m/z$  419.0332, which showed that the molecular formula of this compound  $C_{26}H_{43}O_4$ . On the basis of these results and by comparison with previously published data (Nair *et al.*, 1988; Kumar Verma *et al.*, 2012), TZH-41-49 was identified as ferulic acid ester fatty alcohol. This is the first report of ferulic acid ester fatty alcohol from *T. zanonii*.

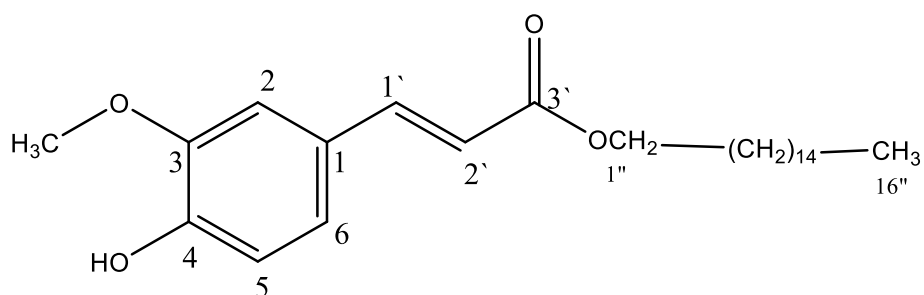
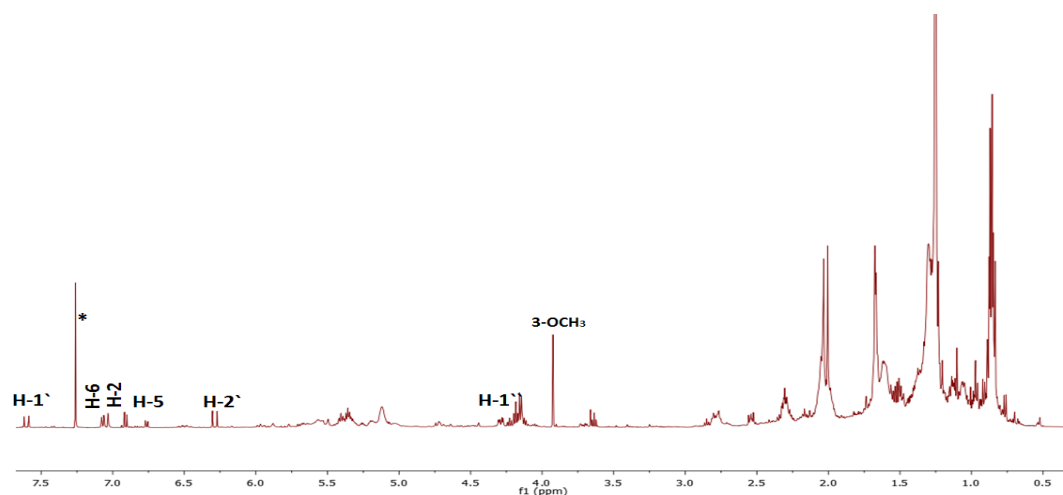


**Figure 3.26:** Structure of ferulic acid ester fatty alcohol.

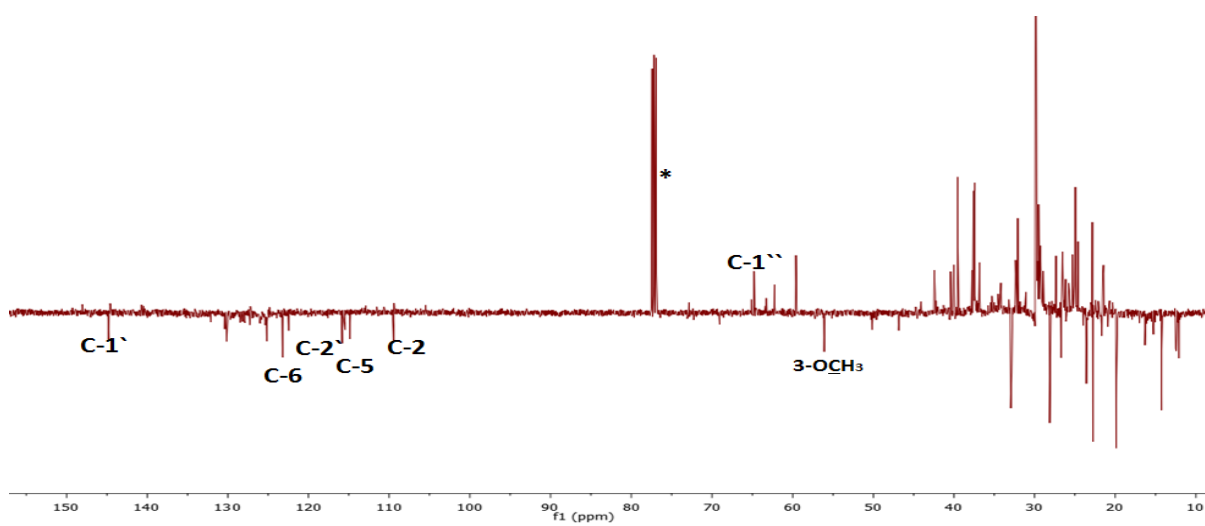
**Table 3.10:**  $^1\text{H}$  (500MHz),  $^{13}\text{C}$  (100MHz), and HMBC data of TZh-41-49 in  $\text{CDCl}_3$ .

Position	$^1\text{H}$ ( $\delta$ ppm)	$^{13}\text{C}$ ( $\delta$ ppm)	HMBC correlations
1	-	126.5	-
2	7.03 (1H, <i>d</i> $J=1.9$ Hz)	109.4	C-6 ( $^3J$ ), C-4 ( $^3J$ ), C-3 ( $^2J$ )
3	-	146.2	-
4	-	148.0	-
5	6.91 (1H, <i>d</i> , $J=8.1$ Hz)	114.6	C-1 ( $^3J$ ), C-4 ( $^2J$ )
6	7.07 (1H, <i>dd</i> , $J=8.1, 1.9$ Hz).	122.9	-
1'	7.60 (1H, <i>d</i> , $J=15.9$ Hz)	144.6	C-2 ( $^3J$ ), C-6( $^3J$ ), C-2' ( $^2J$ ), C-3' ( $^3J$ )
2'	6.28 (1H, <i>d</i> , $J=15.9$ )	115.6	C-1( $^3J$ ), C-3' ( $^2J$ )
3'	-	167.3	-
3-OMe	3.92	56.1	C-3( $^3J$ )
1''	4.13	64.1	C-3' ( $^3J$ )

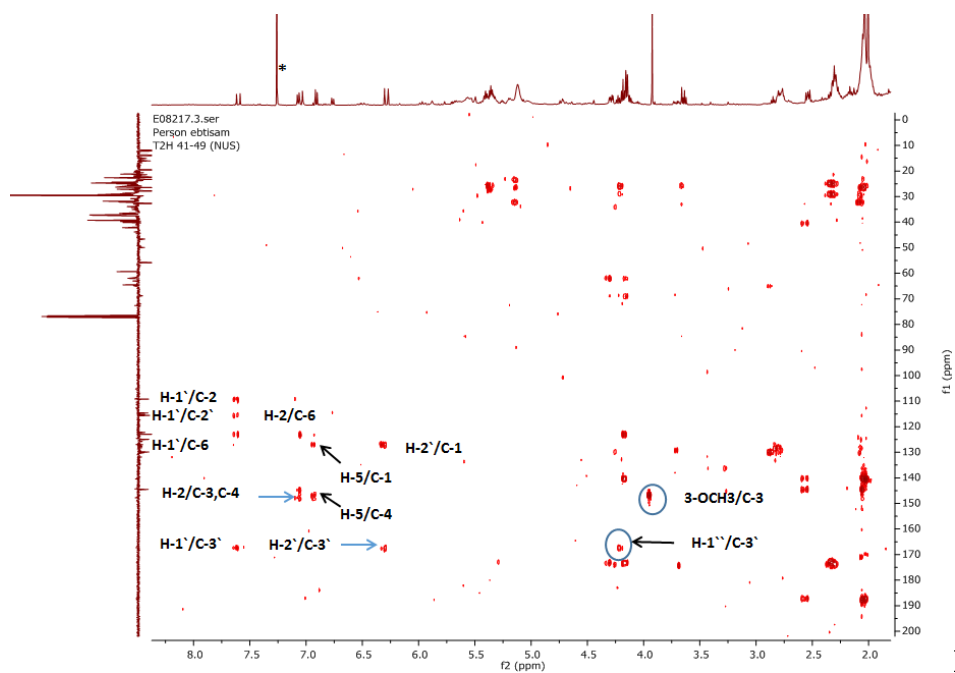
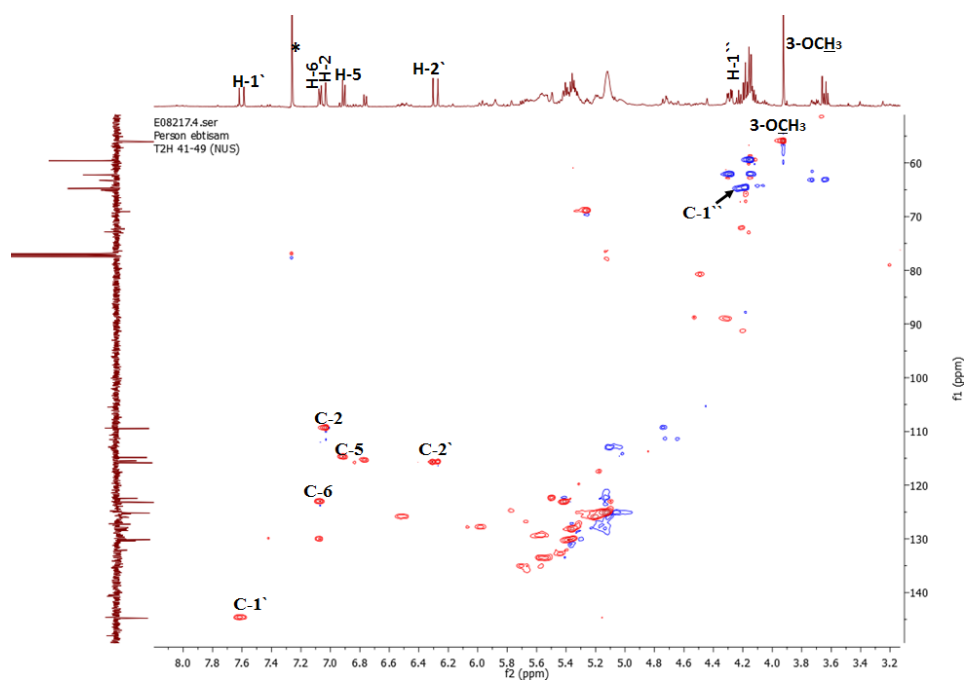
**A**



**B**



**Figure 3.27A:** <sup>1</sup>H NMR and **3.27B:** <sup>13</sup>C NMR spectra (500MHz) of TZH-41-49 in CDCl<sub>3</sub>\*.

**A****B**

**Figure 3.28A:** HMBC and **3.28B:** HSQC (500 MHz) spectra of TZH-41-49 in CDCl<sub>3</sub><sup>\*</sup>.

### 3.5 Fractionation of *H. radicata* crude extracts

The whole plant powdered material (1kg) was macerated with solvents starting from low to high polarity. The hexane extract of *H. radicata* was divided into two parts and separated on two silica gel columns due to the large quantities. The fractions collected were assessed using NMR and enabled elucidation of the structure of fat for example HRH-42. The fractions did not dissolve in deuterated solvents for carrying out NMR analysis, therefore IR helped to elucidate the structure as wax coded HRH-5 (Appendix IV). The EtOAc (5g) and (3g) of *H. radicata* extracts were subjected to silica gel and sephadex columns, respectively. The fractions collected from the silica gel of EtOAc extract were assessed using NMR and enabled elucidation of two structures designated, HRE-94 and HRE-125 and the fractions collected from sephadex of EtOAc extract and lead to the isolation of one compound coded HRE-21. The methanol extract was subjected to sephadex column and the fractions collected were assessed using NMR and enabled elucidation of the structure of one compound coded HRE-50-59.

#### 3.5.1 Characterisation of HRE-21 as 3', 4', 5, 7-tetrahydroxyflavone or luteolin

The compound HRE-21 (Figure 3.29) was isolated from the EtOAc extract of *H. radicata* extract using a sephadex column. On TLC analysis, it gave a yellow spot after spraying with *p*-anisaldehyde-sulphuric acid reagent and heating, with a  $R_f$  value of 0.73 using 20% (v/v) MeOH in EtOAc as the mobile phase.

The  $^1\text{H}$  NMR spectrum (Figure 3.30A, Table 3.11) of HRE-21 showed proton of ring A *meta*-coupled protons at  $\delta_{\text{H}}$  6.26 (1H, *d*,  $J = 2.2$  Hz, H-6) and  $\delta_{\text{H}}$  6.53 (1H, *d*,  $J = 2.2$  Hz, H-8) and the B ring with protons at  $\delta_{\text{H}}$  7.50 (1H, *d*,  $J = 2.3$  Hz, H-2'),  $\delta_{\text{H}}$  7.00 (1H, *d*,  $J = 8.4$  Hz, H-5') and  $\delta_{\text{H}}$  7.47 (1H, *dd*,  $J = 8.4, 2.3$  Hz, H-6'), and proton singlet at  $\delta_{\text{H}}$  6.58 (1H, *s*) H-3 of ring C. The  $^{13}\text{C}$  NMR spectrum (Figure 3.30B) indicated the presence of six aromatic CH at  $\delta_{\text{C}}$  103.2, 98.8, 93.8, 113.8, 115.7 and 119.3 ppm (C-3, C-6, C-8, C-2', C-5' and C-6', respectively). Other carbons were extracted from the HMBC spectrum (Figure 3.31A), two quaternary carbons at  $\delta_{\text{C}}$  103.4, and 122.9

ppm (C-10 and C-1') and six phenolic carbons were observed at  $\delta_c$  164.2, 161.0, 163.0, 157.4, 145.5, and 149.9 ppm (C-2, C-5, C-7, C-9, C-3' and C-4') respectively.

Using 2D NMR (HMBC and HSQC) (Figure 3.31A, Figure 3.31B), the compound was confirmed as follows: The A ring protons at  $\delta_H$  6.26 (H-6) and  $\delta_H$  6.53 (H-8) both showed  $^3J$  correlation to the same quaternary carbon at  $\delta_c$  103.4 (C-10). The proton at  $\delta_H$  6.53 (H-8) displayed a  $^2J$  coupling to a carbon at  $\delta_c$  157.4 (C-9) and  $^3J$  correlation to carbon at  $\delta_c$  98.8 (C-6). The B ring proton at  $\delta_H$  7.00 (H-5') showed  $^3J$  correlation to the quaternary carbon at  $\delta_c$  145.5 (C-3') and  $^2J$  correlation to the carbon at  $\delta_c$  149.9 (C-4'). This proton also showed weak  $^4J$  correlation to a carbon at  $\delta_c$  164.2 (C-2). The proton at  $\delta_H$  7.50 (H-2') correlated via  $^3J$  coupling to C-4' and C-6'. Protons H-2' and H-6' showed  $^3J$  correlation to the carbon C-2 of C ring. The C ring proton at  $\delta_H$  6.58 (H-3) displayed  $^3J$  correlation to the carbon at  $\delta_c$  103.4 (C-10), and  $^2J$  coupling to carbon  $\delta_c$  164.2 (C-2). Protons at  $\delta_H$  6.58 (H-3) and 7.00 (H-5') displayed  $^3J$  correlation to the carbon at  $\delta_c$  122.9 (C-1') and confirmed the assignment of this carbon signal to the C-1' of the aromatic ring B.

The HRESI-MS data showed a molecular ion  $[M]^+$  at  $m/z$  287.0550 which indicated that the molecular formula of this compound was  $C_{15}H_{10}O_6$ . The  $^1H$  &  $^{13}C$  NMR spectral data are agreement with a previous report (Youssef, 2003) and HRE-21 structure identified as 3', 4', 5, 7-tetrahydroxyflavone (luteolin). Luteolin was previously isolated from *H. radicata* (Kim *et al.*, 2014).

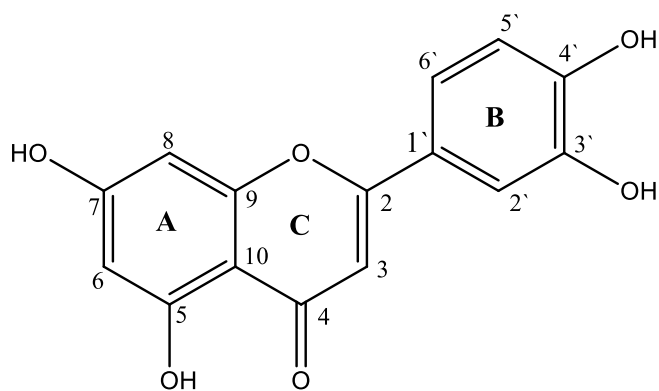
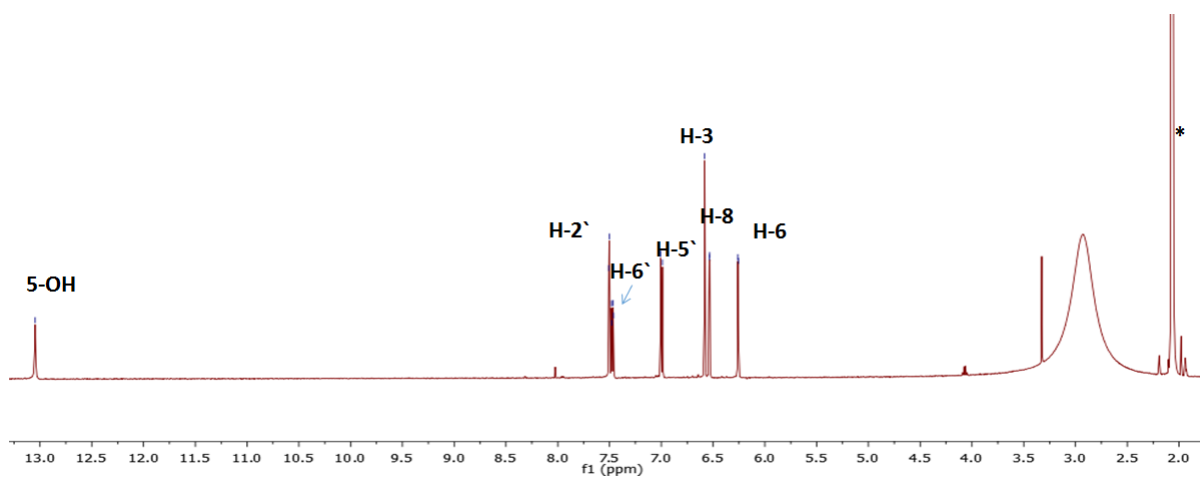


**Figure 3.29:** Structure of luteolin.

**Table 3.11:**  $^1\text{H}$  (400MHz),  $^{13}\text{C}$  (100MHz), and HMBC data of HRE-21 in Acetone- $d_6$ .

Position	$^1\text{H}$ ( $\delta$ ppm)	$^{13}\text{C}$	HMBC correlations
1	-	-	-
2	-	164.2	-
3	6.58 (1H, <i>S</i> )	103.2	C-10( $^3J$ ), C-1'( $^3J$ ), C-2( $^2J$ )
4	-	181.9	-
5	-	161.0	-
6	6.26 (1H, <i>d</i> , $J = 2.2\text{Hz}$ )	98.8	C-8( $^3J$ ), C-10( $^3J$ )
7	-	163.0	-
8	6.53 (1H, <i>d</i> , $J = 2.2\text{ Hz}$ )	93.8	C-6( $^3J$ ), C-10( $^3J$ ), C-9( $^2J$ )
9	-	157.4	-
10	-	103.4	-
1'	-	122.9	-
2'	7.50 (1H, <i>d</i> , $J = 2.2\text{ Hz}$ )	113.8	C-6'( $^3J$ ), C-4'( $^2J$ ), C-2( $^3J$ )
3'	-	145.5	-
4'	-	149.9	-
5'	7.00 (1H, <i>d</i> , $J = 8.4\text{Hz}$ )	115.7	C-1'( $^2J$ ), C-3'( $^4J$ ), C-4'( $^2J$ ), C-4'( $^4J$ )
6'	7.47(1H, <i>dd</i> , $J = 2.2, 8.4\text{ Hz}$ )	119.3	C-2'( $^3J$ ) C-2( $^3J$ ), C-4'( $^3J$ )
5-OH	13.05	-	-

**A**



**B**

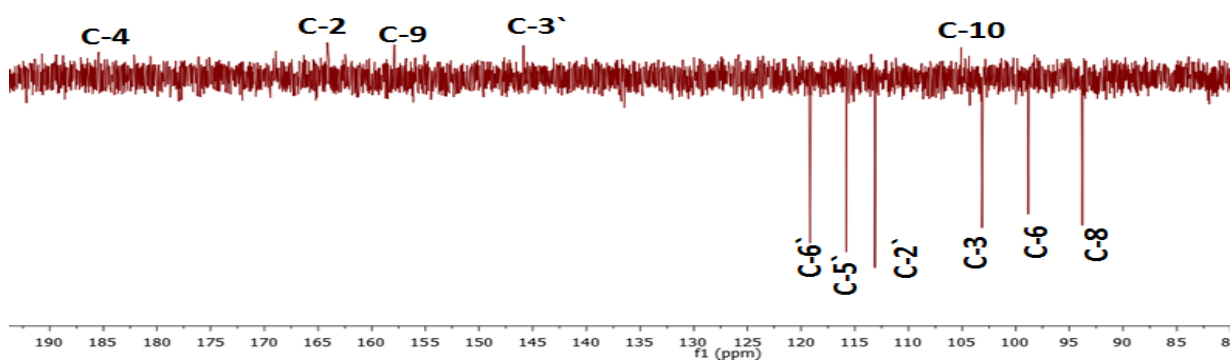
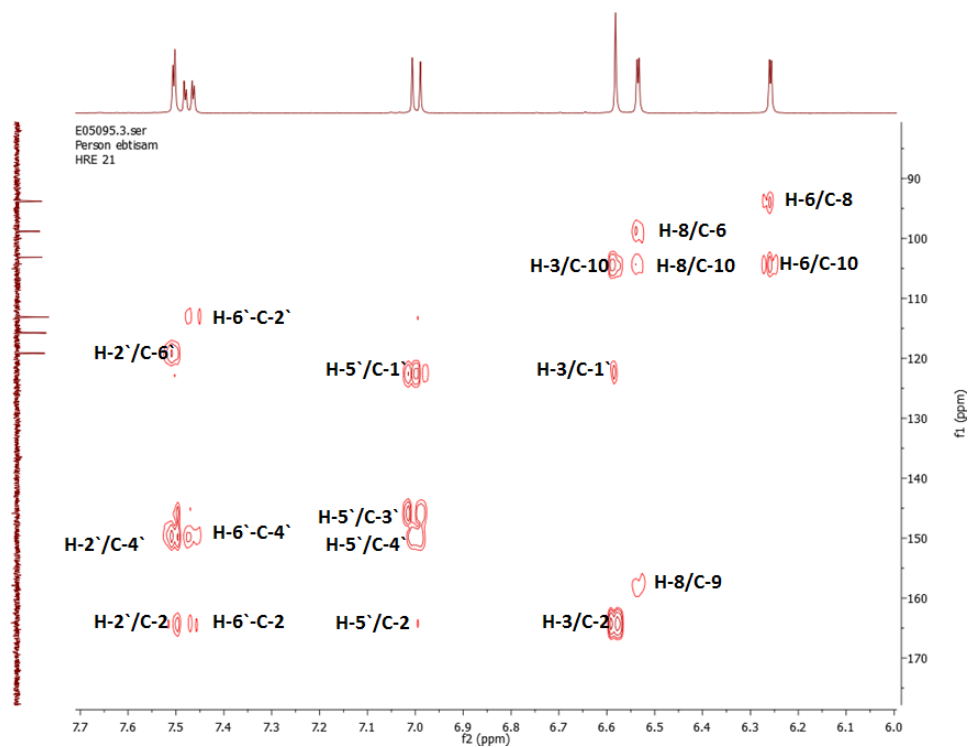


**Figure 3.30A:** <sup>1</sup>H NMR and **3.30B:** <sup>13</sup>C NMR spectra (500 MHz) of HRE-21 in Acetone-*d*<sub>6</sub><sup>\*</sup>.

A



B

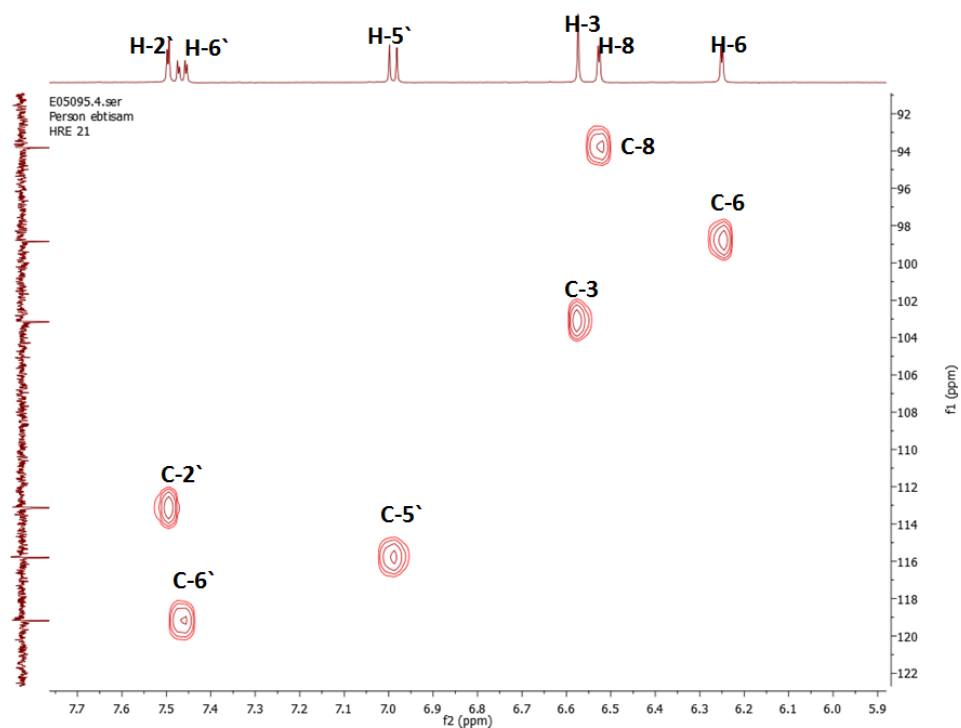


**Figure 3.31A: HMBC and 3.31B: HSQC (500 MHz) spectra of HRE-21 in Acetone- $d_6^*$ .**

### 3.5.2 Characterisation of HRM- 50-59 as Cinaroside (luteolin-7-O-glucoside)

The compound HRM-50 -59 (Figure 3.32), was obtained as a yellow powder from fractions 50 to 59 from Sephadex column of the methanol extract of *H. radicata*. Following TLC, a yellow spot was observed after spraying with *p*-anisaldehyde-sulphuric acid reagent and heating, with a  $R_f$  value of 0.75 using 50% (v/v) MeOH in EtOAc as the mobile phase.

From the  $^1\text{H}$  NMR spectrum (Table 3.12, Figure 3.33A) protons at  $\delta_{\text{H}}$  6.45 (1H, *d*, 2.2 Hz, H-6) and  $\delta_{\text{H}}$  6.80 (1H, *d*, 2.2 Hz, H-8) were *meta*-coupled for A ring, and the presence of an ABX substitution pattern on B ring was established with proton signals at  $\delta_{\text{H}}$  7.46 (1H, *d*,  $J=2.3$  Hz, H-2'),  $\delta_{\text{H}}$  6.94 (1H, *d*,  $J=8.9$  Hz, H-5') and  $\delta_{\text{H}}$  7.45 (1H, *dd*, 8.9, 2.3 Hz, H-6'). The only singlet at  $\delta_{\text{H}}$  6.75, integrating for one proton, was attributed to proton H-3 of flavonoids and a sharp singlet in the region of  $\delta_{\text{H}}$  12.99 for the 5-OH of (H-5). The spectrum also indicated the presence of a sugar unit, with an anomeric proton at  $\delta_{\text{H}}$  5.08 (1H, *d*,  $J=7.4$  Hz, H-1''), signal at  $\delta_{\text{H}}$  3.71 (1H, *m*, H-6a'')/  $\delta_{\text{H}}$  3.49 (1H, *m*, H-6b'') and signals between  $\delta_{\text{H}}$  3.73-3.15, attributable to a sugar moiety.

The  $^{13}\text{C}$  NMR spectrum (Figure 3.33B) indicated the presence of 21 carbons including a carbonyl carbon ( $\delta_{\text{C}}$  181.7), two olefinic carbons (C-2, C-3) ( $\delta_{\text{C}}$  164.4 and 103.4), and four hydroxyl carbons ( $\delta_{\text{C}}$  162.9, 161.0, 149.9 and 145.5) C-7, C-5, C-4' and C-3' respectively and an anomeric carbon at  $\delta_{\text{C}}$  99.9 (C-1'), four oxymethines at  $\delta_{\text{C}}$  73.0 (C-2'), 76.4 (C-3'), 69.5 (C-4') 77.0 (C-5'), and an oxymethylene at  $\delta_{\text{C}}$  60.5 (C-6') was assigned to the glucose unit and sugar units were identified as  $\beta$ -D-glucose due to the large coupling constant (7.4 Hz).

This was further confirmed from the analysis of its 2D NMR (HMBC and HSQC) spectra (Figure 3.34A Figure 3.34B), the A ring protons at  $\delta_{\text{H}}$  6.45 (H-6) and 6.80 (H-8) both showed  $^3J$  correlations to the same quaternary carbon at  $\delta_{\text{C}}$  105.3 (C-10) and  $^2J$  correlation to the olefinic carbon at  $\delta_{\text{C}}$  162.9 (C-7). The  $\delta_{\text{H}}$  6.45 (H-6) showed a  $^3J$  coupling to the carbon at  $\delta_{\text{C}}$  94.8 (C-8). The  $\delta_{\text{H}}$  6.80 (H-8) displayed a  $^2J$  coupling to

a carbon at  $\delta_C$  157.2 (C-9), and  $^3J$  coupling to  $\delta_C$  99.4 (C-6). In the B ring proton at  $\delta_H$  6.94 (H-5') showed  $^3J$  correlations to two quaternary carbons at  $\delta_C$  121.5 (C-1') and  $\delta_C$  145.9 (C-3'). The proton at  $\delta_H$  7.45 (H-6') displayed  $^3J$  couplings to three carbons at  $\delta_C$  114.1 (C-2'), 164.4 (C-2) and 149.9 (C-4') and  $^4J$  couplings to  $\delta_C$  145.9 (C-3'). The proton at  $\delta_H$  7.46 (H-2') displayed  $^3J$  coupling to the carbons at  $\delta_C$  119.6 (C-6'), 149.9 (C-4'). The proton at  $\delta_H$  6.75 (H-3) correlated via  $^2J$  couplings to the carbon at  $\delta_C$  181.7 (C-4) and 164.4 (C-2), and  $^3J$  coupling to  $\delta_C$  121.5 (C-1'), and 105.3 (C-10). The proton at  $\delta_H$  12.99 correlated via  $^2J$  couplings to the carbons at  $\delta_C$  105.3 (C-10) and 99.4 (C-6). An additional  $^3J$  correlation was observed for the anomeric proton of the glucose unit at  $\delta_H$  5.08 (H-1'') to the quaternary carbon at  $\delta_C$  162.9 (C-7). Therefore, HRM 50-59 is likely to be luteolin-7-*O*-glucoside according to the integrations in the NMR spectrum.

The HRESI-MS data showed molecular ion  $[M]^-$  at 447.0934 which showed that the molecular formula of this compound was  $C_{21}H_{20}O_{11}$ . the first time from *H. radicata* plant, The NMR results were in agreement with the literature (Chiruvella *et al.*, 2007).

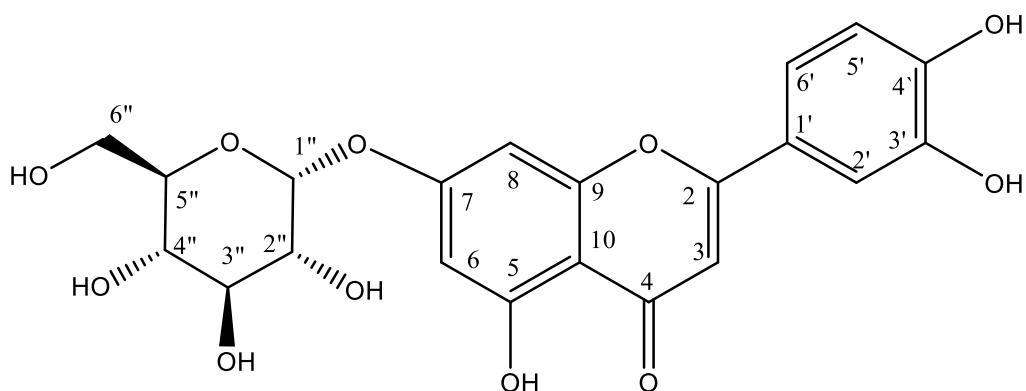
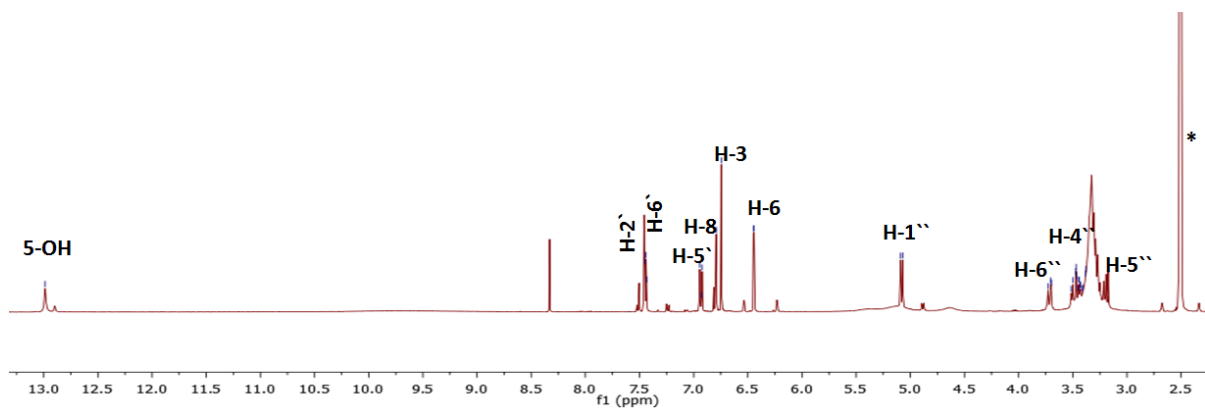


**Figure 3.32:** Structure of luteolin-7-*O*-glucoside.

**Table 3.12:**  $^1\text{H}$  (400MHz),  $^{13}\text{C}$  (100MHz), and HMBC data of HRM-50-59 in DMSO- $d_6$ .

Position	$^1\text{H}$ ( $\delta$ ppm)	$^{13}\text{C}$ ( $\delta$ ppm)	HMBC correlations
1	-	-	-
2	-	164.4	-
3	6.75(1H, <i>s</i> )	103.4	C-10( $^3J$ ), C-1'( $^3J$ ), C-4( $^2J$ ), C-2( $^2J$ )
4	-	181.7	-
5	-	161.0	-
6	6.45(1H, <i>d</i> , $J = 2.2$ Hz)	99.4	C-8( $^3J$ ), C-10( $^3J$ ), C-7( $^2J$ )
7	-	162.9	-
8	6.80(1H, <i>d</i> , $J = 2.2$ Hz)	94.8	C-6( $^3J$ ), C-10( $^3J$ ), C-9( $^2J$ ), C-7( $^2J$ )
9	-	157.2	-
10	-	105.3	-
1'	-	121.5	-
2'	7.46 (1H, <i>d</i> , $J = 2.3$ Hz)	114.1	C-6' ( $^3J$ ), C-4' ( $^3J$ )
3'	-	145.9	-
4'	-	149.9	-
5'	6.94(1H, <i>d</i> , $J = 8.9$ Hz)	116.7	C-1' ( $^3J$ ), C-3' ( $^3J$ )
6'	7.45 (1H, <i>dd</i> , $J = 8.9, 2.3$ Hz)	119.6	C-2' ( $^3J$ ), C-2 ( $^3J$ ), C-4' ( $^3J$ ), C-3' ( $^4J$ ),
1''	5.08	99.9	C-7 ( $^3J$ )
2''	3.27	73.0	C-1'' ( $^2J$ ), C-3'' ( $^2J$ )
3''	3.34	76.4	C-4'' ( $^2J$ ), C-2'' ( $^2J$ )
4''	3.18	69.5	C-3'' ( $^2J$ )
5''	3.47	77.0	-
6''	3.71, 3.49	60.5	-
5-OH	12.9	-	C-10 ( $^2J$ ), C-6 ( $^2J$ )

**A**



**B**

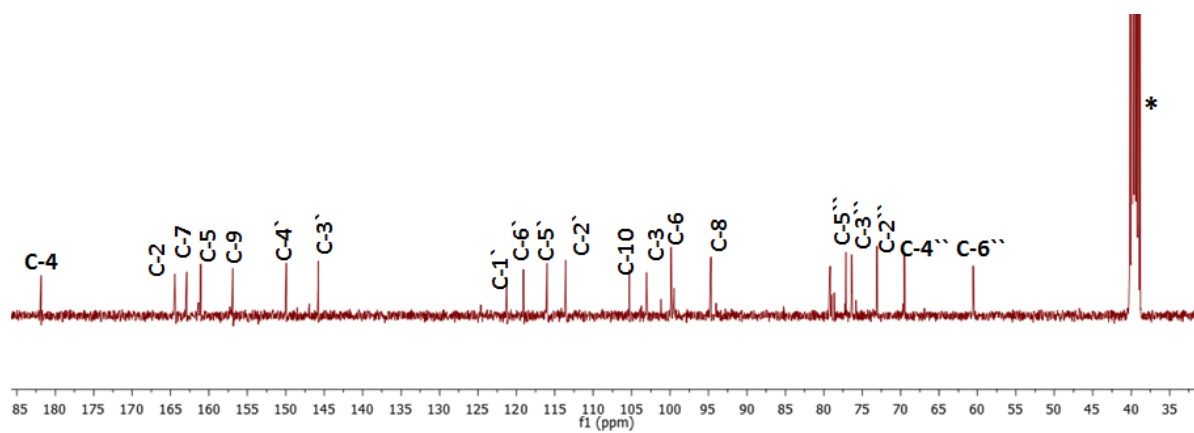


**Figure 3.33A:** <sup>1</sup>H NMR and **3.33B:** <sup>13</sup>C NMR spectra (500 MHz) of HRM-50-59 in DMSO-*d*<sub>6</sub>\*.

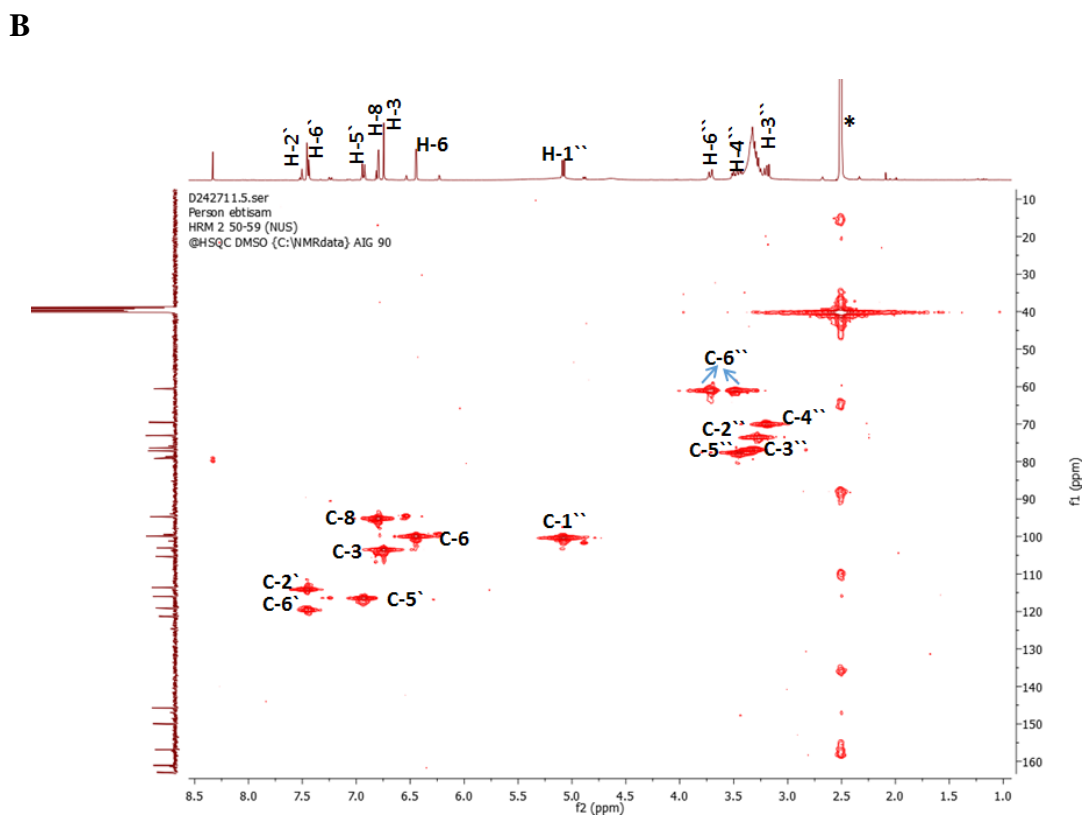
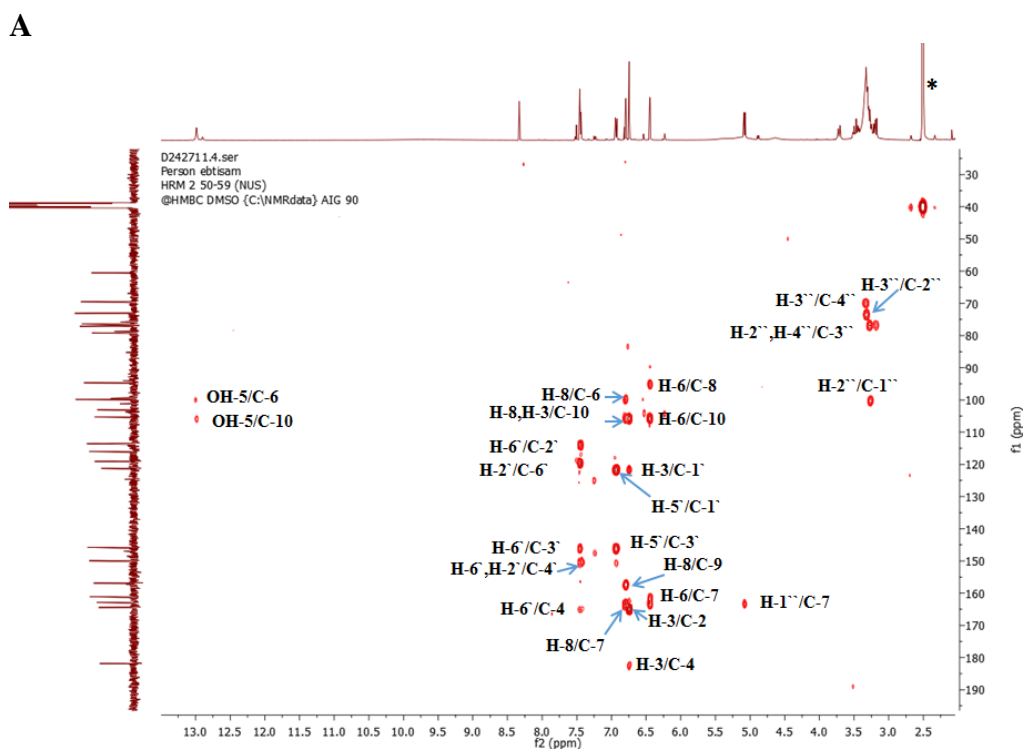


**Figure 3.34A: HMBC and 3.34B: HSQC (500 MHz) spectra of HRM-50-59 DMSO- $d_6$ .\*.**

### 3.5.3 Characterisation of HRE-94 of a novel daucoesterol ester of *trans p-coumaric acid*

The compound HRE-94 (Figure 3.35) was isolated from the EtOAc extract of *H. radicata*. It gave a yellowish-brown color on the TLC plate after treatment with anisaldehyde-sulphuric acid reagent followed by heating with a  $R_f$  value of 0.81 using (v/v) 20% MeOH in EtOAc as the mobile phase.

The  $^1\text{H}$  NMR spectrum (Figure 3.36A, Table 3.13) revealed the presence of a steroidal glycoside skeleton and *trans para*-coumaric acid. It indicated the presence of  $\beta$ -sitosterol due to the distinctive olefinic signal at  $\delta_{\text{H}}$  5.38 (1H, *m*, H-6), an oxymethine proton signal at  $\delta_{\text{H}}$  3.60 (1H, *m*, H-3), and six methyl groups at  $\delta_{\text{H}}$  0.70 (3H, *s*, H-18),  $\delta_{\text{H}}$  0.83 (3H, *d*, H-26),  $\delta_{\text{H}}$  0.85 (3H, *d*,  $J=1.9$  Hz, H-27),  $\delta_{\text{H}}$  0.90 (3H, *t*, H-29),  $\delta_{\text{H}}$  0.94 (3H, *d*,  $J=6.9$  Hz, H-21) and  $\delta_{\text{H}}$  1.03 (3H, *s*, H-19). The sugar unit was identified as  $\beta$ -D-glucose with an anomeric proton at  $\delta_{\text{H}}$  4.38 which appeared as a doublet (1H, *d*,  $J=7.8$  Hz) indicating a H-1'/H-2' *trans* diaxial configuration with an H-1'/H-2' *trans* diaxial configuration. Thus the  $^1\text{H}$  NMR and COSY spectra (Figure 3.36A, Figure 3.36B) revealed the presence of an aromatic ring with protons at  $\delta_{\text{H}}$  7.47 (2H, *d*,  $J=8.7$  Hz, H-2''/6''),  $\delta_{\text{H}}$  6.88 (2H, *d*,  $J=8.6$  Hz, H-3''/5''). Also, the spectrum showed the presence of two *trans* coupled olefinic protons at  $\delta_{\text{H}}$  7.74 (1H, *d*,  $J=15.9$  Hz, H-7'') and  $\delta_{\text{H}}$  6.32 (1H, *d*,  $J=15.90$  Hz, H-8''). In the HMBC spectrum (Figure 3.37A, Table 3.13), the olefinic proton at  $\delta_{\text{H}}$  7.74 (H-7'') showed a  $^3J$  correlation to the methine at  $\delta_{\text{C}}$  130.0 (C-2''/6'') and the carbonyl at  $\delta_{\text{C}}$  170.0 (C-9''). The signal at  $\delta_{\text{H}}$  7.47 (H-2''/6'') showed  $^3J$  coupling to carbons at  $\delta_{\text{C}}$  130.0 (C-6''/2''), and  $\delta_{\text{C}}$  158.21 (C-4'') as well the proton at  $\delta_{\text{H}}$  7.47 (H-2''/6'') showed  $^3J$  correlation to  $\delta_{\text{C}}$  147.7 (C-7'') and the signal at  $\delta_{\text{H}}$  6.88 (H-3''/5'') showed  $^3J$  correlations to carbon at  $\delta_{\text{C}}$  126.2 (C-1'').

The  $^{13}\text{C}$  NMR assignments (Table 3.13) were extracted from the HMBC spectrum. A carbon at  $\delta_{\text{C}}$  101.4 (C-1') was identified as the anomeric carbon while two olefinic carbons were observed at  $\delta_{\text{C}}$  122.9 (C-6) and  $\delta_{\text{C}}$  140.6 (C-5). In the HMBC spectrum (Table 3.13), the anomeric proton at  $\delta_{\text{H}}$  4.38 (H-1') showed  $^3J$  correlation to the methine carbon at  $\delta_{\text{C}}$  79.80 (C-3), and methyl at  $\delta_{\text{H}}$  0.70 (Me-18) showed  $^3J$  correlations to carbons  $\delta_{\text{C}}$  39.26 (C-12), 56.34 (C-14), 56.17 (C-17) and  $^2J$  correlation

to  $\delta_c$  41.62 (C-13). The methyl at  $\delta_H$  1.03 (H-19) showed  $^3J$  correlations to carbons at  $\delta_c$  140.6 (C-5), 50.90 (C-9) and 36.50 (C-1) and  $^2J$  to 37.10 (C-10); the methyl  $\delta_H$  0.85 (H-26) showed  $^3J$  correlations to carbons at  $\delta_c$  19.59 (C-27), 46.30 (C-24), and  $^2J$  to  $\delta_c$  29.21 (C-25) and the methyl  $\delta_H$  0.90 (H-21) to  $\delta_c$  31.68 (C-22) 56.17 (C-17), and 47.2 (C-20).

The above findings were consistent with the published data for daucosterol (Jangwan *et al.*, 2012) except for the presence of two protons at  $\delta_H$  4.51 (1H, *dd*,  $J=$  12.1, 4.7 Hz- H-6'), 4.29 (1H, *dd*,  $J=$  12.1, 2.1 Hz- H-6') representing the 6-CH<sub>2</sub>O- of the glucosyl residue were deshielded by almost one ppm compared to that of 'free' glucose; this indicates that position-6 of the sugar is esterified with the *trans-p*-coumarate.

The HRESI-MS data showed a molecular ion [M]<sup>-</sup> at  $m/z$  721.3284, which showed that the molecular formula of this compound was C<sub>44</sub>H<sub>66</sub>O<sub>8</sub>. The <sup>1</sup>H and <sup>13</sup>C NMR spectral data were consistent with those reported earlier for daucosterol (Lee, 2013) and *p*-coumaric acid (Ren *et al.*, 2013). Kim *et al.*, (2011) reported a derivative of daucosterol with long chain fatty acid with the chemical shifts of the anomeric protons at 4.45 (*dd*,  $J=$  12.2, 1.2 Hz) and 4.29 (*dd*,  $J=$  12.2, 4.4 Hz) and these were similar to the chemical shifts observed for the anomeric protons in HRE-94 which were observed at 4.51 (1H, *dd*,  $J=$  12.1, 4.7 Hz- H-6'), 4.29 (1H, *dd*,  $J=$  12.1, 2.1 Hz- H-6') (Kim *et al.*, 2011).

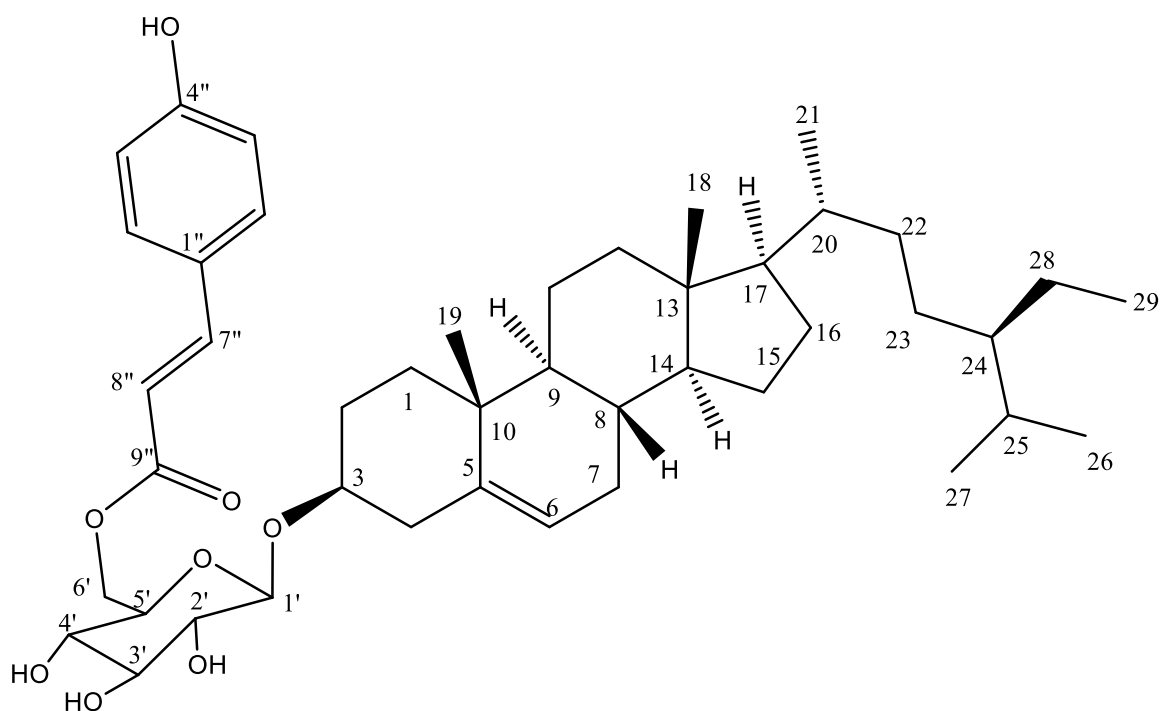


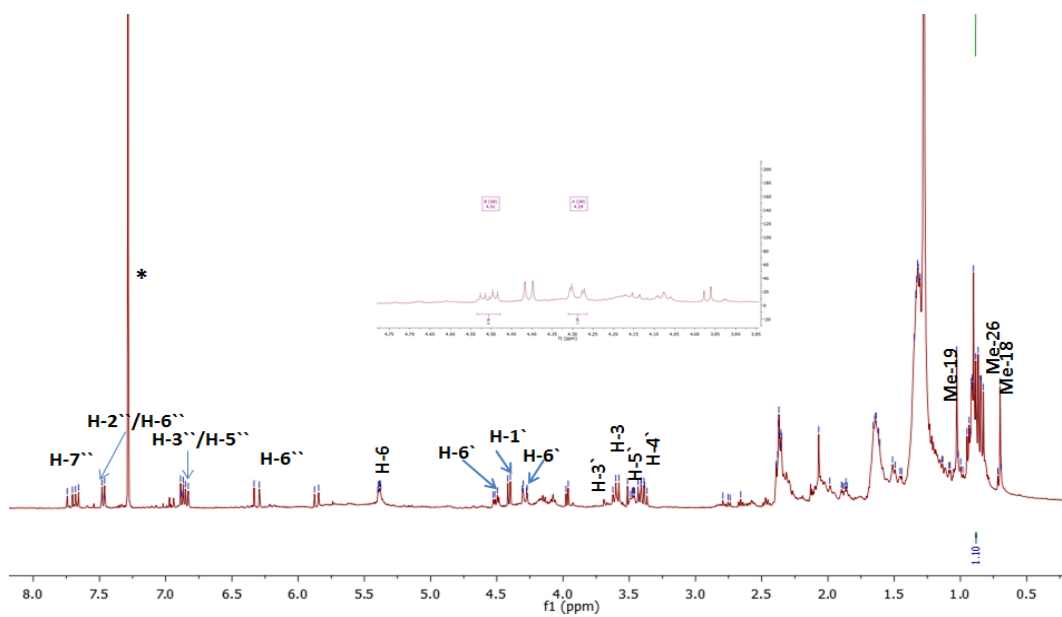
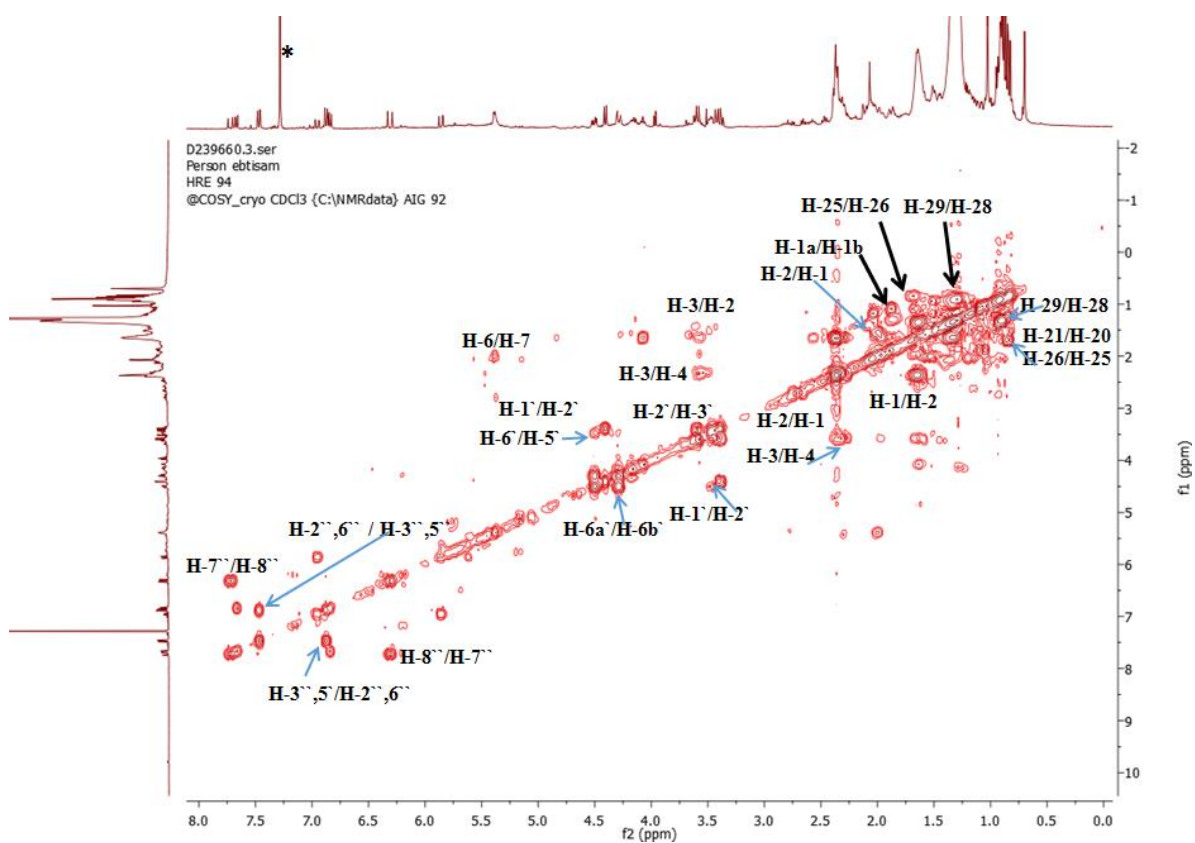
**Figure 3.35:** Structure of daucosterol ester of *trans p*-coumaric acid.

**Table 3.13:**  $^1\text{H}$  (400MHz),  $^{13}\text{C}$  (100MHz), and HMBC data of of HRE-94 in  $\text{CDCl}_3$ .

Position	$^1\text{H}$ ( $\delta$ ppm)	$^{13}\text{C}$ ( $\delta$ ppm)	HMBC correlation
1	1.09 (1H,)/1.89 (1H, <i>m</i> )	36.51	-
2	1.48 (2H)	29.14	-
3	3.60 (1H, <i>m</i> )	79.8	C-1'( $^3J$ )
4	2.07 (1H, <i>m</i> )/2.37 (1H, <i>m</i> )	34.49	-
5	-	140.6	-
6	5.38 (1H, <i>d</i> $J=4.6$ Hz)	122.29	-
7	1.98 (2H, <i>m</i> )	30.0	-
8	1.58 (1H, <i>m</i> )		-
9	0.93 (1H, <i>m</i> )	50.22	-
10	-	37.10	-
11	1.33 (1H, <i>m</i> )/1.50 (1H, <i>m</i> )	22.26	-
12	1.14 (1H, <i>m</i> )/2.04 (1H, <i>m</i> )	39.26	-
13	-	41.62	-
14	1.01 (1H, <i>m</i> )	56.34	-
15	1.03 (1H, <i>m</i> )/1.54 (1H, <i>m</i> )		-
16	1.88 (1H, <i>m</i> )/1.50 (1H, <i>m</i> )	29.01	-
17	1.15 (1H, <i>m</i> )	56.16	C-14 ( $^3J$ )
18	0.70 (3H, <i>s</i> )	11.10	C-12( $^3J$ ), C-13( $^2J$ ), C-17( $^3J$ ),C-14( $^3J$ )
19	1.03 (3H, <i>s</i> )	18.60	C-10( $^2J$ ), C-9( $^3J$ ),, C-5( $^3J$ ), C-1( $^3J$ )
20	1.29 (1H, <i>m</i> )	47.2	-
21	0.94 (3H, <i>d</i> , $J=6.4$ Hz )	18.0	C-17( $^3J$ ), C-20, C-22( $^3J$ )
22	1.00 (1H, <i>m</i> )/1.33 (1H, <i>m</i> )	36.30	-
23	1.16 (2H, <i>m</i> )	22.64	-
24	0.95 (1H, <i>m</i> )	46.30	-
25	1.66 (1H, <i>m</i> )	29.21	-
26	0.83 (3H, <i>d</i> )	18.25	C-24( $^3J$ ), C-25( $^2J$ ),Me-27( $^3J$ )
27	0.84 (3H, <i>d</i> )	19.90	C-24( $^3J$ ), C-25( $^2J$ )
28	1.32 (1H, <i>m</i> )/1.81 (1H, <i>m</i> )	23.0	-
29	0.90 (3H, <i>t</i> )	12.23	C-28( $^3J$ )
1'	4.38 (1H, <i>d</i> , $J=7.8$ Hz)	101.34	C-3( $^3J$ )
2'	3.39 (1H, <i>dd</i> )	73.76	C-1'

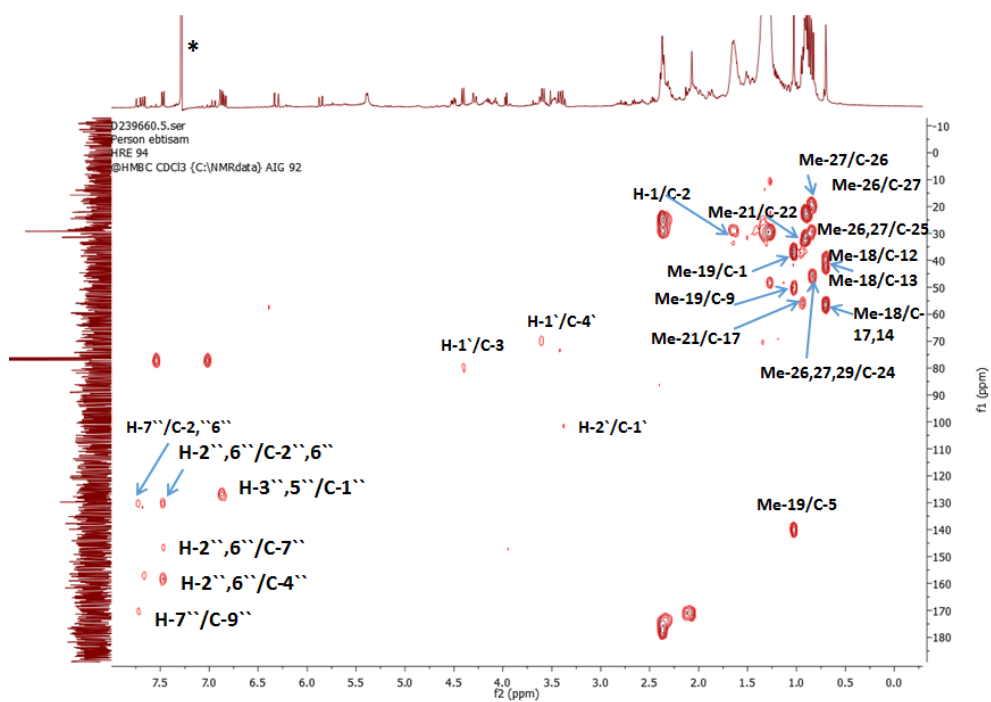
**Table 3.13:** (continued).

3'	3.60 (1H, <i>t</i> )	76.0	C-4'
4'	3.41 (1H, <i>m</i> )	70.37	C-1', C-2'
5'	3.48 (1H, <i>m</i> )	74.62	-
6'	4.51 (1H, <i>dd</i> , $J=12.1$ , 4.7 Hz), 4.29 (1H, <i>dd</i> , $J=12.1$ , 2.1 Hz- H-6')	62.58	-
1''	-	126.20	-
2''	7.47 (1H, <i>d</i> , $J=8.7$ Hz)	130.0	C-6''( <sup>3</sup> <i>J</i> )/C-4''( <sup>3</sup> <i>J</i> ) /C-7''( <sup>3</sup> <i>J</i> )
3''	6.88 (1H, <i>d</i> , $J=8.6$ Hz)	115.8	C-1''( <sup>3</sup> <i>J</i> )
4''	-	158.21	-
5''	6.88 (1H, <i>d</i> , $J=8.6$ Hz)	115.8	C-1''( <sup>3</sup> <i>J</i> )
6''	7.47 (1H, <i>d</i> , $J=8.7$ Hz,)	130.0	C-2''( <sup>3</sup> <i>J</i> )/C-4''( <sup>3</sup> <i>J</i> ) /C-7''( <sup>3</sup> <i>J</i> )
7''	7.74 (1H, <i>d</i> , $J=15.90$ Hz)	147.7	C-2'', 6''( <sup>3</sup> <i>J</i> )/C- 9''( <sup>3</sup> <i>J</i> )
8''	6.32 (1H, <i>d</i> , $J=15.90$ Hz)		-
9''	-	170.0	-

**A****B**

**Figure 3.36A:** <sup>1</sup>H NMR and **3.36B:** COSY spectra (400 MHz) of HRE-94 in CDCl<sub>3</sub>\*.

A



B

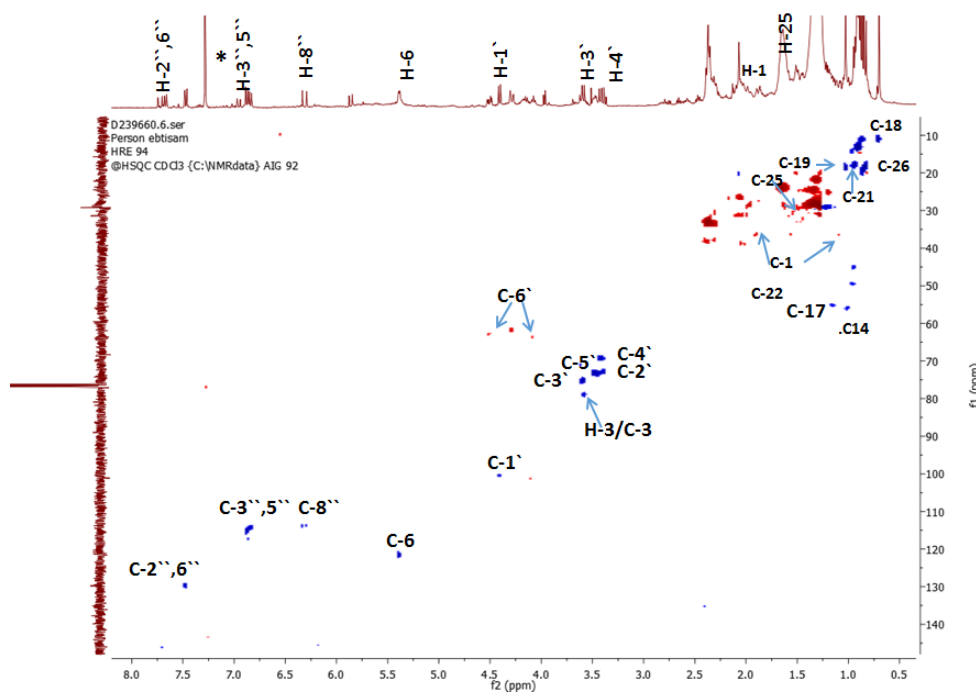


Figure 3.37A: HMBC and 3.37B: HSQC (400 MHz) spectra of HRE-94 in  $\text{CDCl}_3$ .\*

### 3.5.4 Characterisation of HRE-121 as 1-monoacetylglycerol

The compound HRE-121 (Figure 3.38) was isolated from the silica gel column separation of ethyl acetate extract of *H. radicata* as greenish oil; a brown spot appeared with a  $R_f$  value of 0.54 using 20% (v/v) MeOH in EtOAc as the mobile phase on TLC.

The  $^1\text{H}$  NMR spectrum (Figure 3.39) displayed a sharp singlet at  $\delta_{\text{H}}$  2.21 (3H) (H-5) for methyl protons of an acetyl group. The  $^1\text{H}$  NMR also showed proton signals at  $\delta_{\text{H}}$  3.68 (1H, *dd*,  $J=3.9, 11.5$  Hz)/  $\delta_{\text{H}}$  3.78 (1H, *dd*,  $J=3.9, 11.5$  Hz) (H-3a/H-3b) and  $\delta_{\text{H}}$  4.21 (1H, *dd*,  $J=4.7, 11.5$  Hz)/  $\delta_{\text{H}}$  4.27 (1H, *dd*,  $J=4.7, 11.5$  Hz) (H-1a/H-1b) for a pair of two nonequivalent oxymethylene protons. A multiplet proton was detected at  $\delta_{\text{H}}$  3.91 for H-2.

The  $^{13}\text{C}$  NMR spectrum showed one methyl at  $\delta_{\text{C}}$  20.6, two oxymethylenes at  $\delta_{\text{C}}$  62.8 and  $\delta_{\text{C}}$  64.7, one oxymethine at  $\delta_{\text{C}}$  69.6 and a carbonyl at  $\delta_{\text{C}}$  171.3.

In the HMBC spectrum (Table 3.14), the signal at  $\delta_{\text{H}}$  2.21 (C-5) correlated to the carbonyl at  $\delta_{\text{C}}$  171.3 (C-4), establishing the presence of the acetyl group and the proton at  $\delta_{\text{H}}$  3.91(H-2) showed  $^2J$  couplings to carbon at  $\delta_{\text{C}}$  64.7 (C-1). The oxymethylene protons at  $\delta_{\text{H}}$  4.21 (H-1a/b) showed  $^2J$  coupling to carbon at  $\delta_{\text{C}}$  69.6 (C-2) and  $^3J$  coupling to  $\delta_{\text{C}}$  171.3 (C-4). The other oxymethylene protons at  $\delta_{\text{H}}$  3.68/ $\delta_{\text{H}}$  3.78 (H-3a/b) showed  $^3J$  and  $^2J$  correlations to carbons at  $\delta_{\text{C}}$  64.7 (C-1) and  $\delta_{\text{C}}$  69.6(C-2), respectively.

The HRESI-MS data showed a molecular ion  $[\text{M}]^+$  at  $m/z$  135.0651, suggesting a molecular formula of  $\text{C}_5\text{H}_{10}\text{O}_4$ . On the basis of these results and by comparison with previously published data (Homma *et al.*, 2012) HRE-121 was identified as 1-monoacetylglycerol.

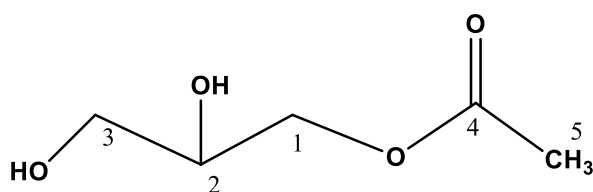


**Figure 3.38:** Structure of 1-monoacetylglycerol.

**Table 3.14:**  $^1\text{H}$  (400MHz),  $^{13}\text{C}$  (100MHz), and HMBC data of HRE-121 in Acetone- $d_6^*$ .

Position	$^1\text{H}$ ( $\delta$ ppm)	$^{13}\text{C}$ ( $\delta$ ppm)	HMBC corelation
1	4.21 (1H, <i>dd</i> , $J=4.7$ , 11.5 Hz)/ 4.27 (1H, <i>dd</i> , $J=4.7$ , 11.5 Hz)	64.7	C-4( $^3J$ ) , C-2( $^2J$ )
2	3.91 (1H, <i>m</i> )	69.6	C-1( $^2J$ )
3	3.68 (1H, <i>dd</i> , $J=3.9$ , 11.5 Hz)/3.78 (1H, <i>dd</i> , $J=3.9$ , 11.5 Hz)	62.8	C-1( $^3J$ ) , C-2( $^2J$ )
4	-	171.3	-
5	2.21(3H, <i>s</i> )	20.6	C-4( $^3J$ )

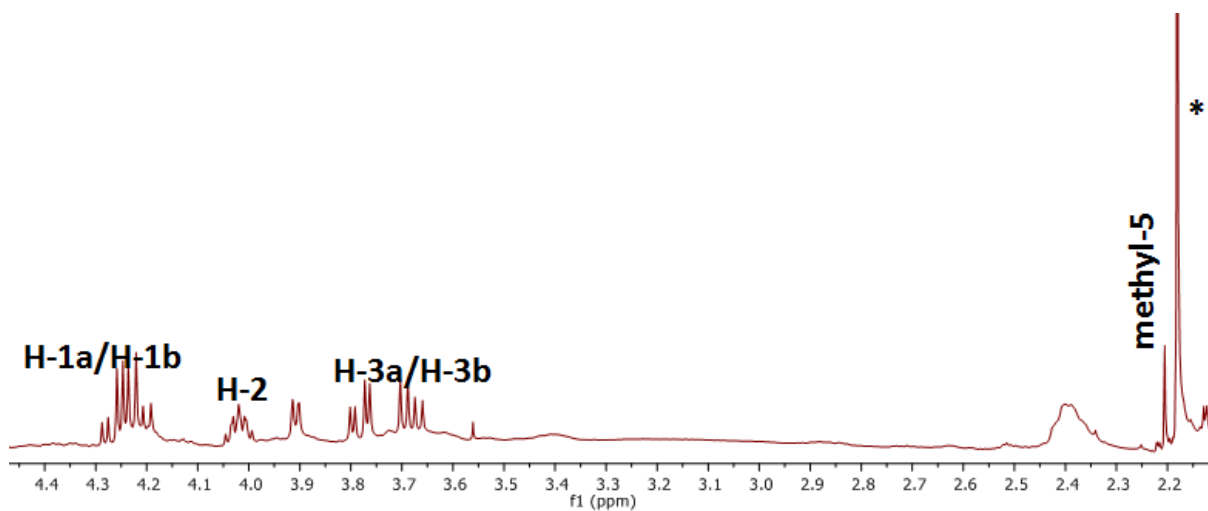


**Figure 3.39:**  $^1\text{H}$  NMR spectrum (400 MHz) of HRE-121 in Acetone- $d_6^*$ .

### 3.5.5 Characterisation of HRH-42 as linoleic acid (undefined)

Compound HRH-42 (Figure 3.40) was isolated from the hexane extract of *H. radicata* as a white amorphous solid. Using (v/v) 70% hexane in EtOAc as the mobile phase for TLC, the compound appeared as a as a yellow spot ( $R_f$  0.60) after spraying with anisaldehyde-sulphuric acid reagent followed by heating. The  $^1\text{H}$  NMR spectrum (Figure 3.41) showed four overlapping olefinic protons (H-9, H-10, H-12, H-13) between  $\delta_{\text{H}}$  5.33-5.36 ppm, two allylic methylenes (H-8, H-14) at  $\delta_{\text{H}}$  2.03 ppm and one bisallylic methylene group at 2.78 ppm (H-11). The terminal methyl (H-18) at  $\delta_{\text{H}}$  0.90, triplet a methylene (H-2) alpha to the carbonyl at  $\delta_{\text{H}}$  2.33 and methylenes distributed between 1.27-1.60 ppm. Thus the compound was identified as 10,13-octadecadienoic acid. The presence for linoleic acid was also reported by (Pajunen *et al.*, 2008).

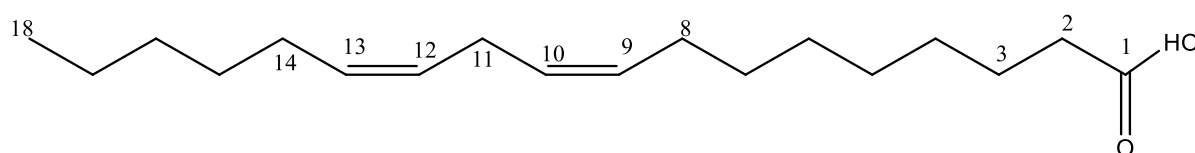


**Figure 3.40:** Structure of linoleic acid.

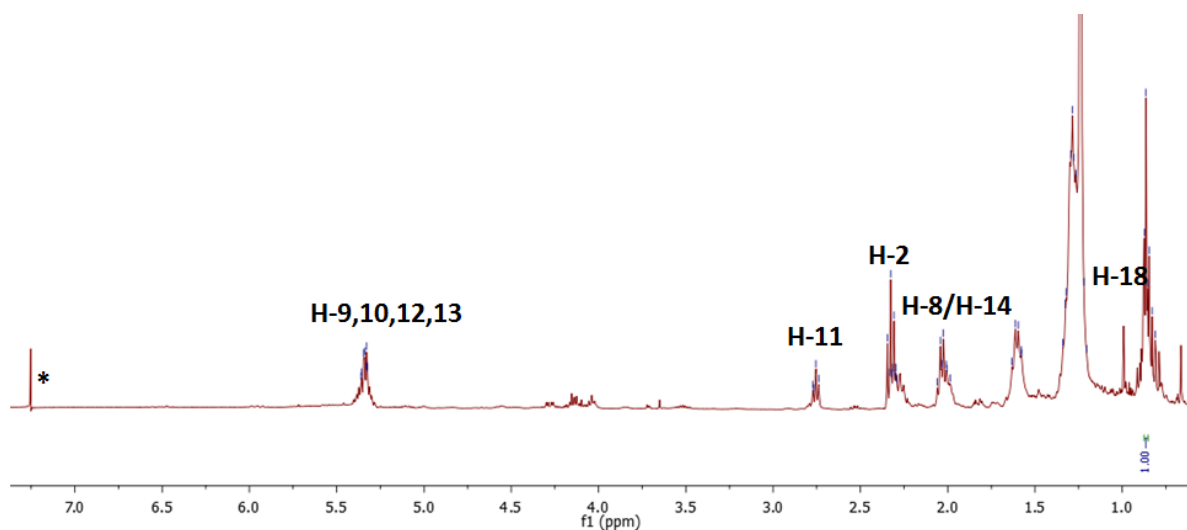


**Figure 3.41:**  $^1\text{H}$  NMR spectrum (400 MHz) of HRH-42 in  $\text{CDCl}_3^*$ .

### 3.6 Fractionation of *S. sodomaeum* crude extracts

The *S. sodomaeum* methanol extract (26g, 7.8% of yield) was divided into two parts for further fractionation. The first part of the methanol extract (15g, 4.5% of yield) was subjected to VLC eluted with hexane increasing the polarity with ethyl acetate and up to 40% methanol. The same fractions from VLC depending on their TLC profiles were combined together and further fractionated by Sephadex. One compound was isolated, coded SSM-30-2. The second part of the extract (3g, 0.9% of yield) was subjected to fractionation using a Sephadex column and lead to the isolation of one compound coded SSM-56. The hexane extract for *S. sodomaeum* produced yellow oil as liquid in the flask after extraction, which weighed 17.3g (5.1% of yield) while the EtOAc extract of *S. sodomaeum* produced oil and powder precipitate in the flask after extraction. The powder was filtered and weighed to yield 1g (0.26% of yield) then it was further purified on a Sephadex. No compounds were separated from it.

#### 3.6.1 Characterisation of SSM-30-2 as solamargine

Compound SSM-30-2 was isolated from VLC then purified by Sephadex LH-20 from the methanol extract of *S. sodomaeum*. After spraying with *p*-anisaldehyde-sulphuric acid reagent and heating, a yellowish brown spot was observed with a  $R_f$  value of 0.43 on TLC using 20% (v/v) MeOH in EtOAc as the mobile phase.

The  $^1\text{H}$  NMR spectrum (Figure 3.43A, Table 3.15) indicated the presence of an aglycon moiety and sugars. The  $^1\text{H}$  NMR showed protons signals for six methyl groups including two methyl singlets at  $\delta_{\text{H}}$  0.73 (3H, *s*, H-18), 0.94 (3H, *s*, H-19) and four doublets methyl at 0.83 (3H, *d*,  $J= 6.4$  Hz, H-27), 0.99 (3H, *d*,  $J= 7.1$  Hz, H-21), 1.08 (3H, *d*,  $J= 6.8$  Hz, Rha 1 H-6), 1.10 (3H, *d*,  $J= 6.8$  Hz, Rha 2 H-6). The  $^1\text{H}$  NMR also showed proton signals due to methylene groups at  $\delta_{\text{H}}$  1.41 (2H, *m*, H-11), 1.57 (2H, H-24), 1.77 (1H, *m*, H-2a), 1.43 (1H, *m*, H-2b), 1.70 (1H, *m*, H-23a), 1.2 (1H, *m*, H-23b), 1.93 (2H, *m*, H-15), 1.77 (1H, *m*, H-1a) 0.96 (1H, *m*, H-1b), 2.13 (1H, *m*, H-4a), 2.38 (1H, *m*, H-4b), 1.69 (2H, *m*, H-12), and 2.78 (1H, *m*, H-26a) and 2.53 (1H, *m*, H-26b). These methylene protons were assigned to the aglycon as their chemical shifts were in the aliphatic or up field region. The olefinic proton at  $\delta_{\text{H}}$  5.31 (1H, *d*,  $J=$

4.7 Hz, H-6) was indicative a double bond in the aglycon. One oxymethine proton signal at  $\delta_{\text{H}}$  4.43 (1H, *d*,  $J=7.6$  Hz, H-16) was assigned to ring E of the aglycone. The proton spectrum also indicated three sugar residues with their anomeric protons at  $\delta_{\text{H}}$  4.38 (1H, *d*,  $J=7.8$  Hz), 4.67 (1H, *br s*) and 5.01 (1H, *d*,  $J=7.6$  Hz).

The  $^{13}\text{C}$  NMR spectrum (Figure 3.43B& C) showed the presence of 45 carbon signals, of which 27 were for the aglycone and 18 for the three hexoses. For the aglycone, there were four methyl signals at  $\delta_{\text{C}}$  15.2 (C-21), 16.2 (C-18), 19.1 (C-27) and 19.4 (C-19) and from the sugars there were two methyl signals at 18.3 (Rha 1 C-6) and 18.2 (Rha 2 C-6). There were ten methylene carbon signals at  $\delta_{\text{C}}$  20.8 (C-11), 28.9 (C-24), 29.5 (C-2), 32.7 (C-23), 31.9 (C-7), 32.2 (C-15), 37.2 (C-1), 38.2 (C-4), 40.6 (C-12) and 46.0 (26). One oxymethine carbon signal was observed at  $\delta_{\text{C}}$  81.3 (C-16) on the ring E of the aglycon. The  $^{13}\text{C}$  NMR spectrum showed the presence of three anomeric carbons at  $\delta_{\text{C}}$  98.7 (Glc C-1'), 100.96, (Rha 1 C-1'') and 100.89 (Rha 2 C-1), sixteen oxymethines between  $\delta_{\text{C}}$  69- 79 ppm and an oxymethylene at  $\delta_{\text{C}}$  61.2 (C-6') was assigned to the glucose unit and two rhamnose units. Four quaternary carbons were observed including one linked to oxygen and nitrogen atom at  $\delta_{\text{C}}$  98.2 (C-22). Other signals were for the quaternaries at  $\delta_{\text{C}}$  36.8 (C-10), 39.1 (C-13), and 140.7 (C-5). The carbon at  $\delta_{\text{C}}$  98.2 (C-22) indicates a linkage to the oxygen atom in ring E and the olefinic carbon at  $\delta_{\text{C}}$  140.7 (C-5) is due to the presence of a double bond in ring B of the aglycone.

The HMBC of SSM 30-2 (Figure 3.44B), revealed the presence of cross peaks between the methyl 0.72 (H-18) and showed  $^2J$  correlation to  $\delta_{\text{C}}$  40.6 ppm (C-12), and  $^3J$  correlation to carbons at  $\delta_{\text{C}}$  56.2 (C-14) and 61.9 (C-17) which indicate the connection between ring C and D. Proton at  $\delta_{\text{H}}$  0.83 (H-27) showed  $^3J$  correlation to carbon at  $\delta_{\text{C}}$  28.9 (C-24) and  $^2J$  coupling to  $\delta_{\text{C}}$  46.0 (C-26). The methyl proton at  $\delta_{\text{H}}$  0.94 (H-19) showed  $^2J$  correlation to the quaternary carbon at  $\delta_{\text{C}}$  36.8 (C-10), and  $^3J$  correlation to the carbons at  $\delta_{\text{C}}$  50.1 (C-9) and 140.7 (C-5), indicating the connectivity of ring A to B. The methyl proton at  $\delta_{\text{H}}$  0.99 (H-21) correlated via  $^2J$  coupling to carbon  $\delta_{\text{C}}$  41.7 (C-20), and  $^3J$  coupling to carbons at  $\delta_{\text{C}}$  61.9 (C-17), and 98.2 (C-22) indicating the connection between ring D to C as well as ring D to E. An olefinic proton at  $\delta_{\text{H}}$  5.32

(H-6) showed  $^3J$  correlation to the carbons at  $\delta_C$  31.4 (C-8) and 36.8 (C-10). Proton at  $\delta_H$  4.38 (Glc H-1') had a  $^3J$  correlation to  $\delta_C$  at 77.60 (C-3) of aglycone, indicating the  $\beta$  Gl C-1 Linked to aglycon. Proton at  $\delta_H$  4.67 (Rha 2 H-1'') showed  $^3J$  correlation to the carbons at  $\delta_C$  68.1 (C-5''), 76.4 (C-3'') and to  $^2J$  coupling at  $\delta_C$  71.1 (C-2'') and proton at  $\delta_H$  5.01 (Rha 1 H-1'') showed  $^3J$  correlation to carbons at  $\delta_C$  69.1 (C-5''), 77.2 (C-4'') and  $^2J$  coupling 71.1 (C-2''). The connectivity of the proton at  $\delta_H$  3.21 (H-2') to the carbon 100.96 (Rha 2 C-1'') indicated the  $\alpha$  Rha 2 (C-1'') was linked to  $\beta$  Gl (C-2'). Proton at  $\delta_H$  3.21 (H-2') also showed  $^2J$  to  $\delta_C$  98.7(C-1') and 76.4 (C-3'). Cross peaks between  $\delta_H$  3.35 (H-4') and  $\delta_C$  100.89 (Rha 1 C-1'') indicated the  $\alpha$  Rha 1 (C-1'') was linked to  $\beta$  Gl (C-4'), in addition,  $\delta_H$  3.35 (H-4') showed  $^2J$  and  $^3J$  coupling to at the carbons  $\delta_C$  at 76.4 (C-3'') and 61.2 (C-6'') respectively. The proton at  $\delta_H$  3.19 (H-4'') showed  $^3J$  correlation to the carbons at  $\delta_C$  18.3 (C-6''), 71.0 (C-2''), and  $^2J$  coupling at  $\delta_C$  69.1(C-5'').

The HRESI-MS data showed a molecular ion  $[M]^+$  at  $m/z$  868.5239 which showed that the molecular formula of this compound was  $C_{45}H_{73}NO_{15}$ . The above data led to the identification of SSM30-2 as solamargine, which was in agreement with previous reports (Cornelius *et al.*, 2010). The NMR spectra were in agreement with literature reports and the compound has previously been reported from *S. sodomaeum* (Cham and Wilson, 1987).

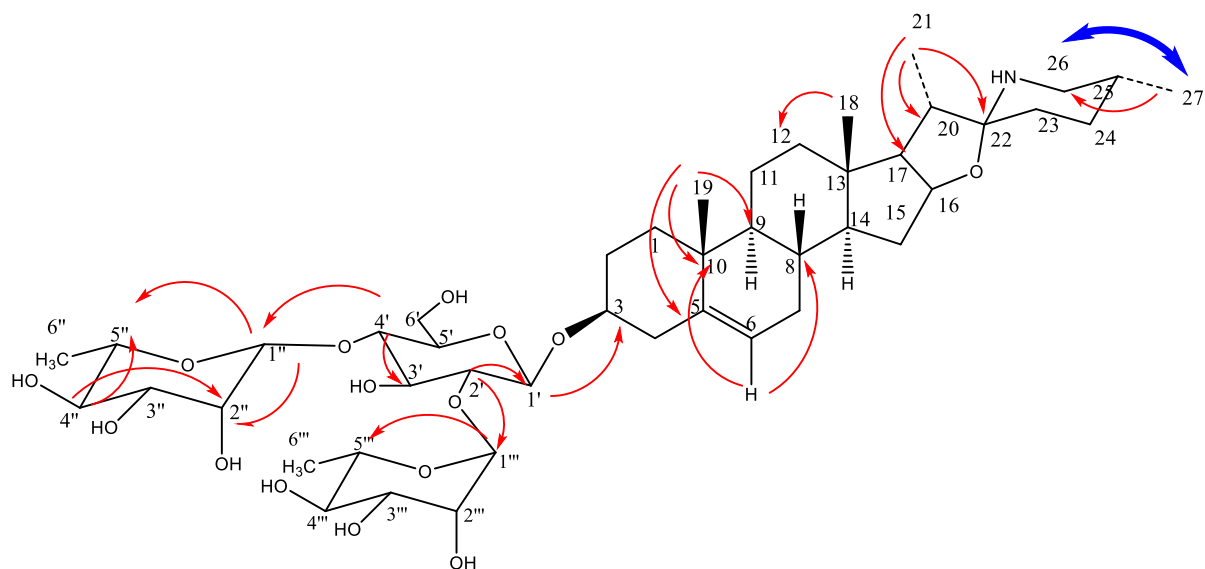


**Figure 3.42:** Structure of solamargine.

Key HMBC (  ) and NOESY (  ) correlations observed in SSM-30-2.

**Table 3.15:**  $^1\text{H}$  (500MHz),  $^{13}\text{C}$  (100MHz), and HMBC data of SSM-30-2 in  $\text{DMSO-}d_6$ .

Position	$^1\text{H}$ (ppm)	$^{13}\text{C}$ (ppm)	HMBC correlations
1	1.77/ 0.96 (2H, <i>m</i> , )	37.2	-
2	1.77/1.43(2H, <i>m</i> , )	29.5	-
3	3.45	77.6	-
4	2.13/2.38(1H, <i>t</i> , $J= 12.4$ Hz, and 1H, <i>m</i> , )	38.2	C-3 ( $^2J$ ), C-5 ( $^2J$ ), C-6, ( $^3J$ ) C-10( $^3J$ )
5	-	140.7	
6	5.31(1H, <i>d</i> , $J= 4.7$ Hz)	121.2	C-8 ( $^3J$ ), C-10, ( $^3J$ )
7	1.91	31.9	C-13 ( $^4J$ ), C-14 ( $^3J$ ),C-17 ( $^4J$ )
8	1.54	31.4	-
9	0.87	50.1	-
10	-	36.8	-
11	1.41	20.8	-
12	1.69/1.12(2H, <i>d</i> , $J= 11.4$ Hz)	40.6	-
13	-	39.1	-
14	1.2	56.2	-
15	1.93	32.2	-
16	4.43(1H, <i>d</i> , $J= 7.6$ Hz)	81.3	-
17	1.78	61.9	C-18 ( $^2J$ )
18	0.73(3H, <i>s</i> )	16.2	C-12 ( $^2J$ ), C-14, ( $^3J$ ) C-17( $^3J$ )
19	0.94(3H, <i>s</i> )	19.4	C-10 ( $^2J$ ), C-4, ( $^3J$ ) C-9( $^3J$ ),C-5( $^3J$ )
20	2.00	41.7	C-13( $^3J$ ), C-17( $^2J$ )
21	0.99(3H, <i>d</i> , $J= 7.1$ Hz)	15.2	C-20 ( $^2J$ ), C-22 ( $^3J$ ), C-17( $^3J$ )
22	-	98.2	-
23	1.70/1.2(2H, <i>m</i> )	32.7	-
24	1.57	28.9	-
25	1.65	28.7	-
26	2.78/2.531H, <i>m</i> , and 1H, <i>d</i> , $J= 11.6$ Hz)	46.0	-
27	0.83(3H, <i>d</i> , $J= 6.4$ Hz)	19.1	C-24( $^3J$ ),C-26( $^3J$ )
1'	4.38 (1H, <i>d</i> , $J=7.8$ Hz,)	98.7	C-3( $^3J$ )
2'	3.21	72.3	C-1' ( $^2J$ ), C-1'' ( $^3J$ ), C-3' ( $^3J$ )
3'	3.42	76.4	
4'	3.35	77.2	C-3' ( $^2J$ ), C-1'' ( $^3J$ ), C-6' ( $^3J$ )

**Table 3.15:** (continued).

5 <sup>ˆ</sup>	3.70	71.8	-
6 <sup>ˆ</sup>	3.45/3.60	61.2	-
1 <sup>ˆˆ</sup>	5.01(1H, <i>d</i> , <i>J</i> =7.6 Hz)	100.8	C-5 <sup>ˆˆ</sup> ( <sup>3</sup> <i>J</i> ), C-2 <sup>ˆˆ</sup> ( <sup>2</sup> <i>J</i> ), C-4 <sup>ˆ</sup> ( <sup>3</sup> <i>J</i> )
2 <sup>ˆˆ</sup>	3.40	71.0	-
3 <sup>ˆˆ</sup>	3.38	75.3	-
4 <sup>ˆˆ</sup>	3.19	72.2	C-6 <sup>ˆˆ</sup> ( <sup>3</sup> <i>J</i> ), C-5 <sup>ˆˆ</sup> ( <sup>2</sup> <i>J</i> ), C-2 <sup>ˆˆ</sup> ( <sup>3</sup> <i>J</i> )
5 <sup>ˆˆ</sup>	3.84	69.1	-
6 <sup>ˆˆ</sup>	1.10(2H, <i>d</i> , <i>J</i> = 6.5 Hz)	18.3	-
1 <sup>ˆˆˆ</sup>	4.67 (1H, <i>br s</i> )	100.96	C-5 <sup>ˆˆˆ</sup> ( <sup>3</sup> <i>J</i> ), C-2 <sup>ˆˆˆ</sup> ( <sup>2</sup> <i>J</i> ), C-3 <sup>ˆ</sup> ( <sup>3</sup> <i>J</i> )
2 <sup>ˆˆˆ</sup>	3.64	71.1	-
3 <sup>ˆˆˆ</sup>	3.16	75.7	-
4 <sup>ˆˆˆ</sup>	3.20	76.4	-
5 <sup>ˆˆˆ</sup>	3.97	68.1	-
6 <sup>ˆˆˆ</sup>	1.18	18.2	-

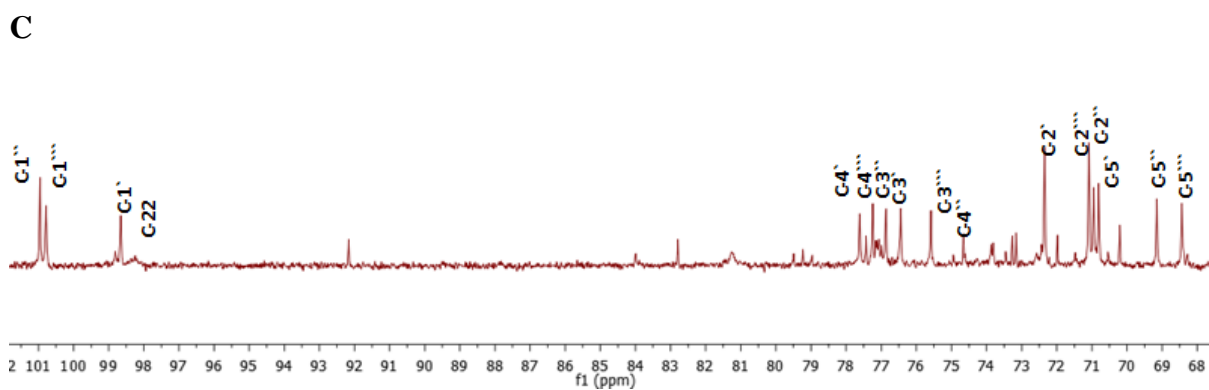
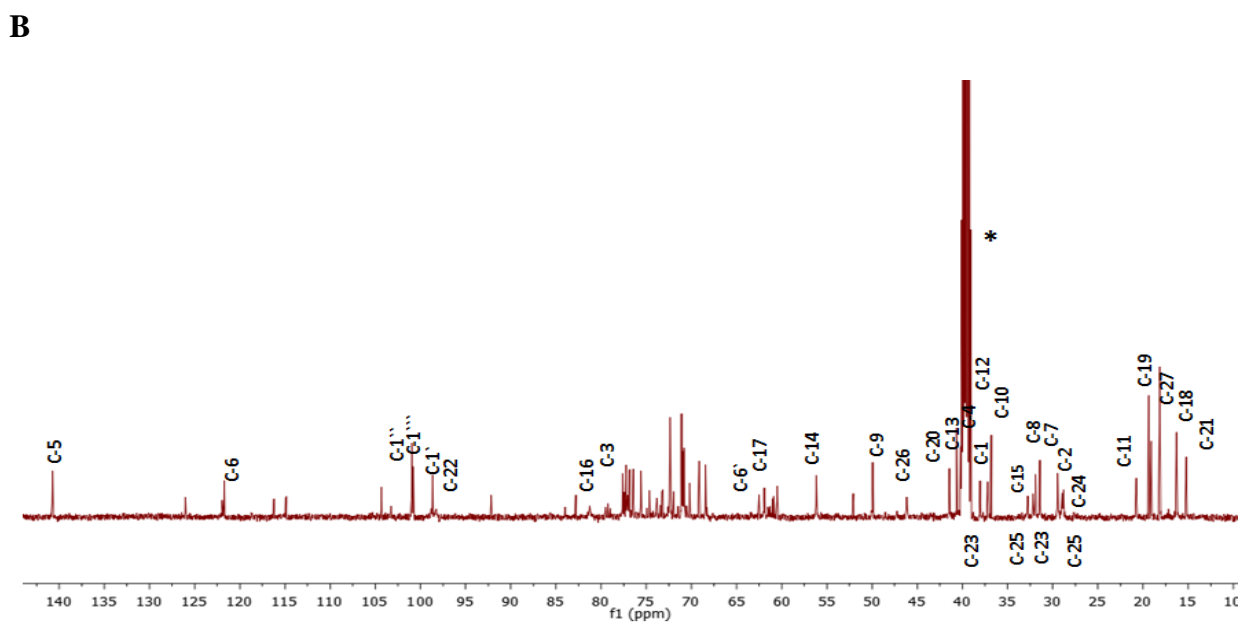
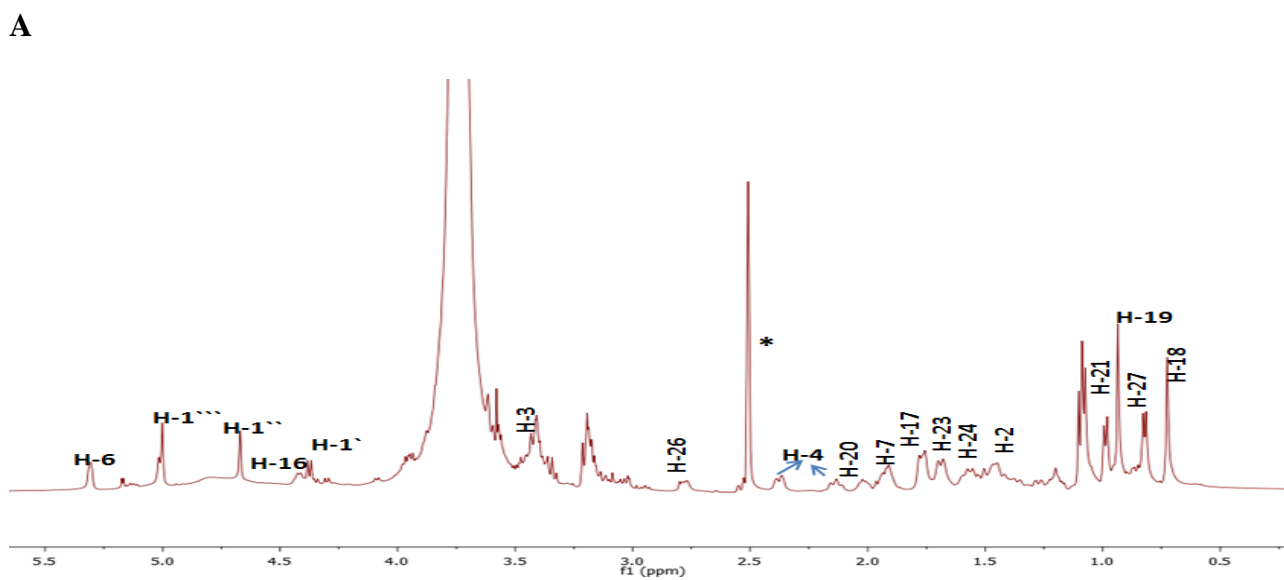
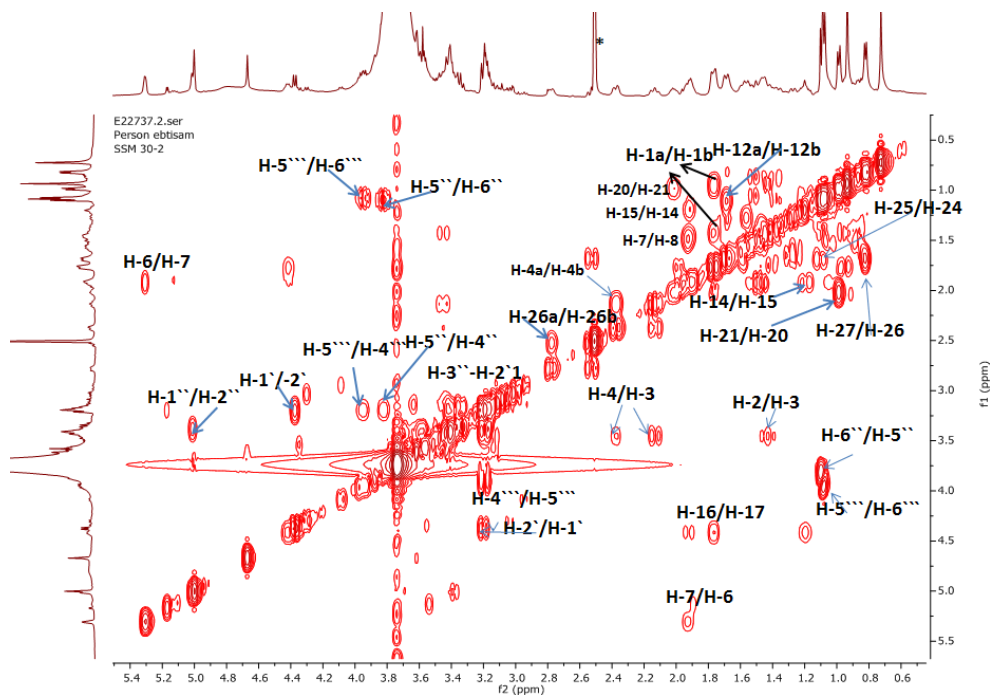


**Figure 3.43A:**  $^1\text{H}$  NMR and **3.43B& C:**  $^{13}\text{C}$  NMR spectra (500 MHz) of SSM-30-2 in  $\text{DMSO-}d_6^*$ .

A



B

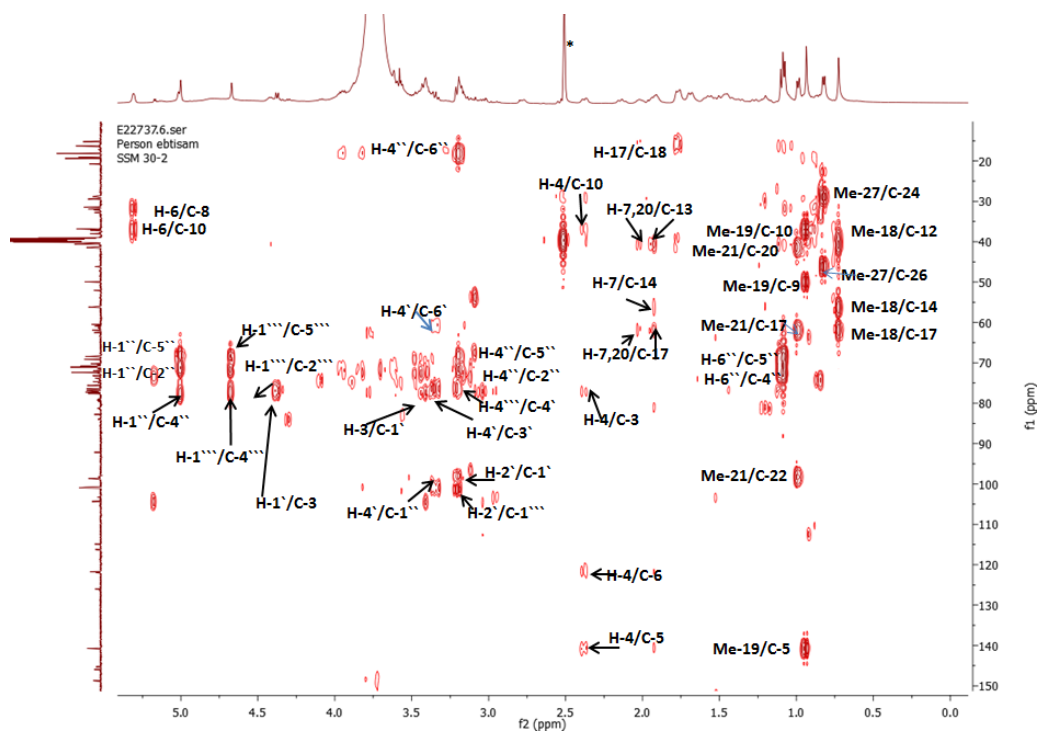
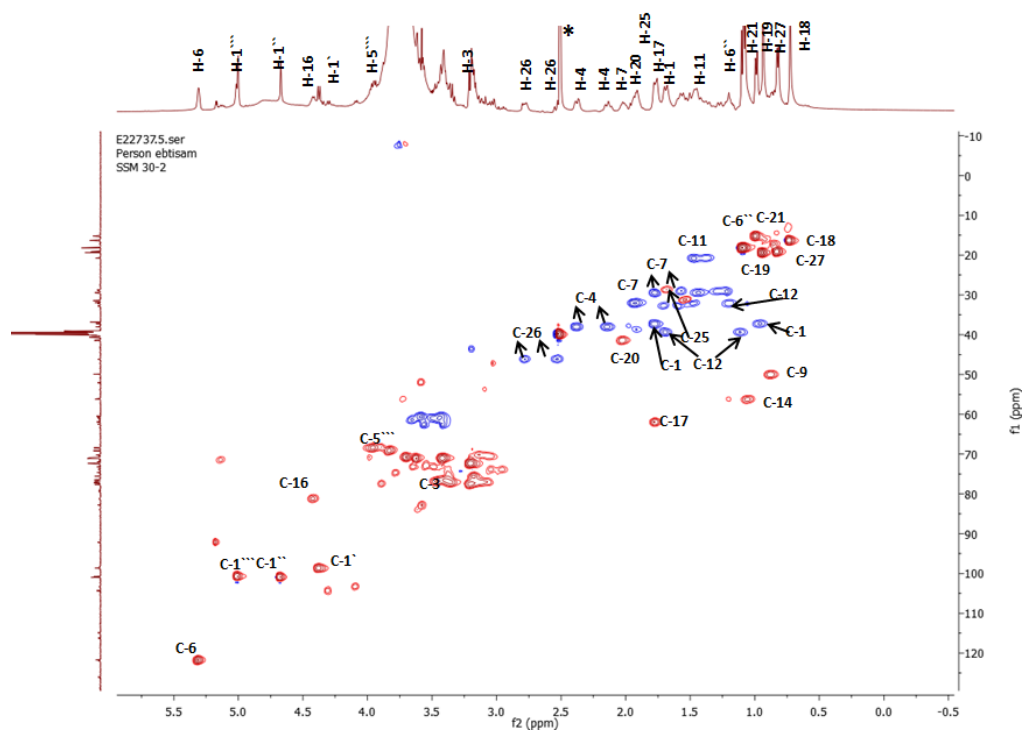


**Figure 3.44A:** COSY and **3.44B:** HMBC spectra (500 MHz) of SSM-30-2 in DMSO-*d*<sub>6</sub>\*.

A



B

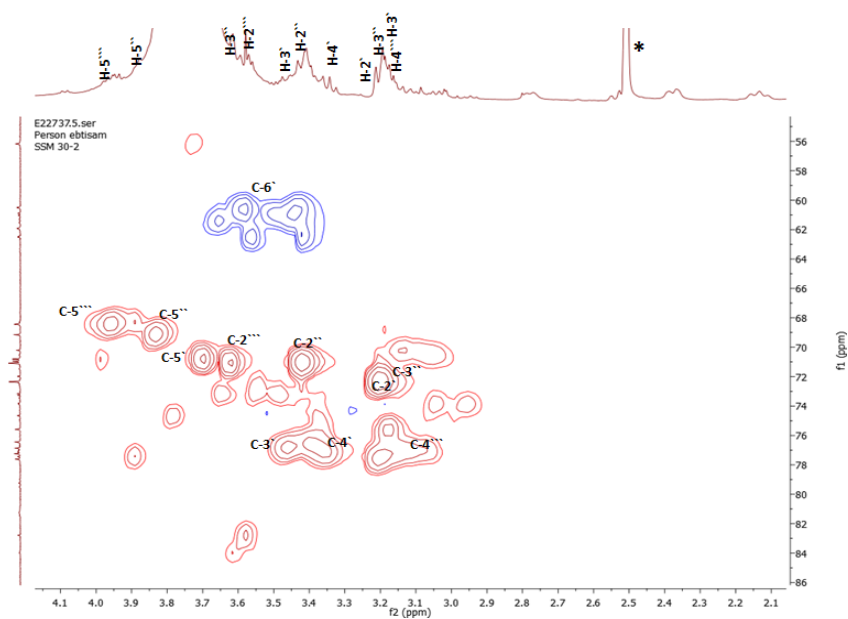


**Figure 3.45A:** HSQC and **3.45B:** expansion HSQC spectra (500 MHz) of SSM-30-2 in  $\text{DMSO-}d_6$ .

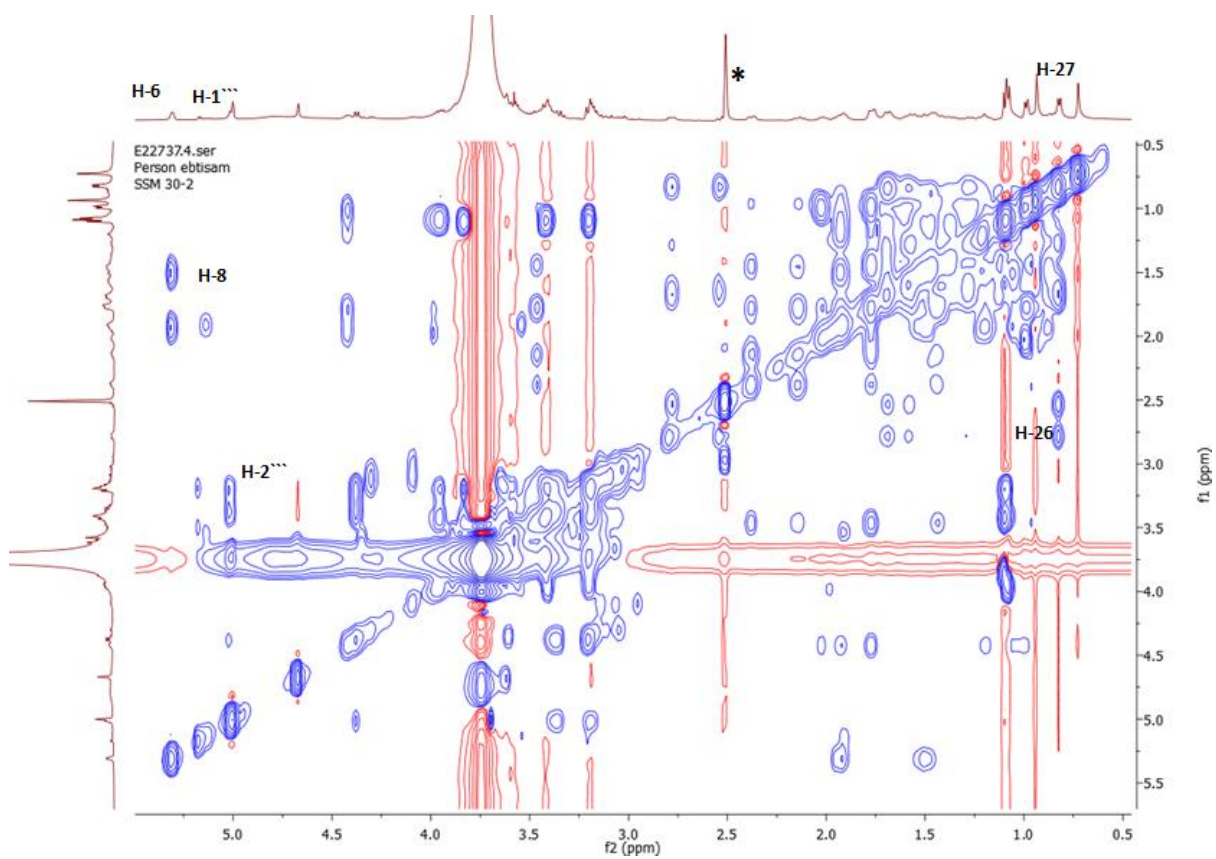


**Figure 3.46:** NOSY spectrum (500 MHz) of SSM-30-2 in DMSO- $d_6^*$ .

### 3.6.2 Characterisation of SSM-56 as 3- *O*-caffeoyl quinic acid or cholorgenic acid

The compound SSM-56 (Figure 3.47) was obtained as a dark greenish yellow solid from the MeOH extract of *S. sodomaeum* using Sephadex LH-20 column separation. After spraying with p-anisaldehyde-sulphuric acid reagent and heating, a yellow spot appeared with a  $R_f$  value of 0.73 on the TLC plate using EtOAc as the mobile phase.

The  $^1\text{H}$  NMR spectra (Figure 3.48A, Table 3.16) revealed one quinic acid moiety with three oxymethines at  $\delta_{\text{H}}$  3.47 (1H, *dd*,  $J = 9.9, 3.1$  Hz, H-3), 3.90 (1H, *d*,  $J = 3.1$  Hz, H-4), and 5.17 (1H, *ddd*,  $J = 11.3, 9.8, 5.2$  Hz, H-5) and two set of methylene at  $\delta_{\text{H}}$  1.61 (1H, *dd*,  $J = 14.3, 3.0$  Hz), 1.99 (1H, *dd*,  $J = 14.4, 3.0$  Hz) (H-2) and 1.76 (1H, *dd*,  $J = 12.7, 5.3, 2.5$  Hz), 1.82 (1H, *d*,  $J = 11.7$  Hz) (H-6). One caffeoyl moiety was established with signals at  $\delta_{\text{H}}$  7.45 (H-7'), 6.23 (H-8'), 6.96 (H-2'), 7.07 (H-6') and 6.76 (H-5').

The  $^{13}\text{C}$  spectrum (Figure 3.48B, Table 3.16) showed sixteen carbon atoms made up of seven carbon atoms of the quinic acid moiety and nine carbons for the caffeoyl moiety. The quinic acid moiety showed two methylene carbons, C-2 and C-6 at 38.1 and 40.05 ppm respectively and three oxymethine carbons (C-1, C-3, C-4 and C-5) as well as a quaternary carbon at 75.23 ppm along with a carboxyl signal (C-7) at 176.3 ppm. The caffeoyl moiety includes a carbonyl at  $\delta_{\text{C}}$  166.4 (C-9') and five methine carbons at 121.2, 114.5, 115.7, 145.7 and 114.3 ppm (C-2', C-5', C-6', C-7' and C-8', respectively). Three quaternary carbons were observed at 125.8, 144.7 and 148.8 ppm (C-1', C-3' and C-4').

Using 2D NMR (HMBC and HSQC) (Figure 3.49A, Figure 3.49B), the compound was elucidated as follows: the correlation (HMBC, Figure 3.49A) of the proton at  $\delta_{\text{H}}$  7.07 (H-6') showed  $^3J$  correlations to the carbons at  $\delta_{\text{C}}$  121.2 (C-2'), 148.8 (C-4') and 145.7 (C-7') while the proton at  $\delta_{\text{H}}$  6.98 (H-2') showed  $^2J$  correlation to  $\delta_{\text{C}}$  144.6 (C-3') and  $^3J$  correlation to  $\delta_{\text{C}}$  148.8 (C-4') and 115.7 (C-6') in the aromatic ring. The proton at  $\delta_{\text{H}}$  6.23 (H-8') had a  $^2J$  correlation to  $\delta_{\text{C}}$  166.8 which was assigned as a

carboxylic acid carbon C-9'. The protons at  $\delta_{\text{H}}$  6.23 (H-8') and at  $\delta_{\text{H}}$  6.75 (H-5') showed  $^3J$  correlation to the carbon at  $\delta_{\text{C}}$  125.28 while the proton at  $\delta_{\text{H}}$  7.45 (H-7') had a  $^2J$  correlation to  $\delta_{\text{C}}$  125.28 which was assigned as C-1' in the aromatic ring. In the quinic acid moiety, the proton at  $\delta_{\text{H}}$  3.90 (H-4) showed  $^2J$  correlations to the oxymethines at  $\delta_{\text{C}}$  72.6(C-5) and  $\delta_{\text{C}}$  73.36 (C-3). The methylene protons at  $\delta_{\text{H}}$  1.61/1.97 (H-2a/b) and  $\delta_{\text{H}}$  1.75/1.84 (H-6a/b) displayed a  $^2J$  correlation to the carbon at  $\delta_{\text{C}}$  75.23 (C-1). The proton signal (H-2b) had  $^3J$  correlation to the carbonyl at  $\delta_{\text{C}}$  176.3 (C-7). The deshielded proton at  $\delta_{\text{H}}$  5.17 (H-5) correlated via  $^2J$  coupling to C-6 at  $\delta_{\text{C}}$  40.04 and  $^3J$  coupling to carbon at  $\delta_{\text{C}}$  73.6 (C-3). H-5 showed a  $^3J$  correlation to the caffeoyl carbonyl at  $\delta_{\text{C}}$  166.4 (C-9'), confirming the presence of one caffeic acid unit in SSM-56.

The HRESI-MS data showed a molecular ion  $[\text{M}]^-$  at  $m/z$  353.0985 which showed that the molecular formula of this compound was  $\text{C}_{16}\text{H}_{18}\text{O}_9$ . The  $^1\text{H}$  &  $^{13}\text{C}$  NMR spectral data are in agreement with those reported earlier (Amin *et al.*, 2013; Lopez-Martinez *et al.*, 2015; Matthias *et al.*, 2014). This is the first report of the isolation of cholorgenic acid from *S. sodomaeum*.

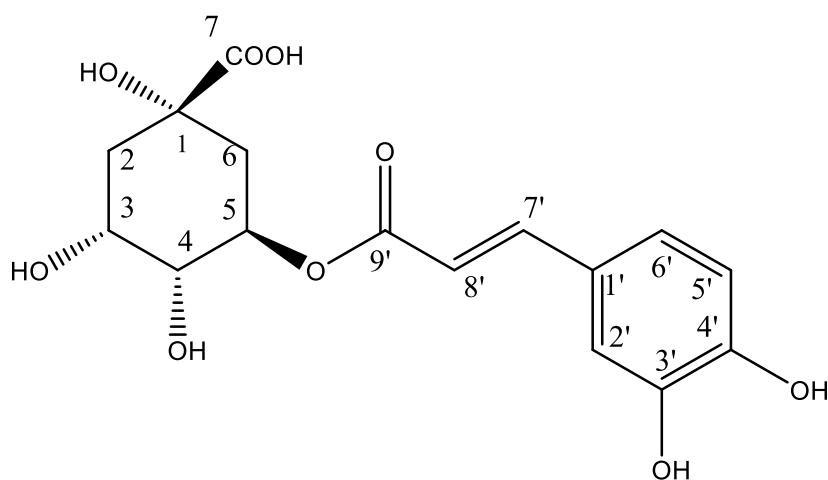
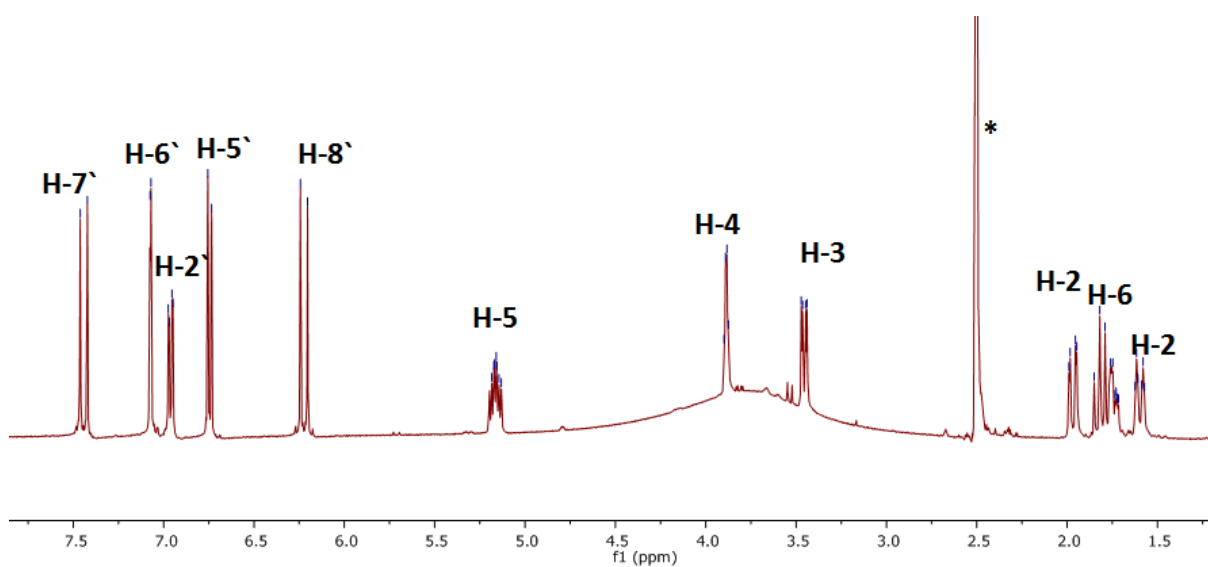


**Figure 3.47:** Structure of cholorgenic acid.

**Table 3.16:**  $^1\text{H}$  (400MHz),  $^{13}\text{C}$  (100MHz), and HMBC data of SSM-56 in DMSO- $d_6$ .

Position	$^1\text{H}$ (ppm)	$^{13}\text{C}$ (ppm)	HMBC correlations
1	-	75.23	
2	1.61 (1H, <i>dd</i> , $J = 14.3, 3.1$ Hz) 1.98 (1H, <i>dd</i> , $J = 14.3, 3.1$ Hz)	38.10	C-1( $^2J$ ),C-5( $^4J$ ),C-3( $^2J$ ),C-6 ( $^3J$ )
3	3.47 (1H, <i>dd</i> , $J = 9.9, 3.1$ Hz)	73.36	C-4( $^2J$ )
4	3.90 (1H, <i>d</i> , $J = 3.1$ Hz)	71.50	C-3( $^2J$ ),C-5 ( $^2J$ )
5	5.17 (1H, <i>ddd</i> , $J = 11.3, 9.8, 5.2$ Hz)	71.60	C-6( $^2J$ ),C-3 ( $^3J$ ),C-9'( $^3J$ )
6	1.76 (1H, <i>dd</i> , $J = 12.7, 5.3, 2.5$ Hz) 1.82 (1H, <i>dd</i> , $J = 12.7, 11.1$ Hz)	40.05	C-2( $^3J$ ),C-5( $^2J$ ),C-3( $^4J$ ),C-1 ( $^2J$ )
7	-	176.3	-
1'	-	125.28	-
2'	6.96 (1H, <i>dd</i> , $J = 8.2, 2.1$ Hz)	121.22	C-3'( $^2J$ ),C-6'( $^3J$ ),C-4'( $^3J$ )
3'	-	144.7	-
4'	-	148.2	-
5'	6.76 (1H, <i>d</i> , $J = 8.2$ Hz)	114.5	C-2'( $^4J$ ),C-1'( $^3J$ ),C-4', C-7'( $^2J$ )
6'	7.07 (1H, <i>d</i> , $J = 2.1$ Hz)	115.7	C-4'( $^3J$ ),C-2'( $^3J$ ),C7'( $^3J$ )
7'	7.45 (1H, <i>d</i> , $J = 15.8$ Hz)	145.7	C-6'( $^3J$ ), C-2'( $^3J$ ),C9'( $^3J$ ), C-1'( $^2J$ )
8'	6.23 (1H, <i>d</i> , $J = 15.8$ Hz)	114.3	C-1'( $^3J$ ),C-9' ( $^2J$ )
9'	-	166.4	-

A



B

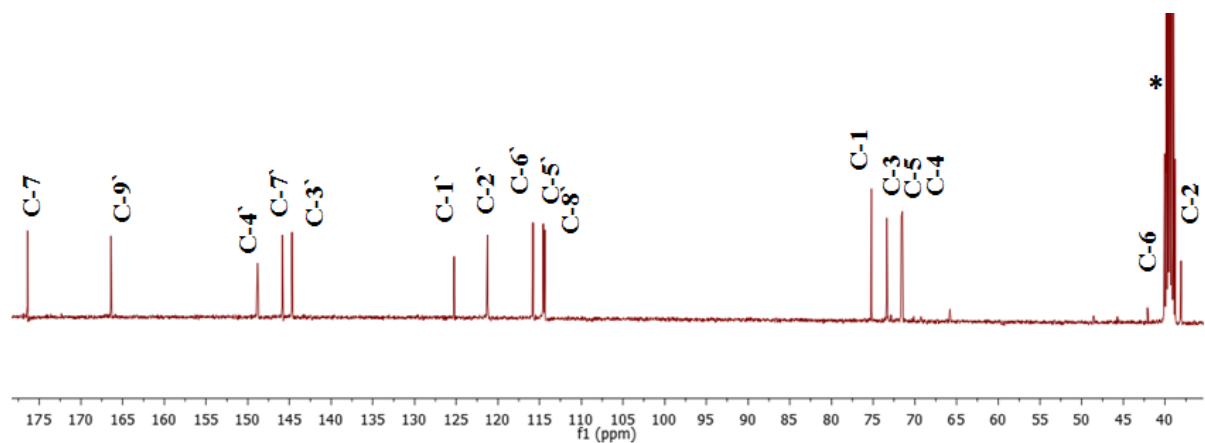
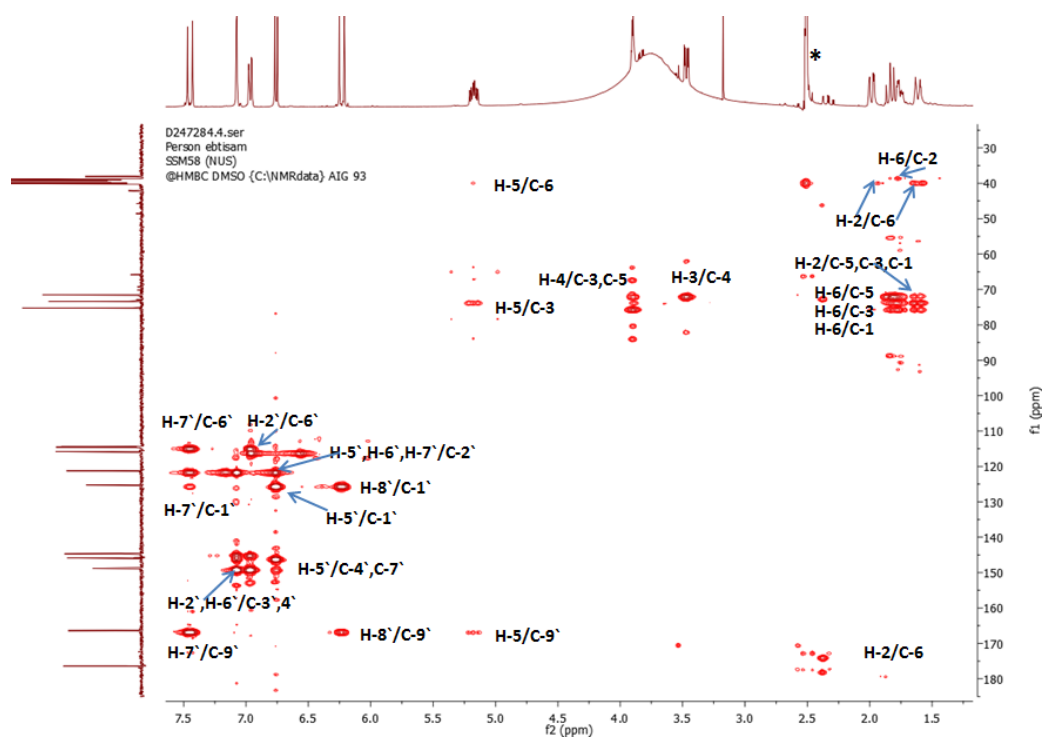


**Figure 3.48A:**  $^1\text{H}$  NMR and **3.48B:**  $^{13}\text{C}$  NMR spectra (400 MHz) of SSM-56 in  $\text{DMSO-}d_6^*$ .

A



B

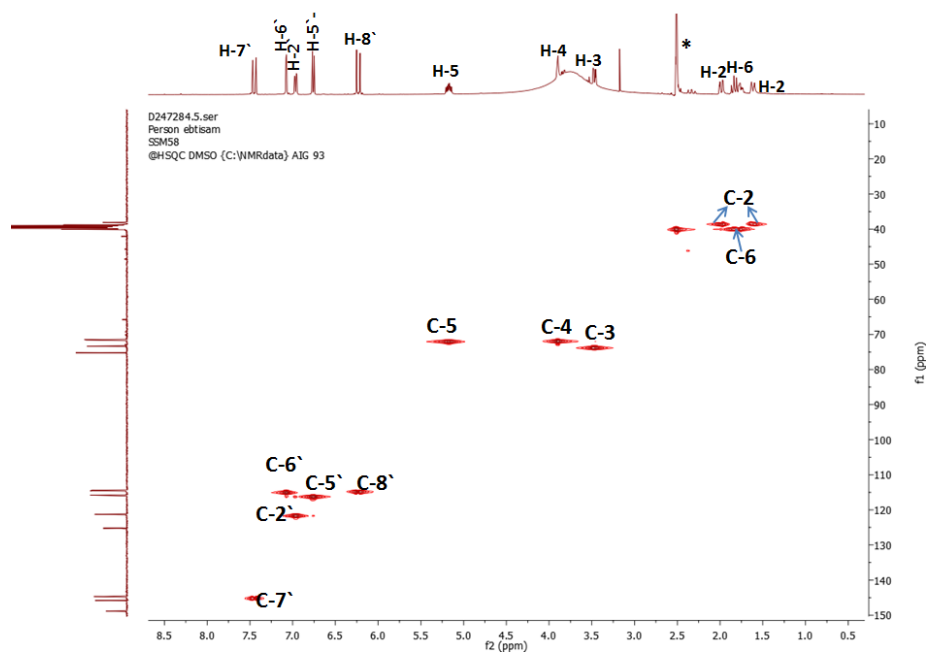


**Figure 3.49A: HMBC and 3.49B: HSQC spectra (400 MHz) of SSM-56 in DMSO- $d_6^*$ .**

### 3.4.3 Characterisation SSH and SSE as trilinolein

The compounds SSH-1 and SSE-1 (Figure 3.50) were isolated from the hexane and ethyl acetate crude extract of *S. sodomaeum*. On TLC, they appeared as purple spots after development with anisaldehyde sulphuric acid reagent and heating.

The  $^1\text{H}$  NMR spectrum (Figure 3.51) exhibited overlapping olefinic proton (H-9', H-10', H-12', H-13') signals at  $\delta$  5.36-5.33 ppm (12H, *m*) and  $\delta$  5.25 ppm (1H, *m*) owing to methine protons in a triglycerol. Signals at  $\delta$  4.28 ppm (2H, *dd*) indicated H-1a and H-3a and proton H-3b and H-1b at  $\delta$  4.13 ppm (2H, *dd*), assigned four methylene protons in the triglyceride. Signal at  $\delta_{\text{H}}$  2.75 ppm (6H, *t*) (H-11') due to divinyl methylene protons. Signal at  $\delta_{\text{H}}$  at  $\delta$  2.02 ppm (12H, q4,  $J=7.56$  Hz) (H-8', H-14') revealed allyl methylene groups, proton at  $\delta$  2.29 ppm H-2' (6H, *t*) revealed methylene protons attached to a carbonyl carbon. Protons at  $\delta$  1.59 ppm (6 H, *t*,  $J=6.6$  Hz) (H-3') indicating six  $\beta$  methylene protons. Protons at  $\delta$  1.27 ppm (21H, *m*,) were due to the methylene protons on a saturated carbon. Signal at  $\delta$  0.87 ppm (9H, *t*) (H-18') revealed to methyl groups. These data for trilinolein were also supported by (Vlahov, 1999) and Carneiro *et al.* (2005).

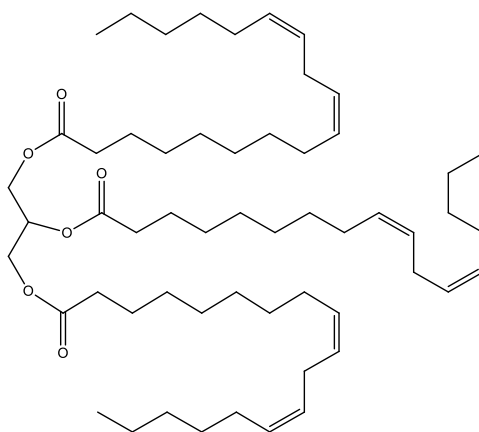


**Figure 3.50:** Structure of SSH as triglyceride.

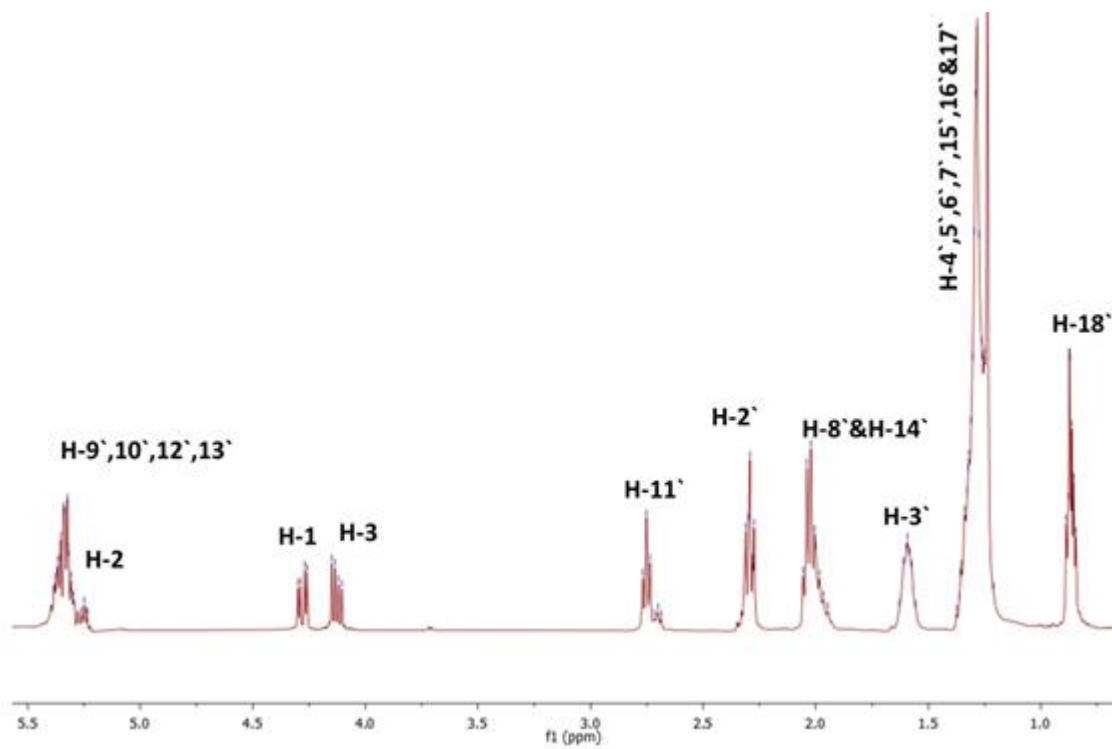


**Figure 3.51:**  $^1\text{H}$  NMR spectrum (400 MHz) of SSH  $\text{CDCl}_3$ .

## Part 2: Biological Results

### 3.7 Cytotoxicity screening of crude extracts and isolated compounds using AlamarBlue® assay

Cytotoxicity assessment was carried out against cancer cells A375, HeLa, LNCaP, PC-3M, PANC-1 and HepG2 and non-cancer PNT2 and HEKa (normal) cell lines using an AlamarBlue® assay. It was used to evaluate the toxicity of different plants *A. cyrenaicum*, *P. tortuosus*, *T. zanonii*, *H. radicata* and *S. sodomaeum* extracts and their constituents (section 3.7.1, section 3.7.2 section 3.7.3, section 3.7.4 and section 3.7.5) respectively. Any crude extract or compound that caused cell viability to decrease to less than 50% was considered cytotoxic and the concentration of each crude or compound which gave 50% of the maximum response and the (IC<sub>50</sub>) was calculated. In addition, as shown in Figure 3.52, a 5 % (v/v) (63.99 uM) of DMSO was used to dissolve samples without killing the cells in contrast with high concentration 50 % DMSO (639.95 uM) that had a cytotoxic effect on the cells (Table. 3.17). Use of 5uM staurosporine a positive control to induce apoptosis in the cells (Figure 3.53), and 250 µg/ml (833.30 uM) to 1.9 µg/ml (6.33uM) of cisplatin as positive controls (chemotherapy drug) on the cells showed that the staurosporine had a significant ( $p < 0.0001$ ) cytotoxic effect on cells while the cisplatin was resistant to the cells.

**Table 3.17:** IC<sub>50</sub> of 50% DMSO on normal and cancer cell lines. The values are means ± SEM of at least three independent experiments performed in triplicates

Cells	IC <sub>50</sub> (μM)
A375	47.83±1.620 μg/ml (612.18 uM)
PANC-1	131.7± 1.86 μg/ml (1685.65 uM)
PC-3M	53.38±0.4024 μg/ml (683.22 Um)
LNCaP	15.66±1.125 μg/ml (200.435 uM)
HeLa	27.67+1.393 μg/ml (354.15 uM)
HepG2	180.8 ±0.1552 μg/ml (2314.09 uM)
PNT2	72.94 ±1.823 μg/ml (933.57 uM)
HEKa	48.63 ±1.586 μg/ml (622.42 uM)

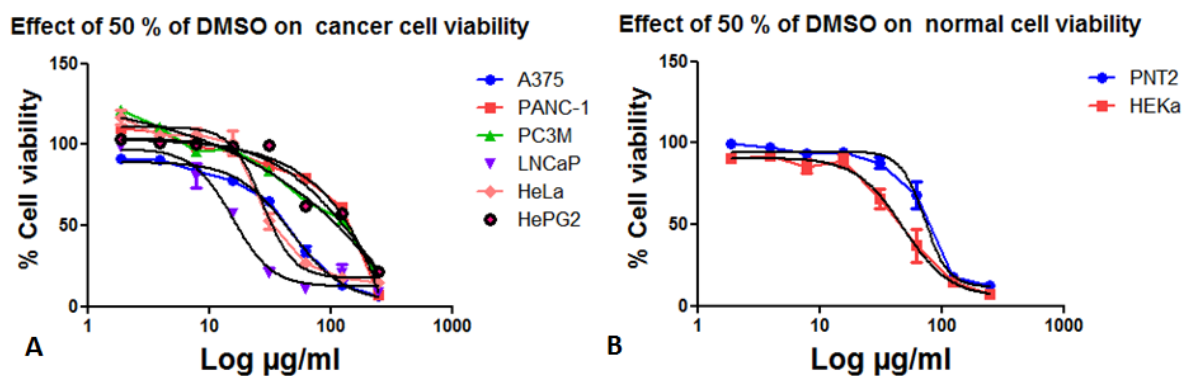


**Figure 3.52:** Effect 50% of DMSO on cell viability of (A) cancers cells and (B) normal cells after 48h. Cell viability was measured using an AlamarBlue® assay at 560nm and 590nm. Values represent the mean ± SEM of 3 values. Statistical analysis was performed using the dose response curves.

### Effect of 5 $\mu$ M Staurosporine on cell viability of cells

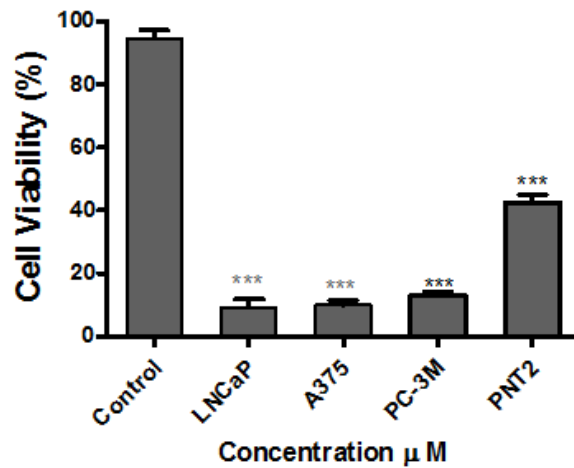


**Figure 3.53:** Effect of 5 $\mu$ M of staurosporine on cell viability of LNCaP, A375, PC-3M and PNT2 cells. Cell viability was measured using an AlamarBlue® assay at 560nm and 590nm after 48 h. Values represent the mean  $\pm$  SEM of 3 values. Statistical analysis was performed using one way ANOVA with Dunnett's multiple comparison test. \*\*\* indicates significantly ( $p < 0.0001$ ) lower values compared with the untreated control.

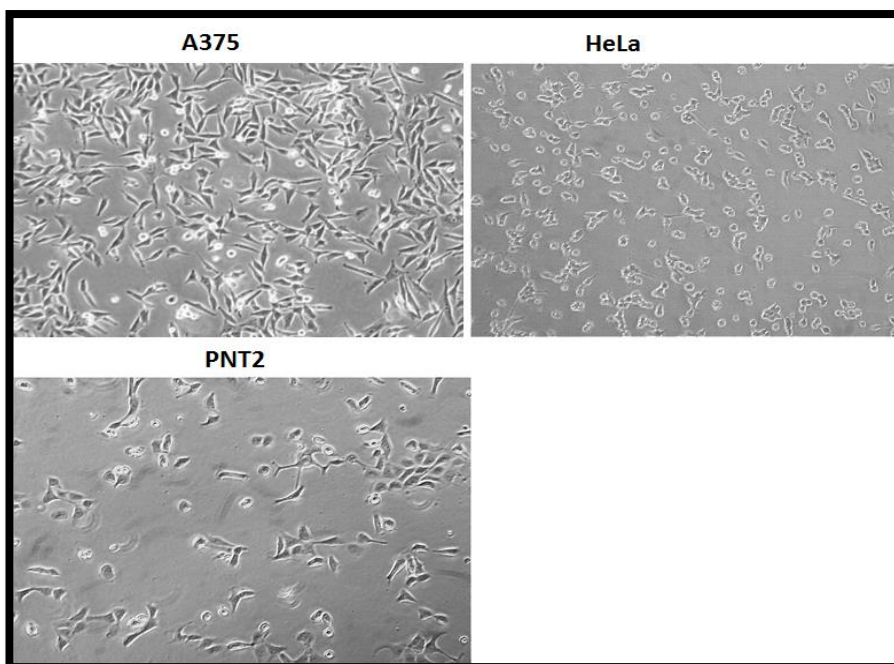
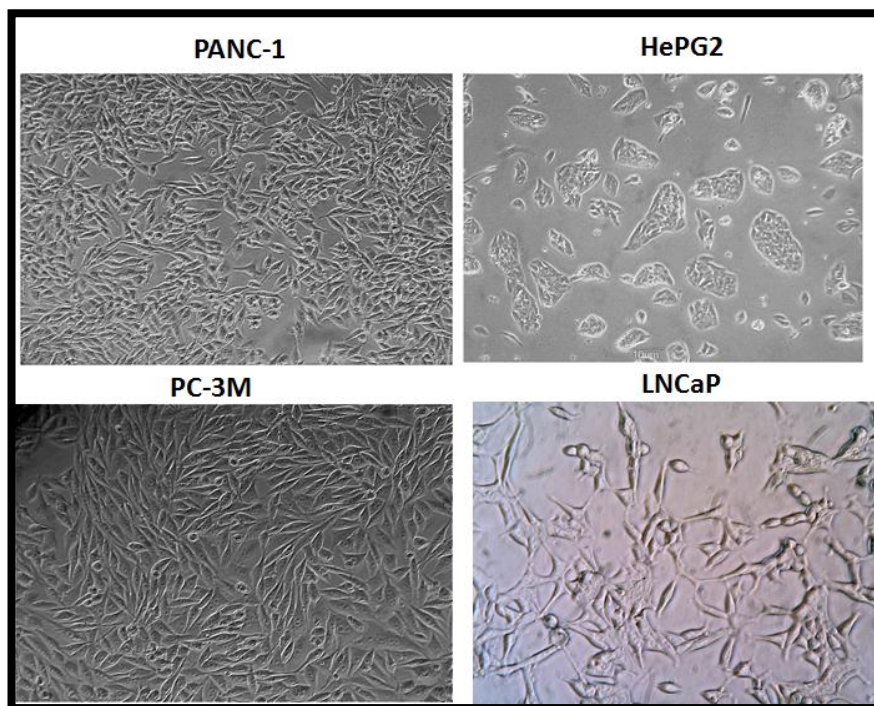


**Figure 3.54:** Morphology and substrate coverage of the cells for the cytotoxicity assay, the images show that  $1 \times 10^5$  cells per well were used as an optimum number to be used in a 96 well plate. The magnification bar represents  $50 \mu\text{m}$ . Objective lens  $\times 20$ .

### 3.7.1 Cytotoxicity of *A. cyrenaicum* crude extracts and isolated compounds

Results of the cytotoxicity activity of *A. cyrenaicum* extracts and its constituents against cancer and normal cells are presented in Table 3.18. The all extracts and the isolated compounds showed no cytotoxic activity on the cells except *A. cyrenaicum* root hexane extract that was toxic to cancer and normal cells (HeLa, HepG2, HEKa and PNT2) cells at 250 µg/ml with IC<sub>50</sub> of 181.3, 128.3, 136.6 and 140.7 µg/ml, respectively. *A. cyrenaicum* fruit extracts showed toxicity only against normal cells, therefore they were considered not promising for future work; results not shown.

**Table 3.18:** Summary of IC<sub>50</sub> of *A. cyrenaicum* extracts and compounds on each cell line. The values are means ± SEM of at least three independent experiments performed in triplicates. ND: not determined. (---): not active up to 250 µg/ ml.

Treatment	Cancer Cell Lines						Normal Cell Line	
	A375	HeLa	LNCaP	PC-3M	PANC-1	HepG2	HEKa	PNT2
<i>A. cyrenaicum</i> root hexane	---	181.3	---	---	---	128.3	136.6	140.7
<i>A. cyrenaicum</i> root EtOAc	---	---	---	---	---	---	---	---
<i>A. cyrenaicum</i> root MeOH	---	---	---	---	---	---	---	---
<i>A. cyrenaicum</i> aerial hexane	---	---	---	---	---	---	---	---
<i>A. cyrenaicum</i> aerial EtOAc	---	---	---	ND	ND	---	---	---
<i>A. cyrenaicum</i> aerial MeOH	---	---	---	---	---	---	---	---
<i>A. cyrenaicum</i> fruit <i>H</i>	---	---	---	---	---	---	215.8	---
<i>A. cyrenaicum</i> fruit. EtOAc	---	---	---	---	---	---	116.3	---
<i>A. cyrenaicum</i> fruit MeOH	---	---	---	---	---	---	219.3	---

### 3.7.2 Cytotoxicity of *P. tortuosus* crude extracts and isolated compounds

Results of the cytotoxicity activity of *P. tortuosus* extracts and its constituents against cancer and normal cells are presented in Table 3.19. The methanol extract of *P. tortuosus* and PTM-1 showed no cytotoxic effects on both normal and cancer cells. On the other hand, *P. tortuosus* EtOAc extract was toxic to A375, PANC-1 and PNT2 at 250µg/ml; data not shown. However, the *P. tortuosus* hexane extract was toxic to cancer and normal cells (A375, PANC-1 and PNT2) at 125 µg/ml with IC<sub>50</sub> values of 76.97± 1.77 µg/ml, 86.57± 1.82 µg/ml and 80.30± 1.99 µg/ml, respectively and this extract was toxic to LNCaP, PC-3M and HepG2 at 250 µg/ml (Figure 3.55). PTH-6-7 was toxic against A375, PC-3M, PANC-1 and HepG2 at 125µg/ml with IC<sub>50</sub> values of 70.11± 1.93 µg/ml, 72.20 ±1.77 µg/ml, 75.88± 1.98 µg/ml and 90.29 ±2.14 µg/ml, respectively, while the PTH 6-7 was toxic to PNT2 at 250 µg/ml with IC<sub>50</sub> value of 136.16 µg/ml (Figure 3.56).

This preliminary cytotoxic screening of *P. tortuosus* extracts and its constituents had effects on both cancer and normal cells at same concentrations and therefore there was no need for further investigation except for the PTH6-7 because it was slightly toxic to cancer cells at 125µg/ml.

**Table 3.19:** Summary of IC<sub>50</sub> of *P. tortuosus* extracts and compounds on each cell line. The values are means ± SEM of at least three independent experiments performed in triplicates. ND: not determined. (---): not active up to 250 µg/ ml.

Treatment	Cancer Cell Lines						Normal Cell Line	
	A375	HeLa	LNCaP	PC-3M	PANC-1	HepG2	HEK a	PNT2
<i>P. tortuosus</i> hexane	76.97	ND	195.5	154.3	86.57	140.2	ND	80.30
<i>P. tortuosus</i> EtOAc	203	ND	---	---	174.33	---	ND	216.3
<i>P. tortuosus</i> MeOH	---	ND	---	---	---	---	ND	---
PTH-6-7	70.11	ND	---	72.20	75.88	90.29	ND	136.16
PTM-1	---	ND	---	---	---		ND	---

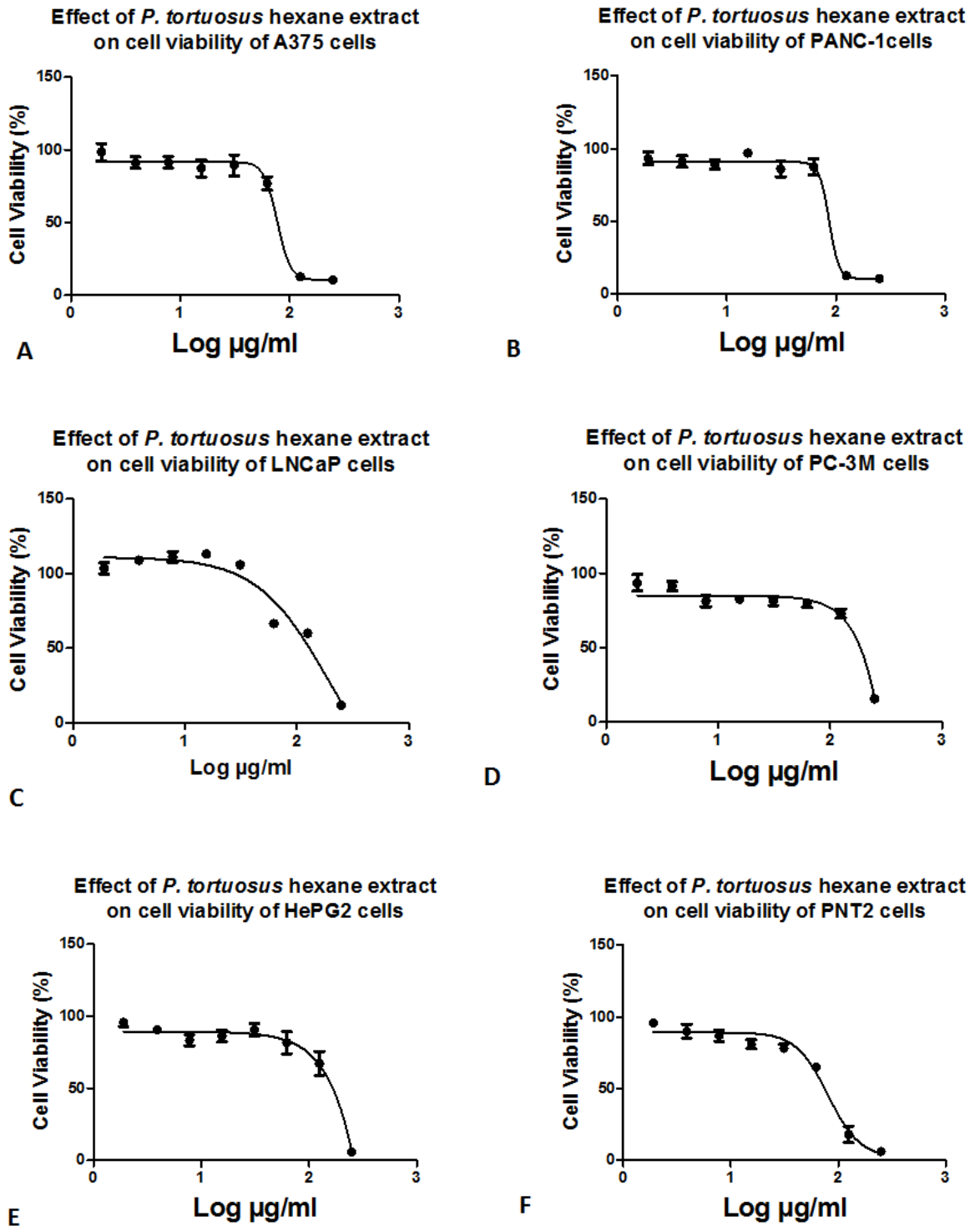


**Figure 3.55:** Effect of *P. tortuosus* hexane on cell viability of (A) A375 cells, (B) PANC-1 cells, (C) LNCaP cells, (D) PC-3M cells, (E) HepG2 cells, and (F) PNT2 cells after 48 h. Cell viability was measured using an AlamarBlue® assay at 560nm and 590nm and calculated as a % of untreated controls. Values are the means of  $n = 3 \pm \text{SEM}$ .

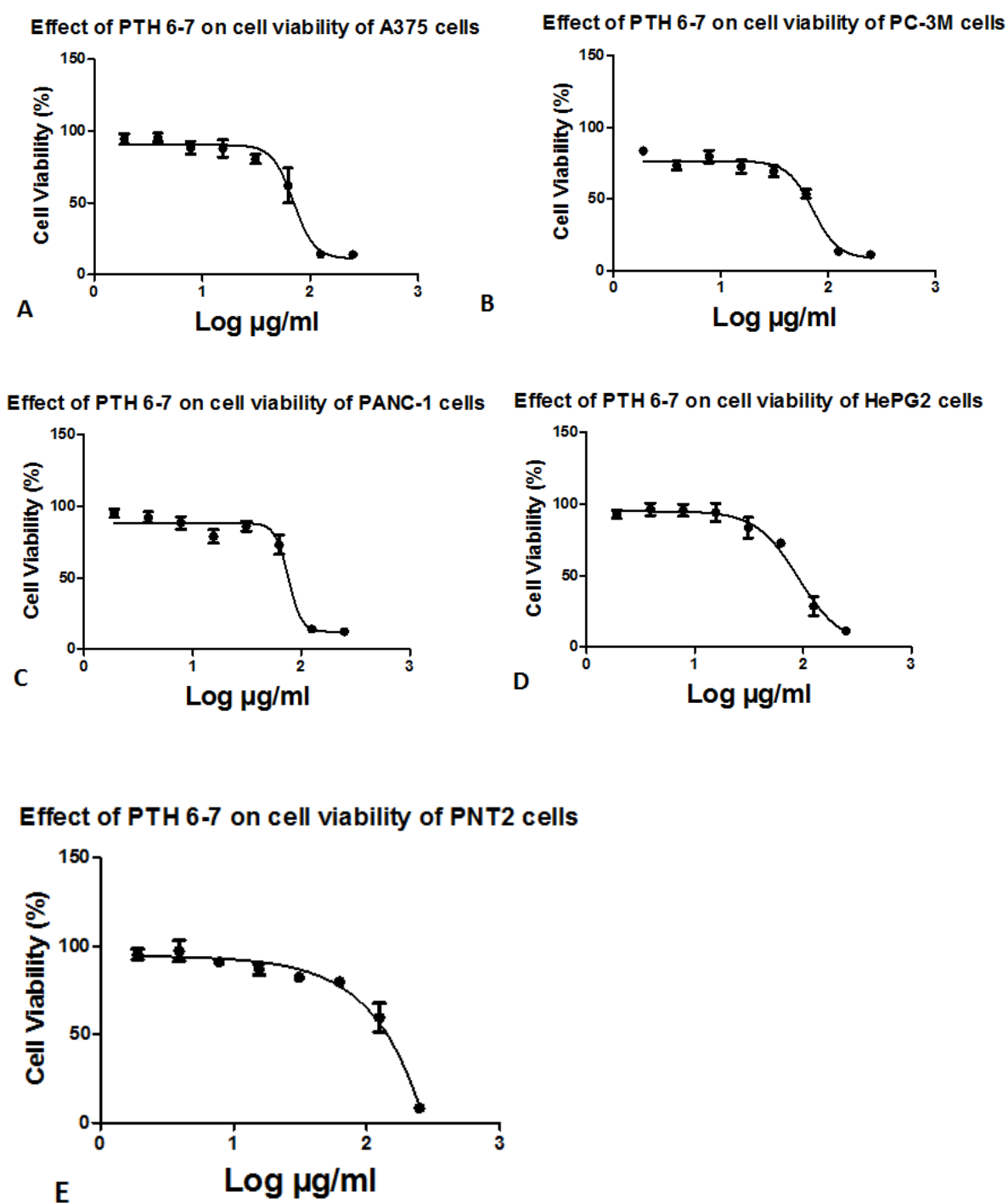


**Figure 3.56:** Effect of PTH-6-7 on cell viability of (A) A375 cells, (B) PC-3M cells, (C) PANC-1 cells, (D) HepG2 cells and (E) PNT2 cells after 48 h. Cell viability was measured using an AlamarBlue® assay at 560nm and 590nm and calculated as a % of untreated controls. Values are the means of  $n = 3 \pm \text{SEM}$ .

### 3.7.3 Cytotoxicity of *T. zanonii* crude extracts and isolated compounds

Results of the cytotoxicity activity of *T. zanonii* extracts and its constituents against cancer and normal cells are presented in Table 3.20. Only the ethyl acetate extract was toxic to A375 and LNCaP with IC<sub>50</sub> values of 47.24±1.13, and 61.60±1.62 µg/ml, respectively (Figure 3.57) and to PANC-1 and normal cells (PNT2 and HEKa) at the highest concentration tested, 250µg/ml 174.1±1.03 µg/ml, 143.1± 2.48 µg/ml and 145.8 ±1.79 µg/ml, respectively. On the other hand it had no toxicity on HeLa, PC-3M and HepG2 cells even at 250µg/ml.

The hexane extract showed toxicity to PANC-1 and normal cells (PNT2 and HEKa) at 250 µg/ml with IC<sub>50</sub> values of 132.9±2.25 µg/ml, 157.3±1.929 µg/ml and 113.1±1.98 µg/ml; respectively (data not shown). The methanol extract of *T. zanonii* was toxic to PANC-1 at 125µg/ml with IC<sub>50</sub> value of 62.02±1.41 µg/ml and was toxic to LNCaP and normal cells (HEKa PNT2) at 250 µg/ml with IC<sub>50</sub> value of 135.99±1.83 µg/ml, 141.9±1.27 µg/ml and 195.1 µg/ml, respectively (Figure 3.58). The compounds, TZH-150-170-7 and TZH 68 showed no cytotoxic effects on any cells, while TZH-103-107-9 showed toxicity only to PANC-1 and PNT2 cells at 250µg/ml with IC<sub>50</sub> values of 148.9±2.65 µg/ml (455.23µM) and 179.8±2.83 µg/ml (549.70 µM) respectively (Figure 3.59) and TZH-41-49 showed toxicity to HeLa cells at 250 µg/ml with IC<sub>50</sub> value of 156.90 µg/ml (374.43 µM) (Figure 3.60). The compound TZH-24 was not assessed for cytotoxicity due to time constraints.

This preliminary cytotoxic screening of *T. zanonii* extracts and its constituents showed some extracts had effects on both cancer and normal cells, while with others no cytotoxicity was observed and therefore there was no need for further investigation except for the ethyl acetate extract because it was highly toxic to A375 and LNCaP cells, but had toxicity on normal cells above 250 µg/ml. This would be considered essential for future work as this is the first time for screening cytotoxicity of *T. zanonii*.

**Table 3.20:** Summary of IC<sub>50</sub> of *T. zanonii* extracts and compounds on each cell line. The values are means ± SEM of at least three independent experiments performed in triplicates. ND: not determined. (----): not active up to 250 µg/ ml.

Treatment	Cancer Cell Lines						Normal Cell Line	
	A375	HeLa	LNCaP	PC-3M	PANC-1	HepG2	HEK a	PNT2
TZH	-	---	---	---	132.9	---	113.1	157.3
TZ EtOAc	47.24	---	61.60	----	174.1	---	145.8	143.1
TZ MeOH	---	---	135.99	---	62.02	---	141.9	195.1
TZH 103-107-9	---	---	---	---	148.9	ND	---	179.8
TZH 150-170-7	ND	ND	----	----	----	---	ND	---
TZH-68	----	---	---	---	---	---	---	---
TZM-24	ND	ND	ND	ND	ND	ND	ND	ND
TZH-41-49	----	156.90	----	----	----	ND	----	ND

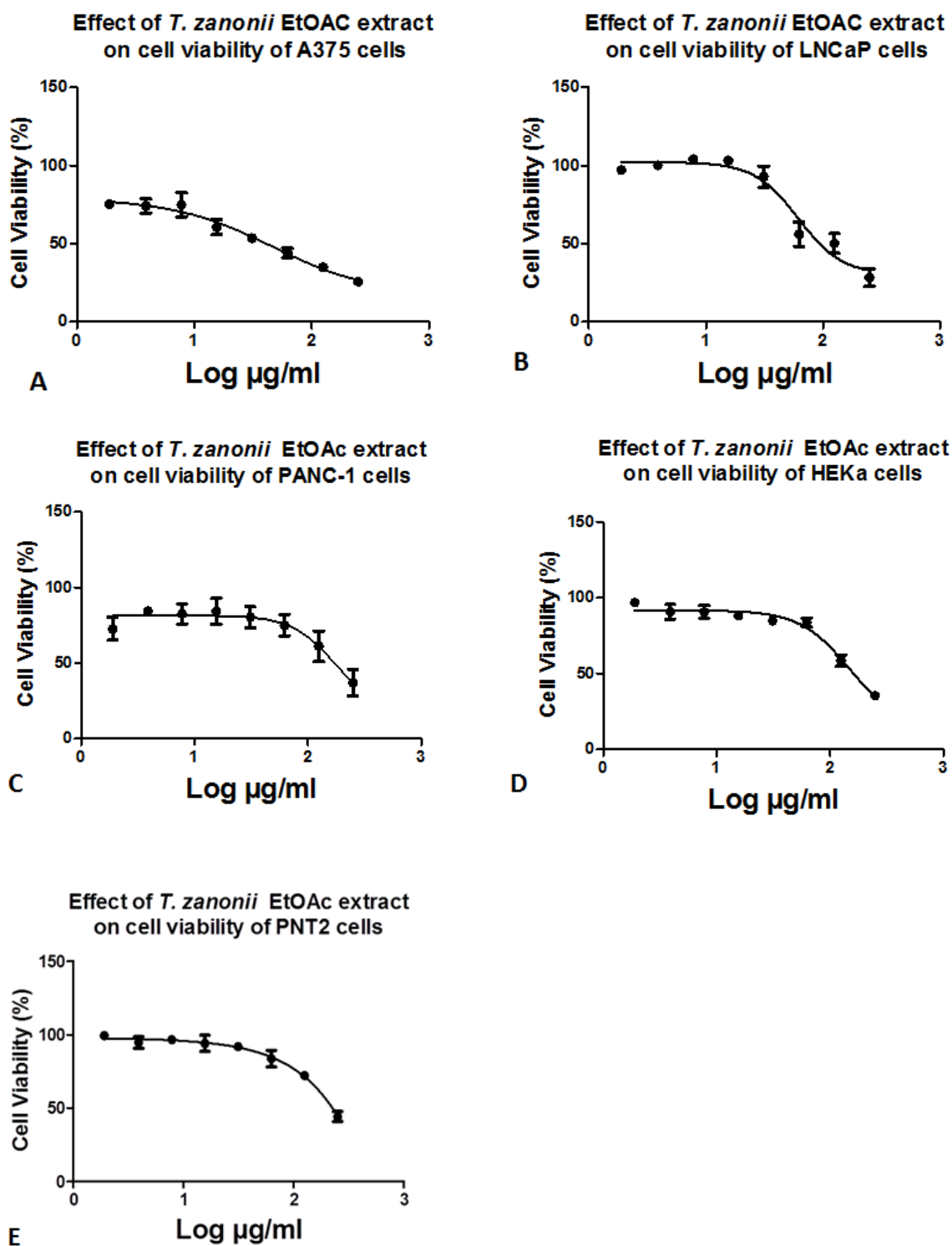


**Figure 3.57:** Effect of *T. zanonii* EtOAc extract on cell viability of (A) A375 cells, (B) LNCaP cells, (C) PANC-1 cells, (D) HEKa cells and (E) PNT2 cells after 48 h. Cell viability was measured using an AlamarBlue® assay at 560nm and 590nm and calculated as a % of untreated controls. Values are the means of  $n = 3 \pm \text{SEM}$ .

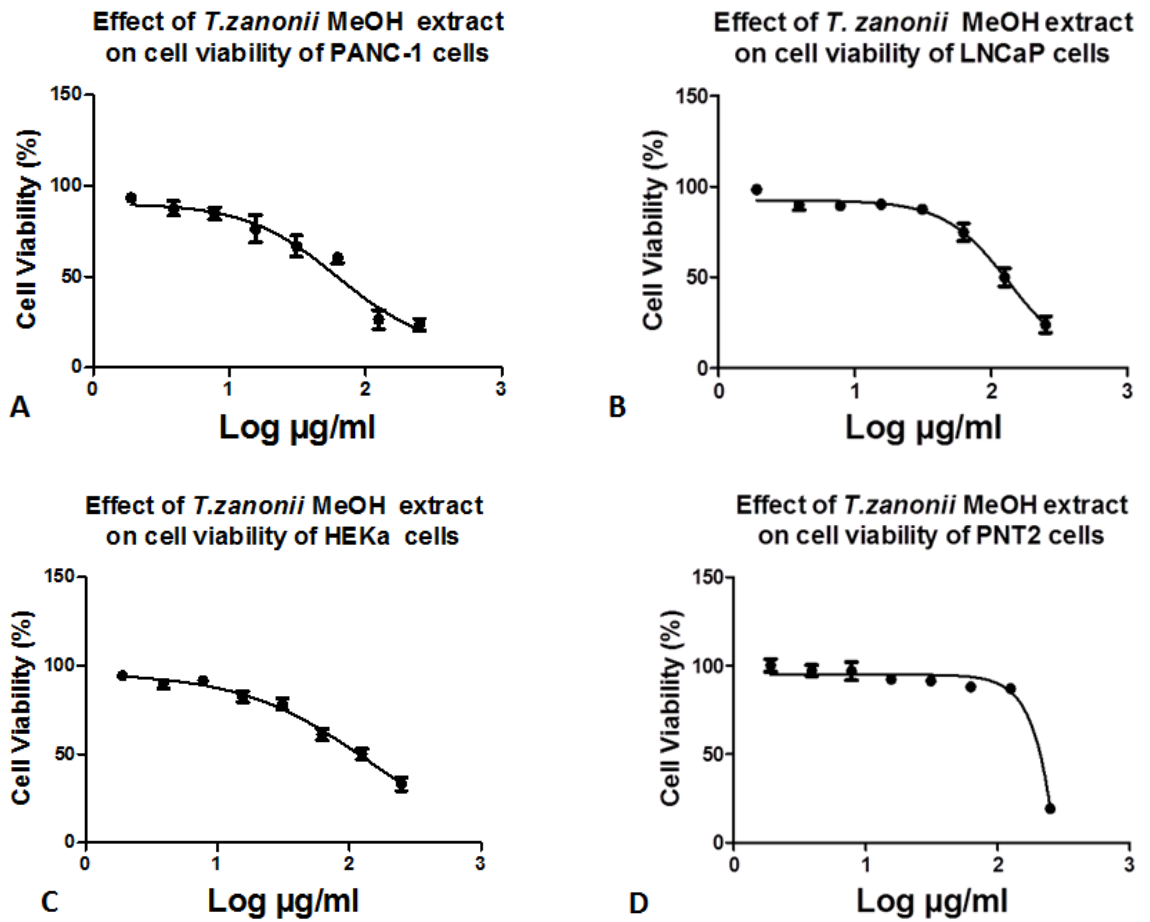


**Figure 3.58:** Effect of *T. zanonii* MeOH extract on cell viability of (A) PANC-1 cells, (B) LNCaP cells, (C) HEKa cells and (D) PNT2 cells after 48 h. Cell viability was measured using an AlamarBlue® assay at 560nm and 590nm and calculated as a % of untreated controls. Values are the means of  $n = 3 \pm \text{SEM}$ .

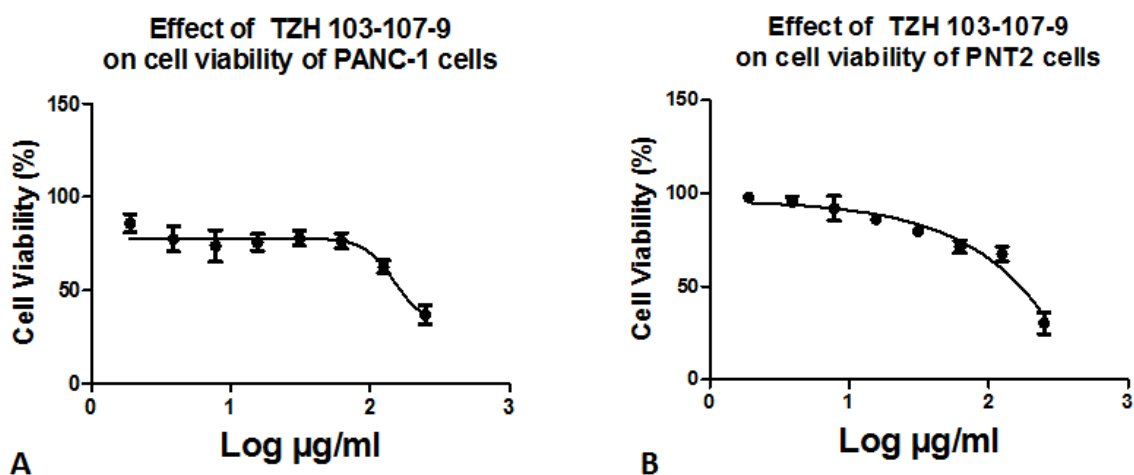


**Figure 3.59:** Effect of TZH-103-107-9 on cell viability of (A) PANC-1 cells and (B) PNT2 cells after 48 h. Cell viability was measured using an AlamarBlue® assay at 560nm and 590nm and calculated as a % of untreated controls. Values are the means of  $n = 3 \pm \text{SEM}$ .

**Effect of TZH 41-49 on cell viability of HeLa cells**

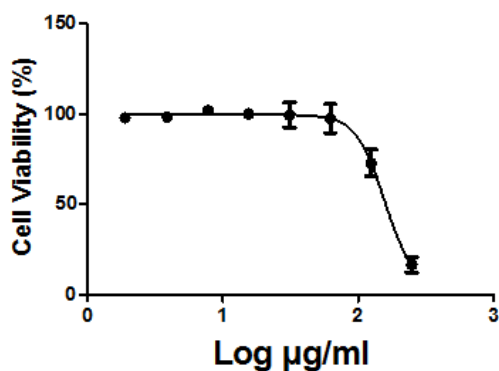


**Figure 3.60:** Effect of TZH-41-49 on HeLa cells after 48 h. Cell viability was measured using an AlamarBlue® assay at 560nm and 590nm and calculated as a % of untreated controls. Values are the means of  $n = 3 \pm \text{SEM}$ .

### 3.7.4 Cytotoxicity of *H. radicata* crude extracts and isolated compounds

Results of the cytotoxicity activity of *H. radicata* extracts and its constituents against cancer and normal cells are presented in Table 3.21. Only the hexane extract *H. radicata* was toxic on all cancer and normal cells and it was highly toxic to LNCaP, PANC-1, PC-3M, HepG2, A375, HeLa and PNT2, with IC<sub>50</sub> values of 24.59 ±1.46 µg/ml, 39.08± 1.638 µg/ml, 38.70± 1.68 µg/ml, 40.18 ±1.66 µg/ml, 76.35±1.75 µg/ml, 55.11±1.63 µg/ml and 11.02±1.08 µg/ml, respectively (Figure 3.61, Figure 3.62 ). It was also toxic to HEKa cells at 250µg/ml with an IC<sub>50</sub> value of 144.5±1.21 µg/ml (Figure 3.62).

On the other hand, *H. radicata* EtOAc extract was toxic to HeLa, PC-3M, PANC-1 and HEKa cells at 250 µg/ml (Figure 3.64), with IC<sub>50</sub> values of 137.45±2.57 µg/ml, 163.13±2.54 µg/ml, 145.39±3.39 µg/ml, and 135.90 µg/ml, and to HepG2 and PNT2 at 125 µg/ml, with IC<sub>50</sub> values of 63.43±1.73 µg/ml and 74.99±1.75 µg/ml respectively (Figure 3.64). This extract was not toxic to A375 and LNCaP. The methanol extract was only toxic to PNT2 at 250µg/ml with IC<sub>50</sub> value of 184.5±3.92 µg/ml (Figure 3.63).

For the HRM-50-59 no cytotoxic effects on both cancer and non-cancer cells were observed, while HRE-21 showed toxicity against PC-3M at 250µg/ml with an IC<sub>50</sub> value of 122.3± 3.28 µg/ml (427.26 µM) and to PNT2 at 125 µg/ml with IC<sub>50</sub> value of 88.25 ±1.73 µg/ml (308.30 µM), and to HepG2 with an IC<sub>50</sub> of 36.59 ±1.11 µg/ml (127.82 µM) (Figure 3.65).

The new daucosterol derivative, HRE-94, showed toxicity to cancer and normal cells A375, LNCaP, HepG2 and PNT2 at 250µg/ml, with IC<sub>50</sub> values of 122.95 µg/ml (170.45 µM), 162.5 µg/ml (255.28 µM), 156.9 µg/ml (217.51 µM) and 156.0 µg/ml (220.43 µM) , respectively and showed no toxicity to PANC-1 and PC-3M cells (Figure 3.66).

The above observations indicate that the hexane extract of *H. radicata* was found to be not selective against the cancer cells due to high toxicity to normal cells. Only the ethyl acetate and HRE-21 seemed to possess selective activity against HepG2 with IC<sub>50</sub> of 63.43±1.73 µg/ml and 36.59 ±1.1µg/ml, respectively compared to normal

cells. In this study some samples (HRE-121) were not assessed due to limited quantities.

**Table 3.21:** Summary IC<sub>50</sub> of cytotoxicity of *H. radicata* extracts and compounds on each cell line. The values are means ± SEM of at least three independent experiments performed in triplicates. ND: not determined. (----): not active up to 250 µg/ ml.

Treatment	Cancer Cell Lines						Normal Cell Line	
	A375	HeLa	LNCaP	PC-3M	PANC-1	HepG2	HEK a	PNT2
<i>H. radicata</i> hexane	76.35	55.11	24.59	38.70	39.08	40.18	144.5	11.02
<i>H. radicata</i> EtOAc	---	137.45	---	163.13	145.39	63.43	135.90	74.99
<i>H. radicata</i> MeOH	---	---	---	---	---	---	---	184.5
HRE-21	---	---	---	122.3	---	36.59	---	88.25
HRM-50-59	---	---	---	---	---	ND	---	---
HRE-94	122.95	ND	162.5	---	---	156.9	ND	156.0

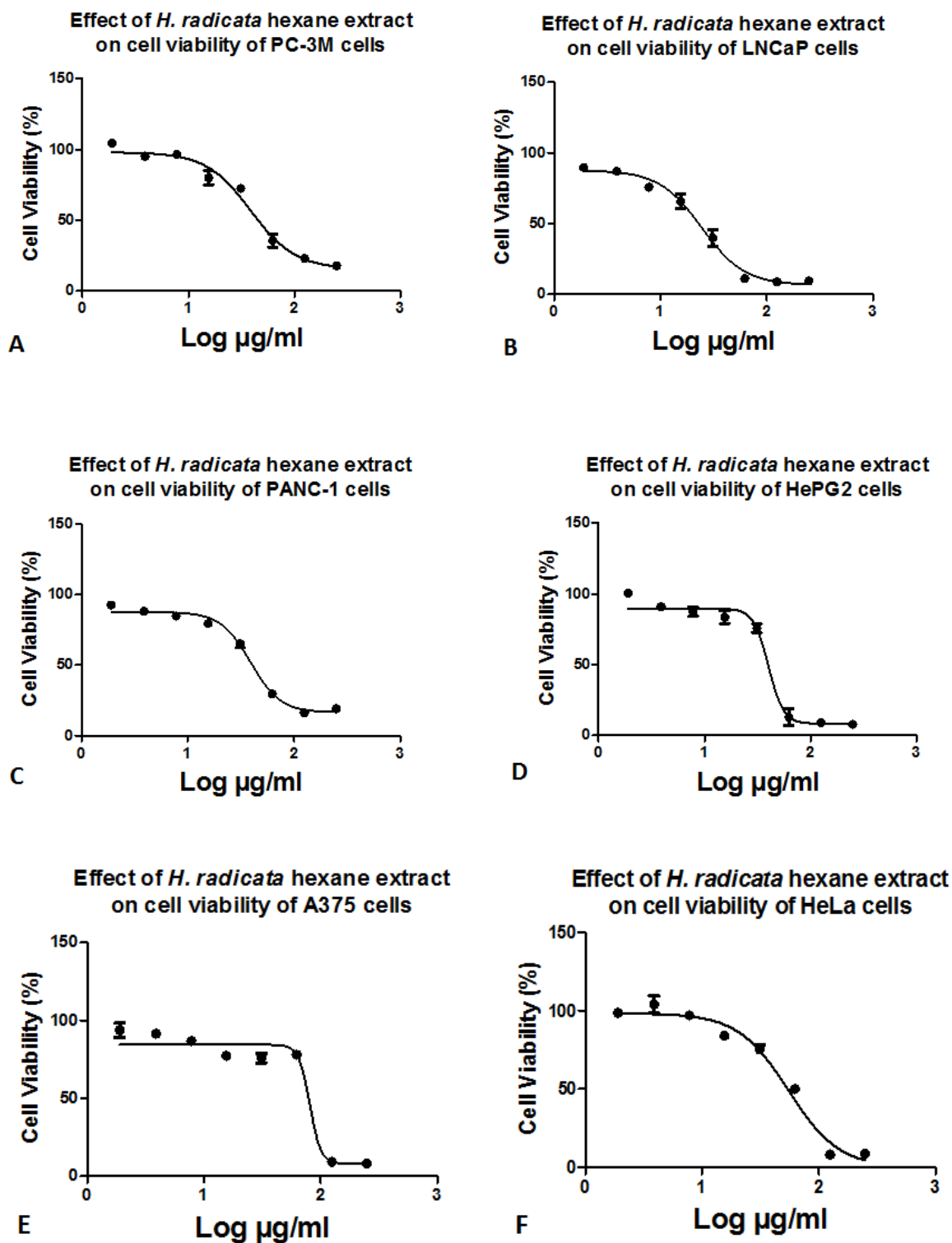


**Figure 3.61:** Effect of *H. radicata* hexane on cell viability of (A) PC-3M cells, (B) LNCap cells, (C) PANC-1 cells, (D) HepG2 cells, (E) A375 cells and (F) HeLa cells after 48 h. Cell viability was measured using an AlamarBlue® assay at 560nm and 590nm and calculated as a % of untreated controls. Values are the means of  $n = 3 \pm$  SEM.

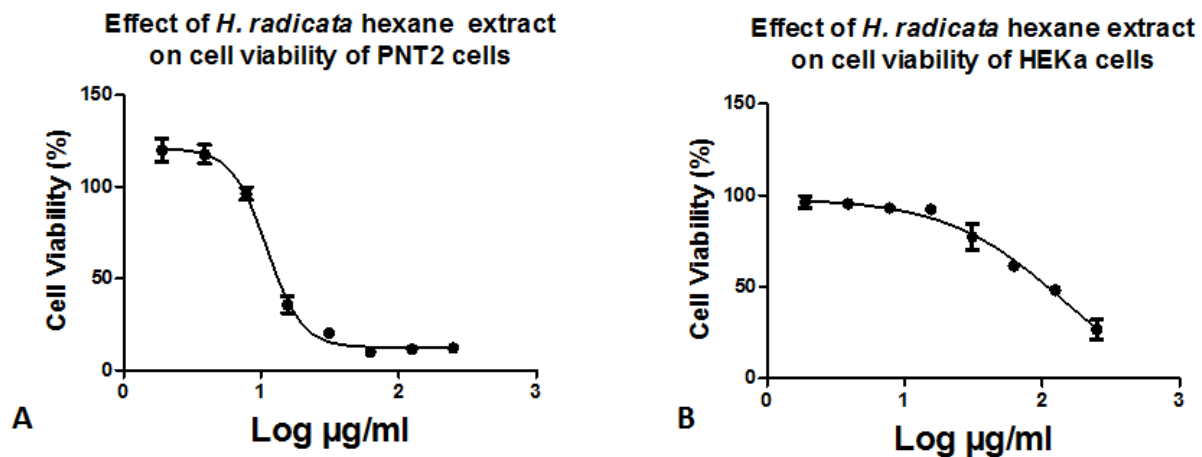


**Figure 3.62:** Effect of *H. radicata* hexane extract on cell viability of (A) PNT2 cells and (B) HEKa cells after 48 h. Cell viability was measured using an AlamarBlue® assay at 560nm and 590nm and calculated as a % of untreated controls. Values are the means of  $n = 3 \pm \text{SEM}$ .

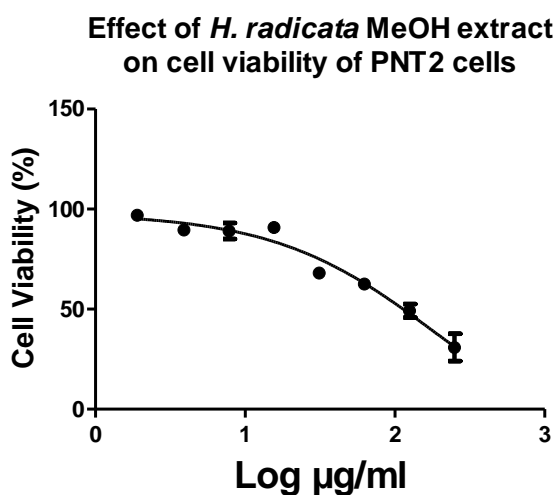


**Figure 3.63:** Effect of *H. radicata* MeOH extract on cell viability of PNT2 cells after 48 h. Cell viability was measured using an AlamarBlue® assay at 560nm and 590nm and calculated as a % of untreated controls. Values are the means of  $n = 3 \pm \text{SEM}$ .

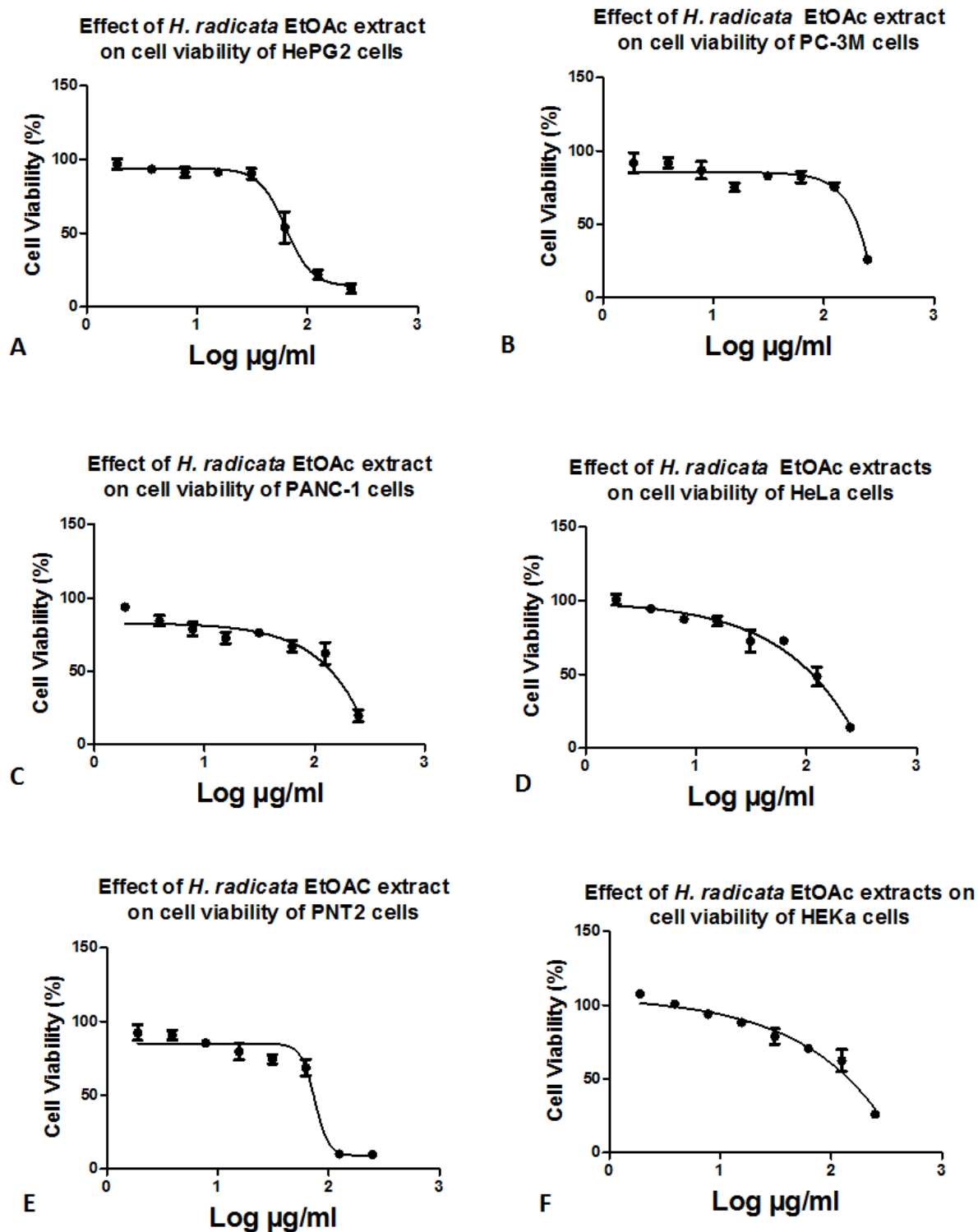


**Figure 3.64:** Effect of *H. radicata* EtOAc extract on cell viability of (A) HepG2, (B) PC-3M, (C) PANC-1, (D) HeLa, (E) PNT2 and (F) HEKa cells after 48 h. Cell viability was measured using an AlamarBlue® assay at 560nm and 590nm and calculated as a % of untreated controls. Values are the means of  $n = 3 \pm \text{SEM}$ .

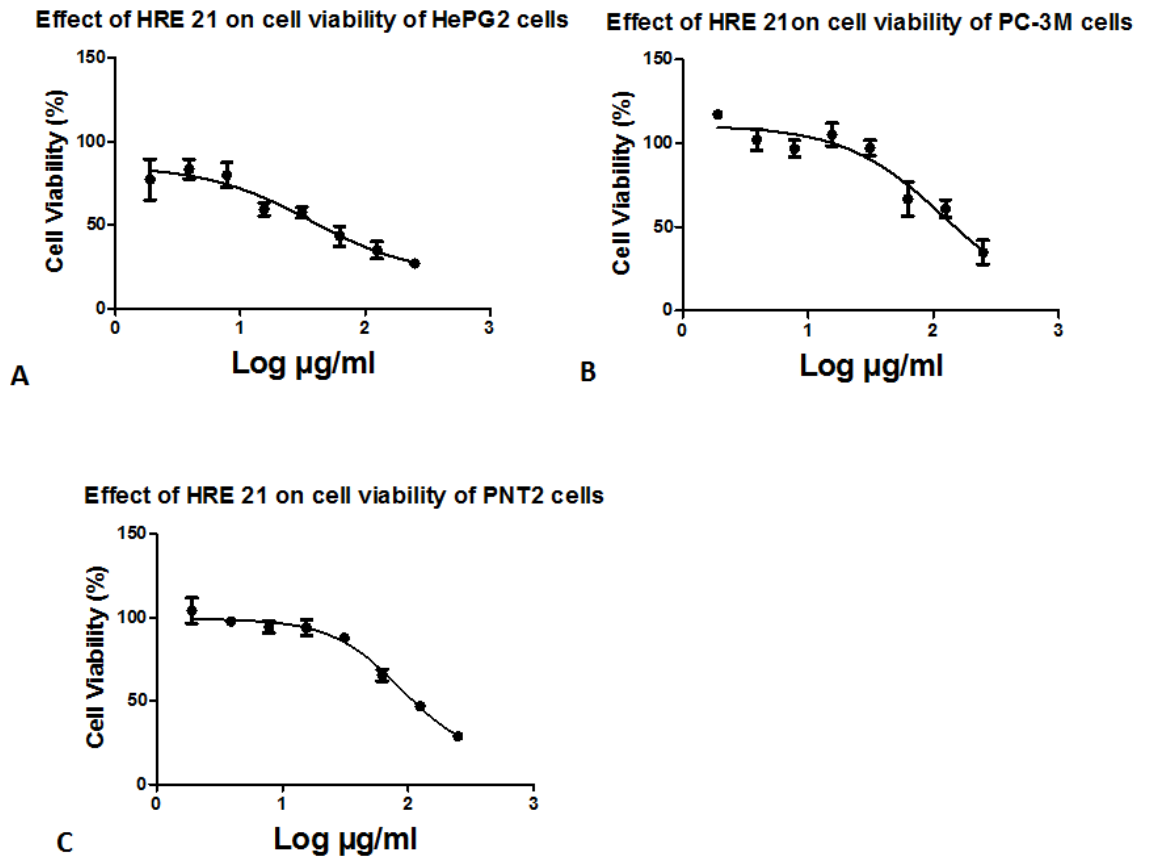


**Figure 3.65:** Effect HRE-21 on cell viability of (A) HepG2 cells, (B) PC-3M cells and (C) PNT2 cells after 48 h. Cell viability was measured using an AlamarBlue® assay at 560 nm and 590 nm and calculated as a % of untreated controls. Values are the means of  $n = 3 \pm \text{SEM}$ .

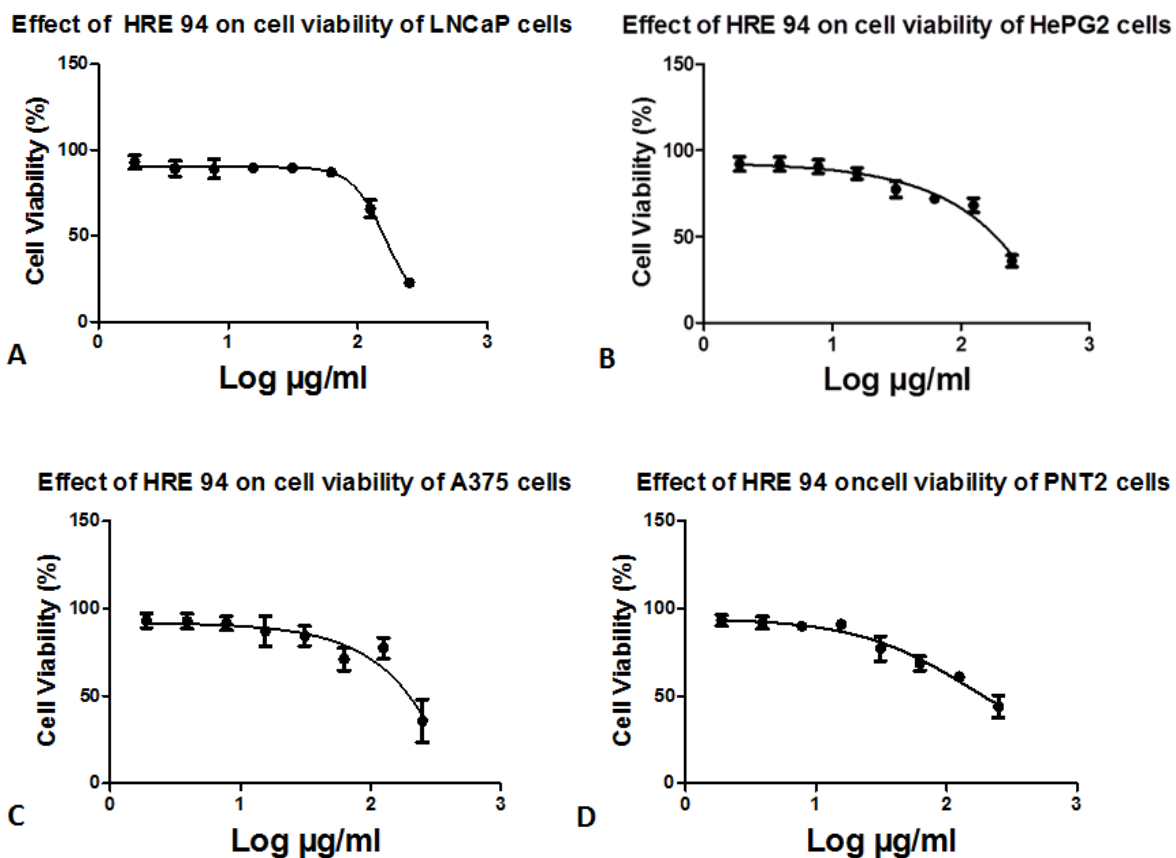


**Figure 3.66:** Effect of HRE-94 on cell viability of (A) LNCaP cells, (B) HepG2 cells, (C) A375 cells and (D) PNT2 cells after 48 h. Cell viability was measured using an AlamarBlue® assay at 560 nm and 590 nm and calculated as a % of untreated controls. Values are the means of  $n = 3 \pm \text{SEM}$ .

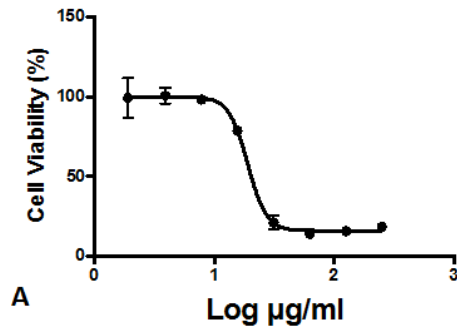
### 3.7.5 Cytotoxicity of *S. Sodomaeum* crude extracts and isolated compounds

Results of the cytotoxicity activity of *S. sodomaeum* extracts and its constituents against cancer and normal cells are presented in Table 3.22. The *S. sodomaeum* hexane extract (SS H) showed no toxicity to either normal or cancer cells at the highest concentrations tested but the *S. sodomaeum* ETOAc extract (SS ETOAc) had toxic effects on LNCaP at 250µg/ml (data not shown). On the other hand, the results show that *S. sodomaeum* methanol crude extract (SSM) had toxicity against LNCaP, PC-3M, A375, HeLa, PANC-1 and HepG2 cells at different concentrations with different IC<sub>50</sub> values 18.95±1.29 µg/ml, 18.37±1.01 µg/ml, 93.58±1.04 µg/ml, 29.20± 1.38 µg/ml, 8.72±0.04 µg/ml and 18.98±1.25, respectively (Table 3.22, Figure 3.67). However, SSM extract was most toxic to PANC-1 cells at 250, 125, 62.5, 31.2, 15.6µg/ml and toxic to normal cells (HEKa), at 250 µg/ml with IC<sub>50</sub> value of 139.9± 4.43 µg/ml and to PNT2 at 125µg/ml with IC<sub>50</sub> value of 67.17±1.66 µg/ml (Figure 3.68) that may indicate selective toxicity at concentrations above 125 µg/ml on cancer cell lines only. Compound SSM-56 was toxic to LNCaP at 250 µg/ml with IC<sub>50</sub> value of 131.77 µg/ml (371.90 µM) and toxic to PC-3M and HepG2 at 125µg/ml with IC<sub>50</sub> values of 80.42± 1.83 µg/ml (266.97 µM) and 119.7 ± 2.01 µg/ml (337.83 µM), respectively, but was highly toxic to PANC-1 with an IC<sub>50</sub> of 20.19 ± 1.25 µg/ml (56.98 µM) (Figure 3.69) while it did not show toxic activity on normal cells. SSM-30-2 was not assessed for cytotoxicity due to time constraints. According to the cytotoxicity assessment, SSM extract and SSM-56 gave the best results for preliminary cytotoxicity screening against cancer cells when compared with normal cells and PANC-1 cells was chosen to evaluate their activities on metastasis of cancer (adhesion, migration and invasion) because of the highly potent cytotoxicity activity with SSM and SSM-56.

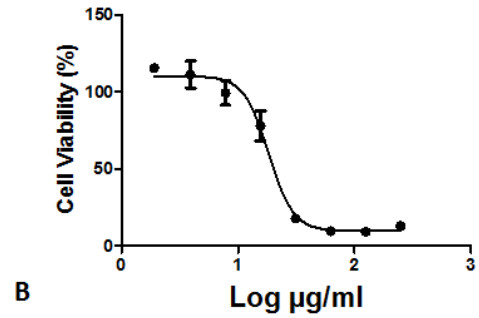
**Table 3.22:** Summary IC<sub>50</sub> of cytotoxicity of *S. sodomaeum* extracts and compounds on each cell line. The values are means ± SEM of at least three independent experiments performed in triplicate. (----): not active up to 250 µg/ ml.

Treatment	Cancer Cell Lines						Normal Cell Line	
	A375	HeLa	LNCaP	PC-3M	PANC-1	HepG2	HEK a	PNT2
SS H	---	---	---	---	---	---	---	---
SS ETOAc	---	---	250	---	---	---	---	---
SSM	93.58	29.20	18.95	18.37	8.72	18.98	139.9	67.17
SSM-56	---	---	131.77	80.42	20.19	119.7	---	---

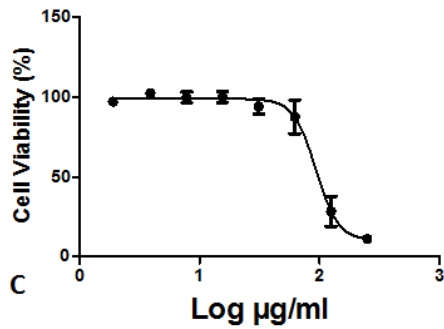
Effect of SSM extract on cell viability of LNCaP cells



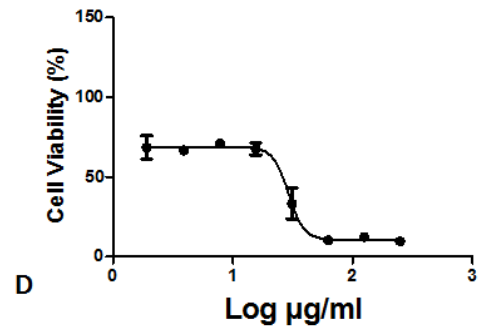
Effect of SSM extract on cell viability of PC-3M cells



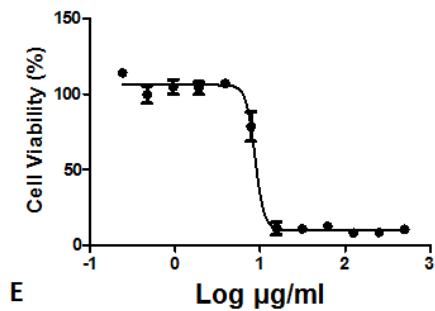
Effect of SSM extract on cell viability of A375 cells



Effect of SSM extract on cell viability of HeLa cells



Effect of SSM extract on cell viability of PANC-1 cells



The effect of SSM extract on cell viability of HepG2 cells

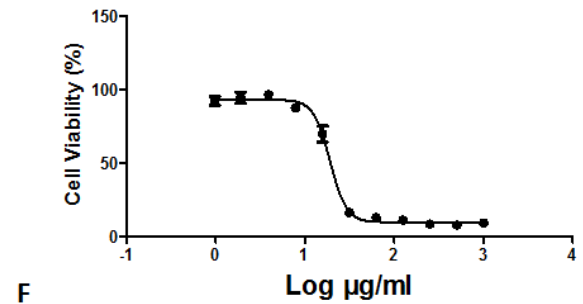


**Figure 3.67:** Effect of SSM extract on cell viability of (A) LNCaP cells, (B) PC-3M cells, (C) A375 cells, (D) HeLa cells, (E) PANC-1 cells and (F) HepG2 cells after 48 h. Cell viability was measured using an AlamarBlue® assay at 560 nm and 590 nm and calculated as a % of untreated controls. Values are the means of  $n = 3 \pm \text{SEM}$ .

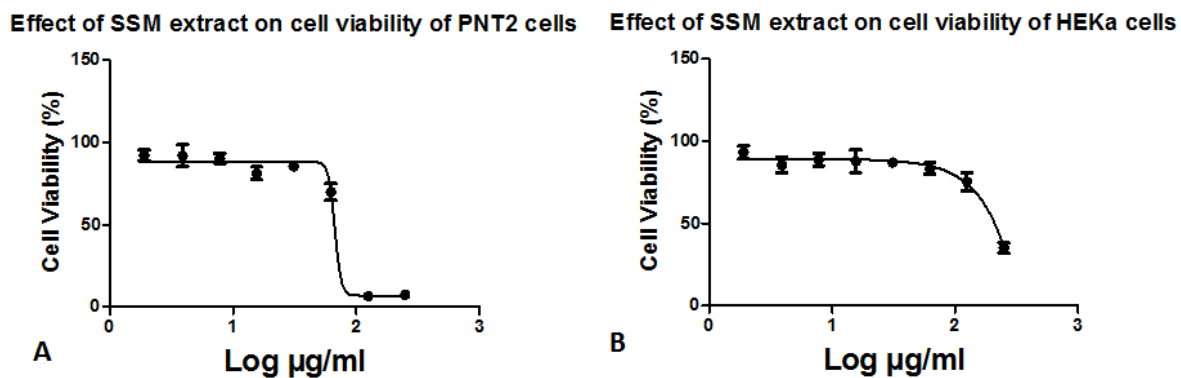
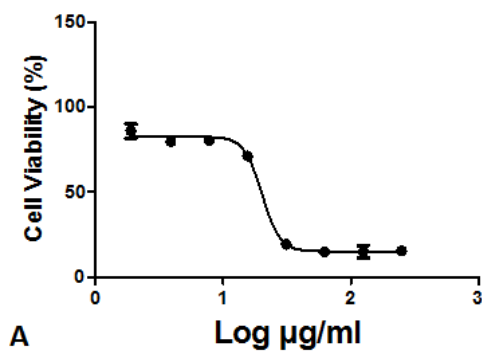
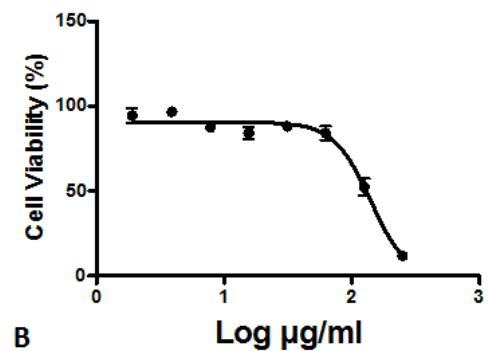


**Figure 3.68:** Effect of SSM extract on cell viability of normal cells (A) PNT2 cells and (B) HEKa cells after 48 h. Cell viability was measured using an AlamarBlue® assay at 560 nm and 590 nm and calculated as a % of untreated controls. Values are the means of  $n = 3 \pm \text{SEM}$ .

Effect of SSM 56 on cell viability of PANC-1 cells



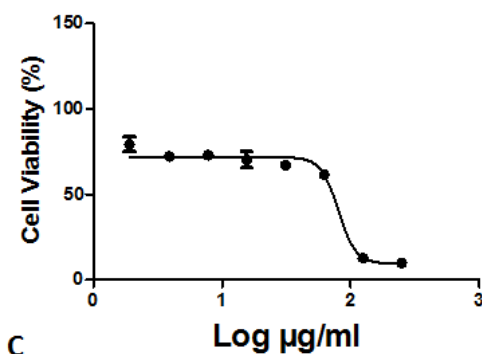
Effect of SSM 56 on cell viability of HepG2 cells



A

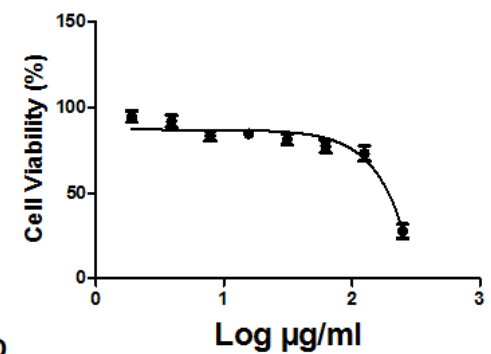
B

Effect of SSM56 on cell viability of PC-3M cells



C

Effect of SSM56 on cell viability of LNCaP cells



D

**Figure 3.69:** Effect of SSM-56 on cell viability of (A) PANC-1 cells, (B) HepG2 cells, (C) PC-3M cells and (D) LNCaP cells after 48 h. Cell viability was measured using an AlamarBlue® assay at 560 nm and 590 nm and calculated as a % of untreated controls. Values are the means of  $n = 3 \pm \text{SEM}$ .

### **3.7.5.1 Effects of *S. sodomaeum* methanol extract (SSM) and chlorogenic acid (SSM-56) on PANC-1 cells**

The overall aim of this section was to examine the effect of SSM and SSM-56 on morphology, viability, adhesion, migration and invasion PANC-1 cells as these provided the best results in the preliminary cytotoxicity screening.

#### **3.7.5.1.1 Effect of SSM and SSM 56 on PANC-1 and PNT2 cells viability after 48 h**

The effect of different concentrations of SSM extract and SSM-56 the viability of PANC-1 cells and PNT2 cells were examined. SSM extract was found to have a significant (p value <0.0001) effect on the viability of the PANC-1 cells at concentrations between 250 µg/ml to 15.6 µg/ml after 48 h but the viability of the PNT2 cells was affected (p value <0.0001) only at 250 and 125 µg/ml. Therefore, these concentrations of SSM extract 62.5, 31.2, and 15.6 µg/ml were chosen for further experiments because they did not kill the normal cells (Figure 3.70). On the other hand, the viability of the PANC-1 cells was significantly affected (p value <0.0001) at 31.2 µg/ml and above of SSM-56 after 48 h, but the viability of the PNT 2 cells was not affected at high concentrations of SSM-56 at 48 h (Figure 3.71). In comparison with the positive control 5µM staurosporine had an effect on PANC-1 cells with an IC<sub>50</sub> value 60.28±1.264 µg/ml, while cisplatin also had an effect with an IC<sub>50</sub> value of 64.80± 1.33 µg/ml on PANC-1 cells (Figure 3.72). This result was confirmed quantitatively with an AlamarBlue® assay.

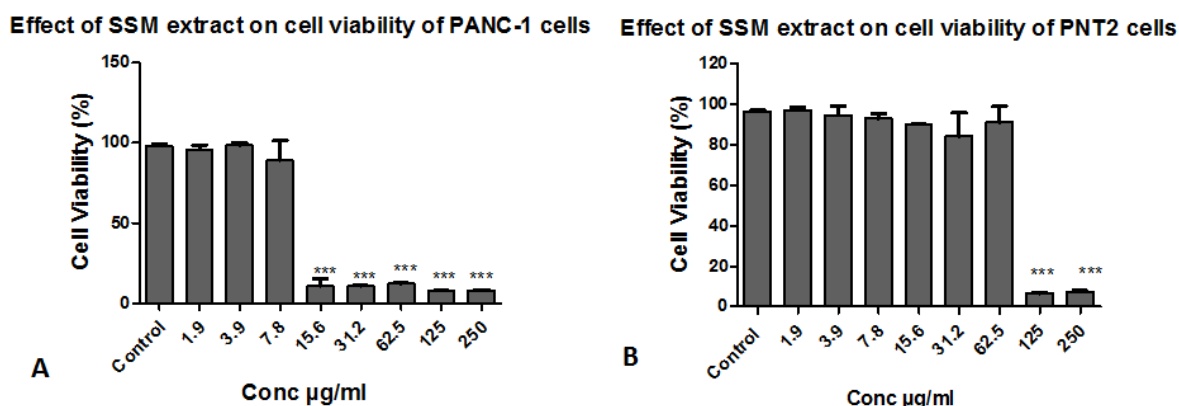


**Figure 3.70:** Effect of SSM on viability of (A) PANC-1 cells and (B) PNT2 cells after 48 h. Statistical analysis was performed using one way ANOVA with Tukey's Multiple Comparison test. \*\*\* and \*\*\* indicates significantly ( $p < 0.0001$ ,  $p < 0.0001$ ) lower values compared with the untreated control, respectively.

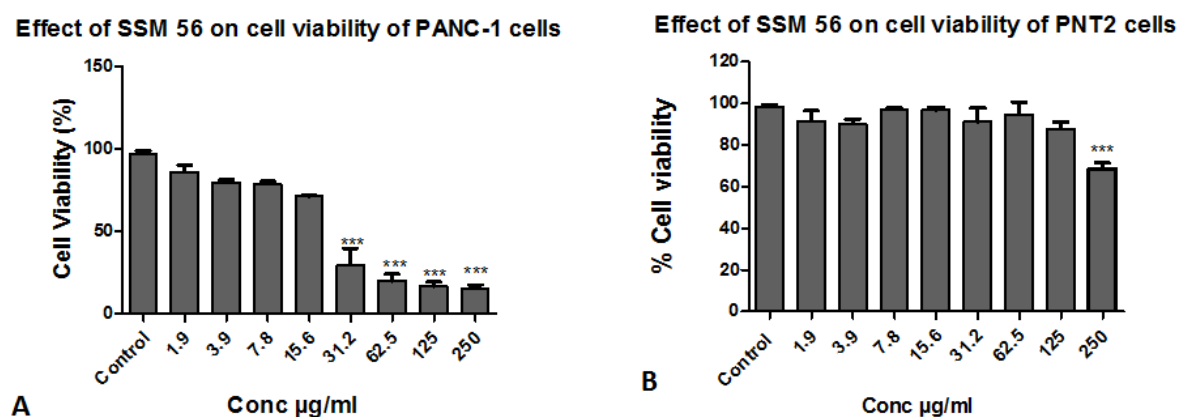


**Figure 3.71:** Effect of SSM 56 on viability of (A) PANC-1 cells and (B) PNT2 cells after 48 h. Statistical analysis was performed using one way ANOVA with Tukey's Multiple Comparison test. \*\*\* and \*\*\* indicates significantly ( $p < 0.0001$ ,  $p < 0.0001$ ) lower values compared with the untreated control, respectively.

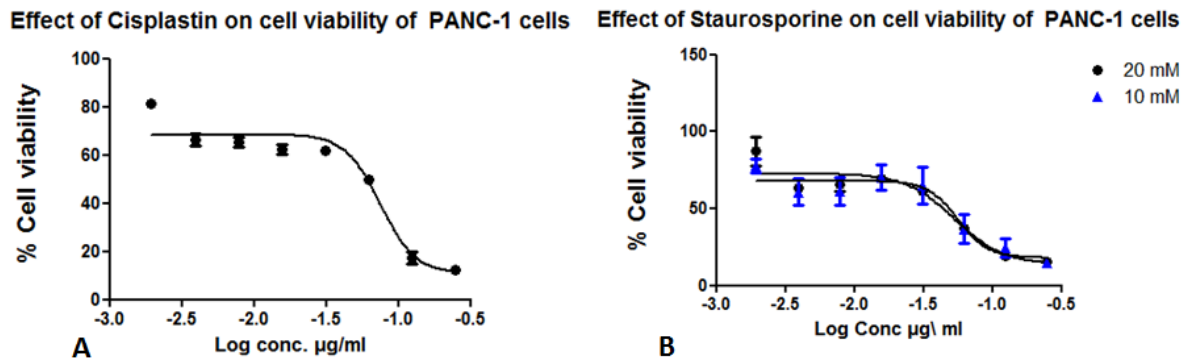


**Figure 3.72:** Effect of (A) 250µg/ml cisplatin and (B) staurosporine on cell viability of PANC-1 cells after 48 h. Cell viability was measured using an AlamarBlue® assay at 560nm and 690nm and calculated as a % of untreated controls. Values are the means of  $n = 3 \pm \text{SEM}$ . Using the dose-response curve.

### 3.7.5.1.2 Effect of SSM and SSM-56 on the morphology of PANC-1 cells after 48 h

This experiment was carried out to determine the effect of SSM and SSM 56 at 62.5µg/ml on the morphology of PANC-1 cells after 48 h. There was a difference in the morphology of PANC-1 cells after treatment with SSM and SSM-56 compared with the non-treated cells which appeared oval in shape with good attachment and spreading (Figure 3.73). While cells that were treated with SSM and SSM-56 appeared small in size and were poorly spread, suggesting there was an effect on adhesion of the cells.

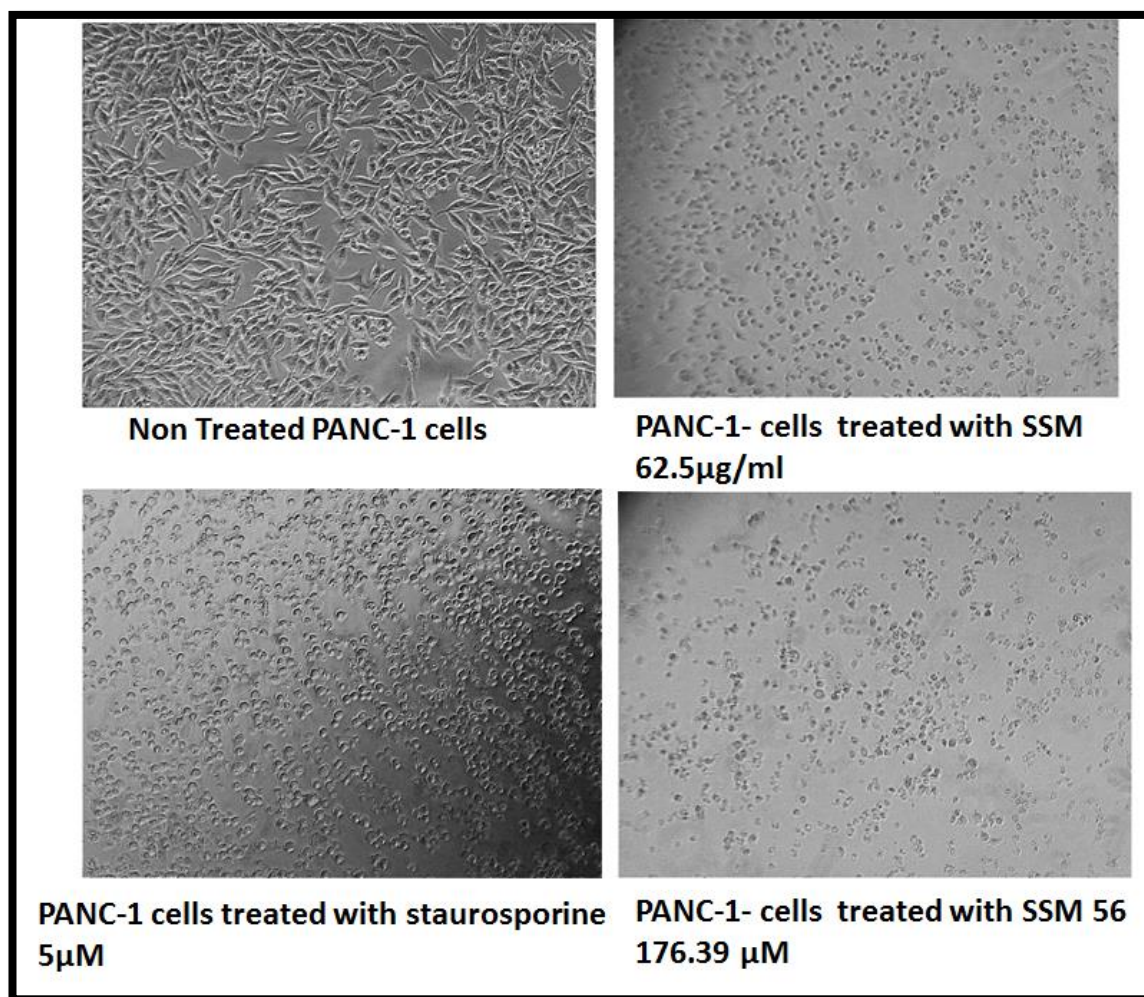


**Figure 3.73:** Morphology of PANC-1 cells before and after treatment with SSM, SSM56 and staurosporine after 48 h. The magnification bar represents 50µm. Objective lens x20.

### **3.7.5.1.3 Effect of SSM and SSM 56 on membrane integrity of PANC-1 cells after 24 h**

This experiment was carried out to evaluate cell viability using SYTOX®Green in order to examine whether after adding samples SYTOX®Green penetrated non-viable cells compared with un-treated cells (control) and to prove the morphological alterations of PANC-1 cells after adding SSM extract and SSM-56 was not due to cytotoxicity. Staurosporine (5 $\mu$ M) was used as the positive control. In the case of SSM, there was no effect on membrane integrity at concentrations between 1.9-7.8  $\mu$ g/ml, but there was an effect between 62.5 and 250  $\mu$ g/ml, and changes in morphology were observed at 31.2 and 15.6  $\mu$ g/ml, while in the case of SSM-56, there was an effect on membrane integrity at high concentrations 250  $\mu$ g/ml (705.59  $\mu$ M) and changes in morphology were observed with 125  $\mu$ g/ml (352.79  $\mu$ M) and 15.6  $\mu$ g/ml (44.31 $\mu$ M) after 24 h (Figure 3.74). By comparison the effect of SSM, SSM-56 and staurosporine on PNT2 cells in the presence of SYTOX®Green are shown in Figure 3.75. Staurosporine had a significant ( $p < 0.0001$ ) effect on the membrane integrity of PNT2 compared with SSM and SSM-56 which had no effect on the membrane integrity of these normal cells.

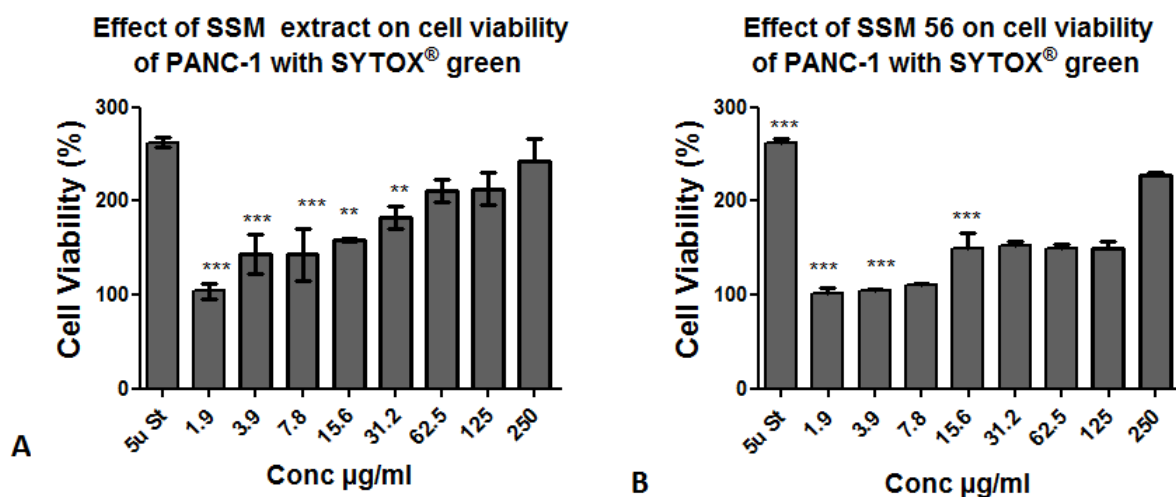


**Figure 3.74:** Effect of (A) SSM extract and (B) SSM-56 on PANC-1 cell membrane integrity after 24 h. Cells were seeded in a 96 well plate at a density of  $1 \times 10^5$  cells per well in complete medium (100µl) and incubated overnight. After which SSM and SSM 56 were prepared in complete medium and added to the wells (100µl) at final concentrations between 1.9-250 µg/ml for 24 h. SYTOX<sup>®</sup> Green was used at a final concentration of 5 µM in each well and incubated for 15 min at 37°C. The fluorescence intensity was measured at 485-535 nm. Values represent the mean  $\pm$  SEM of 3 values. Statistical analysis was performed using one way ANOVA with Tukey test. \*\*\* and \*\*\* indicates significantly ( $p < 0.0001$ ,  $p < 0.0001$ ) lower values compared with the untreated control, respectively.

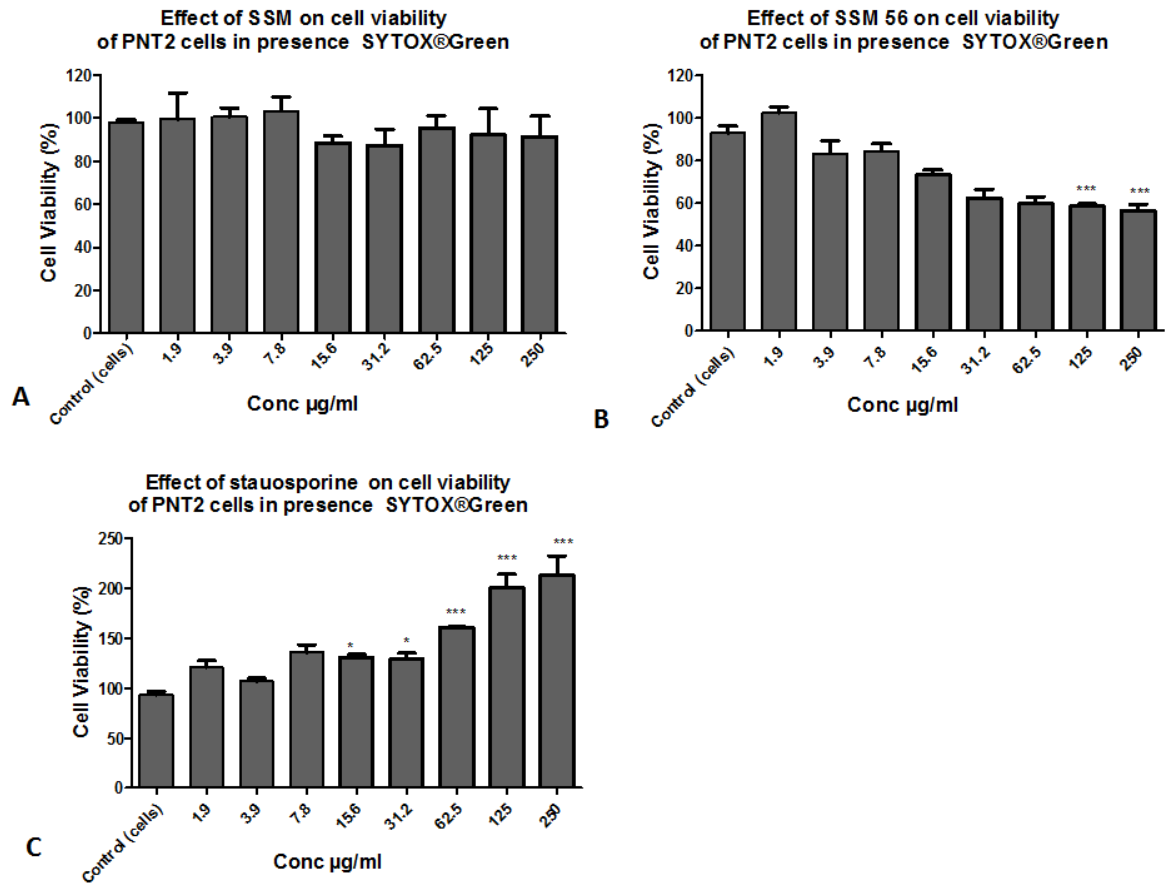


**Figure 3.75:** Effect of (A) SSM extract, (B) SSM-56 and (C) 5 µM staurosporine on PNT2 cell membrane integrity after 24 h. Cells were seeded in a 96 well plate at a density of  $1 \times 10^5$  cells per well in complete medium (100 µl) and incubated overnight. After which SSM and SSM 56 were prepared in complete medium and added to the wells (100 µl) at final concentrations between 1.9-250 µg/ml for 24 h. SYTOX®Green was used at a final concentration of 5 µM in each well and incubated for 15 min at 37°C. The fluorescence intensity was measured at 485-535nm. Values represent the mean  $\pm$  SEM of 3 values. Statistical analysis was performed using one way ANOVA with Tukey test.

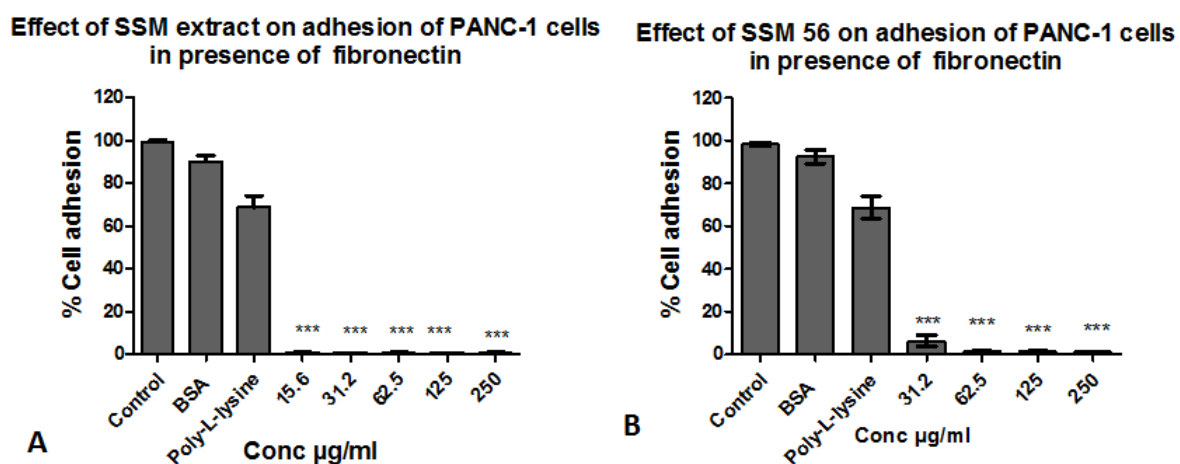
#### **3.7.5.1.4 Effects of SSM and SSM-56 on adhesion, migration and invasion of PANC-1 cells**

Metastasis is an important hallmark of cancer progression, which involves numerous factors including the degradation of the extracellular matrix (ECM), tumor angiogenesis and defects in programmed cell death such as apoptosis, autophagy and necrosis. The ECM is an essential component of the tumor microenvironment. The chemical and physical signals elicited from ECM are necessary for cancer cell proliferation and invasion. ECM is primarily composed of laminin and collagen type IV. In addition, the ECM also consists of many non-collagenous molecules such as bone sialoprotein (BSP), osteopontin (OPN), osteonectin, osteocalcin (OC), fibronectin, vitronectin (VN). Type IV collagen is a protein, and important component of the basement membrane, is highly expressed by pancreatic cancer cells. Fibronectin is a glycoprotein of the ECM, and together with type IV collagen plays a major role in cell adhesion, growth, migration, and differentiation in cancer cells. Therefore the purpose of this experiment was to assess the effect of SSM and SSM-56 on adhesion of PANC-1 cells to fibronectin and collagen IV coated plates.

##### **3.7.5.1.4.1 Effect of SSM and SSM-56 on adhesion of PANC-1 cells to ECM (fibronectin and collagen IV)**

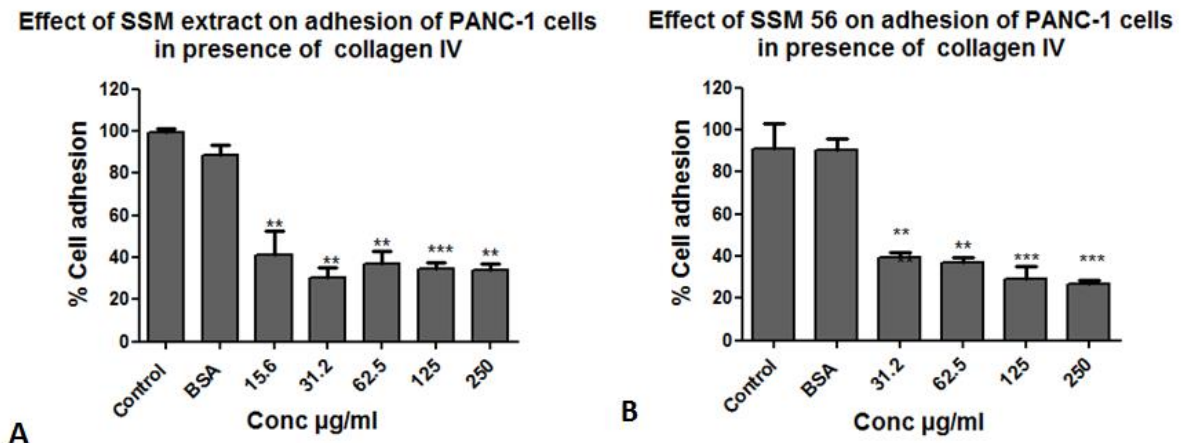
The result, which can be seen in Figure 3.76, showed that the large % of untreated PANC-1 cells compared with treated cells was significantly affected ( $p < 0.0001$ ) because the cells adhered and spread well on fibronectin, while cells treated with SSM and SSM-56, lost their adherence to fibronectin. Therefore, SSM extract concentrations 15.6  $\mu\text{g/ml}$  to 250  $\mu\text{g/ml}$  had greater significant ( $p < 0.0001$ ) effect on adhesion (Figure 3.76) and the % of adhesion of PANC-1 treated with 15.6 to 250  $\mu\text{g/ml}$  of SSM was 0.9% to 3%, respectively. In the case of SSM-56, there was decreased adhesion of PANC-1 cells to fibronectin in a dose-dependent manner and the % adhesion was 2% to 12% at 31.2 to 250  $\mu\text{g/ml}$ . On the other hand, as shown in Figure 3.77, the effect of both SSM and SSM-56 on adhesion of PANC-1 cells to collagen IV was significant ( $p < 0.0001$ ), but with a lower effect than on fibronectin.

However, SSM decreased adhesion of PANC-1 cells to collagen IV at 15.6-250  $\mu\text{g/ml}$ . The % adhesion of PANC-1 cells treated with 15.6-250  $\mu\text{g/ml}$  of SSM was 29-60% respectively, although SSM-56 concentrations 31.2- 250  $\mu\text{g/ml}$  decreased adhesion to collagen IV in a dose-dependent manner. The % adhesion of PANC-1 cells treated with 31.2- 250  $\mu\text{g/ml}$  of SSM-56 was 23-42% ,respectively (Figure 3. 77). The effect of SSM and SSM-56 on adhesion of PANC-1 cells to fibronectin was more potent than to collagen IV. As shown in Figure 3.76, there was no effect of SSM and SSM-56 on adhesion of PANC-1 to poly-L-lysine, suggesting that the effect of the SSM and SSM-56 is specific for the integrin family of adhesion receptors.



**Figure 3.76:** Effect of (A) SSM extract and (B) SSM-56 on adhesion of PANC-1 cells coated plates of fibronectin, with BSA as a negative.

A suspension consisting of 100µl of  $5 \times 10^5$  cells/ml in serum-free media with SSM and SSM 56 at a final concentration of 15.6-250 µg/ml and 31.2-250 µg/ml, respectively was added to a 96 well plate coated with fibronectin and incubated at 37°C. After 2 h, the plate was washed, and 100 µl of calcein-AM was added and incubated 1 h at 37°C. The fluorescence was measured at 485 and 520nm. The values are means  $\pm$  SEM of 3 values. Statistical analysis was performed using one way ANOVA with Tukey test. \*\*\* and\*\*\* indicates significantly ( $p < 0.0001$ ,  $p < 0.0001$ ) lower values compared with the untreated control.

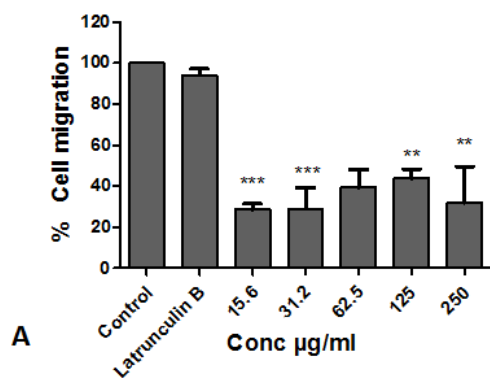
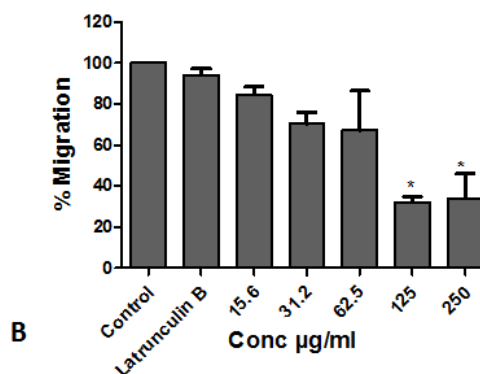


**Figure 3.77:** Effect of (A) SSM extract (B) SSM-56 on adhesion of PANC-1 cells to a collagen IV coated plate, with BSA as a negative control.

A 48 well plate coated with collagen IV was warmed up for 10 min, before adding 150  $\mu\text{l}$  of  $0.5 \times 10^6$  cells/ml in serum-free media with SSM and SSM-56 at a final concentration 15.6-250  $\mu\text{g/ml}$  and 31.2-250  $\mu\text{g/ml}$ , respectively in a 48 well plate and incubated at 37°C. After 90 min, the plate was washed, fixed, stained and lysed with 200  $\mu\text{l}$  extraction solution. After incubation 10min, the absorbance was measured at 560 nm. The values are means  $\pm$  SEM of 3 values. Statistical analysis was performed using one way ANOVA with Tukey test. \*\*\* and \*\*\* indicates significantly ( $p < 0.0001$ ,  $p = 0.0001$ ) lower values compared with the untreated control.

#### **3.7.5.1.4.2 Effect of SSM and SSM56 on migration of PANC-1 cells using a Cytoselect<sup>TM</sup> 24-well Cell Migration Assay**

The aim of this experiment was to determine the effect of SSM and SSM-56 on migration of PANC-1 cells using a Cytoselect<sup>TM</sup> 24-well Cell Migration Assay. As seen in Figure 3.78, SSM had a significant ( $p < 0.0001$ ) inhibitory effect on migration between 15.6 and 250  $\mu\text{g/ml}$  and the % migratory inhibition of PANC-1 cells treated with SSM between 40%-20%. While SSM-56 inhibited the migration of PANC-1 cells at 125 and 250  $\mu\text{g/ml}$  (30 and 40%, respectively).

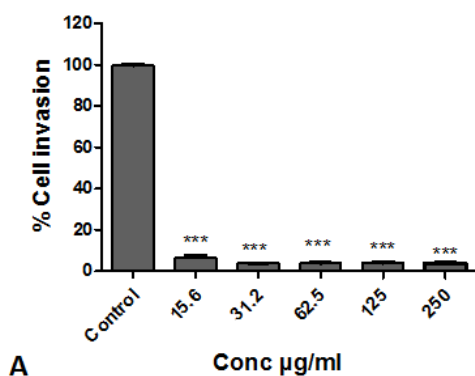
**Effect of SSM extract on migration of PANC-1 cells****Effect of SSM 56 on migration of PANC-1 cells****Figure 3.78:** Effect of (A) SSM extract and (B) SSM-56 on migration of PANC-1 cells.

Three hundred and fifty  $\mu\text{l}$  of a cell suspension containing  $5 \times 10^5$  cells/ml in serum-free media with the SSM and SSM-56 at a final concentration of 15.6 or 250  $\mu\text{g/ml}$  was added to the inside of each insert in a 24 well plate. One  $\mu\text{M}$  of Latrunculin B was added as a negative control. The cells were incubated at 37°C. After 24 h, the cells inside the insert were treated with detachment solution for 20 min at 37°C then the insets were removed by forceps and each inset gently tap against the bottom of the well to ensure complete dislodged cells and the plate containing dislodged cells incubated for 40 min at 37°C. The fluorescence was measured at 485 and 520nm. The values are means  $\pm$  SEM of 3 values. Statistical analysis was performed using one way ANOVA with Tukey test. \*\*\* and \*\* indicates significantly ( $p < 0.0001$ ,  $p = 0.0082$ ) lower values compared with the untreated control, respectively.

#### **3.7.5.1.4.3 Effect of SSM and SSM-56 on invasion of PANC-1 cells across the basement membrane using a Cytoselect™ 24-well Cell Invasion Assay**

The effect of SSM and SSM-56 on invasion of PANC-1 cells across a basement membrane was assessed using a Cytoselect™ 24-well Cell Invasion Assay. As shown in Figure 3.79, the number of PANC-1 cells which invaded after exposure to SSM was markedly less than the untreated control. SSM between 15.6 and 250 µg/ml significantly ( $p < 0.0001$ ) inhibited the invasion of PANC-1 cells across the basement membrane, while SSM-56 between 62.5 and 250 µg/ml significantly ( $p=0.0009$ ) inhibited the invasion of PANC-1 cells across the basement membrane (Figure 3. 79B). In the case of SSM, the concentration between 15.6 and 62.5 µg/ml and in the case of SSM-56, the concentration between 62.5 and 250 µg/ml did not kill normal cells thus these concentrations are recommended in future work for treatment of PANC-1 cells.

Effect of SSM extract on invasion of PANC-1 cells



Effect of SSM 56 on invasion of PANC-1 cells

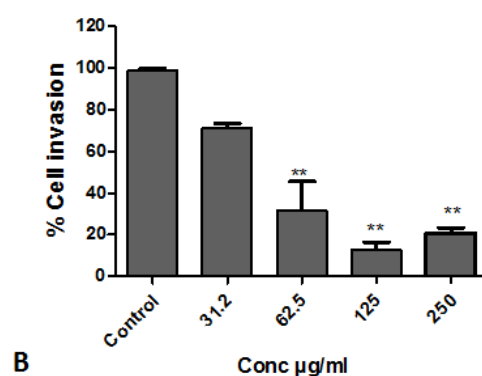


**Figure 3.79:** Effect of (A) SSM and (B) SSM-56 on invasion of PANC-1 cells. Cells were adjusted to  $1 \times 10^6$  cells /ml in serum-free media and 300µl of cell suspension was added to each insert in a 24 well plate with SSM and SSM-56 at a final concentration of 15.6-250 µg/ml. Incubation was carried out for 48 h and those cells that invaded into the lower surface of the membrane were stained and quantified. The absorbance was measured at 560 nm. The values are means  $\pm$  SEM of 2 values. Statistical analysis was performed using one way ANOVA with Tukey test. \*\*\* and \*\* indicates significantly ( $P < 0.0001$ ,  $p = 0.0009$ ) lower values compared with the untreated control, respectively.

### 3.7.5.1.4 Effect of SSM and SSM-56 on viability, cytotoxicity and apoptosis of PANC-1 cells using the ApoTox-Glo™ Triplex Assay

This experiment was carried out to measure the viability, cytotoxicity and apoptosis of SSM and SSM-56 on PANC-1 cells. The results (Figure 3.80) showed that SSM caused a dose-dependent decrease in viability, an increase in cytotoxicity, with an increase in caspase-3/7 activity that was consistent with apoptosis. On the other hand, SSM-56 caused a decrease in viability, increase in cytotoxicity with no caspase-3/7 activation, which is consistent with primary necrosis.

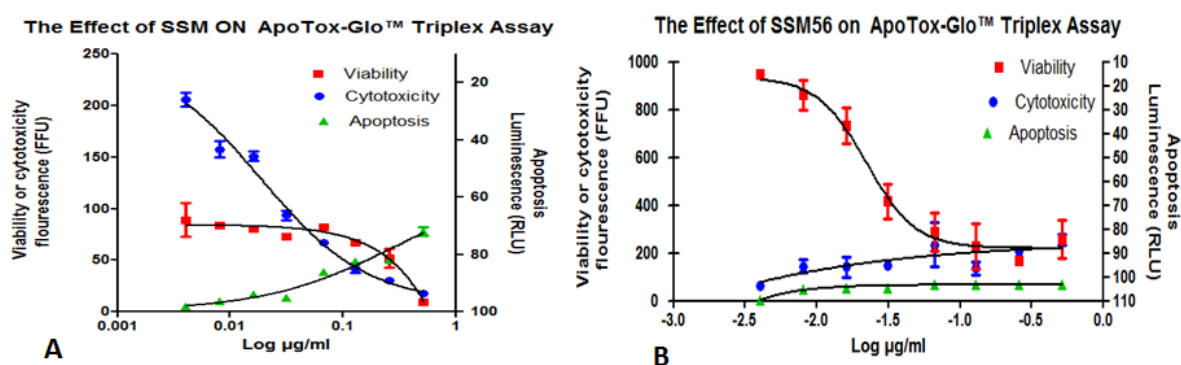


**Figure 3.80:** Effect of (A) SSM and (B) SSM-56 on PANC-1 cells by measuring viability, cytotoxicity and apoptosis. Cells were seeded in a 96 well plate at  $1 \times 10^6$  cells per well in complete medium (100 µl) and incubated for 24 h, following which, SSM and SSM-56 was prepared and added to the cells at 125 µg/ml certain concentration incubated for 2 h. After which, 20 µl of viability/cytotoxicity reagent was added to each well for 30 min. The fluorescence was measured at 400-505 nm for viability and 485-520 for cytotoxicity. After reading, 100 µl of Caspase-Glo was added to each well and incubated 30 min at room temperature then luminescence was measured. The values are means  $\pm$  SEM of 3 values.

#### **3.7.5.1.5 Effect of SSM and SSM-56 on PANC-1 cells by measuring the ADP and ATP using of ADP/ATP Ratio Assay Kit and**

An ADP/ATP assay was carried out to confirm the previous experiment by calculating the ADP/ATP ratio, changes in the ADP and ATP have been used to differentiate modes of cell death and viability. Increased levels of ATP and decreased levels of ADP indicate proliferating cells. On the other hand, decreased levels of ATP and increased levels of ADP represent apoptotic or necrotic cells where the decrease in ATP and increase in ADP are much more noticeable in necrosis versus apoptosis. The result (Figure 3.81) showed that SSM lowered ATP levels (0.3 %) with a slight increase in ADP levels (1%) in comparison to control cells; often seen in apoptosis. SSM-56 exhibited markedly lower ATP levels (20%) with greatly increased ADP levels (60%) compared with control cells; often seen in necrosis. Therefore, this confirmed that SSM causes apoptosis and SSM-56 causes necrosis in PANC-1 cells.

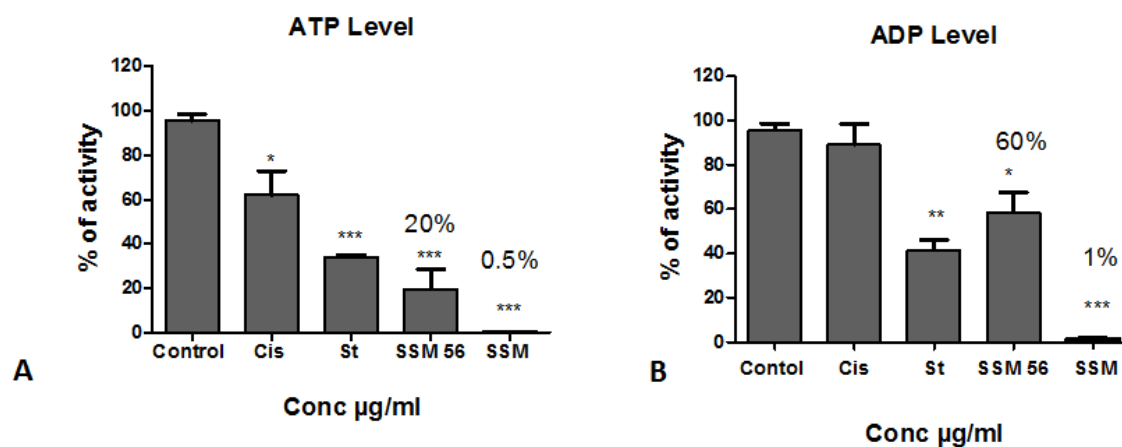


**Figure 3.81:** Effect of SSM extract and SSM-56 on PANC-1 cells with (A) ATP and (B) ADP level. The SSM Test with lower ATP levels (0.5%) with slightly an increase in ADP levels (0.1%) in comparison to control cells is often seen in apoptosis and the SSM 56 with markedly lower ATP levels (20%) with greatly increased ADP levels (60%) in control cells is often seen in necrosis. The values are means  $\pm$  SEM of 3 values and statistical analysis was performed using one way ANOVA with Tukey test. \*\*\* and \*\* indicates significantly ( $p < 0.0001$ ,  $p = 0.0001$ ) lower values compared with the untreated control, respectively.

### 3.7.5.1.6 Effect of SSM and SSM-56 on PANC-1 cells by measuring an apoptosis, necrosis and Healthy Cell Quantitation Kit Plus

This experiment was carried out to confirm the previous experiment and to provide a convenient assay for detecting apoptotic (green) and necrotic (red) cells. Green fluorescent plasma membrane staining identifies apoptotic cells, while necrotic cells are identified by red fluorescent nuclear staining. Both Annexin V and Ethidium Homodimer III rely upon the presence of intact membranes in healthy cells to accurately distinguish them from apoptotic or necrotic cells. During apoptosis, phosphatidylserine (PS) is translocated from the inner to the outer surface of the cell, allowing the dying cell to be engulfed by phagocytic cells. Annexin V is a 35 kD  $\text{Ca}^{2+}$ -dependent phospholipid binding protein with a high affinity for PS. Annexin V labeled with CF<sup>TM</sup>488A (excitation/emission: 490/515 nm) stains apoptotic cells with green fluorescence by binding to PS exposed on the cell surface. On the other hand, the Ethidium Homodimer III (EthD-III) is a highly positively charged nucleic acid probe that stains necrotic cells and late apoptotic cells with red fluorescence due to its significantly higher affinity for DNA and higher fluorescence quantum yield. Figure 3.82 shows that the PANC-1 cells showed green fluorescence with SSM and red fluorescence with SSM 56.

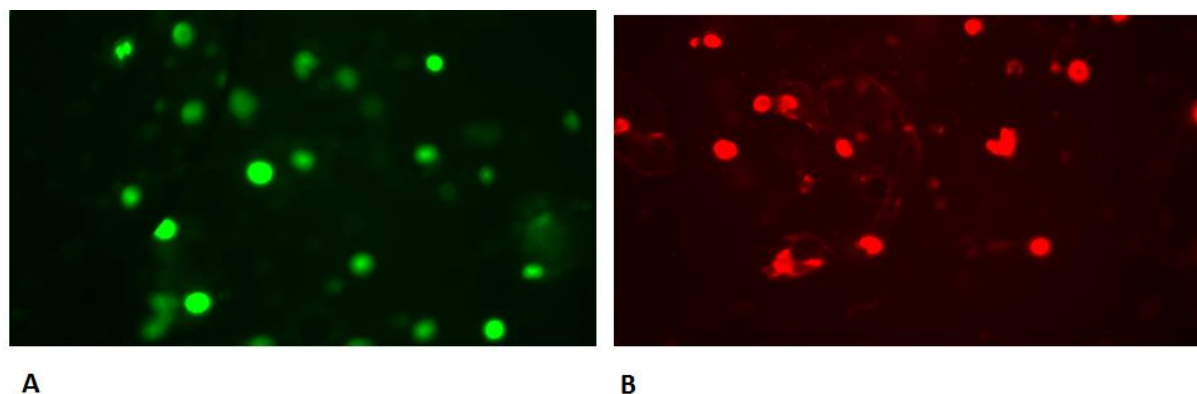


**Figure 3.82:** Shows the PANC-1 cells exhibiting green fluorescence with (A) SSM and red fluorescence with (B) SSM-56. Images were taken using an Epi fluorescence upright microscope (Nikon Eclipse) E600 under X60 1.40 NA. The objective lens was used under the following settings; Alexa555: TRITC, YFP: FITC, Nuclei: Dapi.

### **3.8 *In vitro* antidiabetic activity assessment**

#### **3.8.1 Screening of antidiabetic assays, of PTP1B, $\alpha$ -glucosidase and $\alpha$ -amylase enzymes**

In this study, according to the cytotoxicity results in section 3.7, the *T. zanonii*, *H. radicata*, *P. tortuosus* and *A. cyrenaicum* crude extracts and their constituents did not show any/ or weak cytotoxicity activity on the cells. Therefore preliminary screening for antidiabetic activity was carried out using 30  $\mu\text{g/ml}$  which did not kill the cells as determined by the cytotoxicity assays (section 3.7.1 to 3.7.4).

#### **3.8.2 PTP1B enzyme**

##### **3.8.2.1 Z-factor of PTP1B and TFMS Reference Standard Curve**

The Z-factor shows the reliability of an assay. In these experiments the Z-factor was 0.99 with the addition of catalase in the buffer and thus the result was considered reliable. Figure 3.83 shows the difference between the positive and negative controls and the assay and its conditions were excellent and can be highly recommended to be followed in further screening tests. TFMS, Bis(4-trifluoromethylsulfonamidophenyl)-1,4-diisopropylbenzine (PTP Inhibiter IV) was used as a positive control as it is an inhibitor of PTP1B and Figure 3.84 shows a typical standard curve with catalase with a  $K_i$  value of  $4.6 \pm 007 \mu\text{M}$ .

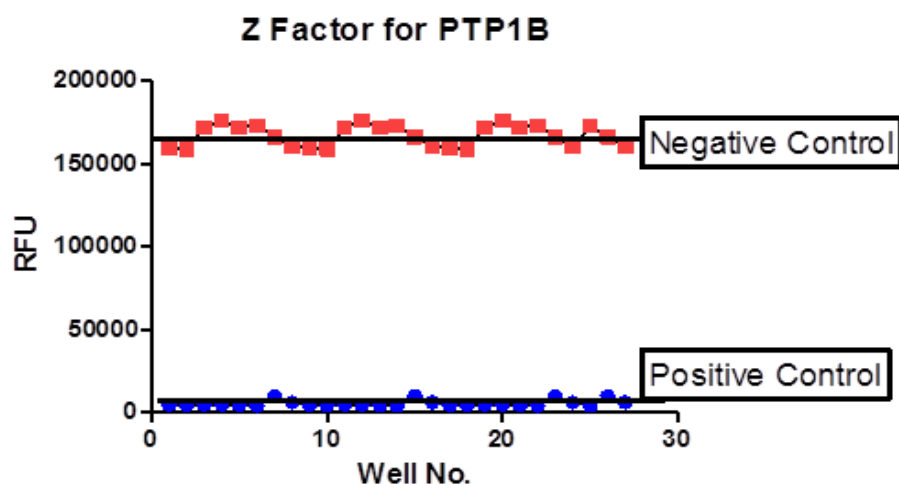


**Figure 3.83:** Z factor for PTP1B inhibition assay. The positive control was the highest concentration of TFMS (100 $\mu$ M) and the negative control was assay buffer only, with the addition of catalase. All other assay conditions remained the same.

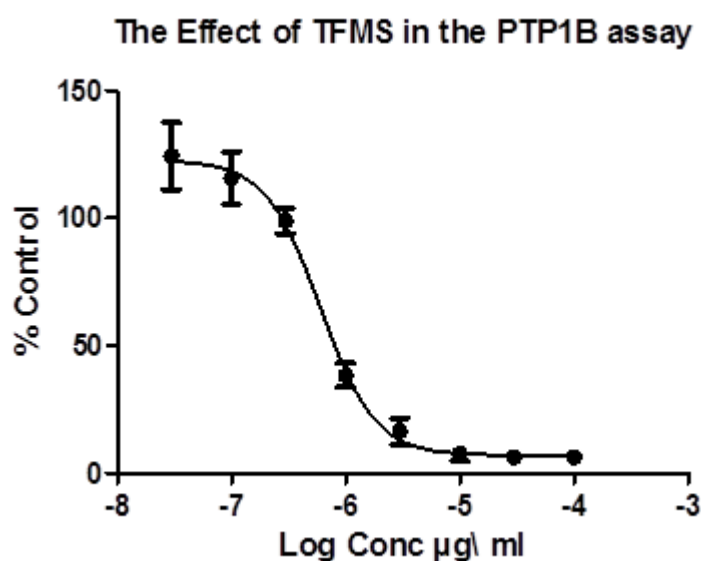


**Figure 3.84:** Effect of TFMS inhibitor on PTP1B enzyme in the presence of DiFMUP substrate. The inhibitor at a range of concentrations was incubated with PTP1B enzyme for 30 min at 37°C in an atmosphere containing 5% CO<sub>2</sub>. DiFMUP (10  $\mu$ M) was then added and incubated for 10 min at 37°C. The fluorescence was measured at 355-460 nm. Data represents the mean  $\pm$  3 of PTP1B enzyme hydrolysis (% control). The K<sub>i</sub> for TFMS was 4.6 $\pm$  007  $\mu$ M.

### 3.8.2.2 PTP1B inhibition by crude extracts and isolated compounds

All the samples from *T. zanonii*, *H. radicata*, *P. tortuosus* and *A. cyrenaicum* (hexane, ethyl acetate crude methanol extract and their constituents) were tested in the PTP1B enzyme assay at 30 µg/ml and compared with the standard inhibitor, TFMS, which produced a concentration-dependent inhibition with a  $K_i$  value of  $4.6 \pm 0.07$  µM (Figure 3.84). In comparison the control, DMSO, did not produce any effect on PTP1B enzyme. The results from *T. zanonii* (hexane, ethyl acetate crude methanol extract and their constituents) were tested on the PTP1B enzyme assay (Figure 3.85), and showed that only the *T. zanonii* hexane extract significantly ( $p = 0.0011$ ) inhibited PTP1B enzyme with a 65 % inhibition of PTP1B.

In addition, all the samples from *H. radicata* (hexane, ethyl acetate and methanol crude extract and their constituents) showed that the hexane and ethyl acetate of *H. radicata* crude extracts significantly ( $p < 0.0001$ ) inhibited PTP1B enzyme (Figure 3.85B). A 85% inhibition of PTP1B was observed by the crude extracts (hexane and ethyl acetate).

Among the *A. cyrenaicum* extracts and its constituents, the root hexane extract and aerial part hexane extract significantly ( $p < 0.0001$ ) inhibited PTP1B enzyme (Figure 3.85C). A 90 % inhibition of PTP1B was observed by the crude extract of root and 70% inhibition was observed by the aerial part. Moreover, other samples at 30 µg/ml did not produce inhibition of enzyme in comparison to the control (Figure not shown).

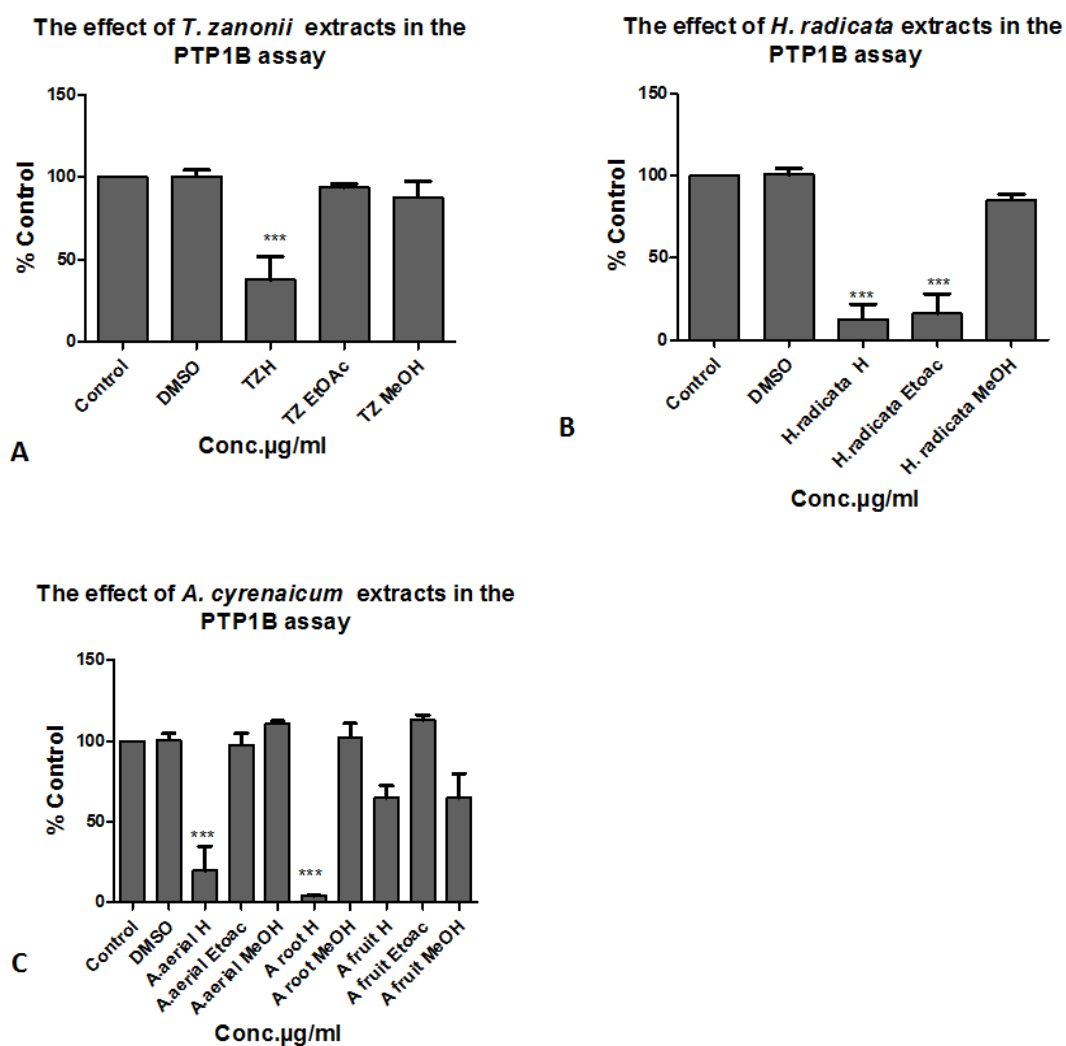


**Figure 3.85:** Effect (A) *T. zanonii* (hexane, ethyl acetate crude methanol crude extracts) on PTP1B enzyme in the presence of DiFMUP substrate, (B) *H. radicata* (hexane, ethyl acetate and methanol crude extracts) and (C) *A. cyrenaicum* (hexane, ethyl acetate crude methanol extracts). Extracts at 30 µg/ml were incubated with PTP1B enzyme for 30 min at 37°C in an atmosphere containing 5% CO<sub>2</sub>. DiFMUP (10 µM) was then added and incubated for 10 min at 37°C. The hydrolysis of DiFMUP by PTP1B enzyme was measured at 355/460 nm. Data represent mean ± 3 of PTP1B enzyme hydrolysis (% control). The data were analysed by Dunnett's Multiple Comparison Test. \*\*, \*\*\* and \*\*\* indicates significantly (p= 0.0011, p<0.0001 and p<0.0001) lower values compared with the untreated control, respectively.

### 3.8.2.3 Concentration dependent inhibition of crude extracts

TFMS produced a concentration-dependent inhibition of PTP1B enzyme with a  $K_i$  value of  $4.6 \pm 0.07 \mu\text{M}$ . Samples showing more than 60% inhibition of PTP1B enzyme at  $30 \mu\text{g/ml}$  are presented in Figure 3.85. The effect of a range (0.1-30  $\mu\text{M}$ ) of concentrations of these crudes was tested on the hydrolysis of PTP1B enzyme using DiFMUP as the substrate. The hexane crude extract of *A. cyrenaicum* root and the hexane crude extract of *A. cyrenaicum* aerial part produced a concentration-dependent inhibition of PTP1B enzyme with  $K_i$  values of  $1.902 \pm 1.51 \mu\text{g/ml}$  and  $1.65 \pm 1.37 \mu\text{g/ml}$ , respectively (Figure 3.86).

The hexane and ethyl acetate of *H. radicata* crude extracts produced a concentration-dependent inhibition of PTP1B enzyme with  $K_i$  values of  $1.207 \pm 0.008$  and  $1.301 \pm 0.006 \mu\text{g/ml}$ , respectively (Figure 3.87).

The hexane crude extract of *T. zanonii* produced a concentration-dependent inhibition of PTP1B enzyme with a  $K_i$  value of  $1.18 \pm 0.006$  (Figure 3.88).

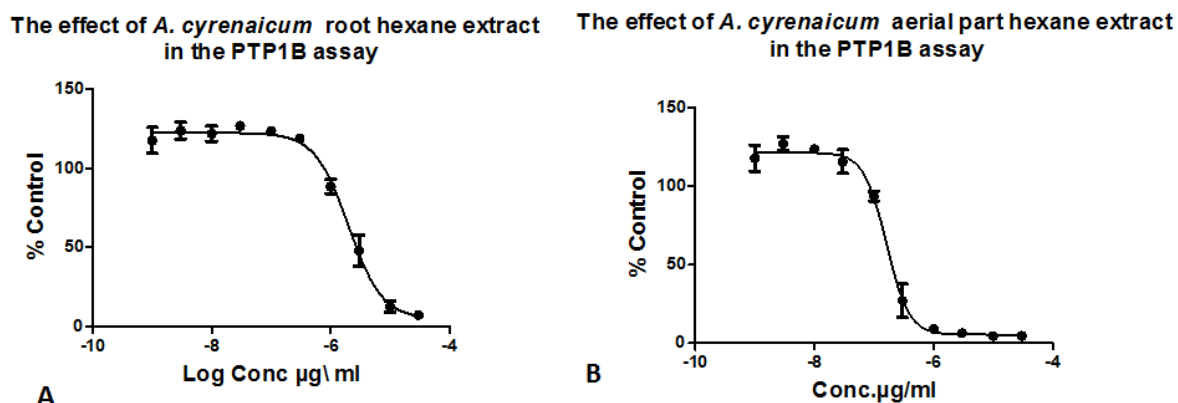


**Figure 3.86:** The effect of (A) root and (B) aerial part of hexane crude extract of *A. cyrenaicum* on PTP1B enzyme. Extracts were incubated with PTP1B enzyme for 30 min at 37°C in an atmosphere containing 5% CO<sub>2</sub>. DiFMUP (10 µM) was then added and incubated for 10 min at 37°C. The hydrolysis of DiFMUP by PTP1B enzyme was measured at 355/460 nm. Data represent mean ± 3 of PTP1B enzyme hydrolysis (% control).

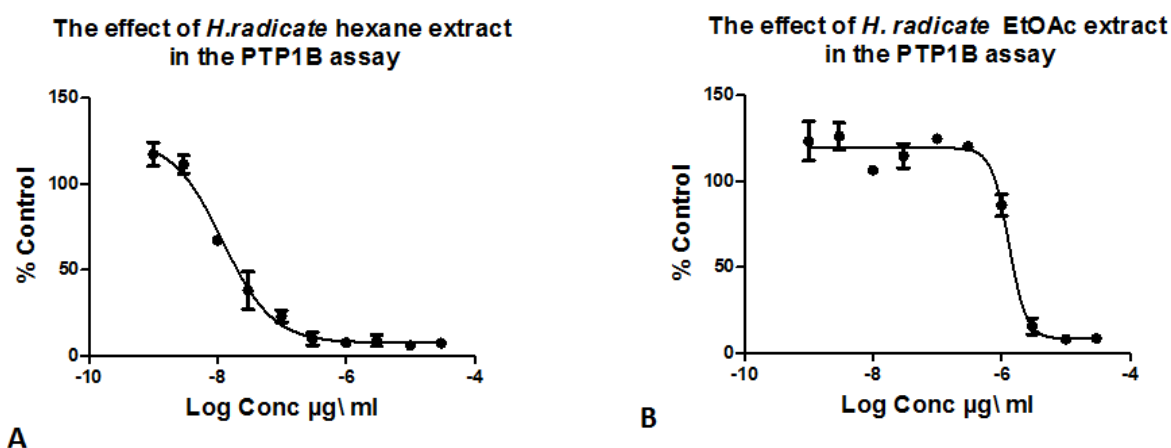


**Figure 3.87:** The effect of (A) hexane and (B) EtOAc of crude extract of *H. radicata* on the PTP1B enzyme. Extracts were incubated with PTP1B enzyme for 30 min at 37°C in an atmosphere containing 5% CO<sub>2</sub>. DiFMUP (10 µM) was then added and incubated for 10 min at 37°C. The hydrolysis of DiFMUP by PTP1B enzyme was measured at 355/460 nm. Data represent mean ± 3 of PTP1B enzyme hydrolysis (% control).

The effect of *T. zanonii* hexane extract  
in the PTP1B assay

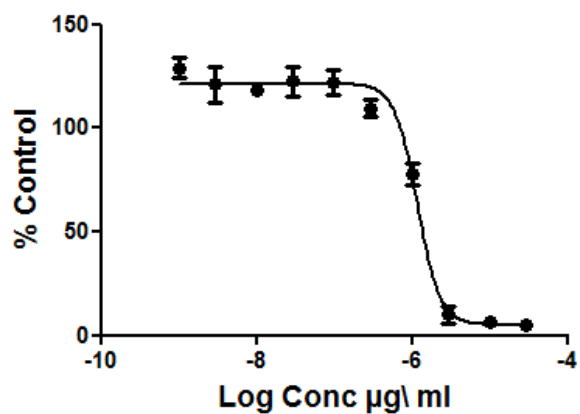


**Figure 3.88:** The effect of hexane crude extract of *T. zanonii* on the PTP1B enzyme. Extract was incubated with PTP1B enzyme for 30 min at 37°C in an atmosphere containing 5% CO<sub>2</sub>. DiFMUP (10 µM) was then added and incubated for 10 min at 37°C. The hydrolysis of DiFMUP by PTP1B enzyme was measured at 355/460 nm. Data represent mean ± 3 of PTP1B enzyme hydrolysis (% control).

### 3.8.3 $\alpha$ -Glucosidase enzyme

#### 3.8.3.1 Z-Factor of $\alpha$ -Glucosidase assay and Acarbose Reference Standard

##### Curve

$\alpha$ -Glucosidase enzyme assay was screened using  $\alpha$ -glucosidase enzyme at 0.2 units/ml in the presence of 1 mM 4-nitrophenyl- $\alpha$ -D-glucopyranoside as the substrate. The positive control included both substrate and  $\alpha$ -glucosidase enzyme, while the negative control used the substrate only. For the  $\alpha$ -glucosidase assay (Figure 3.89), the Z-factor was 0.94. Acarbose is an important inhibitor of  $\alpha$ -glucosidase, and was used as a positive control as a reference standard and Figure 3.90 shows the standard curve produced from acarbose, where the  $K_i = 0.11 \pm 0.0002$  mg/ml.

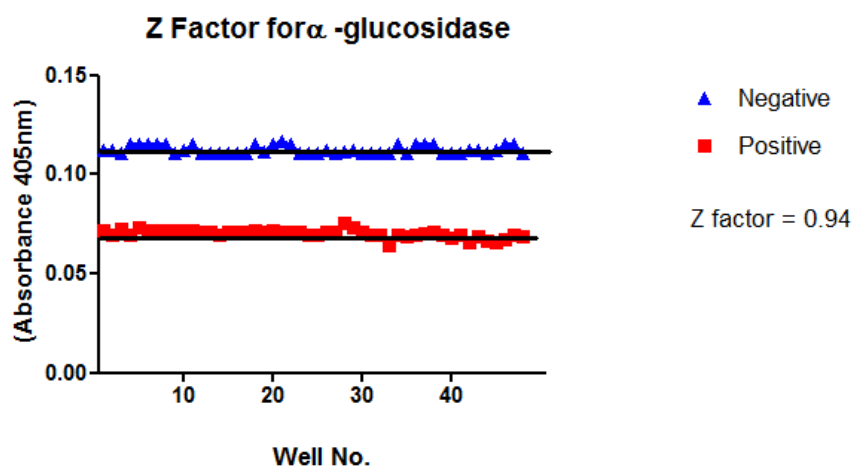


**Figure 3.89:** Z factor for  $\alpha$ -glucosidase assay using 4-nitrophenyl-  $\alpha$ -D-glucopyranoside as substrate and  $\alpha$ -glucosidase enzyme.

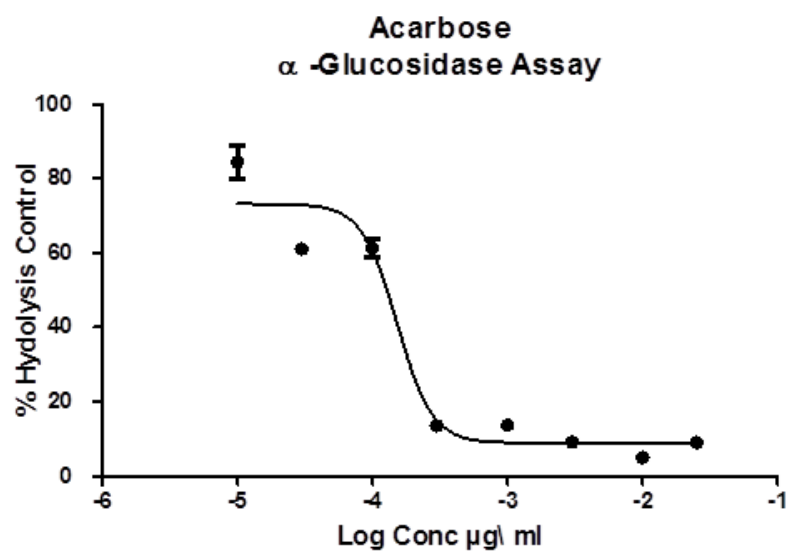


**Figure 3.90:** Effect of acarbose on the  $\alpha$ -glucosidase assay in the presence of 4-nitrophenyl-glucopyranoside (substrate). Acarbose at different concentrations (10  $\mu\text{g/ml}$  –30  $\text{mg/ml}$ ) was incubated with  $\alpha$ -glucosidase enzyme for 10 min at 37°C. 4-nitrophenyl-glucopyranoside (4 mM) was then added and incubated for 10 min at 37°C. The absorbance was measured at 405 nm. Data represent mean  $\pm$  3 of  $\alpha$ -glucosidase enzyme hydrolysis (% control) of experiments.  $K_i$  for acarbose was  $0.11 \pm 0.0002$   $\text{mg/ml}$ .

### 3.8.3.2 Effect of crude extracts and isolated compounds

Only the hexane extract of *H. radicate* showed 60% of inhibition on  $\alpha$ -glucosidase enzyme at 30  $\mu\text{g/ml}$  (Figure 3.90). Ethyl acetate and methanol crude extracts of *H. radicate* and all other samples had no significant effect on  $\alpha$ -glucosidase enzyme by comparison with the control. DMSO (1%) did not produce inhibition of the enzyme.

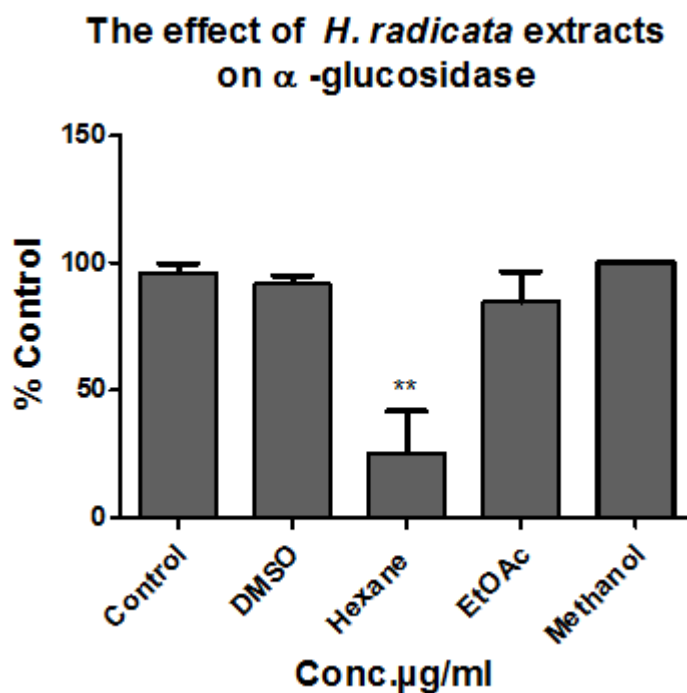


**Figure 3.91:** Effect of *H. radicata* from hexane, ethyl acetate and methanol crude extract on the  $\alpha$ -glucosidase enzyme. Extracts at 30 $\mu\text{g/ml}$  were incubated with  $\alpha$ -glucosidase enzyme for 10 min at 37°C in an atmosphere containing 5%  $\text{CO}_2$ . 4-nitrophenyl-glucopyranoside (4 mM) was then added and incubated for 10 min at 37°C. The hydrolysis of the substrate by  $\alpha$ -glucosidase enzyme was measured at 405 nm. DMSO is a negative control and acarbose is a positive control. The values are means  $\pm$  SEM of 3 values. The data were analysed by Dunnett's Multiple Comparison Test, \*\* p value =0.0027 versus control.

### 3.8.3.3 Concentration dependent inhibition of crude extracts

To study the effect of concentration of the extract on  $\alpha$ -glucosidase enzyme, acarbose produced a concentration-dependent inhibition of  $\alpha$ -glucosidase with a  $K_i$  value of  $0.11 \pm 0.0002$  mg/ml (Figure 3.90). While the hexane extract of *H. radicate* produced a concentration-dependent inhibition of the enzyme with  $K_i$  value of  $2.160 \pm 1.007$   $\mu$ g/ml (Figure 3.92).

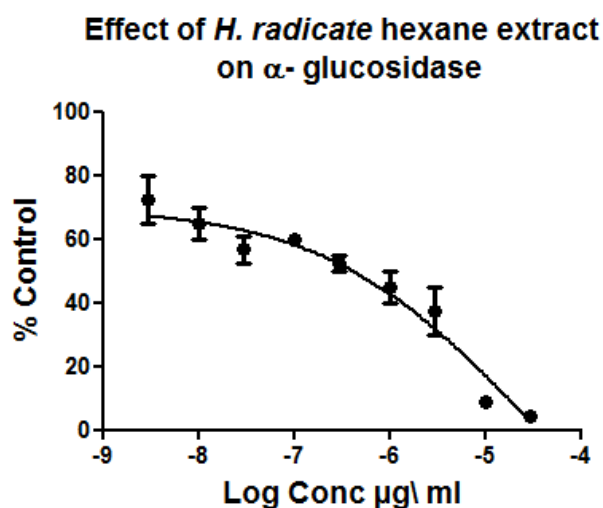


**Figure 3.92:** The effect of the hexane extract of *H. radicate* on  $\alpha$ -glucosidase enzyme. Extract were incubated with  $\alpha$ - glucosidase enzyme for 10 min at 37°C in an atmosphere containing 5% CO<sub>2</sub>. 4-nitrophenyl-glucopyranoside (4 mM) was then added and incubated for 10 min at 37°C. The hydrolysis of the substrate by  $\alpha$ -glucosidase enzyme was measured at 405 nm. Data represent mean  $\pm$  3 of  $\alpha$ -glucosidase enzyme hydrolysis (% control) of experiments.

### 3.8.4 $\alpha$ -Amylase enzyme

#### 3.8.4.1 Z-factor of $\alpha$ -Amylase assay and A carbose Reference Standard Curve

$\alpha$ -Amylase enzyme assay was screened using  $\alpha$ -amylase enzyme at 125 units/ml in the presence of 4-nitrophenyl- $\alpha$ -D-maltohexaside as substrate (1.5 mM). Positive control included both substrate and  $\alpha$ -amylase enzyme, while the negative control used the substrate only. For the  $\alpha$ -amylase assay (Figure 3.93), the Z-factor was 0.73.

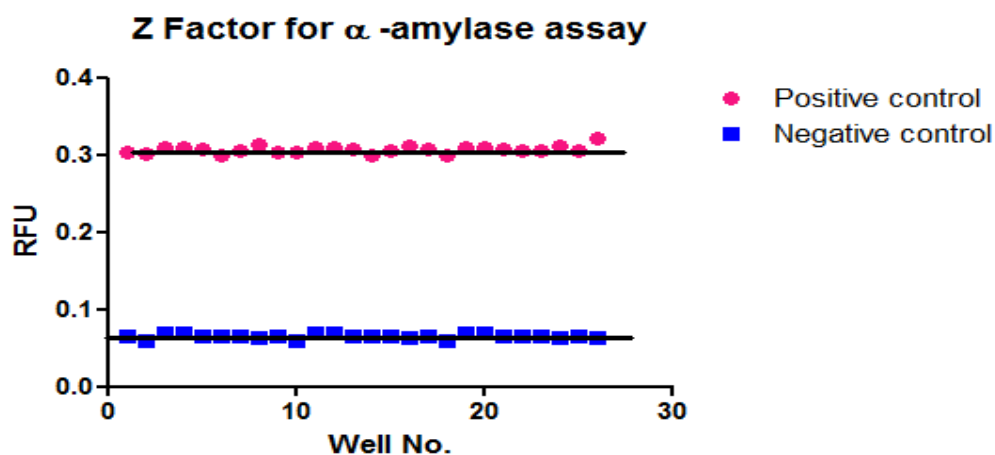


**Figure 3.93:** High-throughput screening fitness for  $\alpha$ -amylase assay using 4-nitrophenyl- $\alpha$ -D-maltohexaside as substrate and  $\alpha$ -amylase enzyme

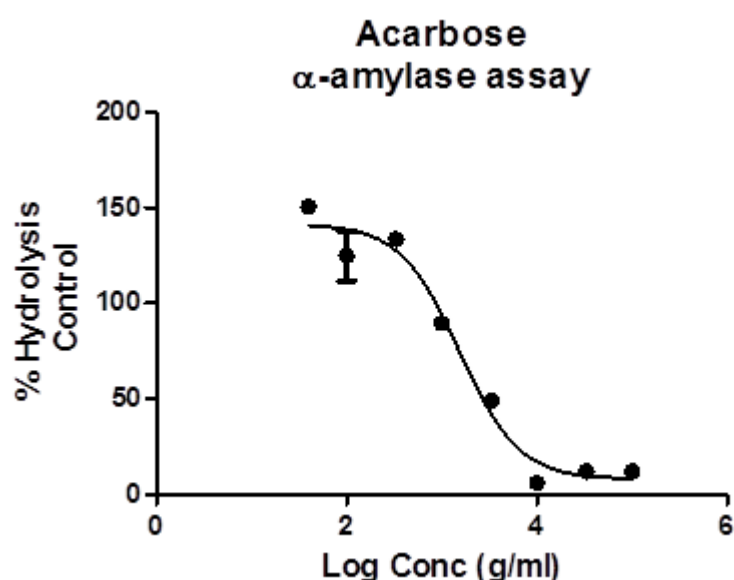


**Figure 3.94:** Effect of acarbose on  $\alpha$ -amylase enzyme in the presence of 4-nitrophenyl- $\alpha$ -D-maltohexaside substrate. Acarbose at different concentrations (10  $\mu$ M – 30 mM) was incubated with  $\alpha$ -amylase enzyme for 30 min at 37°C in an atmosphere containing 5% CO<sub>2</sub>. 4-nitrophenyl- $\alpha$ -D-maltohexaside (1.5 mM) was then added and incubated for 30 min at 37°C. The hydrolysis of the substrate by enzyme was measured at 450 nm. Data represent mean  $\pm$  SEM of enzyme hydrolysis (% control) of three independent experiments.

#### **3.8.4.2 $\alpha$ -amylase inhibition by crude extracts**

Acarbose produced a concentration-dependent inhibition of  $\alpha$ -amylase enzyme with a  $K_i$  value of  $0.26 \pm 0.05$  mg/ml (Figure 3.94). All the samples from *T. zanonii*, *H. radicata*, *P. tortuosus* and *A. cyrenaicum* (hexane, ethyl acetate crude methanol extract and their constituents) were tested on  $\alpha$ -amylase enzyme at 30 $\mu$ g/ml. DMSO (1%) did not produce inhibition of  $\alpha$ -enzyme in comparison to the control. However, none of these extracts was considered to be active on  $\alpha$ -amylase enzyme (results not shown).

## **Chapter 4**

### ***Discussion, Future work and Conclusions***

## 4.1 Discussion

The main objective of this study was to investigate five Libyan medicinal plants for their potential anticancer and/or antidiabetic properties. Therefore, isolation and identification of bioactive compounds from the plants was carried out followed by an investigation into their bioactivity.

To achieve this goal, the plants *T. zanonii*, *S. sodomaeum*, *A. cyrenaicum* and *P. tortuosus* were extracted using Soxhlet apparatus, while *H. radicata* was treated by a maceration method. Different solvents (hexane, ethyl acetate and methanol) were used to obtain crude extracts, which were then subjected to numerous chromatographic techniques in order to isolate pure compounds. Furthermore, biological activity of the crude extracts and isolated compounds was evaluated to fill in the knowledge gap about previously reported biological activities and traditional uses of these plants.

Firstly, the crude extracts and isolated compounds in sufficient quantities were evaluated for potential cytotoxicity against a range of human cancer and normal cell lines. Secondly, the crude extracts and the isolated compounds which were non-toxic were tested in three different enzyme inhibition assays to assess for potential anti-diabetic potential.

## 4.2 *In vitro* cytotoxicity activity assessment

### 4.2.1 Effects of crude extracts from the *A. cyrenaicum* and its components on cell viability

This is first time the phytochemical investigation of *A. cyrenaicum* plant (aerial parts, roots and fruits) has been reported. The <sup>1</sup>H NMR spectra of the fractions showed signals suggesting the presence of mixtures of cycloartane, pheophytin A, a mixture of  $\beta$ -sitosterol and stigmasterol compounds associated with fats (data not shown, Appendix IV). Attempting to increase the quantities of these compounds, the remaining extracts were subjected to different columns to obtain sufficient quantities, but these further separation methods failed to obtain enough quantities of these compounds. Due to low quantities of these compounds in the fractions, it was difficult to purify them. Further work is required to separate and isolate the pure compounds in sufficient quantities, using another purification method such as HPLC, and to enable

biological tests to be carried out on the pure compounds and increasing the initial amount of the plant is required to improve the compound yield followed by further work to purify these compounds as it has impurities which may also be interesting. However, from the ethyl acetate extract of the aerial part simple phenolic compounds, *para*-hydroxybenzoic acid ARE6-6 and mixture of *p*-coumaric acid (a) and 3, 4-dimethoxycinnamic acid (b) ARE6-18 were obtained. This is the first report of ARE-6-6 and ARE-6-18 from *A. cyrenaicum*. The cytotoxicity assessment of ARE6-6 and ARE 6-18 was not carried out because of low yield.

In this study, the cytotoxicity screening of crude extracts of *A. cyrenaicum* was carried out (Results Section: 3.7.1), and all extracts showed no cytotoxic activity against the cells (cancer and normal) except the root hexane extract that was toxic to HeLa, HepG2, HEK293 and PNT2. Although the fruit extracts showed toxicity only to normal cells, according to a number of references, (Husein *et al.*, 2014; Farid *et al.*, 2015; Naseef - shtaya *et al.*, 2017), *Arum* species are considered a promising source of anticancer agents. For example, Farid *et al.* (2015) showed that diethyl ether and dichloromethane extracts of *A. palaestinum* aerial parts had toxicity against larynx (Hep2), cervix (HeLa), liver (HepG2) and breast (MCF7) cell lines, whereas the hexane, ethyl acetate and methanol extracts of *A. cyrenaicum* extract in the present study did not have toxicity against HeLa, HepG2. Similarly, Husein *et al.* (2014) revealed that *A. palaestinum* showed IC<sub>50</sub> in the range between 500 and 600 mg/ml against breast cancer cells (MCF-7). On the other hand, in this study, most of the *A. cyrenaicum* extracts failed to exhibit this level of activity (less than 250 mg/ml) against the tested cancer cells. However, negative results do not mean that the plant extracts are inactive or that there is an absence of bioactive compounds. Active compounds may be present in insufficient quantities in the crude extracts for them to show activity with the concentrations assayed. For example, solubility issues became quite challenging in preliminary screening (Złotek *et al.*, 2016); most of the hexane extracts showed very weak activity at 250 µg/ml against HepG2 and HeLa, or no activity which could have been due to the poor solubility of non-polar ingredients in a water-based medium. Furthermore, the different extraction methods for example in the present study which used hot extraction could have had an effect on the extraction of

the plants. Further, selection of suitable extraction processes is recommended such as maceration, percolation, infusion and decoction in future work of to preserve the original compounds which may have a relatively unstable character ( Dhanani *et al.*, 2017; Zhang *et al.*, 2018). However, further phytochemical experiments or better alternative isolation methods are recommended for future use.

ARE-6-6 was previously isolated from rice (*Oryza sativa*) (Cho *et al.*, 1998) and showed different biological activities such as antimicrobial activity against *E. coli*, *B. aureus*, *Staph. aureus*, *P. aeruginosa*, hypoglycemic, anti-inflammatory, antiplatelet aggregating, nematocidal, antiviral and antioxidant activities (Peungvicha *et al.*, 1998; Cueva *et al.*, 2010; Velika and Kron, 2012; Chaudhary *et al.*, 2013). ARE 6-18 was a mixture of two compounds *p*-coumaric acid and 3, 4-dimethoxycinnamic acid (ARE 6-18a and ARE 6-18b). Compound ARE 6-18a was isolated previously from the plant *Cynodon dactylon* (Karthikeyan *et al.*, 2015). The evaluation of antioxidant activity of *p*-coumaric acid was carried out by Kilic and Yesiloglu. (2013), the compound showed strong antioxidant activity in a DPPH assay and exhibited 78.3% chelation of ferrous ion (Kilic and Yesiloglu, 2013). In addition, the study revealed that the compound caused <99.9% inhibition of *E. coli* at 1000 µg/ml, *Staph.aureus* at 500 µg/ml, and *B. cereus* at 500 µg/ml (Herald and Davidson, 1983). It would be interesting to investigate the activity of these compounds present in extracts in the future.

#### **4.2.2 Effects of crude extracts from the *P. tortuosus* and its components on cell viability**

The hexane extract of *P. tortuosus* presented cytotoxic activities against six cancer cell lines and two normal cell lines. Only PTH-6-7 isolated from this extract, at 125 µg/ml, exerted inhibitory effects on the PANC-1, PC-3M and A375 cells, with IC<sub>50</sub> values of 75.88, 72.20 and 70.11 µg/ml, respectively compared to the control. These observations suggest that this compound could be preferentially selective to PANC-1, PC-3M and A375 cells and further tests need to be carried out on other cancer cells to confirm this anti-tumour activity. On the other hand, the methanol extract and PTM-1 showed no toxicity to either cell line used in the present study. No studies have described any cytotoxicity for compound PTM-1; the lack of the cytotoxicity of PTM-1 may be due to the presence of a sugar moiety, given previous report flavonoid

glycosides to be less active than the 'free' aglycones. It has been used for the treatment of chronic venous insufficiency (CVI) (Ramelet, 2001), haemorrhoids (Meshikhes, 2002), lymphedema (Pecking *et al.*, 1997), venous leg ulcers (Coleridge Smith, 2003), anti-inflammatory activity (Crespo *et al.*, 1999) antioxidant and anti-apoptotic activity (Shalkami *et al.*, 2018). While the ethyl acetate extract exhibited cell toxicity against A375, PANC-1 and PNT2 in the present study. Hexane, chloroform and ethyl acetate extracts of *P. tortuosus* showed cytotoxic effects with IC<sub>50</sub> values of 106, 110, 670 µg/mL on K562 leukemia cells while ethyl acetate, methanol, acetone, and aqueous extracts exhibited no significant cytotoxic effect on L1210 leukemia cell line by Abdelwahed *et al.* (2008) using a cold extraction water/acetone mixture (Abdelwahed *et al.*, 2008a).

The <sup>1</sup>HNMR spectrum of the hexane extract of *P. tortuosus* revealed the presence of phenolic compounds as minor constituents and fats. Therefore, according to the aforementioned observations, the activity of this extract could be attributable to the combined effects of these phenolic compounds with fat. However, the activity observed for the isolated compound PTH-6-7 was stronger than that for the hexane extract, suggesting that their activities might be decreased by the presence of other (non-purified) phytochemical(s) or the compounds acting antagonistically. However, this extract is causing killing of the normal cells over cancer cells and is not selective to cancer cells, but the isolated compound is selective to cancer cells. Therefore since the PNT2 cells are normal mammalian cells, toxicity against these cells most likely predicts lack of selectivity and thus it will be toxic to mammalian cells, and therefore the traditional healers and patients should be informed on the risk of toxicity that might arise following use of the extract of this plant. These results, even being preliminary, provide some scientific basis for the ethnomedicinal use of *P. tortuosus* as an anti-tumour agent.

#### **4.2.3 Effects of crude extracts from the *T. zanonii* and their components on cell viability**

Fractionation of the hexane extract of *T. zanonii* led to the isolation of two flavonoid compounds, salvigenin (TZH-103-107-9) and 5-hydroxy-3, 4, 7, 8-tetramethoxyflavone (TZH-150-170-7). In addition, pheophytin A (TZH-68), and a

simple phenolic ester (TZH 41-49) a ferulic acid ester of fatty alcohol were isolated. Fractionation of the methanol extract led to the isolation and characterisation of one compound poliumoside (TZM-24). All of the isolated compounds in this study were identified for first time from *T. zanonii*.

There is no data in the literature concerning the cytotoxicity of the *T. zanonii* plant. Therefore, from the literature other species in the genus *Teucrium* were examined for comparative antiproliferative agents. Table 4.1 summarises a number of studies that have reported the cytotoxicity of species in the genus *Teucrium* against several cancer cell lines.

In this study, the ethyl acetate extract *T. zanonii* had a toxic effect against A375 (melanoma), LNCaP (prostate) and PNT2 (normal). On the PNT2 normal cells, this extract showed toxicity at concentrations  $\geq 250$   $\mu\text{g/ml}$ . However, at  $47.24 \pm 1.137$   $\mu\text{g/ml}$  and  $61.60 \pm 1.62$   $\mu\text{g/ml}$ , the ethyl acetate extract was toxic to the A375 and LNCaP cells respectively, but with no toxicity to the PNT2 cells. This could be an indicator of the potential selective effect on the melanoma and prostate cancer cells. Both cells are adherent, epithelial cells. In this study, no compound was obtained from this extract that was present in sufficient quantities, so only the crude extract was tested. Considering all the above data, the moderate and more selective cytotoxic activity of the ethyl acetate extract could therefore be attributed to other phytochemical(s) that were not isolated.

The hexane and ethyl acetate extracts showed weak toxicity against PANC-1 cells  $132.9 \pm 2.255$   $\mu\text{g/ml}$  and  $174.1 \pm 1.035$   $\mu\text{g/ml}$ , respectively. Of the four isolated compounds from the hexane extract, only salvigenin, showed toxic effects on the PANC-1 cell line. However, TZH-103-107-9, showed weak cytotoxic activity against PNT2 cells and did not show cytotoxicity up to  $250 \mu\text{g/ml}$  in A375, HeLa, LNCaP, PC-3M and HEKa cells; it was not tested against HepG2 due to inadequate quantities. TZH-103-107-9 was also reported in the literature against human cancer cell lines HeLa (cervical), PC-3 (prostate) and MCF-7 (breast) and L-929 (normal) by Sen *et al.*, (2017) using a MTT assay and was shown to be non-cytotoxic (Sen *et al.*, 2017).

However, this compound showed moderate activity against MCF-7 cells with an  $IC_{50}$  value of  $67.78 \pm 3.78$   $\mu\text{g/ml}$  when screened by Kamatou *et al.* (2008) using a SRB assay (Kamatou *et al.*, 2008). The combination of salvigenin with doxorubicin (a cancer drug) induced apoptosis in HT-29 and SW948 colon cancer cells through changes in mitochondrial membrane permeability by enhancing the Bax/Bcl-2 ratio and increasing the Bax/Bcl-2 ratio, caspase-3 expression and enhanced poly ADP ribose polymerase (PARP) cleavage enzyme during apoptosis (Sarvestani *et al.*, 2018). The results in the present work seem to correlate well with these reports as TZH-103-107-9 was weak/or not toxic to cancer cells within the tested concentration range, and only at 148.9  $\mu\text{g/ml}$  showed toxicity on PANC-1 cells and decreased the number of the viable cells by 12%. Therefore, TZH-103-107-9 may possess selective activity against particular cell lines. Noori *et al.* (2013) suggested that a possible mechanism of antitumor activity of salvigenin may be due to modulation of the immune response. The cytotoxic and immunomodulatory properties of salvigenin *in vivo* has been reported in that it significantly caused a decrease in the level of IL-4 (pleiotropic cytokine), increase in interferon  $IFN-\gamma$  and decreased the level of splenic  $CD4+CD25+Foxp3+$  (T regulatory cells) then decreased the rate of tumour growth. They suggested that the a possible mechanism of antitumor activity of salvigenin may be due to its involvement in modulation of the immune responses (Noori *et al.*, 2013). It has been reported to have anti-inflammatory and analgesic properties at doses of 50 and 100 mg/kg resulting in increasing pain inhibition (Mansourabadi *et al.*, 2015). Additionally, Esfandabadi *et al.* (2013) reported salvigenin as a good neuroprotective compound, inhibiting apoptosis and oxidative stress in the hippocampus and cortex of  $A\beta$ -injected rats ( $\beta$ -amyloid) by decreasing induction of apoptosis factors such as Bax/Bcl-2 ratio, caspase-3 and decreasing the level of Heme oxygenase-1 (HO-1) 1 about 1.2 and 1.1% in hippocampus and cortex respectively. Therefore it prevented the decrease of superoxide dismutase (SOD) and choline acetyltransferase (CAT) enzyme activity with more effective antioxidant defences in the cortex (Esfandabadi *et al.*, 2013). It is also reported to have antidepressant and anxiolytic activities (Abdelhalim *et al.*, 2015) and it was found to have *in vitro* antimalarial properties (Kamatou *et al.*, 2008).

Of the two tested compounds 5-hydroxy-3', 4', 6, 7-tetramethoxyflavone (TZH-150-170-7) and pheophytin A (TZH-68), they were not toxic against the cell lines in this work. TZH-150-170-7 has no previous reported biological activities. Thus for future work, screening of this compound for various biological activities needs to be carried out. The cytotoxicity of TZH-68 has been evaluated on different cell lines in the literature and the results vary. She *et al.* (2017) showed that pheophytin A exhibited significant ( $p < 0.05$ ) inhibitory activity towards the AGS (stomach) cell line with an  $IC_{50}$  of 3.69  $\mu$ M and was toxic against DU145 (prostate), SCC9 (tongue), A375 (melanoma) K562 (leukaemia) cancer cell lines with  $IC_{50}$  values of 6.6, 5.8, 35.3, 64.2  $\mu$ M, respectively (She *et al.*, 2017) compared to cisplatin, the positive control, using a XTT assay. While Liu *et al.* (2014) found that pheophytin A was inactive against A375.S2 (melanoma), DU-145 (prostate), WiDr (colon), HepG2 (liver), H441 (lung) and AGS (stomach) (Liu *et al.*, 2014). Generally, it seems that the preliminary results in the present work correlate well with Liu and co-workers regarding the cancer cells and it could be concluded that TZH-68 may possess selective activity against particular cell lines. Pheophytin A has been reported to have antioxidant and anti-inflammatory activity (Okai and Higashi-Okai, 1997; Lin *et al.*, 2014; Kusmita *et al.*, 2015). In this study, TZH-41-49 showed weak cytotoxic activity against HeLa cells (374.43  $\mu$ M) and showed no activity against A375, LNCaP, PC-3M, and PANC-1 and HEKa cells. It was not tested against HepG2 and PNT2 cells due to inadequate quantities. Ferulic acid alkyl esters have previously shown antioxidant activity (Anselmi *et al.*, 2004). In a study by Murakami *et al.* (2002), synthesised alkyl ferulate (2-methyl-1-butyl ferulic acid), *in vitro* markedly suppressed iNOS and COX-2, and also inhibited the release of TNF- $\alpha$  accompanied by suppression of I- $\kappa$ B degradation in RAW264.7 murine macrophage cells compared with ferulic acid (Murakami *et al.*, 2002). Similarly to the previous compound, TZH-41-49 could have selective activity against particular cell lines rather than others.

The methanol extract had apparent selective activity against PANC-1 cells with an  $IC_{50}$  value of 62.02  $\mu$ g/ml, while it produced less toxicity in HEKa and PNT2 normal cells with higher  $IC_{50}$  values of  $141.9 \pm 1.27$   $\mu$ g/ml and  $195.1 \pm 1.41$   $\mu$ g/ml, respectively. Its activity could be due to the presence of poliumoside (phenolic) compounds. Therefore,

the inhibitory effect, particularly in PANC-1 cells, produced by the methanol extract was suggested to be related to the presence of poliumoside TZM-24 and/ or to unidentified phytochemical(s). However this extract showed weak toxicity towards LNCaP. The cytotoxicity assessment for poliumoside was not carried out in this work because of time limitations. The anticancer activity of TZM-24 in the literature is controversial as it is uncertain whether the compound has been shown to possess an antioxidant activity in DPPH test with an IC<sub>50</sub> value of 4.23 µg/ml (Boghrati *et al.*, 2016a). The poliumoside is a phenylethanoid glycoside, structurally characterised with a hydroxyl-phenylethyl moiety attached to a β- glucopyranose through glycosidic linkage and it has been suggested that the importance of chemical structures of phenylethanoid glycosides is matched by diversity of biological activities, including antibacterial, antitumor, antiviral, anti-inflammatory, neuroprotective, antioxidant, hepatoprotective, immunomodulatory, and tyrosinase inhibitory actions (Fu *et al.*, 2008). Structure-activity relationship analysis indicates the importance the number and position of the phenolic hydroxyls play in the antioxidative activity of phenylpropanoid glycosides (Shi *et al.*, 1997; Fu *et al.*, 2008). Poliumoside showed high inhibitory activity with IC<sub>50</sub> values ranging from 9–42 µM against DNA polymerases, indicating the potential of using this compound as a lead candidate for the development of an antitumor agent targeting DNA polymerases.

On the other hand, all the extracts of *T. zanonii* were found to be inactive in terms of potential anti-cervical (HeLa) and anti-hepatoma (HepG2) drugs. In the literature, the methanol/water leaves extract of *T. sandrasicum* caused apoptosis induction and there were observed changes in the mitochondrial membrane with increased caspase-9 activities against HeLa cells; and they found that the plant contained flavonoids (Tarhan *et al.*, 2016). Another study showed that the ethyl acetate and methanol extracts of *T. polium* showed low toxicity against HepG2 cells at the 200 Mm; and this was due to *neo*-clerodane diterpenes (teupolin X) compounds. Teupolin X (200 µM) caused a weak inhibition of the cells viability (46.7%) after 48 h (Fiorentino *et al.*, 2011). Generally, the different results in the present study and Fiorentino co-worker and Tarhan co-worker studies may be due to difference of the nature and composition of phytochemical extracts in these studies. The results in the present work correlate

well with Bai *et al.* (2010), who found that flavonoids did not show cytotoxic activity against HepG2 cells (Bai *et al.*, 2010). In a study by Chow *et al.* (2008) it was suggested that the anticancer activity of flavonoids could be effective due to the position methoxy-substituted flavones in the A ring (Chow *et al.*, 2008).

Therefore, in view of the foregoing findings, the inactivity of hexane extract could be related to the presence of the flavonoids alone or together with pheophytin A if these compounds did not possess activity at higher concentration or to the other unknown phytochemical(s). While the ethyl acetate and methanol extracts activities could be attributed to its isolates components as well as to the presence of other phytochemical(s). The <sup>1</sup>H NMR spectrum of the hexane extract of the *T. zanonii* indicated that the dominant types of compounds were mainly flavonoids, pheophytin A as well as ferulic acid ester fatty alcohol. In general, the isolated compounds under these categories were found to be inactive within the tested range of concentrations, however, the hexane extract and its component, TZH-103-107-9 were found to be weakly toxic and not selective against the pancreatic cells at 132.9 and 148.9 µg/ml, respectively. While the methanol extract was toxic and selective against the pancreatic cells (PANC-1) with an IC<sub>50</sub> value of 62.02 µg/ml, and this extract indicated the presence of phenolic compound TzM-24. In the present study, since no reports were found about the activity of ethyl acetate on A37S and LNCaP and no compound obtained from this extract in the present work therefore, further work needs to be carried out on the purified compounds to correlate the activity of this extract to it; otherwise it might be due to the presence of other unknown minor components.

**Table 4.1:** Cytotoxicity activity of *T. zanonii* extracts and other species of *Teucrium* on different cancer cell lines.

Cancer type	<i>T. zanonii</i>	Other species of <i>Teucrium</i>	References
Melanoma	Tested on A375 cells only activity from ethyl acetate extract	The combination the methanol extract of <i>T. polium</i> with vincristine resulted in a massive apoptosis (>80%) compared to the effect of individual drugs (vincristine) (0-3%) against Skmel-3 cells	(Rajabalian, 2008; Stankovic`e <i>tal.</i> , 2015)
Cervical	No activity against HeLa cells from all extracts	Methanol/water extract of <i>T. sandrasicum</i> flower inhibited cell proliferation in HeLa with an IC <sub>50</sub> value of 46.46±0.2145 due to flavonoid content	(Tarhan <i>et al.</i> , 2016)
Prostate	Tested on LNCaP the ethyl acetate and methanol had activity. And no activity against PC-3M cells from all extract	Methanol extract of <i>T. persicum</i> (200 µg/ml) decreased 60% in the number of viable cells of PC-3 cells with an IC <sub>50</sub> value of 142 µg/ml	(Tafrihi <i>et al.</i> , 2014)
Liver	No activity against HepG2 cells from all extracts	Ethyl acetate and methanol extracts of <i>T. polium</i> caused regulation of biochemical markers, alanine aminotransferase (ALT), aspartate aminotransferase (AST), alpha-fetoprotein tumor marker (AFP), corticosteroid binding globulin (CBG), alkaline phosphatase (ALP), homocysteine (HCY), tumor necrosis factor-alpha (TNF-α), alpha-2-macroglobulin (α2MG), and corticosteroid binding globulin of hepatocellular carcinoma (neo-clerodanes compounds)	(Movahedi <i>et al.</i> , 2014)

**Table 4.2:** (continued).

<b>Cancer type</b>	<b><i>T. zanonii</i></b>	<b>Other species of <i>Teucrium</i></b>	<b>References</b>
Pancreas	All extracts had activity on PANC-1 cells	Essential oil ( $\beta$ -limonene, $\alpha$ -bisabolol, humulene and thymol) of <i>T. alopecurus</i> inhibited the proliferation of Panc28 (pancreatic carcinoma)	(Guesmi <i>et al.</i> , 2018)
Normal	All extracts had activity on PNT2 and HEKa	<i>T. persicum</i> extract reduced the viability of NIH-3T3 cells (mouse fibroblast) with an IC <sub>50</sub> value of 143 $\mu$ g/ml.	(Tafrihi <i>et al.</i> , 2014; Stankovic` <i>et al.</i> , 2015)

#### 4.2.4 Effects of crude extracts from the *H. radicata* and its components on cell viability

In the literature, few scientific reports have been made for *H. radicata* species in terms of its medicinal uses, but have included antioxidant (Senguttuvan *et al.*, 2014a), antibacterial (Senguttuvan *et al.*, 2013) and antifungal activities (Jamuna *et al.*, 2013). However, the cytotoxicity evaluation of this species of the *Hypochoeris* genus has not been investigated previously and no work has been done for other species in the genus in terms of cytotoxicity. Therefore, this is the first report on cytotoxicity for this species and genus.

From the ethyl acetate and methanol extracts of *H. radicata*, four compounds were isolated: luteolin (HRE-21), daucosterol ester of *trans* *p*-coumaric acid (HRE-94), 1-monoacetyl glycerol (HRE-121) and luteolin-7-O-glucoside (HRM-50-59). From the hexane extract, linoleic acid (HRH-42) and waxes (HRH5) were identified. In this study, the hexane extract exhibited high toxicity against both cancer and normal cells at all the tested concentrations compared to the control as explained in section 3.7.4. This extract caused a decrease of the cell viability of cancer cells as following for A375 (35%) at 125 µg/ml, HeLa (60%) at 125 µg/ml, HepG2 (20%) at 62.5 µg/ml, PC-3M (25%) at 62.5 µg/ml, PANC-1 (20%) at 62.5 µg/ml, LNCaP (45%) at 62.5 µg/ml and to normal cells PNT2 (15%) at 31.2 µg/ml. Therefore, this extract was not selective because it was highly potent against normal cells compared to cancer cells with an IC<sub>50</sub> of 11.02±1.084 µg/ml. The dominant types of compounds in the hexane extract were mainly fat and wax. Therefore, the activity of the hexane extract of the *H. radicata* could be attributable to the previous components and/or to other non-purified phytochemical(s). This extract caused killing of the normal over cancer cells and is not selective to cancer cells therefore all studies reporting anticancer properties need rethinking and more investigation is needed into phytochemical and antitumor activities. In the literature, *O*-hydroxy-2-decenoic acid (fat) obtained from royal jelly inhibited the microphthalmia-associated transcription factor (MITF) protein expression (IC<sub>50</sub> =0.86 mM) in B16F1 melanoma cells. It inhibited the activity of

tyrosinase and the expression of tyrosinase-related protein 1 (TRP-1), TRP-2, and MITF in B16F1 melanoma cells (Peng *et al.*, 2017). Lu *et al.* (2010), reported that linoleic acid inhibited tumour cell growth at high concentrations ( $\geq 300 \mu\text{mol/L}$ ), while low concentrations (100–200  $\mu\text{mol/l}$ ) seemed to promote cell proliferation in LoVo and Rko colorectal cancer cell (Lu *et al.*, 2010). Oleic, linoleic and palmitic acids obtained from almond oil were found to be active against Colo-320 and Colo-741 colon adenocarcinoma cells using MTT assay as cited by Mericli *et al.* (2017) (Mericli *et al.*, 2017). The suggestions of considering all the above data, the lack of selectivity for cancer cells because of cytotoxic activity of the hexane extract to normal cells could therefore be attributed to wax and fat as well as to the presence of other phytochemical(s).

While, ethyl acetate extract presented cytotoxic activity towards HeLa, PC-3M, PANC-1, HepG2, PNT2 and HEK293T cell lines as explained in section 3.7.4. On the hepatoma cancer cells, the ethyl acetate extract and HRE-21 (luteolin) were perfectly selective to HepG2 at a concentration at 63.43  $\mu\text{g/ml}$  and 36.59  $\mu\text{g/ml}$ , respectively. They gave lower  $\text{IC}_{50}$  values of 74.99 and 88.25  $\mu\text{g/ml}$  on PNT2 cells, respectively and no activity on (HEK293T) normal cells. This could be an indicator of the potential selectivity to hepatoma cancer cells. On the other hand, HRE-21 showed weak or no effects on the other cell lines. Therefore, the inhibitory effect, particularly in HepG2 cells, produced by the ethyl acetate extract was suggested to be related to the presence of HRE-21 compound and/ or to those unidentified phytochemical(s).

These results correlate well with those found by Wang *et al.* (2007). Using a MTT assay, luteolin showed an inhibition of the cell proliferation of MCF-7 (breast) and (HepG2) cancer cells in 125-200  $\mu\text{M}$  (Wang *et al.*, 2007). It has been reported to possess anti-proliferative activity on HepG2 cells via G1 cell cycle arrest (Yee *et al.*, 2003). While in this study, HRE -21 showed toxicity against PC-3M and no toxicity against LNCaP; this could be due the PC-3 cells being an androgen independent prostate cancer and LNCaP androgen-dependent (Singh *et al.*, 2012). In contrast with this result, luteolin inhibited proliferation and induced apoptosis in PC3 and LNCaP cancer cells at 31.44 and 32.05  $\mu\text{M}$ , respectively (Han *et al.*, 2016). The results demonstrated that luteolin

inhibited cell proliferation and induced apoptosis through down-regulation of miR-301 by increasing the expression of death effector domain-containing protein 2 (DEDD2), a potent inducer of apoptosis in various cell types. This difference in the results could be due to a different assay used by Han and colleagues to measure cell viability in which they used a CCK-8 assay rather than the AlamarBlue® assay used in the present study. CCK-8 is (2-(2-methoxy-4-nitrophenyl)-3-(4-nitrophenyl)-5-(2,4-disulfophenyl)-2H tetrazolium, monosodium salt), a highly stable and water-soluble WST, is utilized in Cell Counting Kit-8 (CCK-8) WST-8 assay, it is a colorimetric assay for the determination of viable cell numbers and can be used for cell proliferation assays as well as cytotoxicity assays but, Alamar Blue is a Fluorometric assay. A study by Pratheeshkumar *et al.* (2012) reported that HRE-21 is a potent inhibitor of angiogenesis by inhibiting the activation of VEGF stimulated endothelial cell proliferation, suppressed the ERK, mammalian target of rapamycin (mTOR), ribosomal protein S6 kinase (p70S6K) mediated angiogenesis signaling pathways leading to the suppression of prostate cancer (PC-3) (Pratheeshkumar *et al.*, 2012). It was indicated that the importance of the presence of double bonds between carbon atoms C2 and C3 is probably essential for cytotoxic activity of luteolin in breast, prostate, colon cancers (Chang *et al.*, 2009). It also inhibits proliferation of various tumour cell lines *in vitro* (Fotsis *et al.*, 1997). Various studies have demonstrated the anti-cancer properties of luteolin in several cancer cell lines through different mechanisms including; induction of cell cycle arrest and apoptosis in HT-29 human colon cancer cells (Lim *et al.*, 2007), apoptosis through cleavage of B-cell lymphoma 2 (Bcl-2) family in human leukemia HL-60 cells (Cheng *et al.*, 2005), induction of G2 phase cell cycle arrest and apoptosis in non-small cell lung cancer cells (Cai *et al.*, 2011), lung cancer cells (NCI-H460) through Sirt1-mediated apoptosis (Ma *et al.*, 2015), depression of the malignancy of highly invasive Du145 prostate tumour cells (Tsai *et al.*, 2016). The lack of time prevented to study the mechanism of HRE-21 on the HepG2 cells, thus, this can be considered for future.

The new daucosterol esterified derivative (HRE-94) showed moderate cytotoxic activity against A375 cells (170.45  $\mu$ M), and weak activity against LNCaP (255.28  $\mu$ M), HepG2 (217.51  $\mu$ M) and PNT2 (220.43  $\mu$ M) cells. These observations suggest

that a concentration at 122.95  $\mu\text{g/ml}$  for HRE-94 could have a selective effect on melanoma cells. The  $^1\text{H}$ - $^1\text{H}$  and COSY spectra confirmed the assignments of the protons. This data in comparison with the literature suggests that HRE-94 is a daucosterol esterified derivative as the  $^1\text{H}$  and  $^{13}\text{C}$  NMR data were identical to daucosterol (Manayi *et al.*, 2013), with identical olefinic, oxymethine, six methyls and a glucose protons, except the two protons the glucose  $-\text{CH}_2\text{OH}$  unit appeared at  $\delta_{\text{H}}$  4.51 and 4.29 ppm which are unusual deshielded chemical shifts for these protons. A carbonyl carbon was also observed at  $\delta_{\text{C}}$  170.0 ppm. These can only be as a result of esterification of the  $-\text{OH}$  thus deshielding the protons. This is confirmed by the chemical shifts observed for these protons at  $\delta_{\text{H}}$  4.49 and 4.27 and the carbonyl carbon at  $\delta_{\text{C}}$  174.0 ppm by Sultana and Afolayan, (2007) for the daucosterol derivative 3-O- $[\beta\text{-D-(6' -nonadecanoate) glucopyranosyl}]-\beta\text{-sitosterol}$ . The only moiety that can be attached to the ester is *p*-coumaric acid as it is the only residue present in the compound. Lack of correlations in HMBC between proton number (H-6') and carbon (C-1'') may be due to insufficient sample used in the NMR analysis and the increase of number of scan to show all the correlation that expected in HMBC is not affected. Further work is required to obtain the compound in sufficient quantities, using another purification method such as HPLC, and to enable biological tests to be carried out on other cells and complete analysis of 2D NMR.

Daucosterol is also reported to have cytotoxic effects against many human cancer cell lines including breast cancer (MCF-7), gastric cancer (MGC803, BGC823 and AGS) colon cancer (HCT-116) hepatocellular carcinoma (HepG2 and SMMC-7721) (Zhao *et al.*, 2015; Wang *et al.*, 2016; Zeng *et al.*, 2017). However, the activity observed for the ethyl acetate extract could be attributable to the previous components and/ or to other non-purified phytochemical(s) without disregarding the possibility of the synergistic effect among these constituents. Therefore, according to the aforementioned observations, the moderate cytotoxic activity of this extract could be attributable to the combined effects of these. However, the selective cytotoxic activity observed for the isolated compound (HRE-21) was stronger than that for the ethyl acetate extract, suggesting that their activities might be decreased by the presence of other (non-purified) phytochemical(s)

On the other hand, the methanol extract of *H. radicata* had poor selectivity on cancer cells as it was cytotoxic to the PNT2 normal cell line with an IC<sub>50</sub> of 184.5µg/ml. HRM-50-59 obtained from the methanol extract, showed no toxicity against the cancer cell lines used in the present study. There are no previous reported biological activities of this compound, thus for future work, screening of this compound for various biological activities needs to be carried out. The <sup>1</sup>H NMR spectrum of the methanol extract indicated that the dominant types of compounds were mainly flavonoid glycoside. In general, the isolated compounds under these categories were found to be inactive within the tested range of concentrations, therefore, in view of these findings, lack of cytotoxicity activity of methanol extract could be attributable to the presence of these flavonoid glycoside and/ or to other unidentified phytochemical(s), flavonoid glycosides of their attached sugar units are less active than their free flavonoid (Plochmann *et al.*, 2007). The significant effect of the plant extract on PNT2 cells might also suggest cytotoxic effect toward prostate cancer cells it is not possible to say for definite whether they are anticancer or simply cytotoxic. In the literature, *H. radicata* is medicinally important by having antiinflammatory, anticancer, antioxidant, antibacterial, antifungal and antidiuretic properties (Senguttuvan *et al.*, 2014b), therefore it is needed to consider about the *H. radicata* for the anticancer activity because of the toxicity on normal cells in future.

#### **4.2.5 Effects of crude extracts from the *S. sodomaeum* and its components on cell viability**

The *S. sodomaeum* hexane extract showed no toxicity to either cancer or normal cell lines while the ethyl acetate extract showed toxicity only against LNCaP at 250µg/ml. These extracts are highly rich with trilinolein, which has been reported to have antioxidant activity (Chan *et al.*, 1996). It has also been reported to inhibit A549 lung carcinoma cells through the modulation of the PI3K/Akt pathway (Chou *et al.*, 2011). In the present study, *S. sodomaeum* methanol extract (SSM) showed toxicity against all cancer cell lines, but it was most potent against PANC-1 (8.72±0.04 µg/ml) cells. On PNT2 cells, the SSM extract showed toxicity at concentrations ≥ (125 µg/ml). At 67.17±1.665 µg/ml, this extract showed no effects on PNT2 cells. These observations

suggest that a concentration range between 62.5- 8.72  $\mu\text{g/ml}$  for the SSM extract could have a selective effect on the PANC-1 pancreas cells. In the literature, a cream formulation containing glycoalkaloids from this plant has proven effective in the treatment of malignant human skin tumors and antineoplastic activity against Sarcoma 180 in human skin cancers (Cham and Wilson, 1987; Cham and Meares, 1987) and there is no literature for other cancer cell lines. Two compounds were isolated from the SSM extract; solamargine (SSM-30-2) and chlorogenic acid (SSM-56). This is the first report of SSM-56 from *S. sodomaicum* while, SSM-30-2 was isolated previously from this plant.

The isolated phenolic compound chlorogenic acid (SSM-56) showed apparent selective activity against PANC-1 cells with an  $\text{IC}_{50}$  of  $20.19 \pm 1.25 \mu\text{g/ml}$  ( $56.98 \mu\text{M}$ ), and it showed moderate and selective effects on PC-3M cells with an  $\text{IC}_{50}$  of  $80.42 \mu\text{g/ml}$  ( $266.97 \mu\text{M}$ ) and weak activity toward LNCaP and HepG2 cell lines. On the other hand, SSM-56 showed no toxicity to A375, HeLa and the normal cell lines in this work. While it showed limited sensitivity to HeLa ( $\text{IC}_{50}=1.4 \text{ mg/ml}$ ) and HepG2 ( $\text{IC}_{50}=4.1 \text{ mg/ml}$ ) cancer cells when screened by Gouthamchandra *et al.* (2017) using a MTT assay. Li *et al.* (2014) showed SSM-56 had a significant ( $p < 0.05$ ), inhibitory activity against B16 melanoma cells at 30 and 60  $\mu\text{M}$  compared to 8-methoxypsoralen (8-MOP) as the control (Li *et al.*, 2014a). Also, SSM-56 at 100  $\mu\text{M}$  reduced cell viability and induced apoptosis in U937 leukemia cells by promoting production of ROS and reduced mitochondrial membrane potential ( $\Delta\Psi\text{m}$ ) (Yang *et al.*, 2012). Therefore, SSM-56 could have selective activity on particular cell lines. This conclusion was also reached by Yang *et al.* (2012) where this compound possessed selective and significant ( $p < 0.001$ ) inhibitory activity against a leukemia cell line. SSM-56 appears to act through different mechanisms, including: inhibition of cell growth, regulation of cell cycle, and induction of apoptosis pathways. Xu *et al.* (2013) suggested that the multimeric protein complex of  $\beta$ -catenin could be increased by chlorogenic acid upregulated genes glycogen synthase kinase ( $\text{GSK-3}\beta$ ) and adenomatous polyposis coli (APC), which could inhibit the free  $\beta$ -catenin into the nucleus to connect with Transcription factors (TCF). So the transcriptional expression of the target genes will be cut to abnormal cell proliferation. It is probably one of the

ways that can stop tumour increase by chlorogenic acid (Xu *et al.*, 2013). Table 4.2 summarises some studies, which show the mechanism of action of chlorogenic acid in different cancer cell lines.

SSM-30-2 (solamargine) was obtained in very small quantities, which prevented it from being tested for cytotoxic activity. A number of studies have reported the cytotoxicity of SSM-30-2 against several cancer cell lines. Table 4.3 summarises these studies, which showed that solamargine exhibits a broad spectrum inhibition on all the tested cancer cell lines. In a report by Munari *et al.* (2014), SSM-30-2 has inhibitory effects on the proliferation of many cancer cells such as B16F10 murine melanoma, HT29 colon, MCF-7 breast, HeLa cervical, HepG2 liver and MO59J, U343 and U251 glioblastoma tumour cell lines (Munari *et al.*, 2014b). Lee *et al.* (2004) also found it to be more toxic against liver (HepG2) than colon (HT29) cancer cells because solamargine at 0.1, 1, 10 and 100  $\mu\text{g}/\text{mL}$  concentrations caused % of inhibition in HepG2 cell viability 5.2, 59.9, 81.4 and 83.6 % while the % growth inhibition in HT29 was 1.3, 28.9, 71.8 and 82.0 respectively (Lee *et al.*, 2004). Chang *et al.* (1998) reported that SSM-30-2 had remarkable anticancer activity against hepatoma (Hep3B) cells compared with khasianine (steroidal alkaloids) with  $\text{IC}_{50}$  values of 3.0 and 20 mg/ml respectively, due to the different sugar moieties; the difference was SSM-30-2 contains two rhamnose sugars, while khasianine contains one (Chang *et al.*, 1998a). Wang *et al.* (2011) showed that rhamnose plays an important role in solamargine's anticancer activity. Accordingly, the strongly observed anti-cancer activities of the SSM extract were linked to these isolated components SSM 30-2 and SSM 56, which could be acting synergistically.

**Table 4.3:** Mechanism of action of SSM-56 on selected tumour cell lines.

<b>Organ</b>	<b>Mechanism of action</b>	<b>Refences</b>
Blood	Induced cell-cycle arrest, inhibited growth proliferation and induced apoptosis in human acute promyelocytic leukemia HL-60 cells	(Liu <i>et al.</i> , 2013)
Colon	Inhibited the cell viability, induced ROS generation, caused S-phase arrest and ERK inactivation in HCT116 and HT29 cells	(Hou <i>et al.</i> , 2017)
Liver	Combination of of 250 $\mu\text{mol/L}$ chlorogenic acid and 20 $\mu\text{mol/L}$ 5-florouracil inhibited cell proliferation and inactivated ERK1/2 via ROS overproduction in HepG2 and Hep3B cells	(Yan <i>et al.</i> , 2015)
Oral	Induction of apoptosis in human oral squamous cell carcinoma (HSC-2) and salivary gland tumor (HSG)	(Jiang <i>et al.</i> , 2000)
Colorectal	Decreases proliferation by 50% ( $\text{EC}_{50}$ ) ( $758 \pm 19.09 \mu\text{M}$ ). It induced cell-cycle arrest at the S-phase by 250 $\mu\text{M}$ , activation of caspase-3 (1000 $\mu\text{M}$ ) in Caco-2 cells	(Sadeghi Ekbatan <i>et al.</i> , 2018)
Breast	Increased the multimeric protein complex of $\beta$ -catenin upregulated genes glycogen synthase kinase 3 beta (GSK-3 $\beta$ ) and adenomatous polyposis coli (APC), which could inhibit the free $\beta$ -catenin into the nucleus to connect with TCF. So the transcriptional expression of the target genes could be cut to abnormal cell proliferation in EMT-6 mice breast tumor lines	(Xu <i>et al.</i> , 2013)

**Table 4.2:** (continued).

<b>Organ</b>	<b>Mechanism of action</b>	<b>Refences</b>
Breast	Killing cancer cells MDAMB-231 and MCF-7 in a dose-dependent manner with an IC <sub>50</sub> of 75.88±4.54µg/ml and 52.5±4.72µg/ml, respectively and induces apoptosis by ethidium bromide/acridine orange (AO/EtBr) staining and degradation of genomic DNA to give a laddering pattern	(Deka <i>et al.</i> , 2017)
In a rat carcinogenesis model	Inhibit the formation of one type of oxidative DNA damage, and inhibit 8-hydroxydeoxyguanosine (8-OH-dG) level in the DNA of the rat tongue	(Kasai <i>et al.</i> , 2000)
Liver	Decreased ROS formation and increased glutathione levels. It did not induce the caspase cascade for apoptosis nor affect expression levels of Bcl-xL or Bax, so did not have an effect on apoptosis. No enhanced AKT/PI-3-kinase and ERK. It might act through limiting apoptosis related to oxidative stress by a reduced ROS production and, also by an increase in cellular antioxidant potential (GSH) in HepG2 cells	(Granado-Serrano <i>et al.</i> , 2007)

**Table 4.3:** Cytotoxic activity of SSM-30-2 on human tumour cell lines.

<b>Cell line</b>	<b>Mechanism of action</b>	<b>References</b>
Hep3B liver cancer cells	Triggers gene expression of human TNFR I lead to cell apoptosis	(Hsu <i>et al.</i> , 1996)
U2OS osteosarcoma cells	Activation of caspase	(Li <i>et al.</i> , 2011)
SMMC-7721 hepatoma cancer	Activation of caspase-3, induction of apoptosis and inhibits hepatoma cell proliferation	(Ding <i>et al.</i> , 2012)
NSCLC lung carcinoma	Inhibits protein expression of SP1 and NF- $\kappa$ B subunit p65, inactivation of PI3-K/Akt, suppressing EP4 expression in human lung cancer cells	(Chen <i>et al.</i> , 2015)
HBL-100, ZR-75-1 and SK-BR-3 breast cancer cells	Induces apoptosis by up-regulating the expression of external death receptors, such as TNFR-I, Fas receptor (Fas), TNFR-I-associated death domain (TRADD) cytochrome <i>c</i> , caspase-8, -9 and -3, also inhibits the anti-apoptotic Bcl-2 and Bcl-xL proteins in human breast cancer cells	(Shiu <i>et al.</i> , 2007)
MGC-803 gastric cancer	Decreases mutation p53, increases the ratio of Bax to Bcl-2 and the activation of caspase-3	(Ding <i>et al.</i> , 2013b)
ZR-75-1 breast cancer cells	Downregulation of human epidermal growth factor receptor 2 (HER2/neu). However, patients with HER2/neu overexpression exhibit resistance to anticancer drugs, particularly, combinations of methotrexate, 5-florouracil, and cisplatin with SSM-30-2 individually increasing the susceptibility of breast cancer cells to these chemotherapeutic agents.	(Shiu <i>et al.</i> , 2008)

#### **4.2.5.1 SSM extract and SSM-56 had an inhibitory effect on morphology, adhesion, migration and invasion of PANC-1 cells**

From these preliminary findings, SSM extract and SSM-56 were chosen for further examination due to the selective cytotoxicity on PANC-1 cells. Therefore the SSM extract and SSM-56 were chosen to investigate the effect on anti-adhesion properties of PANC-1 cells.

Cancer metastasis is a complex process which causes spread of cancer cells from the primary tumour to surrounding tissues and to distant organs (Gupta and Massague, 2006; Lv *et al.*, 2014a). It is involved in loss of cellular adhesion, increased migration and invasion, circulation through the vascular/lymphatic systems at distant sites (Chambers *et al.*, 2002). In order for metastasis to occur to new sites, through cell adhesion molecules, migration and invasion is required (Keleg *et al.*, 2003). Degradation of the ECM and BM by proteolytic enzymes and invasion are essential for metastasis (Bogenrieder and Herlyn, 2003). ECM components have been demonstrated to play an important role in cancer cell invasion and metastasis (Müller-Pillasch *et al.*, 1997). The ECM is composed of two main classes of macromolecules: fibrous proteins and proteoglycans (Frantz *et al.*, 2010). So this study focussed on the effect of SSM extract and SSM-56 viability, adhesion to ECM proteins (collagen IV and fibronectin), migration and invasion of PANC-1 cells. To date, there has not been a study of the effect of SSM extract and SSM-56 on the morphology of PANC-1 cells. Both SSM extract and SSM-56 had an effect on the morphology of the cells as explained in section 3.7.5.1.2. It was demonstrated that these morphological changes were associated with the anti-adhesion properties of the SSM extract and SSM-56. The result of the current work is similar to the result by Liu *et al.* (2013) who reported that chlorogenic acid, showed irregular changes in morphology at 48 h, including shrinkage of the cell membrane at 1  $\mu\text{M}$  against HL-60 leukemia cells (Liu *et al.*, 2013). Another study demonstrated that chlorogenic acid at 50, 100, 150 or 200 $\mu\text{M}$  reduced cell viability and induced cell morphological alterations of U937 myelocytic leukemic cell compared to control un-treated cells for 48 h (Yang *et al.*, 2012). To clarify that the actions of SSM-56 on morphology were due to their effect on adhesion, the effect on

viability after 48 h was tested. Moreover, chlorogenic acid at 500  $\mu$ M and 1 mM decreased cell viability of HepG2 cells by 50.92% and 23.17%, respectively using Trypan blue dye-exclusion assay. In the same study, it caused S-phase arrest, reduced phosphorylation of ERK1/2, matrix metalloproteinases (MMP-2/TIMP-2) in both HepG2 cells and HepG2 xenografts and decreased the expression MMP-9 in HepG2 xenografts only. It has been shown *in vivo*, that chlorogenic acid treatment also suppressed the progression of HepG2 xenografts with 30 and 60 mg/kg of SSM-56 causing a tumour volume decrease by 64.3% and 91.4%, and tumour weight decrease by 26.6% and 77.2%, separately (Yan *et al.*, 2017). Therefore, the MMPs play an important role in tumour invasion and metastasis by degeneration of ECM proteins such as collagens (Fassina *et al.*, 2000). Therefore, in this study, the effect of SSM extract and SSM-56 on interaction between collagen IV or fibronectin ECM proteins with PANC-1 cells was studied.

A concentration between 62.5 and 15.6  $\mu$ g/ml, SSM extract caused significant ( $p < 0.01$ ) loss of cell adhesion (95%) in PANC-1 cell lines to fibronectin and a concentration between 250 and 15.6  $\mu$ g/ml SSM-56 caused a loss of cell adhesion of 90% in a dose-dependent manner. There was no effect on their adhesion to poly-L-lysine, because the poly-L-lysine is a positively charged synthetic amino acid. It is commonly used as a thin coating on tissue culture surfaces. The poly-L-lysine coating promotes the attachment and adhesion of many cells *in vitro*. It does this by increasing the electrostatic attraction between the surface and the cells. The poly-L-lysine enhances cell binding to polystyrene surfaces for certain cell-based assays and procedures, therefore, suggesting that the effect of the SSM extract and SSM-56 is specific for the adhesion receptors. SSM extract caused a loss of cell adhesion of more than 65% and SSM 56 60% in PANC-1 cell lines in a dose dependent manner to collagen IV. It can be concluded that the SSM extract and SSM-56 are specific at least for the fibronectin receptor more than collagen IV. These results correlate well with those found by Bouzaiene *et al.* (2015). Using phenolic compounds (caffeic, coumaric and ferulic acids), they inhibited the adhesion of A549 lung and HT29-D4 colon cells by 77.9% and 79.8%, respectively to collagen IV at 200  $\mu$ M. In the same study, at the (200  $\mu$ M), caused inhibition of migration of A549 cells by 7.7%, 9.5% and 35% for caffeic, coumaric or ferulic acids, respectively. The mechanism of action was through

the inhibition effect of phenolic compounds on cell migration and it is likely due to the reduced attachment to ECM proteins (Bouzaiene *et al.*, 2015). This work on phenolic compounds correlates to the result of the current work since SSM extract and SSM-56 inhibited the adhesion of the cells to fibronectin and collagen IV. The current work also demonstrated that both SSM extract and SSM-56 had an inhibitory effect on migration and invasion of PANC-1 cells as explained in section 3.7.5.1.4.1. This result was similar to a study carried out by Belkaid *et al.* (2006), which demonstrated that chlorogenic acid inhibited glucose-6-phosphatase (G6PT). G6PT triggers cancer cell migration in U-87glioma cells (Belkaid *et al.*, 2006). This result was also similar to a study carried out by Yagasaki *et al.* (2000), which found that chlorogenic acid, quinic acid and caffeic acid at 10  $\mu$ M inhibited significantly ( $p < 0.05$ ) AH109A hepatoma cell invasion by 68%, 31% and 36%, respectively. Thus, the suppressive effect of chlorogenic acid on AH109A cell invasion might result from the additive effects of its quinic acid (31%) and caffeic acid (36%) constituents. However, in this study, the invasion assay (CytoSelect™ 24-Well Cell Invasion Assay) used was different from Yagasaki *et al.* (2000) who used a co-culture system invasion assay (Yagasaki *et al.*, 2000). A study by Yamagata *et al.* (2018) found that chlorogenic acid reduced significantly ( $p < 0.05$ ) the gene expression of Bcl-2, but significantly ( $p < 0.05$ ) increased apoptosis regulator (BAX) and caspase protein (CASP3) in apoptosis of A549 lung cancer cells. Yamagata *et al.* (2018) reported that it enhanced annexin V expression, using fluorescently labelled annexin V, indicating increased levels of apoptosis (Yamagata *et al.*, 2018). The result from the present study showed that SSM-56 stained red fluorescence with an Annexin V and Ethidium Homodimer III stain, which indicates that it could be acting as a necrotic agent on PANC-1 cells. However, the difference in results could be the difference in mechanism of action. On the other hand, the work of Yang *et al.* (2012) showed that chlorogenic acid induced apoptosis by promoting ROS production and reduced the  $\Delta\Psi_m$  and increased the activation of caspase-3 pathways in human leukemia U937 cells (Yang *et al.*, 2012). An experiment *in vitro* showed that the anti-cancer activity of SSM-56 comes through reduction in cell viability, changes in the cell cycle and increases in apoptosis in HT-29 colon adenocarcinoma cells (Murad *et al.*, 2015). Liu *et al.* (2013), showed that SSM-56 at 10  $\mu$ M inhibited proliferation and induced apoptosis in HL-60 promyelocytic leukemia

cells. While Granado-Serrano *et al.* (2007) found that SSM-56 did not induce the caspase cascade and did not affect expression levels of Bcl-xL or Bax in HepG2 cells, therefore, SSM-56 showed no effect on apoptosis in HepG2 cells. Generally, it seems that the results in the present work regarding apoptosis correlate well with Granado-Serrano and co-workers which showed no effect on apoptosis except they used different cell lines in both studies (Granado-Serrano *et al.*, 2007). This suggestion could be due to different mechanisms based on the cell type. It has been reported that phenolic compounds such as chlorogenic acid, curcumin, epigallocatechin-3-gallate, resveratrol and gallic acid affect different tumour cells for example, A549 lung, RKO and HCT116 colorectal, OC2 oral, RPMI 8226, U266, and KM3 myeloma and HeLa cervical cancer cells are affected through adhesion, migration and invasion (Sun *et al.*, 2006; Ho *et al.*, 2007; Chen *et al.*, 2008; Zhao and Hu, 2013; Maruyama *et al.*, 2014; Shi *et al.*, 2015; Li *et al.*, 2017; ), and that SSM-56 could be a promising target to treat pancreatic cancer by inhibition of cell migration and invasion as a result of reduced or inhibited attachment to ECM proteins (collagen IV and fibronectin).

### **4.3 *In vitro* antidiabetic activity assessment**

Due to lack of cytotoxicity, *A. cyrenaicum*, *P. tortuosus*, *T. zanonii* and *H. radicata* extracts and their isolated compounds were tested to determine whether these crude extracts and isolated compounds have any antidiabetic effects.

A major goal in the treatment of diabetes mellitus is to maintain near normal blood glucose levels in both the fasting and postprandial state. One therapeutic approach to decrease postprandial hyperglycemia is to suppress the production and/or absorption of glucose from the gastrointestinal tract through inhibition of either PTP1B or  $\alpha$ -amylase or  $\alpha$ -glucosidase enzymes (Cheng and Fantus, 2005; Kim *et al.*, 2005; Bhandari *et al.*, 2008). Alpha amylase catalyses polysaccharides (starch) into various oligosaccharides and disaccharides. Disaccharides produced by  $\alpha$ -amylase are hydrolysed further by  $\alpha$ -glucosidases to produce glucose and other monosaccharides, which are readily absorbed in the small intestines (Janeček and Baláž, 1992; Ross *et al.*, 2004). PTP1B is the main principle underlying the type of approach according to the activation of glucose uptake (Cho, 2013). PTP1B negatively regulates insulin signalling by dephosphorylating phosphotyrosine residues on the insulin receptor (Cho, 2013). Antidiabetic and hypoglycemic potential of several plants have been reported

( Raju *et al.*, 2001; Kooti *et al.*, 2016). The most common herbal active ingredients include flavonoids, tannins, phenolic and alkaloids that are used in treating diabetes (Sen and Dash, 2014).

Experimental animal studies and clinical studies have shown that inhibitors of PTP1B or  $\alpha$ -amylase and  $\alpha$ -glucosidase can suppress the production and absorption of glucose from the small intestine (Hara and Honda, 1990; Kumar *et al.*, 2011b; Thilagam *et al.*, 2013; Ali Asgar, 2013; Liu *et al.*, 2015). Furthermore, some enzyme inhibitors such as  $\alpha$ -amylase and  $\alpha$ -glucosidases are currently used to suppress postprandial glucose levels in diabetic patients (Kim *et al.*, 2005; Kavimani *et al.*, 2014). Enzyme inhibitors for PTP1B such as thiazolidinediones (glitazones) and benzofuran directly catalyse insulin receptor (IR) and insulin receptor substrate (IRS) dephosphorylation, coordinate the balance between phosphorylation and dephosphorylation of tyrosine residues, resulting in the downregulation of insulin signal transduction. PTP1B has also been shown to negatively regulate leptin receptor signalling by dephosphorylating Janus kinase JAK2 receptor, which and prevented leptin signal transduction. Therefore, PTP1B inhibitors may enhance insulin sensitivity by blocking the PTP1B-mediated negative insulin and leptin signalling pathways (Tamrakar *et al.*, 2014). According to the literature, a number of studies have reported that traditional Indian and Chinese medicines have used plant and herbal extracts as anti-diabetic agents (Chen *et al.*, 2001; Grover *et al.*, 2002).

In this study, among all the extracts of *T. zanonii*, only the hexane extract inhibited PTP1B enzyme at 30  $\mu$ g/ml. Compounds TZH-103-107-9, TZH-150-170-7, TZH-68 and TZH-41-49 did not show activity against PTP1B enzyme. On the basis of the results of the above mentioned studies, it was hypothesised in the current study that *T. zanonii* hexane extract may inhibit the activity of PTP1B enzyme due to the presence of flavonoids (TZH-103-107-9, TZH-150-170-7) and pheophytin A (TZH-68) which suggests that these compounds are only active in synergy. This confirms that this extract can be reported as a PTP1B enzyme inhibitor because of the flavonoids. Phenolic, flavonoids and other compounds have been reported previously as classes of PTP1B inhibitory compounds from plants (Jiang *et al.*, 2012). Pongamol and karanjin

are phenolic compounds, isolated from *Pongamia pinnata* fruits possesses significant anti-hyperglycemic activity in streptozotocin-induced diabetic rats (Tamrakar *et al.*, 2008). According to the literature, flavonoids with less polar substituents (isoprenyl, methylation or acylation of hydroxyl groups) on their skeletons are usually beneficial to activity, while the addition of one hydroxyl group may lead to decreased activity (Jiang *et al.*, 2012). A study by Semaan *et al.* (2017) supported the findings of the current study on the synergism effect of flavonoids and pheophytins on PTP1B activity (Semaan *et al.*, 2017).

The hexane extract of the root and aerial part of *A. cyrenaicum* inhibited PTP1B;  $K_i$  values very similar to that of TFMS. The results of the current study are similar to those reported elsewhere in the literature (Afifi *et al.*, 2016). The highest inhibitory activity towards PTP1B was found in hexane extract of the root and aerial part of *A. cyrenaicum* (90% and 70%, respectively). Both the root and aerial part hexane extracts of *A. cyrenaicum* produced a concentration-dependent inhibition of PTP1B enzyme with  $K_i$  values of  $1.902 \pm 1.51$   $\mu\text{g/ml}$  and  $1.65 \pm 1.37$   $\mu\text{g/ml}$ , respectively.  $K_i$  value of  $4.6 \pm 007$   $\mu\text{M}$  was obtained for the positive control (TFMS). This observation suggests that PTP1B is inhibited mostly by the less polar chemical components of the roots and aerial parts of *A. cyrenaicum*. Phytochemical screening of *A. cyrenaicum* root and aerial parts hexane extracts suggested the presence of phenolic compounds. Taking into consideration the results of other similar *in vitro* studies, which have attributed the PTP1B inhibitory activity of some plant material extracts to the presence of flavonoids, polyphenols as well as their glycoside derivatives (Cai *et al.*, 2015; Uddin *et al.*, 2018). The inhibition of PTP1B enzyme by the roots and aerial parts of *A. cyrenaicum* might be due to the presence the parahydroxybenzoic acid in addition to other secondary metabolites in the plant, which may be responsible for the activity of the plant extract. However, these findings seemed to correlate well with those reported in the literature regarding antidiabetic properties of *p*-hydroxybenzoic acid. In spite of the differences in the assays used for their assessment in those studies, it caused a decrease plasma glucose level in a dose dependent manner by increasing peripheral glucose consumption upon oral administration to streptozotocin induced diabetic rats (Peungvicha *et al.*, 1998). To conclude, it is reasonable to suggest that the PTP1B

inhibitory effect of *A. cyrenaicum* root and aerial parts hexane extract observed in the current study could also be due to the presence of less polar phenolic or other phenolic compounds. Of interest is the fact that the ethyl acetate and methanol extracts of *A. cyrenaicum* did not display any *in vitro* hypoglycaemic activity.

In addition, in this study, hexane and ethyl acetate of *H. radicata* extracts inhibited PTP1B, but the methanol extract of *H. radicata* did not display any activity. However, this is the first report for the potential hypoglycaemic activity for it. On the other hand, no activity was observed from any compound that was obtained from the plant. Both extracts produced a concentration-dependent inhibition of PTP1B enzyme with  $K_i$  values of  $1.207 \pm 0.008 \mu\text{g/ml}$  for the hexane extract and  $1.301 \pm 0.006 \mu\text{g/ml}$  for the ethyl acetate extract. These low  $K_i$  values reflect the high potencies of these extracts. Kinetic studies demonstrated that the inhibition of both hexane and ethyl acetate extracts, as well as the TFMS inhibitor of PTP1B enzyme, were competitive inhibitors. This confirms that these extracts can be reported as PTP1B enzyme inhibitors. Their activity is probably due to the presence of fat, luteolin and daucosterol ester derivatives. Various chemical classes of PTP1B inhibitory compounds from plants including phenols, flavonoids and other compounds have been reported previously (Chen *et al.*, 2002; Feng *et al.*, 2007; Jiang *et al.*, 2012; Li *et al.*, 2010a). In this study, these extracts contain fat, flavonoid (luteolin), triterpenoid (daucosterol ester of *trans p*-coumaric acid). In the literature according to Zang *et al.* (2016) luteolin improved blood glucose, hemoglobin A1c (HbA1c), insulin, and homeostasis model assessment of insulin resistance (HOMR-IR) levels in KK-Ay mice (Zang *et al.*, 2016). However, another study by Matsui *et al.* (2002), found that luteolin had a weak activity on  $\alpha$ -glucosidase compared to the control, acarbose ( $IC_{50}$   $430 \mu\text{M}$ ) (Matsui *et al.*, 2002). The positive results obtained in the present study could be attributed to the above mentioned isolated compounds in these extracts. The presence of fatty acids and flavonoids (Zang *et al.*, 2016) increased the activity of the inhibition of the extracts.

Only the hexane extract of *H. radicata* containing fats inhibited  $\alpha$ -glucosidase enzyme. The hexane extract produced a concentration-dependent inhibition of  $\alpha$ -glucosidase with a  $K_i$  value of  $2.160 \pm 1.007 \mu\text{g/ml}$ . Many studies have shown potential  $\alpha$ -

glucosidase inhibitors from extracts of plants that contain active components such as terpenoids, phenolics, alkaloids, flavonoids (Kumar *et al.*, 2011a; Yin *et al.*, 2014b).

$\alpha$ -Amylase enzyme plays an important role in the digestion of starch and glycogen. Inhibition of  $\alpha$ -amylase enzyme was considered an important approach for the management of carbohydrate uptake-related problems (such as diabetes and obesity). All the extracts of *T. zanonii*, *H. radicata*, *A. cyrenaicum* and *P. tortuosus* and the isolated compounds at 30  $\mu\text{g/ml}$  did not show  $\alpha$ -amylase enzyme. In the literature, among the phyto-constituents that have been investigated, flavonoids had the highest inhibitory effect on  $\alpha$ -amylase enzyme and the potential of inhibition was related to the number of hydroxyl groups in the molecule of the compound (Pm *et al.*, 2012). A study demonstrated that luteolin also inhibited  $\alpha$ -amylase effectively although it was less potent than the control acarbose (Kim *et al.*, 2000).

Some anti-diabetic drugs act through inhibition of digestion of complex carbohydrates in the gastrointestinal tract. To determine if some of the plant extracts could act at this level, they were tested to determine their inhibition of PTP1B, alpha-glucosidase and alpha-amylase. The results obtained for PTP1B indicated that the plant extracts of hexane of *T. zanonii* ( $K_i$   $1.18 \pm 0.006$ ), hexane and ethyl acetate of *H. radicata* ( $K_i$   $1.207 \pm 0.008$  and  $1.301 \pm 0.006$   $\mu\text{g/ml}$ ) and the root hexane extract and aerial part hexane extract of *A. cyrenaicum* ( $K_i$   $1.902 \pm 1.51$   $\mu\text{g/ml}$  and  $1.65 \pm 1.37$   $\mu\text{g/ml}$ ) displayed PTP1B inhibition. The results obtained for  $\alpha$ -glucosidase indicated that plant extract of *H. radicata* ( $K_i$  value of  $2.160 \pm 1.007$   $\mu\text{g/ml}$ ) displayed  $\alpha$ -glucosidase inhibition. The results obtained for  $\alpha$ -amylase indicated that no any plant extract displayed activity. Based on previous phytochemical and studies and the results from this study, it can be concluded that *T. zanonii*, *A. cyrenaicum* and *H. radicata* should be further investigated to identify the compounds responsible for its promising *in vitro* antidiabetic activity.

#### **4.2.4 Overall evaluation of the cytotoxicity and antidiabetic activities of the crude extracts**

The summarising results of the cytotoxicity and the antidiabetic activities in this study are presented in Table 4.4. The hexane, ethyl acetate and methanol extracts of *A. cyrenaicum* showed a lack of toxicity against cancer cells as explained in section 3.7.1. The isolated compounds were low in quantity with impurities. The purification work on these compounds has not yet been completed because of the limited quantities of plant materials. Thus, for future work, the same chromatographic procedures could be repeated with larger amounts of the fractions to improve the yields. Also, further separation and subsequent purification have to be continued to purify the isolated compounds. However, the activity of the extracts containing these compounds was evaluated as discussed earlier and the results were very not promising. These findings may be attributed to the extraction procedures and different seasonal variation of the plant; for example, the localities and time of collection could be affected on constituents of the plant. While the root and aerial part hexane extracts of *A. cyrenaicum* possessed high antidiabetic activity on PTP1B enzyme. Therefore, further work is required to isolate and test a pure compound for their inhibition of the enzyme PTP1B.

**Table 4.4:** Summary of the cytotoxicity effects of crude extracts and their constituents from the plants in this study.

Plant Name	Extract /or Compound	Code	Cancer cells	Normal cells	Anti-diabetic
<i>A. cyrenaicum</i>	Aerial part hexane extract	aerial part H	---	---	PTP1B
	Root hexane extract	root H	HeLa (181.3µg/ml) and HepG2 (128.3 µg/ml)	HEKa (136.6 µg/ml) and PNT2 (140.7 µg/ml)	PTP1B
	Fruit hexane extract		---	HEKa (215.8 µg/ml)	---
	Fruit. EtOAc extract	fruit EtOAc	---	HEKa (116.3 µg/ml)	---
	Fruit MeOH extract	fruit MeOH	---	HEKa (219.3 µg/ml)	
<i>P. tortuosus</i>	Hexane extract	PTH	A375 (76.97 µg/ml), PANC-1(86.57 µg/ml), LNCaP (195.5 µg/ml), PC-3M(154.3 µg/ml)and HepG2(140.2 µg/ml)	PNT2 (80.30 µg/ml)	---
	Ethyl acetate extract	PTEtOAc	PANC-1 (174.33 µg/ml)	PNT2 (216.3 µg/ml)	---
	Vanillic acid	PTH-6-7	A375 (70.11 µg/ml), PC-3M (72.20 µg/ml), PANC-1 (75.88 µg/ml)and HepG2 (90.29 µg/ml)	PNT2 (136.16 µg/ml)	---
<i>T. zanonii</i>	Hexane extract	TZH	PANC-1 (132.9 µg/ml)	HEKa (113.1 µg/ml) and PNT2 (157.3 µg/ml)	PTP1B
	Ethyl acetate extract	TZ EtOAc	A375 (47.24 µg/ml), LNCaP 61.60 µg/ml), and PANC-1 (174.1 µg/ml)	HEKa (145.8 µg/ml) and PNT2 (143.1 µg/ml)	---
	Methanol extract	TZ MeOH	PANC-1 (62.02 µg/ml) and LNCaP (135.99 µg/ml)	HEKa (141.9 µg/ml), PNT2 (195.1 µg/ml)	---
	Salvigenin	TZH-103-107-9	PANC-1 (148.9 µg/ml)	PNT2 (179.8 µg/ml)	---
	Ferulic acid ester of fatty alcohol(s)	TZH-41-49	HeLa (156.90 µg/ml)	---	---

**Table 4.4:** (continued).

Plant Name	Extract /or Compound	Code	Cancer cells	Normal cells	anti-diabetic
<i>H. radicata</i>	Hexane extract	HRH	LNCaP (24.59 µg/ml), PANC-1 (39.08 µg/ml), PC-3M, HepG2 (40.18 µg/ml), A375 (76.35 µg/ml) and HeLa (55.11 µg/ml)	HEKa (144.5 µg/ml) and PNT2 (11.02 µg/ml)	PTP1B and α-glucosidase
	Ethyl acetate extract	HR EtOAc	HeLa (137.45 µg/ml), PC-3M (163.13 µg/ml), PANC-1 (145.39 µg/ml) and HepG2 (63.43 µg/ml)	HEKa (135.9 µg/ml) and PNT2 (74.99 µg/ml)	PTP1B
	Methanol extract	HR MeOH	---	PNT2 (184.5 µg/ml)	---
	Luteolin	HRE-21	PC-3M (122.3 µg/ml) and HepG2 (36.59 µg/ml)	PNT2 (88.25µg/ml)	---
	Daucosterol ester of <i>trans p</i> - coumaric acid	HRE-94	A375 (122.9 µg/ml), LNCaP (162.5 µg/ml) and HepG2 (156.9 µg/ml)	PNT2 (156.0 µg/ml)	---
<i>S. sodomaeum</i>	Ethyl acetate	SS EtOAc	LNCaP (250 µg/ml)		---
	Methanol	SSM	LNCaP 18.95, µg/ml PC-3M 18.37 µg/ml), A375 (93.58 µg/ml), HeLa (29.20, PANC-1 (8.72 µg/ml) and HepG2 (18.98 µg/ml)	HEKa (139.9 µg/ml) and PNT2 (67.17 µg/ml)	---
	Cholorgenic acid	SSM-56	LNCaP (131.77 µg/ml), PC-3M (80.42 µg/ml), HepG2 (119.7 and PANC-1(20.19 µg/ml)		---

The hexane extract of *P. tortuosus* mainly composed of phenolic compounds and fats as explained earlier. One compound (PH6-7) was isolated from this extract. The preliminary results for the hexane extract were found to be highly active at both cancer and normal cells at tested concentrations. Vanillic acid (PH6-7) showed that only the former exhibited high activity on A375, PC-3M, PANC-1 and HepG2.

The hexane extract of *T. zanonii* mainly composed of flavonoid compounds, fats, in addition to pheophytins, as explained earlier. The EtOA of *T. zanonii* extract had selective anti-melanoma and anti-prostate activity as explained in section 3.7.3. The activity of the The EtOA crude extract of the *T. zanonii* could be attributable to other non-purified phytochemicals and the methanol extract had selective activity to pancreatic cancer and it mainly composed of phenylethanoid glycosides type compounds (poliumoside). In the literature poliumoside was found to possess antioxidant and anti-inflammatory activities (Guo *et al.*, 2014). However, it could be particular activity of TZM-24. Only the hexane extract of *T. zanonii* possessed high anti-diabetic activity on PTP1B enzyme. These results provide scientific evidence to support the traditional use of *T. zanonii* and demonstrate that the inhibitory effect might be attributable to the flavonoids or ferulic acid has the ability to inhibit a PTP1B enzyme.

Positive results were obtained from this study. It is however, recommended that further assays be performed on the *T. zanonii* plant evaluated for their hypoglycaemic activity and toxicity. This should be done by using an aqueous extracts as used by traditional healers and herbalists because in this study, hypoglycaemic activity comes from the hexane extract.

On the other hand, the EtOAc extract of *H. radicata* was selective toward liver (HepG2) cancer cells than other cancer cells. The preliminary results for luteolin (HRE-21) showed selective activity against HepG2 at 127.82  $\mu$ M. By considering all the aforementioned data, the anti-hepatoma activity of the EtOAc extract of the *H. radicata* could be attributed to the isolated compound HRE-21, and the results were very promising. For anti-diabetic screening, the hexane and ethyl acetate of *H.*

*radicata* inhibited PTP1B. Only *H. radicate* hexane extract inhibited alpha-glucosidase.

The methanol extract of the *S. sodomaeum* was selective against cancer cells. This extract had anti-pancreatic activity against PANC-1 cells by inhibiting adhesion on fibronectin and collagen IV in the ECM and inhibited their migration and invasion. The methanol extract of the *S. sodomaeum* was mainly composed of phenolic compounds and steroidal glycoalkaloids. This activity of antiadhesion, migration and invasion of this extract was due to the presence of SSM-56.

This study also gave an indication of the toxicity of some of the plant extracts where this information was available. The method of preparation and administration of medicines used by traditional healers is the starting point to design experimental protocols aimed at finding scientific evidence of efficacy and toxicity. The ability to produce safe, standardised medicinal plant products for further clinical evaluation is a major stumbling block in most countries wishing to enhance the quality of their traditional medicines.

### **5.1 Recommendations for future**

The most significant issue in this study was the impact on the work of limited quantities of *A. cyrenaicum*, dried plant stocks and the lack of fresh plant material. Therefore, if further work is to be carried out large quantities of fresh plant material should be made available for an in-depth study. The lack toxicity of this plant could be time of collection of the plant therefore; this could be collected plant from different location and time of year (season) provide different results, therefore future work could be targeted for further separation and purification with choosing, a suitable time of collection the plant during the year and locations. Future work would entail isolating the phenolic derivative as well as evaluating the antidiabetic activity of the pure isolates. The future work will involve a detailed study on the antidiabetic activity of the hexane extract in a diabetes model of rats as well as the purified compounds should be tested for their inhibition of the enzyme alpha-amylase and alpha-glucosidase.

It is also recommended that the hexane extract of *T. zanonii* should be tested *in vivo* in a rat or mouse model for its hypoglycaemic activity as the activity of some of the plant extracts may differ *in vitro* and *in vivo*.

The hexane extract of *H. radicata* exhibited highly toxic on both cancer and normal cells but not selective, therefore using nano-sized drug delivery system (nanoparticles) such as ligand–receptor interactions (“active targeting”) to deliver it to cancer cells and nanoparticles can be programmed for recognizing the cancerous cells and giving selective and accurate drug delivery avoiding interaction with the normal cells (Bae and Park, 2011) is recommended to use in future work as well as a more detailed phytochemistry in the hexane fraction of *H. radicata*. Based on previous phytochemical studies and the results from this study, we conclude that *H. radicata* should be further investigated to identify the compounds responsible for its promising *in vitro* antidiabetic activity.

The ethyl acetate extract of *H. radicata* showed had selective effects on the hepatoma cells; however, more work will be required to be carried out on these cells and on other types of cancer cell lines using different protocols such as MTT assay, especially for the isolated compound (luteolin) which exerted potent activity, even at the lowest tested concentration. It is also important to investigate the mechanism of action applied by the active compound to determine whether the mode of cell death is apoptosis or necrosis by observing the morphological and the biochemical features of the cells.

Further work could focus on *H. radicata* plant extracts to isolate the new compound HRE-94 in sufficient quantities to complete analysis of 2D NMR and carried out to test it on other cell lines.

The SSM extract and pure compound SSM-56 may have anti-metastatic effect on pancreatic cancer and could be used for production of safer, natural and active anti-metastatic lead candidate drugs. It has been explored that the pancreatic cancer cells are resistance to chemotherapy more than single cells (Gnanamony and Gondi, 2017), so future work could focus on three-dimensional (3D) *in vitro* models (Weiswald *et*

*al.*, 2015). Furthermore, future work would need to focus on *in vivo* assessment, initially using a suitable rodent experimental model to improve pancreatic cancer patient outcomes.

## 5.2 Conclusion

The aim of this project was to investigate the anticancer or antidiabetic activity of five Libyan plants. A total of 17 compounds, including triterpenes, flavonoids, pheophytin, simple phenolics, phenylethanoid glycoside, phenolic acids, fatty acid, flavonoid glycosides and steroid-glycoalkaloid were isolated from these plants. Most of these compounds were isolated for the first time from these plants.

Cytotoxic activity was carried out for the plant extracts and the isolated compounds. Only the root hexane extract of *A. cyrenaicum* showed weak toxicity to the normal and cancer cells at 250 µg/ml and the fruit of *A. cyrenaicum* extracts showed toxicity on normal cells. While the hexane extract of *P. tortuosus* showed toxicity against normal and cancer cells but the ethyl acetate extract of *P. tortuosus* showed only toxicity against A375, PANC-1 and PNT2 cell lines at 250 µg/ml. However, vanillic acid (PTH-6-7) from hexane extract presented preferable effects on the melanoma, pancreatic and hepatoma cells with IC<sub>50</sub> of 70.11, 75.88 and 72.20 µg/ml, respectively. The ethyl acetate extract of *T. zanonii* showed selective effects on the melanoma and prostate cancer cells with IC<sub>50</sub> of 47.24 µg/ml and 61.60 µg/ml, respectively, while the methanol extract of *T. zanonii* showed selective cytotoxicity to the pancreatic cancer cells with IC<sub>50</sub> of 62.02 µg/ml. On the other hand, the hexane extract of *H. radicata* exhibited highly toxicity toward both normal and cancer cells; but the ethyl acetate extract showed only selective effects on the hepatoma cells with IC<sub>50</sub> of 63.43 µg/ml. Luteolin (HRE-21) from the ethyl acetate extract showed selective effects on the hepatoma cells with IC<sub>50</sub> of 36.59 µg/ml. However, the methanol extract of *S. sodomaicum* (SSM) was most toxic against PANC-1 cells (8.72 µg/ml) and toxic to normal cells PNT2 and HEKa (139.9 µg/ml) and (67.17 µg/ml). Cholorogenic acid (SSM-56) showed highly toxicity against PANC-1 cells (56.98 µM) while SSM-56 did not show toxicity against the normal cell line. Due to lack or highly toxicity of extracts

or compounds on cells, therefore, SSM extract and SSM-56 were chosen anti-metastatic against PANC-1 cells. Both SSM extract and SSM-56 showed anti-metastatic against PANC-1 cells. So SSM extract and SSM-56 are promising anticancer therapeutics against PANC-1 cells. Furthermore, we were able to identify one lead compound from *S. sodomaicum*, SSM-56, with promising anticancer activity for pancreatic cancer. Thus, SSM-56 could be a source of promising treatments for pancreas cancers in the near future.

The hexane extracts of *T. zanonii*, *H. radicata* and the root and aerial part of *A. cyrenaicum* and the ethyl acetate extracts of *H. radicata* inhibited PTP1B enzyme at 30µg/ml. Only the hexane extract of *H. radicate* inhibited  $\alpha$ -glucosidase. The current study appear to be the first to investigate the inhibitory effects of *T. zanonii* *H. radicata* *A. cyrenaicum* extracts on the activity of diabetes related carbohydrate metabolizing enzymes.

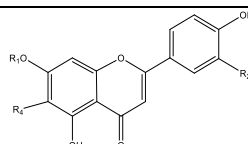
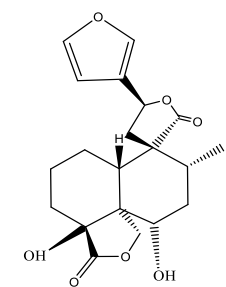
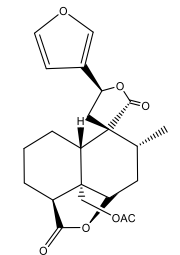
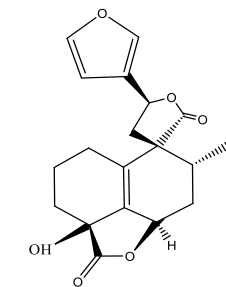
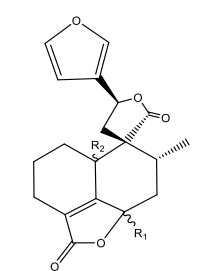
This provides some scientific support for the traditional use of *T. zanonii* (aerial parts in particular) as anti- diabetic therapy.

Overall, these results reveal that traditional medicinal plants such as this one have potential as a source of natural anticancer agents available to fight cancer or others have anti-diabetic agent.

## *Appendices*

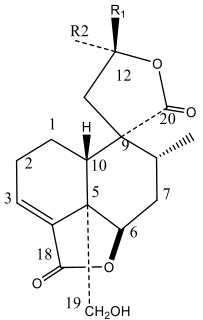
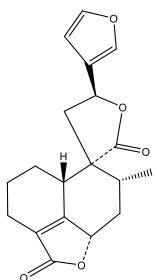
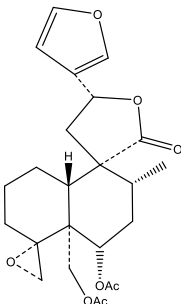
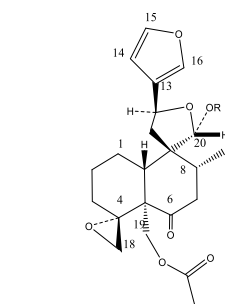
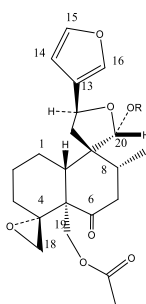
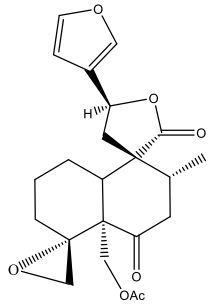
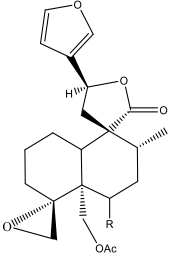
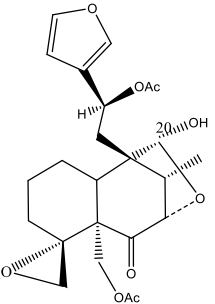
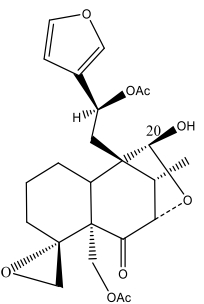
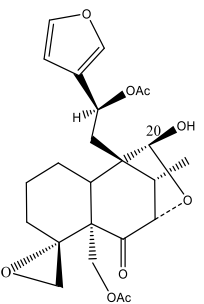
Appendix I

**Table 1.6 :** Selection of phytochemicals previously isolated from the Lamiaceae family. *Teucrium* (T) species

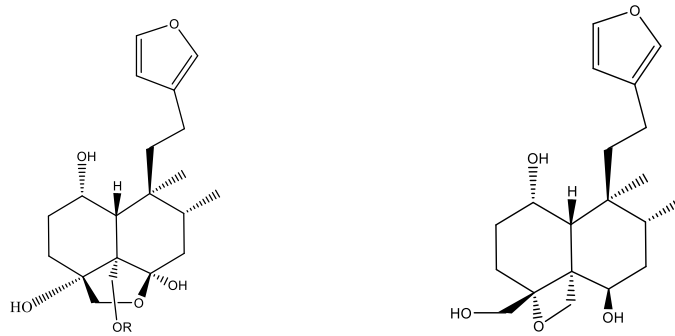
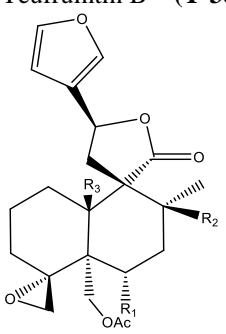
Classification	Compound	Parts of the plant	Reference
			(Elmasri <i>et al.</i> , 2015b; Lv <i>et al.</i> , 2014b)
	Acacetin (T-17)	R <sub>1</sub> H	Aerial parts of <i>T. polium</i> and whole plant of <i>T. viscidum</i>
	Cirsimaritin (T-18)	R <sub>2</sub> H	
	Apigenin 7-O-glucoside (T-19)	R <sub>3</sub> OMe	
	3',4',5-trihydroxy-6,7-dimethoxy-flavone (T-20)	R <sub>4</sub> H	
	5,6,7,3',4'-pentahydroxyflavone (T-21)	R <sub>1</sub> OMe, R <sub>2</sub> OH, R <sub>3</sub> OH, R <sub>4</sub> OH	
<b>Terpenoids</b>			
<b>19-nor-neoclerodane diterpenoids</b>			
			
			
		R <sub>1</sub> β-OH, R <sub>2</sub> β-H R <sub>1</sub> α-H, R <sub>2</sub> α-OH	

Appendix I

Table 1.6 (continued): Selection of phytochemicals previously isolated from the Lamiaceae family. *Teucrium* (T) species

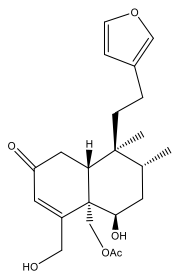
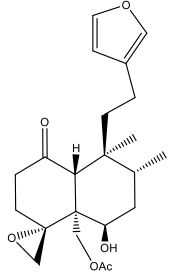
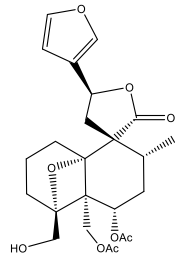
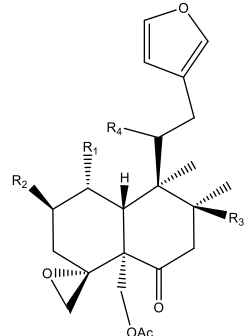
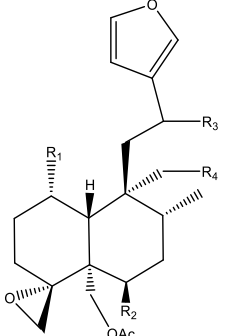
Classification	Compound	Parts of the plant	Reference
	 <p>(12R)-epi-teuscordonin R<sub>1</sub>=H, R<sub>2</sub>=β-furyl (T-27)</p>		Labbe <i>et al.</i> , 1989
	 <p>Teucvin (T-28)</p>		(Venditti <i>et al.</i> , 2017, Bruno <i>et al.</i> , 2004)
	 <p>Montanin C (T-29)</p>		
	 <p>Teucrasiatin (T-30) R = H</p>		
	 <p>20-O-acetyl-teucrasiatin (T-31) R = Ac</p>		
	 <p>19-acetyl-gnaphalin (T-32)</p>		
	 <p>Auropolin (T-33)</p>		
	 <p>20-epi-auropolin (T-34)</p>		
	 <p>Isoeriocephalin (T-35)</p>		
	 <p>6-acetyl-picropolin (T-36)</p>		

**Table 1.6 (continued):** Selection of phytochemicals previously isolated from the Lamiaceae family. *Teucrium* (T) species

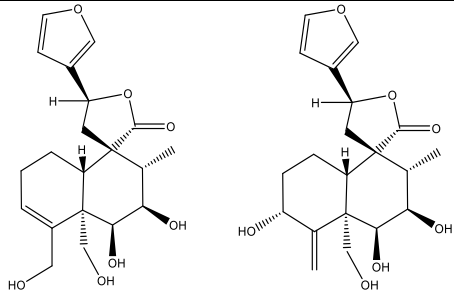
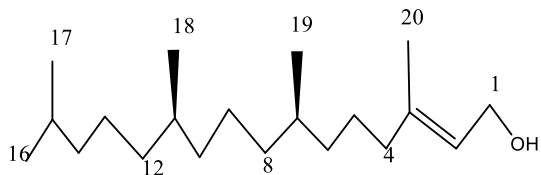
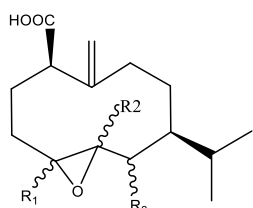
Classification	Compound	Parts of the plant	Reference												
		Aerial parts of <i>T. fruticans</i>	(Lv <i>et al.</i> , 2015)												
	<p>TeufruintinA(T-37)R=A Teufruintin B (T-38) R = H</p> 														
	<p>Teufruintin E (T-40) 6-acetyl-10-hydroxyteucjaponin B (T-41) 6-acetyl-teucjaponin B (T-42)</p>	<table border="0"> <thead> <tr> <th><b>R<sub>1</sub></b></th> <th><b>R<sub>2</sub></b></th> <th><b>R<sub>3</sub></b></th> </tr> </thead> <tbody> <tr> <td>αOAc</td> <td>OH</td> <td>H</td> </tr> <tr> <td>βOAc</td> <td>H</td> <td>OH</td> </tr> <tr> <td>βOAc</td> <td>H</td> <td>H</td> </tr> </tbody> </table>	<b>R<sub>1</sub></b>	<b>R<sub>2</sub></b>	<b>R<sub>3</sub></b>	αOAc	OH	H	βOAc	H	OH	βOAc	H	H	
<b>R<sub>1</sub></b>	<b>R<sub>2</sub></b>	<b>R<sub>3</sub></b>													
αOAc	OH	H													
βOAc	H	OH													
βOAc	H	H													

Appendix I

Table 1.6 (continued): Selection of phytochemicals previously isolated from the Lamiaceae family. *Teucrium* (T) species

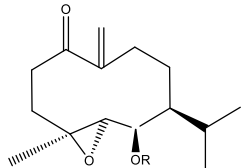
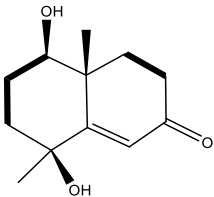
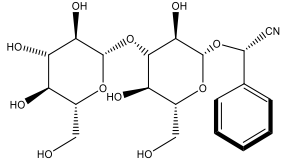
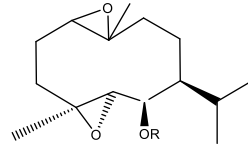
Classification	Compound	Parts of the plant	Reference																																																
		Aerial parts and whole plants of <i>T. polium</i>	(Bedir <i>et al.</i> , 1999, Venditti <i>et al.</i> , 2017)																																																
																																																			
																																																			
																																																			
																																																			
	<table border="0"> <tr> <td>Teufruintin G (T-46)</td> <td>R<sub>1</sub></td> <td>R<sub>2</sub></td> <td>R<sub>3</sub></td> <td>R<sub>4</sub></td> <td></td> </tr> <tr> <td></td> <td>H</td> <td>OH</td> <td>H</td> <td>H</td> <td></td> </tr> <tr> <td>Fruticolone (T-47)</td> <td></td> <td></td> <td></td> <td></td> <td></td> </tr> <tr> <td></td> <td>OH</td> <td>H</td> <td>H</td> <td>H</td> <td></td> </tr> <tr> <td>8β-hydroxyfruticolone (T-48)</td> <td></td> <td></td> <td></td> <td></td> <td></td> </tr> <tr> <td></td> <td>OH</td> <td>H</td> <td>OH</td> <td>H</td> <td></td> </tr> <tr> <td>11-hydroxyfruticolone(T-49)</td> <td></td> <td></td> <td></td> <td></td> <td></td> </tr> <tr> <td></td> <td>OH</td> <td>H</td> <td>H</td> <td>OH</td> <td></td> </tr> </table>	Teufruintin G (T-46)	R <sub>1</sub>	R <sub>2</sub>	R <sub>3</sub>	R <sub>4</sub>			H	OH	H	H		Fruticolone (T-47)							OH	H	H	H		8β-hydroxyfruticolone (T-48)							OH	H	OH	H		11-hydroxyfruticolone(T-49)							OH	H	H	OH			
Teufruintin G (T-46)	R <sub>1</sub>	R <sub>2</sub>	R <sub>3</sub>	R <sub>4</sub>																																															
	H	OH	H	H																																															
Fruticolone (T-47)																																																			
	OH	H	H	H																																															
8β-hydroxyfruticolone (T-48)																																																			
	OH	H	OH	H																																															
11-hydroxyfruticolone(T-49)																																																			
	OH	H	H	OH																																															
	<table border="0"> <tr> <td>Teucretol (T-50)</td> <td>R<sub>1</sub></td> <td>R<sub>2</sub></td> <td>R<sub>3</sub></td> <td>R<sub>4</sub></td> <td></td> </tr> <tr> <td></td> <td></td> <td></td> <td></td> <td></td> <td></td> </tr> <tr> <td>6α-hydroxyfruticolone(T-51)</td> <td></td> <td></td> <td></td> <td></td> <td></td> </tr> </table>	Teucretol (T-50)	R <sub>1</sub>	R <sub>2</sub>	R <sub>3</sub>	R <sub>4</sub>								6α-hydroxyfruticolone(T-51)																																					
Teucretol (T-50)	R <sub>1</sub>	R <sub>2</sub>	R <sub>3</sub>	R <sub>4</sub>																																															
6α-hydroxyfruticolone(T-51)																																																			

**Table 1.6 (continued):** Selection of phytochemicals previously isolated from the Lamiaceae family. *Teucrium* (T) species

Classification	Compound	Parts of the plant	Reference
		Aerial parts and whole plants of <i>T. polium</i>	(Bedir <i>et al.</i> , 1999, Venditti <i>et al.</i> , 2017)
			
	<p>Teulolin A (T-52)      Teulolin B (T-53)      (E)-Phytol (T-54)</p>		
Sesquiterpenes			
	<p>4<math>\beta</math>,5<math>\alpha</math>-epoxy-7<math>\alpha</math>H-germacr-10(14)-en,1<math>\beta</math>-hydroperoxyl,6<math>\beta</math>-ol; <b>R<sub>1</sub></b> <b>R<sub>2</sub></b> <b>R<sub>3</sub></b>  <math>\alpha</math>-Me <math>\beta</math>-H <math>\beta</math>-OH (T-55)  4<math>\beta</math>,5<math>\beta</math>-epoxy-7<math>\alpha</math>H-germacr-10(14)-en,1<math>\beta</math>-hydroperoxyl,6<math>\beta</math>-ol; <b>R<sub>1</sub></b> <b>R<sub>2</sub></b> <b>R<sub>3</sub></b>  <math>\alpha</math>-Me <math>\alpha</math>-H <math>\beta</math>-OH (T-56)  4<math>\alpha</math>,5<math>\beta</math>-epoxy-7<math>\alpha</math>H-germacr-10(14)-en,1<math>\beta</math>-hydroperoxyl,6<math>\alpha</math>-ol, <b>R<sub>1</sub></b> <b>R<sub>2</sub></b> <b>R<sub>3</sub></b>  <math>\beta</math>-Me <math>\alpha</math>-H <math>\alpha</math>-OH (T-57)</p>		(Elmasri <i>et al.</i> , 2014a) (Elmasri <i>et al.</i> , 2016)

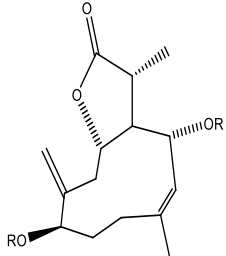
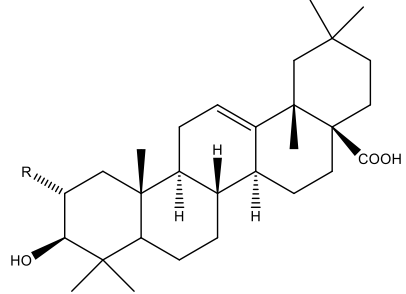
*Appendix I*

**Table 1.6 (continued):** Selection of phytochemicals previously isolated from the Lamiaceae family. *Teucrium* (T) species

Classification	Compound	Parts of the plant	Reference
	 <p>4β,5α-epoxy-7αH-germacr- 10(14)-en-6β-ol-1-one(<b>T-58</b>)  <b>R</b>            1b S-MTPA            1a R-MTPA</p>	Aerial parts <i>T.polium</i>	(Elmasri <i>et al.</i> , 2014a) (Elmasri <i>et al.</i> , 2016)
	 <p>(1<i>R</i>, 4<i>S</i>, 10<i>R</i>)            10,11-dimethyl-dicyclohex-5(6)-            en-1,4-diol-7-one (<b>T-59</b>)</p>		
Sesquiterpenes	 <p>(<i>R</i>)-mandelonitrile-β-laminaribioside (<b>T-60</b>)</p>		
	 <p>(10<i>R</i>,1<i>R</i>,4<i>S</i>,5<i>S</i>,6<i>R</i>,7<i>S</i>)-4,10-diepoxygermacran-6-            Ol (<b>T-61</b>)</p>		

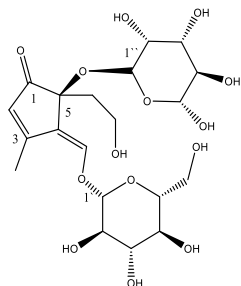
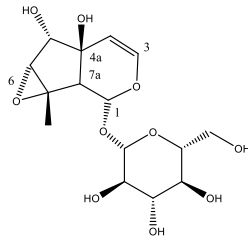
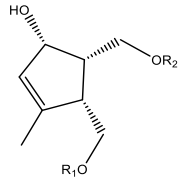
**Appendix I**

**Table 1.6 (continued):** Selection of phytochemicals previously isolated from the Lamiaceae family. *Teucrium* species T: refers to the name of the *Teucrium*

Classification	Compound	Parts of the plant	Reference
	 <p>(1<i>R</i>,6<i>R</i>,7<i>R</i>,8<i>S</i>,11<i>R</i>)-1,6-dihydroxy-4,11-dimethyl- germacran-4(5), 10(14)-dien-8,12-olide(<b>T-62</b>)</p>	Aerial parts of <i>T. polium</i>	(Elmasri <i>et al.</i> , 2016)
<b>Triterpenoids</b>	 <p>Oleanolic acid (<b>T-63</b>)      R=H  Maslinic acid (<b>T-64</b>)      R=OH</p>		

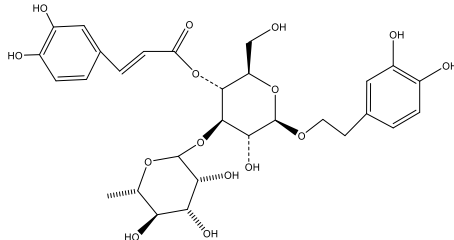
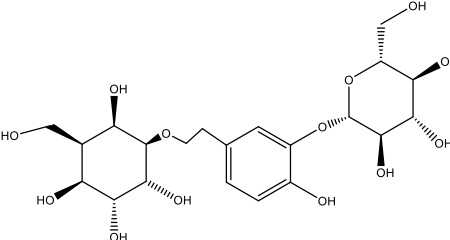
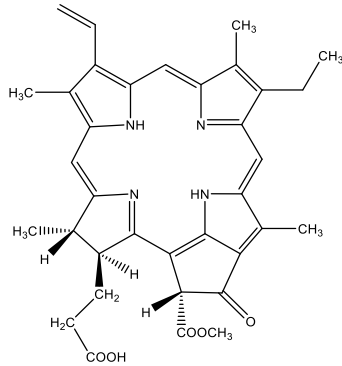
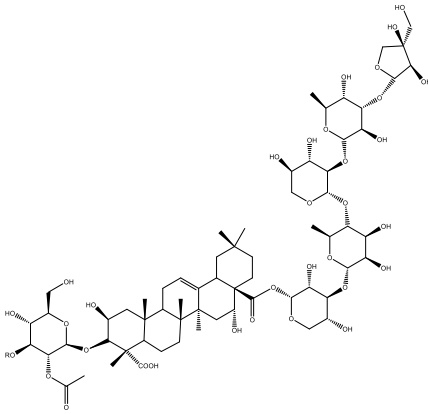
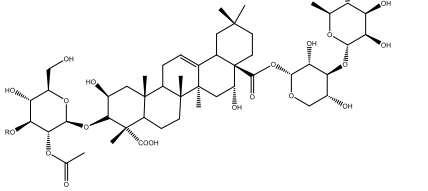
Appendix I

**Table 1.6 (continued):** Selection of phytochemicals previously isolated from the Lamiaceae family. *Teucrium* species T: refers to the name of the *Teucrium*

Classification	Compound	Parts of the plant	Reference
Iridoid derivatives	 <p>4-[(β-D-glucopyranosyloxy)methylene]-5α-(2-hydroxyethyl)-5-(α-L-rhamnopyranosyloxy)-3-methylcyclopent-2-en-1-one (<b>T-65</b>)</p>	Aerial parts of <i>T. polium</i>	(Elmasri <i>et al.</i> , 2015b)
	 <p>1α-(β-D-glucopyranosyloxy)-6α,7α-epoxy-4αβ,5α-dihydroxy-7-methyl-1,4a,5,6,7,7aβ-hexahydrocyclopenta[c]pyran (<b>T-66</b>)</p>		
	 <p>4α-[(β-D-glucopyranosyloxy)methyl]-5α-(2-hydroxyethyl)-3-methylcyclopent-2-en-1-one; (<b>T-67</b>) <b>R<sub>1</sub></b> =Glc<b>R<sub>2</sub></b>=H</p>		
	<p>5α-[2-(β-D-glucopyranosyloxy)ethyl]-4α-hydroxymethyl-3-methylcyclopent-2-en-1-one; (<b>T-68</b>) <b>R<sub>2</sub></b>=Glc, <b>R<sub>1</sub></b>=H</p>		
	<p>5α-(2-hydroxyethyl)-4α-hydroxymethyl-3-methylcyclopent-2-en-1-one; (<b>T-69</b>) <b>R<sub>1</sub></b> =H, <b>R<sub>2</sub></b>=H</p>		

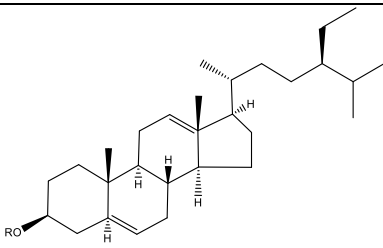
**Appendix I**

**Table 1.6 (continued):** Selection of phytochemicals previously isolated from the Lamiaceae family. *Teucrium* species T: refers to the name of the *Teucrium*

Classification	Compound	Parts of the plant	Reference
Phenylethanoid glycosides	 <p align="center">Verbascoside (<b>T-70</b>)</p>	Whole plants and aerial parts of <i>T. polium</i>	(Elmasri <i>et al.</i> , 2015a, Venditti <i>et al.</i> , 2017)
	 <p align="center">3-(<i>O</i>-<math>\beta</math>-D-glucopyranosyl)-<math>\alpha</math>-(<i>O</i>-<math>\beta</math>-D-glucopyranosyl)-4-hydroxyphenylethanol (<b>T-71</b>)</p>		
Saponins	 <p align="center">Pheophorbide a (<b>T-72</b>)</p>		
	 <p align="center">Poliusaposide A <b>R =Glu (T-73)</b></p>		
	 <p align="center">Poliusaposide B <b>R =H(T-74)</b></p>		

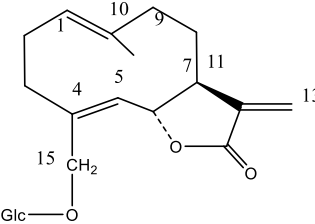
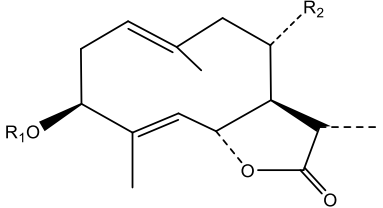
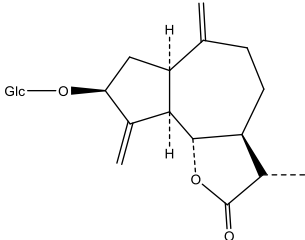
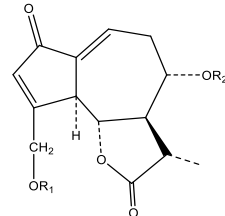
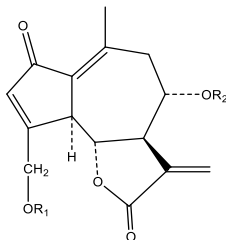
## Appendix I

**Table 1.6 (continued):** Selection of phytochemicals previously isolated from the Lamiaceae family. *Teucrium* species T: refers to the name of the *Teucrium*

Classification	Compound	Parts of the plant	Reference
Steroids	 <p style="text-align: center;"> <math>\beta</math>-sitosterol                      Daucosterol;                 </p> <p style="text-align: center;"> <b>R=H (T-75)</b>  <b>R= Glc(T-76)</b> </p>		

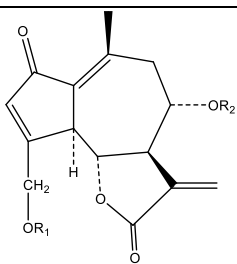
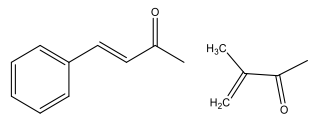
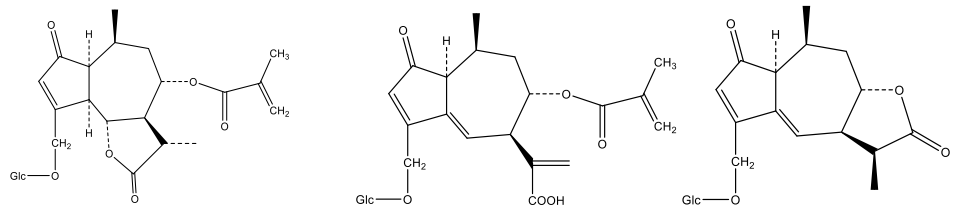
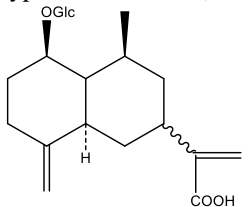
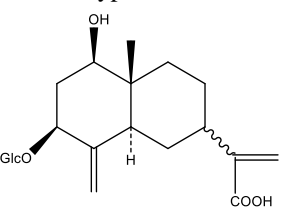
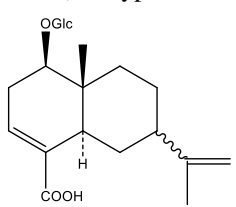
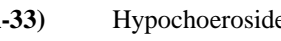
Appendix II

**Table 1.7:** Selection of phytochemicals previously isolated from Asteraceae. HR: refers to the name of the *H. radicata*

Classification	Compound	Parts of the plant	Reference								
Terpenoids Sesquiterpenes	 <p>Picriside B (<b>HR-17</b>)</p>	leaves and roots <i>H. radicata</i>	(Jamuna <i>et al.</i> , 2015; Ohmura <i>et al.</i> , 1989)								
	 <p>Sonchuside A (<b>HR-18</b>)</p> <p>Cichorioside C (<b>HR-19</b>)</p> <p>Hypochoeroside A (<b>HR-20</b>)</p> <table border="0" style="margin-left: auto; margin-right: auto;"> <tr> <td><b>R<sub>1</sub></b></td> <td><b>R<sub>2</sub></b></td> </tr> <tr> <td>Glc</td> <td>H</td> </tr> <tr> <td>Glc</td> <td>OH</td> </tr> <tr> <td>H</td> <td>OGlc</td> </tr> </table>			<b>R<sub>1</sub></b>	<b>R<sub>2</sub></b>	Glc	H	Glc	OH	H	OGlc
<b>R<sub>1</sub></b>	<b>R<sub>2</sub></b>										
Glc	H										
Glc	OH										
H	OGlc										
	 <p>IxerinF (<b>HR-21</b>)</p>										
	 <p>11,13-dihydrolactucin (<b>HR-22</b>)</p> <p>Cichorioside B (<b>HR-23</b>)</p> <p>Hypochoeroside B (<b>HR-24</b>)</p> <table border="0" style="margin-left: auto; margin-right: auto;"> <tr> <td><b>R<sub>1</sub></b></td> <td><b>R<sub>2</sub></b></td> </tr> <tr> <td>H,</td> <td>H</td> </tr> <tr> <td>Glc,</td> <td>H</td> </tr> <tr> <td>Glc,</td> <td>M</td> </tr> </table>	<b>R<sub>1</sub></b>	<b>R<sub>2</sub></b>	H,	H	Glc,	H	Glc,	M		
<b>R<sub>1</sub></b>	<b>R<sub>2</sub></b>										
H,	H										
Glc,	H										
Glc,	M										
	 <p>Hypochoeroside C (<b>HR-25</b>)</p> <p>Picriside A (<b>HR-26</b>)</p> <p>Hypochoeroside D (<b>HR-27</b>)</p> <table border="0" style="margin-left: auto; margin-right: auto;"> <tr> <td><b>R<sub>1</sub></b></td> <td><b>R<sub>2</sub></b></td> </tr> <tr> <td>Glc,</td> <td>M</td> </tr> <tr> <td>Glc,</td> <td>H</td> </tr> <tr> <td>Glc,</td> <td>C</td> </tr> </table>	<b>R<sub>1</sub></b>	<b>R<sub>2</sub></b>	Glc,	M	Glc,	H	Glc,	C		
<b>R<sub>1</sub></b>	<b>R<sub>2</sub></b>										
Glc,	M										
Glc,	H										
Glc,	C										

Appendix II

Table 1.7: Selection of phytochemicals previously isolated from Asteraceae. HR: refers to the name of the *H. radicata*

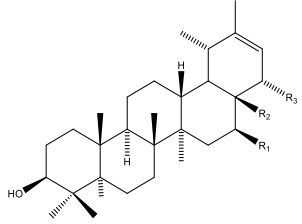
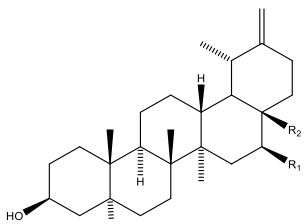
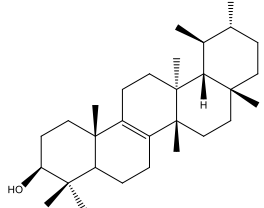
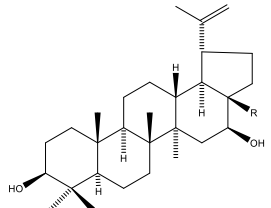
Classification	Compound	Parts of the plant	Reference
Terpenoids Sesquiterpenes		leaves and roots <i>H. radicata</i>	(Jamuna <i>et al.</i> , 2015; Ohmura <i>et al.</i> , 1989)
		Leaves and flower heads of <i>S. balsamita c</i>	(Mukhametzhanov <i>et al.</i> , 1971; Adekenov, 1995; Ivanescu <i>et al.</i> , 2015)
	<p>Hypochoeroside E (HR-28); R<sub>1</sub>= Glc, R<sub>2</sub>= M</p> <p>Hypochoeroside F (HR-29); R<sub>1</sub>=Glc, R<sub>2</sub>= C</p> 		
	<p>Hypochoeroside G (HR-30)</p> 		
	<p>Hypochoeroside H (HR-31)</p> 		
	<p>Hypochoeroside I (HR-32)</p> 		
	<p>Hypochoeroside J (HR-33)</p> 		
	<p>Hypochoeroside K (HR-34)</p> 		
	<p>Hypochoeroside L (HR-35)</p> 		

**Appendix II Table 1.7:** Selection of phytochemicals previously isolated from Asteraceae. HR: refers to the name of the *H. radicata*

Classification	Compound	Parts of the plant	Reference
Terpenoids Sesquiterpenes		Leaves and flower heads of <i>S. balsamita c</i>	(Mukhametz hanov <i>et al.</i> , 1971; Adekenov, 1995;
	<p>Stizolin (HR-36)      Anobin (HR-37)      Anolide (HR-38)      Achimicrin (HR-39)</p>	And Genus <i>Achillea</i>	Ivanescu <i>et al.</i> , 2015)
	<p>Artausin (HR-40)      Arglabin (HR-41)      Argolide (HR-42)      Cnicin (HR-43)</p>	Aerial parts of <i>Inula aucheriana</i> and aerial parts of <i>Tanacetum parthenium</i>	(Gohari <i>et al.</i> , 2015; Tiuman <i>et al.</i> , 2005)
	<p>Salonltenolide (HR-44)      Grosshemin (HR-45)      Yomogin (HR-46)      6- deoxychamissonolide (HR-47) (stevin)</p>		

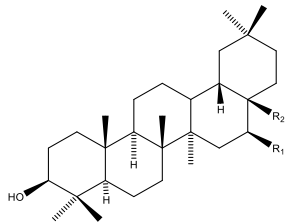
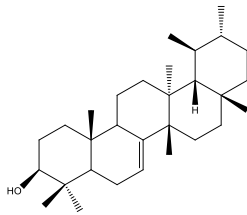
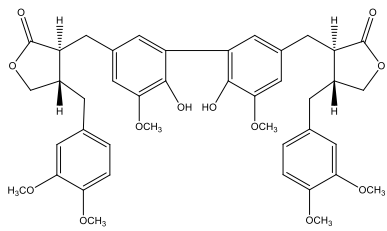
## Appendix II

**Table 1.7:** Selection of phytochemicals previously isolated from Asteraceae. HR: refers to the name of the *H. radicata*

Classification	Compound	Parts of the plant	Reference																									
Triterpenoids		Root of <i>Arctium-lappa</i> L and genus <i>Calendula</i>	(Barbosa Filho <i>et al.</i> , 1993; Arora <i>et al.</i> , 2013)																									
																												
	<table style="width: 100%; border: none;"> <tr> <td style="width: 33%;"></td> <td style="text-align: center;"><b>R<sub>1</sub></b></td> <td style="text-align: center;"><b>R<sub>2</sub></b></td> <td style="text-align: center;"><b>R<sub>3</sub></b></td> <td style="width: 33%;"></td> </tr> <tr> <td style="text-align: left;">γ-Taraxasterol (<b>HR-48</b>)</td> <td style="text-align: center;">H</td> <td style="text-align: center;">CH<sub>3</sub></td> <td style="text-align: center;">H</td> <td style="text-align: left;">Taraxasterol (<b>HR-52</b>)</td> </tr> <tr> <td style="text-align: left;">Faradiol (<b>HR-49</b>)</td> <td style="text-align: center;">OH</td> <td style="text-align: center;">CH<sub>3</sub></td> <td style="text-align: center;">H</td> <td style="text-align: left;">Heliantriol B<sub>1</sub> (<b>HR-53</b>)</td> </tr> <tr> <td style="text-align: left;">Heliantriol B<sub>0</sub> (<b>HR-50</b>)</td> <td style="text-align: center;">OH</td> <td style="text-align: center;">CH<sub>2</sub>OH</td> <td style="text-align: center;">H</td> <td style="text-align: left;"><b>R<sub>1</sub></b></td> </tr> <tr> <td style="text-align: left;">Heliantriol C (<b>HR-51</b>)</td> <td style="text-align: center;">OH</td> <td style="text-align: center;">CH<sub>2</sub>OH</td> <td style="text-align: center;">OH</td> <td style="text-align: left;"><b>R<sub>2</sub></b></td> </tr> </table>		<b>R<sub>1</sub></b>	<b>R<sub>2</sub></b>	<b>R<sub>3</sub></b>		γ-Taraxasterol ( <b>HR-48</b> )	H	CH <sub>3</sub>	H	Taraxasterol ( <b>HR-52</b> )	Faradiol ( <b>HR-49</b> )	OH	CH <sub>3</sub>	H	Heliantriol B <sub>1</sub> ( <b>HR-53</b> )	Heliantriol B <sub>0</sub> ( <b>HR-50</b> )	OH	CH <sub>2</sub> OH	H	<b>R<sub>1</sub></b>	Heliantriol C ( <b>HR-51</b> )	OH	CH <sub>2</sub> OH	OH	<b>R<sub>2</sub></b>		
	<b>R<sub>1</sub></b>	<b>R<sub>2</sub></b>	<b>R<sub>3</sub></b>																									
γ-Taraxasterol ( <b>HR-48</b> )	H	CH <sub>3</sub>	H	Taraxasterol ( <b>HR-52</b> )																								
Faradiol ( <b>HR-49</b> )	OH	CH <sub>3</sub>	H	Heliantriol B <sub>1</sub> ( <b>HR-53</b> )																								
Heliantriol B <sub>0</sub> ( <b>HR-50</b> )	OH	CH <sub>2</sub> OH	H	<b>R<sub>1</sub></b>																								
Heliantriol C ( <b>HR-51</b> )	OH	CH <sub>2</sub> OH	OH	<b>R<sub>2</sub></b>																								
																												
																												
	Isobauerenol( <b>HR-54</b> )																											
	Calenduladiol ( <b>HR-55</b> ); <b>R=CH<sub>3</sub></b> Heliantriol B <sub>2</sub> ( <b>HR-56</b> ); <b>R=CH<sub>2</sub>OH</b>																											

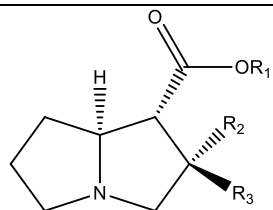
## Appendix II

**Table 1.7:** Selection of phytochemicals previously isolated from Asteraceae. HR: refers to the name of the *H. radicata*.

Classification	Compound	Parts of the plant	Reference
	 <p> <math>\beta</math>-Amyrin (HR- 57); R<sub>1</sub>= H, R<sub>2</sub>= CH<sub>3</sub>            Maniladiol (HR- 58 ); R<sub>1</sub>= OH, R<sub>2</sub>= CH<sub>3</sub>            Logispinogenin (HR- 59); R<sub>1</sub>=OH, R<sub>2</sub>=CH<sub>2</sub>OH            Erythrodiol (HR- 60 ); R<sub>1</sub>= H, R<sub>2</sub>=CH<sub>2</sub>OH         </p>		
	 <p>Bauerenol (HR- 61)</p>		
Lignans	 <p>Diarctigenin(HR- 62)</p>	Seeds of <i>Centaurea</i> <i>vlachorum</i>	(Hodaj <i>et al.</i> , 2017)

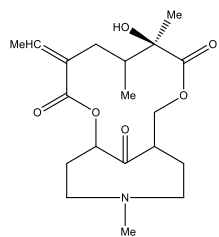
---

**Alkaloid**

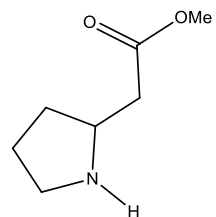


Tussilagine (**HR- 63**)  
Isotussilagine (**HR- 64**)

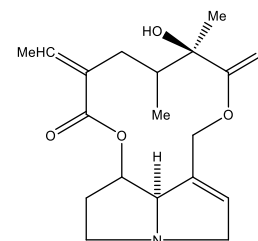
<b>R<sub>1</sub></b>	<b>R<sub>2</sub></b>	<b>R<sub>3</sub></b>
Me	OH	Me
Me	Me	OH



Senkirkine (**HR-65**)



2-Methylpyrrolidine (**HR-66**)

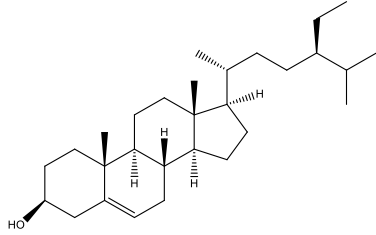
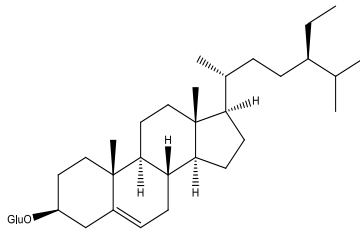
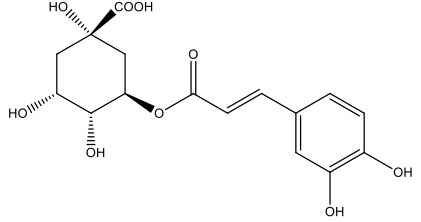
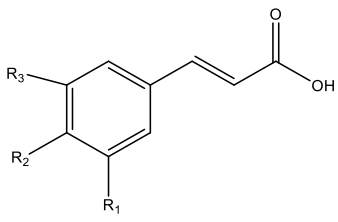
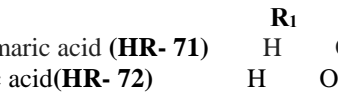
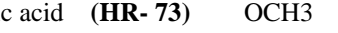
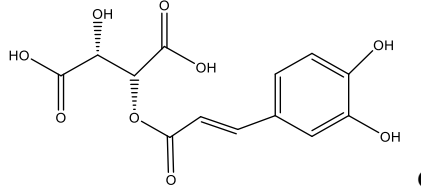


Senecionine (**HR- 67**)

---

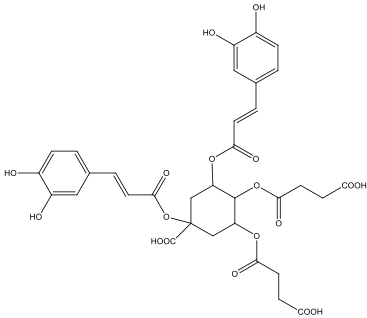
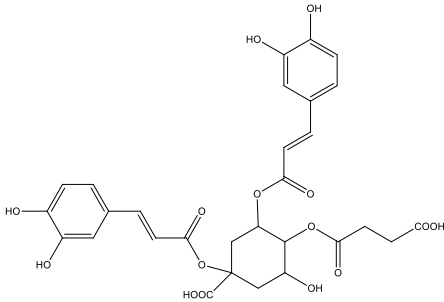
## Appendix II

**Table 1.7:** Selection of phytochemicals previously isolated from Asteraceae. HR: refers to the name of the *H. radicata*

Classification	Compound	Parts of the plant	Reference											
Sterols	 $\beta$ -sitosterol (HR- 68)	Seeds of <i>Centaurea vlachorum</i>	(Hodaj <i>et al.</i> , 2017)											
	 Sitosterol- $\beta$ -D-glucopyranoside (HR- 69)													
Polyphenol	 Chlorogenic acid (HR- 70)	Plant of <i>Artemisia dracunculus</i>	(Jaiswal <i>et al.</i> , 2011; Bohm and Stuessy, 2013)											
	 $p$ -Coumaric acid (HR- 71)													
	 Caffeic acid (HR- 72)													
	 Ferulic acid (HR- 73)													
	<table style="margin-left: auto; margin-right: auto;"> <thead> <tr> <th style="text-align: center;">R<sub>1</sub></th> <th style="text-align: center;">R<sub>2</sub></th> <th style="text-align: center;">R<sub>3</sub></th> </tr> </thead> <tbody> <tr> <td style="text-align: center;">H</td> <td style="text-align: center;">OH</td> <td style="text-align: center;">H</td> </tr> <tr> <td style="text-align: center;">H</td> <td style="text-align: center;">OH</td> <td style="text-align: center;">OH</td> </tr> <tr> <td style="text-align: center;">OCH<sub>3</sub></td> <td style="text-align: center;">OH</td> <td style="text-align: center;">H</td> </tr> </tbody> </table>	R <sub>1</sub>	R <sub>2</sub>	R <sub>3</sub>	H	OH	H	H	OH	OH	OCH <sub>3</sub>	OH	H	
R <sub>1</sub>	R <sub>2</sub>	R <sub>3</sub>												
H	OH	H												
H	OH	OH												
OCH <sub>3</sub>	OH	H												
	 Caftaric acid (HR- 74)													

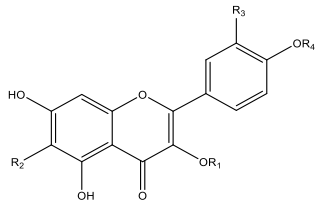
## Appendix II

**Table 1.7:** Selection of phytochemicals previously isolated from Asteraceae. HR: refers to the name of the *H. radicata*

Classification	Compound	Parts of the plant	Reference
<b>Polyphenol</b>	 <p style="text-align: center;">1-<i>O</i>-,5-<i>O</i>-dicaffeoyl-3-<i>O</i>-, 4-<i>O</i>-disuccinylquinic acid (<b>HR- 75</b>)</p>	Plant of	(Jaiswal <i>et al.</i> , 2011; Bohm and Stuessy, 2013)
	 <p style="text-align: center;">1-<i>O</i>-,5-<i>O</i>-dicaffeoyl-4-<i>O</i>-succinylquinic acid (<b>HR- 76</b>)</p>	Plant of	(Jaiswal <i>et al.</i> , 2011; Bohm and Stuessy, 2013)

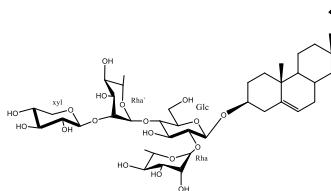
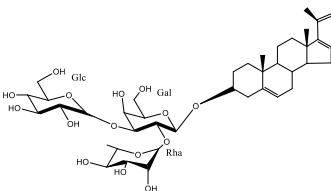
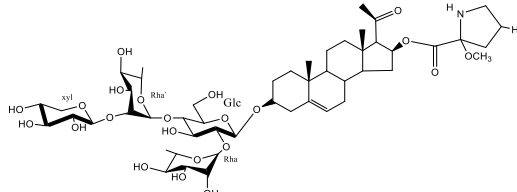
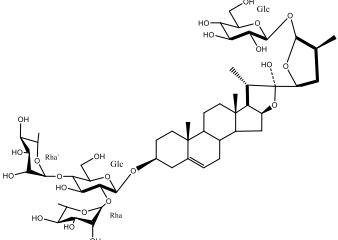
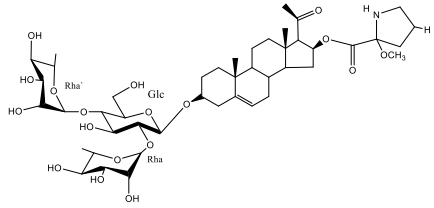
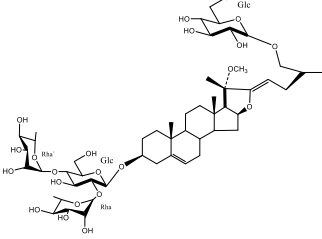
## Appendix II

**Table 1.7:** Selection of phytochemicals previously isolated from Asteraceae. HR: refers to the name of the *H. radicata*

Classification	Compound	Parts of the plant	Reference																																									
<b>Polyphenol</b>		<table style="margin-left: auto; margin-right: auto;"> <thead> <tr> <th>R<sub>1</sub></th> <th>R<sub>2</sub></th> <th>R<sub>3</sub></th> <th>R<sub>4</sub></th> </tr> </thead> <tbody> <tr> <td>H</td> <td>H</td> <td>H</td> <td>H</td> </tr> <tr> <td>rut</td> <td>H</td> <td>OH</td> <td>H</td> </tr> <tr> <td>gal</td> <td>H</td> <td>OH</td> <td>H</td> </tr> <tr> <td>H</td> <td>H</td> <td>OH</td> <td>H</td> </tr> <tr> <td>ara</td> <td>H</td> <td>OH</td> <td>H</td> </tr> <tr> <td>ara</td> <td>H</td> <td>H</td> <td>H</td> </tr> <tr> <td>H</td> <td>H</td> <td>OH</td> <td>glu</td> </tr> <tr> <td>glu</td> <td>H</td> <td>H</td> <td>H</td> </tr> <tr> <td>rut</td> <td>H</td> <td>H</td> <td>H</td> </tr> </tbody> </table>	R <sub>1</sub>	R <sub>2</sub>	R <sub>3</sub>	R <sub>4</sub>	H	H	H	H	rut	H	OH	H	gal	H	OH	H	H	H	OH	H	ara	H	OH	H	ara	H	H	H	H	H	OH	glu	glu	H	H	H	rut	H	H	H	Flowers of <i>H. radicata</i>	(Jaiswal <i>et al.</i> , 2011; Kim <i>et al.</i> , 2014; Ferracane <i>et al.</i> , 2010; Liu <i>et al.</i> , 2006)
	R <sub>1</sub>	R <sub>2</sub>	R <sub>3</sub>	R <sub>4</sub>																																								
	H	H	H	H																																								
	rut	H	OH	H																																								
	gal	H	OH	H																																								
	H	H	OH	H																																								
	ara	H	OH	H																																								
	ara	H	H	H																																								
H	H	OH	glu																																									
glu	H	H	H																																									
rut	H	H	H																																									
	Kaempferol ( <b>HR- 77</b> )																																											
	Rutin ( <b>HR- 78</b> )																																											
	Hyperin ( <b>HR- 79</b> )																																											
	Quercetin ( <b>HR- 80</b> )																																											
	Quercetin-3- <i>O</i> -arabinoside ( <b>HR- 81</b> )																																											
	Kaempferol-3- <i>O</i> -arabinoside ( <b>HR- 82</b> )																																											
	Quercetin-4'- <i>O</i> -glucoside ( <b>HR- 83</b> )																																											
	Kaempferol-3- <i>O</i> -glucoside ( <b>HR- 85</b> )																																											
	Kaempferol-3- <i>O</i> -rutinoside ( <b>HR-86</b> )																																											

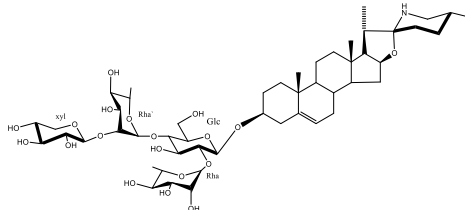
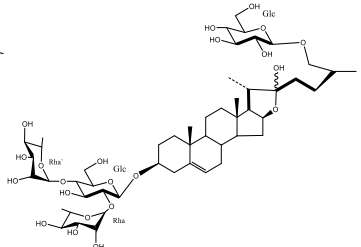
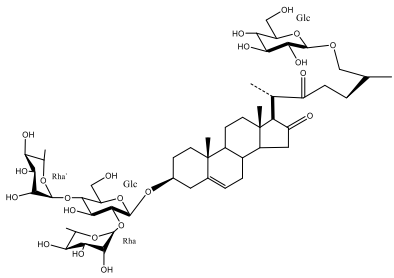
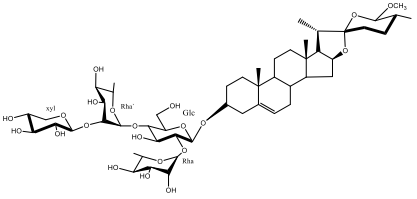
### Appendix III

**Table 1.8:** Selection of phytochemicals previously isolated from *S.sodomaeum*. SS: refers to the name of the plant *Solanum*.

Classification	Compound	Parts of the plant	Reference		
Steroidal glycosides			Stems of <i>S. sodomaeum</i>	Ono <i>et al.</i> , 2009)	
	Solasodaside B (SS-12)	Solasodaside C (SS-13)			Solasodaside D (SS-14)
					
	Solasodaside E (SS-15)	Solasodaside F (SS-16)			
					
	Abutiloside O (SS-17)	Dioscoreside E (SS-18)			

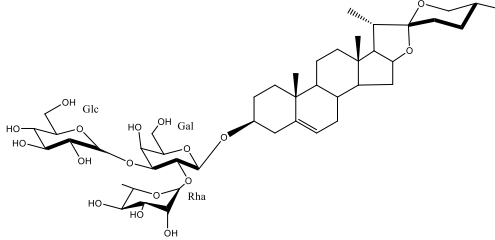
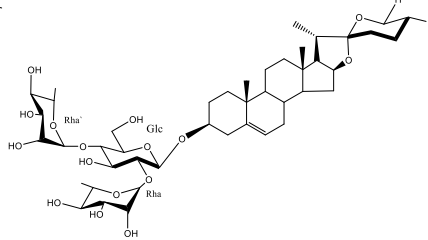
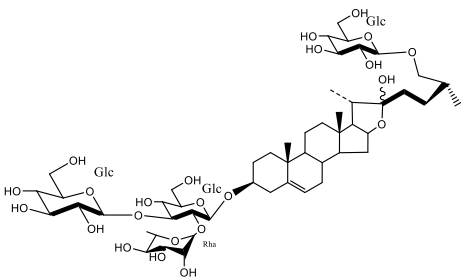
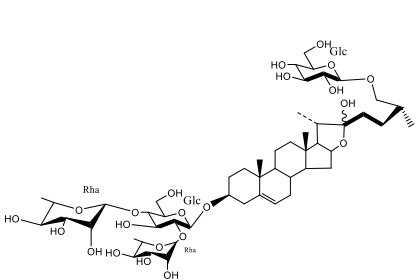
### Appendix III

**Table 1.8:** Selection of phytochemicals previously isolated from *S. sodomaeum*. SS: refers to the name of the plant *Solanum*.

Classification	Compound	Parts of the plant	Reference
Steroidal glycosides	 <p>Sycophantine (SS-19)</p>	Stems of <i>S. sodomaeum</i>	(Ono <i>et al.</i> , 2009)
	 <p>Protodioscin (SS-20)</p>		
	 <p>Anguivioside XV (SS-21)</p>		
	 <p>Solasodoside A (SS-22)</p>		

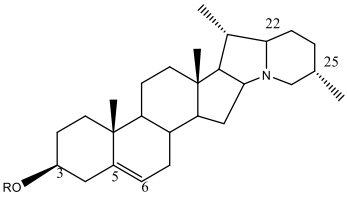
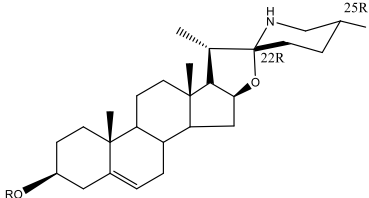
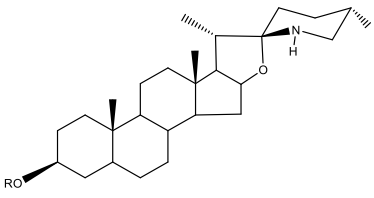
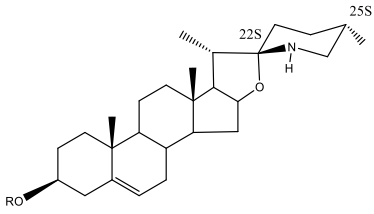
*Appendix III*

**Table 1.8(continued):** Selection of phytochemicals previously isolated from *S. sodomaeum*. SS: refers to the name of the plant *Solanum*.

Classification	Compound	Parts of the plant	Reference	
Steroidal glycosides			Underground parts of <i>S. sodomaeum</i>	(Ono <i>et al.</i> , 2009)
	Diosgenin 3- <i>O</i> - $\beta$ -solatrioside(SS-23)	Dioscin (SS-24)		
				
	IndiosideD (SS-25)	Protodioscin (SS-26)		

Appendix III

**Table 1.8 (continued):** Selection of phytochemicals previously isolated from *S..sodomaemum*. SS: refers to the name of the plant *Solanum*.

Classification	Compound	Parts of the plant	Reference	
Steroidal glycosides	 <p>Solanidine (SS-27)  <math>\alpha</math>-Solanine (SS-28)  <math>\alpha</math>-Chaconine (SS-29)                      Chacotriose</p>	<p><b>R</b> H Solatriose Chacotriosa Chacotriose</p>	<p><i>S. tuberosum</i> (potato plants),  <i>S. melongena</i> (eggplants) and  <i>Lycopersicon esculentum</i> Mill (tomato plants)</p>	<p>(Chowanski <i>et al.</i>, 2016)</p>
	 <p>Solasodine (SS-30)                      Solasonine (SS-31)                      Solamargine (SS-32)</p>	<p><b>R</b> H Salatriose Chacotriose</p>		
	 <p>Tomatidine (SS-33)  <math>\alpha</math>-Tomatine (SS-34)</p>	<p><b>R</b> H Lycotetrose</p>		
	 <p>Tomatidenol (SS-35)                      Dehydrotomatine (SS-36)</p>	<p><b>R</b> H Lycotetrose</p>		

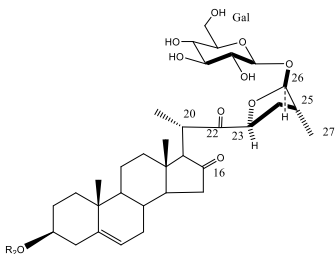
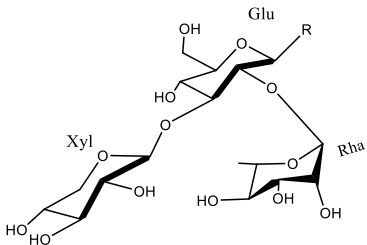
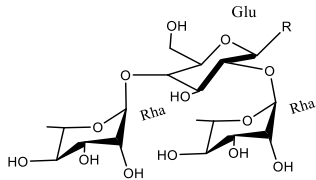
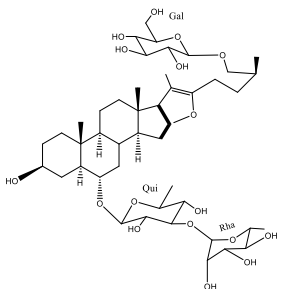
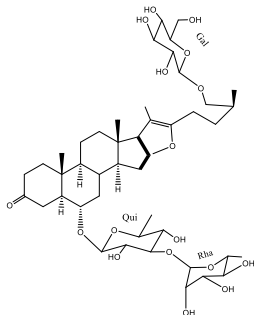
**Appendix III**

**Table 1.8 (continued):** Selection of phytochemicals previously isolated from *S. sodomaeum*. SS: refers to the name of the plant *Solanum*.

Classification	Compound	Parts of the plant	Reference	
Steroidal glycosides		Fruits of <i>S.anguivi</i>	(Honbu <i>et al.</i> , 2002)	
	Solatriose			
				Chacotriose
				Lycotetrose
				Anguivoside III(SS-37)
				Anguivoside XI(SS-38)
	Anguivoside XV(SS-39)			

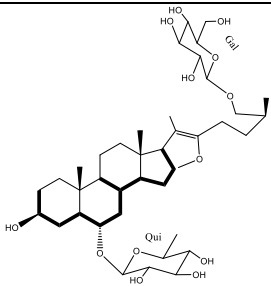
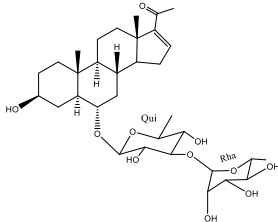
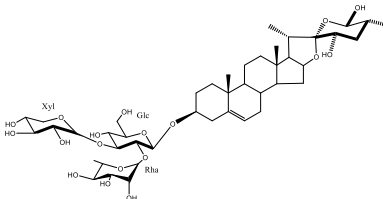
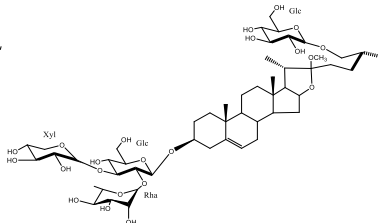
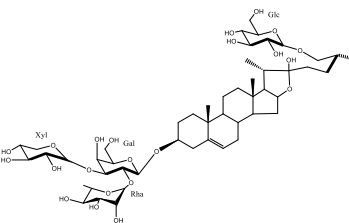
Appendix III

Table 1.8 (continued): Selection of phytochemicals previously isolated from *S. sodomaeum*. SS: refers to the name of the plant *Solanum*.

Classification	Compound	Parts of the plant	Reference
Steroidal glycosides	 <p>Anguivioside XVI (SS-40)</p>	Fruits of <i>S. torvum</i>	(Li <i>et al.</i> , 2014b)
	 <p><b>R<sub>1</sub></b></p>		
	 <p><b>R<sub>2</sub></b></p>		
	 <p>25(<i>S</i>)-26-<i>O</i>-β-D-glucopyranosyl-5α-furost-22(20)-en-3β,6α,26-triol 6-<i>O</i>-[α-L-rhamnopyranosyl-(1 → 3)-<i>O</i>-β-D-quinovopyranoside] (SS-41)</p>		
	 <p>25(<i>S</i>)-26-<i>O</i>-β-D-glucopyranosyl-5α-furost-22(20)-en-3-one-6α,26-diol 6-<i>O</i>-[α-L-rhamnopyranosyl-(1 → 3)-<i>O</i>-β-D-quinovopyranoside] (SS-42)</p>		

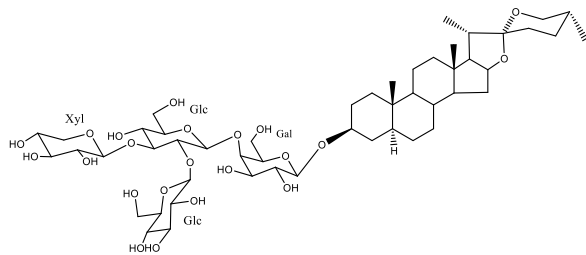
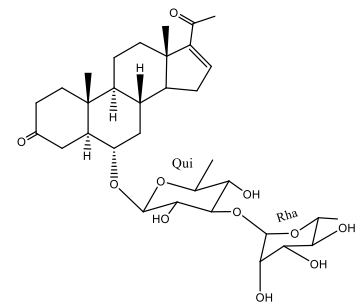
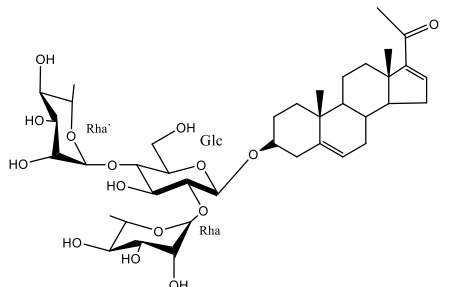
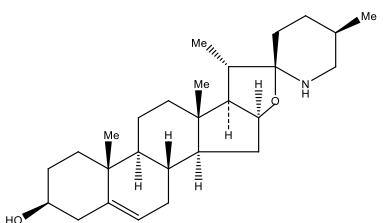
Appendix III

**Table 1.8 (continued):** Selection of phytochemicals previously isolated from *S. sodomaeum*. SS: refers to the name of the plant *Solanum*.

Classification	Compound	Parts of the plant	Reference		
Steroidal glycosides	 <p>25(S)-26-O-<math>\beta</math>-D-glucopyranosyl-5<math>\alpha</math>-furost-22(20)-en-3<math>\beta</math>,6<math>\alpha</math>,26-triol 6-O-<math>\beta</math>-D-quinovopyranoside. -[quinovopyranoside(SS-43)]</p>	Fruits of <i>S. torvum</i>	(Li <i>et al.</i> , 2014b)		
	 <p>5<math>\alpha</math>-pregn-16-en-20-one-3<math>\beta</math>,6<math>\alpha</math>-diol-6-O-<math>\alpha</math>-L-rhamnopyranosyl-(1 <math>\rightarrow</math> 3)-<math>\beta</math>-D-quinovopyranoside] (SS-44)</p>				
	 <p>Indioside A(SS-45)</p>			Fruits and roots of <i>S. indicum</i> , whole plant of <i>S. nigrum</i> and fruits of <i>S. torvum</i>	(Yahara <i>et al.</i> , 1996;Zhou <i>et al.</i> , 2006; Li <i>et al.</i> , 2014b)
	 <p>Indioside B (SS-46)</p>				
	 <p>Indioside C (SS-47)</p>				

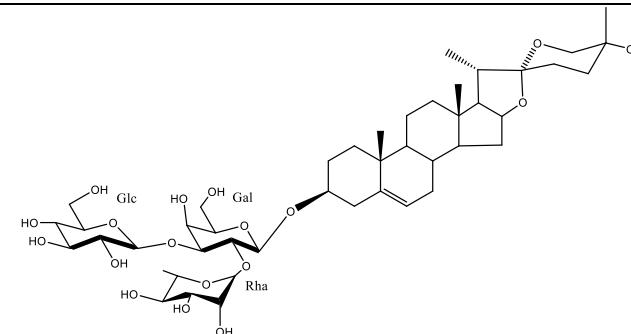
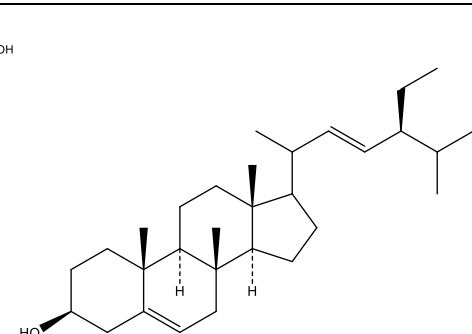
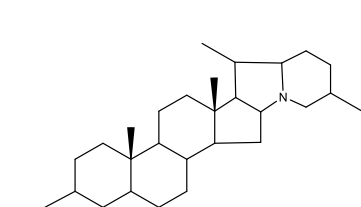
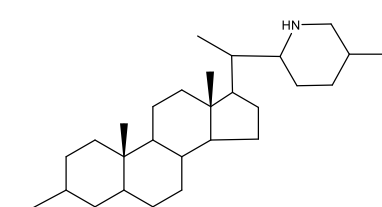
### Appendix III

**Table 1.8 (continued):** Selection of phytochemicals previously isolated from *S. sodomaeum*. SS: refers to the name of the plant *Solanum*.

Classification	Compound	Parts of the plant	Reference
Steroidal glycosides		Fruits and roots of <i>S. indicum</i> , whole plant of <i>S. nigrum</i> and fruits of <i>S. torvum</i>	(Yahara <i>et al.</i> , 1996; Zhou <i>et al.</i> , 2006; Li <i>et al.</i> , 2014b)
	Degalactotigonin (SS-48)		
			
	5α-pregn-16-en-3,20-dione-6α-ol-6-O-[α-L-rhamnopyranosyl-(1→3)-β-D-quinovopyranoside] (SS-49)		
			
	pregna-5,16-dien-3β-ol-20-one 3-O-α-L-rhamnopyranosyl(1→2)-[α-L-rhamnopyranosyl-(1→4)]-β-D-glucopyranoside (SS-50)		
			
	Solasodine (SS-51)		

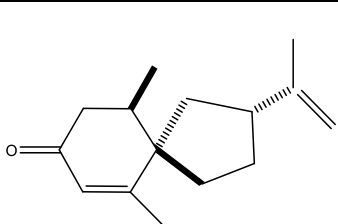
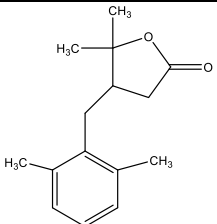
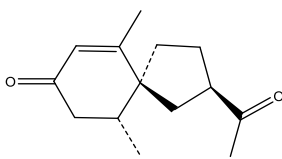
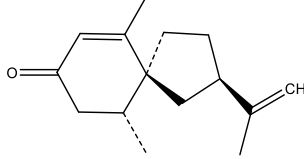
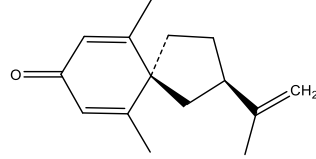
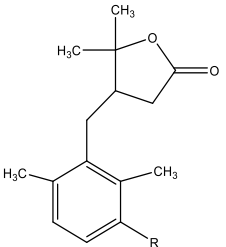
Appendix III

**Table 1.8 (continued):** Selection of phytochemicals previously isolated from *S. sodomaeum*. SS: refers to the name of the plant *Solanum*.

Classification	Compound	Parts of the Reference plant
Steroidal glycosides	 <p data-bbox="584 863 1099 895">Isonuatigenin-3-O-<math>\beta</math>-solatriose(steroid) (SS-52)</p>	<p data-bbox="1906 496 2063 528">(Niño <i>et al.</i>,</p> <p data-bbox="1682 544 2085 975">Berries <i>S.</i> 2009; Ramos and de roots of <i>S. erianthum</i>, seeds of <i>S. indicum</i> and aerial parts of <i>S. leucocarpum</i></p>
	 <p data-bbox="1234 863 1525 927"><math>\beta</math>-sitosterol (SS-53) and stigmasterol <math>\Delta^{22}</math>(SS-54)</p>	
Alkaloids	 <p data-bbox="651 1214 875 1246">Demissidine(SS-55)</p>	 <p data-bbox="987 1214 1368 1246">Dihydrosolacongestidine (SS-56)</p>

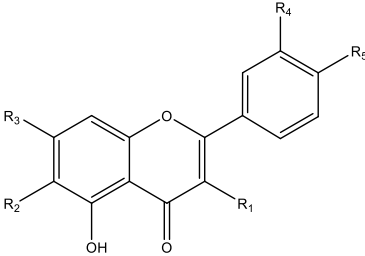
**Appendix III**

**Table 1.8 (continued):** Selection of phytochemicals previously isolated from *S. sodomaeum*. SS: refers to the name of the plant *Solanum*.

Classification	Compound	Parts of the plant	Reference	
Sesquiterpenoids			Roots <i>S. indicum</i> and roots of <i>S. erianthum</i> (Syu <i>et al.</i> , 2001; Chen <i>et al.</i> , 2013)	
	Solavetivone (SS-57)	Solafuranone (SS-58)		Solanerianones A (SS-59)
				
	SolanerianonesB (SS-60)	(-)-Solavetivone (SS-61)		(+)-Anhydro- $\beta$ -rotunol (SS-62)
		Solafuranone (SS-63) R=H		
		Lycifuranone A (SS-64) R=OH		

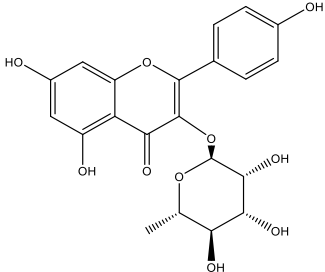
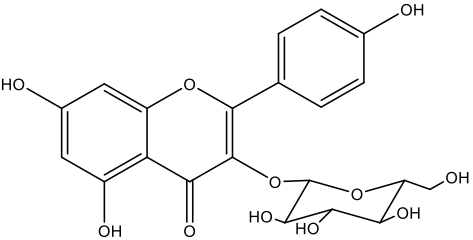
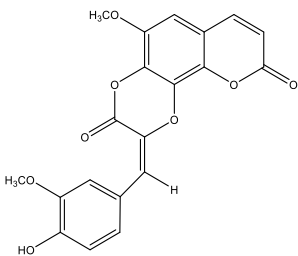
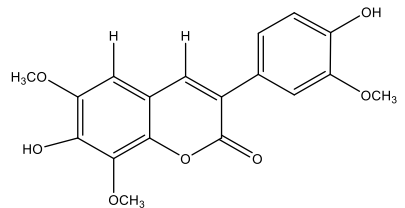
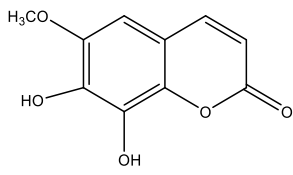
### Appendix III

**Table 1.8 (continued):** Selection of phytochemicals previously isolated from *S. sodomaeum*. SS: refers to the name of the plant *Solanum*.

Classification	Compound	Parts of the plant	Reference
Flavonoids		Aerial parts of <i>S. incanum</i> and <i>S. torvum</i>	(Lin <i>et al.</i> , 2000; Lu <i>et al.</i> , 2011)
	Kaempferol (SS-65); $R_1 = OH, R_2 = H, R_3 = OH, R_4 = H, R_5 = OH$		
	Quercetin (SS-66); $R_1 = OH, R_2 = H, R_3 = OH, R_4 = OH, R_5 = OH$		
	Baicalin (SS-67); $R_1 = H, R_2 = OH, R_3 = O\text{-glucopyranuronyl}, R_4 = H, R_5 = H$		
	Astragalin (SS-68); $R_1 = O\text{-}\beta\text{-D-glucopyranosyl}, R_2 = H, R_3 = OH, R_4 = H, R_5 = OH$		
	Isoquercitrin (SS-69); $R_1 = O\text{-}\beta\text{-D-glucopyranosyl}, R_2 = H, R_3 = OH, R_4 = OH, R_5 = OH$		
	Luteolin 7- $O\text{-}\beta\text{-D-glucopyranoside}$ (SS-70); $R_1, R_2 = H, R_3 = O\text{-}\beta\text{-D-glucopyranosyl}, R_4, R_5 = OH$		
	Isorhamnetin 3- $O\text{-}\beta\text{-D-glucopyranoside}$ (SS-71); $R_1 = O\text{-}\beta\text{-D-glucopyranosyl}, R_2 = H, R_3 = OH, R_4 = OCH_3, R_5 = OH$		
	Kaempferol 3- $O\text{-}\beta\text{-D-glucopyranosyl}$ (1 $\rightarrow$ 2) $\beta\text{-Dglucopyranoside}$ (SS-72); $R_1 = O\text{-}\beta\text{-D-glucopyranosyl}$ (1 $\rightarrow$ 2) $\beta\text{-D-glucopyranosyl}, R_2 = H, R_3 = OH, R_4 = H, R_5 = OH$		
	Quercetin 3- $O\text{-}\beta\text{-D-glucopyranosyl}$ (1 $\rightarrow$ 2) $\beta\text{-Dglucopyranoside}$ (SS-73); $R_1 = O\text{-}\beta\text{-D-glucopyranosyl}$ (1 $\rightarrow$ 2) $\beta\text{-D-glucopyranosyl}, R_2 = H, R_3 = OH, R_4 = OH, R_5 = OH$		
	Rutin (SS-74); $R_1 = \alpha\text{-L-rhamnopyranosyl-(1}\rightarrow\text{6)-}\beta\text{-D-glucopyranose), R_2 = H, R_3 = OH, R_4 = OH, R_5 = OH$		

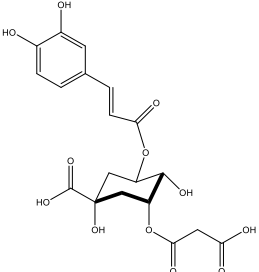
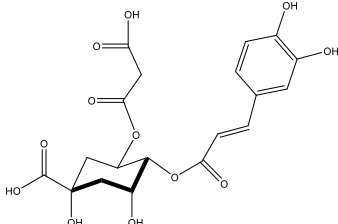
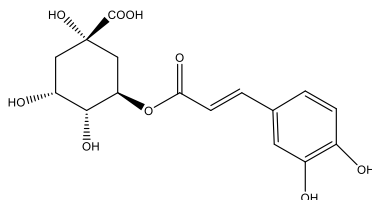
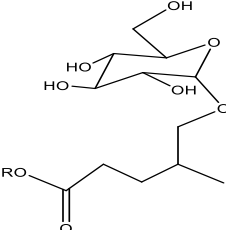
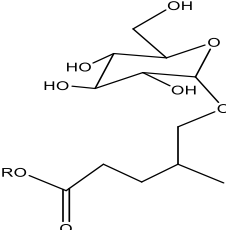
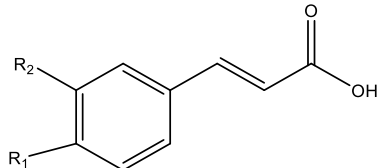
**Appendix III**

**Table 1.8 (continued):** Selection of phytochemicals previously isolated from *S. sodomaeum*. SS: refers to the name of the plant *Solanum*.

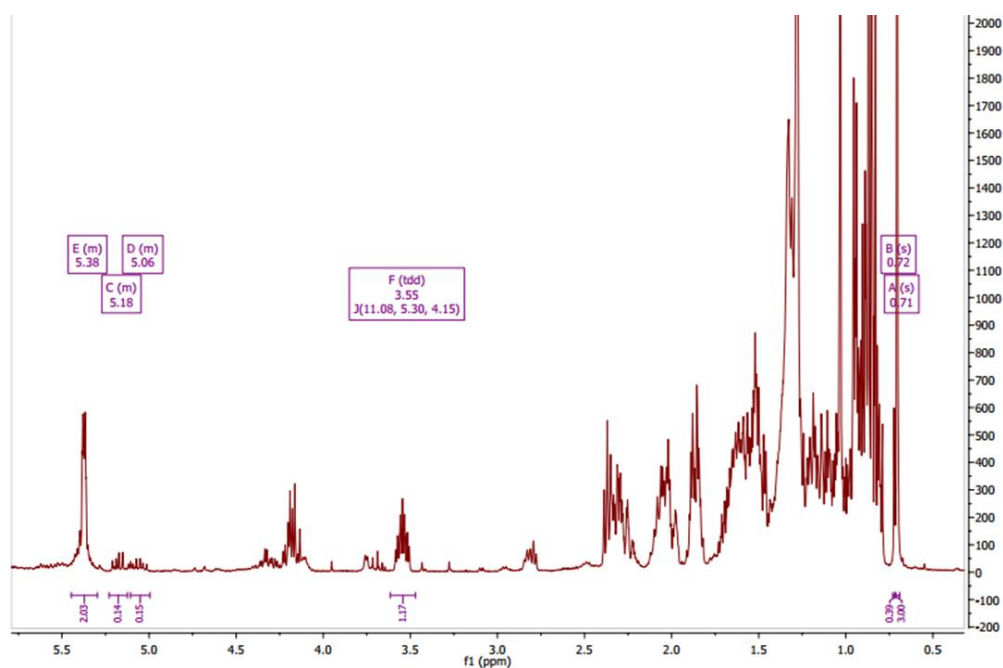
Classification	Compound	Parts of the plant	Reference
Flavonoids	 <p>Afzelin (SS-75)</p>	Leaves of <i>S. cernuum</i>	(Ramos and de Oliveira, 2017)
	 <p>Astragalin (SS-76)</p>		
Coumarins	 <p>Indicumin E (SS-77)</p>	Seeds of <i>S. indicum</i>	(Yin <i>et al.</i> , 2014a)
	 <p>7-hydroxy-6,8-dimethoxy-3-(4-hydroxy-30-methoxyphenyl)-coumarin (SS-78)</p>		
	 <p>Fraxetin (SS-79)</p>		

### Appendix III

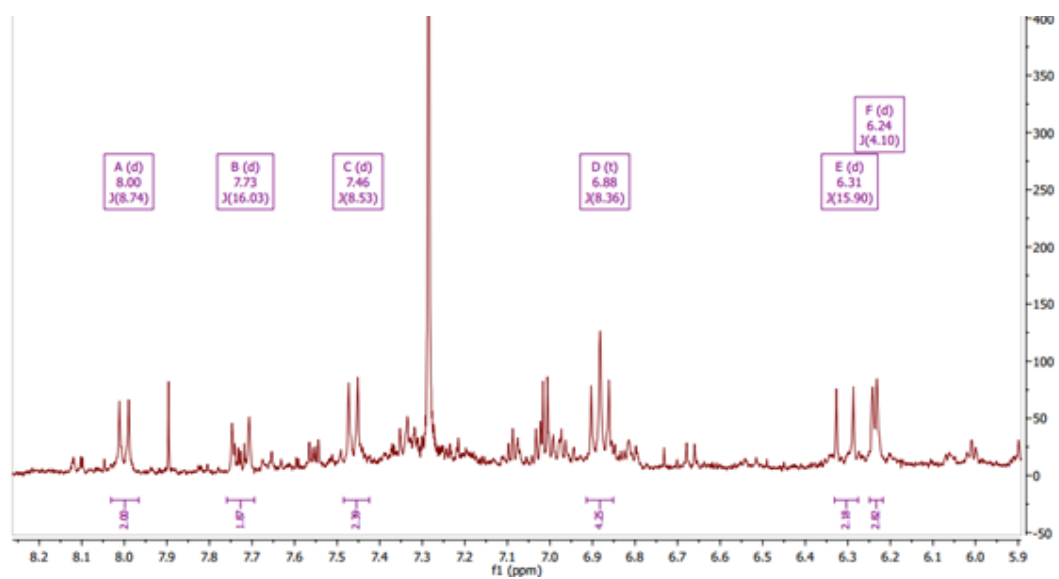
**Table 1.8 (continued):** Selection of phytochemicals previously isolated from *S. sodomaeum*. SS: refers to the name of the plant *Solanum*.

Classification	Compound	Parts of the plant	Reference
Phenolic acid	 <p>3-<i>O</i>-malonyl-5-<i>O</i>-(<i>E</i>)-caffeoylquinic acid (SS-81)</p>	Fruits of the eggplant species <i>S. melongena</i> , potato ( <i>S. tuberosum</i> ), aerial parts of <i>S. incanum</i> and stems of <i>S. sodomaeum</i>	(Ma <i>et al.</i> , 2011; Li <i>et al.</i> , 2014b; Ono <i>et al.</i> , 2009; Valiñas <i>et al.</i> , 2015)
	 <p>4-<i>O</i>-(<i>E</i>)-caffeoyl-5-<i>O</i>-malonylquinic acid (SS-82)</p>		
	 <p>Chlorogenic acid (SS-83)</p>		
	 <p><math>\gamma</math>-methyl-<math>\delta</math>-hydroxy pentanoic acid glucoside (SS-84) R=H</p>		
	 <p>methyl <math>\gamma</math>-methyl-<math>\delta</math>-hydroxy pentanoate glucoside (SS-85) R=CH<sub>3</sub></p>		
	 <p><math>\text{R}_1</math> <math>\text{R}_2</math>  <math>\text{OH}</math> <math>\text{H}</math>  <math>\text{OH}</math> <math>\text{OH}</math></p>		
	 <p>(3<i>S</i>,6<i>E</i>)-8-hydroxylinalool 3-<i>O</i>-<math>\beta</math>-D-glucopyranoside (SS-88)</p>		

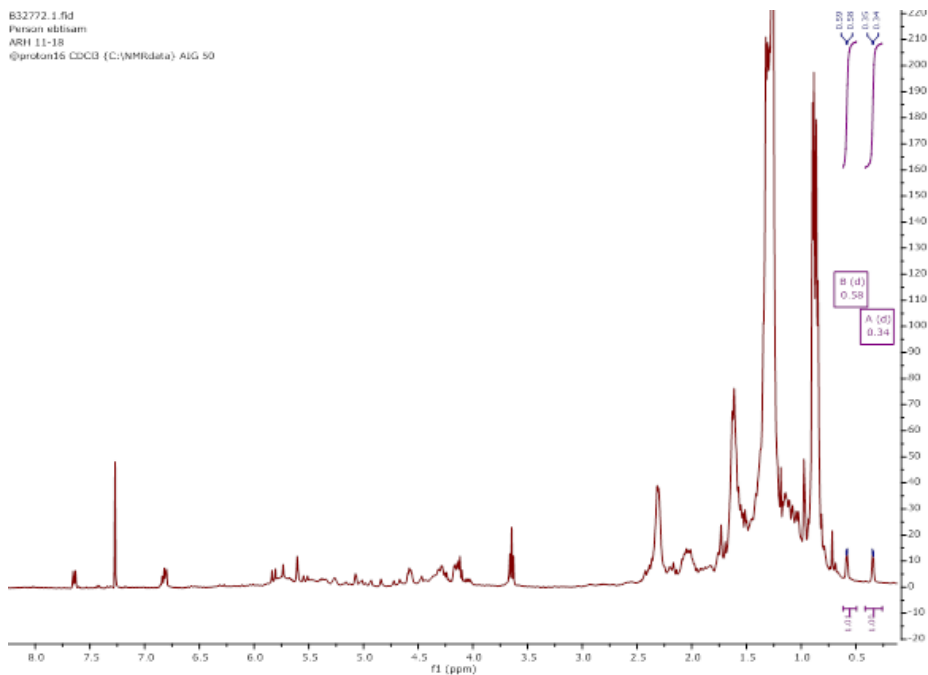
Appendix IV (A) *Arum cyrenaicum*



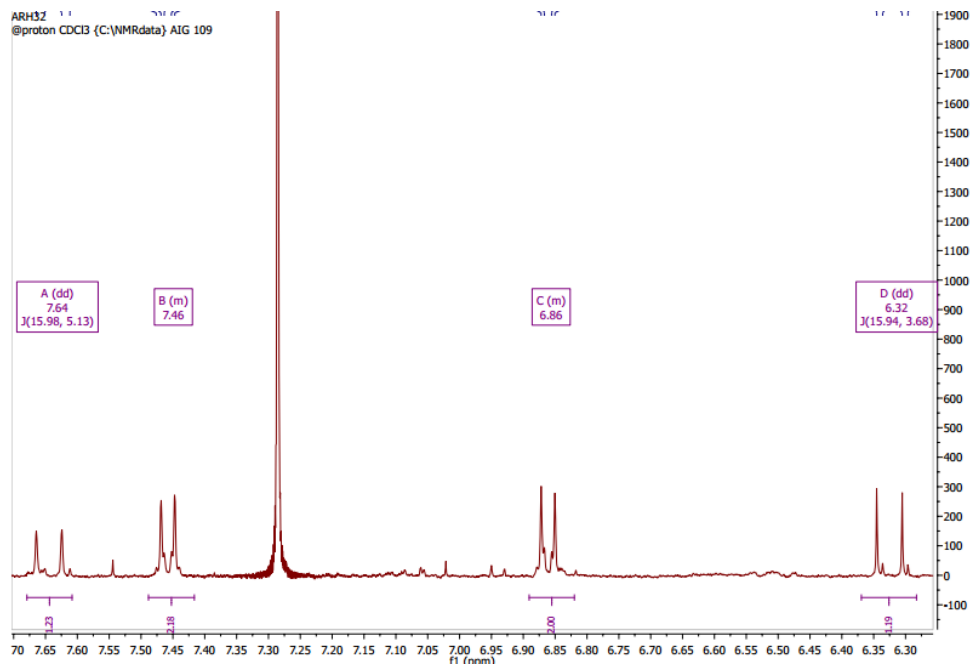
$^1\text{H}$  NMR spectrum (400 MHz) ARH 38 a mixture of  $\beta$ -sitosterol and stigmasterol with fatty acid in  $\text{CDCl}_3$



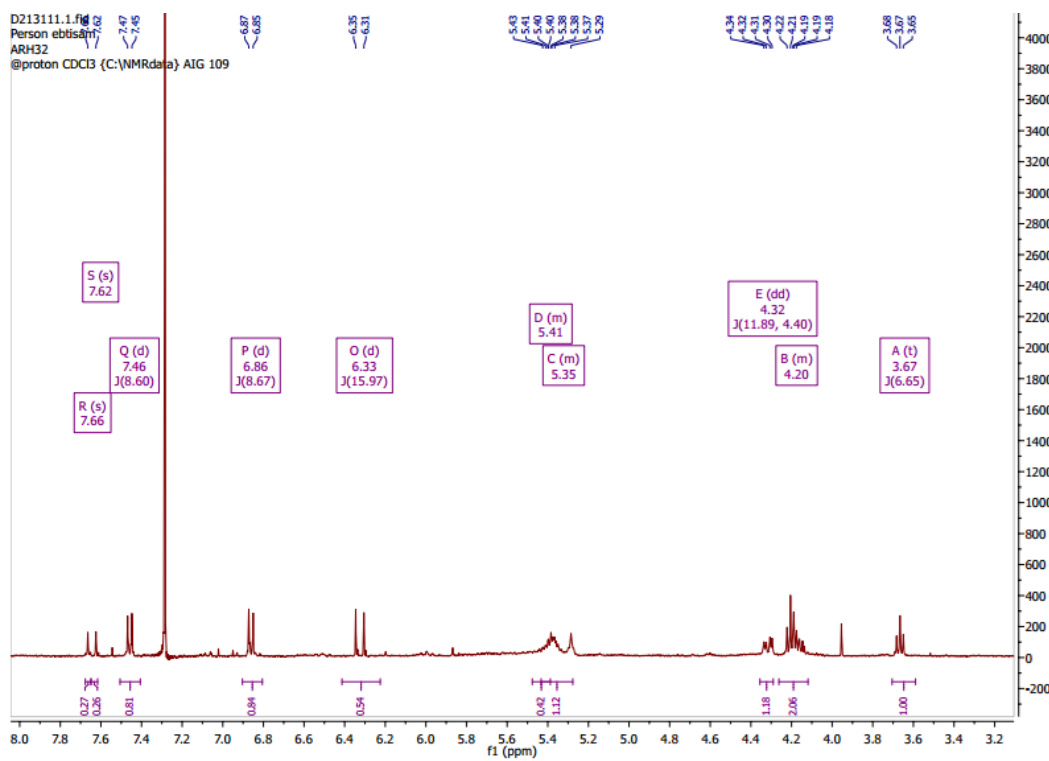
$^1\text{H}$  NMR spectrum (400 MHz) ARE6 as mixtures of *p*-coumaric acid with a long chain fatty and *p*-hydroxybenzaldehyde



$^1\text{H}$  NMR spectrum (400 MHz) ARH 11-18 as cycloartane with unsaturated fatty acid

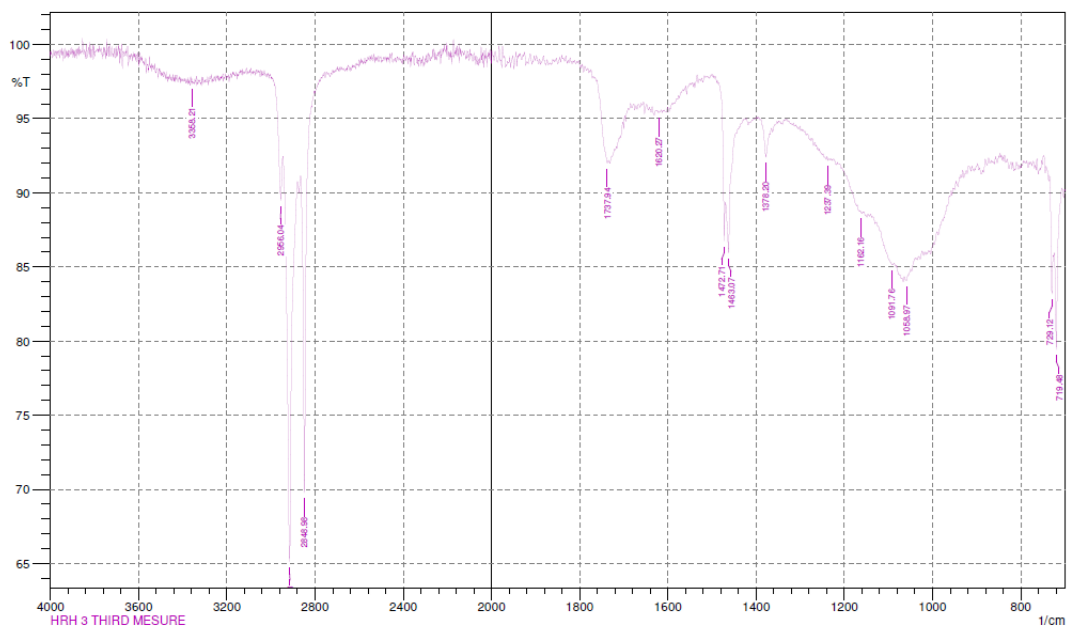


$^1\text{H}$  NMR spectrum (400 MHz) ARH32 as *p*-coumaric acid substitution with unsaturated fatty alcohol

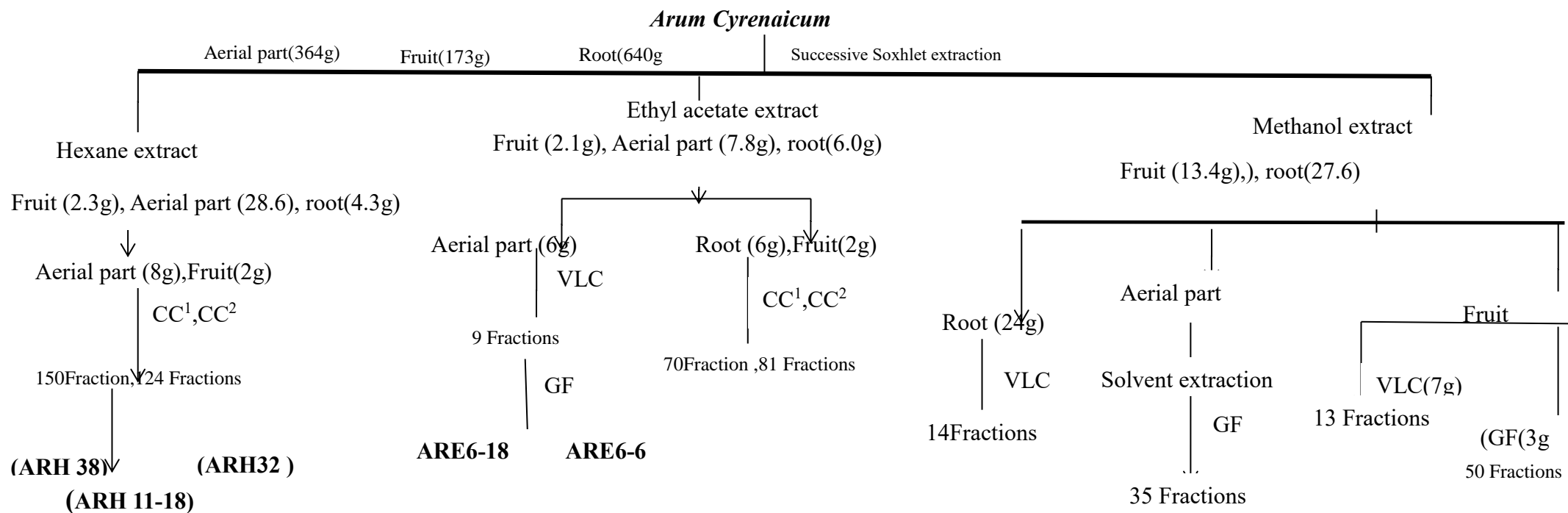


<sup>1</sup>H NMR spectrum (400 MHz) ARH32 as p-coumaric acid substitution with unsaturated fatty alcohol

Appendix V *H. radicata*



Infrared spectroscopy of HRH-5as wax long chain fatty acid esterified into long chain alcohol, these fractions seem to contain wax. IR , peaks were 3358, 2956, 2915, 2848, 1738, 1620, 1472, 1463, 1378, 1237, 1162, 1091, 1058, 729, 719  $\text{cm}^{-1}$ ., 1162 indicate to ester group, bands at 729  $\text{cm}^{-1}$  and 719  $\text{cm}^{-1}$  indicate showed the long chain methylene. Band at 3358  $\text{cm}^{-1}$  was indicated the presence of hydroxyl group (OH), band 1472, 1463  $\text{cm}^{-1}$  indicated to  $\text{CH}_2$ , 1378  $\text{cm}^{-1}$  for (CH<sub>3</sub>), Peaks at 1738  $\text{cm}^{-1}$  for (C=O), peaka at 2956, 2915, 2848, for (CH).

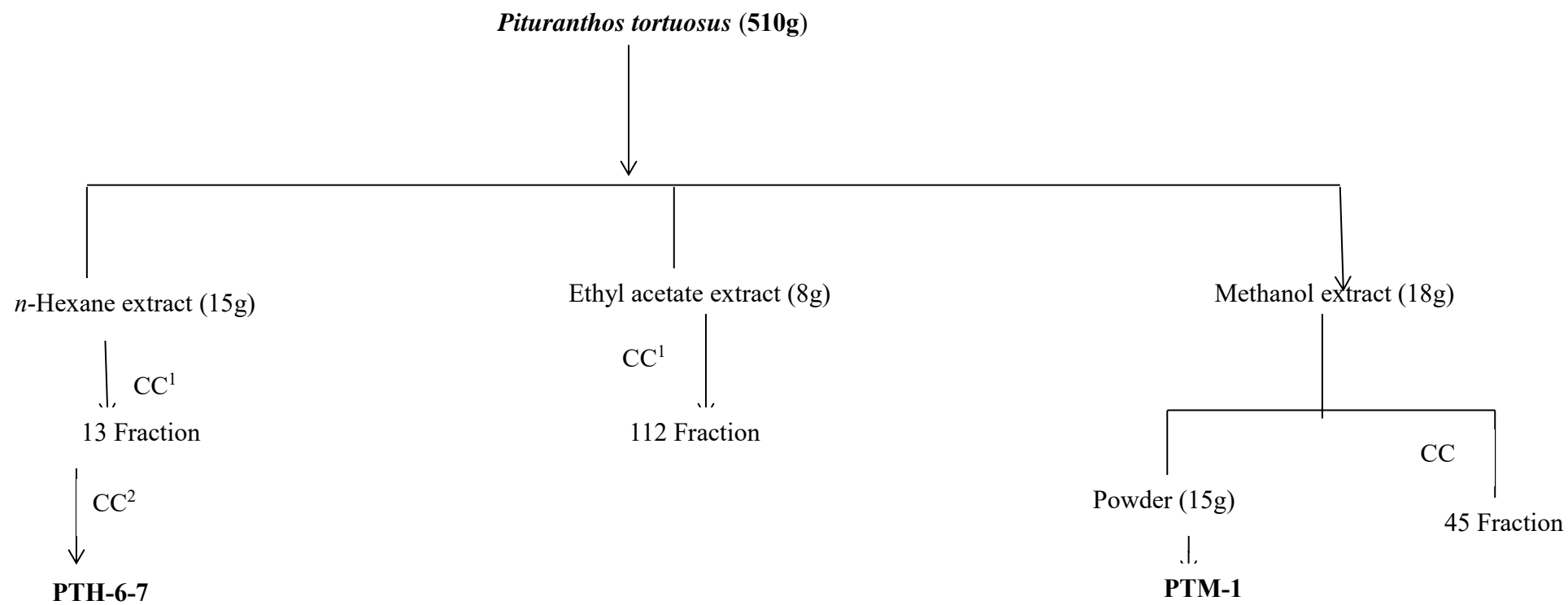


VLC: Vacuum liquid chromatography eluted with 100% *n*-hexane, with the gradual increase of ethyl acetate, followed by the increase of methanol; CC<sup>1</sup> and

CC<sup>2</sup>: Gradient column eluted with 10% *n*-hexane, increasing polarity by addition of EtOAc.

GF: Gel filtration eluted with 100% methanol.

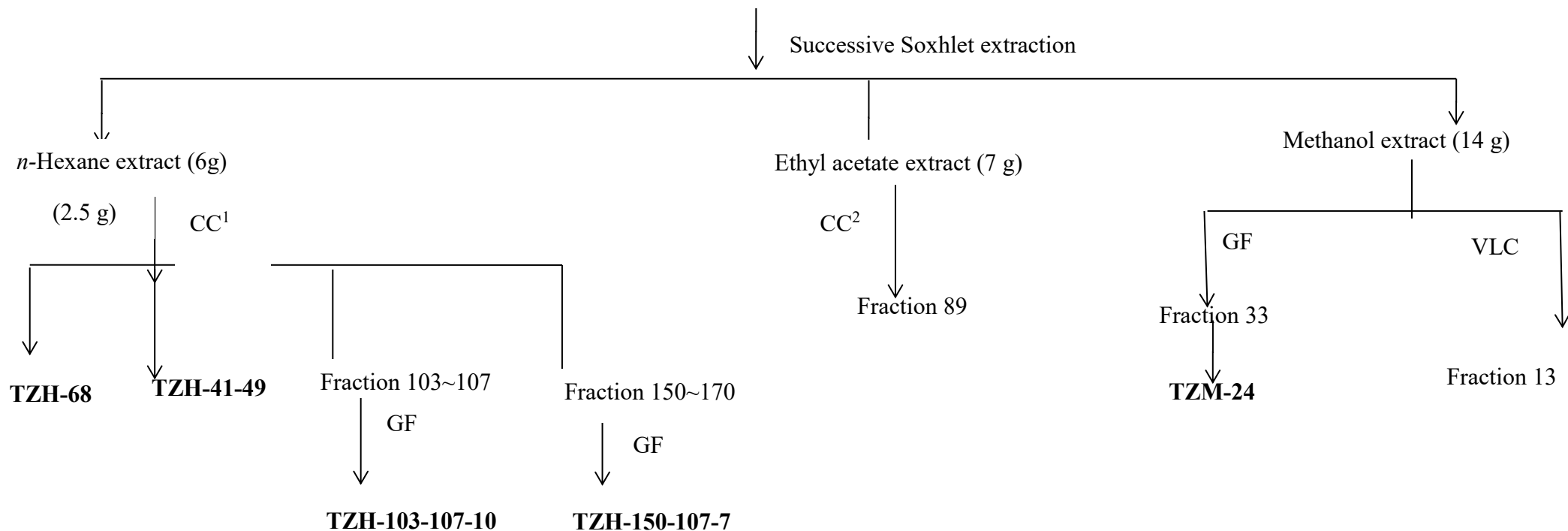
**Scheme 1: Isolation of compounds from the extracts of *Arum Cyrenaicum***



CC<sup>1</sup> and CC<sup>2</sup>: Gradient column eluted with 10% n-hexane, increasing polarity by addition of EtOAc.

**Scheme 2: Isolation of compounds from the extracts of *Pituranthos tortuosus***

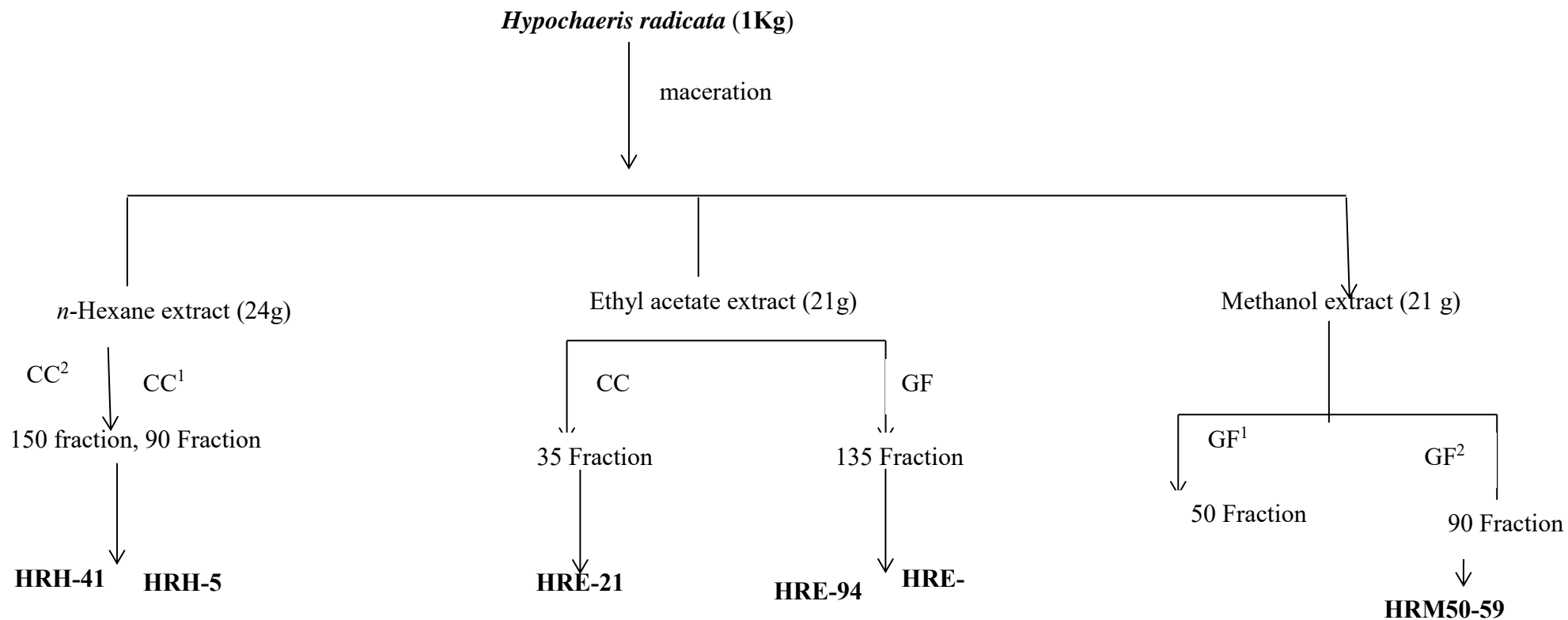
*Teucrium zanonii* (400g)



VLC: Vacuum liquid chromatography eluted with 100% *n*-hexane, with the gradual increase of ethyl acetate, followed by the increase of methanol GF:

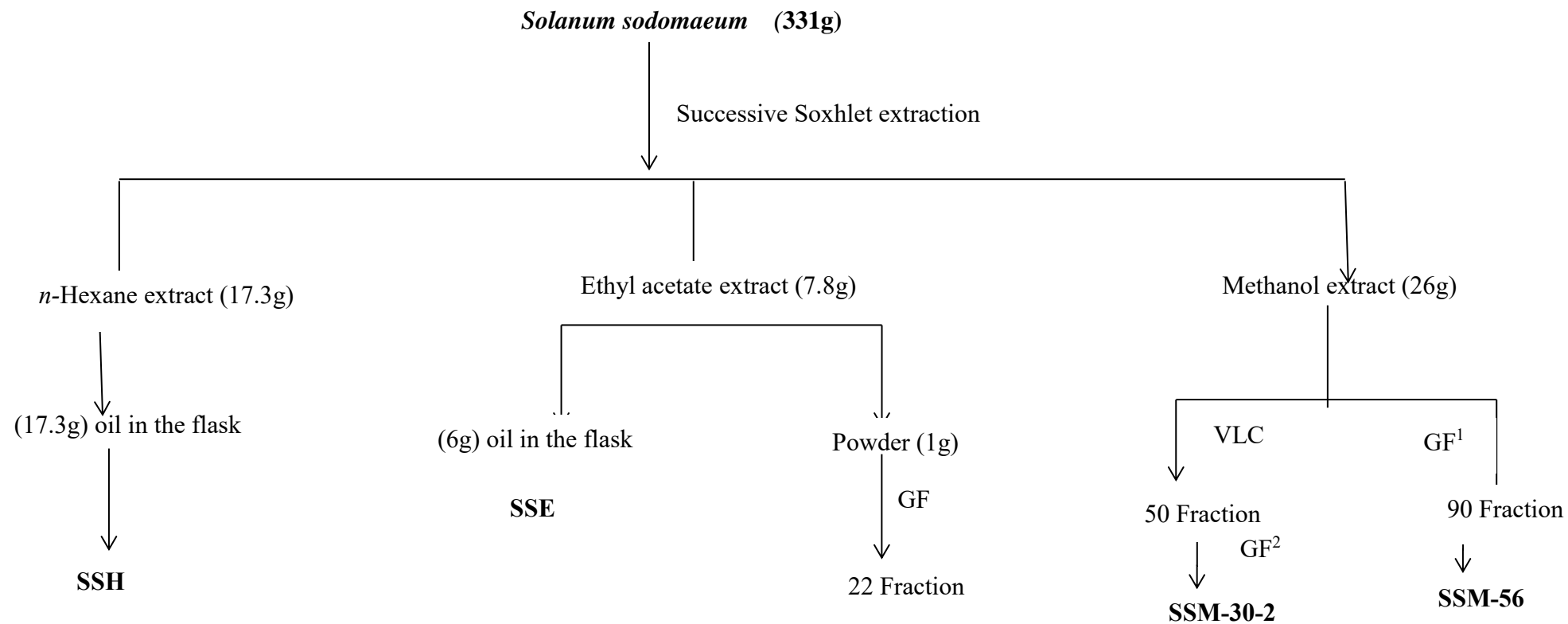
Gel filtration eluted with 100% methanol; CC<sup>1</sup> and CC<sup>2</sup>: Gradient column eluted with 10% *n*-hexane, increasing polarity by addition of EtOAc.

**Scheme 3: Isolation of compounds from the extracts of *Teucrium zanonii***



GF<sup>1</sup> and GF<sup>2</sup>: Gel filtration eluted with methanol; GF<sup>2</sup>: Gel filtration eluted with 100% methanol; CC<sup>1</sup> and CC<sup>2</sup>: Gradient column eluted with 10% n-hexane, increasing polarity by addition of EtOAc.

**Scheme 4: Isolation of compounds from the extracts of *Hypochaeris radicata***



VLC: Vacuum liquid chromatography eluted with 100% *n*-hexane, with the gradual increase of ethyl acetate, followed by the increase of methanol

GF<sup>1</sup>, GF<sup>2</sup> : Gel filtration eluted with 100% methanol;

**Scheme 5: Isolation of compounds from the extracts of *Solanum sodomaeum***

## References

- A., A., N., H., S., K., A., M., J., C., M., H., L., C. G. & K., G. 2006. Chemical composition and antimicrobial activity of essential oils from Tunisian *Pituranthos tortuosus* (Coss.) Maire. *Flavour and Fragrance Journal*, 21, 129-133.
- A., T. L., FREDDIE, B., L., S. R., JACQUES, F., JOANNIE, L. T. & AHMEDIN, J. 2015. Global cancer statistics, 2012. *CA: A Cancer Journal for Clinicians*, 65, 87-108.
- ABDALLAH, H. M. & EZZAT, S. M. 2011. Effect of the method of preparation on the composition and cytotoxic activity of the essential oil of *Pituranthos tortuosus*. *Z Naturforsch C*, 66, 143-8.
- ABDEL-KADER, M. S. 2003. New ester and furocoumarins from the roots of *Pituranthos tortuosus*. *Journal of the Brazilian Chemical Society*, 14, 48-51.
- ABDELHALIM, A., KARIM, N., CHEBIB, M., ABURJAI, T., KHAN, I., JOHNSTON, G. A. & HANRAHAN, J. 2015. Antidepressant, Anxiolytic and Antinociceptive Activities of Constituents from *Rosmarinus Officinalis*. *Journal of Pharmacy and Pharmaceutical Sciences*, 18, 448-59.
- ABDELSHAFEEK, K., ABDELRAHEM, F., ELWAHSH, M. & ABDELKHALEK, I. 2009. Investigation of the flavonoidal constituents and insecticidal activity of *Teucrium zanonii*. *Pharmacognosy Research*, 1, 410-416.
- ABDELSHAFEEK, K., ISMAIL, I. A. & ALWAHSH, M. A. 2006. *Flavonoids and insecticidal activity of Teucrium zanonii*.
- ABDELWAHED, A., HAYDER, N., KILANI, S., MAHMOUD, A., CHIBANI, J., HAMMAMI, M., CHEKIR-GHEDIRA, L. & GHEDIRA, K. 2006. Chemical composition and antimicrobial activity of essential oils from Tunisian *Pituranthos tortuosus* (Coss.) Maire. *Flavour and Fragrance Journal*, 21, 129-133.
- ABDELWAHED, A., SKANDRANI, I., KILANI, S., NEFFATI, A., BEN SGHAIER, M., BOUHLEL, I., BOUBAKER, J., BEN AMMAR, R., MAHMOUD, A., GHEDIRA, K. & CHEKIR-GHEDIRA, L. 2008a. *Mutagenic, Antimutagenic, Cytotoxic, and Apoptotic Activities of Extracts from Pituranthos tortuosus*.

- ABDELWAHED, A., SKANDRANI, I., KILANI, S., NEFFATI, A., SGHAIER, M. B., BOUHLEL, I., BOUBAKER, J., AMMAR, R. B., MAHMOUD, A., GHEDIRA, K. & CHEKIR-GHEDIRA, L. 2008b. Mutagenic, antimutagenic, cytotoxic, and apoptotic activities of extracts from *Pituranthos tortuosus*. *Drug and Chemical Toxicology*, 31, 37-60.
- ADEKENOV, S. M. 1995. Sesquiterpene lactones from plants of the family Asteraceae in the Kazakhstan flora and their biological activity. *Chemistry of Natural Compounds*, 31, 21-25.
- AFIFI, F. U., KASABRI, V., LITESCU, S. C. & ABAZA, I. M. 2016. In vitro and in vivo comparison of the biological activities of two traditionally and widely used Arum species from Jordan: *Arum dioscoridis* Sibth & Sm. and *Arum palaestinum* Boiss. *Natural Product Research*, 30, 1777-1786.
- AHMED, S. B., SGHAIER, R. M., GUESMI, F., KAABI, B., MEJRI, M., ATTIA, H., LAOUINI, D. & SMAALI, I. 2011. Evaluation of antileishmanial, cytotoxic and antioxidant activities of essential oils extracted from plants issued from the leishmaniasis-endemic region of Sned (Tunisia). *Natural Product Research*, 25, 1195-201.
- AHN, E.-M., BANG, M.-H., SONG, M.-C., PARK, M.-H., KIM, H.-Y., KWON, B.-M. & BAEK, N.-I. 2006. Cytotoxic and ACAT-inhibitory sesquiterpene lactones from the root of *Ixeris dentata forma albiflora*. *Archives of Pharmacal Research*, 29, 937.
- AL-BAYATI, F. A. & MOHAMMED, M. J. 2009. Isolation, identification, and purification of cinnamaldehyde from *Cinnamomum zeylanicum* bark oil. An antibacterial study. *Pharmaceutical Biology*, 47, 61-66.
- AL-GABY, A. M. & ALLAM, R. R. 2000. Chemical Analysis, Antimicrobial Activity, and the Essential Oils from Some Wild Herbs in Egypt. *Journal of Herbs, Spices & Medicinal Plants*, 7, 15-23.
- AL SINANI, S. S., ELTAYEB, E. A., COOMBER, B. L. & ADHAM, S. A. 2016. Solamargine triggers cellular necrosis selectively in different types of human melanoma cancer cells through extrinsic lysosomal mitochondrial death pathway. *Cancer Cell International*, 16, 11.
- ALAMGEER, -, RASHID, M., BASHIR, S., MUSHTAQ, M. N., KHAN, H. U., MALIK, M. N. H., QAYYUM, A. & RAHAMAN, M. S. U. 2013.

Comparative hypoglycemic activity of different extracts of *Teucrium stocksianum* in diabetic rabbits. 2013, 8, 8.

ALI ASGAR, M. 2013. Anti-Diabetic Potential of Phenolic Compounds: A Review. *International Journal of Food Properties*, 16, 91-103.

ALI, M., AL-QATTAN, K. K., AL-ENEZI, F., KHANAFER, R. M. & MUSTAFA, T. 2000. Effect of allicin from garlic powder on serum lipids and blood pressure in rats fed with a high cholesterol diet. *Prostaglandins Leukot Essent Fatty Acids*, 62, 253-9.

ALI, N., SHAH, S. W., SHAH, I., AHMED, G., GHIAS, M. & KHAN, I. 2011. Cytotoxic and anthelmintic potential of crude saponins isolated from *Achillea Wilhelmsii* C. Koch and *Teucrium Stocksianum* boiss. *BMC Complement The Journal of Alternative and Complementary Medicine*, 11, 106.

ALIMOVA, I. N., LIU, B., FAN, Z., EDGERTON, S. M., DILLON, T., LIND, S. E. & THOR, A. D. 2009. Metformin inhibits breast cancer cell growth, colony formation and induces cell cycle arrest in vitro. *Cell Cycle*, 8, 909-915.

ALIZADEH, A., MOSHIRI, M., ALIZADEH, J. & BALALI-MOOD, M. 2014. Black henbane and its toxicity - a descriptive review. *Avicenna Journal of Phytomedicine*, 4, 297-311.

ALJAIYASH, A., H GONAIID, M., ISLAM, M. & CHAOUCH, A. 2014. *Antibacterial and cytotoxic activities of some Libyan medicinal plants*.

ALMEIDA, C. A. & BARRY, S. A. 2011. *Cancer: Basic Science and Clinical Aspects*, Wiley.

AMIN, R. P., KUNAPARAJU, N., KUMAR, S., TALDONE, T., BARLETTA, M. A. & ZITO, S. W. 2013. Structure elucidation and inhibitory effects on human platelet aggregation of chlorogenic acid from *Wrightia tinctoria*. *Journal of Complementary and Integrative Medicine*, 10.

AMIRI, H. 2010. Antioxidant Activity of the Essential Oil and Methanolic Extract of *Teucrium orientale* (L.) subsp. *taylori* (Boiss.) Rech. f. *Iranian Journal of Pharmaceutical Research*, 9, 417-23.

ANSELMINI, C., CENTINI, M., GRANATA, P., SEGA, A., BUONOCORE, A., BERNINI, A. & FACINO, R. M. 2004. Antioxidant activity of ferulic acid

- alkyl esters in a heterophasic system: a mechanistic insight. *J Agric Food Chem*, 52, 6425-32.
- ARORA, D., RANI, A. & SHARMA, A. 2013. A review on phytochemistry and ethnopharmacological aspects of genus *Calendula*. *Pharmacognosy Reviews*, 7, 179-87.
- ARUMUGAM, G., MANJULA, P. & PAARI, N. 2013. A review: Anti diabetic medicinal plants used for diabetes mellitus. *Journal of Acute Disease*, 2, 196-200.
- AYATOLLAHI, A. M., GHANADIAN, M., ATT-UR-RAHMAN, R., MESAİK, M. A., KHALID, A. S. & ADELI, F. 2015. Methoxylated Flavones from *Salvia Mirzayanii* Rech. f. and *Esfand* with Immunosuppressive Properties. *Iranian Journal of Pharmaceutical Research*, 14, 955-60.
- BAE, Y. H. & PARK, K. 2011. Targeted drug delivery to tumors: myths, reality and possibility. *Journal Control Release*, 153, 198-205.
- BAI, N., HE, K., ZHOU, Z., LAI, C.-S., ZHANG, L., QUAN, Z., SHAO, X., PAN, M.-H. & HO, C.-T. 2010. Flavonoids from *Rabdosia rubescens* exert anti-inflammatory and growth inhibitory effect against human leukemia HL-60 cells. *Food Chemistry*, 122, 831-835.
- BALANDRIN, M. F., KINGHORN, A. D. & FARNSWORTH, N. R. 1993. Plant-Derived Natural Products in Drug Discovery and Development. *Human Medicinal Agents from Plants*. American Chemical Society.
- BARBOSA FILHO, J., COSTA, M., GOMES, C. & TROLIN, G. 1993. *Isolation of Onopordopicrin, the Toxic Constituent of Arctium lappa L.*
- BARONE, B. B., YEH, H. C., SNYDER, C. F., PEAIRS, K. S., STEIN, K. B., DERR, R. L., WOLFF, A. C. & BRANCATI, F. L. 2010. Postoperative mortality in cancer patients with preexisting diabetes: systematic review and meta-analysis. *Diabetes Care*, 33, 931-9.
- BASCH, E., GABARDI, S. & ULBRICHT, C. 2003. Bitter melon (*Momordica charantia*): a review of efficacy and safety. *American Journal of Health-System Pharmacy*, 60, 356-9.
- BEDIR, E., TASDEMİR, D., ÇALIS, I., ZERBE, O. & OTTO, S. 1999. Neo-clerodane diterpenoids from *Teucrium polium*. *Phytochemistry*, 51, 921-925.

- BEL HADJ SALAH-FATNASSI, K., HASSAYOUN, F., CHERAIF, I., KHAN, S., JANNET, H. B., HAMMAMI, M., AOUNI, M. & HARZALLAH-SKHIRI, F. 2017. Chemical composition, antibacterial and antifungal activities of flowerhead and root essential oils of *Santolina chamaecyparissus* L., growing wild in Tunisia. *Saudi Journal of Biological Sciences*, 24, 875-882.
- BELKAID, A., CURRIE, J. C., DESGAGNES, J. & ANNABI, B. 2006. The chemopreventive properties of chlorogenic acid reveal a potential new role for the microsomal glucose-6-phosphate translocase in brain tumor progression. *Cancer Cell International*, 6, 7.
- BEN SAHRA, I., REGAZZETTI, C., ROBERT, G., LAURENT, K., LE MARCHAND-BRUSTEL, Y., AUBERGER, P., TANTI, J. F., GIORGETTI-PERALDI, S. & BOST, F. 2011. Metformin, independent of AMPK, induces mTOR inhibition and cell-cycle arrest through REDD1. *Cancer Research*, 71, 4366-72.
- BHANDARI, M. R., JONG-ANURAKKUN, N., HONG, G. & KAWABATA, J. 2008.  $\alpha$ -Glucosidase and  $\alpha$ -amylase inhibitory activities of Nepalese medicinal herb Pakhanbhed (*Bergenia ciliata*, Haw.). *Food Chemistry*, 106, 247-252.
- BHARTI, S. K., KRISHNAN, S., KUMAR, A. & KUMAR, A. 2018. Antidiabetic phytoconstituents and their mode of action on metabolic pathways. *Therapeutic Advances in Endocrinology and Metabolism*, 9, 81-100.
- BLACK, S. E. 2017. Doctors on Drugs: Medical Professionals and the Proliferation of Morphine Addiction in Nineteenth-Century France. *Social History of Medicine*, 30, 114-136.
- BOGENRIEDER, T. & HERLYN, M. 2003. Axis of evil: molecular mechanisms of cancer metastasis. *Oncogene*, 22, 6524-36.
- BOGHRATI, Z., NASERI, M., REZAIE, M., PHAM, N., QUINN, R. J., TAYARANI-NAJARAN, Z. & IRANSHAHI, M. 2016a. Tyrosinase inhibitory properties of phenylpropanoid glycosides and flavonoids from *Teucrium polium* L. var. *gnaphalodes*. *Iranian journal of basic medical sciences*, 19, 804-811.
- BOGHRATI, Z., NASERI, M., REZAIE, M., PHAM, N., QUINN, R. J., TAYARANI-NAJARAN, Z. & IRANSHAHI, M. 2016b. Tyrosinase inhibitory properties of

phenylpropanoid glycosides and flavonoids from *Teucrium polium* L. var. *gnaphalodes*. *Iranian Journal of Basic Medical Sciences*, 19, 804-811.

BOHM, B. A. & STUESSY, T. F. 2013. *Flavonoids of the Sunflower Family (Asteraceae)*, Springer Vienna.

BOHS, L. & OLMSTEAD, R. 1997. *Phylogenetic Relationships in Solanum (Solanaceae) Based on ndhF Sequences*.

BOUSSAADA, O., BEN HALIMA KAMEL, M., AMMAR, S., HAOUAS, D., GANNOUN, S. & HELAL, A. N. 2008. *Insecticidal activity of some Asteraceae plant extracts against Tribolium confusum*.

BRUNO, M., PIOZZI, F., ROSSELLI, S., MAGGIO, A., ALANIA, M., LAMARA, K., AL HILLO, M. R. Y. & SERVETTAZ, O. 2004. Phytochemical Investigation of Four *Teucrium* Species. *Journal of the Mexican Chemical Society*, 48, 137-138.

CAI, J., ZHAO, L. & TAO, W. 2015. Potent protein tyrosine phosphatase 1B (PTP1B) inhibiting constituents from *Anoectochilus chapaensis* and molecular docking studies. *Journal of Pharmaceutical Biology*, 53, 1030-4.

CAI, X., YE, T., LIU, C., LU, W., LU, M., ZHANG, J., WANG, M. & CAO, P. 2011. Luteolin induced G2 phase cell cycle arrest and apoptosis on non-small cell lung cancer cells. *Toxicol In Vitro*, 25, 1385-91.

CAO, J., HAN, J., XIAO, H., QIAO, J. & HAN, M. 2016. Effect of Tea Polyphenol Compounds on Anticancer Drugs in Terms of AntiTumor Activity, Toxicology, and Pharmacokinetics. *Nutrients*, 8, 762.

CHAM, B. E., GILLIVER, M. & WILSON, L. 1987. Antitumour effects of glycoalkaloids isolated from *Solanum sodomaeum*. *Planta Med*, 53, 34-6.

CHAM, B. E. & MEARES, H. M. 1987. Glycoalkaloids from *Solanum sodomaeum* are effective in the treatment of skin cancers in man. *Cancer Letters*, 36, 111-118.

CHAM, B. E. & WILSON, L. 1987. HPLC of Glycoalkaloids from *Solanum sodomaeum*. *Planta Med*, 53, 59-62.

- CHAMBERS, A. F., GROOM, A. C. & MACDONALD, I. C. 2002. Dissemination and growth of cancer cells in metastatic sites. *Nature Reviews Cancer*, 2, 563-72.
- CHAMIKARA, M., DISSANAYAKE, D. R. R. P., ISHAN, M. & SOORIYAPATHIRANA, S. 2016. *Dietary, Anticancer and Medicinal Properties of the Phytochemicals in Chili Pepper (Capsicum spp.)*.
- CHAN, L. K., KOH, W. Y. & TENGKU-MUHAMMAD, T. S. 2005. Comparison of cytotoxic activities between in vitro and field grown plants of *Typhonium flagelliforme* (Lodd.) blume. *Journal of Plant Biology*, 48, 25-31.
- CHAN, P., CHENG, J. T., TSAO, C. W., NIU, C. S. & HONG, C. Y. 1996. The in vitro antioxidant activity of trilinolein and other lipid-related natural substances as measured by enhanced chemiluminescence. *Life Sciences*, 59, 2067-73.
- CHANG, H., MI, M., LING, W., ZHU, J., ZHANG, Q., WEI, N., ZHOU, Y., TANG, Y. & YUAN, J. 2009. Structurally related cytotoxic effects of flavonoids on human cancer cells *in vitro*. *Archives of Pharmacal Research*, 31, 1137.
- CHANG, L.-C., TSAI, T.-R., WANG, J.-J., LIN, C.-N. & KUO, K.-W. 1998a. The Rhamnose Moiety of Solamargine Plays a Crucial Role in Triggering Cell Death by Apoptosis. *Biochemical and Biophysical Research Communications*, 242, 21-25.
- CHANG, L. C., TSAI, T. R., WANG, J. J., LIN, C. N. & KUO, K. W. 1998b. The rhamnose moiety of solamargine plays a crucial role in triggering cell death by apoptosis. *Biochem Biophys Res Commun*, 242, 21-5.
- CHAUDHARY, J., JAIN, A., MANUJA, R. & SACHDEVA, S. 2013. *A Comprehensive Review on Biological activities of p-hydroxy benzoic acid and its derivatives*.
- CHAUHAN, K., SHETH, N., RANPARIYA, V. & PARMAR, S. 2011. Anticonvulsant activity of solasodine isolated from *Solanum sisymbriifolium* fruits in rodents. *Pharmaceutical Biology*, 49, 194-199.
- CHEN, H.-W., LEE, J.-Y., HUANG, J.-Y., WANG, C.-C., CHEN, W.-J., SU, S.-F., HUANG, C.-W., HO, C.-C., J W CHEN, J., TSAI, M.-F., YU, S.-L. & YANG, P.-C. 2008. *Curcumin Inhibits Lung Cancer Cell Invasion and Metastasis through the Tumor Suppressor HLJ1*.

- CHEN, H., FENG, R., GUO, Y., SUN, L. & JIANG, J. 2001. Hypoglycemic effects of aqueous extract of *Rhizoma Polygonati Odorati* in mice and rats. *J Ethnopharmacol*, 74, 225-9.
- CHEN, R. M., HU, L. H., AN, T. Y., LI, J. & SHEN, Q. 2002. Natural PTP1B inhibitors from *Broussonetia papyrifera*. *Bioorganic & Medicinal Chemistry Letters*, 12, 3387-90.
- CHEN, Y.-C., LEE, H.-Z., CHEN, H.-C., WEN, C.-L., KUO, Y.-H. & WANG, G.-J. 2013. Anti-Inflammatory Components from the Root of *Solanum erianthum*. *International Journal of Molecular Sciences*, 14, 12581.
- CHEN, Y., LI, S., SUN, F., HAN, H., ZHANG, X., FAN, Y., TAI, G. & ZHOU, Y. 2010. In vivo antimalarial activities of glycoalkaloids isolated from Solanaceae plants. *Pharmaceutical Biology*, 48, 1018-1024.
- CHEN, Y., TANG, Q., WU, J., ZHENG, F., YANG, L. & HANN, S. S. 2015. Inactivation of PI3-K/Akt and reduction of SP1 and p65 expression increase the effect of solamargine on suppressing EP4 expression in human lung cancer cells. *Journal of Experimental & Clinical Cancer Research*, 34, 154.
- CHENG, A. C., HUANG, T. C., LAI, C. S. & PAN, M. H. 2005. Induction of apoptosis by luteolin through cleavage of Bcl-2 family in human leukemia HL-60 cells. *European Journal of Pharmacology*, 509, 1-10.
- CHENG, A. Y. & FANTUS, I. G. 2005. Oral antihyperglycemic therapy for type 2 diabetes mellitus. *Canadian Medical Association Journal*, 172, 213-26.
- CHIRUVELLA, K. K., MOHAMMED, A., DAMPURI, G., GHANTA, R. G. & RAGHAVAN, S. C. 2007. Phytochemical and Antimicrobial Studies of Methyl Angolensate and Luteolin-7-O-glucoside Isolated from Callus Cultures of *Soymida febrifuga*. *International Journal of Biomedical Science*, 3, 269-78.
- CHO, H. 2013. Chapter Seventeen - Protein Tyrosine Phosphatase 1B (PTP1B) and Obesity. In: LITWACK, G. (ed.) *Vitamins & Hormones*. Academic Press.
- CHO, J.-Y., MOON, J.-H., SEONG, K.-Y. & PARK, K.-H. 1998. Antimicrobial Activity of 4-Hydroxybenzoic Acid and trans 4-Hydroxycinnamic Acid Isolated and Identified from Rice Hull. *Bioscience, Biotechnology, and Biochemistry*, 62, 2273-2276.

- CHOU, P.-Y., HUANG, G. J., PAN, C.-H., CHIEN, Y. C., CHEN, Y.-Y., WU, J. P., SHEU, M.-J. & CHENG, H.-C. 2011. *Trilinolein Inhibits Proliferation of Human Non-Small Cell Lung Carcinoma A549 Through the Modulation of PI3K/Akt Pathway*.
- CHOW, J.-M., HUANG, G.-C., SHEN, S.-C., WU, C.-Y., LIN, C.-W. & CHEN, Y.-C. 2008. Differential apoptotic effect of wogonin and nor-wogonin via stimulation of ROS production in human leukemia cells. *Journal of Cellular Biochemistry*, 103, 1394-1404.
- CHOWANSKI, S., ADAMSKI, Z., MARCINIAK, P., ROSINSKI, G., BUYUKGUZEL, E., BUYUKGUZEL, K., FALABELLA, P., SCRANO, L., VENTRELLA, E., LELARIO, F. & BUFO, S. A. 2016. A Review of Bioinsecticidal Activity of Solanaceae Alkaloids. *Toxins (Basel)*, 8.
- COLERIDGE SMITH, P. D. 2003. From skin disorders to venous leg ulcers: pathophysiology and efficacy of Daflon 500 mg in ulcer healing. *Angiology*, 54 Suppl 1, S45-50.
- COLL, J. C. & BOWDEN, B. F. 1986. The Application of Vacuum Liquid Chromatography to the Separation of Terpene Mixtures. *Journal of Natural Products*, 49, 934-936.
- COLLINS, K. K. 2014. The diabetes-cancer link. *Diabetes Spectr*, 27, 276-80.
- CRAGG, G. M. & NEWMAN, D. J. 2005. Plants as a source of anti-cancer agents. *Journal of Ethnopharmacology*, 100, 72-79.
- CRAGG, G. M. & NEWMAN, D. J. 2013. Natural products: A continuing source of novel drug leads. *Biochimica et Biophysica Acta (BBA) - General Subjects*, 1830, 3670-3695.
- CRESPO-ORTIZ, M. P. & WEI, M. Q. 2012. Antitumor activity of artemisinin and its derivatives: from a well-known antimalarial agent to a potential anticancer drug. *J Biomed Biotechnol*, 2012, 247597.
- CRESPO, M. E., GALVEZ, J., CRUZ, T., OCETE, M. A. & ZARZUELO, A. 1999. Anti-inflammatory activity of diosmin and hesperidin in rat colitis induced by TNBS. *Planta Med*, 65, 651-3.
- CUEVA, C., MORENO-ARRIBAS, M. V., MARTIN-ALVAREZ, P. J., BILLS, G., VICENTE, M. F., BASILIO, A., RIVAS, C. L., REQUENA, T.,

- RODRIGUEZ, J. M. & BARTOLOME, B. 2010. Antimicrobial activity of phenolic acids against commensal, probiotic and pathogenic bacteria. *Research in Microbiology*, 161, 372-82.
- D'ABROSCA, B., PACIFICO, S., SCOGNAMIGLIO, M., D'ANGELO, G., GALASSO, S., MONACO, P. & FIORENTINO, A. 2013. A new acylated flavone glycoside with antioxidant and radical scavenging activities from *Teucrium polium* leaves. *Nat Prod Res*, 27, 356-63.
- DA ROCHA, A. B., LOPES, R. M. & SCHWARTSMANN, G. 2001. Natural products in anticancer therapy. *Current Opinion in Pharmacology*, 1, 364-369.
- DAS, A., JAWED, J. J., DAS, M. C., SANDHU, P., DE, U. C., DINDA, B., AKHTER, Y. & BHATTACHARJEE, S. 2017. Antileishmanial and immunomodulatory activities of lupeol, a triterpene compound isolated from *Sterculia villosa*. *International Journal of Antimicrobial Agents*, 50, 512-522.
- DE ABREU, I. N., SAWAYA, A. C. H. F., EBERLIN, M. N. & MAZZAFERA, P. 2005. Production of pilocarpine in callus of jaborandi (*pilocarpus microphyllus* stapf). *In Vitro Cellular & Developmental Biology - Plant*, 41, 806-811.
- DEKA, S. J., GORAI, S., MANNA, D. & TRIVEDI, V. 2017. Evidence of PKC Binding and Translocation to Explain the Anticancer Mechanism of Chlorogenic Acid in Breast Cancer Cells. *Curr Mol Med*, 17, 79-89.
- DEWAN, S. M. R., AMIN, M. N., ADNAN, T., UDDIN, S. M. N., SHAHID-UDAULA, A. F. M., SARWAR, G. & HOSSAIN, M. S. 2013. Investigation of analgesic potential and in vitro antioxidant activity of two plants of Asteraceae family growing in Bangladesh. *Journal of Pharmacy Research*, 6, 599-603.
- DHANANI, T., SHAH, S., GAJBHIYE, N. A. & KUMAR, S. 2017. Effect of extraction methods on yield, phytochemical constituents and antioxidant activity of *Withania somnifera*. *Arabian Journal of Chemistry*, 10, S1193-S1199.
- DHOLWANI, K. K., SALUJA, A. K., GUPTA, A. R. & SHAH, D. R. 2008. A review on plant-derived natural products and their analogs with anti-tumor activity. *Indian J Pharmacol*, 40, 49-58.
- DIAB-ASSAF, M., TALEB, R. I., SHEBABY, W., MANSOUR, A., MOUSSA, C. J., DAHER, C. & MROUEH, M. 2012. Antioxidant and anticancer activities of

- methanolic, ethyl acetate and chloroform extracts of *Arum Palaestinum*. *Planta Med*, 78, PI389.
- DIAS, D. A., URBAN, S. & ROESSNER, U. 2012. A historical overview of natural products in drug discovery. *Metabolites*, 2, 303-36.
- DING, X., ZHU, F.-S., LI, M. & GAO, S.-G. 2011. *Induction of apoptosis in human hepatoma SMMC-7721 cells by solamargine from Solanum nigrum L.*
- DING, X., ZHU, F.-S., LI, M. & GAO, S.-G. 2012. Induction of apoptosis in human hepatoma SMMC-7721 cells by solamargine from *Solanum nigrum L.* *Journal of Ethnopharmacology*, 139, 599-604.
- DING, X., ZHU, F., YANG, Y. & LI, M. 2013a. *Purification, antitumor activity in vitro of steroidal glycoalkaloids from black nightshade (Solanum nigrum L.).*
- DING, X., ZHU, F., YANG, Y. & LI, M. 2013b. Purification, antitumor activity in vitro of steroidal glycoalkaloids from black nightshade (*Solanum nigrum L.*). *Food Chemistry*, 141, 1181-6.
- DO NASCIMENTO, P. G., LEMOS, T. L., BIZERRA, A. M., ARRIAGA, A. M., FERREIRA, D. A., SANTIAGO, G. M., BRAZ-FILHO, R. & COSTA, J. G. 2014. Antibacterial and antioxidant activities of ursolic acid and derivatives. *Molecules*, 19, 1317-27.
- DOWLING, R. J., NIRLAULA, S., STAMBOLIC, V. & GOODWIN, P. J. 2012. Metformin in cancer: translational challenges. *J Mol Endocrinol*, 48, R31-43.
- EDDOUKS, M., MAGHRANI, M., LEMHADRI, A., OUAHIDI, M. L. & JOUAD, H. 2002. Ethnopharmacological survey of medicinal plants used for the treatment of diabetes mellitus, hypertension and cardiac diseases in the south-east region of Morocco (Tafilalet). *Journal of Ethnopharmacology*, 82, 97-103.
- EKOR, M. 2014. The growing use of herbal medicines: issues relating to adverse reactions and challenges in monitoring safety. *Front Pharmacol*, 4, 177.
- EL-DESOUKY, S. K., HAWAS, U. W. & KIM, Y.-K. 2014. Two New Diketopiperazines from ARUM Palaestinum. *Chemistry of Natural Compounds*, 50, 1075-1078.
- EL-DESOUKY, S. K., KIM, K. H., RYU, S. Y., EWEAS, A. F., GAMAL-ELDEEN, A. M. & KIM, Y.-K. 2007a. A new pyrrole alkaloid isolated from Arum

- palaestinum Boiss. and its biological activities. *Archives of Pharmacal Research*, 30, 927-931.
- EL-DESOUKY, S. K., RYU, S. Y. & KIM, Y.-K. 2007b. Piperazirum, a novel bioactive alkaloid from *Arum palaestinum* Boiss. *Tetrahedron Letters*, 48, 4015-4017.
- EL-MOKASABI, F. M. 2014. *Floristic composition and traditional uses of plant species at Wadi Alkuf, Al-Jabal Al-Akhder, Libya*.
- EL SAYED, K. A., HAMANN, M. T., ABD EL-RAHMAN, H. A. & ZAGHLOUL, A. M. 1998. New pyrrole alkaloids from *Solanum sodomaeum*. *Journal of Natural Products*, 61, 848-50.
- ELEKOFEHINTI, O. O. 2015. Saponins: Anti-diabetic principles from medicinal plants & 2013; A review. *Pathophysiology*, 22, 95-103.
- ELEKOFEHINTI, O. O., KAMDEM, J. P., KADE, I. J., ROCHA, J. B. T. & ADANLAWO, I. G. 2013. Hypoglycemic, antiperoxidative and antihyperlipidemic effects of saponins from *Solanum anguivi* Lam. fruits in alloxan-induced diabetic rats. *South African Journal of Botany*, 88, 56-61.
- ELMASRI, W. A., HEGAZY, M.-E. F., AZIZ, M., KOKSAL, E., AMOR, W., MECHREF, Y., HAMOOD, A. N., CORDES, D. B. & PARÉ, P. W. 2014a. Biofilm blocking sesquiterpenes from *Teucrium polium*. *Phytochemistry*, 103, 107-113.
- ELMASRI, W. A., HEGAZY, M.-E. F., MECHREF, Y. & PARE, P. W. 2015a. Cytotoxic saponin polysapogenin from *Teucrium polium*. *RSC Advances*, 5, 27126-27133.
- ELMASRI, W. A., HEGAZY, M.-E. F., MECHREF, Y. & PARÉ, P. W. 2016. Structure-antioxidant and anti-tumor activity of *Teucrium polium* phytochemicals. *Phytochemistry Letters*, 15, 81-87.
- ELMASRI, W. A., HEGAZY, M. F., AZIZ, M., KOKSAL, E., AMOR, W., MECHREF, Y., HAMOOD, A. N., CORDES, D. B. & PARE, P. W. 2014b. Biofilm blocking sesquiterpenes from *Teucrium polium*. *Phytochemistry*, 103, 107-113.

- ELMASRI, W. A., YANG, T., TRAN, P., HEGAZY, M.-E. F., HAMOOD, A. N., MECHREF, Y. & PARÉ, P. W. 2015b. *Teucrium polium* Phenylethanol and Iridoid Glycoside Characterization and Flavonoid Inhibition of Biofilm-Forming *Staphylococcus aureus*. *Journal of Natural Products*, 78, 2-9.
- ENDO, Y., MITSUI, K., MOTIZUKI, M. & TSURUGI, K. 1987. The mechanism of action of ricin and related toxic lectins on eukaryotic ribosomes. The site and the characteristics of the modification in 28 S ribosomal RNA caused by the toxins. *Journal of Biological Chemistry*, 262, 5908-12.
- ENOKI, T., OHNOGI, H., NAGAMINE, K., KUDO, Y., SUGIYAMA, K., TANABE, M., KOBAYASHI, E., SAGAWA, H. & KATO, I. 2007. Antidiabetic Activities of Chalcones Isolated from a Japanese Herb, *Angelica keiskei*. *Journal of Agricultural and Food Chemistry*, 55, 6013-6017.
- ESFANDABADI, A. O., KHODAGHOLI, F. & SANATI, M. H. 2013. Evaluation of the neuroprotective effect of salvigenin between the hippocampus and cortex of beta-amyloid-injected rats. *Alzheimer's & Dementia: The Journal of the Alzheimer's Association*, 9, P308.
- ESTEVEZ-SOUZA, A., SILVA, T. M. S. D., ALVES, C. C. F., CARVALHO, M. G. D., BRAZ-FILHO, R. & ECHEVARRIA, A. 2002. Cytotoxic activities against Ehrlich carcinoma and human K562 leukaemia of alkaloids and flavonoid from two *Solanum* Species. *Journal of the Brazilian Chemical Society*, 13, 838-842.
- EVANS, J. M., DONNELLY, L. A., EMSLIE-SMITH, A. M., ALESSI, D. R. & MORRIS, A. D. 2005. Metformin and reduced risk of cancer in diabetic patients. *Bmj*, 330, 1304-5.
- FACHINI-QUEIROZ, F. C., KUMMER, R., ESTEV, O-SILVA, C. F., CARVALHO, M. D. D. B., CUNHA, J. M., GRESPAN, R., BERSANI-AMADO, C. A. & CUMAN, R. K. N. 2012. Effects of Thymol and Carvacrol, Constituents of *Thymus vulgaris* L. Essential Oil, on the Inflammatory Response. *Evidence-Based Complementary and Alternative Medicine*, 2012, 10.
- FACUNDO, V. A., AZEVEDO, M. S., RODRIGUES, R. V., NASCIMENTO, L. F. D., MILITÃO, J. S. L. T., SILVA, G. V. J. D. & BRAZ-FILHO, R. 2012. Chemical constituents from three medicinal plants: *Piper renitens*, *Siparuna guianensis* and *Alternanthera brasiliana*. *Revista Brasileira de Farmacognosia*, 22, 1134-1139.

- FARID, M., HUSSEIN, S., TREDAFILOVA, A., MARZOUK, M., EL-OQLAH, A. & SAKER, M. M. 2017. *Phytochemical constituents of the butanol fraction of Arum palaestinum Boiss: Cytotoxic and antiviral screening.*
- FARID, M. M., HUSSEIN, S. R., IBRAHIM, L. F., EL DESOUKY, M. A., ELSAYED, A. M., EL OQLAH, A. A. & SAKER, M. M. 2015. Cytotoxic activity and phytochemical analysis of Arum palaestinum Boiss. *Asian Pacific Journal of Tropical Biomedicine*, 5, 944-947.
- FASSINA, G., FERRARI, N., BRIGATI, C., BENELLI, R., SANTI, L., NOONAN, D. M. & ALBINI, A. 2000. Tissue inhibitors of metalloproteases: regulation and biological activities. *Clin Exp Metastasis*, 18, 111-20.
- FATMA, G., SAMI, B. H. A. & AHMED, L. 2017. Investigation of Extracts from Tunisian Ethnomedicinal Plants as Antioxidants, Cytotoxins, and Antimicrobials. *Biomedical and Environmental Sciences*, 30, 811-824.
- FENG, Y., CARROLL, A. R., ADDEPALLI, R., FECHNER, G. A., AVERY, V. M. & QUINN, R. J. 2007. Vanillic acid derivatives from the green algae *Cladophora socialis* as potent protein tyrosine phosphatase 1B inhibitors. *Journal of Natural Products*, 70, 1790-2.
- FERRACANE, R., GRAZIANI, G., GALLO, M., FOGLIANO, V. & RITIENI, A. 2010. Metabolic profile of the bioactive compounds of burdock (*Arctium lappa*) seeds, roots and leaves. *Journal of Pharmaceutical and Biomedical Analysis*, 51, 399-404.
- FIorentino, A., D'ABROSCA, B., PACIFICO, S., SCOGNAMIGLIO, M., D'ANGELO, G., GALLICCHIO, M., CHAMBERY, A. & MONACO, P. 2011. Structure elucidation and hepatotoxicity evaluation against HepG2 human cells of neo-clerodane diterpenes from *Teucrium polium* L. *Phytochemistry*, 72, 2037-2044.
- FOTSIS, T., PEPPER, M. S., AKTAS, E., BREIT, S., RASKU, S., ADLERCREUTZ, H., WAHALA, K., MONTESANO, R. & SCHWEIGERER, L. 1997. Flavonoids, dietary-derived inhibitors of cell proliferation and in vitro angiogenesis. *Cancer Research*, 57, 2916-21.
- FRANTZ, C., STEWART, K. M. & WEAVER, V. M. 2010. The extracellular matrix at a glance. *Journal of Cell Science*, 123, 4195-200.

- FU, G., PANG, H. & WONG, Y. H. 2008. Naturally occurring phenylethanoid glycosides: potential leads for new therapeutics. *Current Medicinal Chemistry*, 15, 2592-613.
- FULDA, S. 2008. Betulinic Acid for cancer treatment and prevention. *International Journal of Molecular Sciences*, 9, 1096-107.
- GAI, W. T., YU, D. P., WANG, X. S. & WANG, P. T. 2016. Anti-cancer effect of ursolic acid activates apoptosis through ROCK/PTEN mediated mitochondrial translocation of cofilin-1 in prostate cancer. *Oncology Letters*, 12, 2880-2885.
- GILBERT, E. R. & LIU, D. 2013. Anti-diabetic functions of soy isoflavone genistein: mechanisms underlying its effects on pancreatic beta-cell function. *Food Funct*, 4, 200-12.
- GIOVANNUCCI, E., HARLAN, D. M., ARCHER, M. C., BERGENSTAL, R. M., GAPSTUR, S. M., HABEL, L. A., POLLAK, M., REGENSTEINER, J. G. & YEE, D. 2010. Diabetes and cancer: a consensus report. *Diabetes Care*, 33, 1674-85.
- GNANAMONY, M. & GONDI, C. S. 2017. Chemoresistance in pancreatic cancer: Emerging concepts. *Oncology Letters*, 13, 2507-2513.
- GOHARI, A. R., MOSADDEGH, M., NAGHIBI, F., ESLAMI-TEHRANI, B., PIRANI, A., HAMZELOO-MOGHADAM, M. & READ, R. W. 2015. Cytotoxic sesquiterpene lactones from the aerial parts of *Inula aucheriana*. *An Acad Bras Cienc*, 87, 777-85.
- GOPALAKRISHNAN, V., IYYAM PILLAI, S. & SUBRAMANIAN, S. P. 2015. Synthesis, Spectral Characterization, and Biochemical Evaluation of Antidiabetic Properties of a New Zinc-Diosmin Complex Studied in High Fat Diet Fed-Low Dose Streptozotocin Induced Experimental Type 2 Diabetes in Rats. *Biochemistry Research International*, 2015, 350829.
- GOVINDASAMY, C., AL-NUMAIR, K. S., ALSAIF, M. A. & VISWANATHAN, K. P. 2011. Influence of 3-hydroxymethyl xylitol, a novel antidiabetic compound isolated from *Casearia esculenta* (Roxb.) root, on glycoprotein components in streptozotocin-diabetic rats. *Journal of Asian Natural Products Research*, 13, 700-6.

- GRANADO-SERRANO, A. B., ANGELES MARTÍN, M., IZQUIERDO-PULIDO, M., GOYA, L., BRAVO, L. & RAMOS, S. 2007. Molecular Mechanisms of (-)-Epicatechin and Chlorogenic Acid on the Regulation of the Apoptotic and Survival/Proliferation Pathways in a Human Hepatoma Cell Line. *Journal of Agricultural and Food Chemistry*, 55, 2020-2027.
- GRAY, A. I., IGOLI, J. O. & EDRADA-EBEL, R. 2012. Natural products isolation in modern drug discovery programs. *Methods Mol Biol*, 864, 515-34.
- GREGORY, J., MOORE, D. & SIMMONS, J. 2013. *Type 1 Diabetes Mellitus*.
- GROVER, J. K., YADAV, S. & VATS, V. 2002. Medicinal plants of India with anti-diabetic potential. *J Ethnopharmacol*, 81, 81-100.
- GUESMI, F., TYAGI, A. K., PRASAD, S. & LANDOULSI, A. 2018. Terpenes from essential oils and hydrolate of *Teucrium alopecurus* triggered apoptotic events dependent on caspases activation and PARP cleavage in human colon cancer cells through decreased protein expressions. *Oncotarget*, 9, 32305-32320.
- GULLETT, N. P., RUHUL AMIN, A. R. M., BAYRAKTAR, S., PEZZUTO, J. M., SHIN, D. M., KHURI, F. R., AGGARWAL, B. B., SURH, Y.-J. & KUCUK, O. 2010. Cancer Prevention With Natural Compounds. *Seminars in Oncology*, 37, 258-281.
- GUO, Z.-Y., LI, P., HUANG, W., WANG, J.-J., LIU, Y.-J., LIU, B., WANG, Y.-L., WU, S.-B., KENNELLY, E. J. & LONG, C.-L. 2014. Antioxidant and anti-inflammatory caffeoyl phenylpropanoid and secoiridoid glycosides from *Jasminum nervosum* stems, a Chinese folk medicine. *Phytochemistry*, 106, 124-133.
- GUPTA, G. P. & MASSAGUE, J. 2006. Cancer metastasis: building a framework. *Cell*, 127, 679-95.
- GUPTA, M. M., SINGH, D. V., TRIPATHI, A. K., PANDEY, R., VERMA, R. K., SINGH, S., SHASANY, A. K. & KHANUJA, S. P. 2005. Simultaneous determination of vincristine, vinblastine, catharanthine, and vindoline in leaves of *catharanthus roseus* by high-performance liquid chromatography. *Journal of Chromatographic Science*, 43, 450-3.

- GÜRBÜZ ÖZTÜRK, N., KARABEY, F., KURTULUŞ ÖZTÜRK, T., KILINC, A., FRARY, A. & DOGANLAR, S. 2015. *Glycoalkaloid isolation from Solanum linnaeanum berries*.
- GURIB-FAKIM, A. 2006. *Medicinal plants: Traditions of yesterday and drugs of tomorrow*.
- HAMMAMI, S., JMII, H., EL MOKNI, R., KHMIRI, A., FAIDI, K., DHAOUADI, H., EL AOUNI, M. H., AOUNI, M. & JOSHI, R. K. 2015. Essential Oil Composition, Antioxidant, Cytotoxic and Antiviral Activities of *Teucrium pseudochamaepitys* Growing Spontaneously in Tunisia. *Molecules*, 20, 20426-33.
- HAN, K., MENG, W., ZHANG, J. J., ZHOU, Y., WANG, Y. L., SU, Y., LIN, S. C., GAN, Z. H., SUN, Y. N. & MIN, D. L. 2016. Luteolin inhibited proliferation and induced apoptosis of prostate cancer cells through miR-301. *Oncotargets Ther*, 9, 3085-94.
- HAO, X., ZHANG, J., XIA, G., XUE, Y., LUO, Z., SI, Y., YAO, G. & ZHANG, Y. 2013. A new triterpenoid from *Teucrium viscidum*. *Molecules*, 18, 1262-9.
- HARA, Y. & HONDA, M. 1990. The Inhibition of  $\alpha$ -Amylase by Tea Polyphenols. *Agricultural and Biological Chemistry*, 54, 1939-1945.
- HARVEY, A. L. 2008. Natural products in drug discovery. *Drug Discovery Today*, 13, 894-901.
- HAYASHI, K., NARUTAKI, K., NAGAOKA, Y., HAYASHI, T. & UESATO, S. 2010. Therapeutic effect of arctiin and arctigenin in immunocompetent and immunocompromised mice infected with influenza A virus. *Biological and Pharmaceutical Bulletin*, 33, 1199-205.
- HEGAZY, A., BOULOS, L., KABIEL, H. & O S SHARASHY, A. 2011. Vegetation and species altitudinal distribution in Al-Jabal Al-Akhdar landscape, Libya.
- HEILBRUN, L. K., NOMURA, A. & STEMMERMANN, G. N. 1986. Black tea consumption and cancer risk: a prospective study. *British Journal of Cancer*, 54, 677-83.
- HEJMADI, M. 2009. *Introduction to Cancer Biology*, Ventus Publishing.

- HENRIQUEZ, C. L., ARIAS, T., PIRES, J. C., CROAT, T. B. & SCHAAL, B. A. 2014. Phylogenomics of the plant family Araceae. *Mol Phylogenet Evol*, 75, 91-102.
- HO, Y.-C., YANG, S.-F., PENG, C.-Y., CHOU, M.-Y. & CHANG, Y.-C. 2007. *Epigallocatechin-3-gallate inhibits the invasion of human oral cancer cells and decreases the productions of matrix metalloproteinases and urokinase-plasminogen activator.*
- HODAJ, E., TSIFTSOGLU, O., ABAZI, S., HADJIPAVLOU-LITINA, D. & LAZARI, D. 2017. Lignans and indole alkaloids from the seeds of *Centaurea vlachorum* Hartvig (Asteraceae), growing wild in Albania and their biological activity. *Natural Product Research*, 31, 1195-1200.
- HONBU, T., IKEDA, T., ZHU, X.-H., YOSHIHARA, O., OKAWA, M., NAFADY, A. M. & NOHARA, T. 2002. New Steroidal Glycosides from the Fruits of *Solanum anguivi*. *Journal of Natural Products*, 65, 1918-1920.
- HOSSAIN, M. A. & MIZANUR RAHMAN, S. M. 2015. Isolation and characterisation of flavonoids from the leaves of medicinal plant *Orthosiphon stamineus*. *Arabian Journal of Chemistry*, 8, 218-221.
- HOU, N., LIU, N., HAN, J., YAN, Y. & LI, J. 2017. Chlorogenic acid induces reactive oxygen species generation and inhibits the viability of human colon cancer cells. *Anticancer Drugs*, 28, 59-65.
- HSU, S.-H., TSAI, T.-R., LIN, C.-N., YEN, M.-H. & KUO, K.-W. 1996. Solamargine Purified from *Solanum incanum* Chinese Herb Triggers Gene Expression of Human TNFR I Which May Lead to Cell Apoptosis. *Biochemical and Biophysical Research Communications*, 229, 1-5.
- HUANG, D.-M., GUH, J.-H., CHUEH, S.-C. & TENG, C.-M. 2004. Modulation of anti-adhesion molecule MUC-1 is associated with arctiin-induced growth inhibition in PC-3 cells. *The Prostate*, 59, 260-267.
- HUSEIN, A. I., ALI-SHTAYEH, M. S., JONDI, W. J., ZATAR, N. A.-A., ABUREIDAH, I. M. & JAMOUS, R. M. 2014. In vitro antioxidant and antitumor activities of six selected plants used in the Traditional Arabic Palestinian herbal medicine. *Pharmaceutical Biology*, 52, 1249-1255.

- HWANG, J. H., HWANG, I.-S., LIU, Q.-H., WOO, E.-R. & LEE, D. G. 2012. (+)-Medioresinol leads to intracellular ROS accumulation and mitochondria-mediated apoptotic cell death in *Candida albicans*. *Biochimie*, 94, 1784-1793.
- IKEDA, T., TSUMAGARI, H., HONBU, T. & NOHARA, T. 2003. Cytotoxic activity of steroidal glycosides from *solanum* plants. *Biol Pharm Bull*, 26, 1198-201.
- INOUE, M., TAJIMA, K., MIZUTANI, M., IWATA, H., IWASE, T., MIURA, S., HIROSE, K., HAMAJIMA, N. & TOMINAGA, S. 2001. Regular consumption of green tea and the risk of breast cancer recurrence: follow-up study from the Hospital-based Epidemiologic Research Program at Aichi Cancer Center (HERPACC), Japan. *Cancer Letter*, 167, 175-82.
- IQBAL, J., ABBASI, B. A., MAHMOOD, T., KANWAL, S., ALI, B., SHAH, S. A. & KHALIL, A. T. 2017. Plant-derived anticancer agents: A green anticancer approach. *Asian Pacific Journal of Tropical Biomedicine*, 7, 1129-1150.
- IVANESCU, B., MIRON, A. & CORCIOVA, A. 2015. Sesquiterpene Lactones from *Artemisia* Genus: Biological Activities and Methods of Analysis. *Journal of Analytical Methods in Chemistry*, 2015, 21.
- J., H. P. & M., D. P. 1983. Antibacterial Activity of Selected Hydroxycinnamic Acids. *Journal of Food Science*, 48, 1378-1379.
- JACQUES, F., ISABELLE, S., RAJESH, D., SULTAN, E., COLIN, M., MARISE, R., MAXWELL, P. D., DAVID, F. & FREDDIE, B. 2015. Cancer incidence and mortality worldwide: Sources, methods and major patterns in GLOBOCAN 2012. *International Journal of Cancer*, 136, E359-E386.
- JAISWAL, R., KIPROTICH, J. & KUHNERT, N. 2011. Determination of the hydroxycinnamate profile of 12 members of the Asteraceae family. *Phytochemistry*, 72, 781-790.
- JAMUNA, S., KARTHIKA, K., PAULSAMY, S., THENMOZHI, K., KATHIRAVAN, S. & VENKATESH, R. 2015. Confertin and scopoletin from leaf and root extracts of *Hypochaeris radicata* have anti-inflammatory and antioxidant activities. *Industrial Crops and Products*, 70, 221-230.
- JAMUNA, S., PAULSAMY, S. & KARTHIKA, K. 2013. *In vitro* antibacterial activity of leaf and root extracts of *Hypochaeris Radicata* L. (Asteraceae)—a medicinal plant species inhabiting the high hills of Nilgiris, the Western Ghats.

- JANEČEK, Š. & BALÁŽ, Š. 1992.  $\alpha$ -Amylases and approaches leading to their enhanced stability. *FEBS Letters*, 304, 1-3.
- JANGWAN, J. S., AQUINO, R., MENCHERINI, T. & SINGH, R. 2012. *Chemical investigation and in vitro cytotoxic activity of Randia dumetorum lamk. Bark.*
- JBILLOU, R., AMRI, H., BOUAYAD, N., GHAILANI, N., ENNABILI, A. & SAYAH, F. 2008. Insecticidal effects of extracts of seven plant species on larval development,  $\alpha$ -amylase activity and offspring production of *Tribolium castaneum* (Herbst) (Insecta: Coleoptera: Tenebrionidae). *Bioresource Technology*, 99, 959-964.
- JEMAI, H., EL FEKI, A. & SAYADI, S. 2009a. Antidiabetic and antioxidant effects of hydroxytyrosol and oleuropein from olive leaves in alloxan-diabetic rats. *Journal of Agricultural and Food Chemistry*, 57, 8798-804.
- JEMAI, H., EL FEKI, A. & SAYADI, S. 2009b. Antidiabetic and Antioxidant Effects of Hydroxytyrosol and Oleuropein from Olive Leaves in Alloxan-Diabetic Rats. *Journal of Agricultural and Food Chemistry*, 57, 8798-8804.
- JIANG, C. S., LIANG, L. F. & GUO, Y. W. 2012. Natural products possessing protein tyrosine phosphatase 1B (PTP1B) inhibitory activity found in the last decades. *Acta Pharmacol Sin*, 33, 1217-45.
- JIANG, Y., KUSAMA, K., SATOH, K., TAKAYAMA, F., WATANABE, S. & SAKAGAMI, H. 2000. Induction of cytotoxicity by chlorogenic acid in human oral tumor cell lines. *Phytomedicine*, 7, 483-491.
- KALENDER, A., SELVARAJ, A., KIM, S. Y., GULATI, P., BRULE, S., VIOLLET, B., KEMP, B. E., BARDEESY, N., DENNIS, P., SCHLAGER, J. J., MARETTE, A., KOZMA, S. C. & THOMAS, G. 2010. Metformin, independent of AMPK, inhibits mTORC1 in a rag GTPase-dependent manner. *Cell Metabolism*, 11, 390-401.
- KAMAKURA, R., SON, M. J., DE BEER, D., JOUBERT, E., MIURA, Y. & YAGASAKI, K. 2015. Antidiabetic effect of green rooibos (*Aspalathus linearis*) extract in cultured cells and type 2 diabetic model KK-A(y) mice. *Cytotechnology*, 67, 699-710.

- KAMATOU, G. P. P., VAN ZYL, R. L., DAVIDS, H., VAN HEERDEN, F. R., LOURENS, A. C. U. & VILJOEN, A. M. 2008. Antimalarial and anticancer activities of selected South African *Salvia* species and isolated compounds from *S. radula*. *South African Journal of Botany*, 74, 238-243.
- KARAHAN, F., KULAK, M., URLU, E., GÖZÜACIK, H. G., BÖYÜMEZ, T., ŞEKEROĞLU, N. & DOĞANTURK, I. H. 2015. Total phenolic content, ferric reducing and DPPH scavenging activity of *Arum dioscoridis*. *Natural Product Research*, 29, 1678-1683.
- KARTHIKEYAN, R., DEVADASU, C. & SRINIVASA BABU, P. 2015. Isolation, Characterization, and RP-HPLC Estimation of P-Coumaric Acid from Methanolic Extract of Durva Grass (*Cynodon dactylon* Linn.) (Pers.). *International Journal of Analytical Chemistry*, 2015, 7.
- KASAI, H., FUKADA, S., YAMAIZUMI, Z., SUGIE, S. & MORI, H. 2000. Action of chlorogenic acid in vegetables and fruits as an inhibitor of 8-hydroxydeoxyguanosine formation in vitro and in a rat carcinogenesis model. *Food and Chemical Toxicology*, 38, 467-471.
- KASZNICKI, J., SLIWINSKA, A. & DRZEWOSKI, J. 2014. Metformin in cancer prevention and therapy. *Ann Transl Med*, 2, 57.
- KATIYAR, S. K. 2011. Green tea prevents non-melanoma skin cancer by enhancing DNA repair. *Arch Biochem Biophys*, 508, 152-8.
- KAUR, G. & VERMA, N. 2015. Nature curing cancer - review on structural modification studies with natural active compounds having anti-tumor efficiency. *Biotechnol Rep (Amst)*, 6, 64-78.
- KAVIMANI, S., KAYAROHANAM, S. & SENTHIL KUMAR, R. 2014. *In Vitro Antidiabetic Activity of Dolichandrone atrovirens – An Indian Medicinal Plant*.
- KELEG, S., BUCHLER, P., LUDWIG, R., BUCHLER, M. W. & FRIESS, H. 2003. Invasion and metastasis in pancreatic cancer. *Molecular Cancer*, 2, 14.
- KIANINIA, S. & FARJAM, M. H. 2016. Chemical and Biological Evolution of Essential Oil of *Arum maculatum*. *Iranian Journal of Science and Technology, Transactions A: Science*.

- KILIC, I. & YESILOGLU, Y. 2013. *Spectroscopic studies on the antioxidant activity of p-coumaric acid.*
- KIM, J. A., YANG, S. Y., KANG, S. & KIM, Y. H. 2011. *Verticilloside, a new daucosterol derivative from the seeds of Malva verticillata.*
- KIM, J. S., KWON, C. S. & SON, K. H. 2000. Inhibition of alpha-glucosidase and amylase by luteolin, a flavonoid. *Biosci Biotechnol Biochem*, 64, 2458-61.
- KIM, M. J., KIM, S. J., KIM, S. S., LEE, N. H. & HYUN, C. G. 2014. Hypochoeris radicata attenuates LPS-induced inflammation by suppressing p38, ERK, and JNK phosphorylation in RAW 264.7 macrophages. *Excli j*, 13, 123-36.
- KIM, Y.-M., JEONG, Y.-K., WANG, M.-H., LEE, W.-Y. & RHEE, H.-I. 2005. Inhibitory effect of pine extract on  $\alpha$ -glucosidase activity and postprandial hyperglycemia. *Nutrition*, 21, 756-761.
- KINGSTON, D. G. I. 2011. Modern Natural Products Drug Discovery and Its Relevance to Biodiversity Conservation. *Journal of Natural Products*, 74, 496-511.
- KOC, S., ISGOR, B. S., ISGOR, Y. G., SHOMALI MOGHADDAM, N. & YILDIRIM, O. 2015. The potential medicinal value of plants from Asteraceae family with antioxidant defense enzymes as biological targets. *Pharmaceutical Biology*, 53, 746-751.
- KOOTI, W., FAROKHIPOUR, M., ASADZADEH, Z., ASHTARY-LARKY, D. & ASADI-SAMANI, M. 2016. The role of medicinal plants in the treatment of diabetes: a systematic review. *Electron Physician*, 8, 1832-42.
- KUMAR, S., NARWAL, S., KUMAR, V. & PRAKASH, O. 2011a.  $\alpha$ -glucosidase inhibitors from plants: A natural approach to treat diabetes. *Pharmacognosy Reviews*, 5, 19-29.
- KUMAR, S., NARWAL, S., KUMAR, V. & PRAKASH, O. 2011b.  $\alpha$ -glucosidase inhibitors from plants: A natural approach to treat diabetes. *Pharmacognosy Reviews*, 5, 19-29.
- KUMAR VERMA, S., PAREEK, D., SINGHAL, R., KUMAR CHAUHAN, A., PARASHAR, P. & DOBHALL, M. 2012. *Ferulic acid ester from Colebrookea oppositifolia.*

- KUO, K. W., HSU, S. H., LI, Y. P., LIN, W. L., LIU, L. F., CHANG, L. C., LIN, C. C., LIN, C. N. & SHEU, H. M. 2000. Anticancer activity evaluation of the solanum glycoalkaloid solamargine. Triggering apoptosis in human hepatoma cells. *Biochem Pharmacol*, 60, 1865-73.
- KUSMITA, L., PUSPITANINGRUM, I. & LIMANTARA, L. 2015. Identification, Isolation and Antioxidant Activity of Pheophytin from Green Tea (*Camellia Sinensis* (L.) Kuntze). *Procedia Chemistry*, 14, 232-238.
- LABBE, C., POLANCO, M. I. & CASTILLO, M. 1989. 12-epi-Teuscordonin and Other Neoclerodanes from *Teucrium bicolor*. *Journal of Natural Products*, 52, 871-874.
- LARSSON, S. & RONSTED, N. 2014. Reviewing Colchicaceae alkaloids - perspectives of evolution on medicinal chemistry. *Current Topics in Medicinal Chemistry*, 14, 274-89.
- LEE, K.-A., MOON, S. H., KIM, K.-T., MENDONCA, A. F. & PAIK, H.-D. 2010. Antimicrobial effects of various flavonoids on *Escherichia coli* O157:H7 cell growth and lipopolysaccharide production. *Food Science and Biotechnology*, 19, 257-261.
- LEE, K.-R., KOZUKUE, N., HAN, J.-S., PARK, J.-H., CHANG, E.-Y., BAEK, E.-J., CHANG, J.-S. & FRIEDMAN, M. 2004. Glycoalkaloids and Metabolites Inhibit the Growth of Human Colon (HT29) and Liver (HepG2) Cancer Cells. *Journal of Agricultural and Food Chemistry*, 52, 2832-2839.
- LEE, M. 2013. *Isolation and identification of phytochemical constituents from the fruits of Acanthopanax senticosus*.
- LEONELLI, F., LA BELLA, A., MIGNECO, L. M. & BETTOLO, R. M. 2008. Design, synthesis and applications of hyaluronic acid-paclitaxel bioconjugates. *Molecules*, 13, 360-78.
- LEZAMA-DÁVILA, C. M., MCCHESENEY, J. D., BASTOS, J. K., MIRANDA, M. A., TIOSSI, R. F., DA COSTA, J. D. C., BENTLEY, M. V., GAITAN-PUCH, S. E. & ISAAC-MÁRQUEZ, A. P. 2016. A New Antileishmanial Preparation of Combined Solamargine and Solasonine Heals Cutaneous Leishmaniasis through Different Immunochemical Pathways. *Antimicrobial Agents and Chemotherapy*, 60, 2732-2738.

- LI, H.-R., HABASI, M., XIE, L.-Z. & AISA, H. 2014a. Effect of Chlorogenic Acid on Melanogenesis of B16 Melanoma Cells. *Molecules*, 19, 12940.
- LI, H., WU, H., ZHANG, H., LI, Y., LI, S., HOU, Q., WU, S. & YANG, S.-Y. 2017. Identification of curcumin-inhibited extracellular matrix receptors in non-small cell lung cancer A549 cells by RNA sequencing. *Tumor Biology*, 39, 1010428317705334.
- LI, J., ZHANG, L., HUANG, C., GUO, F. & LI, Y. 2014b. Five new cytotoxic steroidal glycosides from the fruits of *Solanum torvum*. *Fitoterapia*, 93, 209-215.
- LI, N., CAO, L., WANG, Y.-R., TAO, X.-Q., DING, G., WANG, Z.-Z. & XIAO, W. 2016. Induction of Solasonine on Apoptosis of Human Breast Cancer Bcap-37 Cells through Mitochondria-Mediated Pathway. *Chinese Herbal Medicines*, 8, 164-172.
- LI, S.-Y., HE, D.-J., ZHANG, X., NI, W.-H., ZHOU, Y.-F. & ZHANG, L.-P. 2007. Modification of Sugar Chains in Glycoalkaloids and Variation of Anticancer Activity. *Chemical Research in Chinese Universities*, 23, 303-309.
- LI, S., LI, W., WANG, Y., ASADA, Y. & KOIKE, K. 2010a. Prenylflavonoids from *Glycyrrhiza uralensis* and their protein tyrosine phosphatase-1B inhibitory activities. *Bioorg Med Chem Lett*, 20, 5398-401.
- LI, X., CUI, X., SUN, X., LI, X., ZHU, Q. & LI, W. 2010b. Mangiferin prevents diabetic nephropathy progression in streptozotocin-induced diabetic rats. *Phytotherapy Research*, 24, 893-9.
- LI, X., ZHAO, Y., WU, W. K. K., LIU, S., CUI, M. & LOU, H. 2011. Solamargine induces apoptosis associated with p53 transcription-dependent and transcription-independent pathways in human osteosarcoma U2OS cells. *Life Sciences*, 88, 314-321.
- LIANG, W., LAI, Y., ZHU, M., HUANG, S., FENG, W. & GU, X. 2016. Combretastatin A4 Regulates Proliferation, Migration, Invasion, and Apoptosis of Thyroid Cancer Cells via PI3K/Akt Signaling Pathway. *Medical Science Monitor*, 22, 4911-4917.
- LIM, D. Y., JEONG, Y., TYNER, A. L. & PARK, J. H. 2007. Induction of cell cycle arrest and apoptosis in HT-29 human colon cancer cells by the dietary compound luteolin. *American Journal of Physiology-Gastrointestinal and Liver Physiology*, 292, G66-75.

- LIN, C. Y., LEE, C. H., CHANG, Y. W., WANG, H. M., CHEN, C. Y. & CHEN, Y. H. 2014. Pheophytin a inhibits inflammation via suppression of LPS-induced nitric oxide synthase-2, prostaglandin E2, and interleukin-1beta of macrophages. *International Journal of Molecular Sciences*, 15, 22819-34.
- LIN, Y.-L., WANG, W.-Y., KUO, Y.-H. & CHEN, C.-F. 2000. Nonsteroidal Constituents from *Solanum Incanum* L. *Journal of the Chinese Chemical Society*, 47, 247-251.
- LIU, B., FAN, Z., EDGERTON, S. M., DENG, X. S., ALIMOVA, I. N., LIND, S. E. & THOR, A. D. 2009. Metformin induces unique biological and molecular responses in triple negative breast cancer cells. *Cell Cycle*, 8, 2031-40.
- LIU, C. M., KAO, C. L., WU, H. M., LI, W. J., HUANG, C. T., LI, H. T. & CHEN, C. Y. 2014. Antioxidant and anticancer aporphine alkaloids from the leaves of *Nelumbo nucifera* Gaertn. cv. Rosa-plena. *Molecules*, 19, 17829-38.
- LIU, C. T., HSE, H., LII, C. K., CHEN, P. S. & SHEEN, L. Y. 2005. Effects of garlic oil and diallyl trisulfide on glycemic control in diabetic rats. *European Journal of Pharmacology*, 516, 165-73.
- LIU, J. D., CHEN, S. H., LIN, C. L., TSAI, S. H. & LIANG, Y. C. 2001. Inhibition of melanoma growth and metastasis by combination with (-)-epigallocatechin-3-gallate and dacarbazine in mice. *Journal of Cellular Biochemistry*, 83, 631-42.
- LIU, K. Y., ZHANG, T. J., GAO, W. Y., CHEN, H. X. & ZHENG, Y. N. 2006. [Phytochemical and pharmacological research progress in *Tussilago farfara*]. *Zhongguo Zhong Yao Za Zhi*, 31, 1837-41.
- LIU, L. F., LIANG, C. H., SHIU, L. Y., LIN, W. L., LIN, C. C. & KUO, K. W. 2004. Action of solamargine on human lung cancer cells--enhancement of the susceptibility of cancer cells to TNFs. *FEBS Lett*, 577, 67-74.
- LIU, Y. J., ZHOU, C. Y., QIU, C. H., LU, X. M. & WANG, Y. T. 2013. Chlorogenic acid induced apoptosis and inhibition of proliferation in human acute promyelocytic leukemia HL60 cells. *Molecular Medicine Reports*, 8, 1106-10.
- LIU, Z. Q., LIU, T., CHEN, C., LI, M. Y., WANG, Z. Y., CHEN, R. S., WEI, G. X., WANG, X. Y. & LUO, D. Q. 2015. Fumosorinone, a novel PTP1B inhibitor,

activates insulin signaling in insulin-resistance HepG2 cells and shows anti-diabetic effect in diabetic KKAY mice. *Toxicol Appl Pharmacol*, 285, 61-70.

LOBAY, D. 2015. Rauwolfia in the Treatment of Hypertension. *Integr Med (Encinitas)*, 14, 40-6.

LOHAR, D. R., BHATIA, R. K., GARG, S. P. & CHAWAN, D. D. 1979. Seasonal variation in the content of sennoside in Senna leaves. *Pharmaceutisch weekblad*, 1, 206-208.

LOPEZ-BIEDMA, A., SANCHEZ-QUESADA, C., BELTRAN, G., DELGADO-RODRIGUEZ, M. & GAFORIO, J. J. 2016. Phytoestrogen (+)-pinoresinol exerts antitumor activity in breast cancer cells with different oestrogen receptor statuses. *BMC Complementary and Alternative Medicine*, 16, 350.

LOPEZ-LAZARO, M. 2009. Distribution and biological activities of the flavonoid luteolin. *Mini-Reviews in Medicinal Chemistry*, 9, 31-59.

LOPEZ-MARTINEZ, L. M., SANTACRUZ-ORTEGA, H., NAVARRO, R. E., SOTELO-MUNDO, R. R. & GONZALEZ-AGUILAR, G. A. 2015. A (1)H NMR Investigation of the Interaction between Phenolic Acids Found in Mango (*Manguifera indica* cv Ataulfo) and Papaya (*Carica papaya* cv Maradol) and 1,1-diphenyl-2-picrylhydrazyl (DPPH) Free Radicals. *PLoS One*, 10, e0140242.

LU, X. F., HE, G. Q., YU, H. N., MA, Q., SHEN, S. R. & DAS, U. N. 2010. Colorectal cancer cell growth inhibition by linoleic acid is related to fatty acid composition changes. *J Zhejiang Univ Sci B*, 11, 923-30.

LU, Y.-Y., LUO, J.-G. & KONG, L.-Y. 2011. Chemical Constituents from *Solanum torvum*. *Chinese Journal of Natural Medicines*, 9, 30-32.

LV, C., KONG, H., DONG, G., LIU, L., TONG, K., SUN, H., CHEN, B., ZHANG, C. & ZHOU, M. 2014a. Antitumor efficacy of alpha-solanine against pancreatic cancer in vitro and in vivo. *PLoS One*, 9, e87868.

LV, F. & XU, X. J. 2008. [Studies on the chemical constituents of *Rabdosia rubescens*]. *Zhong Yao Cai*, 31, 1340-3.

- LV, H.-W., LUO, J.-G., ZHU, M.-D., ZHAO, H.-J. & KONG, L.-Y. 2015. neo-Clerodane diterpenoids from the aerial parts of *Teucrium fruticans* cultivated in China. *Phytochemistry*, 119, 26-31.
- LV, H. W., LUO, J. G., ZHU, M. D., SHAN, S. M. & KONG, L. Y. 2014b. Teucvisins A-E, five new neo-clerodane diterpenes from *Teucrium viscidum*. *Chem Pharm Bull (Tokyo)*, 62, 472-6.
- MA, C., DASTMALCHI, K., WHITAKER, B. D. & KENNELLY, E. J. 2011. Two New Antioxidant Malonated Caffeoylquinic Acid Isomers in Fruits of Wild Eggplant Relatives. *Journal of Agricultural and Food Chemistry*, 59, 9645-9651.
- MA, E.-L., LI, Y.-C., TSUNEKI, H., XIAO, J.-F., XIA, M.-Y., WANG, M.-W. & KIMURA, I. 2008.  $\beta$ -Eudesmol suppresses tumour growth through inhibition of tumour neovascularisation and tumour cell proliferation. *Journal of Asian Natural Products Research*, 10, 159-167.
- MA, L., PENG, H., LI, K., ZHAO, R., LI, L., YU, Y., WANG, X. & HAN, Z. 2015. Luteolin exerts an anticancer effect on NCI-H460 human non-small cell lung cancer cells through the induction of Sirt1-mediated apoptosis. *Molecular Medicine Reports*, 12, 4196-4202.
- MAHADY, G. B., PENDLAND, S. L., YUN, G. S., LU, Z. Z. & STOIA, A. 2003. Ginger (*Zingiber officinale* Roscoe) and the gingerols inhibit the growth of Cag A+ strains of *Helicobacter pylori*. *Anticancer Research*, 23, 3699-702.
- MAJUMDER, P., MONDAL, H. A. & DAS, S. 2005. Insecticidal Activity of *Arum maculatum* Tuber Lectin and Its Binding to the Glycosylated Insect Gut Receptors. *Journal of Agricultural and Food Chemistry*, 53, 6725-6729.
- MANAYI, A., SAEIDNIA, S., OSTAD, S. N., HADJIAKHOONDI, A., ARDEKANI, M. R., VAZIRIAN, M., AKHTAR, Y. & KHANAVI, M. 2013. Chemical constituents and cytotoxic effect of the main compounds of *Lythrum salicaria* L. *Z Naturforsch C*, 68, 367-75.
- MANDAL, P., MISRA, T. K. & SINGH, I. D. 2010. Antioxidant activity in the extracts of two edible aroids. *Indian Journal Pharm Sci*, 72, 105-8.

- MANDAL, S. & MANDAL, M. 2015. Coriander (*Coriandrum sativum* L.) essential oil: Chemistry and biological activity. *Asian Pacific Journal of Tropical Biomedicine*, 5, 421-428.
- MANS, D. R., DA ROCHA, A. B. & SCHWARTSMANN, G. 2000. Anti-cancer drug discovery and development in Brazil: targeted plant collection as a rational strategy to acquire candidate anti-cancer compounds. *Oncologist*, 5, 185-98.
- MANSOURABADI, A. H., SADEGHI, H. M., RAZAVI, N. & REZVANI, E. 2015. Anti-inflammatory and Analgesic Properties of Salvigenin, *Salvia officinalis* Flavonoid Extracted. *Advanced Herbal Medicine*, 1, 31-41.
- MARLES, R. J. & FARNSWORTH, N. R. 1995. Antidiabetic plants and their active constituents. *Phytomedicine*, 2, 137-89.
- MARUYAMA, T., MURATA, S., NAKAYAMA, K., SANO, N., OGAWA, K., NOWATARI, T., TAMURA, T., NOZAKI, R., FUKUNAGA, K. & OHKOHCHI, N. 2014. (-)-Epigallocatechin-3-gallate suppresses liver metastasis of human colorectal cancer. *Oncology Reports*, 31, 625-33.
- MATKOWSKI, A., KUS, P., GORALSKA, E. & WOZNIAK, D. 2013. Mangiferin - a bioactive xanthonoid, not only from mango and not just antioxidant. *Mini-Reviews in Medicinal Chemistry*, 13, 439-55.
- MATSUI, T., KOBAYASHI, M., HAYASHIDA, S. & MATSUMOTO, K. 2002. Luteolin, a flavone, does not suppress postprandial glucose absorption through an inhibition of alpha-glucosidase action. *Bioscience, Biotechnology, and Biochemistry*, 66, 689-92.
- MATTHIAS, A., NNADI, C., UKWUEZE, N. & OKOYE, F. 2014. *Phenolic constituents from Platycerium bifurcatum and their antioxidant properties*.
- MCGUIRE, S. 2016. World Cancer Report 2014. Geneva, Switzerland: World Health Organization, International Agency for Research on Cancer, WHO Press, 2015. *Advances in Nutrition*, 7, 418-9.
- MERICLI, F., BECER, E., KABADAYI, H., HANOGLU, A., YIGIT HANOGLU, D., OZKUM YAVUZ, D., OZEK, T. & VATANSEVER, S. 2017. Fatty acid composition and anticancer activity in colon carcinoma cell lines of *Prunus dulcis* seed oil. *Pharmaceutical Biology*, 55, 1239-1248.

- MESHIKHES, A. W. 2002. Efficacy of Daflon in the treatment of hemorrhoids. *Saudi Medical Journal*, 23, 1496-8.
- MIGHRI, H., SABRI, K., ELJENI, H., NEFFATI, M. & AKROUT, A. 2015. Chemical Composition and Antimicrobial Activity of *Pituranthos chloranthus* (Benth.) Hook and *Pituranthos tortuosus* (Coss.) Maire Essential Oils from Southern Tunisia. *Advances in Biological Chemistry*, Vol.05No.07, 7.
- MIRANDA, M. A., TIOSSI, R. F. J., SILVA, M. R. D., RODRIGUES, K. C., KUEHN, C. C., OLIVEIRA, L. G. R., ALBUQUERQUE, S., MCCHESENEY, J. D., LEZAMA-DAVILA, C. M., ISAAC-MARQUEZ, A. P. & BASTOS, J. K. 2013. In vitro Leishmanicidal and Cytotoxic Activities of the Glycoalkaloids from *Solanum lycocarpum* (Solanaceae) Fruits. *Chemistry & Biodiversity*, 10, 642-648.
- MOHSENZADEH, F., CHEHREGANI, A. & AMIRI, H. 2011. Chemical composition, antibacterial activity and cytotoxicity of essential oils of *Tanacetum parthenium* in different developmental stages. *Pharmaceutical Biology*, 49, 920-6.
- MOONEY, M. H., FOGARTY, S., STEVENSON, C., GALLAGHER, A. M., PALIT, P., HAWLEY, S. A., HARDIE, D. G., COXON, G. D., WAIGH, R. D., TATE, R. J., HARVEY, A. L. & FURMAN, B. L. 2008. Mechanisms underlying the metabolic actions of galegine that contribute to weight loss in mice. *British Journal of Pharmacology*, 153, 1669-77.
- MOORE, H., SUMMERBELL, C., HOOPER, L., CRUICKSHANK, K., VYAS, A., JOHNSTONE, P., ASHTON, V. & KOPELMAN, P. 2004. Dietary advice for treatment of type 2 diabetes mellitus in adults. *Cochrane Database Syst Rev*, CD004097.
- MOUNIRA, K., EL, M. S. E., NAWEL, B., ANTONIO, P., EMILIE, S., LEILA, C. G. & PHILIPPE, R. 2016. In Vitro and In Vivo Anti-Melanoma Effects of *Pituranthos tortuosus* Essential Oil Via Inhibition of FAK and Src Activities. *Journal of Cellular Biochemistry*, 117, 1167-1175.
- MOVAHEDI, A., BASIR, R., RAHMAT, A., CHARAFFEDINE, M. & OTHMAN, F. 2014. Remarkable Anticancer Activity of *Teucrium polium* on Hepatocellular Carcinogenic Rats. *Evidence-Based Complementary and Alternative Medicine*, 2014, 726724.

- MUKHAMETZHANOV, M. N., SHEICHENKO, V. I., BAN'KOVSKII, A. I. & RYBALKO, K. S. 1971. Structure of stizolin — A sesquiterpene lactone from *Stizolophus balsamita*. *Chemistry of Natural Compounds*, 7, 386-391.
- MÜLLER-PILLASCH, F., GRESS, T. & ADLER, G. Extracellular Matrix in Pancreatic Diseases. 1997 Berlin, Heidelberg. Springer Berlin Heidelberg, 291-302.
- MUNARI, C., FRANCIELLI DE OLIVEIRA, P., COSTA LIMA CAMPOS, J., DE PAULA LIMA MARTINS, S., CARVALHO DA COSTA, J., BASTOS, J. & TAVARES, D. 2013. *Antiproliferative activity of Solanum lycocarpum alkaloidic extract and their constituents, solamargine and solasonine, in tumor cell lines.*
- MUNARI, C. C., DE OLIVEIRA, P. F., CAMPOS, J. C., MARTINS SDE, P., DA COSTA, J. C., BASTOS, J. K. & TAVARES, D. C. 2014a. Antiproliferative activity of *Solanum lycocarpum* alkaloidic extract and their constituents, solamargine and solasonine, in tumor cell lines. *Journal of Natural Medicines*, 68, 236-41.
- MUNARI, C. C., DE OLIVEIRA, P. F., CAMPOS, J. C. L., MARTINS, S. D. P. L., DA COSTA, J. C., BASTOS, J. K. & TAVARES, D. C. 2014b. Antiproliferative activity of *Solanum lycocarpum* alkaloidic extract and their constituents, solamargine and solasonine, in tumor cell lines. *Journal of Natural Medicines*, 68, 236-241.
- MURAD, L. D., SOARES NDA, C., BRAND, C., MONTEIRO, M. C. & TEODORO, A. J. 2015. Effects of caffeic and 5-caffeoylquinic acids on cell viability and cellular uptake in human colon adenocarcinoma cells. *Nutr Cancer*, 67, 532-42.
- MURAKAMI, A., NAKAMURA, Y., KOSHIMIZU, K., TAKAHASHI, D., MATSUMOTO, K., HAGIHARA, K., TANIGUCHI, H., NOMURA, E., HOSODA, A., TSUNO, T., MARUTA, Y., KIM, H. W., KAWABATA, K. & OHIGASHI, H. 2002. FA15, a hydrophobic derivative of ferulic acid, suppresses inflammatory responses and skin tumor promotion: comparison with ferulic acid. *Cancer Letters*, 180, 121-129.

- MURUGANANDAN, S., SRINIVASAN, K., GUPTA, S., GUPTA, P. K. & LAL, J. 2005. Effect of mangiferin on hyperglycemia and atherogenicity in streptozotocin diabetic rats. *J Ethnopharmacol*, 97, 497-501.
- NAGAO, Y., ITO, N., KOHNO, T., KURODA, H. & FUJITA, E. 1982. Antitumor activity of Rabdosia and Teucrium diterpenoids against P 388 lymphocytic leukemia in mice. *Chem Pharm Bull (Tokyo)*, 30, 727-9.
- NAGHIBI, F., MOSADDEGH, M., MOHAMMADI MOTAMED, M. & GHORBANI, A. 2010. Labiatae Family in folk Medicine in Iran: from Ethnobotany to Pharmacology. *Iranian Journal of Pharmaceutical Research*, Volume 4, 63-79.
- NAIR, M. G., EPP, M. D. & BURKE, B. A. 1988. Ferulate esters of higher fatty alcohols and allelopathy in *Kalanchöe daigremontiana*. *Journal of Chemical Ecology*, 14, 589-603.
- NAKAMURA, T., KOMORI, C., LEE, Y., HASHIMOTO, F., YAHARA, S., NOHARA, T. & EJIMA, A. 1996. Cytotoxic activities of solanum steroidal glycosides. *Biol Pharm Bull*, 19, 564-6.
- NAMAZI SARVESTANI, N., SEPEHRI, H., DELPHI, L. & MORIDI FARIMANI, M. 2018. Eupatorin and Salvigenin Potentiate Doxorubicin-Induced Apoptosis and Cell Cycle Arrest in HT-29 and SW948 Human Colon Cancer Cells. *Asian Pacific Journal of Cancer Prevention*, 19, 131-139.
- NASEEF - SHTAYA, H., QADADHA, H., ABU ASFOUR, Y., SABRI, I., AL-RIMAWI, F., ABU-QATOUSEH, L. & FARRAJ, M. 2017. ANTICANCER, ANTIBACTERIAL, AND ANTIFUNGAL ACTIVITIES OF ARUM PALAESTINUM PLANT EXTRACTS.
- NASR BOUZAIENE, N., KILANI JAZIRI, S., KOVACIC, H., CHEKIR-GHEDIRA, L., GHEDIRA, K. & LUIS, J. 2015. The effects of caffeic, coumaric and ferulic acids on proliferation, superoxide production, adhesion and migration of human tumor cells in vitro. *Eur J Pharmacol*, 766, 99-105.
- NAUHEIMER, L., METZLER, D. & RENNER, S. S. 2012. Global history of the ancient monocot family Araceae inferred with models accounting for past continental positions and previous ranges based on fossils. *New Phytologist*, 195, 938-50.

- NEWMAN, D. J. & CRAGG, G. M. 2007. Natural Products as Sources of New Drugs over the Last 25 Years. *Journal of Natural Products*, 70, 461-477.
- NEWMAN, D. J. & CRAGG, G. M. 2012. Natural products as sources of new drugs over the 30 years from 1981 to 2010. *Journal of Natural Products*, 75, 311-35.
- NEWMAN, D. J. & CRAGG, G. M. 2016a. Natural Products as Sources of New Drugs from 1981 to 2014. *Journal of Natural Products*, 79, 629-661.
- NEWMAN, D. J. & CRAGG, G. M. 2016b. Natural Products as Sources of New Drugs from 1981 to 2014. *Journal of Natural Products*, 79, 629-61.
- NGUYEN, Q. T., SANDERS, L., MICHAEL, A. P., ANDERSON, S. R., NGUYEN, L. D. & JOHNSON, Z. A. 2012. Diabetes medications and cancer risk: review of the literature. *American Health and Drug Benefits*, 5, 221-9.
- NIÑO, J., CORREA, Y. M. & MOSQUERA, O. M. 2009. Biological activities of steroidal alkaloids isolated from *Solanum leucocarpum*. *Pharmaceutical Biology*, 47, 255-259.
- NIÑO, J., NARVÁEZ, D. M., MOSQUERA, O. M. & CORREA, Y. M. 2006. Antibacterial, antifungal and cytotoxic activities of eight Asteraceae and two Rubiaceae plants from colombian biodiversity. *Brazilian Journal of Microbiology*, 37, 566-570.
- NOORI, S., HASSAN, Z. M., YAGHMAEI, B. & DOLATKHAH, M. 2013. Antitumor and immunomodulatory effects of salvigenin on tumor bearing mice. *Cellular Immunology*, 286, 16-21.
- OBA, T., MASADA, Y. & TAMIAKI, H. 1997. *Convenient Preparation of Pheophytin b from Plant Extract through the C7Reduced Intermediate*.
- ODONTUYA, G., HOULT, J. R. S. & HOUGHTON, P. J. 2005. Structure-activity relationship for antiinflammatory effect of luteolin and its derived glycosides. *Phytotherapy Research*, 19, 782-786.
- OHMURA, K., MIYASE, T. & UENO, A. 1989. Sesquiterpene glucosides and a phenylbutanoid glycoside from *Hypochoeris radicata*. *Phytochemistry*, 28, 1919-1924.

- OKAI, Y. & HIGASHI-OKAI, K. 1997. Potent anti-inflammatory activity of pheophytin a derived from edible green alga, *Enteromorpha prolifera* (Sujiao-nori). *International Journal of Immunopharmacology*, 19, 355-8.
- OLIVEIRA, J. C. S., LIMA, L. S., MEDRADO, H. H. S., DAVID, J. M., DO VALE, A. E., DAVID, J. P. & OLIVEIRA, L. L. D. S. S. 2015. Isolation of Methylxantines from Cacao Beans (*Theobroma cacao*) by Counter-Current Chromatography (CCC). *Journal of Liquid Chromatography & Related Technologies*, 38, 1448-1451.
- OLOKOBA, A. B., OBATERU, O. A. & OLOKOBA, L. B. 2012. Type 2 diabetes mellitus: a review of current trends. *Oman Medical Journal*, 27, 269-73.
- ONG, K. W., HSU, A. & TAN, B. K. 2013a. Anti-diabetic and anti-lipidemic effects of chlorogenic acid are mediated by ampk activation. *Biochemical Pharmacology*, 85, 1341-51.
- ONG, K. W., HSU, A. & TAN, B. K. H. 2013b. Anti-diabetic and anti-lipidemic effects of chlorogenic acid are mediated by ampk activation. *Biochemical Pharmacology*, 85, 1341-1351.
- ONO, M., NISHIMURA, K., SUZUKI, K., FUKUSHIMA, T., IGOSHI, K., YOSHIMITSU, H., IKEDA, T. & NOHARA, T. 2006. Steroidal glycosides from the underground parts of *Solanum sodomaeum*. *Chem Pharm Bull (Tokyo)*, 54, 230-3.
- ONO, M., UENOSONO, Y., UMAOKA, H., SHIONO, Y., IKEDA, T., OKAWA, M., KINJO, J., YOSHIMITSU, H. & NOHARA, T. 2009. Five new steroidal glycosides from the stems of *Solanum sodomaeum*. *Chem Pharm Bull (Tokyo)*, 57, 759-63.
- ORTEGO, F., RODRÍGUEZ, B. & CASTAÑERA, P. 1995. Effects of neo-clerodane diterpenes from *Teucrium* on feeding behavior of colorado potato beetle larvae. *Journal of Chemical Ecology*, 21, 1375-1386.
- OSADEBE, P., ODOH, U. & UZOR, P. 2014. *Natural Products as Potential Sources of Antidiabetic Drugs*.
- PAJUNEN, T. I., KOSKELA, H., HASE, T. & HOPIA, A. 2008. NMR properties of conjugated linoleic acid (CLA) methyl ester hydroperoxides. *Chem Phys Lipids*, 154, 105-14.

- PAL, S. K. & SHUKLA, Y. 2003. Herbal medicine: current status and the future. *Asian Pacific Journal of Cancer Prevention*, 4, 281-8.
- PATEL, D. K., PRASAD, S. K., KUMAR, R. & HEMALATHA, S. 2012. An overview on antidiabetic medicinal plants having insulin mimetic property. *Asian Pacific Journal of Tropical Biomedicine*, 2, 320-30.
- PATEL, K. & PATEL, D. K. 2013. Medicinal importance, pharmacological activities, and analytical aspects of aloin: A concise report. *Journal of Acute Disease*, 2, 262-269.
- PECKING, A. P., FEVRIER, B., WARGON, C. & PILLION, G. 1997. Efficacy of Daflon 500 mg in the treatment of lymphedema (secondary to conventional therapy of breast cancer). *Angiology*, 48, 93-8.
- PENG, C. C., SUN, H. T., LIN, I. P., KUO, P. C. & LI, J. C. 2017. The functional property of royal jelly 10-hydroxy-2-decenoic acid as a melanogenesis inhibitor. *BMC Complementary and Alternative Medicine*, 17, 392.
- PEREZ G, R. M., ZAVALA S, M. A., PEREZ G, S. & PEREZ G, C. 1998. Antidiabetic effect of compounds isolated from plants. *Phytomedicine*, 5, 55-75.
- PERNICOVA, I. & KORBONITS, M. 2014. Metformin--mode of action and clinical implications for diabetes and cancer. *Nature Reviews Endocrinology*, 10, 143-56.
- PERRETT, S. & J. WHITFIELD, P. 1995. *Anthelmintic and pesticidal activity of Acorus gramineus (Araceae) is associated with phenylpropanoid asarones.*
- PEUNGVICHA, P., THIRAWARAPAN, S. S. & WATANABE, H. 1998. Possible mechanism of hypoglycemic effect of 4-hydroxybenzoic acid, a constituent of Pandanus odoratus root. *The Japanese Journal of Pharmacology*, 78, 395-8.
- PI, L., HU, F. & SHI, Z. 2005. [Determination of papaverine in seeds of Papaver somniferum L. and soup of chafing dish by high performance liquid chromatography-fluorescence detection]. *Se Pu*, 23, 639-41.
- PIETRAS, R. J., POEN, J. C., GALLARDO, D., WONGVIPAT, P. N., LEE, H. J. & SLAMON, D. J. 1999. Monoclonal antibody to HER-2/neureceptor modulates

repair of radiation-induced DNA damage and enhances radiosensitivity of human breast cancer cells overexpressing this oncogene. *Cancer Research*, 59, 1347-55.

PLOCHMANN, K., KORTE, G., KOUTSILIERI, E., RICHLING, E., RIEDERER, P., RETHWILM, A., SCHREIER, P. & SCHELLER, C. 2007. Structure–activity relationships of flavonoid-induced cytotoxicity on human leukemia cells. *Archives of Biochemistry and Biophysics*, 460, 1-9.

PM, S., PM, S., SIMEONI, L., MAGALHÃES, P. & SILVEIRA, D. 2012.  *$\alpha$ -Amylase Inhibitors: A Review of Raw Material and Isolated Compounds from Plant Source*.

POPOV, A. M., OSIPOV, A. N., KOREPANOVA, E. A., KRIVOSHAPKO, O. N., ARTYUKOV, A. A. & KLIMOVICH, A. A. 2016. A study of the antioxidant and membranotropic activities of luteolin using different model systems. *Biophysics*, 61, 843-850.

PORNPRASERTPOL, A., SEREEMASPUN, A., SOOKLERT, K., SATIRAPIATKUL, C. & SUKRONG, S. 2015. Anticancer activity of selected *Colocasia gigantea* fractions. *Journal of the Medical Association of Thailand*, 98 Suppl 1, S98-106.

PRAKASH, O., KUMAR, A. & KUMAR, P. 2013. *Anticancer Potential of Plants and Natural Products: A Review*.

PRATHEESHKUMAR, P., SON, Y. O., BUDHRAJA, A., WANG, X., DING, S., WANG, L., HITRON, A., LEE, J. C., KIM, D., DIVYA, S. P., CHEN, G., ZHANG, Z., LUO, J. & SHI, X. 2012. Luteolin inhibits human prostate tumor growth by suppressing vascular endothelial growth factor receptor 2-mediated angiogenesis. *PLoS One*, 7, e52279.

QIAN, X. J., JIN, Y. S., CHEN, H. S., XU, Q. Q., REN, H., ZHU, S. Y., TANG, H. L., WANG, Y., ZHAO, P., QI, Z. T. & ZHU, Y. Z. 2016. Trachelogenin, a novel inhibitor of hepatitis C virus entry through CD81. *Journal of General Virology*, 97, 1134-44.

QUANG, T., NGAN, N., YOON, C.-S., CHO, K.-H., KANG, D., LEE, H., KIM, Y.-C. & OH, H. 2015. Protein Tyrosine Phosphatase 1B Inhibitors from the Roots of *Cudrania tricuspidata*. *Molecules*, 20, 11173.

- RAJABALIAN, S. 2008. Methanolic extract of *Teucrium polium* L. potentiates the cytotoxic and apoptotic effects of anticancer drugs of vincristine, vinblastine and doxorubicin against a panel of cancerous cell lines. *Experimental oncology*, 30, 133-8.
- RAJU, J., GUPTA, D., RAO, A. R., YADAVA, P. K. & BAQUER, N. Z. 2001. *Trigonella foenum graecum* (fenugreek) seed powder improves glucose homeostasis in alloxan diabetic rat tissues by reversing the altered glycolytic, gluconeogenic and lipogenic enzymes. *Molecular and Cellular Biochemistry*, 224, 45-51.
- RAMELET, A. A. 2001. Clinical benefits of Daflon 500 mg in the most severe stages of chronic venous insufficiency. *Angiology*, 52 Suppl 1, S49-56.
- RAMESH, A. S., CHRISTOPHER, J. G., RADHIKA, R., SETTY, C. R. & THANKAMANI, V. 2012. Isolation, characterisation and cytotoxicity study of arjunolic acid from *Terminalia arjuna*. *Natural Product Research*, 26, 1549-52.
- RAMOS, A. C. & DE OLIVEIRA, R. R. 2017. A new alkaloid and flavonoids isolated from *Solanum cernuum* leaves by high-performance countercurrent chromatography. *Natural Product Research*, 31, 2405-2412.
- RASHED, K. N., #X106, IRI, #X107, , A., GLAMO, #X10D, LIJA, J., CALHELHA, R. C., FERREIRA, I. C. F. R., SOKOVI, #X107 & , M. 2013. Antimicrobial Activity, Growth Inhibition of Human Tumour Cell Lines, and Phytochemical Characterization of the Hydromethanolic Extract Obtained from *Sapindus saponaria* L. Aerial Parts. *BioMed Research International*, 2013, 9.
- REN, H., ZHAI, H., ZHANG, Y., JIN, Y. & OMORI, S. 2013. *Isolation of acetosyringone and cinnamic acids from straw soda cooking black liquor and simplified synthesis of hydroxyacetophenones*.
- RIBNICKY, D. M., POULEV, A., WATFORD, M., CEFALU, W. T. & RASKIN, I. 2006. Antihyperglycemic activity of Tarralin, an ethanolic extract of *Artemisia dracuncululus* L. *Phytomedicine*, 13, 550-7.
- ROSS, S. A., GULVE, E. A. & WANG, M. 2004. Chemistry and biochemistry of type 2 diabetes. *Chemical Reviews*, 104, 1255-82.

- ROY, S., M DUTTA, C. & PAUL, S. B. 2013. *Antibacterial activity of araceae: An overview.*
- SABET, Z., ROGHANI, M., NAJAFI, M. & MAGHSOUDI, Z. 2013. Antidiabetic effect of *Teucrium polium* aqueous extract in multiple low-dose streptozotocin-induced model of type 1 diabetes in rat. *Journal of Basic and Clinical Pathophysiology*, 1, 34-38.
- SADEGHI EKBATAN, S., LI, X. Q., GHORBANI, M., AZADI, B. & KUBOW, S. 2018. Chlorogenic Acid and Its Microbial Metabolites Exert Anti-Proliferative Effects, S-Phase Cell-Cycle Arrest and Apoptosis in Human Colon Cancer Caco-2 Cells. *International Journal of Molecular Sciences*, 19.
- SALAKO, O. A., AKINDELE, A. J., SHITTA, O. M., ELEGUNDE, O. O. & ADEYEMI, O. O. 2015. Antidiarrhoeal activity of aqueous leaf extract of *Caladium bicolor* (Araceae) and its possible mechanisms of action. *Journal of ethnopharmacology*, 176, 225-231.
- SEMAAN, D. G., IGOLI, J. O., YOUNG, L., MARRERO, E., GRAY, A. I. & ROWAN, E. G. 2017. In vitro anti-diabetic activity of flavonoids and pheophytins from *Allophylus cominia* Sw . on PTP1B, DPPIV, alpha-glucosidase and alpha-amylase enzymes. *Journal Ethnopharmacol*, 203, 39-46.
- SEN, A., OZBAS TURAN, S. & BITIS, L. 2017. Bioactivity-guided isolation of anti-proliferative compounds from endemic *Centaurea kilaea*. *Pharmaceutical Biology*, 55, 541-546.
- SEN, M. & DASH, B. 2014. *A review on medicinal plants with antidiabetic activity.*
- SENGUTTUVAN, J., PAULSAMY, S. & KARTHIKA, K. 2014a. Phytochemical analysis and evaluation of leaf and root parts of the medicinal herb, *Hypochaeris radicata* L. for in vitro antioxidant activities. *Asian Pacific Journal of Tropical Biomedicine*, 4, S359-67.
- SENGUTTUVAN, J., PAULSAMY, S. & KARTHIKA, K. 2014b. Phytochemical analysis and evaluation of leaf and root parts of the medicinal herb, *Hypochaeris radicata* L. for in vitro antioxidant activities. *Asian Pacific Journal of Tropical Biomedicine*, 4, S359-S367.

- SENGUTTUVAN, J., PAULSAMY, S. & KRISHNAMOORTHY, K. 2013. *In vitro* antifungal activity of leaf and root extracts of the medicinal plant, *Hypochoeris radicata* L.
- SENGUTTUVAN, J. & SUBRAMANIAM, P. 2016. HPTLC Fingerprints of Various Secondary Metabolites in the Traditional Medicinal Herb *Hypochoeris radicata* L. *Journal of Botany*, 2016, 11.
- SEYED FAZEL, N., RAMAN, T., LUCA, R., MARIA, D., EDUARDO, S.-S., HESHMATOLLAH, A. & SEYED MOHAMMAD, N. 2015. Curcumin: A Natural Product for Diabetes and its Complications. *Current Topics in Medicinal Chemistry*, 15, 2445-2455.
- SHAH, S. M., AYAZ, M., KHAN, A. U., ULLAH, F., FARHAN, SHAH, A. U., IQBAL, H. & HUSSAIN, S. 2015. 1,1-Diphenyl,2-picrylhydrazyl free radical scavenging, bactericidal, fungicidal and leishmanicidal properties of *Teucrium stocksianum*. *Toxicol Ind Health*, 31, 1037-43.
- SHALKAMI, A. S., HASSAN, M. & BAKR, A. G. 2018. Anti-inflammatory, antioxidant and anti-apoptotic activity of diosmin in acetic acid-induced ulcerative colitis. *Human & Experimental Toxicology*, 37, 78-86.
- SHARMA, A. & PURKAIT, B. 2012. Identification of Medicinally Active Ingredient in Ultradiluted *Digitalis purpurea*: Fluorescence Spectroscopic and Cyclic-Voltammetric Study. *Journal of Analytical Methods in Chemistry*, 2012, 109058.
- SHE, L. C., LIU, C.-M., CHEN, C. T., LI, H. T., LI, W. J. & CHEN, C. Y. 2017. *The anti-cancer and anti-metastasis effects of phytochemical constituents from leucaena leucocephala*.
- SHENG-JI, P. 2001. Ethnobotanical Approaches of Traditional Medicine Studies: Some Experiences From Asia. *Pharmaceutical Biology*, 39, 74-79.
- SHI, J., LIU, F., ZHANG, W., LIU, X., LIN, B. & TANG, X. 2015. Epigallocatechin-3-gallate inhibits nicotine-induced migration and invasion by the suppression of angiogenesis and epithelial-mesenchymal transition in non-small cell lung cancer cells. *Oncology Reports*, 33, 2972-80.

- SHI, L. F., CAO, Y. Y., CHEN, H. S. & DONG, J. P. 1997. [Isolation and identification of two new secoiridoids of water-soluble chemical constituents from the fruits of *Ligustrum lucidum* Ait]. *Yao Xue Xue Bao*, 32, 442-6.
- SHIKATA, K., NINOMIYA, T. & KIYOHARA, Y. 2013. Diabetes mellitus and cancer risk: review of the epidemiological evidence. *Cancer Science*, 104, 9-14.
- SHIU, L. Y., CHANG, L. C., LIANG, C. H., HUANG, Y. S., SHEU, H. M. & KUO, K. W. 2007. Solamargine induces apoptosis and sensitizes breast cancer cells to cisplatin. *Food and Chemical Toxicology*, 45, 2155-2164.
- SHIU, LI Y., LIANG, CHIA H., CHANG, LI C., SHEU, HAMM M., TSAI, EING M. & KUO, KOU W. 2009. Solamargine induces apoptosis and enhances susceptibility to trastuzumab and epirubicin in breast cancer cells with low or high expression levels of HER2/neu. *Bioscience Reports*, 29, 35-45.
- SHIU, L. Y., LIANG, C. H., HUANG, Y. S., SHEU, H. M. & KUO, K. W. 2008. Downregulation of HER2/neu receptor by solamargine enhances anticancer drug-mediated cytotoxicity in breast cancer cells with high-expressing HER2/neu. *Cell Biology and Toxicology*, 24, 1-10.
- SHOUIP, H. 2014. *Diabetes mellitus*.
- SHUKIA, R., SHARMA, S. B., PURI, D., PRABHU, K. M. & MURTHY, P. S. 2000. Medicinal plants for treatment of diabetes mellitus. *Indian Journal of Clinical Biochemistry*, 15, 169-77.
- SIDDIQUE, H. R. & SALEEM, M. 2011. Beneficial health effects of lupeol triterpene: a review of preclinical studies. *Life Sciences*, 88, 285-93.
- SINGAB, A. N., KHALIFA, T., MAHRAN, G. H., OKADA, Y., MATSUMARU, Y., NISHINO, H. & OKUYAMA, T. 1998. *A new flavonoid glycoside from Pituranthos tortuosus Desf, Benth and Hook.*
- SINGH, S., CHITKARA, D., MEHRAZIN, R., BEHRMAN, S. W., WAKE, R. W. & MAHATO, R. I. 2012. Chemoresistance in prostate cancer cells is regulated by miRNAs and Hedgehog pathway. *PLoS One*, 7, e40021.
- SON, M. J., MIURA, Y. & YAGASAKI, K. 2015. Mechanisms for antidiabetic effect of gingerol in cultured cells and obese diabetic model mice. *Cytotechnology*, 67, 641-52.

- SPECIES, D. A. I. 2008. *Handbook of Alien Species in Europe*, Springer Netherlands.
- SPOONER, D. M., ANDERSON, G. & JANSEN, R. 1993. *Chloroplast DNA Evidence for the Interrelationships of Tomatoes, Potatoes, and Pepinos (Solanaceae)*.
- STANKOVIĆ, M. S., MITROVIĆ, T. L., MATIĆ, I. Z., TOPUZOVIĆ, M. D. & STAMENKOVIĆ, S. M. 2015. New Values of Teucrium species: in Vitro Study of Cytotoxic Activities of Secondary Metabolites. *2015*, 43, 6.
- STIBOROVA, M., POLJAKOVA, J., MARTINKOVA, E., BOREK-DOHALSKA, L., ECKSCHLAGER, T., KIZEK, R. & FREI, E. 2011. Ellipticine cytotoxicity to cancer cell lines - a comparative study. *Interdiscip Toxicol*, 4, 98-105.
- SUBASH BABU, P., PRABUSEENIVASAN, S. & IGNACIMUTHU, S. 2007. Cinnamaldehyde—A potential antidiabetic agent. *Phytomedicine*, 14, 15-22.
- SULTANA, T., RASHID, M. A., ALI, M. A. & MAHMOOD, S. F. 2010. Hepatoprotective and Antibacterial Activity of Ursolic Acid Extracted from *Hedyotis corymbosa* L. *Bangladesh Journal of Scientific and Industrial Research*, 45, 8.
- SUN, C. Y., HU, Y., GUO, T., WANG, H. F., ZHANG, X. P., HE, W. J. & TAN, H. 2006. Resveratrol as a novel agent for treatment of multiple myeloma with matrix metalloproteinase inhibitory activity. *Acta Pharmacol Sin*, 27, 1447-52.
- SUN, L., ZHAO, Y., LI, X., YUAN, H., CHENG, A. & LOU, H. 2010. A lysosomal–mitochondrial death pathway is induced by solamargine in human K562 leukemia cells. *Toxicology in Vitro*, 24, 1504-1511.
- SUN, L., ZHAO, Y., YUAN, H., LI, X., CHENG, A. & LOU, H. 2011. Solamargine, a steroidal alkaloid glycoside, induces oncosis in human K562 leukemia and squamous cell carcinoma KB cells. *Cancer Chemother Pharmacol*, 67, 813-21.
- SÜNTAR, I. 2014. *The medicinal value of asteraceae family plants in terms of wound healing activity*.

- SYU, W., JR., DON, M.-J., LEE, G.-H. & SUN, C.-M. 2001. Cytotoxic and Novel Compounds from *Solanum indicum*. *Journal of Natural Products*, 64, 1232-1233.
- TABATA, K., MOTANI, K., TAKAYANAGI, N., NISHIMURA, R., ASAMI, S., KIMURA, Y., UKIYA, M., HASEGAWA, D., AKIHISA, T. & SUZUKI, T. 2005. Xanthoangelol, a major chalcone constituent of *Angelica keiskei*, induces apoptosis in neuroblastoma and leukemia cells. *Biol Pharm Bull*, 28, 1404-7.
- TAFRIHI, M., TOOSI, S., MINAEI, T., GOHARI, A. R., NIKNAM, V. & ARAB NAJAFI, S. M. 2014. Anticancer properties of *Teucrium persicum* in PC-3 prostate cancer cells. *Asian Pacific Journal of Cancer Prevention*, 15, 785-91.
- TÄHTIHARJU, S., RIJPKEMA, A. S., VETTERLI, A., ALBERT, V. A., TEERI, T. H. & ELOMAA, P. 2012. Evolution and Diversification of the CYC/TB1 Gene Family in Asteraceae—A Comparative Study in *Gerbera* (Mutisieae) and Sunflower (Heliantheae). *Molecular Biology and Evolution*, 29, 1155-1166.
- TAKIMOTO, T., SUZUKI, K., ARISAKA, H., MURATA, T., OZAKI, H. & KOYAMA, N. 2011. Effect of N-(p-coumaroyl)serotonin and N-feruloylserotonin, major anti-atherogenic polyphenols in safflower seed, on vasodilation, proliferation and migration of vascular smooth muscle cells. *Molecular Nutrition & Food Research*, 55, 1561-71.
- TAMRAKAR, A., MAURYA, C. & RAI, A. 2014. *PTP1B inhibitors for type 2 diabetes treatment: A patent review (2011-2014)*.
- TAMRAKAR, A. K., YADAV, P. P., TIWARI, P., MAURYA, R. & SRIVASTAVA, A. K. 2008. Identification of pongamol and karanjin as lead compounds with antihyperglycemic activity from *Pongamia pinnata* fruits. *Journal of Ethnopharmacology*, 118, 435-9.
- TARGETT, N. M., KILCOYNE, J. P. & GREEN, B. 1979. Vacuum liquid chromatography: an alternative to common chromatographic methods. *The Journal of Organic Chemistry*, 44, 4962-4964.
- TARHAN, L., NAKIPOGLU, M., KAVAKCIOGLU, B., TONGUL, B. & NALBANTSOY, A. 2016. The Induction of Growth Inhibition and Apoptosis in HeLa and MCF-7 Cells by *Teucrium sandrasicum*, Having Effective

Antioxidant Properties. *Biotechnology and Applied Biochemistry*, 178, 1028-41.

TATAR, M., QUJEQ, D., FEIZI, F., PARSIAN, H., SOHAN FARAJI, A., HALALKHOR, S., ABASSI, R., ABEDIAN, Z., POURBAGHER, R., AGHAJANPOUR MIR, S. M., MIR, H. & SEYFIZADEH, N. 2012. Effects of Teucrium Polium Aerial Parts extract on oral glucose tolerance tests and pancreas histopathology in Streptozocin-induced diabetic rats. *International Journal of Molecular and Cellular Medicine*, 1, 44-9.

THILAGAM, E., PARIMALADEVI, B., KUMARAPPAN, C. & CHANDRA MANDAL, S. 2013.  $\alpha$ -Glucosidase and  $\alpha$ -Amylase Inhibitory Activity of *Senna surattensis*. *Journal of Acupuncture and Meridian Studies*, 6, 24-30.

THOMPSON, I. R. 2007. *A taxonomic treatment of tribe Lactuceae (Asteraceae) in Australia*.

TIUMAN, T. S., UEDA-NAKAMURA, T., GARCIA CORTEZ, D. A., DIAS FILHO, B. P., MORGADO-DIAZ, J. A., DE SOUZA, W. & NAKAMURA, C. V. 2005. Antileishmanial activity of parthenolide, a sesquiterpene lactone isolated from *Tanacetum parthenium*. *Antimicrob Agents Chemother*, 49, 176-82.

TSAI, P.-H., CHENG, C.-H., LIN, C.-Y., HUANG, Y.-T., LEE, L.-T., KANDASWAMI, C. C., LIN, Y.-C., LEE, K. P.-H., HUNG, C.-C., HWANG, J.-J., KE, F.-C., CHANG, G.-D. & LEE, M.-T. 2016. Dietary Flavonoids Luteolin and Quercetin Suppressed Cancer Stem Cell Properties and Metastatic Potential of Isolated Prostate Cancer Cells. *Anticancer Research*, 36, 6367-6380.

UDDIN, Z., SONG, Y. H., ULLAH, M., LI, Z., KIM, J. Y. & PARK, K. H. 2018. Isolation and Characterization of Protein Tyrosine Phosphatase 1B (PTP1B) Inhibitory Polyphenolic Compounds From *Dodonaea viscosa* and Their Kinetic Analysis. *Front Chem*, 6, 40.

VALIÑAS, M. A., LANTERI, M. L., TEN HAVE, A. & ANDREU, A. B. 2015. Chlorogenic Acid Biosynthesis Appears Linked with Suberin Production in Potato Tuber (*Solanum tuberosum*). *Journal of Agricultural and Food Chemistry*, 63, 4902-4913.

VAN UDEN, W., BOUMA, A. S., BRACHT WAKER, J. F., MIDDEL, O., WICHERS, H. J., DE WAARD, P., WOERDENBAG, H. J., KELLOGG, R.

- M. & PRAS, N. 1995. The production of podophyllotoxin and its 5-methoxy derivative through bioconversion of cyclodextrin-complexed desoxypodophyllotoxin by plant cell cultures. *Plant Cell, Tissue and Organ Culture*, 42, 73-79.
- VARGHESE, G. K., BOSE, L. V. & HABTEMARIAM, S. 2013. Antidiabetic components of Cassia alata leaves: Identification through  $\alpha$ -glucosidase inhibition studies. *Pharmaceutical Biology*, 51, 345-349.
- VELIKA, B. & KRON, I. 2012. Antioxidant properties of benzoic acid derivatives against Superoxide radical. *Free Radicals and Antioxidants*, 2, 62-67.
- VENDITTI, A., FREZZA, C., TRANCANELLA, E., ZADEH, S. M. M., FODDAI, S., SCIUBBA, F., DELFINI, M., SERAFINI, M. & BIANCO, A. 2017. A new natural neo-clerodane from Teucrium polium L. collected in Northern Iran. *Industrial Crops and Products*, 97, 632-638.
- VIGNERI, P., FRASCA, F., SCIACCA, L., PANDINI, G. & VIGNERI, R. 2009. Diabetes and cancer. *Endocr Relat Cancer*, 16, 1103-23.
- VINEIS, P. & WILD, C. P. 2014. Global cancer patterns: causes and prevention. *The Lancet*, 383, 549-557.
- VISINTINI JAIME, M. F., REDKO, F., MUSCHIETTI, L. V., CAMPOS, R. H., MARTINO, V. S. & CAVALLARO, L. V. 2013. In vitro antiviral activity of plant extracts from Asteraceae medicinal plants. *Virology Journal*, 10, 245.
- VLAHOV, G. 1999. Application of NMR to the study of olive oils. *Progress in Nuclear Magnetic Resonance Spectroscopy*, 35, 341-357.
- VLASE, L., BENEDEC, D., HANGANU, D., DAMIAN, G., CSILLAG, I., SEVASTRE, B., MOT, A. C., SILAGHI-DUMITRESCU, R. & TILEA, I. 2014. Evaluation of antioxidant and antimicrobial activities and phenolic profile for Hyssopus officinalis, Ocimum basilicum and Teucrium chamaedrys. *Molecules*, 19, 5490-507.
- WACHTEL-GALOR, S. & BENZIE, I. F. F. 2011. Herbal Medicine: An Introduction to Its History, Usage, Regulation, Current Trends, and Research Needs. In: ND, BENZIE, I. F. F. & WACHTEL-GALOR, S. (eds.) *Herbal Medicine: Biomolecular and Clinical Aspects*. Boca Raton (FL): CRC Press/Taylor & Francis Llc.

- WANG, G.-Q., GU, J.-F., GAO, Y.-C. & DAI, Y.-J. 2016. *Daucosterol inhibits colon cancer growth by inducing apoptosis, inhibiting cell migration and invasion and targeting caspase signalling pathway.*
- WANG, Q. & XIE, M. 2010. [Antibacterial activity and mechanism of luteolin on *Staphylococcus aureus*]. *Wei Sheng Wu Xue Bao*, 50, 1180-4.
- WANG, R., PADDON-ROW, M. N. & SHERBURN, M. S. 2013. Short Synthesis of 3-(Hydroxymethyl)xylitol and Structure Revision of the Anti-diabetic Natural Product from *Casearia esculenta*. *Organic Letters*, 15, 5610-5612.
- WANG, T., ZHANG, J. C., CHEN, Y., HUANG, F., YANG, M. S. & XIAO, P. G. 2007. [Comparison of antioxidative and antitumor activities of six flavonoids from *Epimedium koreanum*]. *Zhongguo Zhong Yao Za Zhi*, 32, 715-8.
- WANG, Z. Y., HUANG, M. T., FERRARO, T., WONG, C. Q., LOU, Y. R., REUHL, K., IATROPOULOS, M., YANG, C. S. & CONNEY, A. H. 1992. Inhibitory effect of green tea in the drinking water on tumorigenesis by ultraviolet light and 12-O-tetradecanoylphorbol-13-acetate in the skin of SKH-1 mice. *Cancer Research*, 52, 1162-70.
- WANI, S. A. & KUMAR, P. 2018. Fenugreek: A review on its nutraceutical properties and utilization in various food products. *Journal of the Saudi Society of Agricultural Sciences*, 17, 97-106.
- WEESE, T. L. & BOHS, L. 2007. A Three-Gene Phylogeny of the Genus *Solanum* (Solanaceae). *Systematic Botany*, 32, 445-463.
- WEISWALD, L.-B., BELLET, D. & DANGLES-MARIE, V. 2015. Spherical Cancer Models in Tumor Biology. *Neoplasia*, 17, 1-15.
- WESOŁOWSKA, A., NIKIFORUK, A., MICHALSKA, K., KISIEL, W. & CHOJNACKA-WÓJCIK, E. 2006. Analgesic and sedative activities of lactucin and some lactucin-like guaianolides in mice. *Journal of Ethnopharmacology*, 107, 254-258.
- WU, C. H., LIANG, C. H., SHIU, L. Y., CHANG, L. C., LIN, T. S., LAN, C. C., TSAI, J. C., WONG, T. W., WEI, K. J., LIN, T. K., CHANG, N. S. & SHEU, H. M. 2011. *Solanum incanum* extract (SR-T100) induces human cutaneous squamous cell carcinoma apoptosis through modulating tumor necrosis factor receptor signaling pathway. *J Dermatol Sci*, 63, 83-92.

- XIONG, Z.-Q., WANG, J.-F., HAO, Y.-Y. & WANG, Y. 2013. Recent Advances in the Discovery and Development of Marine Microbial Natural Products. *Marine Drugs*, 11, 700.
- XU, R., KANG, Q., REN, J., LI, Z. & XU, X. 2013. Antitumor Molecular Mechanism of Chlorogenic Acid on Inducing Genes GSK-3 beta and APC and Inhibiting Gene beta -Catenin. *Journal of Analytical Methods in Chemistry*, 2013, 951319.
- YAGASAKI, K., MIURA, Y., OKAUCHI, R. & FURUSE, T. 2000. Inhibitory effects of chlorogenic acid and its related compounds on the invasion of hepatoma cells in culture. *Cytotechnology*, 33, 229-235.
- YAHARA, S., NAKAMURA, T., SOMEYA, Y., MATSUMOTO, T., YAMASHITA, T. & NOHARA, T. 1996. Steroidal glycosides, indiosides A-E, from *Solanum indicum*. *Phytochemistry*, 43, 1319-1323.
- YAMAGATA, K., IZAWA, Y., ONODERA, D. & TAGAMI, M. 2018. Chlorogenic acid regulates apoptosis and stem cell marker-related gene expression in A549 human lung cancer cells. *Molecular and Cellular Biochemistry*, 441, 9-19.
- YAN, Y., LI, J., HAN, J., HOU, N., SONG, Y. & DONG, L. 2015. Chlorogenic acid enhances the effects of 5-fluorouracil in human hepatocellular carcinoma cells through the inhibition of extracellular signal-regulated kinases. *Anticancer Drugs*, 26, 540-6.
- YAN, Y., LIU, N., HOU, N., DONG, L. & LI, J. 2017. Chlorogenic acid inhibits hepatocellular carcinoma in vitro and in vivo. *The Journal of Nutritional Biochemistry*, 46, 68-73.
- YANG, J.-S., LIU, C.-W., MA, Y.-S., WENG, S.-W., TANG, N.-Y., WU, S.-H., JI, B.-C., MA, C.-Y., KO, Y.-C., FUNAYAMA, S. & KUO, C.-L. 2012. Chlorogenic Acid Induces Apoptotic Cell Death in U937 Leukemia Cells through Caspase- and Mitochondria-dependent Pathways. *In Vivo*, 26, 971-978.
- YAZDANPARAS, R., ESMAEILI, M. A. & ASHRAFI HELAN, J. 2005. Teucrium polium Extract Effects Pancreatic Function of Streptozotocin Diabetic Rats: A Histopathological Examination. *Iranian Biomedical Journal*, 9, 81-85.

- YEE, S. B., LEE, J. H., CHUNG, H. Y., IM, K. S., BAE, S. J., CHOI, J. S. & KIM, N. D. 2003. Inhibitory effects of luteolin isolated from *Ixeris sonchifolia* Hance on the proliferation of HepG2 human hepatocellular carcinoma cells. *Archives of Pharmacal Research*, 26, 151-6.
- YI, B., HU, L., MEI, W., ZHOU, K., WANG, H., LUO, Y., WEI, X. & DAI, H. 2011. Antioxidant phenolic compounds of cassava (*Manihot esculenta*) from Hainan. *Molecules*, 16, 10157-67.
- YIN, H.-L., LI, J.-H., LI, B., CHEN, L., LI, J., TIAN, Y., LIU, S.-J., ZHAO, Y.-K., XIAO, Y.-H. & DONG, J.-X. 2014a. Two new coumarins from the seeds of *Solanum indicum*. *Journal of Asian Natural Products Research*, 16, 153-157.
- YIN, H.-L., LI, J.-H., LI, J., LI, B., CHEN, L., TIAN, Y., LIU, S.-J., ZHANG, T. & DONG, J.-X. 2013. Four new coumarinolignoids from seeds of *Solanum indicum*. *Fitoterapia*, 84, 360-365.
- YIN, J., XING, H. & YE, J. 2008. Efficacy of berberine in patients with type 2 diabetes mellitus. *Metabolism*, 57, 712-7.
- YIN, R., LI, T., TIAN, J. X., XI, P. & LIU, R. H. 2018. Ursolic acid, a potential anticancer compound for breast cancer therapy. *Critical Reviews in Food Science and Nutrition*, 58, 568-574.
- YIN, Z., ZHANG, W., FENG, F., ZHANG, Y. & KANG, W. 2014b.  $\alpha$ -Glucosidase inhibitors isolated from medicinal plants. *Food Science and Human Wellness*, 3, 136-174.
- YU, X., MAO, W., ZHAI, Y., TONG, C., LIU, M., MA, L., YU, X. & LI, S. 2017. Anti-tumor activity of metformin: from metabolic and epigenetic perspectives. *Oncotarget*, 8, 5619-5628.
- ZAKIKHANI, M., DOWLING, R., FANTUS, I. G., SONENBERG, N. & POLLAK, M. 2006. Metformin is an AMP kinase-dependent growth inhibitor for breast cancer cells. *Cancer Research*, 66, 10269-73.
- ZANG, Y., IGARASHI, K. & LI, Y. 2016. Anti-diabetic effects of luteolin and luteolin-7-O-glucoside on KK-A(y) mice. *Bioscience, Biotechnology, and Biochemistry*, 80, 1580-6.

- ZAORSKY, N. G., CHURILLA, T. M., EGLESTON, B. L., FISHER, S. G., RIDGE, J. A., HORWITZ, E. M. & MEYER, J. E. 2017. Causes of death among cancer patients. *Annals of Oncology*, 28, 400-407.
- ZAPATA, B., DURAN, C., STASHENKO, E., BETANCUR-GALVIS, L. & MESA-ARANGO, A. C. 2010. [Antifungal activity, cytotoxicity and composition of essential oils from the Asteraceae plant family]. *Rev Iberoam Micol*, 27, 101-3.
- ZENG, J., LIU, X., LI, X., ZHENG, Y., LIU, B. & XIAO, Y. 2017. Daucosterol Inhibits the Proliferation, Migration, and Invasion of Hepatocellular Carcinoma Cells via Wnt/beta-Catenin Signaling. *Molecules*, 22.
- ZHANG, D. W., FU, M., GAO, S. H. & LIU, J. L. 2013. Curcumin and diabetes: a systematic review. *Evid Based Complement Alternat Med*, 2013, 636053.
- ZHANG, H. H. & GUO, X. L. 2016. Combinational strategies of metformin and chemotherapy in cancers. *Cancer Chemother Pharmacol*, 78, 13-26.
- ZHANG, Q. W., LIN, L. G. & YE, W. C. 2018. Techniques for extraction and isolation of natural products: a comprehensive review. *Chinese Medicine*, 13, 20.
- ZHAO, B. & HU, M. 2013. Gallic acid reduces cell viability, proliferation, invasion and angiogenesis in human cervical cancer cells. *Oncol Lett*, 6, 1749-1755.
- ZHAO, C., SHE, T., WANG, L., SU, Y., QU, L., GAO, Y., XU, S., CAI, S. & SHOU, C. 2015. Daucosterol inhibits cancer cell proliferation by inducing autophagy through reactive oxygen species-dependent manner. *Life Sciences*, 137, 37-43.
- ZHOU, H., REN, J. & LI, Z. 2017. Antibacterial activity and mechanism of pinoresinol from *Cinnamomum Camphora* leaves against food-related bacteria. *Food Control*, 79, 192-199.
- ZHOU, X., HE, X., WANG, G., GAO, H., ZHOU, G., YE, W. & YAO, X. 2006. Steroidal saponins from *Solanum nigrum*. *Journal of Natural Products*, 69, 1158-63.
- ZŁOTEK, U., MIKULSKA, S., NAGAJEK, M. & ŚWIECA, M. 2016. The effect of different solvents and number of extraction steps on the polyphenol content and antioxidant capacity of basil leaves (*Ocimum basilicum* L.) extracts. *Saudi Journal of Biological Sciences*, 23, 628-633.

- ZOU, L. B. & ZHAN, J. B. 2005. [Purification and anti-cancer activity of ricin]. *Zhejiang Da Xue Xue Bao Yi Xue Ban*, 34, 217-9.
- ZOUITEN, H., ABBASSI, K., ATAY-KADIRI, Z., MZARI, M., MAHI, M. E. & ESSASSI, E. M. 2006. Insecticidal activity of *Solanum sodomaeum* (Solanaceae) extracts on *Schistocerca gregaria* (Forskål) larvae. *Journal of Orthoptera Research*, 15, 171-173.
- ZU, Y., WANG, D., ZHAO, X., JIANG, R., ZHANG, Q., ZHAO, D., LI, Y., ZU, B. & SUN, Z. 2011. A novel preparation method for camptothecin (CPT) loaded folic acid conjugated dextran tumor-targeted nanoparticles. *International Journal of Molecular Sciences*, 12, 4237-49.